UNIVERSITAT DE BARCELONA

Global evaluation of the fitness and virulence determinants in the phytopathogen *Ralstonia solanacearum*

Roger de Pedro Jové

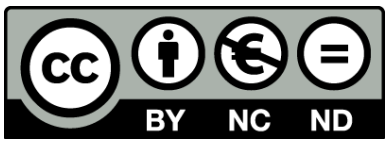

Global evaluation of fitness and virulence determinants in the phytopathogen *Ralstonia solanacearum*

Roger de Pedro Jové

Facultat de Biologia

Departament de Genètica, Microbiologia i Estadística

Programa de Doctorat: Genètica

“Global evaluation of fitness and virulence determinants in the phytopathogen *Ralstonia solanacearum*”

(Avaluació global dels determinants de virulència i d’eficàcia biològica en el fitopatogen *Ralstonia solanacearum*)

Memòria presentada per Roger de Pedro Jové per optar al grau de doctor per la Universitat de Barcelona. Tesi doctoral realitzada sota la direcció del Dr. Marc Valls i Matheu al Departament de Genètica, Microbiologia i Estadística de la Facultat de Biologia (UB) i al Centre de Recerca en Agrigenòmica (CRAG).

Signatura del Director i Tutor,

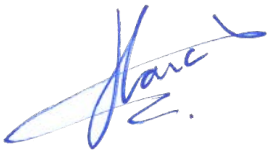

Dr. Marc Valls i Matheu

Signatura del Doctorand,

Roger de Pedro Jové

Barcelona, març de 2023

Global evaluation of fitness and virulence determinants in the phytopathogen *Ralstonia solanacearum*

Roger de Pedro Jové

Roger de Pedro Jové

"Global evaluation of fitness and virulence determinants in the phytopathogen *Ralstonia solanacearum*"

PhD thesis, March 2020

Universitat de Barcelona & Centre de Recerca en Agrigenòmica

Cover design: Ra Paredes

AGRAÏMENTS – ACKNOWLEDGEMENTS

Toca posar punt i final a una etapa de la meva vida marcada per la tesis doctoral. En perspectiva, crec que he estat molt afortunat d'aterrar en un laboratori que m'ha permès conèixer gent nova i compartir espais amb gent meravellosa. Alhora he pogut tornar a viure a la ciutat que m'ha vist créixer, prop de la gent que considero els pilars de la meva vida. En resum, durant aquests quatre anys (o més), he conegut i compartit moments i espais amb gent de dins i fora del laboratori a qui sempre estaré agraït pel seu suport, amistat i comprensió. Si una cosa he après, és que una tesis no és cosa d'una sola persona.

Per començar, al meu director i tutor de tesis, **Marc Valls**, gràcies per donar-me la oportunitat de conèixer el grup mentre feia el grau i el TFG i de plantar les llavors que han esdevingut aquesta tesis. Gràcies per ajudar-me a decidir anar a estudiar el màster fora i al teu suport rebut a l'hora de buscar la beca i durant la tesis. A tu també **Núria Sánchez**, gràcies per co-tutoritzar no oficialment la meva tesis. Les múltiples reunions, però sobretot les teves idees i opinions sinceres m'han fet aprendre i millorar com a científic i persona. També, no voldria deixar d'agrair la confiança dipositada en mi per poder organitzar fins cert punt el dia a dia del laboratori. Han estat quatre anys on m'heu donat la oportunitat d'aprendre, créixer i conèixer nous llocs i persones excepcionals.

A la gent del laboratori, Biobact, laboratori 105, 101 o 103 depèn de quan ens trobéssim. Amb tots vosaltres vull compartir el mèrit de que aquesta tesis arribi a bon port. Estaré eternament agraït a tota la gent que han fet d'aquesta etapa una experiència única. **Marina**, la meva gran supervisora i millor persona, mai oblidaré la teva ajuda i companyia durant el grau. Realment va ser un xoc tornar al laboratori i que tu no hi fossis. Gràcies per ser-hi sempre i donar-me suport en els moments de crisis. **Marc**, a tu també et considero de la primera generació. Gràcies per tots els moments compartits durant aquests anys tant al P2 com als ordinadors colze a colze. **Alex**, la alegria del laboratori i ara l'etern suport per quan els tomàquets decideixen no créixer bé. Gràcies per la teva felicitat contagiosa i pels viatges en cotxe de tornada a Barcelona. **Pau**, gràcies per la teva ajuda durant tota la tesis. Has estat una persona amb qui he confiat i que m'ha acompanyat en tot moment. Gràcies sobretot per fer l'etapa de la quarantena una mica menys desagradable i amena. **Ben**, I'm sad I missed your first months in the lab, but I am happy for those that we were together. You were always there to talk, gossip and make the lab a little bit funnier. J'espère que vous trouverez votre chemin en Nouvelle-Calédonie loin des influences françaises. **Anurag**, I am happy I got to share so many happy moment with you working in the lab but also outside it. Your happiness was contagious and my belly remembers with great pleasure the food you and Munmi (sorry if I misspelled the name) prepared for us multiple times. See you soon in awesome Assam. **Eugenia**, my dear dearest Eugenia. I've missed you a lot this last year, You've been a friend to whom I've always felt safe to come to talk and share my stuff. You are and always will be the public relations and the most friendly person in any lab you go. Τα λέμε σύντομα Ευγενία, σου εύχομαι τα καλύτερα. No em vull oblidar de ningú amb qui he compartit el laboratori; **Liang**, **Ujjal**, **Montse Solé**, **Fernanda**, **Saul**, **Irma**, **Pedro**, **Crina**, **Jenna** i **Marta**, gràcies per tots els moments compartits. Also, to those that have visited us and from whom I've had the oportunity to learn a lot; **Eri**, **Saki**, and **Liang Yang**. No puc acabar sense donar les gràcies als estudiants que han contribuït en els diferents projectes relacionats amb la tesis, gràcies **Fatima**, **Melis**, **Sofia**, i **Jordi** per la vostra dedicació i entusiasme.

Als que encara continueu al laboratori, espero que acabeu el doctorat d'una sola peça i de la millor manera possible. Jo marxo físicament, però us vull continuar veient i sapigueu que sempre em podreu trobar quan vulgueu. **Jose**, sempre recordaré amb alegria el teu entusiasme i les converses sobre ciència o on trobar el millor menjar de Barcelona. Et desitjo tot el millor per la teva nova aventura a Anglaterra. **Weiqi**, you are the next in line to finish with the PhD. I wish you all the luck of the world, although I am sure you'll manage. Thanks for the help and the happiness you always shared. Before you leave, we must do a proper farewell in a Chinese restaurant. **非常感**谢你的友谊. **Nerea**, la teva

arribada va ser un cop d'aire fresc i diversitat al grup. Gràcies per tot. Per ser una persona amb qui poder parlar i en català, que també s'agraeix de tant en tant. Espero que ens puguem continuar veient i trobant més enllà del laboratori. D'una cosa pots estar segura, sempre em tindràs de fan als teus concerts sempre que vulguis! **Jordi**, el meu estimat Jordi, o com t'agrada autoanomenar-te, el meu estimat Dobby. Ja tens el mitjó que tant anhelaves tot i que espero que no et vulguis desenganxar tant de mi. Espero que facis el que facis, i vagis on vagis tinguis un lloc per mi i ens continuem veient (o vinc a matar els teus cucs). **Laia**, una pena que haguem tingut tant poc temps per conèixer-nos. Gràcies per fer d'aquest pixapí una persona feliç idealitzant per un dia el treball al camp collint olives. Moltes gràcies per la teva companyia i experiència en la vida i la ciència. No et desenganxaràs tant fàcilment de mi, i si mai necessiteu un altre parell de mans pel que sigui, aquí em teniu. **Mario**, l'ànima de la festa. Gràcies per dinamitzar el laboratori, les trobades, i animar la gent en tot moment. Ens trobem pel barri o on sigui, de festa o per xerrar. **Álvaro**, al meu veí de laboratori, molta sort en tots els teus experiments i gràcies per la teva energia contagiosa. **Mercè**, el relleu i futur de Bacteriology. Espero que tot vagi molt bé i et desitjo molta sort amb els teus maxiexperiments. M'ha agradat poder tornar a compartir espai al laboratori amb tu després de Wageningen. Si mai tens qualsevol dubte ja saps on trobar-me. Moltes gràcies també a **Fernando**, **Azahar**, **Montse Capellades** i **Joel** per tots els moments compartits.

No podia acabar els agraïments del CRAG sense mencionar a la resta de gent amb qui he compartit espais i que han permès que tot vagi sobre rodes. Als nostres veïns de laboratori, **Nacho**, gràcies per ajudar-nos en tots els moments de crisis. **Unai**, sempre m'has semblat una persona molt accessible, gràcies per animar el passadissos amb el teu somriure. Però sobretot gràcies a la gent que treballa des de l'ombra per a que el CRAG no pari i continuï funcionant. A tot el personal d'hivernacles (**Glòria** i **Alejandro**), als d'administració, als informàtics que tants dubtes m'heu resolt (**Victor** i **Martí**), a la gent de comandes (gràcies **Natàlia** per sempre estar disposada a ajudar) i a la gent de neteja. Sense la vostra feina molts cops invisible i invisibilitzada, res podria funcionar.

I would like to thank **Gunther** and **Johana** for hosting me and giving me the chance to work in a lab with such a great environment. **Ute**, thanks for all the help, guidance, and input in all my experiments. And mostly I'd like to thank to all the people from the laboratory that made my stay memorable, an experience I will always retain in my memory. **Janina**, thanks a lot for your kindness and friendship, I was lucky to be your neighbour. Also, many thanks to **Anna**, **Sina**, **Bilal**, **Andrea**, **Daniel**, **Maurice**, **Wei**, **Yoon Joo**, **Weiliang** and **Luyao** for hosting me, helping me, and for all the gatherings and bouldering excursions. **Jasper**, I was very happy to meet you again after Wageningen, the world is indeed very small. I wish you and your family all the luck in UK. I'd also like to thank **Pitter**, **Melissa** and **Maithy** for hosting me in Jülich, and teaching me a little bit of the proteomics world. Thanks for making my first time living in Germany such a great experience. Vielen Dank, dass Sie meine erste Wohnerfahrung in Deutschland zu einer so großartigen Erfahrung gemacht haben.

Per sort, tot i que de vegades no ho sembli, hi ha vida més enllà del doctorat i del CRAG. Gràcies als amics amb qui en menor o major mesura m'heu acompanyat durant aquest viatge. Sobretot gràcies a les meves amigues de l'institut i biologia. Amb vosaltres he trobat amb qui poder compartir inquietuds i dubtes laborals i vitals. Gràcies de tot cor, espero seguir celebrant molts més sopars amb vosaltres. També em sento afortunat de totes aquelles persones que he anat coneixent durant aquests últims anys, en gran mesura (per no dir en la totalitat) gràcies al Gela (de tu parlaré després). Gràcies per acollir-me sempre amb els braços oberts. Una persona en especial, Ra, gràcies per ser com ets i per aquesta portada tant fenomenal.

Gràcies a tu, Gela, també he pogut conèixer una segona família amb qui he pogut compartir estones de tot. Gràcies **Txus**, **Mireia** i **Kike** per les tardes de jocs i de menjar (que espero que la meva panxa permeti tornar a celebrar amb normalitat). No em podria oblidar del mai Bacon, però sobretot de la Brie, tant de bo sempre tenir la seva energia. Ja que parlem d'animals que t'han canviat la vida, gràcies a les dues gates que han portat amor, companyia i distracció als meus dies d'escriptura. Onix i Deku, crec que som tots molt afortunats d'haver-nos trobat.

A la meva família, no em vull deixar de dir-vos com d'afortunat em sento de tenir-vos. A les meves tietes, cosins i avis. Espero poder continuar celebrant durant molts més anys dinars, sopars i trobades. Iaia, espero que d'aquí poc pugui tornar a gaudir del teu menjar com sempre ho he fet. A la meva família més pròxima, **papa**, **mama** i **Marc**, us dec tot. En tot moment m'heu acompanyat, aconsellat, ajudat i recolzat a cada decisió i pas important de la meva vida. Amb el pas dels anys me n'he adonat que això que jo pensava que era la norma, de vegades, és excepció, així que us vull agrair tots i cadascun dels moments, viatges i anys passats junts. Espero poder retornar-vos d'alguna forma tot el temps i paciència dipositada en mi, una persona de vegades críptica i difícil d'entendre (jo molts cops tampoc m'entenc a mi mateix). Us estimo moltíssim.

Finalment, **Gela**, no sé per on començar. La veritat és que em pensava que seria més fàcil però no em puc posar a escriure sense plorar una mica. Gràcies per aguantar-me. Gràcies per estar amb mi en cada pas del camí de principi a final. Gràcies per no defallir i continuar endavant i creient en mi en tot moment. Crec que mai t'agrairé suficient el fet de no haver-me enviat a la merda en els moments on davant tenies una pedra sense sentiments, compassió, ni capacitat de comunicació. Per sort, aquesta aventura ha estat molt més. He compartit amb tu l'aventura de descobrir-me (o si més no acceptar-me) a mi mateix i de descobrir nous mons i experiències. Vull continuar vivint moltes més aventures, experiències i descobertes amb tu, però sense oblidar-nos del dia a dia. Vull continuar construint això que tenim entre nosaltres, que no sé que és ni serà, però que serà el que nosaltres voldrem. Gràcies per tot, t'estimo amb tot el meu cos.

Gràcies a tothom de tot cor!

SYNOPSIS

Losses to plant pathogens pose a major threat to global agriculture and food security worldwide. In the context of globalisation and climate change, the emergence and dispersion of pathogens resistant to conventional management strategies causes destructive outbreaks. One of the most important bacterial phytopathogen is *R. solanacearum*, the causal agent of the bacterial wilt disease, infecting over 200 plant species. *R. solanacearum* colonises the vascular system of the plants and blocks the water flow by secreting exopolysaccharides, which causes the wilting symptoms. Moreover, it can persist and easily disperse through contaminated soil and waterways. Many different virulence factors have been studied to date but a comprehensive understanding of the transcriptional regulation during the life cycle of this pathogen is lacking. The huge genetic and phenotypic variability of this traditionally tropical pathogen has led to its spread and establishment in temperate regions. To prevent its dispersal and design efficient management strategies, inexistent to date, a thorough understanding of the pathogen infection and dispersion process is of paramount importance.

In this thesis we set to characterise the transcriptomic landscape of *R. solanacearum* to unravel novel virulence and fitness determinants deployed by the pathogen throughout its life cycle. In the first two chapters, we studied the gene expression profile of the bacterium during in different stages of plant infection (Chapter 1 or C1) and the environmental soil and water stages (Chapter 2 or C2). Overall, we have identified a dynamic expression profile of different metabolism and virulence genes along the life cycle of the pathogen. Consistent with previous analysis, we identified that the Type III secretion system (T3SS) is also transcriptionally active at late stages of infection but also in water. Interestingly, we identified the alkali pH as a cue triggering T3SS expression in water, which links to the pH alkalinisation along infection inside the plant. Moreover, we validated the expression of different virulence factors *in planta* such as the flagellar or T4P motility along infection. In soil, we identified the expression of multiple metabolic pathways and stress-related genes that are required for the life of the bacterium in the soil. Among them, we described the induction of genes related to lignin degradation, and alternative metabolic pathways to synthetise carbon molecules related to stress tolerance.

The last two chapters have the objective to characterise and describe specific genes potentially involved in virulence and/or fitness of *R. solanacearum*. In Chapter 3 (C3), we studied the role of the catalase KatE in detail. We proved its importance for the detoxification of the hydrogen peroxide but discovered that, possibly to redundancy, its mutation has no biological effect on the virulence or the life of the bacterium inside the plant. Finally, in Chapter 4 (C4), we took a different approach studying the secretome of *R. solanacearum* inside the apoplast and xylem sap of the plant. Many potential proteins related to virulence were discovered but we focused on the description of the S8 serine protease protein family. Preliminary results suggest that highly accumulated S8 proteases might be involved in the life of the bacterium inside the plant.

To sum up, this thesis provides with a solid background to further study and characterise virulence and fitness factors important for the life cycle of the bacterium. Additionally, we started the description and characterisation of different potential virulence factors important for the bacterium. All this information might be of use in the future to have a comprehensive knowledge of the pathogen and to design novel and efficient management and control strategies.

TABLE OF CONTENTS

INDEX

List of Abbreviations

Abbreviation	Description
3-OH PAME/MAME	(R)-methyl 3-hydroxypalmitate or (R)-methyl 3-hydroxymyristate
AHL	Acyl-homoserine lactones
CFU	Colony forming units
CWDE	Cell wall degrading enzymes
DAMP	Damage-associated molecular pattern
DEG	Differentially expressed genes
Dpi/Hpi	Days/Hours post inoculation
eATP	Extracellular ATP
EPPO	European Plant Protection Organisation
EPS	Exopolysaccharide I
ETI	Effector-triggered immunity
FDR	False discovery rate
GABA	Gamma (γ)-Aminobutyric acid
GB1	Protein G B1 domain
GO	Gene Ontology
HGT	Horizontal gene transfer
HR	Hypersensitive response
Hrc	Hrp conserved
Hrp	Hypersensitive response and pathogenicity
IPTG	Isopropyl β-D-1-thiogalactopyranoside
KEGG	Kyoto Encyclopaedia of Genes and Genomes
LFQ	Label-free quantification
LPS	Lipopolysaccharides
MAMP	Microbe-associated molecular pattern
MAPK	Mitogen-activated protein kinase
MBP	Maltose binding protein
NLR	**Nucleotide-binding leucin rich-repeat**
OG	Oligogalacturonides
ON	Over night
PAMP	Pathogen-associated molecular pattern
PC/Phc	Phenotype conversion
PCA	Principal Component Analysis
Prh	Plant regulatory *hrp*
PRR	Pattern recognition receptor
PTI	PAMP-triggered immunity
PTM	Post-translational modification
QS	Quorum sensing
RH	Relative humidity
Rip	*Ralstonia* protein injected into plant cells
RLU	Relative light units
ROS	Reactive Oxygen Species
RSSC	Ralstonia solanacearum species complex
SOD	Superoxide dismutase
SP	Signal Peptide
T2SS	Type II secretion system
T3E	Type III effectors
T3SS	Type III secretion system
T4P	Type IV pilus
T5SS	Type V secretion system
T6SS	Type VI secretion system
Tat	Twin arginine translocation system
TCA	Tricarboxylic acid cycle
TOR	Target of rapamycin
VBNC	Viable but non-culturable

1. INTRODUCTION

1. INTRODUCTION

1.1 Plant-pathogen interactions

In nature, plants cohabit with multiple and diverse microorganisms, both above and below the ground, such as archaea, bacteria, and fungi (Berendsen, Pieterse and Bakker, 2012; Vorholt, 2012). This complex consortium termed as the plant microbiota has a tremendous impact on plant growth, environment adaptation and productivity. For the microbiota, plants are perceived as a natural and valuable source of nutrients and water from which they have evolved to profit from. This coevolution between symbionts can ultimately have a positive, neutral or negative effect on the plant fitness (Hassani, Durán and Hacquard, 2018; Thoms, Liang and Haney, 2021). The benefits on plant health range from enhanced nutrient acquisition (Singh *et al.*, 2022), priming of plant defence and disease suppression (Westman *et al.*, 2019; Zhou *et al.*, 2022) or higher tolerance to abiotic stresses (Omae and Tsuda, 2022). However, plant immunity must integrate multiple and complex environmental signals to tolerate and associate with nonharmful or even beneficial microbes and block the negative interactions. Luckily for plants, the deleterious (or pathogenic) interactions are an exceptional event, which success is dependent on multiple parameters condensed in the disease triangle (Figure 1). This triangle consists of three interconnected participants that rule the outcome of a plant-pathogen interaction: the host, the pathogen and the environment (Francl, 2001; Scholthof, 2007). Only when the pathogen is present (pathogen dispersal, pathogenicity, and fitness), the host plant is susceptible (age, developmental stage, and general nutrition and health state), and there is a favourable environment (temperature, humidity, and soil properties) the pathogen infection will occur, and the disease symptoms appear.

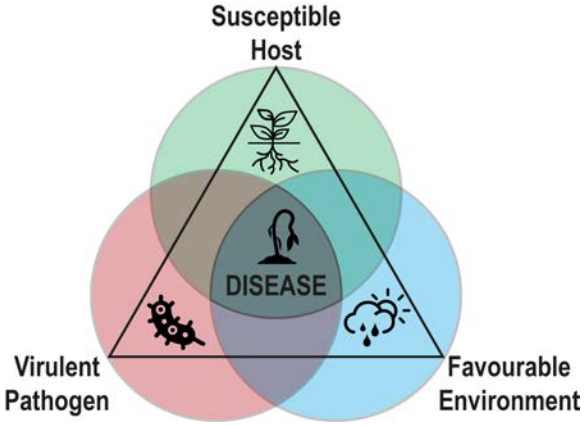

Figure 1. Disease triangle. Three factors determine the outcome of any plant-pathogen interaction: the host, the pathogen, and the environment.

Plant diseases are caused by a plethora of microorganisms that result in losses of 10 to 40 percent in different staple crops, posing a threat to food security (Oerke and Dehne, 2004; Savary *et al.*, 2019). It is estimated that over 150 bacterial species can cause disease by deploying different strategies to successfully colonise the plant (Aguilar-Marcelino *et al.*, 2020). Among the most important bacterial phytopathogens (Mansfield *et al.*, 2012), we have different foliar pathogens that proliferate in the apoplastic (or intercellular) spaces by entering through natural openings, such as stomata, after colonising the leaf surface. *Pseudomonas syringae* pathovars and the different species of *Xanthomonas* spp. (Xin, Kvitko and He, 2018; An *et al.*, 2019) are the most important representatives of this strategy. These bacterial pathogens can cause diseases ranging from leaf spots, cankers, and bacterial blight. Other soil-borne pathogens take advantage of the wounds naturally occurring in the plant due to adverse weather conditions, pests, or plant root development. In this group we can find the famous *Agrobacterium tumefaciens* and, of relevance for this thesis, *Ralstonia solanacearum*. *A. tumefaciens* is famous for its ability to inject fragments of DNA into the host cells that cause the typical crown gall tumours (Chilton *et al.*, 1977). This rare ability to genetically transform plants became a valuable and widely used tool for plant biotechnology and research soon after its discovery (Thompson *et al.*, 2020). Finally, the deadly bacterium *R. solanacearum* is a vascular pathogen that profusely proliferate in the xylem vessels causing an abrupt wilting of the host (Genin and Denny, 2012). Overall, pathogens have evolved numerous strategies to access and colonise the plant to survive and endure to infect new host plants.

Plants are aware of the constant threat posed by pathogens, both above and below ground. To defend themselves, plants have developed multiple physical and chemical barriers to prevent and monitor

pathogen entry, its spreading and subsequent disease development (Bacete *et al.*, 2018; Kaur *et al.*, 2022). As sessile organisms without mobile cells, plants rely on the innate immune response of individual cells and the radiating signalling to systemically activate plant defences (Figure 2) (Jones and Dangl, 2006). To recognise pathogens, plants deploy an arsenal of cell surface pattern recognition receptors (PRR) and mostly intracellular nucleotide-binding leucin rich-repeat (NLR). PRRs recognise nonself-ligands known as pathogen- or microbe-associated molecular patterns (P/MAMP) or endogenous signals product of cell damage and disintegration called damage-associated molecular patterns (DAMP). Typical MAMPs such as bacterial flagellin and fungal chitin are recognised by the well described FLS2 (Chinchilla *et al.*, 2006) and CERK1 (Miya *et al.*, 2007) receptors, respectively. In the same direction, DAMPs such as extracellular ATP (eATP), released upon wounding, or oligogalacturonides (OG), product of cell wall hydrolysis, are recognised by DORN1 (Choi *et al.*, 2014) and WAK1 (Brutus *et al.*, 2010) receptors, respectively. Recognition of elicitors by PRRs leads to the activation of an immune response traditionally named PAMP-triggered immunity (or PTI). PTI response is characterised by the rapid production of apoplastic reactive oxygen species (ROS) and increase of cytosolic Ca^{2+}, which serves as a signal molecule to activate the mitogen-activated protein kinase (MAPK) and the downstream defence response and metabolic reprogramming (Yu *et al.*, 2017). However, some pathogens can hide or interfere with the plant basal PTI responses through the production of a wide array of secreted effectors. Effectors have the main role in promoting plant colonisation by supressing plant immunity and alter plant physiological state (Toruño, Stergiopoulos and Coaker, 2016). In turn, plants can recognise these effectors (directly) or their functions (indirectly) via NLRs. NLR activation triggers the effector-triggered immunity (or ETI) which deploys a similar response as PTI but more robust and amplified that is often followed by localised cell death called hypersensitive response (HR) (Salguero-Linares and Coll, 2019). Traditionally, ETI and PTI were seen as two separate branches of the immune response but nowadays they are conceived as intertwined processes working synergically in pose of plant defence (Ngou *et al.*, 2021) (Figure 2).

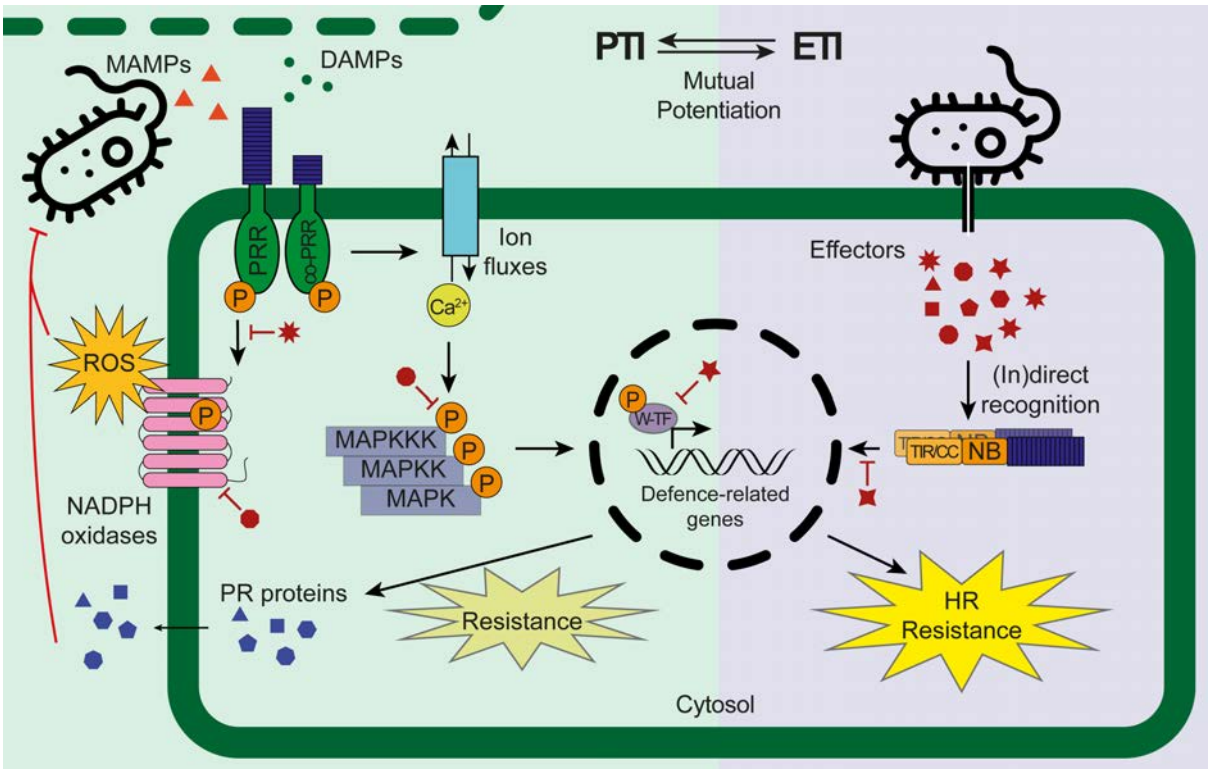

Figure 2. Schematic representation of Pattern-triggered immunity (PTI) and Effector-triggered immunity (ETI) in plants and interference of bacterial effector proteins. Arrows indicate activation of downstream proteins. Red T-shaped head arrows pinpoints a representation of the multiple sites where effectors can interfere with the defence response of the host plant both during PTI and ETI. Abbreviations can be found in the text except for W-TF, WRKY transcription factors; TIR/CC, Toll-interleukin 1-like receptor/coiled-coil; NLR, Nucleotide-binding (NB) and Leucine-rich-repeat (LRR) containing receptors.

Plant-pathogen infection models still disregard the importance of the environment as the third vertex of the disease triangle (Figure 1). Environmental abiotic parameters such as humidity, nutrients and temperature dramatically influence pathogen survival and plant colonisation (Scholthof, 2007; Saijo, Loo and Yasuda, 2018). Fortunately, the gaps on the functional link between environmental conditions and plant immunity are starting to be filled. One example is temperature, an environmental factor that has long been studied as a key determinant of disease development, which influences both pathogens and plants in a species dependent manner. For instance, in *Arabidopsis thaliana*, high temperatures favour PTI at expense of ETI (Cheng *et al.*, 2013; Cheng, Zhang and He, 2019). Overall, in the context of climate change, temperature rise seems to negatively affect plant immunity while it place many pathogens close to their optimal growth temperature (Desaint *et al.*, 2021). Another abiotic parameter, humidity, is known to supress HR in different plant-pathogen interactions and to generally help the pathogen by promoting bacterial virulence and survival inside the plant (Wright and Beattie, 2004; Xin *et al.*, 2016). The effect of nutrient status on plant-pathogen interactions is yet a mystery, although different studies hint to its importance in the modulation of these relations (Hacquard *et al.*, 2016; Yamada *et al.*, 2016; Cheng, Zhang and He, 2019). Integration of these environmental cues on the plant-pathogen (and microbe) interplay will help to move forward to understand and prepare for the challenges of climate change.

1.2 *Ralstonia solanacearum*, the causal agent of the bacterial wilt disease

R. solanacearum is a gram-negative bacterium responsible of the rapid and lethal bacterial wilt disease, considered one of the highest impact bacterial diseases worldwide (Elphinstone, 2005). This vascular pathogen was first described in 1896 by Erwin F. Smith in the Solanaceous species tomato, potato and eggplant and thus named *Bacillus solanacearum* (Smith, 1896; Osdaghi, 2020). Since then, the bacterium has been reassigned to different genera until 1995, when it was finally assigned to the β-proteobacterium genera of *Ralstonia* (Yabuuchi *et al.*, 1995). Recently, the genome taxonomy database team demoted the genus to within the class γ-proteobacterium based on genome evolutionary distances (Parks *et al.*, 2018).

1.2.1 *R. solanacearum* species complex, host range and agronomic importance

R. solanacearum is part of a genotypically and phenotypically heterogeneous group of species and strains grouped under the *R. solanacearum* species complex (RSSC) (Prior and Fegan, 2005). Before the genomic era, the diversity within the RSSC was classified into races and biovars based on, respectively, their host range and their capability to use different carbon sources (Buddenhagen, Sequeira and Kelman, 1962; Hayward, 1964). With the appearance of molecular tools, RSSC race-biovar classification was replaced by a more reliable phylotype-sequevar system based on gene sequence analysis. RSSC was classified into four monophyletic phylotypes (I-IV) and further subdivided into 23 sequevars, concordant with their geographical origin and distribution (Prior and Fegan, 2005; Villa *et al.*, 2005). Phylotype I included strains from Asia, phylotype II from America, phylotype III from Africa and phylotype IV from Australia, Indonesia and Japan, which also contained the closely related species *Ralstonia syzygii* (Remenant *et al.*, 2011). Further phylogenomic studies subdivided the phylotype II into A and B groups (Castillo and Greenberg, 2007). Recent taxonomic revisions consider that RSSC is constituted of three different species although throughout the thesis the phylotype system will be used for convenience. In this classification, only phylotype II strains remain as *R. solanacearum*. Phylotype I and III strains have been reassigned to the new species *R. pseudosolanacearum* and all phylotype IV strains are now part of *R. syzigii* (Safni *et al.*, 2014; Prior *et al.*, 2016). Despite most RSSC strains are endemic to the warm tropical and subtropical regions, outbreaks of cold adapted strains have been increasingly reported over the years (Siri, Sanabria and Pianzzola, 2011; Janse, 2012). These genetically related strains belonging to the phylotype II-B, sequevar 1 (or race 3 biovar 2), such as UY031, were introduced and are nowadays present in highlands of South and North America and in many European countries (Figure 3). Hence, this pathogen is included in the A2 (high risk) list of quarantine organisms by the European Plant Protection Organisation (EPPO) (EPPO, 2018) due to its major risk to cause outbreaks amid the temperature raise context (Cellier and Prior, 2010).

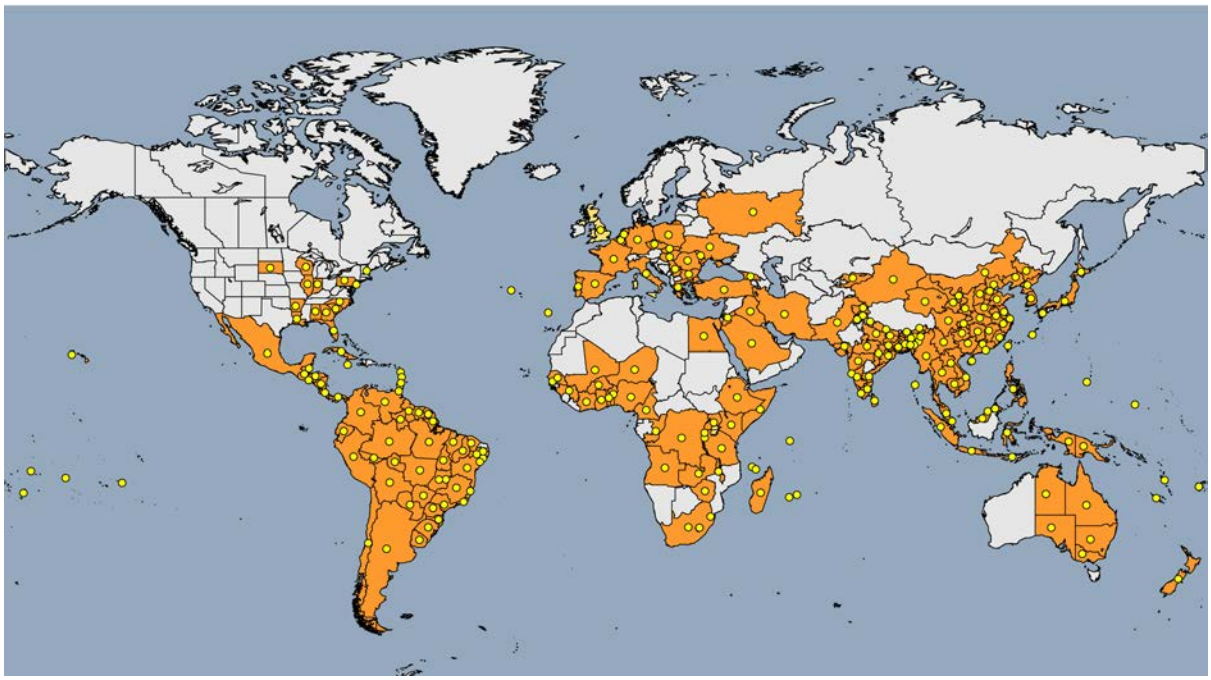

Figure 3. Worldwide geographical distribution of the RSSC. Countries where any species from the RSSC have been detected is indicated by a yellow point and orange colour. Map downloaded and adapted from the EPPO Global Database (EPPO, 2023).

The RSSC has an exceptionally broad host range affecting more than 250 mono and dicotyledonous plant species from 50 different botanical families, most of them from the Solanaceous family (Elphinstone, 2005). This should not come as a shock when we take into account the vast genotypic diversity and geographic distribution of the RSSC. However, no clear association between the host range and the different genetic determinants of the different strains has been found to date (Lebeau *et al.*, 2011; Cellier *et al.*, 2012; Ailloud *et al.*, 2015; Bocsanczy *et al.*, 2022). Among the different species affected by the bacterial wilt disease (Osdaghi, 2020), there are many economically important crops such as potato, tomato, tobacco, banana (moko disease), pepper, peanut or eggplant (García, Kerns and Thiessen, 2019). The lack of efficient control and eradication strategies combined with its survival in soil, waterways and wild asymptomatic plants pose a threat to agricultural systems worldwide (Hayward, 1991). Overall, the agronomic impact of the disease is difficult to quantify but the production losses of infected fields can go up to 90% in tomato, potato and even to 100% in banana cultivars (Yuliar, Nion and Toyota, 2015). Altogether, the wide host range and broad geographic distribution evidence the genotypic flexibility of RSSC species to adapt to new environments and overcome plant resistance. This great biodiversity can be partially explained by the ability of the different species to incorporate long sequences of exogenous DNA into its genome by natural transformation. This suggests an important contribution of recombination and horizontal gene transfer (HGT) events within and between phylotypes to potentially exchange virulence genes, and expand the host range (Guidot *et al.*, 2009; Wicker *et al.*, 2009, 2012; Coupat-Goutaland *et al.*, 2011).

1.2.2 *R. solanacearum* life cycle and infection process

R. solanacearum lifestyle can be split in two, (I) an environmental phase where the pathogen survives in the soil and waterways, which allows its dissemination, and (II) a pathogenic phase inside the host plant (Figure 4). In the soil, the bacterium senses, migrates and adheres to the roots of the host plants by detecting its exudates (Kang *et al.*, 2002; Yao and Allen, 2006). Once in the rhizosphere, the bacterium invades the host through natural wounds caused by the root elongation and the emergence of lateral roots, or wounds produced by other organisms such as nematodes (Vasse, Frey and Trigalet, 1995; Furusawa *et al.*, 2019). Once inside the host, the pathogen rapidly colonises the apoplast of the cortical cells and moves towards the xylem vessels (Digonnet *et al.*, 2012). Inside the xylem, *R.*

solanacearum profusely proliferates and invades the plant systemically reaching concentrations of 10^{10} colony forming units (CFU)/ml (Vasse, Frey and Trigalet, 1995; Clough, Flavier, *et al.*, 1997). When reaching high densities, the pathogen produces exopolysaccharide I (EPS), which blocks the water and nutrient flow in the xylem vessels and causes the characteristic wilting symptoms (McGarvey, Denny and Schell, 2007). At the latest stages of the infection, the pathogen escapes from the vessels and invades the parenchyma before being released back to the soil after the plant death (Planas-Marquès *et al.*, 2020) (Figure 4).

Back in the environment, *R solanacearum* can survive free-living in soil, water, or associated with reservoir hosts. As a soil-borne bacterium, *R. solanacearum* can persist for long periods of time in soil as deep as 75 cm as a saprophyte associated to plant debris or in contaminated tubers for up to four years (Graham and Lloyd, 1979; Graham, Lloyd and Jones, 1979). Contaminated irrigation waters are also an important route for pathogen dispersal, there *R. solanacearum* is able not only to survive for years but also to proliferate and remain infective (Van Elsas *et al.*, 2000; Caruso *et al.*, 2005). To survive in these adverse environments, *R. solanacearum* can enter a viable but non-culturable (VBNC) state (Grey and Steck, 2001; Van Elsas *et al.*, 2001). Many factors such as temperature and starvation influence the entrance and survival in a VBNC state that can be reverted (Álvarez, López and Biosca, 2007; Um *et al.*, 2013). The resuscitation of the pathogen is not well understood but it allows the infection of new host plants with no penalty associated (Grey and Steck, 2001; Caruso *et al.*, 2005; Kong *et al.*, 2014; Kan *et al.*, 2019). Therefore, the capability of strains IIB-1 to survive in cooler environments increases their potential to disseminate and cause outbreaks in temperate regions. Ultimately, reservoir hosts are great allies in the spread and survival of the bacterium over seasons (or overwinter) (Hayward, 1991). *Solanum dulcamara, S. nigrum* or *Urtica dioica* that grow on river edges or close to crop fields can harbour high amounts of bacteria and become a source of inoculum for disease outbreaks (Olsson, 1976; Wenneker *et al.*, 1999; Caruso *et al.*, 2005; Sebastià *et al.*, 2021) (Figure 4).

1.2.3 Control strategies and plant resistance against the bacterial wilt disease

To summarise, the broad host range, the worldwide distribution, and the pathogen persistence in soil and waterways, combined with its aggressiveness led to the cataloguing of *R. solanacearum* as the second most important phytopathogen and a threat to agriculture (Mansfield *et al.*, 2012). Additionally, vascular pathogens are more difficult to detect and control as they are sheltered deep inside the plants (Yadeta and Thomma, 2013). Thus, there is currently a significant effort focused on the development of efficient management strategies to counter *R. solanacearum*. As expected, handling of the bacterial wilt disease has proven to be very challenging, but crop losses can be diminished by employing multiple parallel disease management strategies, a tactic termed as integrated disease management. This include strategies such as good management practices, use of pathogen-free material, use of resistant plant varieties and crop rotation (Denny, 2006).

In the past, chemicals were used to control *R. solanacearum* outbreaks but, in addition to their low efficacy to eradicate the bacterium, fumigation has a severe impact on the environment (Fortnum and Martin, 1998; Ajwa *et al.*, 2010). Also, the heating of the fields known as solarisation was used to free infected fields from the pathogen. But again, it was proven to be inefficient as *R. solanacearum* can survive deep into the soil or sheltered in reservoir plants (Wenneker *et al.*, 1999; Denny, 2006). An alternative is the use of biological agents such as other microorganisms to hinder the pathogen survival. Multiple organisms have been proposed to compete in different ways with *R. solanacearum* and ameliorate the disease progression (Cao *et al.*, 2018; Ma *et al.*, 2018; Wang *et al.*, 2019; Elsayed *et al.*, 2020; Ahmed *et al.*, 2022). One biocontrol strategy is the use of bacteriophages that specifically infect and lysate the bacterial cells in contaminated waterways (Álvarez, López and Biosca, 2019). Despite the promising results, many times these cannot be extrapolated to the fields, where biological agents are exposed and affected by many biotic and abiotic factors (Ahmed *et al.*, 2022).

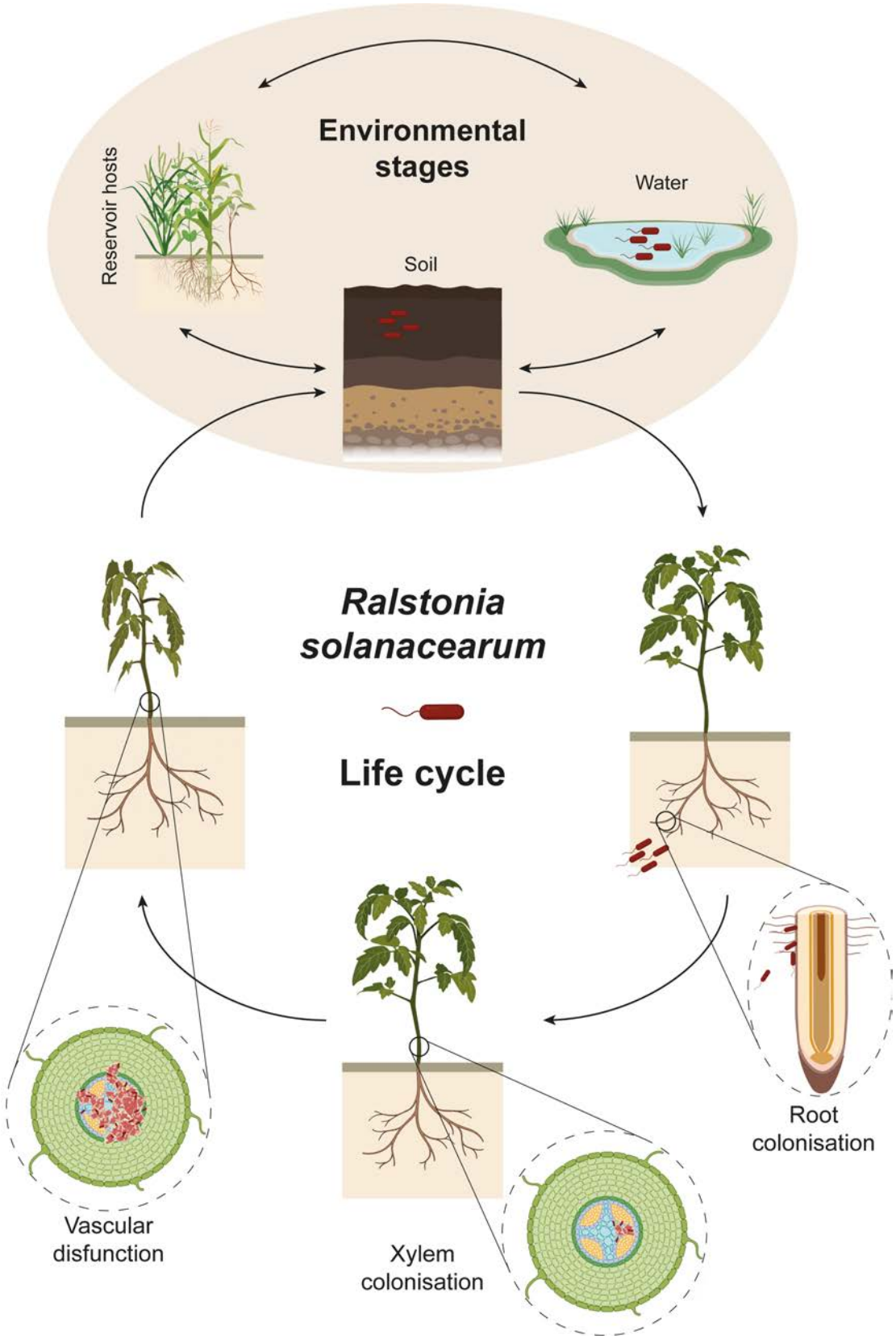

Figure 4. Life cycle of *R. solanacearum*. *R. solanacearum* can survive long periods of time in the soil, waterways, or asymptomatic reservoir hosts until environmental conditions are favourable for plant infection. Once it finds a suitable host, the pathogen will enter through wounds or secondary roots, colonise the root cortical cells apoplast, and move towards the plant xylem vessels. There it will systemically colonise the vasculature of the plant, and profusely proliferate. The secretion of exopolysaccharides (EPS) will clog the vascular system, blocking the water flow and eventually causing the distinctive wilting symptoms. Once the plant dies, the bacteria will be release back to the soil.

In those agricultural fields where the pathogen has not been detected, prevention is the best strategy. To this aim, regulatory agencies like the EPPO have endorsed strict regulations regarding plant management, disease monitoring and eradication in order to control the spread of the pathogen (Denny, 2006). In those regions where *R. solanacearum* is endemic, cultural practices can be applied to alleviate disease incidence. The use of non-contaminated plant material (Álvarez *et al.*, 2015), monitoring of irrigation waters, elimination of weeds that can harbour the bacteria, soil amendments, and mostly crop rotation can help to reduce infection levels (Lemaga *et al.*, 2005; Osdaghi, 2020). Rotation and introduction of grasses or non-hosts such as sweet potato is desirable, unfortunately, rotation is sometimes impossible to apply due to the pressure to produce subsistence crops or limited land (Lemaga *et al.*, 2005; Denny, 2006; Yuliar, Nion and Toyota, 2015). Related with irrigation water, a recent report describes the filtration of aquifer waters through natural sediment under oxygenation as an strategy to remove plant pathogenic bacteria (Eisfeld *et al.*, 2022). In absence of efficient ways to fully control the spread of the disease, one of the most suitable strategies is the development or use of naturally resistant cultivars.

Important advances have been made thanks to the increasing genomic information on commercial crops and of their wild relatives, an important natural source of resistance. Many studies have identified genomic QTLs or genes linked to resistance in different plants such as potato, tomato or eggplant (Salgon *et al.*, 2017; Habe *et al.*, 2019; Lavale *et al.*, 2022). Breeding strategies mostly focus on the introgression of natural source of resistances or known QTLs into economically important crops. For example, breeding strategies in potato (*Solanum tuberosum*) include the use of the wild *Solanum commersonii* (Ferreira *et al.*, 2017) or the wild *Solanum aethiopicum* for eggplant (*Solanum melongena*) breeding (Yuliar, Nion and Toyota, 2015). Unfortunately, the development of resistant crop is limited by the sources of resistance, the difficulty of transferring the genes of interest to the crops and the avoidances of undesirable traits (Lavale *et al.*, 2022). Moreover, resistances found in different plant species are thought to be strain specific, exemplifying the difficulty to reach a worldwide resistant variety (Wang *et al.*, 2000; Carmeille *et al.*, 2006). Interestingly, the use of resistant rootstocks and grafting of the desirable scions have been successfully employed in tomato and eggplant varieties to bypass the breeding process (Rivard and Louws, 2008; Rakha *et al.*, 2020). Overall, different management strategies and resistant plants can be used to minimise the impact of the pathogen in the fields, even though more efficient control strategies are needed to stop the spread of *R. solanacearum*.

1.3 Virulence determinants of *R. solanacearum*

During the last decades, the improvement of the available genetic tools and the genome sequencing of multiple RSSC strains has quicken the identification and functional characterisation of key virulence factors of *R. solanacearum* (Denny, 2006; Genin, 2010). An outline of the different virulence determinants described to date are depicted in the following sections.

1.3.1 Secretion and translocation systems

Secretion systems are essential bacterial tools to interact with both the environment and the hosts. Remarkably, *R. solanacearum* possesses all six secretion systems present in gram negative bacteria, which correlates with the versatility and ecological diversity of this plant pathogen (Genin and Boucher, 2004) (Figure 5). To date, no knowledge is available about the required secretion systems for the life of the bacteria in the environment, but many have been shown to be essential for its pathogenicity. Mutants defective in the Type II, III, VI secretion systems (T2SS, T3SS, and T6SS) and the twin arginine translocation (tat) system have impaired colonisation or proliferation *in planta* (Boucher *et al.*, 1985; Kang Yaowei *et al.*, 1994; González *et al.*, 2007; Zhang *et al.*, 2012). Interestingly, these phenotypes are mild or non-existent when individual exported proteins are mutated, illustrating the redundant and collective effect of the different secreted proteins.

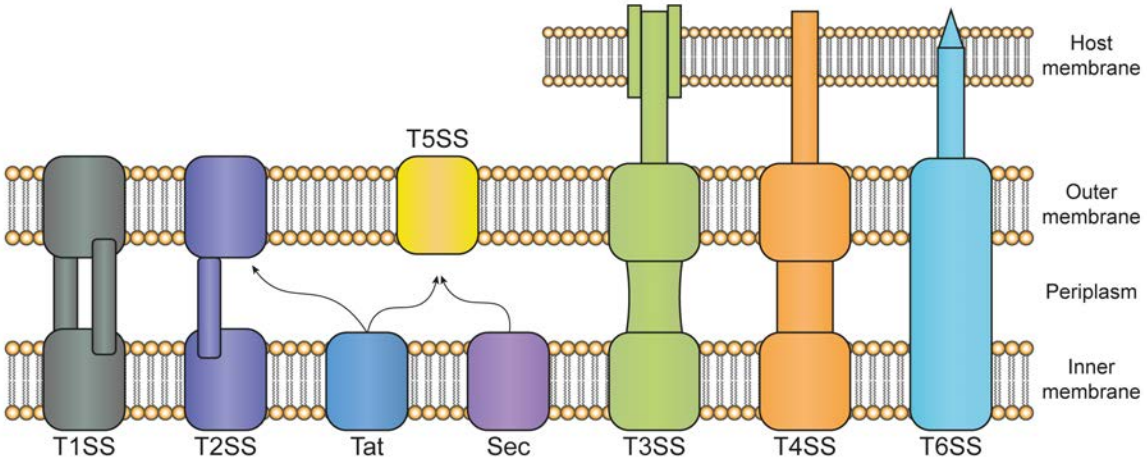

Figure 5. Diversity of protein secretion systems in *R. solanacearum*. Graphical representation of the secretion systems encoded in the genome of *R. solanacearum*. Tat and Sec systems allow the periplasmic transfer of proteins later secreted by the type II (T2SS) or type V secretion systems (T5SS).

T2SS and cell wall degrading enzymes

This system, highly conserved among gram-negative bacteria, allows the export of proteins to the extracellular space. The T2SS, encoded by the *gsp* gene cluster, is responsible of the secretion, among other proteins, of the cell wall degrading enzymes (CWDE). These enzymes are involved in the depolymerisation of cell wall polysaccharides, a basic defence layer of plant hosts (Kubicek, Starr and Glass, 2014). Six CWDE have been characterised in *R. solanacearum*: three polygalacturonases (PehA or PglA, PehB and PehC) (Schell, Roberts and Denny, 1988; Huang and Allen, 1997; González and Allen, 2003), the Pme pectin methyl esterase (Tans-Kersten, Guan and Allen, 1998), the Egl 1,4-β-endoglucanase (Roberts, Denny and Schell, 1988), and the CbhA 1,4-β-cellobiohydrolase (Liu *et al.*, 2005). Interestingly, while T2SS deficient mutants lost their ability to naturally infect the plant and showed a dramatic decrease in their ability to colonise the stem (Kang Yaowei *et al.*, 1994), the mutant lacking all six CWDE was affected to a lesser extent and it was still capable of infecting the plant (Liu *et al.*, 2005). These results suggest that additional secreted proteins by the T2SS contribute to the virulence of *R. solanacearum*.

T3SS and secreted effectors

The T3SS is considered the main virulence determinant of pathogenic gram-negative bacteria. This syringe-like structure, evolutionary related to the flagella, allows the direct injection of so called Type 3 Effectors (T3E) inside the host cells (Coburn, Sekirov and Finlay, 2007; Notti *et al.*, 2015). The genes coding for the T3SS in *R. solanacearum* are located in a single cluster in the megaplasmid expanding 23 Kb that include five transcriptional units and more than 20 different genes (van Gijsegem *et al.*, 1995; Van Gijsegem *et al.*, 2002). These genes were named hypersensitive response and pathogenicity (*hrp*) cluster as they were discovered in a screening to identify avirulent mutants that triggered hypersensitive response in plants, thus crucial for bacterial virulence (Boucher *et al.*, 1985; Arlat *et al.*, 1992). The gene cluster contains the *hrc* (*hrp* conserved) genes that are essential machinery for the syringe apparatus of all known T3SS, and the *hrp* genes, more species-specific, which aid in the effector protein translocation (Denny, 2006).

The T3E translocated into the host cell are required to supress plant defence, modulate host metabolism, or avoid bacterial recognition. However, T3E can also be recognised by plant defence leading to a strong immune response (Landry *et al.*, 2020). Since T3SS was discovered, many studies have tried to unravel the full T3E repertoire of RSSC (Peeters *et al.*, 2013; Landry *et al.*, 2020; De Ryck, Van Damme and Goormachtig, 2023). A recent study on effector diversity on the RSSC identified over 100 T3E, with each strain carrying between 50 and 70 effectors (Peeters *et al.*, 2013; Rubenstein Sabbagh *et al.*, 2019). This contrasts with other plant pathogens such *P. syringae* or *X. campestris* with

30 or 20 T3E genes on average (Roux *et al.*, 2015; Dillon *et al.*, 2019). Even though the T3E repertoires share a core of 16 T3E, there is no clear link between the huge effector diversity and the host specificity (Ailloud *et al.*, 2015; Cho *et al.*, 2019; Rubenstein Sabbagh *et al.*, 2019). To date, more than 50 T3E have been characterised to different degrees (Landry *et al.*, 2020) and the subcellular localisation determined for some of them (Denne *et al.*, 2021). T3Es can interfere with basal plant immunity by preventing transcription of plant defence genes (RipP2, (Le Roux *et al.*, 2015)), regulating the calcium signalling pathway (RipAB, (Zheng *et al.*, 2019; Qi *et al.*, 2022)) or by modulating plant hormone levels (RipAL, (Nakano and Mukaihara, 2018)). Also, effectors such as RipAY can suppress the defence response triggered by the recognition of other effectors (Sang *et al.*, 2020), which allows the bacteria to maintain important virulence functions. Finally, effectors can also manipulate host metabolic processes, which leads to the release of nutrients and creates a favourable niche for the pathogen survival (Macho, 2016). For example, by enhancing the secretion of plant polyamines to prevent proliferation of competitors (RipTAL, (Wu *et al.*, 2019)), by inhibiting enzymatic activities that contribute to plant tolerance to infection (RipAK, (Wang *et al.*, 2021)) or directly hijacking plant metabolism to produce γ-aminobutyric acid (GABA) to support bacterial nutrition (RipI, (Xian *et al.*, 2020)). The functional redundancy that shows some effectors by targeting similar host processes, ensure a robust and durable virulence (Ghosh and O'Connor, 2017; Landry *et al.*, 2020), but hinders effector characterisation and masks their impact on the global bacterial virulence (Lei *et al.*, 2020).

Other secretion systems involved in pathogenicity

The Tat system is predicted to translocate around 70 proteins to the periplasm before they can be secreted to the extracellular space by other secretion systems such as T2SS or T5SS (van Ulsen *et al.*, 2014) (Figure 5). Mutation of one crucial gene of the tat pathway caused an attenuation of the disease severity (González *et al.*, 2007). However, the mutation of the Tat system most likely cause a pleiotropic effect as translocated proteins include not only virulence genes such as CWDE (secreted through the T2SS), but also genes related to cell division, nitrate utilisation or membrane stability. Recently, presence of contact dependent inhibition loci belonging to the T5SS was described in *R. solanacearum*. These loci usually mediate direct competition with other microorganisms, but their specific role in competition or pathogenicity has not been studied (Prokchorchik *et al.*, 2020).

The last secretion system known to affect the virulence of *R. solanacearum* is the T6SS. This system, similar to the T4 bacteriophage tail spike, is also capable of injecting proteins inside the host plant or competitors. The search for orthologs of known T6SS in *R. solanacearum* allowed the discovery of this secretion system (Shrivastava and Mande, 2008). Deletion mutants of one of the essential components of the T6SS showed attenuated virulence, defects in biofilm formation and reduced motility (Zhang *et al.*, 2014).

1.3.2 Extracellular polysaccharides

One of the major virulence factors of *R. solanacearum* is the EPS. This highly heterogenous acidic polymer is composed by a repetition of three different sugar moieties that combine to create a high molecular weight slimy structure (Orgambide *et al.*, 1991). This polymer is synthesised by the *eps* operon that comprises more than 12 genes under a tight transcriptional control (Huang and Schell, 1995; Huang *et al.*, 1995). The secretion of EPS is triggered both *in vitro* and inside the xylem vessels where it responsible of the typical wilting symptoms (Denny and Baek, 1991). Interestingly, non-mucoid mutants that do not produce EPS can naturally infect the plants but show delayed or no wilting symptoms (Kao, Barlow and Sequeira, 1992; Saile *et al.*, 1997). Microscopic observations showed that mutant strains agglutinated and degenerated within the cortical cells triggering plant defences (Araud-Razou *et al.*, 1998). This fact suggested that EPS might have a masking and protective role as not all EPS is released but some remain cell-bond forming a capsule as biofilm (Denny, 1995; McGarvey *et al.*, 1998). However, a study also pointed out the elicitor role of EPS on the resistant tomato cultivars (Milling, Babujee and Allen, 2011). To sum up it seems that EPS might be a recurrent strategy to avoid plant recognition that some resistant varieties have evolved to bypass.

Lipopolysaccharides (LPS) are components of the outer membrane controlling the permeability in gram-negative bacteria that are crucial for the bacterial fitness (Raetz and Whitfield, 2002). LPS consist of a conserved lipid A, a core polysaccharide, and a variable oligosaccharide called the O-antigen that is mostly conserved in *R. solanacaerum* (Kocharova *et al.*, 1993). These components have crucial roles in the plant-pathogen interaction by enhancing colonisation, biofilm formation, survival of the bacteria in adverse niches and by modulating host defence (Newman *et al.*, 2007). In fact, It was described that *R. solanacearum* LPS can supress the plant HR (Graham, Sequeira and Huang, 1977). Removal of the O-polysaccharide was enough to cause the HR but the complete LPS was required for the systemic infection and bacterial proliferation inside the plant (Li *et al.*, 2014).

1.3.3 Motility and host adhesion

Motility is a key factor for many bacterial pathogens as well as for *R. solanacearum*, that possesses the ability to move through flagellum and type IV pilus (T4P), both required for virulence (Corral *et al.*, 2020). Flagellar appendage is responsible for both the swarming and swimming motility, which are multicellular coordinated movements on semisolid medium or individual movements on liquid medium, respectively. Early studies mutated the flagellum components of the filament (*fliC*) or the motor protein (*fliM*) to discover the role of flagella in virulence (Tans-Kersten, Huang and Allen, 2001). They found out that these non-flagellar mutants were not affected on virulence if injected directly inside the plant. However, they showed a reduced infective capacity when inoculated on soil. These results confirm the crucial role of flagellar movement in early environmental stages of plant colonisation, but not for the vascular proferation (Tans-Kersten, Huang and Allen, 2001). Similar to non-flagellate mutants, motile bacteria deficient in the chemotactic sensors (CheA and CheW) required to properly regulate the flagellum, only showed an effect on virulence after soil drenching (Yao and Allen, 2006). Thus, highlighting the importance of chemotaxis together with flagellar movement for the early stages of infection.

T4P is a retractile appendix that will extend, attach and retract on solid or semisolid surfaces in an organised multicellular way, controlling the so-called twitching motility (Mattick, 2002). The deletion of structural genes of the T4P (*pilQ*, *pilT* and *pilA*) were severely impaired in their ability to cause disease in soil or plant inoculation (Liu *et al.*, 2001; Kang *et al.*, 2002). Related to the importance of twitching for both root invasion and *in planta* proliferation, it was not surprising to find out that mutants were also affected in cell aggregation, migration and adherence to the host roots, and in biofilm formation (Kang *et al.*, 2002). Interestingly, twitching mutants also lost their ability to naturally transform as T4P is crucial for DNA internalisation (Kang *et al.*, 2002). Recently, pilus-mediated chemotaxis regulators were discovered (*pilI* and *chpA*), and their disruption also altered biofilm, twitching, transformation efficiency and root adhesion. Moreover, they were affected in virulence when soil inoculated but not when bacteria was directly inoculated inside the plant, like the swimming chemotaxis mutants (Corral *et al.*, 2020). A different T4P gene cluster was discovered to code for Flp pilus, which contributes to virulence in potato by affecting bacterial cell aggregation (Wairuri *et al.*, 2012).

A crucial structure for adhesion to host surfaces is the biofilm, a matrix formed by bacteria cells and extracellular components such as polysaccharides, proteins, and DNA (Montanaro *et al.*, 2011). The capacity of *R. solanacearum* to form biofilm has been reported *in vitro* and inside the plant apoplast and xylem vessels (Mori *et al.*, 2016; Tran *et al.*, 2016). As reported before, biofilm formation is dependent on the T4P (Kang *et al.*, 2002), but also requires lectins. Lectins are carbohydrate binding proteins localised on the cell surface that promote aggregation and adherence of bacterial cells to the extracellular matrices like EPS, providing mechanical stability (Gabius, 2002; Flemming and Wingender, 2010). To date, three different lectins have been identified in *R. solanacearum* (Sudakevitz, Imberty and Gilboa-Garber, 2002; Sudakevitz *et al.*, 2004; Meng *et al.*, 2015). Remarkably, the mutant lacking the lectin *lecM* showed impaired biofilm formation, EPS secretion, reduced attachment ability, and overall deficient plant colonisation (Meng *et al.*, 2015; Mori *et al.*, 2016). Other players modulating biofilm formation are extracellular DNAses, which help on the maturation of the biofilm to help on the bacterium dispersal. The lack of extracellular nucleases produced non-dispersing colonies with abnormal and thick biofilms, showing a reduced ability to colonise plants (Tran *et al.*, 2016).

1.3.4 Protective enzymes and efflux transport

Once *R. solanacearum* enters inside the host plant, it encounters a hostile environment and a harsh plant defence response intended to destroy invaders. The plant ROS burst, deposition of different phenolic and antimicrobial compounds have to be countered or avoided by the bacteria (Saijo, Loo and Yasuda, 2018; Kashyap *et al.*, 2021, 2022). *R. solanacearum* responds to these stresses by deploying an arsenal of protective detoxifying enzymes. Among the genes to resist oxidative stress we find superoxide dismutases (*sodBC*), peroxidases such as *bcp* or the alkyl hydroperoxide reductases (*aphDCF*), the catalse *katE* and the bifunctional catalase-peroxidases *katGab* (Flores-Cruz and Allen, 2009; Colburn-Clifford, Scherf and Allen, 2010) (Figure 6). Most of these genes are under control of the oxidative stress regulator OxyR (Flores-Cruz and Allen, 2011). The deletion of *oxyR* or some other stress related genes cause hypersensitivity to oxidative stress and reduced virulence (Flores-Cruz and Allen, 2009, 2011; Colburn-Clifford, Scherf and Allen, 2010). *R. solanacearum* can also degrade phenolic compounds by utilizing polyphenol oxidases (Hernández-Romero, Solano and Sanchez-Amat, 2005) or degrade the toxic hydroxycinnamic acid by feruloyl-CoA synthetase (Lowe, Ailloud and Allen, 2015; Zhang *et al.*, 2019). Additionally, two multidrug efflux pumps, AcrA and DinF, are required by the pathogen to resist antimicrobial compounds deployed by the plant called phytoalexins. Mutants lacking the efflux pumps showed reduced virulence during infection (Brown, Swanson and Allen, 2007).

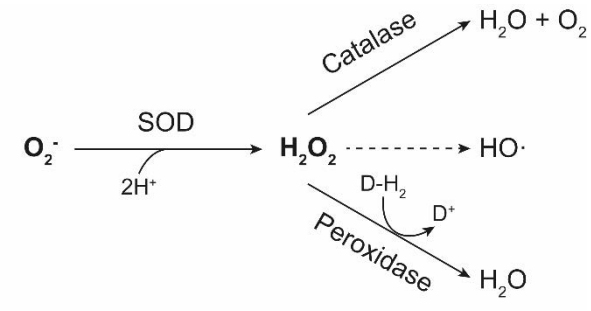

Figure 6. Plant ROS (O_2^- and H_2O_2) detoxification. Superoxide dismutase (SOD) catalyses the dismutation of superoxide into hydrogen peroxide, degraded by catalases and peroxidases. Peroxidases need reduced donors such as NADH or Glutathione (GSH). The non-scavenged hydrogen peroxide can yield hydroxyl radicals, which can damage DNA and lead to mutations (Fasnacht and Polacek, 2021).

1.3.5 Metabolic adaptation, phytohormones and metabolite biosynthesis

R. solanacearum changes its metabolism and modulates the one of the hosts to create an ideal niche for colonisation and dispersion. For example, upon infection, the core virulence HrpG regulator induces the expression of *metE*, which codes for the enzyme responsible of the methionine biosynthesis. This enzyme is induced instead of the isoenzyme *metH* that requires cobalamin (vitamin B12) cofactor to function, a molecule absent in the xylem. Mutation of *metE* caused reduced virulence without affecting bacterial growth, suggesting the importance of methionine as precursor of other metabolites involved in pathogenicity (González *et al.*, 2011; Plener *et al.*, 2012). Inside the xylem vessels, *R. solanacearum* must cope with relatively low oxygen levels. One strategy employed by the pathogen is the oxygen scavenging through the *cco* high-affinity oxidase operon (cytochrome C oxidase *cbb*-3 type), whose mutation caused a delayed wilting symptomatology (Colburn-Clifford and Allen, 2010). Another strategy is the respiration of nitrate (NO_3^-). Remarkably, nitrate concentration in the xylem is optimal for the growth of *R solanacearum*. Its genome encodes for the required enzymes to respirate nitrate to nitrite (NO_2^-), which produces most of the ATP, and of the subsequent reduction and detoxification of reactive nitrogen species to nitric oxide (NO), nitrous oxide (N_2O) and eventually, in some cases, to nitrogen gas (N_2) (Dalsing *et al.*, 2015; Prior *et al.*, 2016). Also, *R solanacearum* genome codes for the necessary genes to assimilate nitrate and incorporate the nitrogen into other compounds (Dalsing and Allen, 2014). Overall, nitrate assimilation and respiration contributes to root attachment, stem colonisation and virulence (Dalsing and Allen, 2014; Dalsing *et al.*, 2015). Interestingly, only phylotypes I and III code for the *nosZ* enzyme in charge of the final reduction to N_2. This enzymatic reaction is required for growth under anaerobic conditions in phylotypes I and III, whereas the partially denitrifying phylotypes II and IV can perfectly grow in these conditions. These findings indicate that within the RSSC two different metabolic strategies evolved to survive in the xylem (Truchon *et al.*, 2023).

Putrescine is a virulence secondary metabolite produced by *R. solanacearum* in the xylem. Even though this polyamine cannot be used as a sole carbon or nitrogen source, it is 70-fold increase upon infection and plays an important role in enhancing disease progression. Also, the deletion of putrescine biosynthesis gene (*speC*) impaired the growth of the bacterium in the xylem (Lowe-Power *et al.*, 2018). Recently, a T3E has been identified to target the plant putrescine biosynthesis pathway to enhance its production. This accumulation of putrescine production creates the perfect niche for *R. solanacearum* as putrescine will trigger defence response that will only inhibit bacterial competitors (Wu *et al.*, 2019). *R. solanacearum* also produces ralfuranones and ralstonins (or ralsolamycins) during infection. These two secondary metabolites induced by plant glucose or galactose are required for full virulence of the pathogen (Ishikawa *et al.*, 2019).

Many phytopathogenic bacteria can produce plant hormones to modulate and hijack plant physiology. *R. solanacearum* can produce ethylene, auxin and citokynins (Genin and Boucher, 2002; Valls, Genin and Boucher, 2006). Production of ethylene (*efe*) and auxin is positively regulated by the core virulence regulator HrpG and seem to be accumulated in the host plant during infection. However, their role has never been elucidated as deletion mutants are not affected in virulence (Hirsch *et al.*, 2002; Ratnayake, 2002; Valls, Genin and Boucher, 2006). In contrast, the inactivation of the cytokinin biosynthesis, coded by the *tzs* gene, has been linked to reduced virulence (Ratnayake, 2002). Besides synthesising hormones, the *nag* gene cluster was described to degrade salicylic acid to avoid its inhibitory effect and toxicity on *R. solanacearum* (Lowe-Power *et al.*, 2016).

1.4 Genome structure and gene regulatory networks

The genome of the *R.solanacearum* (nowadays *R. pseudosolanacearum*) GMI1000 strain (phylotype I) was first sequenced in 2002, becoming the first reference genome of the RSSC and one of the first bacterial plant pathogen genome ever sequenced (Salanoubat *et al.*, 2002). Since then, more than 100 genomes from different strains have been completely sequenced, allowing a deeper understanding of RSSC complexity (Xu *et al.*, 2011; Meng, 2013; Chen *et al.*, 2017; Tan *et al.*, 2019; Geng *et al.*, 2022). Among them, cold-adapted strains from the phylotype II-B such as UY031 and UW551 (Guarischi-Sousa *et al.*, 2016; Hayes, MacIntyre and Allen, 2017). *R. solanacearum* has a bipartite genome organisation with two replicons so-called the chromosome (~3.7 Mb) and the megaplasmid (~2 Mb) yielding a genome size of ~5.7 Mb (Salanoubat *et al.*, 2002). However, both replicons contain essential and pathogenicity-related genes for the bacteria so their names should not confuse us about their essentiality for the bacterium.

R. solanacearum has become a model organism for the study of the plant-pathogen interactions as many genetic tools are available, it can be naturally transformed and infect model organisms such as *A. thaliana* (Bertolla *et al.*, 1997; Digonnet *et al.*, 2012). Moreover, the complex regulatory network controlling the different virulence factors has been historically studied and partially elucidated. Many different cues affect the gene regulation such as multiple environmental factors, host availability and bacterial density (Schell, 2000; Coll and Valls, 2013). In the following sections, an overview of the main regulatory networks modulating gene expression are described (Figure 7).

1.4.1 The phenotype conversion (*phc*) sensing system

R. solanacearum is prone to spontaneously mutate producing non-mucous colonies associated with loss of virulence, a phenomenon that was named phenotype conversion (PC) (Kelman, 1954). PC was puzzling the scientists until the discovery of a LysR-type transcriptional regulator PhcA, which showed a high mutation rate upon stressful conditions (Brumbley, Carney and Denny, 1993; Denny *et al.*, 1994). Subsequent studies found out that PC mutants showed enhanced motility and siderophore production, attributes more suitable to survive in stressing environments, while reduced EPS and CWDE secretion (Brumbley and Denny, 1990; Huang *et al.*, 1995; Bhatt and Denny, 2004; Liu *et al.*, 2022). Additionally, recent transcriptomic studies discovered that PhcA can modulate the expression of over 12% of *R. solanacearum* genes with major impacts not only in virulence genes but also nitrogen metabolism among many others (Khokhani *et al.*, 2017). Interestingly, levels of functional PhcA are controlled in a

cell density manner by the *phcBSR* operon. This unique quorum sensing (QS) system relies on the production by PhcB of (R)-methyl 3-hydroxypalmitate (3-OH PAME) or (R)-methyl 3-hydroxymyristate (3-OH MAME) depending on the strain (Flavier, Clough, *et al.*, 1997; Kai *et al.*, 2015; Ujita *et al.*, 2019). At high cell densities, the local accumulation of these small molecules in the extracellular space, will be sensed by the two component system PhcS/PhcR that will activate the PhcA (Clough, Lee, *et al.*, 1997). Then, functional PhcA will directly regulate expression of genes such as the CWDE *egl* or the EPS core regulator *xpsR* by binding to their promoter regions (Huang *et al.*, 1995, 1998), and indirectly regulate many other through other regulatory systems (Genin and Denny, 2012). Parallel studies added more layers of complexity to the coordinated regulation of the EPS expression. The VsrA/VsrD two-component system was reported to induce *xpsR* together with the PhcA, while VsrB/VsrC system was described to induce the *eps* operon together with XpsR (Huang *et al.*, 1995, 1998; Garg *et al.*, 2000). In contrast, the EpsR regulator linked to the T3SS cascade inhibits the expression of the *eps* operon (Chapman and Kao, 1998). VsrBC and VsrAD two component systems regulate other traits besides the EPS. On one hand, VsrD together with PhcA induced the expression of *cbhA* and of the genes responsible for the synthesis of ralfuranones, which contribute to create a positive feedback loop with the *phc* cascade and the VsrBC and VsrAD systems (Schell, 2000; Mori *et al.*, 2018). On the other hand, the VsrBC represses the production of PglA, which is positively regulated by the two component system PehSR. This system also positively regulates different motility and chemotaxis systems, that are indirectly repressed by the inhibitory effect of PhcA on PehSR (Huang, Denny and Schell, 1993; Kang *et al.*, 2002; Meng, Yao and Allen, 2011) (Figure 7).

Overall, the PhcA and its satellite systems, act as the master switch that control the trade-off between virulence gene induction and bacterial multiplication in a cell density dependent manner (Peyraud *et al.*, 2016). In early stages of infection, when bacterial densities are below 10^7 cells/ml, bacterial cells are mostly motile and do not produce EPS as PhcA is inactive. At later stages of infection, when bacterial densities rise above 10^7 cells/ml, and thus the 3-OH PAME/MAME accumulate, the PhcA is activated leading to the production of EPS and repression of bacterial motility (Khokhani *et al.*, 2017). However, except for the EPS production, most traits regulated by PhcA have only been validated *in vitro* suggesting that they cannot be extrapolated to the plant context. A clear example is the repression of the T3SS by PhcA in cultures but not *in plata*, where T3SS is highly expressed throughout infection (Genin *et al.*, 2005; Jacobs *et al.*, 2012; Monteiro *et al.*, 2012). These results suggest a complex multilayer regulation dependent on many environmental signals that are integrated *in planta*.

1.4.2 The canonical quorum sensing systems

R. solanacearum possesses a second QS system named SolR/SolI, homologous to the common LuxR/LuxI system widespread in bacteria (Flavier, Ganova-Raeva, *et al.*, 1997). SolI is required for the biosynthesis of the autoinducer molecules N-hexanoyl and N-octanoyl-homoserine lactones (Acyl-homoserine lactones, AHL) that can freely diffuse to the extracellular space. When AHL accumulates with increasing bacterial densities, the transcription factor SolR is activated and its target genes induced (Flavier, Ganova-Raeva, *et al.*, 1997). Only *aidA* gene, with an unknown function, was identified to be regulated by SolR. Despite the autoinducer nature of the system, *solRI* is also induced by the core regulator PhcA. The two-layer regulation of SolRI system allows for a hierarchical control of its activation. First, it is induced through the PhcA by accumulation of 3-OH PAME/MAME when cells reach 10^7 cells/ml, and in a second phase, at 10^8 cells/ml, SolR is activated by the produced AHL by SolI (Flavier, Ganova-Raeva, *et al.*, 1997). This suggests that downstream genes induced by the SolRI system have a role during the last stages of infection, and thus, the *solRI* mutants show no impact on virulence under regular infection conditions (Flavier, Ganova-Raeva, *et al.*, 1997; Schell, 2000). However, this system was reported to contribute to virulence in cold adapted strains at low temperatures (Meng *et al.*, 2015). Consistent with this hypothesis, the SolRI system was also modulated by RpoS sigma factor, associated with stress survival and stationary growth phase (Flavier, Schell and Denny, 1998) (Figure 7).

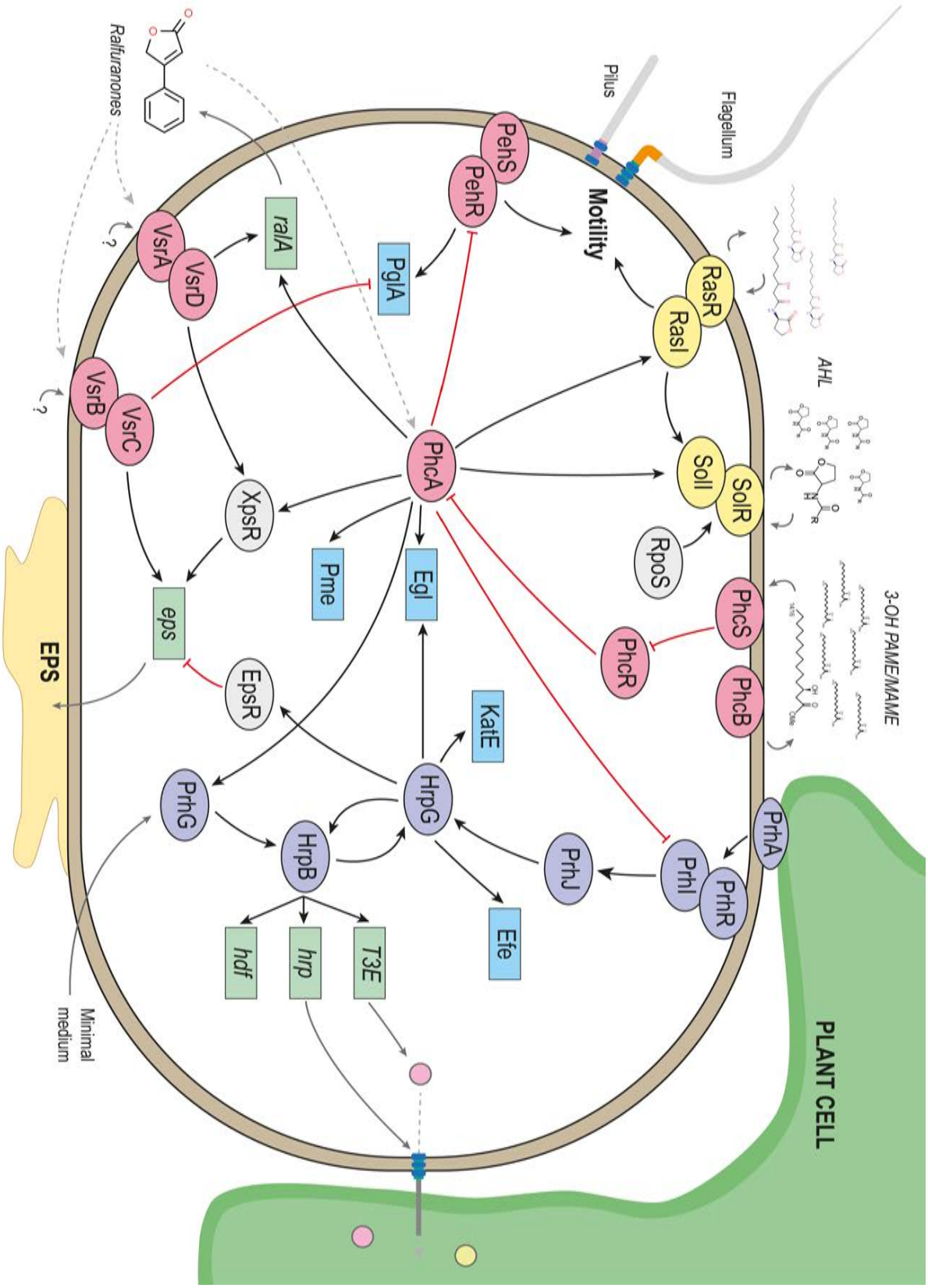

Figure 7: Schematic representation of the *phc*, *sol*, *ras*, and *hrp* regulatory networks described in *R. solanacearum*. Regulatory proteins are marked by different coloured circles depending on the regulatory network: pink – *phc* network, yellow – *sol*/*ras* network, purple – *hrp* network, and in grey other regulatory proteins. Rectangles depict downstream activated or repressed gene products (blue) or gene/operons (green). Black arrows indicate activation, red T-shaped arrows indicate inhibition and grey dashed arrows indicate a positive effect through an unknown pathway. Abbreviations meaning are given in the text.

Recently, another uncharacterised QS system homologous to the LuxR/LuxI designated RasR/RasI was identified. Similar to the other systems, the RasI produce an autoinducer AHL molecule called N-(3-hydroxydodecanoyl)-homoserine lactone (3-OH-C12-HSL), which are sensed by RasR. In contrast with the SolRI system, RasRI was shown to be critical for the virulence and fitness of the bacteria, controlling the production of CWDE, motility and biofilm formation. Moreover, it is another player in the complex hierarchical control of the QS network in *R. solanacearum*, in which PhcA controls the expression of RasIR, and this of the SolIR (Yan *et al.*, 2022) (Figure 7).

1.4.3 The T3SS regulatory cascade

Once the *hrp* operon was identified to code for the T3SS in *R. solanacearum* and its crucial role in virulence elucidated, all efforts focused on unravelling the regulation of this virulence factor. Early studies discovered that expression of *hrp* genes was highly dependent on the growth environment, being induced when grown in minimal media but repressed in rich media or in the presence of different carbon or nitrogen sources (Arlat *et al.*, 1992). The first gene described from the *hrp* operon was *hrpB*, encoding a transcriptional activator controlling not only the *hrp* operon but also genes outside the cluster (Genin *et al.*, 1992). It was not until the first co-cultures of *R. solanacearum* with plant cells that the upstream receptors and regulators could be uncovered. First, the PrhA receptor (named for plant regulatory *hrp*) was identified to sense an unknown molecule to date related to plant cell contact (Marenda *et al.*, 1998; Aldon *et al.*, 2000). This signal was found to transduce to the two-component regulatory system PrhR/PrhI that induces the expression of *prhJ*. The PrhJ protein will drive the expression of HrpG, core regulator of the T3SS, required for the *hrpB* activation and subsequent *hrp* genes expression (Brito *et al.*, 1999, 2002). However, this cascade representation was seen from the beginning as a simplification of a more complex regulatory network. Early on, it was already discovered that other unknown signals were regulating *prhJ* independently from PrhA signalling and that growth in minimal media was also inducing the T3SS cascade at the HrpB level, although the disruption of the *hrpG* also abolished the downstream response (Brito *et al.*, 1999; Zuluaga, Puigvert and Valls, 2013). A partial explanation was given with the discovery of PrhG, a regulator controlling *hrpB* expression under environmental signals found under minimal medium growth (Plener *et al.*, 2010). Also, a positive feedback loop from HrpB to *hrpG* transcription was described (Occhialini *et al.*, 2005). Moreover, the QS controlled PhcA regulator was found to repress expression of the *prhRI* signalling genes while inducing *prhG*, linking the two main virulence regulatory networks of *R. solanacearum* (Yoshimochi *et al.*, 2009; Zhang *et al.*, 2013) (Figure 7).

The HrpB and HrpG are the two master T3SS regulators, and their regulons include many crucial genes for *R. solanacearum* virulence and fitness *in planta*. Both genes are required for full virulence, but mutant strains showed different infection abilities. Whereas *hrpB* mutant showed reduced infection, and colonisation ability, *hrpG* mutant could not transit through the endodermis (Vasse *et al.*, 2000). This illustrates that each regulon activates the expression of genes required in different stages of plant colonisation. The HrpB protein mostly regulates the expression of genes containing the hrp_{II} box in the promoter region (Cunnac, Boucher and Genin, 2004), which can be found in around 200 different genes (Occhialini *et al.*, 2005). Positively HrpB-regulated genes comprise all the T3SS machinery, all the T3E, and different helper T3SS proteins such as type III chaperons which aid during the effector translocation (Occhialini *et al.*, 2005; Mukaihara, Tamura and Iwabuchi, 2010; Lonjon *et al.*, 2016). Additional genes without the hrp_{II} box like some T3E were also induced, meaning that HrpB indirectly induce them or target other regulatory regions (Mukaihara, Tamura and Iwabuchi, 2010). HrpB also regulates the expression of genes beyond the T3SS and T3E, such as the *hrpB*-dependent diffusible factor operon (*hdf*) (Delaspre *et al.*, 2007). The final product of the *hdf* operon could be secreted to interfere with the QS singling of competitors. Interestingly, the other gene of the operon was identified to be required for full fitness of *R. solanacearum* during mixed infections *in planta* (Macho *et al.*, 2010). The HrpG regulon consists of around 400 genes, of which approximately 180 are solely regulated by HrpG independently from HrpB, whereas the others are regulated by HrpG through HrpB (Valls, Genin and Boucher, 2006). The HrpG independently regulated genes include phytohormones, CWDE (e.g. *egl*), oxidative stress

response genes, cell attachment proteins, and the EPS repressor *epsR* (Valls, Genin and Boucher, 2006) (Figure 7).

This complex multi-layered regulation network can be understood if we think of *R. solanacearum* as a pathogen that has to survive in different environments within and outside the host plant (Schell, 2000). However, we still lack a comprehensive knowledge of the pathogen gene regulation as many times *in vitro* discoveries cannot be extrapolated to phenotypes *in planta* and only part of the intricate life cycle has been studied in detail. Answers on how the pathogen survives not only inside the host plant but also in the soil and water environments should open new opportunities for research and eventually, disease control.

2. OBJECTIVES

2. OBJECTIVES

This thesis is part of the long-term efforts to comprehend and elucidate the genetic program that governs *R. solanacearum* adaptation to the plant host and environment. The primary objective of this research is to establish a foundation for future studies by investigating and providing novel insights into gene expression of key virulence and fitness determinants deployed throughout the life cycle of the destructive *R. solanacearum*. By accomplishing the following objectives, this research may contribute to the development of innovative management strategies for controlling *R. solanacearum* and mitigating its impact on global food security.

The main objectives of this thesis are presented below:

I. To determine *R. solanacearum* transcriptomic landscape during infection

II. To determine *R. solanacearum* transcriptomic landscape in the environment

III. To functionally characterise candidate *R. solanacearum* virulence and/or fitness genes

IIIa. To functionally characterise the catalase KatE

IIIb. To decipher the function of the serine proteases during infection

Informe del director de tesi del factor d'impacte i la contribució de l'estudiant en els articles publicats

(PhD supervisor report on the student contribution and impact factor of the publications)

La memòria de la tesi doctoral "Global evaluation of the fitness and virulence determinants in the phytopathogen *Ralstonia solanacearum*" (Avaluació global dels determinants de virulència i d'eficàcia biològica en el fitopatogen *Ralstonia solanacearum*) presentada per Roger de Pedro Jové conté dues publicacions, incloses en els capítols 1 i 3, i dos capítols addicionals (2 i 4). La participació del doctorand en cadascuna de les publicacions és la que es detalla a continuació:

Capítol 1: Publicació 1

Títol: Dynamic expression of *Ralstonia solanacearum* virulence factors and metabolism-controlling genes during plant infection
Autors: **R. de Pedro-Jové**†, M. Puigvert†, P. Sebastià†, A. P. Macho, J. S. Monteiro, N. S. Coll, J. C. Setúbal, and M. Valls
Revista: BMC Genomics
Índex d'impacte: 4,558 (2021) – Q2 (Biotechnology & Applied Microbiology and Genetics & Heredity)

El doctorand ha ajudat a la recol·lecció del material i a la posada a punt de la part experimental junt amb la doctoranda Marina Puigvert. El doctorand també ha dut a terme l'anàlisi bioinformàtic, la preparació del manuscrit i les figures junt amb el doctorand Pau Sebastià. El doctorand també ha participat activament en la planificació del projecte i la resposta als *referees*.

Capítol 3: Publicació 2

Títol: KatE From the Bacterial Plant Pathogen *Ralstonia solanacearum* Is a Monofunctional Catalase Controlled by HrpG That Plays a Major Role in Bacterial Survival to Hydrogen Peroxide
Autors: Tondo ML†, **de Pedro-Jové R**†, Vandecaveye A, Piskulic L, Orellano EG and Valls M
Revista: Frontiers in Plant Sciences (Front Plant Sci)
Índex d'impacte: 5.754 (2020) – Q1 (Plant Sciences)

El doctorand ha estat responsable de part de la planificació i realització dels experiments detallats a continuació: PCRs quantitatives a temps real en els diferents medis de cultiu i estadis de creixement en diferents mutants, quantificació del biofilm i tests de patogenicitat. El doctorand ha redactat els resultats, discussió i materials i mètodes de la seva part experimental i ha contribuït a la correcció i redacció de la resta de l'article. El doctorand també ha participat activament en la planificació del projecte i la resposta als *referees*.

El director,

Marc Valls Matheu
Barcelona, març de 2023

3. CHAPTER 1

PUBLICATION 1

Dynamic expression of *Ralstonia solanacearum* virulence factors and metabolism-controlling genes during plant infection

Resum de la publicació 1 en català

“Dynamic expression of *Ralstonia solanacearum* virulence factors and metabolism-controlling genes during plant infection”

“Expressió dinàmica de factors de virulència i gens reguladors del metabolisme de *Ralstonia solanacearum* durant la infecció”

R. de Pedro-Jové†, M. Puigvert†, P. Sebastià†, A. P. Macho, J. S. Monteiro, N. S. Coll, J. C. Setúbal, i M. Valls

Referència: *BMC Genomics* **22**, 170 (2021). https://doi.org/10.1186/s12864-021-07457-w

Antecedents

Ralstonia solanacearum és l'agent causal del marciment bacterià, una malaltia devastadora en plantes responsable de greus pèrdues econòmiques en espècies com la patatera, tomaquera i altres plantes solanàcies en països de clima temperat. L'anàlisi de l'expressió gènica en *R. solanacearum* ha estat clau per desxifrar molts determinants de la virulència, així com les seves xarxes reguladores. No obstant això, la majoria d'aquests anàlisis s'han realitzat utilitzant bacteris cultivats en medi mínim o dins la planta després de l'aparició de símptomes, que es produeixen en les fases tardanes de la infecció. Per tant, hi ha poca informació sobre el programa genètic que coordina l'expressió de gens de virulència i l'adaptació metabòlica de *R. solanacearum* al llarg de les diferents fases d'infecció de la planta.

Resultats

Hem realitzat un anàlisi de seqüenciació del ARN del transcriptoma de bacteris recuperats de l'apoplast i del xilema de patateres asimptomàtiques o marcides, que corresponen a tres condicions diferents durant la infecció (Apoplast, Xilema primerenc i tardà). Els nostres resultats mostren una expressió dinàmica de gens que controlen el metabolisme i factors de virulència durant el creixement parasitari dins de la planta. Els gens de la motilitat flagel·lar van ser especialment sobre-expressats a l'apoplast i els gens de motilitat per contracció (*twitching*) van mostrar una expressió més sostinguda dins la planta independentment de la condició. Els gens induïts al xilema van incloure gens de virulència, com el sistema de secreció de tipus III (T3SS) i la majoria dels seus efectors, i gens d'utilització del nitrogen. Els reguladors riu amunt del T3SS només van ser sobre-expressats a l'apoplast, precedint la inducció dels seus gens diana riu avall. Finalment, un gran subconjunt de gens involucrats en el metabolisme central del bacteri van ser trobats reprimit exclusivament en el xilema en les fases tardanes d'infecció.

Conclusions

Aquest és el primer informe que descriu els canvis dinàmics transcripcionals durant la infecció de *R. solanacearum* dins de la planta. Les nostres dades descriuen quatre programes genètics principals que defineixen la fisiologia dels gens del patogen durant la colonització de plantes. L'expressió descrita dels gens de virulència, que podria reflectir estats bacterians en diferents fases d'infecció, proporciona informació clau sobre el procés d'infecció de la patatera per *R. solanacearum*.

Pedro-Jové et al. BMC Genomics (2021) 22:170
https://doi.org/10.1186/s12864-021-07457-w

BMC Genomics

RESEARCH ARTICLE Open Access

Dynamic expression of *Ralstonia solanacearum* virulence factors and metabolism-controlling genes during plant infection

R. de Pedro-Jové[1,2†], M. Puigvert[1,2†], P. Sebastià[2†], A. P. Macho[3], J. S. Monteiro[4], N. S. Coll[2], J. C. Setúbal[4] and M. Valls[1,2*]

Abstract

Background: *Ralstonia solanacearum* is the causal agent of bacterial wilt, a devastating plant disease responsible for serious economic losses especially on potato, tomato, and other solanaceous plant species in temperate countries. In *R. solanacearum*, gene expression analysis has been key to unravel many virulence determinants as well as their regulatory networks. However, most of these assays have been performed using either bacteria grown in minimal medium or *in planta*, after symptom onset, which occurs at late stages of colonization. Thus, little is known about the genetic program that coordinates virulence gene expression and metabolic adaptation along the different stages of plant infection by *R. solanacearum*.

Results: We performed an RNA-sequencing analysis of the transcriptome of bacteria recovered from potato apoplast and from the xylem of asymptomatic or wilted potato plants, which correspond to three different conditions (Apoplast, Early and Late xylem). Our results show dynamic expression of metabolism-controlling genes and virulence factors during parasitic growth inside the plant. Flagellar motility genes were especially up-regulated in the apoplast and twitching motility genes showed a more sustained expression *in planta* regardless of the condition. Xylem-induced genes included virulence genes, such as the type III secretion system (T3SS) and most of its related effectors and nitrogen utilisation genes. The upstream regulators of the T3SS were exclusively up-regulated in the apoplast, preceding the induction of their downstream targets. Finally, a large subset of genes involved in central metabolism was exclusively down-regulated in the xylem at late infection stages.

(Continued on next page)

* Correspondence: marcvalls@ub.edu
†R. de Pedro-Jové, M. Puigvert and P. Sebastià contributed equally to this work.
[1]Department of Genetics, University of Barcelona, Barcelona, Catalonia, Spain
[2]Centre for Research in Agricultural Genomics (CSIC-IRTA-UAB-UB), Bellaterra, Catalonia, Spain
Full list of author information is available at the end of the article

(Continued from previous page)
Conclusions: This is the first report describing *R. solanacearum* dynamic transcriptional changes within the plant during infection. Our data define four main genetic programmes that define gene pathogen physiology during plant colonisation. The described expression of virulence genes, which might reflect bacterial states in different infection stages, provides key information on the *R. solanacearum* potato infection process.

Keywords: *Ralstonia solanacearum*, Bacterial wilt, RNAseq, Virulence factors, Dynamic gene expression, Metabolism, T3SS, Effectors, Xylem, Apoplast

Background

Brown rot or bacterial wilt of potato is a vascular disease caused by the bacterial phytopathogen *Ralstonia solanacearum*. This gram-negative β-proteobacterium is among the most threatening bacterial phytopathogens worldwide, as it can infect over 200 different plant species, including many important crops such as potato, tomato, peanut, eggplant and banana [1–3]. Although *R. solanacearum* is endemic of tropical and sub-tropical regions, phylotype IIB-1 strains such as UY031 are acclimated to lower temperatures and have caused important outbreaks in temperate areas [4–6].

R. solanacearum has a complex life cycle. The pathogen survives in soil and water for long periods of time [7]. When *R. solanacearum* senses the roots of natural hosts by plant exudates [8], it penetrates the host through the root elongation zone, root wounds or secondary root emerging points [9]. The root intercellular spaces (the apoplast) constitutes a front line in the arms race in plant-pathogen interactions and it is thus a hostile environment to phytopathogens [10]. Therefore, colonisation of the apoplast is key for *R. solanacearum* pathogenicity [11–13]. Successful infections involve entry into the vascular cylinder and extensive colonisation of the xylem vessels [14, 15]. Occlusion of the vasculature due to massive exopolysaccharide (EPS) production and bacterial multiplication ultimately cause wilting symptoms and plant death [9, 16].

To progress across the different plant tissues, *R. solanacearum* uses a panoply of virulence determinants [17, 18]. The main virulence factor in this and many other pathogenic bacteria is the Type III Secretion System (T3SS) [19, 20], which delivers effector proteins inside the plant cells, hijacking the cellular machinery for bacterial benefit [21]. Another key virulence determinant is EPS. EPS leads to the clogging of the xylem vessels and plant symptom appearance, and it can also bind to the cell wall and protect the bacterium from plant defences [22, 23]. In addition, the general secretion system (type II) secretes important virulence factors into the apoplast, including cell wall degrading enzymes [24]. These enzymes are collectively important for *R. solanacearum* plant colonisation, since multiple deletion of the *egl*, *pehA/B/C*, *pme* and *cbhA* genes compromised pathogenicity [25]. Bacterial motility also plays important roles during parasitic life *in planta*. For instance, *R. solanacearum* flagellar components were shown to be essential at early stages of infection [26] and mutants in the main twitching gene *pilA* were less pathogenic [27]. On the other hand, the *R. solanacearum* genome encodes the necessary enzymes to use nitrate as an energy source (i.e. dissimilatory nitrate reduction), to incorporate nitrate as a molecular building block (i.e. assimilatory nitrate reduction) [28] and to detoxify reactive nitrogen species (i.e. denitrification) [29]. The ability to use nitrate as terminal electron acceptor has been proposed to sustain rapid bacterial growth in the xylem, a hypoxic environment that is nonetheless rich in nitrate [29, 30].

Gene regulation analyses are essential to decipher how *R. solanacearum* finely tunes its pathogenicity. For instance, transcription of the *hrp* genes -encoding the T3SS- and its related effectors was found to be controlled by the HrpB transcriptional activator. HrpB lies downstream of a regulatory cascade induced by bacterial contact with the plant cell wall [31] . The cascade includes the membrane receptor PrhA, the signal transducer PrhI and the transcriptional regulators PrhJ and HrpG, the latter directly activating *hrpB* transcription [32, 33]. Gene expression studies demonstrated that the *R. solanacearum hrp* genes and T3SS effectors were transcribed *in planta* at late infection stages [34]. Based on these results, it was speculated that *R. solanacearum* could inject T3Es to the xylem parenchyma cells in order to hijack plant defences and manipulate the host metabolism [34]. These findings were later confirmed in gene expression studies using bacteria extracted from infected tomato and banana plants [14, 35] or bacterial transcripts isolated from infected potato roots [36]. Similar to the T3SS, EPS production is also stringently controlled through the expression of the *eps* operon, which encodes all EPS biosynthesis genes [37]. The *eps* operon promoter is dependent on the global regulator PhcA, whose production is induced at bacterial densities above 10^7 CFU/ml [37–39] . Finally, it has been described that

some crosstalk exists between the *eps* and the *hrp* gene regulation, since *hrpG* is negatively regulated by *phcA* [32, 40].

Bacterial interactions in plant hosts do not consist on one static phase, but rather in a dynamic interaction during disease development. However, all *R. solanacearum in planta* transcriptomic studies have focused so far on a specific stage of the infection process: xylem colonisation at the onset of disease symptoms [14, 35, 41, 42], with the exception of a single study indirectly analysing bacterial reads from infected roots [36]. Among the differentially expressed (DE) genes identified in these previous studies, the T3SS, T3Es, motility genes, ROS detoxifying enzymes and cell wall degrading enzymes were found up-regulated in most cases. Dynamic transcriptomic studies of the model plant pathogen *Pseudomonas syringae* analysing different moments of the disease development have recently revealed a changing bacterial behaviour. For example, flagellar motility and chemotaxis-related genes were transcribed in the epiphytic phase, while genes controlling metabolism were expressed in the apoplast [43]. In another study, gene expression of virulent and avirulent *P. syringae* strains was studied at different time points after inoculation of various *Arabidopsis thaliana* defence-related mutants. This work identified an iron response regulator that was induced at early infection stages, counteracting plant immunity [44]. Other time course transcriptomes in *P. syringae* have described an up-regulation of flagellar, chemotaxis and two-component system genes and a down-regulation of bacterial secretion systems and general metabolism at late infection stages in bacteria recovered from plants with pre-induced immunity compared to naïve plants [45]. Together, these studies have started revealing the complex landscape of transcriptomic changes occurring over time during the course of a bacterial infection.

Due to the various environments it encounters along the infection process and because of its economic relevance, *R. solanacearum* is an excellent model to analyse gene expression in different plant tissues, which correspond to distinct phases of the infection process. Here, we have analysed the transcriptome of the cold adapted *R. solanacearum* UY031 at three different conditions. We have used the economically important crop potato plant where the *R. solanacearum* UY031 was naturally identified a decade ago [46]. Our data clearly shows that *R. solanacearum* genes behave dynamically inside the plant during the course of infection. We have identified condition-specific expression of virulence and metabolic genes, providing a new dynamic perspective of the *R. solanacearum* infection process.

Results

R. solanacearum transcriptomes reflect four main genetic programmes inside the plant

To elucidate the genes deployed by *R. solanacearum* throughout infection, we profiled the gene expression of strain UY031 in its natural susceptible potato host. We collected bacterial samples from the apoplast —a condition mimicking early root infection, when the bacterium traverses and multiplies in this compartment [47]— and from the xylem of infected plants at six and ten days post-inoculation, which correspond to the onset of the disease (early xylem) or to the final stages when plants are completely wilted (late xylem) (Additional File 1 B and 2A). *R. solanacearum* plant infection through roots is highly variable due to stochastic changes in the physiological state of the plant, the initial inoculum and available root entry sites. To overcome this problem, we took advantage of a luminescent *R. solanacearum* reporter strain previously developed in our group to measure bacterial colonisation and we normalized values for tissues containing comparable bacterial loads at different times of infection [48]. The *in planta* transcriptomes were compared with that obtained from bacteria grown in liquid rich B medium, a reference condition known to repress many of the pathogen's virulence determinants [49]. Principal component analysis (PCA) of the transcripts from each sample showed a clear clustering of the biological replicates and a clear differentiation of the xylem samples from the reference and apoplast samples (PC1, explaining 65% of the variation) (Additional File 2 C). Comparison of the *in planta* transcriptomes with that obtained in axenic growth in rich medium identified 418 differentially expressed genes (DEGs) in the apoplast, 531 in the early xylem and 922 in the late xylem ($\log_2$ fold change ≥ |1.5| and adjusted *p-value* ≤ 0.01). Of these genes, 226 and 192 were up- and down-regulated, respectively, in the apoplast, 290 and 241 in the early xylem, and 378 and 544 in the late xylem (Fig. 1a and Additional File 3).

Comparison of the DEGs in each *in planta* condition is in agreement with the previously published *R. solanacearum in planta* transcriptomic studies (Additional File 4 A). DE transcripts from the same UY031 strain retrieved from total RNAs of infected wild potato roots [36] showed up to 17–18% overlap with the apoplast condition and lower overlap with the other conditions assayed in the present study, and the gene expression values showed a high correlation (Additional File 4 B). This is logical, since the transcriptome previously obtained from roots of asymptomatic plants corresponds to an early time of infection where most bacteria grow apoplastically and only a small proportion of bacteria have already reached the xylem. The highest overlap (34% overlap in up- and 36% in down-regulated genes,

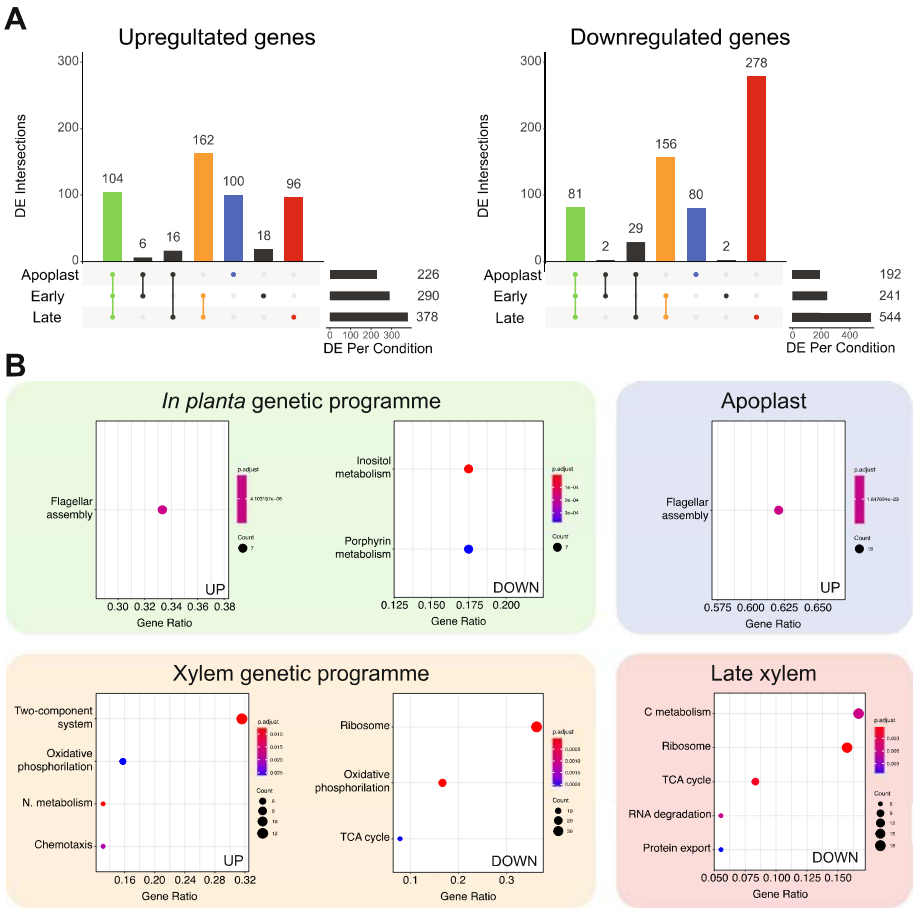

Fig. 1 Transcriptomic profile of *R. solanacearum* UY031 *in planta*. a. Shared and unique DE genes across the three *in planta* conditions for the up-regulated (left) and down-regulated (right) genes. Each vertical bar plot represents the number of shared DE between the conditions indicated by the lines and dots in the schematic below. The horizontal bar plots on the right indicate the total DE genes per *in planta* condition compared to rich medium. **b.** For the intersection of Apoplast, Early and Late (*in planta* genetic programme), Early and Late (Xylem genetic programme), Apoplast and Late xylem alone, the list of genes was extracted and surveyed for enriched KEGG pathways. Dot plots of the enriched KEGG pathways for the up- (left) and down-regulated (right) genes in each environment are shown below. DE genes were identified with DEseq2 (*p-adj* > 0.01, $\log_2$ FC ± 1.5) and plotted using the R package UpsetR

respectively) was found between our early xylem conditions and the microarray transcriptome of the phylogenetically close strain UW551 isolated from tomato plants at a comparable infection time (onset of wilting symptoms) [14], which further validates our results (Additional File 4). The overlap is obviously lower with comparable transcriptomes obtained using the distantly related GMI1000 strain.

To discover the DEGs common or unique to the different plant environments, we analysed the shared genes among the different conditions studied. As can be observed in Fig. 1a, two intersections (i.e. *in planta* and xylem) and two conditions (i.e. apoplast and late xylem) that correspond to bacterial growth in precise environments included most of the DEGs. On this basis, we defined four genetic programmes where *R. solanacearum* expresses exclusive gene sets: *in planta* (genes shared in all *in planta* conditions: apoplast, early and late xylem), the xylem (genes shared in early and late xylem), the apoplast, and the late xylem. Similarly, DE in all *in planta* conditions were 104 up- and 81 down-regulated genes. The differentially expressed genes in the xylem genetic programme (both time points analysed) included a total of 162 and 156 up- and down-regulated genes. Finally, 100 and 80 genes were, respectively, up- or down-regulated solely in the plant apoplast and 96 and 278 only in the late xylem condition, when plants are mostly dead. The remaining conditions or overlaps between conditions included fewer than 30 specifically DEGs (Fig. 1a) and we did not consider them a proper "genetic programme". Overall, as hinted by the PCA analysis, the apoplast showed the most divergent transcriptome of the *in planta* conditions, whereas the samples extracted from the xylem (early and late) were the

most similar. However, a substantial fraction of genes was only differentially expressed in the late xylem (40% of those DE in this condition).

R. solanacearum upregulates a variety of virulence factors *in planta*

Functional enrichment of gene annotations is a powerful tool to evaluate the genes involved in similar roles or pathways in each experimental condition. Thus, we investigated the enrichment of KEGG pathways and GO terms in the genes that appeared DE in all *in planta* conditions. Since the KEGG database contains metabolic pathways and terms specifically for prokaryotes, we ocused on its categories for enrichment analysis. Among the genes up-regulated in all *in planta* conditions, only the KEGG flagellar assembly pathway was enriched (Fig. 1b). This result was confirmed by the GO enrichment analysis, where the bacterial flagellum-dependent cell motility term was similarly over-represented, together with transposase activity and DNA-mediated transposition (Additional File 5). On the other hand, the enriched KEGG terms amongst the genes down-regulated in all *in planta* conditions were all related to metabolism: inositol phosphate metabolism, and porphyrin and chlorophyll metabolism (Fig. 1b), and the GO term cobalamin biosynthetic process (Additional File 5).

Manual curation of gene annotations enabled us to pinpoint a high number of pathogenicity-related functions up-regulated in all *in planta* conditions. These genes had been overlooked by the global enrichment analysis because virulence genes are not in a KEGG pathway and pathogenicity-related terms in GO are too general and have not been widely used. Thus, we used genomic and bibliographic information to create the gene category "virulence and parasitic fitness" for the UY031 strain and calculated its enrichment in all conditions or genetic programmes analysed in this work (see Methods). The new category included all genes encoding the type III secretion system (T3SS) and its associated effectors (T3Es), genes involved in motility, EPS and phytohormone biosynthesis, ROS scavenging, cell-wall degrading enzymes, and nitrogen metabolism (Additional File 5). As expected, the created "virulence and parasitic fitness" category was clearly enriched in the up-regulated genes in the *in planta* genetic programme (*p-value* = $1.4{\cdot}10^{-14}$). Detailed analysis of the subcategories included in "virulence and parasitic fitness" indicated that T3SS and T3Es (*p-value* = $2.4{\cdot}10^{-12}$) and motility (*p-value* = $5.7{\cdot}10^{-5}$) were also significantly enriched among the up-regulated genes. For instance, 20% (12 out of 60) of the genes annotated as T3Es were overexpressed in all *in planta* conditions. The enriched motility subcategory included a total of 11 genes, containing both flagellar and type IV pili. Similarly, the polygalacturonase gene *pglA,* encoding one out of the six cell-wall degrading enzymes in the genome was also up-regulated in the plant. Other virulence genes up-regulated in bacteria growing in any of the studied *in planta* conditions included *efe,* responsible for ethylene formation, the reactive oxygen species (ROS) scavenging superoxide dismutase *sodC*, and *epsR,* encoding the exopolysaccharide (EPS) repressor. Finally, only the EPS subcategory was under-represented *in planta* (*p-value* = $1.25{\cdot}10^{-2}$), which can be explained by the high expression of the exopolysaccharide synthesis operon in the reference rich medium [38].

Flagellar genes and the upstream regulators of the T3SS are exclusively up-regulated in the apoplast

Once *R. solanacearum* has infected the roots of a susceptible host plant it must cross the root cortex through the apoplast. The KEGG flagellar assembly pathway was enriched in the genes exclusively up-regulated in the apoplast (Fig. 1b). Similarly, the four GO terms referring to the flagellum (bacterial-type flagellum-dependent cell motility, bacterial-type flagellum basal body, bacterial-type flagellum and bacterial-type flagellum assembly) and phosphopantetheine binding were also enriched in this genetic programme (Additional File 5). A closer perusal of the list of up-regulated genes in the apoplast genetic programme also revealed that the "virulence and parasitic fitness" category was enriched (*p-value* = $4.2{\cdot}10^{-15}$). *PrhJ* and *hrpG*, key upstream regulators of the T3SS activation cascade [31], were up-regulated in this genetic programme. On the other hand, none of the downstream T3SS transcriptional activators and only two of 60 T3E genes (*ripE2* and *ripAD)* were exclusively up-regulated in this genetic programme. None of the KEGG pathways nor GO terms were enriched amongst the genes down-regulated in the apoplast.

R. solanacearum adapts to the xylem environment by inducing virulence, chemotaxis and nitrogen metabolism genes

After travelling through the root apoplast, *R. solanacearum* crosses the Casparian strip, reaching the plant vasculature and heavily colonising the xylem vessels. As mentioned before, a substantial number of *R. solanacearum* genes was DE in the xylem genetic programme, both at early and late conditions (Fig. 1a). Almost one third (12 out of 38) of the genes with associated KEGG pathways differentially up-regulated in the xylem irrespective of the condition belonged to the enriched category two-component system (Fig. 1b). This includes genes that participate in chemotaxis signal transduction, nitrate reduction, and oxidative phosphorylation. Three other categories were enriched in the genes up-regulated

in the xylem: oxidative phosphorylation (six genes), bacterial chemotaxis (five genes) and nitrogen metabolism (five genes). The up-regulated nitrogen metabolism genes included nitrate transporters (*nark1*/2), enzymes involved in the denitrification pathway (*aniA*, *norB*) and in the dissimilatory nitrate reduction pathway (*narG/H/I, nirB/D*) as well as in reactive nitrogen species detoxification (*hmpX*). The enriched term bacterial chemotaxis included genes involved in different steps of swimming motility, including membrane chemosensors, signal transduction components (i.e. *cheZ1, cheA, cheR*) and flagellar motor genes (i.e. *motB*). The "virulence and parasitic fitness" category was also enriched in the xylem genetic programme up-regulated genes (*p-value* = $8.8{\cdot}10^{-5}$). Amongst these genes were 9 out of 60 T3Es annotated in strain UY031 genome (*ripAE, ripY, ripAN, ripC1, ripN, ripAP, ripF2, ripBH,* and *ripS5),* and one out of six cell wall degrading enzymes (*pme).* Other overexpressed genes in the category included 10 motility genes and the cytokinin biosynthesis gene *tzs*. Finally, amongst the 102 KEGG tagged down-regulated genes in the xylem, the enriched categories were: ribosome, oxidative phosphorylation and citrate (TCA) cycle (Fig. 1b). GO enrichment in down-regulated genes similarly showed the over-represented categories translation, ribosome, structural constituent of ribosome, RNA binding, rRNA binding (Additional File 5). In summary, a large set of *R. solanacearum* genes was found DE in the xylem throughout infection, including up-regulation of nitrogen utilisation and virulence genes, such as T3Es and down-regulation of genes encoding the citrate cycle enzymes and the electron transport chain.

R. solanacearum inhibits a large number of metabolic pathways at late infection stages

Besides the DE genes in the xylem throughout infection, a large set of *R. solanacearum* genes was exclusively DE in the Late xylem genetic programme, at late stages of infection when plants are already wilted (Fig. 1a). Surprisingly, no KEGG category was enriched in this abundant set of up-regulated genes, but our "virulence and parasitic fitness" category was enriched in the up-regulated genes (*p-value* = $5{\cdot}10^{-3}$). Within this category, two subcategories were also enriched: T3SS & T3Es, including six effectors, three of the GALA family (*ripG3, ripG4* and *ripG6*) (*p-value* = $8.5{\cdot}10^{-3}$), and motility, with six involved in chemosensing and signal transduction (*p-value* = $3.68{\cdot}10^{-2}$). In the genes differentially down-regulated in the late xylem condition, five KEGG categories were enriched: carbon metabolism (18 out of 108 genes tagged), ribosome (17 genes), TCA cycle (9 genes), RNA degradation (six genes) and protein export (six genes) (Fig. 1b). GO enrichment analysis also showed similar results with the overrepresented categories translation, ribosome, structural constituent of ribosome, RNA binding and tricarboxylic acid cycle (Additional File 5). In sum, *R. solanacearum* exclusively downregulates at late infection stages in the xylem a large subset of genes involved in the central metabolism and its derived metabolic pathways.

Expression profiles reinforce the existence of specific genetic programmes in the apoplast and the xylem

The findings described so far strongly suggest that *R. solanacearum* expresses specific sets of genes at each step of the infection process. To better understand this dynamic process, we obtained the expression profiles of the *R. solanacearum* UY031 genes in the three *in planta* conditions: apoplast, early and late xylem. To this end, fold-change values of DE genes in each condition in relation to growth in rich culture medium were used as input to the Mfuzz clustering package. Six different gene expression profile clusters were identified according to the condition or temporal progression, considering that the apoplast is the earliest stage during infection, followed by early and late xylem (Fig. 2, Additional File 7). According to this, the profile named "specific apoplast" contained 807 genes up-regulated in the apoplast but down-regulated in early and late xylem (Fig. 2a), and the profile "specific xylem" contained 1286 genes down-regulated in the apoplast but up-regulated in the other conditions (Fig. 2b). We identified two additional profiles, including genes that continuously decreased (561 genes up-regulated in the apoplast with transcripts gradually decreasing in xylem) (Fig. 2c) or increased (334 genes, opposite profile) (Fig. 2d) their expression over the infection period. Finally, the genes specifically repressed (Fig. 2e) or induced (Fig. 2f) in the early xylem that showed the opposite trend in the apoplast and late xylem were 105 and 107, respectively.

To unveil the biological functions behind each expression profile, we performed enrichment analyses. Enriched KEGG pathways in the "specific apoplast" expression profile included various biosynthetic processes, especially biosynthesis of secondary metabolites (99 out of 308 tagged genes) and related pathways such as biosynthesis of amino acids (53 genes) and flagellar assembly (25 genes) (Fig. 2a). Our manually-defined motility subcategory was enriched in this expression profile (*p-value* = $1.78{\cdot}10^{-2}$). In the "specific xylem" profile, the KEGG enrichment analysis yielded terms related with metabolism adaptation such as microbial metabolism in diverse environments (106 out of 411 tagged genes), ABC transporters (63 genes), and nitrogen metabolism (19 genes) among others (Fig. 2b). Our manually-defined subcategories T3SS & T3Es (*p-value* = $5.2{\cdot}10^{-3}$), phytohormones (*p-value* = $2.5{\cdot}10^{-3}$) and nitrogen metabolism (*p-value* = $2{\cdot}10^{-6}$) were also significantly enriched in this

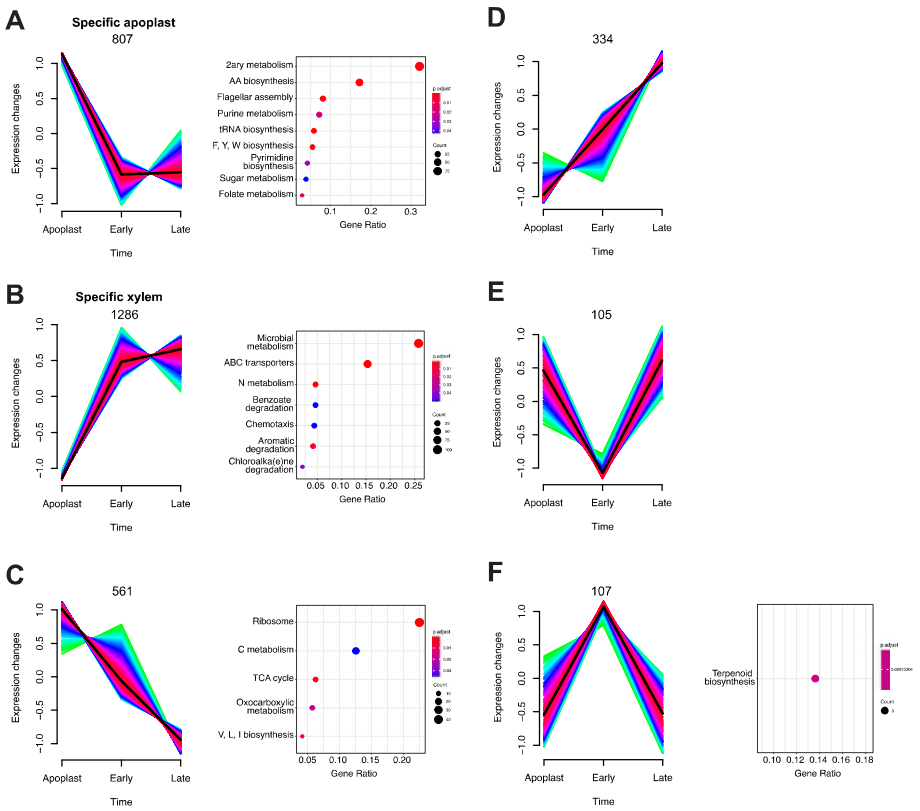

Fig. 2 Gene expression dynamics of *R. solanacearum* throughout infection. Six clusters were obtained through Mfuzz clustering of log_2-fold-change data of the apoplast, early and late xylem conditions normalised to the reference rich liquid media. Clusters include the genes with a membership higher than 70% and consistently associated to the same cluster on at least 30 out of 40 iterations. Number of genes indicated above each graph. The list of genes associated to each cluster was extracted and surveyed for enriched KEGG pathways. Dot plots of the enriched KEGG pathways in each cluster are shown next to the cluster

profile. KEGG enriched terms within the continuous decrease profile were linked to transcription and carbohydrate metabolism such as ribosome (43 out of 191 tagged genes) and carbon metabolism (24 genes) (Fig. 2c). Finally, the profile containing genes with specific up-regulation in the early xylem, was enriched in the ubiquinone and other terpenoid-quinone biosynthesis pathway (3 out of 22 tagged genes). The subcategory T3SS & T3Es was significantly enriched in this expression profile as well ($p\text{-}value = 1.34{\cdot}10^{-2}$), containing genes such as the master regulator *hrpB,* and three T3 effectors (Fig. 2f). GO enrichment analysis confirmed these results, showing over-represented categories with similar biological functions (Additional File 8).

R. solanacearum specifically activates different sets of virulence factors in different plant environments

As described above, key virulence activities were induced in specific plant environments or at specific disease stages. To analyse in further detail the genes in this "virulence and parasitic fitness" (Additional File 6) and its subcategories we graphically represented their normalised read counts in all assayed conditions, including the reference condition in rich medium. This provided an unbiased view on the gene expression data avoiding the effect of the reference condition in the DESeq analysis. Detailed observation of gene expression values in heatmap representations for the T3SS (*hrp* and *hrc* genes) and T3E (*rip* genes) reinforced the above-described enrichment in various genetic programmes or conditions (Fig. 3, Additional File 9). Both the *rip* T3Es and the *hrp/hrc* genes displayed a very homogeneous expression pattern with high expression levels in the xylem genetic programme (early and late) and low expression levels in the apoplast. The only exceptions among the effectors were the two *ripI* genes, with low expression levels in all studied conditions, *ripE2*, with higher expression in the apoplast, and a cluster of effector genes (i.e. *ripAD* and *ripD*), showing high transcript levels in all conditions (Fig. 3). Heatmap visualisation of the normalised transcriptomic data also indicated that flagellar genes —essential for swimming motility— were highly expressed in all *in planta* conditions, but to a higher extent in the apoplast (Fig. 4 top panel). This is in

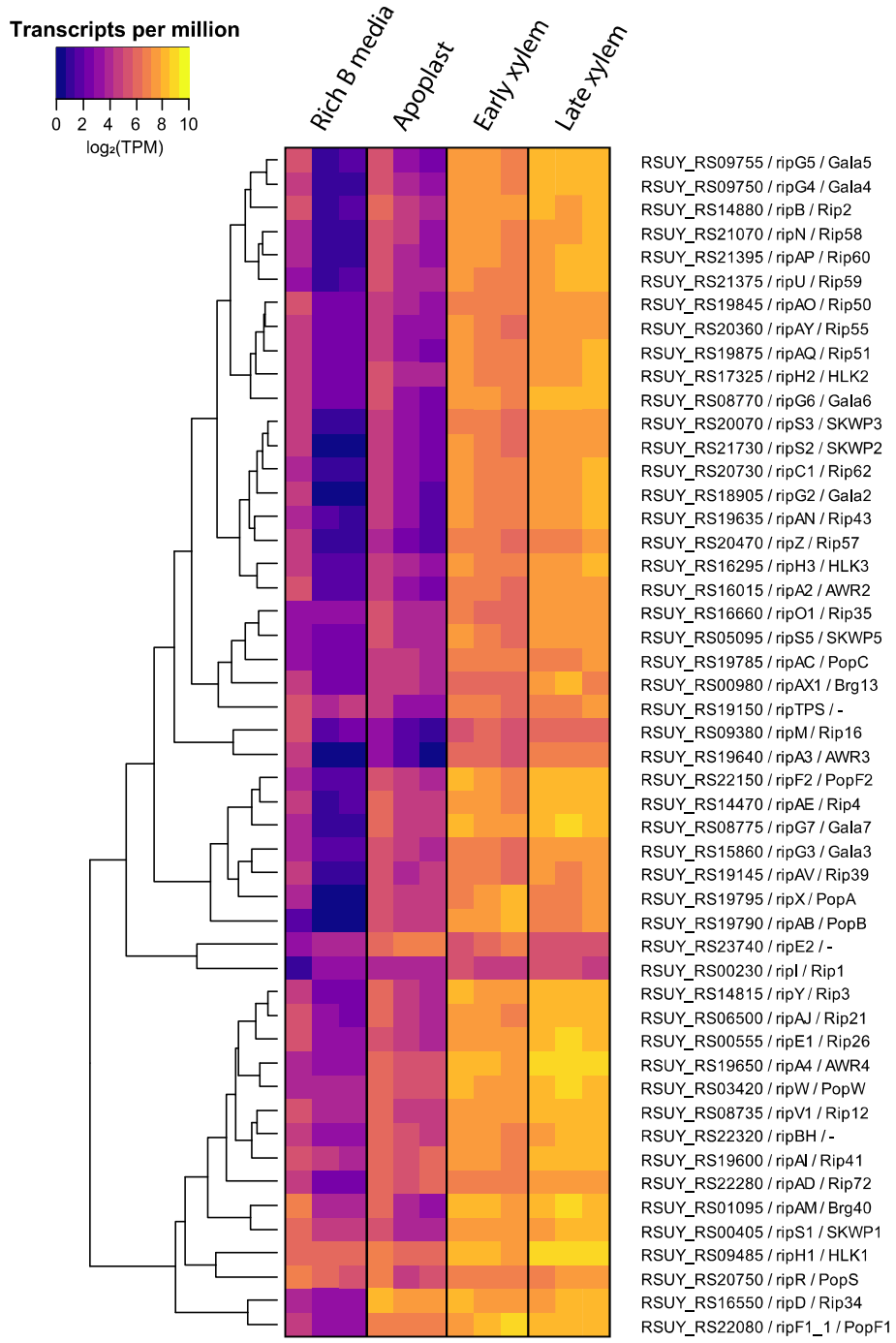

Fig. 3 T3E gene expression profile. Heatmaps showing the normalised transcripts per million (TPM) of the genes coding the 60 T3E described in *R. solanacearum* UY031 in the reference condition and *in planta* apoplast, early and late conditions. Only putatively functional T3E genes are included according to Peeters et al., 2013

accordance with the enrichment of this category *in planta* and in the late xylem genetic programmes up-regulated genes, as well as in the specific apoplast profile. The *pil* twitching motility genes encoding type IV pili followed a similar trend, although their expression was more similar in the apoplast and the xylem (Fig. 4 bottom panel), suggesting that the bacterium is using the pilus appendix in all assayed plant environments. Exceptions to this trend were the flagellar genes (i.e. *fliM, fliS, fliD, fliT, motA, motB, fliC, fliO*) and the type IV pilus genes (e.g. *pilE1, pilY1, pilW, pilV, pilX*), which were down-regulated in the apoplast compared to the xylem

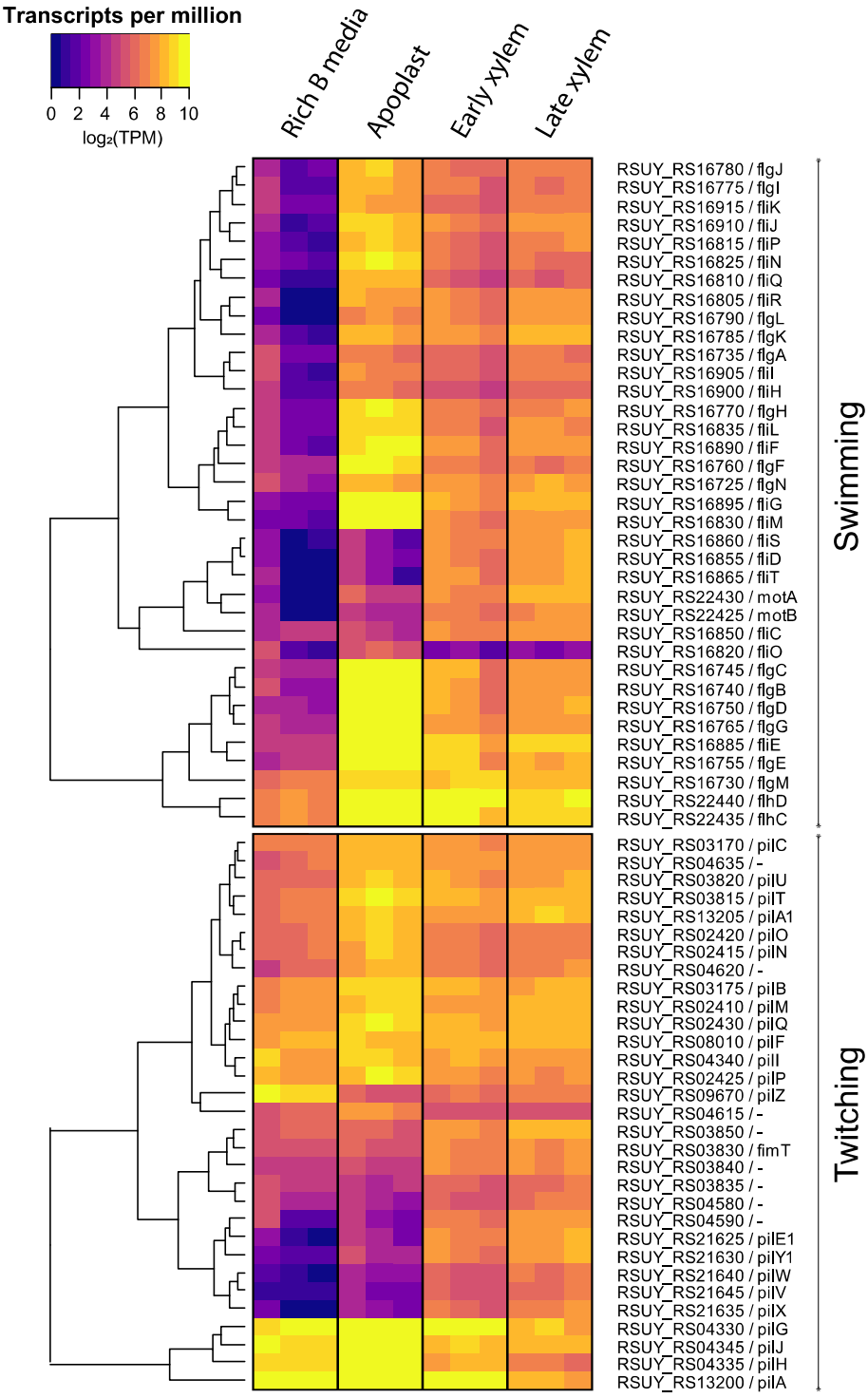

Fig. 4 Motility gene expression profile. Heatmaps showing the normalised transcripts per million (TPM) of the genes involved in motility in the reference (rich Medium), apoplast, early and late xylem conditions. Two heatmaps are shown to differentiate the swimming (top panel) and twitching (bottom panel)

genetic programme. The genes encoding chemotactic sensors and chemotaxis signal transduction proteins showed low expression levels in the apoplast and progressive induction in the early and late xylem conditions (Additional File 10) in accordance with the enrichment of these specific genes in the late xylem genetic programme. Finally, all the UY031 genes that synthetize the plant hormones ethylene (*efe*), cytokinin (*tzs*), and auxin (*RSUY_RS1835* to *RSUY_RS18970*) [33] were highly expressed in the xylem genetic programme and to a lower extent in the apoplast, *efe* and *tsz* displaying a more sustained expression in the apoplast. This stable expression in all *in planta* conditions was also observed in the differential expression analysis (Additional File 12).

Discussion

R. solanacearum gene expression displays a behavioural differentiation into four plant genetic programmes that develop over time during in planta infection

Previous *R. solanacearum* transcriptomic studies compared gene expression profiles obtained using a specific *in planta* condition, such as root apoplast [36] or early xylem colonisation [14], to reference bacteria grown in rich medium. In our study, we analysed the whole infection process, including three different *in planta* conditions: apoplast, early and late xylem, which typify paradigmatic stages of infection. Intersection of the DEGs of each of the three *in planta* experimental conditions showed that most of the DEGs of *R. solanacearum* during the infection are grouped in four biologically relevant genetic programmes: genes commonly DE in all *in planta* conditions, genes exclusively DE in the apoplast, genes expressed in the xylem at any stage of the disease and genes exclusively DE in the xylem when plants are already wilted (Fig. 1). One of the previous transcriptomic studies sampled bacteria from plants 5 days post-inoculation [14], similar to our early xylem condition. With the addition of our novel late xylem condition 10 days after inoculation, and the apoplast condition, we provide a more detailed expression landscape of *R. solanacearum*, encompassing important different stages of the infection process. To study the transcriptomic data from a tissue-specific perspective, we clustered the DEGs based on their expression profile across the three *in planta* experimental conditions (i.e. apoplast, early and late xylem) (Fig. 2). Reinforcing the concept of a specific behaviour of *R. solanacearum* in different genetic programmes, the largest number of DEGs appeared exclusively up-regulated in the xylem genetic programme (1286 genes) and the apoplast (807 genes). This finding confirms that *R. solanacearum* has different sets of genes that are deployed to infect the plant and adapt to the environments encountered along the infection. It should be noted that our gene expression experiments *in planta* were all performed at comparable bacterial loads. The reason for this is that *R. solanacearum* forms microcolonies and biofilms at early infection stages in the apoplast [50], so that neither the effective local bacterial concentrations nor if density-dependent regulatory circuits are already induced at these early stages are known. Consequently, although our results perfectly reflect *R. solanacearum* adaptation to different plant environments, the influence that bacterial cell densities have on their gene expression during disease progression is not reflected in our results.

T3Es expression is prevalent throughout the *in planta* infection process, especially in the xylem

Here, we carefully investigated the expression pattern of the most important virulence factors to elucidate the bacterial strategies used to rewire the plant environments to its own benefit. The T3SS is the main pathogenicity determinant in *R. solanacearum*, as *hrp* mutants are completely avirulent [51]. The T3SS is tightly regulated by a transcriptional regulatory cascade that contains the constitutive receptor and transducer elements PrhA and PrhR and the transcriptional regulators PrhJ, HrpG and HrpB [31]. Interestingly, in this work we found that this cascade appears sequentially induced during infection. As depicted in Fig. 5, *prhI* and *prhJ* are exclusively induced in the apoplast, *hrpG* expression also peaks in this environment but is sustained at lower levels in the early xylem and *hrpB* is expressed in the apoplast but highly induced in the early xylem, preceding the expression of the T3SS and most T3E, which is maximal at all xylem stages (Additional File 9).

Our gene expression dataset also shows that most of the 60 T3Es are highly induced in the xylem genetic programme, confirming our previous results [34] that challenged the view of T3Es as key only early after infection [32, 40]. In agreement our finding that almost all T3Es are simultaneously expressed in the xylem, a recently published study showed that deletion of 42 *R. solanacearum* T3E genes was required to compromise virulence of the bacteria on tobacco and eggplant and proliferation inside the xylem [52].

Interestingly, all *R. solanacearum* T3Es belonging to gene families (*PopA/B/C*, *AWR2/3/4/5_1/5_2*, *SKWP1/2/3/5/7*, *HLK1/2/3* and *GALA2/3/4/5/6/7*) [53] were clearly induced in the xylem throughout infection (Fig. 3). The *GALA* effectors (e.g. *ripG2 to ripG7*) and the *AWR* effectors (e.g. *ripA2 to RipA5*) have both been shown to be collectively required for full bacterial virulence and to target the proteasome or inhibit the Target Of Rapamycin (TOR) pathway, respectively [54–56]. Their expression pattern suggests that these biochemical activities are likely carried out in the

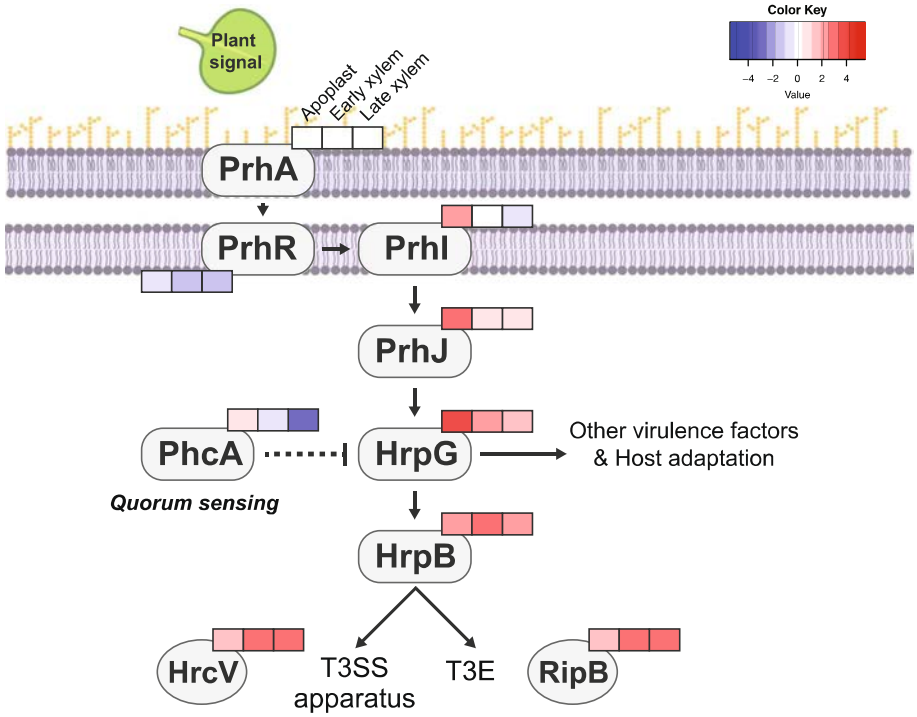

Fig. 5 T3SS regulatory cascade. Log_2 fold-change expression profile in the Apoplast, Early and Late Xylem of the genes involved in the T3SS regulatory cascade and downstream activated genes. Log_2 fold changes in transcript levels with respect to the control condition (axenic growth in rich medium) are indicated in the boxes (left to right: Apoplast, Early and Late Xylem conditions) in colour gradients according to the Colour Key

xylem. Similarly, The T3E *ripAY*, which has been proven to impair the redox status of the plant cell degrading glutathione through its gamma-glutamyl cyclotransferase activity [57–60], was clearly induced in the xylem (Fig. 3). This points to the xylem as a stressing redox environment *R. solanacearum* must cope with.

In contrast, a few T3Es showed alternative induction patterns to the one described above. For instance, *ripE2* can be clearly classified as an "early effector" since it was highly induced in the apoplast compared to the other conditions, while *ripD* and *ripAD* were highly induced in all *in planta* conditions (Fig. 3). *RipD* localizes in vesicle-like structures and blocks the flg22-induced ROS response in *Nicotiana benthamiana* [61]. This fact, linked with its high expression in the apoplast and the activation of flagellar genes in this condition, suggests that *R. solanacearum* counteracts flg22 plant defence responses from the first stages of infection onwards. On the contrary, *ripI*, which was shown to enhance plant production of gamma-aminobutyric acid (GABA), was lowly expressed in all *in planta* conditions (Fig. 3) [62]. Although GABA catabolization by *R. solanacearum* enhances its infection capacity, the overproduction of GABA in plant cells in the absence of sufficient bacteria to consume it has been shown to induce cell death [62]. Therefore, we hypothesize that RipI expression inside the plant must be tightly regulated to induce the production of nutrients without triggering plant stress signals.

R. solanacearum modulates twitching and swimming in different plant environments

R. solanacearum uses two types of motility during the colonisation of plant tissues: swimming [26] and twitching [27]. Swimming motility is an individual bacterial movement through liquid environments in which flagella rotate by a proton-driven motor that is directed by chemosensor proteins [63]. Previous research showed that both flagella (*fliC*) and chemosensor (*cheA* and *cheW*) mutants were less virulent than the wild-type *R. solanacearum*, demonstrating that not just the flagellar movement but also the ability to direct it are essential for full virulence *in planta* [8]. Interestingly, full virulence was restored when the chemotactic mutants were directly inoculated in the plant stem, indicating that swimming motility is of crucial importance at the very early stages of infection [8]. In our data (Fig. 4), most of the flagellar-encoding genes were highly induced in the

apoplast and, to a lower extent, in the early and late xylem, supporting the previously mentioned hypothesis. A small subset of flagellar genes including the motor (*motA, motB*), the flagellin subunit (*fliC*) and the filament cap (*fliD*) among others showed low expression in the apoplast, for which we have no plausible explanation.

R. solanacearum displays twitching motility, which involves the extension and retraction of type IV pili to move on solid or viscous surfaces [64]. This motility is involved in natural transformation, biofilm formation and virulence [27]. Inactivation of the genes encoding the pilin protein (*pilA*), the secretin involved in the pilus extrusion (*pilQ*) or the protein required for pilus retraction (*pilT*) reduced *R. solanacearum* virulence [65]. In our transcriptomic data, twitching motility genes showed a similar expression pattern than swimming motility, but they were less induced in the apoplast and their expression was often maintained in early and late xylem (Fig. 4). This emphasizes the importance of twitching motility throughout the plant infection process, as showed by the effect on virulence of *pil* deletion mutants [27, 65, 66]. Finally, *pilI*, which encodes the type IV pili chemosensor protein, was especially induced in the apoplast (Fig. 4 bottom panel), in agreement with our recent findings that it is involved in virulence especially during the early infection stages [66].

R. solanacearum specifically activates different nitrogen metabolism genes to thrive in the xylem

R. solanacearum encounters a hypoxic environment in the plant xylem, which could limit its growth as the bacterium usually uses oxygen as the main terminal electron acceptor. However, the xylem contains an optimal concentration of nitrate that *R. solanacearum* can use as terminal electron acceptor to maintain its growth rates in this environment [29]. Our gene expression dataset shows a faint induction of the nitrogen metabolism in the apoplast, reaching its expression peak in the xylem (Fig. 6). When nitrate is available in the extracellular space, it diffuses the outer membrane and is imported to the cytoplasm by NarK1/2. Once nitrate enters the cytoplasm, the nitrate reductase (NarG/H/I) converts it to nitrite and then to ammonia through nitrite reductase (NirB/D). We found both the transporters- and reductase-encoding genes induced in the xylem (Fig. 6), suggesting that both import and dissimilatory nitrate reduction are active in this compartment (Fig. 6).

Nitrite diffusing back to the periplasm allows *R. solanacearum* to perform denitrification, first by reducing nitrite to nitric oxide via the nitrite reductase AniA and finally by reducing nitric oxide to nitrous oxide via the nitric oxide reductase NorB. Expression of these denitrification pathway genes is also induced in the xylem (Fig. 6), suggesting that *R. solanacearum* has the ability to detoxify the

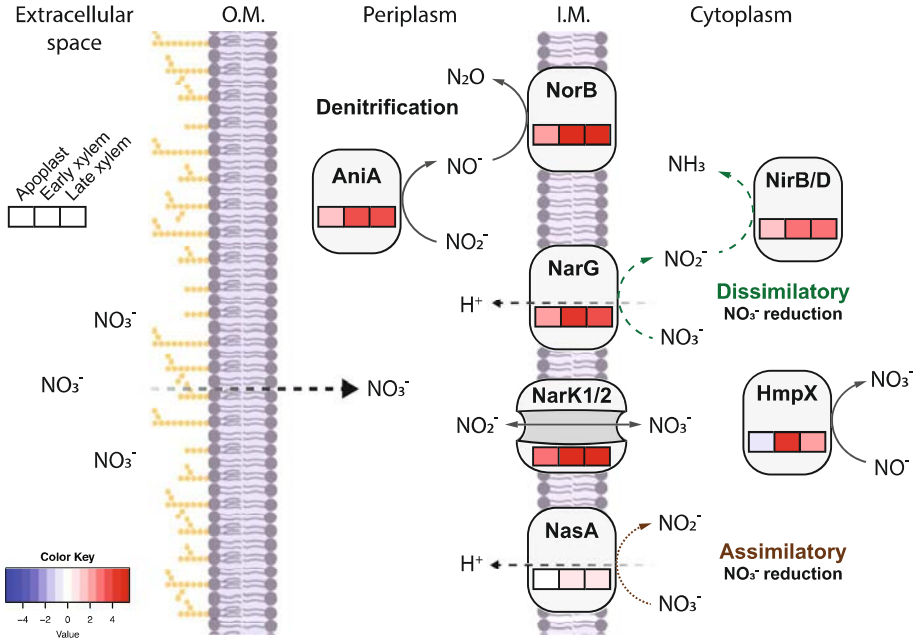

Fig. 6 Nitrogen metabolism expression profile. Log_2 fold-change expression profile in the Apoplast, Early and Late Xylem of the genes involved in the denitrification (*aniA, norB*), assimilatory (*nasA*), dissimilatory (*narK1/2, narG, nirB/D*) and nitrite detoxification (*hmpX*) pathways of nitrogen in *R. solanacearum* UY031. Log_2 fold changes in transcript levels with respect to the control condition (axenic growth in rich medium) are indicated in the boxes (left to right: Apoplast, Early and Late Xylem conditions) in colour gradients according to the Colour Key. O. M = Outer membrane, I.M. = Inner membrane

reactive nitrogen species produced during nitrate dissimilatory pathway in the anaerobic xylem vessels [29].

Moreover, *R. solanacearum* can also incorporate nitrogen to its central metabolism through the assimilatory nitrate reduction. The nitrate present in the cytoplasm is reduced to nitrite by NasA/B. A previous study showed that nitrate assimilation was essential for initial root attachment but was dispensable for growth, virulence, and competitive fitness [28]. The fact that *nasA* is induced in the xylem and not in the apoplast is in disagreement with these results and may indicate strain- or condition-specific roles of N genes in *R. solanacearum*. Finally, the nitric oxide anion in the cytoplasm can be detoxified using HmpX, whose expression is also highly induced in the xylem genetic programme (Fig. 6), an indicator of a highly active N metabolism in this plant environment.

Phytohormone and ROS scavenging enzymes are expressed along the infection

R. solanacearum genome codes for phytohormone biosynthetic genes that drive the production of auxin [33], cytokinin [67] and ethylene [68]. Interestingly, bacterially-produced auxin was described to block plant defences against the plant pathogen *Pseudomonas syringae* pv *savastanoi* [69] and ethylene was involved in wilting development in the pathosystem *A. thaliana-R. solanacearum* [70]. In this study, we observed induction of the cytokinin (*tzs*) and the ethylene (*efe*) biosynthetic genes as well as the auxin operon in the xylem (Additional File 11). Apoplastic induction of the master regulator *hrpG*, which also controls auxin and ethylene synthesis genes [33], precedes the xylematic expression of phytohormone biosynthesis genes as was observed for the T3SS (Fig. 5).

After pathogen infection, plant cells respond with ROS production to create a hostile environment against the bacterium [71]. Interestingly, *R. solanacearum* contains several genes that code for ROS scavenging enzymes, helping the bacterium survive in the plant apoplast and xylem [72]. Amongst them, alkyl hydroperoxide reductase genes (*ahpC1/C2/D/F*) were mostly induced in the xylem (Additional File 12). Several studies have linked the induction of *ahp* genes in biofilm-forming cells in different bacterial pathogens, contributing to protection against oxidative stress, epiphytic survival and attachment in the intercellular spaces or to the xylem vessels [73–77].

Conclusion

In summary, we performed a transcriptomic analysis of *R. solanacearum* at different conditions in potato plants. DEG analysis revealed that *R. solanacearum* deploys inside the plant host four different genetic programmes. Functional enrichment analysis showed that *R. solanacearum* has the highest expression of motility genes in the apoplast, while the majority of T3Es and nitrogen metabolism genes are highly induced in the xylem environment. This study provides for the first time a dynamic gene expression landscape of the bacterial plant pathogen *R. solanacearum* and is a first step towards the transcriptomic characterisation of its complete infection cycle.

Methods

Bacterial strains and plant growth conditions

The highly aggressive *Ralstonia solanacearum* strain UY031 (phylotype IIB, sequevar 1) isolated from potato tubers in Uruguay [46] carrying the synthetic *luxCDABE* operon under the control of the *psbA* promoter was used in this study [34]. The luminescence allowed indirect but precise quantification of bacteria and to track bacterial proliferation *in planta* [48]. Bacteria were routinely grown at 30 °C in rich B medium supplemented with 0.5% glucose [34].

Solanum tuberosum cv. Desirée potato plants were propagated in vitro [36] and 2-week old apexes were transferred to a soil:silica sand mixture in a 1:1 ratio for RNA-seq sampling or moved to a substrate:perlite:vermiculite mixture in a 30:1:1 ratio for *in planta* visualisation. Plants were grown at 22 °C under long day (16 h / 8 h light/dark) conditions for 3 weeks.

Bacterial sampling

For liquid medium samples, bacterial cultures were set to an starting $OD_{600} = 0.1$ (10^8 CFU/ml) and grown for 5 h in rich B medium (10 g/L bacteriological peptone, 1 g/L yeast extract, 1 g/L casamino acids), until they reached exponential growth phase ($OD_{600} \sim 0.4–0.5$). Bacteria were then centrifuged at 4 °C for 2 min at maximum speed and the pellet was immediately frozen in liquid nitrogen.

To assess bacterial colonisation levels, especially in asymptomatic plants, stems were placed under a luminometer to visualize bacterial densities within the vascular system, and only plants showing luminescence were used. To avoid bias of quorum sensing signals in the xylem stages and not in the apoplast, similar bacterial yields were infiltrated in potato leaves for the initial stage. Finally, to identify the best time point at which bacterial colonisation within xylem vessels of almost asymptomatic plants was most similar to that in dead plants, we monitored bacterial growth, luminescence and disease symptoms over time (Additional File 1 A). As shown in Additional File 2 A, bacterial densities recovered from the three *in planta* conditions were in the same order of magnitude (between 10^7 and 10^8 CFUs/ml). The in vitro reference condition corresponding to bacteria grown in liquid rich medium, was also obtained to better define *R.*

solanacearum gene expression. We ensured that the difference of the final bacterial yields from the different conditions was not higher than one log (Additional File 2 A). These conditions allowed us to obtain enough *R. solanacearum* RNA-seq reads to have a robust representation of the whole genome (Additional File 13). Principal component analysis revealed that these conditions are consistent among biological replicates and sensitive enough to detect biological differences between conditions (Additional File 2 C).

To obtain more reproducible samples, leaf apoplast was used as a mimic condition of root apoplast, since it has been reported that *R. solanacearum* behaves similarly in these two apoplastic spaces [47].

To obtain leaf apoplast samples, bacterial cells from an overnight culture were washed with water and resuspended to a final concentration of 5×10^8 CFU/ml. The aerial part of the plants was vacuum-infiltrated for 30 s to 1 min and the leaves were dried in paper towel before incubating the plants in the inoculation chamber (27 °C, 12 h / 12 h). After 6 h, leaves were vacuum-infiltrated with sterile distilled water, dried in paper towel, rolled in a cut tip and centrifuged inside a 50 ml tube at 4 °C for 5 min at 2000 rpm. Apoplast fluid extract was pooled (each pool representing approximately 15 plants) and centrifuged at 4 °C at maximum speed for 2 min. Bacterial pellets were frozen in liquid nitrogen.

For early and late xylem samples, potato roots were injured with a 1 ml tip before inoculation. A total of 40 ml of a 10^8 CFU/ml *R. solanacearum* suspension was used to soil-inoculate each plant. After inoculation, plants were kept inside the inoculation chamber (27 °C, 12 h / 12 h) for 6 days (mean disease index = 0–1) for early xylem condition, or 10 days (disease index = 4 in all the plants) for late xylem condition. Plants were photographed in a Fuji Film LAS4000 light imager system to check individual infection levels and only plants showing luminescence were used. Stem pieces of 2 cm were cut from each plant, placed in a 1.5 ml tube containing 500 µl of sterile distilled water and centrifuged 2 min at maximum speed at 4 °C to release bacteria from the xylem vessels. In all cases, bacterial densities were measured by luminescence before freezing and dilutions were plated to measure CFUs before addition of 5% of an ice-cold transcriptional stop solution (5% [vol/vol] water saturated phenol in ethanol). This enabled normalisation of early or late xylem samples for bacterial concentrations comparable to those of apoplast and reference medium samples. Bacterial pellets were pooled together for each biological replicate and frozen in liquid nitrogen. Approximately 30 plants were used for each early xylem replicate and 7 plants for every late xylem replicate (Additional File 2 A).

RNA extraction, sequencing and library preparation

Total RNA was extracted using the SV Total RNA Isolation System kit (Promega) following manufacturer's instructions for Gram-negative Bacteria. RNA concentration was measured with a ND-8000 Nanodrop and RNA integrity was validated for all samples using the Agilent 2100 Bioanalyzer. For rRNA depletion, 2.5 µg of total RNA were treated with the Ribo-zero (TM) magnetic kit for bacteria (Epicentre). Three biological replicates per condition were subjected to sequencing on a HiSeq2000 Illumina System apparatus using multiplexing and kits specially adapted to obtain 100 bp paired-end reads in stranded libraries. Rich media reference samples were sequenced by Macrogen Inc. In all other cases, RNA-sequencing was performed in the Shanghai PSC Genomics facility. Raw sequencing data will be available upon publication in the Sequence Read Archive under Bio Project: PRJNA660623 (accession codes SAMN15955133 to SAMN15955144).

Read alignment, mapping and differential gene expression analysis

RNA-seq raw data quality was evaluated using FAST QC (version 0.11.4, [78]). *R. solanacearum* reads were mapped using Bowtie2 (version 2.3.3, [79]) with stringent parameters [36] using as reference the completely sequenced genome of UY031 strain [80]. Alignment files were quantified with HTSeq-count (version 0.11.3, [81]) using NCBI's RefSeq sequences NZ_CP012687.1 (chromosome) and NZ_CP012688.1 (megaplasmid). The DESeq2 package (version 1.28.1, [82]) in R ([83], ver. 3.6.3) was employed to perform differential expression (DE) analysis of high quality RNAseq reads. Genes with $|\log_2(\text{fold-change})| > 1.5$ and adjusted *p-value* < 0.01 were considered as DE *in planta* when compared to bacteria grown on liquid rich medium as reference condition (Additional File 2 C). The results of the DeSeq2 analysis is shown in Additional File 3. The UpSetR [84] R package was used to visualise the intersection of DE genes in the different *in planta* conditions. For gene expression comparison, gene counts were also normalised to transcripts per million (TPM) (Additional File 14).

Gene expression pattern clustering and enrichment analysis

To obtain expression profiles of *R. solanacearum* UY031 genes, a soft clustering analysis was performed using Mfuzz package (version 2.48, [85]) in R. Input data corresponds to the DE fold-change values yielded by DESeq2 of apoplast, early and late xylem samples normalised to the reference liquid rich medium. The cluster number was manually set at c = 6. To be more stringent, a gene was considered to belong to a specific cluster if

the gene was allocated in the same cluster in 30 out of 40 iterations with the membership value set to $\mu \geq 0.75$.

To further characterise the genes differentially expressed or belonging to any of the clusters, we looked for enriched Gene Ontology (GO) terms or Kyoto Encyclopaedia of Genes and Genomes (KEGG) pathways among our genes. Since no GO terms had been previously associated to UY031 strain genes, we used Blast2GO [86] software to annotate the UY031 genome. For the KEGG and GO enrichment analysis, we used the enricher function of the ClusterProfiler package [87] in R having previously created the TERM2GENE and TERM2NAME lists to do the hypergeometric test.

Because KEGG enrichment analysis is limited to a number of pre-established pathways or terms that do not include important virulence categories, and because pathogenicity-related terms in GO are too general and have not been widely used, we decided to create a manually curated category that we defined as "virulence and parasitic fitness (Additional File 6). This category included the T3SS and type III effectors, motility genes, exopolysaccharides secretion, phytohormone biosynthesis, ROS scavenging, nitrogen metabolism and cell-wall degrading enzymes. After defining the genes included in this category, we conducted a hypergeometric test using the R stats package on the differentially expressed genes or the gene clusters to find out whether the "virulence and parasitic fitness" or any of the subcategories was overrepresented.

In planta visualisation of *R. solanacearum*

To visualize *R. solanacearum* bacterial cells in early (6 days post-inoculation, d.p.i) and late (10 d.p.i.) xylem stages, UY031 with the *psbA* constitutive promoter was fused to the GFP gene. This reporter strain was soil-inoculated with root wounding at $OD_{600} = 0.1$ (10^8 CFUs/ml) in 3 week-old potato plants. Potato stem slices from the first node of infected plants with GFP-containing bacteria were observed in the SZX16 stereomicroscope equipped with a DP71 camera system (Olympus). Pictures were obtained using the following settings: GFP filter, 10 s exposure time, ISO 1/800. Control plants were soil-inoculated with water (Additional File 1 B).

Abbreviations

CFU: Colony forming units; Cv: Cultivar; d.p.i.: Days post inoculation; DEG: Differentially Expressed Genes; DI: Disease index; DNA: desoxyribonucleic acid; EPS: exopolysaccharide; GABA: gamma-aminobutyric acid; GFP: Green Fluorescent Protein; GO: Gene Ontology; *Hrp*: Hypersensitive response and pathogenicity; IVET: In vivo expression technology; KEGG: Kyoto Encyclopedia of Genes and Genomes; OD: Optical Density; PCA: Principal component analysis; RLU: Relative Light Unit; RNA: Ribonucleic acid; ROS: Reactive Oxygen Species; rRNA: Ribosomal ribonucleic acid; T3E: Type 3 Effector; T3SS: Type III Secretion System; TCA: Tricarboxylic acid

Supplementary Information

The online version contains supplementary material available at https://doi.org/10.1186/s12864-021-07457-w.

Additional file 1: *R. solanacearum* reporter strains and bacterial growth show equivalent infection rates. (A) Luminescence levels or bacterial growth (bar plot) and symptom development (line plot) in potato plants were monitored over time to detect the precise time points at which similar bacterial yields but different symptoms could be detected. The disease index scale (DI) ranges from 0 to 4 being 0 symptomless plants and 4 plants completely wilted. Luminescence measurement were conducted on stem sections of infected plants. (B) GFP-labelled bacteria were monitored at the sampled time points in potato plants. RLU = Relative light units.

Additional file 2: RNAseq experimental set-up and bioinformatic pipeline. (A) Experimental set-up for the three *in planta* conditions, corresponding to an early (leaf apoplast), mid (xylem from asymptomatic plants) and late stages (xylem from dead plants) of the disease. As reference condition, bacteria grown in rich liquid media were used. The average of bacterial yields recovered in each condition are indicated as CFU/ml. The grey background section of the figure contains the representation of how bacteria was enriched in each condition (see M&Ms). (B) Transcriptomic analysis pipeline. (C) Two-dimensional Principal Component Analysis representation of the expression data of the conditions' biological replicates used in the study.

Additional file 3: DEGs in the three *in planta* conditions. Differentially expressed genes of *R. solanacearum* in apoplast, early and late xylem compared to liquid rich medium obtained with DESeq2 (*p-adj* > 0.01, $\log_2$ FC ± 1.5).

Additional file 4: Overlap of DEGs in apoplast, early and late xylem compared to previous gene expression analysis. (A) Percentage of common DE genes in each *in planta* condition (versus rich medium) compared to previous *in planta* gene expression analyses (– Puigvert et al. 2017; –Jacobs et al. 2012; –Khokhani et al. 2017). Fractions represent the overlapping genes from the total of DEGs in each of our conditions compared to a given previous gene expression analysis. Colors were plotted using the Conditional Formatting tool in Microsoft Excel. (B) Expression correlation of the DE data of the common genes between our Apoplast data and the RNAseq data from the potato root (Puigvert et al. 20,107).

Additional file 5: Transcriptomic profile of *R. solanacearum* in *in planta* genetic programmes. Up-regulated (left) and down-regulated (right) genes shared and unique across the three *in planta* conditions. Each vertical bar plot represents the number of shared DE between the conditions indicated by the lines and dots in the schematic below. The horizontal bar plots on the right indicate the total DE genes per *in planta* condition compared to rich medium. For the intersection of Apoplast, Early and Late (*in planta* environment), Early and Late (Xylem environment), Apoplast and Late xylem alone, the list of genes was extracted and surveyed for enriched GO terms. Dot plots of the enriched GO terms for the up- (left) and down-regulated (right) genes in each environment is shown below. DE genes were identified with DEseq2 (*p-adj* > 0.01, $\log_2$ FC ± 1.5) and plotted using the R package UpsetR.

Additional file 6: "Virulence and parasitic fitness" manually defined category. Genes belonging to specific virulence categories (T3SS & T3Es, Motility, ROS scavenging enzymes, phytohormone biosynthesis, EPS, nitrogen metabolism, cell wall degrading enzymes) of *R. solanacearum* are listed showing information related to: UY031 NCBI locus tag (first column), gene name (second column), gene description (third column), category, (forth column), reference (fifth column).

Additional file 7: List of genes included in each of the six expression profiles.

Additional file 8: Gene expression dynamics of *R. solanacearum* throughout infection. Six clusters were obtained through Mfuzz clustering of $\log_2$- fold-change data of the apoplast, early and late xylem conditions normalised to the reference rich liquid media. Clusters include the genes (number indicated above each graph) with a membership higher than 70% and consistently associated to the same cluster on at least 30 out of

40 iterations. The list of genes associated to each cluster was extracted and surveyed for enriched GO terms. Dot plots of the enriched GO terms in each cluster is shown next to the cluster.

Additional file 9: T3SS regulatory cascade and apparatus gene expression profile. Heatmap showing the normalised transcripts per million (TPM) of the genes involved in the T3SS regulatory cascade and the T3SS apparatus in the reference and in the *in planta* conditions.

Additional file 10: hemosensors and signal transduction gene expression profile. Heatmap showing the normalised transcripts per million (TPM) of the genes involved in chemosensing and signal transduction in the reference and in the *in planta* conditions.

Additional file 11: Phytohormones biosynthesis gene expression profile. Heatmap showing the normalised transcripts per million (TPM) of the genes involved in phytohormones biosynthesis in the reference and in the *in planta* conditions.

Additional file 12: ROS scavenging enzymes gene expression profile. Heatmap showing the normalised transcripts per million (TPM) of the genes coding for ROS scavenging enzymes in the reference condition and *in planta* apoplast, early and late condition.

Additional file 13: Proportion of reads aligned to *R. solanacearum* UY031 genome. Total number of reads obtained in each biological replicate for each condition (first column). Total number of reads aligned to *R. solanacearum* UY031 genome (second column). Proportion of reads aligned to *R. solanacearum* genome expressed as percentage (third column).

Additional file 14: Transcripts Per Million of each gene in rich medium, apoplast, early and late xylem. Reads normalized per Transcripts Per Million for each *R. solanacearum* gene in every condition: rich medium (philiq1, 2, 3), apoplast (Apo.10, .7, .9), early xylem (Early.D, .E, .G) and late xylem (Xylem.E, .O, Fresh.xylem). (CSV 986 kb)

Acknowledgements
We thank C. Balsalobre and C. Madrid, from the Microbiology Section of the University of Barcelona for their assistance in interpreting the RNAseq data and their interesting suggestions. Also, we would like to thank L. Tondo and E. Orellano from CONACYT Rosario for their useful advice, and CM Piroupo for help in submitting the sequence datasets to the Short Read Archive.

Authors' contributions
MV and JCS designed the study. APM sequenced the bacterial samples. RdeP, PS and MP performed the experimental work. RdeP, PS, MP, NSC, JSM, JCS, APM and MV analysed the data. RdeP, PS, MP, and MV wrote the paper. All authors have read and approved the manuscript.

Funding
This work was funded by project PID2019-108595RB-I00 from the Spanish Ministry of Economy and Competitiveness. We also acknowledge financial support from the "Severo Ochoa Program for Centres of Excellence in R&D" 2016–2019 (SEV-2015-0533) and the CERCA Program of the Catalan Government (Generalitat de Catalunya). R. de Pedro-Jové received FI and FPU fellowships from Generalitat de Catalunya and the Spanish Ministry of Economy and Competitiveness. P. Sebastià received the support of a fellowship (code is LCF/BQ/IN17/11620004) from la Caixa Foundation (identifier [ID] 100010434). This project has received funding from the European Union's Horizon 2020 research and innovation program under Marie Skłodowska-Curie grant agreement no. 713673. M. Puigvert received an APIF doctoral fellowship from Universitat de Barcelona and travel fellowship funded by Fundació Montcelimar and Universitat de Barcelona to carry out a short stay in J.C. Setubal's lab. J.C. Setubal holds a CNPq senior researcher fellowship. J.S. Monteiro is funded by a FAPESP doctoral fellowship under process number 2019/05287–2. A.P. Macho is funded by the Chinese Academy of Sciences and the Chinese 1000 Talents Program. The funder had no role in study design, data collection and analysis, decision to publish, or preparation of the manuscript.

Availability of data and materials
All data generated or analysed during this study are included in this published article and its supplementary information files and the supporting datasets are available in Sequence Read Archive repository under Bio Project: PRJNA660623 (accession codes SAMN15955133 to SAMN15955144) in https://www.ncbi.nlm.nih.gov/sra.

Declarations

Ethics approval and consent to participate
Not applicable.

Consent for publication
Not applicable.

Competing interests
The authors declare that they have no competing interests.

Author details
[1]Department of Genetics, University of Barcelona, Barcelona, Catalonia, Spain. [2]Centre for Research in Agricultural Genomics (CSIC-IRTA-UAB-UB), Bellaterra, Catalonia, Spain. [3]Shanghai Center for Plant Stress Biology, CAS Center for Excellence in Molecular Plant Sciences, Chinese Academy of Sciences, Shanghai 201602, China. [4]Departamento de Bioquímica, Universidade de São Paulo, São Paulo, Brazil.

Received: 21 September 2020 Accepted: 19 February 2021
Published online: 09 March 2021

References
1. Coll NS, Valls M. Current knowledge on the Ralstonia solanacearum type III secretion system. Microb Biotechnol [Internet]. 2013 Nov [cited 2020 Sep 18];6(6):614–20. Available from: https://www.ncbi.nlm.nih.gov/pmc/articles/PMC3815929/
2. Peeters N, Guidot A, Vailleau F, Valls M. Ralstonia solanacearum, a widespread bacterial plant pathogen in the post-genomic era. Mol Plant Pathol [Internet]. 2013 Sep 1 [cited 2020 Sep 18];14(7):651–62. Available from: https://bsppjournals.onlinelibrary.wiley.com/doi/full/10.1111/mpp.12038
3. Hayward AC. Bacterial wilt caused by pseudomonas solanacearum. Annu Rev Phytopathol. 1991;29:65–87.
4. Ciampi L, Sequeira L, French ER. Latent infection of potato tubers by Pseudomonas solanacearum. Am Potato J. 1980;57(8):377–86.
5. Janse JD, Van Den Beld HE, Elphinstone J, Simpkins S, Tjou-Tam-Sin NNA, Van Vaerenbergh J. Introduction to Europe of Ralstonia solanacearum biovar 2, race 3 in Pelargonium zonale cuttings. J Plant Pathol. 2004;86(2):147–55.
6. Champoiseau PG, Jones JB, Allen C. Ralstonia solanacearum race 3 Biovar 2 causes tropical losses and temperate anxieties. Plant Heal Prog. 2009;10(1):35.
7. Álvarez B, López MM, Biosca EG. Influence of native microbiota on survival of Ralstonia solanacearum phylotype II in river water microcosms. Appl Environ Microbiol. 2007;73(22):7210–7.
8. Yao J, Allen C. Chemotaxis is required for virulence and competitive fitness of the bacterial wilt pathogen Ralstonia solanacearum. J Bacteriol. 2006;188(10):3697–708.
9. Vasse J, Frey P, Trigalet A. Microscopic studies of intercellular infection and protoxylem invasion of tomato roots by Pseudomonas solanacearum. Mol Plant-Microbe Interact. 1995;8(2):241–51.
10. Du Y, Stegmann M, Misas-Villamil JC. Meetings the apoplast as battleground for plant – microbe interactions; 2015.
11. Hikichi Y, Yoshimochi T, Tsujimoto S, Shinohara R, Nakaho K, Kanda A, et al. Global regulation of pathogenicity mechanism of Ralstonia solanacearum. Plant Biotechnol. 2007;24(1):149–54.
12. Planas-Marquès M, Bernardo-Faura M, Paulus J, Kaschani F, Kaiser M, Valls M, et al. Protease Activities Triggered by Ralstonia solanacearum Infection in Susceptible and Tolerant Tomato Lines. Mol Cell Proteomics [Internet]. 2018 Jun 1 [cited 2020 Sep 18];17(6):1112–25. Available from: https://pubmed.ncbi.nlm.nih.gov/29523767/
13. Zuluaga AP, Puigvert M, Valls M. Novel plant inputs influencing Ralstonia solanacearum during infection. Front Microbiol [Internet]. 2013 Nov 20 [cited 2020 Sep 18];4(NOV):349. Available from: http://journal.frontiersin.org/article/10.3389/fmicb.2013.00349/abstract
14. Jacobs JM, Babujee L, Meng F, Physiological C, Strategies V, Wilt B, et al. The In Planta Transcriptome of Ralstonia solanacearum. Conserved. 2012;3(4):1–11.

15. Planas-Marquès M, Kressin JP, Kashyap A, Panthee DR, Louws FJ, Coll NS, et al. Four bottlenecks restrict colonization and invasion by the pathogen Ralstonia solanacearum in resistant tomato. J Exp Bot [Internet]. 2020 Mar 1 [cited 2020 Sep 18];71(6):2157–71. Available from: https://academic.oup.com/jxb/article/71/6/2157/5686149
16. Genin S. Molecular traits controlling host range and adaptation to plants in Ralstonia solanacearum. New Phytol. 2010;187(4):920–8.
17. Vasse J, Genin S, Frey P, Boucher C, Brito B. The hrpB and hrpG regulatory genes of Ralstonia solanacearum are required for different stages of the tomato root infection process. Mol Plant-Microbe Interact. 2000;
18. Lu H, Lema SA, Planas-Marquès M, Alonso-Díaz A, Valls M, Coll NS. Type III secretion-dependent and-independent phenotypes caused by Ralstonia solanacearum in Arabidopsis roots. Mol Plant-Microbe Interact. 2018;31(1):175–84.
19. Büttner D, He SY. Type III protein secretion in plant pathogenic bacteria. Plant Physiol. 2009;150(4):1656–64.
20. Coburn B, Sekirov I, Finlay BB. Type III secretion systems and disease. Clin Microbiol Rev. 2007;20(4):535–49.
21. Peeters N, Carrère S, Anisimova M, Plener L, Cazalé AC, Genin S. Repertoire, unified nomenclature and evolution of the Type III effector gene set in the Ralstonia solanacearum species complex. BMC Genomics. 2013;14:1.
22. Prior P, et al. 1998. Molecular and Ecological Aspects: Bacterial Wilt Disease; 2013. 449 p.
23. Huang J, Denny TP, Schell MA. VsrB, a regulator of virulence genes of Pseudomonas solanacearum, is homologous to sensors of the two-component regulator family. J Bacteriol. 1993;175(19):6169–78.
24. Yaowei K, Jianzhong H, Mao G, Yuan HL, Schell MA. Dramatically reduced virulence of mutants of Pseudomonas solanacearum defective in export of extracellular proteins across the outer membrane. Mol Plant-Microbe Interact. 1994;7(3):370–7.
25. Liu H, Zhang S, Schell MA, Denny TP. Pyramiding unmarked deletions in Ralstonia solanacearum shows that secreted proteins in addition to plant cell-wall-degrading enzymes contribute to virulence. Mol Plant-Microbe Interact. 2005;18(12):1296–305.
26. Tans-Kersten J, Brown D, Allen C. Swimming motility, a virulence trait of Ralstonia solanacearum, is regulated by FlhDC and the plant host environment. Mol Plant-Microbe Interact. 2004 Feb;17(6):686–95.
27. Kang Y, Liu H, Genin S, Schell MA, Denny TP. *Ralstonia solanacearum* requires type 4 pili to adhere to multiple surfaces and for natural transformation and virulence. Mol Microbiol. 2002 Oct;46(2):427–37.
28. Dalsing BL, Allen C. Nitrate assimilation contributes to Ralstonia solanacearum root attachment, stem colonization, and virulence. J Bacteriol. 2014;196(5):949–60.
29. Dalsing BL, Truchon AN, Gonzalez-Orta ET, Milling AS, Allen C. Ralstonia solanacearum uses inorganic nitrogen metabolism for virulence, ATP production, and detoxification in the oxygen-limited host xylem environment. MBio. 2015;6(2):1–13.
30. Pegg GF. Life in a black hole — the micro-environment of the vascular pathogen. Trans Br Mycol Soc. 1985;85(1):IN1–20.
31. Brito B, Marenda M, Barberis P, Boucher C, Genin S. PrhJ and hrpG, two new components of the plant signal-dependent regulatory cascade controlled by PrhA in Ralstonia solanacearum. Mol Microbiol. 1999;31(1):237–51.
32. Genin S, Brito B, Denny TP, Boucher C. Control of the Ralstonia solanacearum type III secretion system (Hrp) genes by the global virulence regulator PhcA. FEBS Lett. 2005;579(10):2077–81.
33. Valls M, Genin S, Boucher C. Integrated regulation of the type III secretion system and other virulence determinants in Ralstonia solanacearum. PLoS Pathog. 2006;2(8):0798–807.
34. Monteiro F, Genin S, van Dijk I, Valls M. A luminescent reporter evidences active expression of Ralstonia solanacearum type III secretion system genes throughout plant infection. Microbiol (United Kingdom). 2012;158(8):2107–16.
35. Ailloud F, Lowe TM, Robène I, Cruveiller S, Allen C, Prior P. In planta comparative transcriptomics of host-adapted strains of Ralstonia solanacearum. Peer J. 2016;2016:1.
36. Puigvert M, Guarischi-Sousa R, Zuluaga P, Coll NS, Macho AP, Setubal JC, et al. Transcriptomes of ralstonia solanacearum during root colonization of solanum commersonii. Front Plant Sci. 2017;8.
37. Garg RP, Huang J, Yindeeyoungyeon W, Denny TP, Schell MA. Multicomponent transcriptional regulation at the complex promoter of the exopolysaccharide I biosynthetic operon of Ralstonia solanacearum. J Bacteriol. 2000;182(23):6659–66.
38. Clough SJ, Flavier AB, Schell MA, Denny TP. Differential expression of virulence genes and motility in Ralstonia (Pseudomonas) solanacearum during exponential growth. Appl Environ Microbiol. 1997;63(3):844–50.
39. Huang J, Carney BF, Denny TP, Weissinger AK, Schell MA. A complex network regulates expression of eps and other virulence genes of Pseudomonas solanacearum. J Bacteriol. 1995;177(5):1259–67.
40. Yoshimochi T, Hikichi Y, Kiba A, Ohnishi K. The global virulence regulator PhcA negatively controls the Ralstonia solanacearum hrp regulatory cascade by repressing expression of the PrhIR signaling proteins. J Bacteriol. 2009;191(10):3424–8.
41. Meng F, Babujee L, Jacobs JM, Allen C. Comparative transcriptome analysis reveals cool virulence factors of Ralstonia solanacearum race 3 biovar 2. PLoS One. 2015;10:10.
42. Khokhani D, Lowe-Power TM, Tran TM, Allen C. A single regulator mediates strategic switching between attachment/spread and growth/virulence in the plant pathogen Ralstonia solanacearum. MBio. 2017;8:5.
43. Yu X, Lund SP, Scott RA, Greenwald JW, Records AH, Nettleton D, et al. Transcriptional responses of Pseudomonas syringae to growth in epiphytic versus apoplastic leaf sites. Proc Natl Acad Sci U S A. 2013;110:5.
44. Nobori T, Velásquez AC, Wu J, Kvitko BH, Kremer JM, Wang Y, et al. Transcriptome landscape of a bacterial pathogen under plant immunity. Proc Natl Acad Sci U S A. 2018;115(13):E3055–64.
45. Lovelace AH, Smith A, Kvitko BH. Pattern-triggered immunity alters the transcriptional regulation of virulence-associated genes and induces the sulfur starvation response in pseudomonas syringae pv. Tomato DC3000. Mol Plant-Microbe Interact. 2018;31(7):750–65.
46. Siri MI, Sanabria A, Pianzzola MJ. Genetic diversity and aggressiveness of Ralstonia solanacearum strains causing bacterial wilt of potato in Uruguay. Plant Dis. 2011;95(10):1292–301.
47. Hikichi Y. Interactions between plant pathogenic bacteria and host plants during the establishment of susceptibility [Internet]. Vol. 82, Journal of General Plant Pathology. Springer Tokyo; 2016 [cited 2020 Aug 18]. p. 326–31. Available from: https://link.springer.com/article/10.1007/s10327-016-0680-9
48. Cruz APZ, Ferreira V, Pianzzola MJ, Siri MI, Coll NS, Valls M. A novel, sensitive method to evaluate potato germplasm for bacterial wilt resistance using a luminescent ralstonia solanacearum reporter strain. Mol Plant-Microbe Interact. 2014;27(3):277–85.
49. Arlat M, Gough CL, Zischek C, Barberis PA, Trigalet A, Boucher CA. Transcriptional organization and expression of the large hrp gene cluster of Pseudomonas solanacearum. Molecular plant-microbe interactions : MPMI. 1992;5:187–93.
50. Mori Y, Inoue K, Ikeda K, Nakayashiki H, Higashimoto C, Ohnishi K, et al. The vascular plant-pathogenic bacterium Ralstonia solanacearum produces biofilms required for its virulence on the surfaces of tomato cells adjacent to intercellular spaces. Mol Plant Pathol. 2016.
51. Boucher CA, Barberis PA, Trigalet AP, Demery DA. Transposon mutagenesis of Pseudomonas solanacearum: isolation of Tn5-induced avirulent mutants. J Gen Microbiol. 1985;131(9):2449–57.
52. Lei N, Chen L, Kiba A, Hikichi Y, Zhang Y, Ohnishi K, et al. Super-Multiple Deletion Analysis of Type III Effectors in Ralstonia solanacearum OE1–1 for Full Virulence Toward Host Plants Bacterial Strains and Culture Conditions. 2020;11(July):1–10.
53. Poueymiro M, Genin S. Secreted proteins from Ralstonia solanacearum: a hundred tricks to kill a plant. Curr Opin Microbiol. 2009;12(1):44–52.
54. Remigi P, Anisimova M, Guidot A, Genin S, Peeters N. Functional diversification of the GALA type III effector family contributes to Ralstonia solanacearum adaptation on different plant hosts. New Phytol. 2011;192(4):976–87.
55. Solé M, Popa C, Mith O, Sohn KH, Jones JDG, Deslandes L, et al. Type III effectors displaying virulence and Avirulence activities. Mol Plant-Microbe Interact. 2012;25(7):941–53.
56. Popa C, Li L, Gil S, Tatjer L, Hashii K, Tabuchi M, et al. The effector AWR5 from the plant pathogen Ralstonia solanacearum is an inhibitor of the TOR signalling pathway. Sci Rep. 2016.
57. Sang Y, Wang Y, Ni H, Cazalé AC, She YM, Peeters N, et al. The ralstonia solanacearum type III effector ripay targets plant redox regulators to suppress immune responses. Mol Plant Pathol. 2018;19(1):129–42.
58. Wei Y, Sang Y, Macho AP. The ralstonia solanacearum type III effector RipAY is phosphorylated in plant cells to modulate its enzymatic activity. Front Plant Sci. 2017;8(November):1–7.
59. Mukaihara T, Hatanaka T, Nakano M, Oda K. Ralstonia solanacearum type III effector RipAY is a glutathione-degrading enzyme that is activated by plant

cytosolic thioredoxins and suppresses plant immunity. MBio [Internet]. 2016 Apr 12 [cited 2020 Aug 18];7(2). Available from: https://pubmed.ncbi.nlm.nih.gov/27073091/
60. Fujiwara S, Kawazoe T, Ohnishi K, Kitagawa T, Popa C, Valls M, et al. RipAY, a Plant Pathogen Effector Protein, Exhibits Robust γ-Glutamyl Cyclotransferase Activity When Stimulated by Eukaryotic Thioredoxins. J Biol Chem [Internet]. 2016 Mar 25 [cited 2020 Aug 18];291(13):6813–30. Available from: https://pubmed.ncbi.nlm.nih.gov/26823466/
61. Jeon H, Kim W, Kim B, Lee S, Jayaraman J, Jung G, et al. Erratum: Ralstonia solanacearum Type III effectors with predicted nuclear localization signal localize to various cell compartments and modulate immune responses in Nicotiana spp. (Plant Pathol. J., (2020) 36(1), (43–53), https://doi.org/10.5423/PPJ.OA.08.2019.0227). Plant Pathol J. 2020;36(3):303.
62. Xian L, Yu G, Wei Y, Rufian JS, Li Y, Zhuang H, et al. A Bacterial Effector Protein Hijacks Plant Metabolism to Support Pathogen Nutrition. Cell Host Microbe [Internet]. 2020 Jul 30 [cited 2020 Aug 18];1–10. Available from: https://doi.org/10.1016/j.chom.2020.07.003.
63. Sampedro I, Parales RE, Krell T, Hill JE. Pseudomonas chemotaxis. FEMS Microbiol Rev. 2015;39(1):17–46.
64. Mattick JS. Type IV pili and twitching motility. Annu Rev Microbiol 2002;56:289–314.
65. Liu H, Kang Y, Genin S, Schell MA, Denny TP. Twitching motility of Ralstonia solanacearum requires a type IV pilus system. Microbiology. 2001;147(12):3215–29.
66. Corral J, Sebastià P, Coll NS, Barbé J, Aranda J, Valls M. Twitching and Swimming Motility Play a Role in Ralstonia solanacearum Pathogenicity. mSphere. 2020;5(2):1–16.
67. Genin S, Denny TP. Pathogenomics of the ralstonia solanacearum species complex. Annu Rev Phytopathol. 2012;50:67–89.
68. Freebairn HT, Buddenhagen IW. Ethylene production by Pseudomonas solanacearum. Nature. 1964;313(314).
69. Robinette D, Matthysse AG. Inhibition by agrobacterium tumefaciens and Pseudomonas savastanoi of development of the hypersensitive response elicited by Pseudomonas syringae pv. Phaseolicola. J Bacteriol. 1990;172(10):5742–9.
70. Hirsch J, Deslandes L, Feng DX, Balagué C, Marco Y. Delayed symptom development in ein2-1, an Arabidopsis ethylene-insensitive mutant, in response to bacterial wilt caused by Ralstonia solanacearum. Phytopathology. 2002;92(10):1142–8.
71. Bolwell GP. The apoplastic oxidative burst in response to biotic stress in plants: a three-component system. J Exp Bot. 2002;53(372):1367–76.
72. Flores-Cruz Z, Allen C. Ralstonia solanacearum encounters an oxidative environment during tomato infection. Mol Plant-Microbe Interact. 2009;22(7):773–82.
73. Büttner D, Bonas U. Regulation and secretion of Xanthomonas virulence factors. FEMS Microbiol Rev. 2010;34(2):107–33.
74. Jang IA, Kim J, Park W. Endogenous hydrogen peroxide increases biofilm formation by inducing exopolysaccharide production in Acinetobacter oleivorans DR1. Sci Rep. 2016;6(February):1–12.
75. Oh E, Jeon B. Role of alkyl hydroperoxide reductase (AhpC) in the biofilm formation of Campylobacter jejuni. PLoS One. 2014;9:1.
76. Panmanee W, Hassett DJ. Differential roles of OxyR-controlled antioxidant enzymes alkyl hydroperoxide reductase (AhpCF) and catalase (KatB) in the protection of Pseudomonas aeruginosa against hydrogen peroxide in biofilm vs. planktonic culture. FEMS Microbiol Lett. 2009;295(2):238–44.
77. Wasim M, Bible AN, Xie Z, Alexandre G. Alkyl hydroperoxide reductase has a role in oxidative stress resistance and in modulating changes in cell-surface properties in Azospirillum brasilense Sp245. Microbiology. 2009;155(4):1192–202.
78. Andrews S, Krueger F, Seconds-Pichon A, Biggins F, Wingett S. FastQC. A quality control tool for high throughput sequence data. Babraham Bioinformatics [Internet]. Vol. 1, Babraham Institute. 2015. p. 1. Available from: https://www.bioinformatics.babraham.ac.uk/projects/fastqc/, http://www.bioinformatics.bbsrc.ac.uk/projects/fastqc/
79. Langmead B, Bowtie SS. Nat Methods [Internet]. 2013;9(4):357–9 Available from: https://www.ncbi.nlm.nih.gov/pmc/articles/PMC3322381/pdf/nihms-366740.pdf.
80. Guarischi-Sousa R, Puigvert M, Coll NS, Siri MI, Pianzzola MJ, Valls M, et al. Complete genome sequence of the potato pathogen Ralstonia solanacearum UY031. Stand Genomic Sci 2016;11(1):1–8.
81. Anders S, Pyl PT, Huber W. HTSeq-A Python framework to work with high-throughput sequencing data. Bioinformatics. 2015;31(2):166–9.
82. Love MI, Huber W, Anders S. Moderated estimation of fold change and dispersion for RNA-seq data with DESeq2. Genome Biol. 2014;15(12):1–21.
83. R Team C. R Core Team (2017). R: a language and environment for statistical computing. R Found Stat Comput Vienna, Austria URL http//www R-project org/, page R Found Stat Comput 2017;
84. Conway JR, Lex A, Gehlenborg N. UpSetR: an R package for the visualization of intersecting sets and their properties. Bioinformatics. 2017;33(18):2938–40.
85. Kumar L, Futschik ME. Mfuzz: A software package for soft clustering of microarray data. Bioinformation. 2007.
86. Götz S, García-Gómez JM, Terol J, Williams TD, Nagaraj SH, Nueda MJ, et al. High-throughput functional annotation and data mining with the Blast2GO suite. Nucleic Acids Res. 2008;36(10):3420–35.
87. Yu G, Wang LG, Han Y, He QY. ClusterProfiler: an R package for comparing biological themes among gene clusters. Omi A J Integr Biol. 2012;16(5):284–7.

Publisher's Note

Supplementary Data

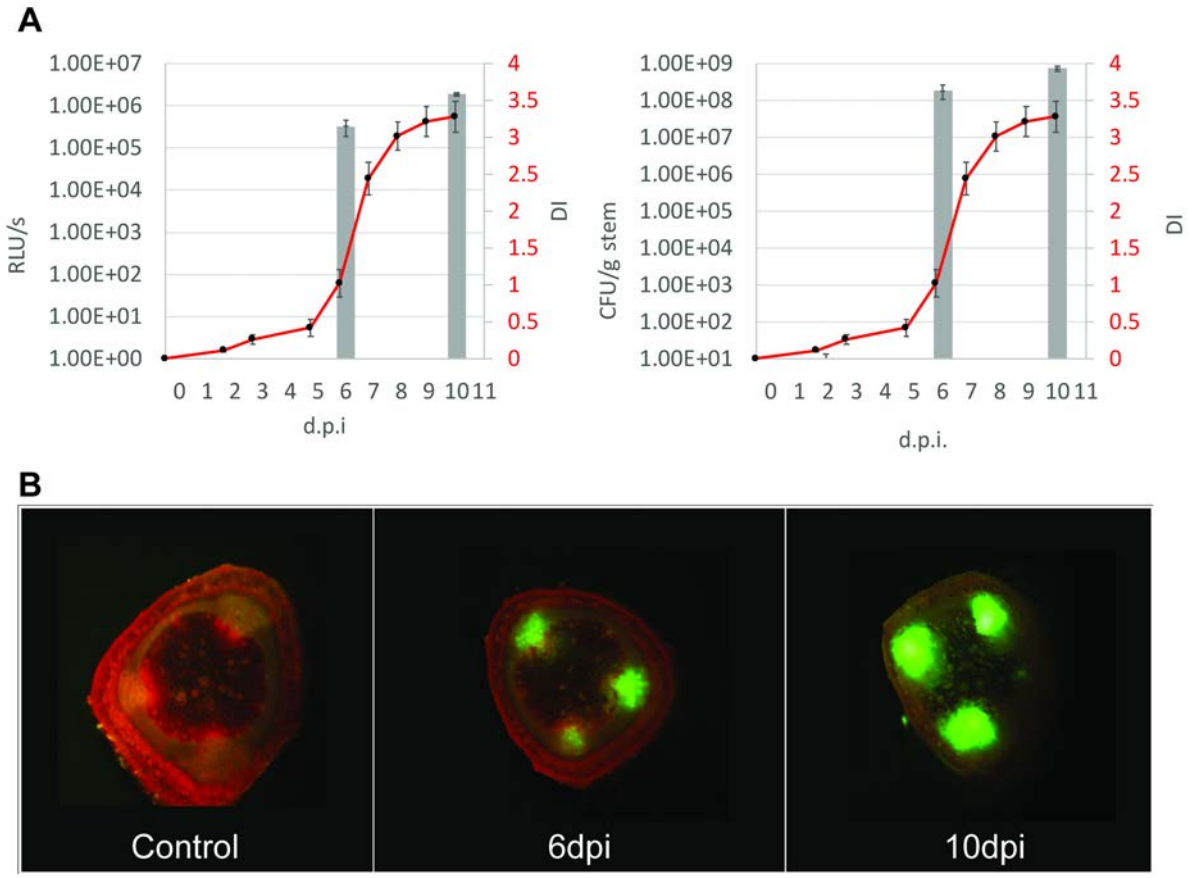

Additional file 1: *R. solanacearum* reporter strains and bacterial growth show equivalent infection rates. (A) Luminescence levels or bacterial growth (bar plot) and symptom development (line plot) in potato plants were monitored over time to detect the precise time points at which similar bacterial yields but different symptoms could be detected. The disease index scale (DI) ranges from 0 to 4 being 0 symptomless plants and 4 plants completely wilted. Luminescence measurement were conducted on stem sections of infected plants. (B) GFP-labelled bacteria were monitored at the sampled time points in potato plants. RLU = Relative light units.

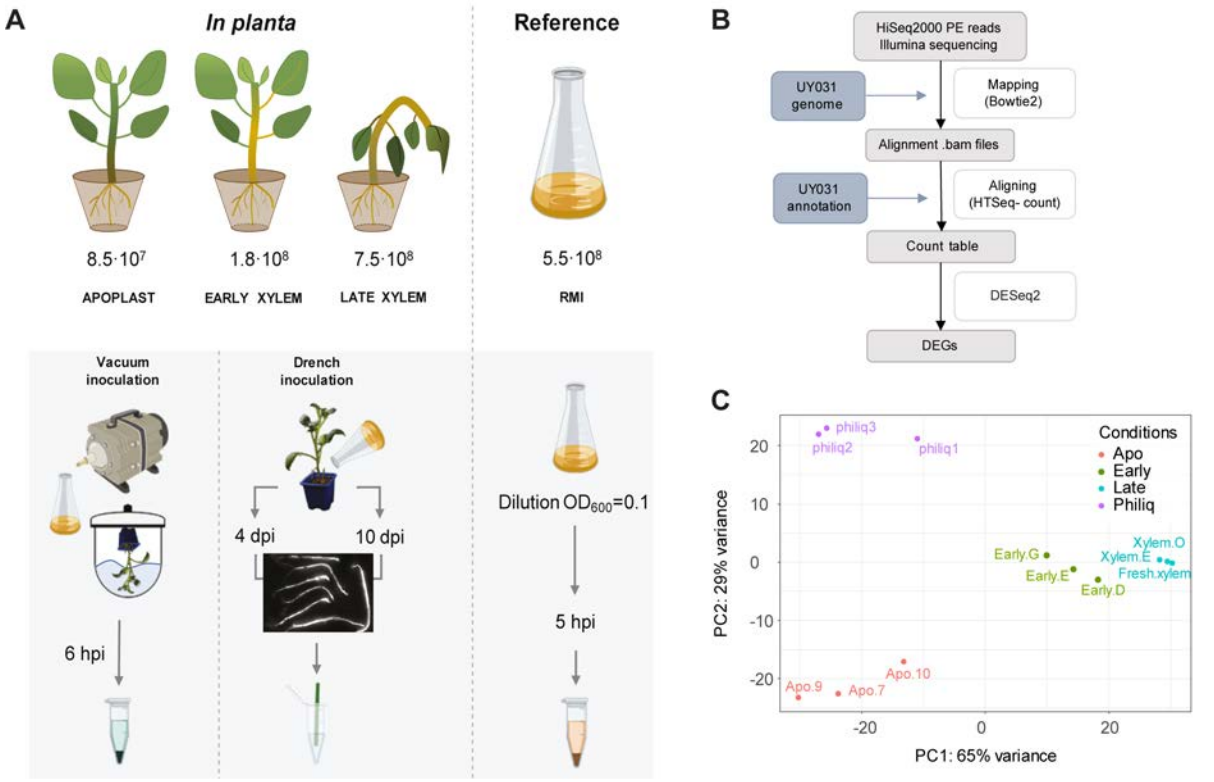

Additional file 2: RNAseq experimental set-up and bioinformatic pipeline. (A) Experimental set-up for the three in planta conditions, corresponding to an early (leaf apoplast), mid (xylem from asymptomatic plants) and late stages (xylem from dead plants) of the disease. As reference condition, bacteria grown in rich liquid media were used. The average of bacterial yields recovered in each condition are indicated as CFU/ ml. The grey background section of the figure contains the representation of how bacteria was enriched in each condition (see M&Ms). (B) Transcriptomic analysis pipeline. (C) Two-dimensional Principal Component Analysis representation of the expression data of the conditions' biological replicates used in the study.

A

Induced - UP			Repressed - DOWN				
Apoplast	Early Xylem	Late Xylem	Apoplast	Early Xylem	Late Xylem		Ref
18% (40/226)	9% (27/290)	5% (20/378)	0% (0)	1% (3/241)	5% (26/544)	RNAseq UY031 - Potato root UP	(36)
0% (0)	0% (1/290)	0% (1/378)	17% (32/192)	9% (21/241)	5% (26/544)	RNAseq UY031 - Potato root DOWN	(36)
33% (74/226)	34% (100/290)	27% (102/378)	6% (11/192)	3% (8/241)	2% (12/544)	µarray UW551 - Tomato UP	(14)
1% (2/226)	1% (4/290)	1% (4/378)	32% (61/192)	36% (86/241)	26% (142/544)	µarray UW551 - Tomato DOWN	(14)
13% (30/226)	20% (58/290)	15% (56/378)	5% (9/192)	3% (8/241)	2% (9/544)	µarray GMI1000 - Tomato UP	(14)
1% (2/226)	1% (2/290)	1% (2/378)	16% (31/226)	21% (50/241)	16% (86/544)	µarray GMI1000 - Tomato DOWN	(14)
8% (17/226)	9% (27/290)	7% (27/378)	6% (12/226)	5% (11/241)	3% (16/544)	RNAseq GMI1000 - Tomato UP	(42)
5% (12/226)	5% (14/290)	4% (15/378)	15% (29/226)	8% (19/241)	12% (63/544)	RNAseq GMI1000 - Tomato DOWN	(42)

B

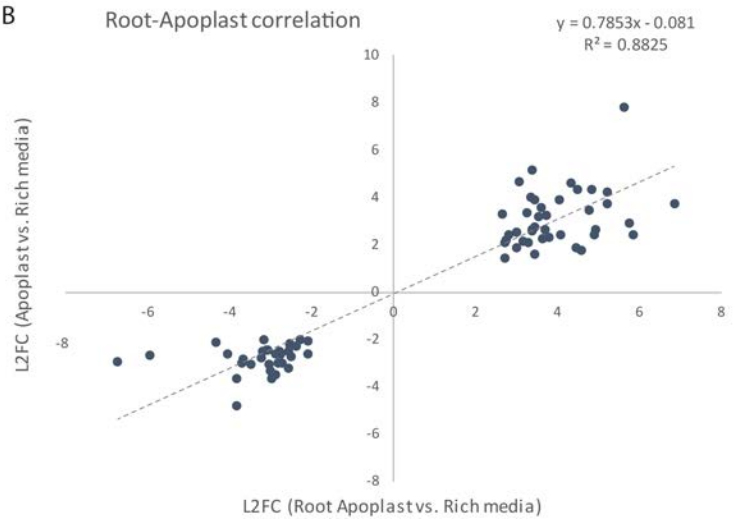

Additional file 4: Overlap of DEGs in apoplast, early and late xylem compared to previous gene expression analysis. (A) Percentage of common DE genes in each in planta condition (versus rich medium) compared to previous in planta gene expression analyses (− Puigvert et al. 2017; −Jacobs et al. 2012; −Khokhani et al. 2017). Fractions represent the overlapping genes from the total of DEGs in each of our conditions compared to a given previous gene expression analysis. Colors were plotted using the Conditional Formatting tool in Microsoft Excel. (B) Expression correlation of the DE data of the common genes between our Apoplast data and the RNAseq data from the potato root (Puigvert et al. 20,107).

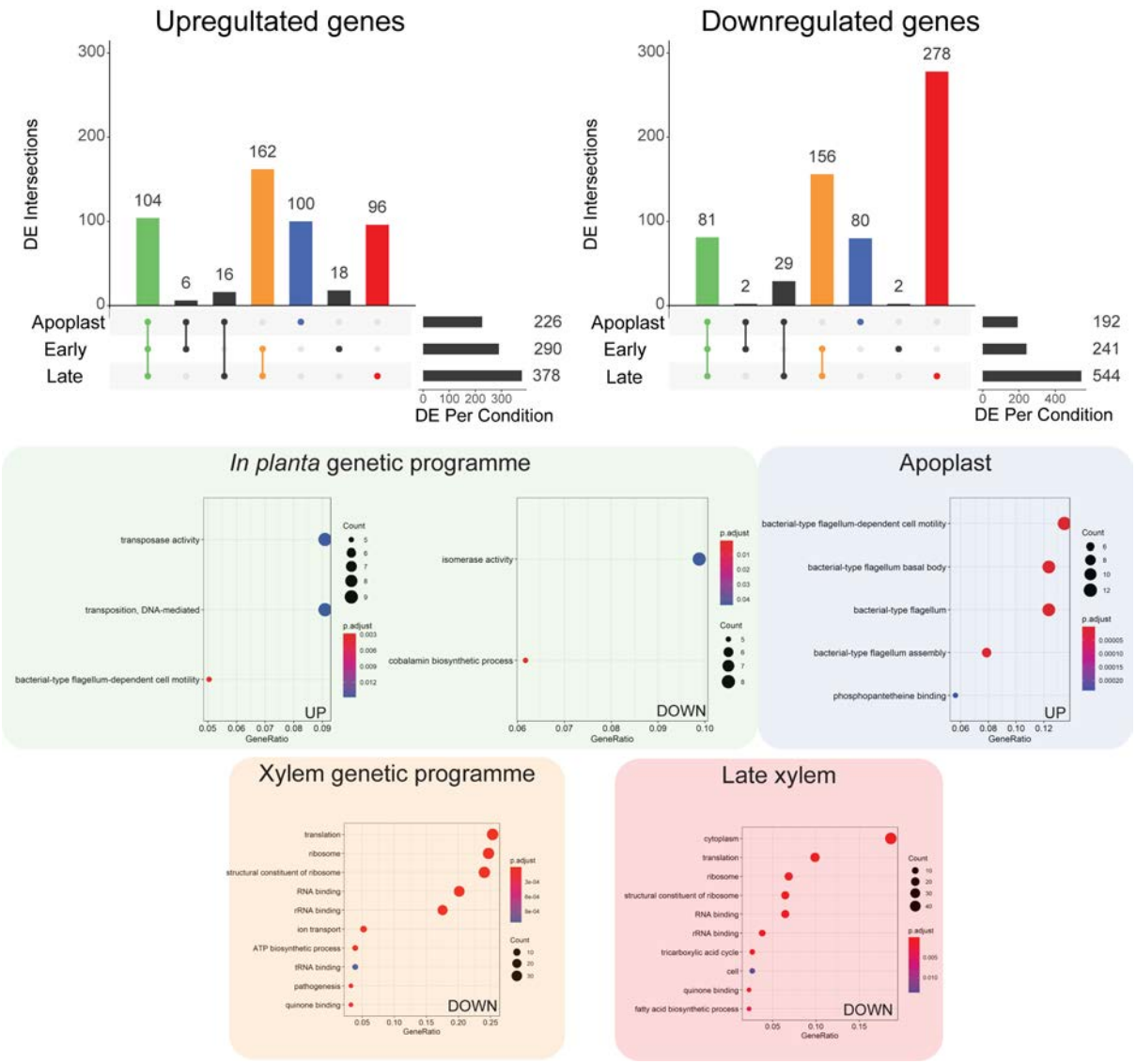

Additional file 5: Transcriptomic profile of *R. solanacearum* in in planta genetic programmes. Up-regulated (left) and down-regulated (right) genes shared and unique across the three in planta conditions. Each vertical bar plot represents the number of shared DE between the conditions indicated by the lines and dots in the schematic below. The horizontal bar plots on the right indicate the total DE genes per in planta condition compared to rich medium. For the intersection of Apoplast, Early and Late (in planta environment), Early and Late (Xylem environment), Apoplast and Late xylem alone, the list of genes was extracted and surveyed for enriched GO terms. Dot plots of the enriched GO terms for the up- (left) and down-regulated (right) genes in each environment is shown below. DE genes were identified with DEseq2 (p-adj > 0.01, log2 FC ± 1.5) and plotted using the R package UpsetR.

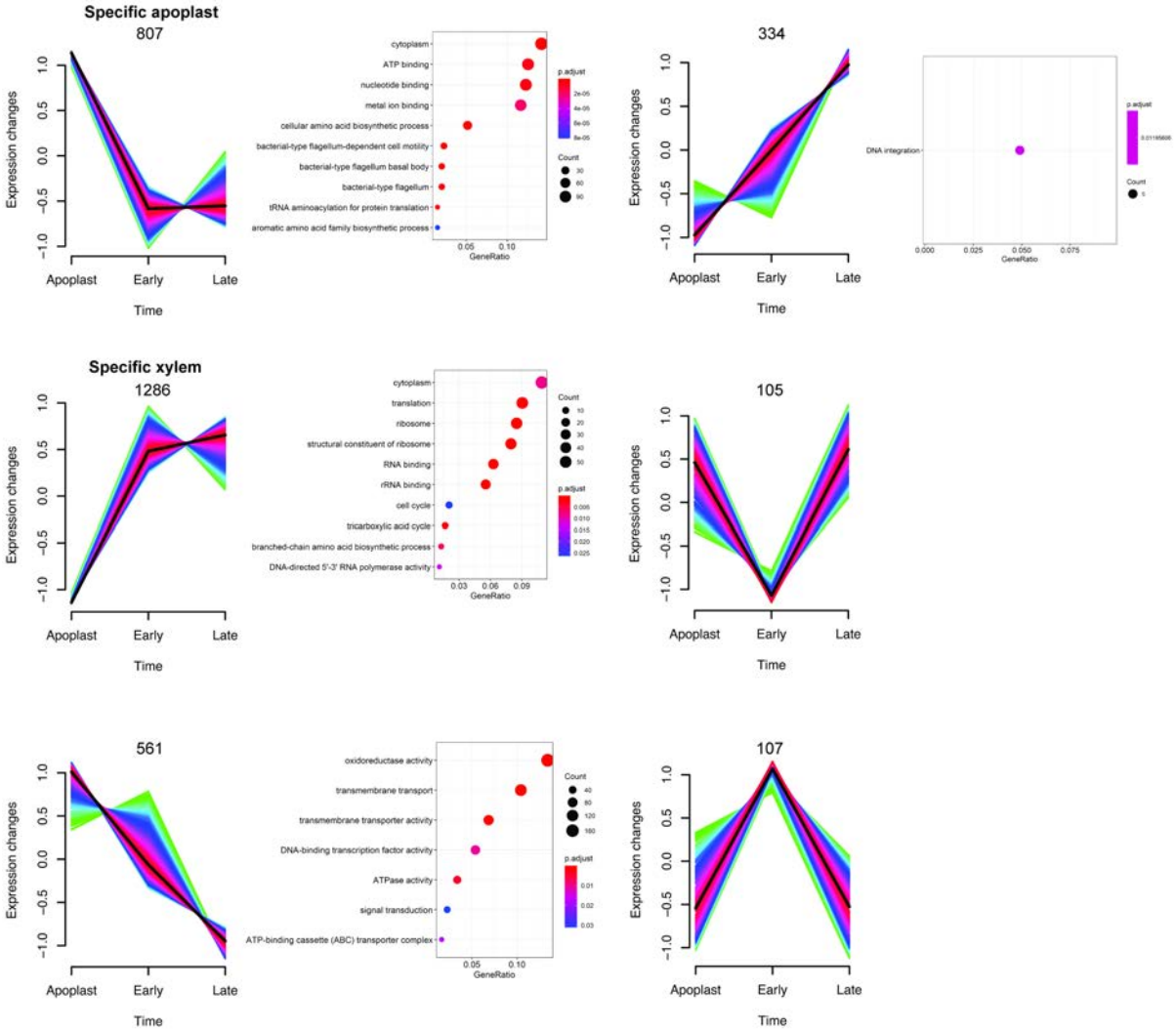

Additional file 8: Gene expression dynamics of *R. solanacearum* throughout infection. Six clusters were obtained through Mfuzz clustering of log2- fold-change data of the apoplast, early and late xylem conditions normalised to the reference rich liquid media. Clusters include the genes (number indicated above each graph) with a membership higher than 70% and consistently associated to the same cluster on at least 30 out of 40 iterations. The list of genes associated to each cluster was extracted and surveyed for enriched GO terms. Dot plots of the enriched GO terms in each cluster is shown next to the cluster.

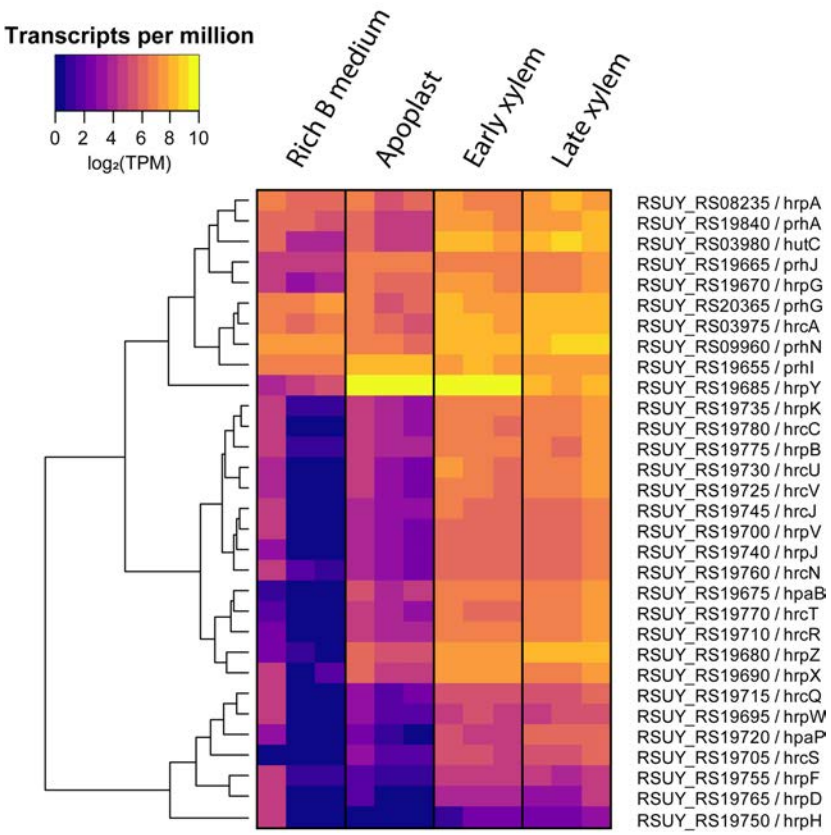

Additional file 9: T3SS regulatory cascade and apparatus gene expression profile. Heatmap showing the normalised transcripts per million (TPM) of the genes involved in the T3SS regulatory cascade and the T3SS apparatus in the reference and in the in planta conditions.

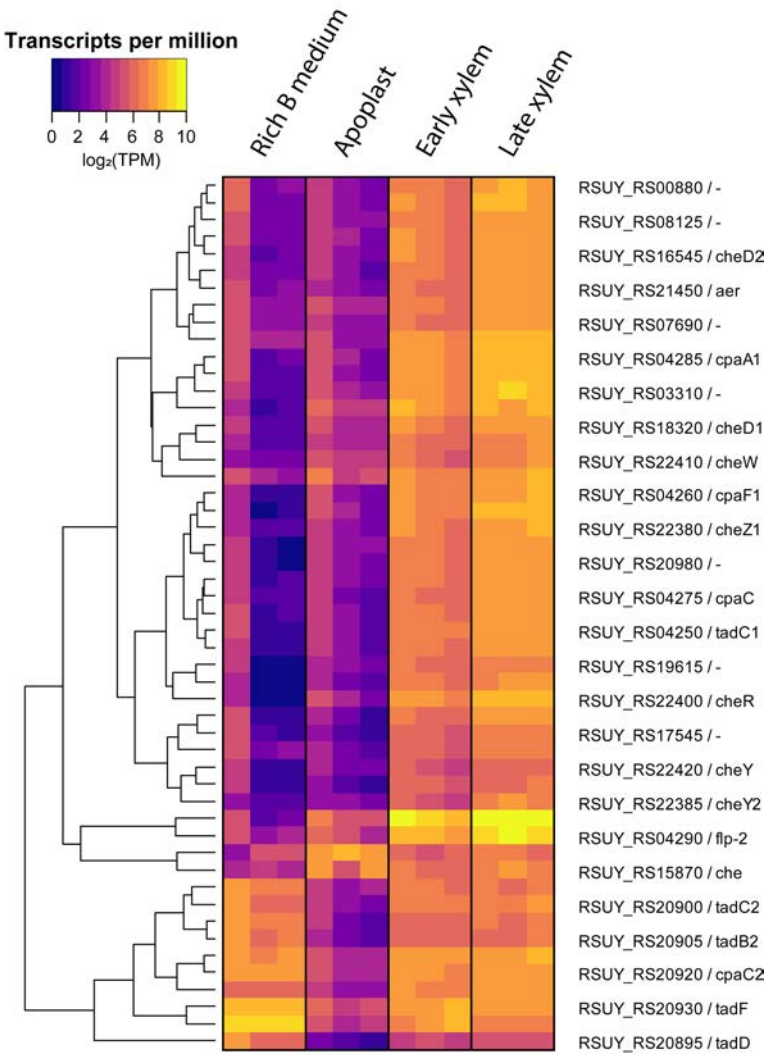

Additional file 10: Chemosensors and signal transduction gene expression profile. Heatmap showing the normalised transcripts per million (TPM) of the genes involved in chemosensing and signal transduction in the reference and in the in planta conditions.

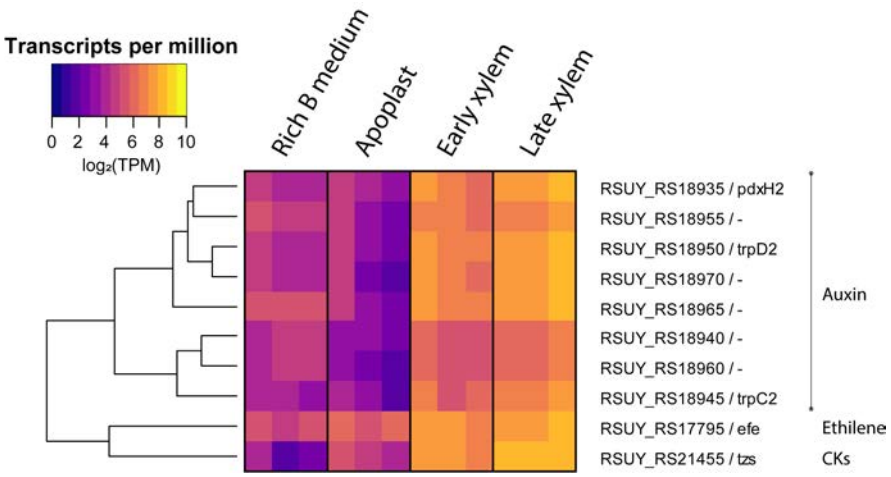

Additional file 11: Phytohormones biosynthesis gene expression profile. Heatmap showing the normalised transcripts per million (TPM) of the genes involved in phytohormones biosynthesis in the reference and in the in planta conditions.

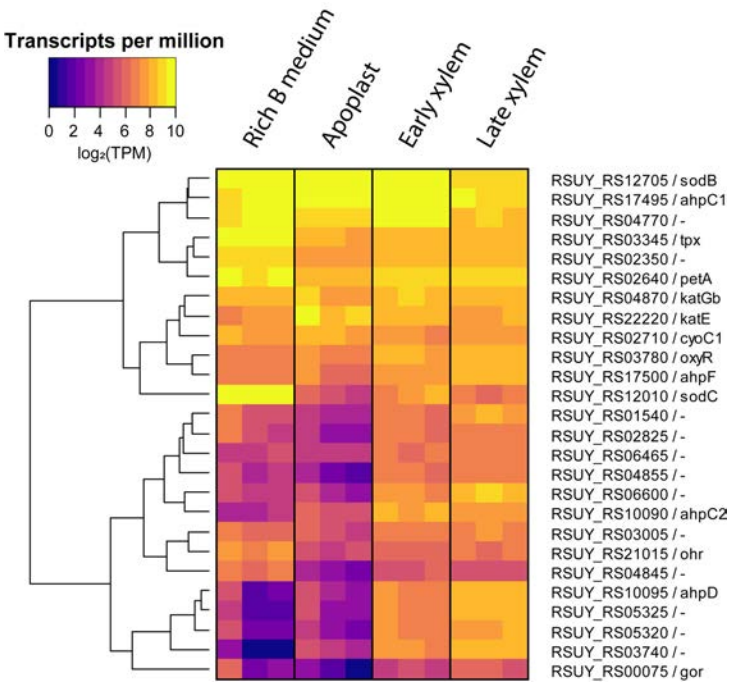

Additional file 12: ROS scavenging enzymes gene expression profile. Heatmap showing the normalised transcripts per million (TPM) of the genes coding for ROS scavenging enzymes in the reference condition and in planta apoplast, early and late condition.

Additional file 13: Proportion of reads aligned to *R. solanacearum* UY031 genome. Total number of reads obtained in each biological replicate for each condition (first column). Total number of reads aligned to *R. solanacearum* UY031 genome (second column). Proportion of reads aligned to *R. solanacearum* genome expressed as percentage (third column).

Sample ID	Total reads	Aligned reads	% Aligned reads
Apoplast1	21879209	18225945	83.30
Apoplast2	26766576	22641780	84.59
Apoplast3	24945027	20106785	80.60
Early xylem1	23554394	19887599	84.43
Early xylem2	24102624	20115780	83.46
Early xylem3	25157995	18506738	73.56
Late xylem1	23270138	21909969	94.15
Late xylem2	23309741	21562241	92.50
Late xylem3	24741904	23166640	93.63
RMliq1	28623378	20467036	71.50
RMliq2	32546088	28018378	86.09
RMliq3	30741621	26841635	87.31

Due to their length, the following Additional Files may be found in the online version of this article: https://doi.org/10.1186/s12864-021-07457-w.

Additional file 3: DEGs in the three in planta conditions. Differentially expressed genes of *R. solanacearum* in apoplast, early and late xylem compared to liquid rich medium obtained with DESeq2 (p-adj > 0.01, log2 FC ± 1.5).

Additional file 6: "Virulence and parasitic fitness" manually defined category. Genes belonging to specific virulence categories (T3SS & T3Es, Motility, ROS scavenging enzymes, phytohormone biosynthesis, EPS, nitrogen metabolism, cell wall degrading enzymes) of *R. solanacearum* are listed showing information related to: UY031 NCBI locus tag (first column), gene name (second column), gene description (third column), category, (forth column), reference (fifth column).

Additional file 7: List of genes included in each of the six expression profiles.

Additional file 14: Transcripts Per Million of each gene in rich medium, apoplast, early and late xylem. Reads normalized per Transcripts Per Million for each *R. solanacearum* gene in every condition: rich medium (philiq1, 2, 3), apoplast (Apo.10, .7, .9), early xylem (Early.D, .E, .G) and late xylem (Xylem.E, .O, Fresh.xylem).

4. CHAPTER 2

DRAFT 1

Gene expression in unexplored environmental niches reveals *Ralstonia solanacearum* genes essential to complete its life cycle

Resum de l’esborrany 1 en català

“Gene expression in unexplored environmental niches reveals *Ralstonia solanacearum* genes essential to complete its life cycle”

“L’estudi de l’expressió gènica en els nínxols ambiental inexplorats de *Ralstonia solanacearum* revelen gens essencials per completar el seu cicle vital”

Roger de Pedro-Jové[†], Jordi Corral[†], Mercedes Rocafort, Marina Puigvert, Fatima Waqar, Cristina Vandecaveye, Alberto P. Macho, Núria S. Coll, Elena Orellano, i Marc Valls

Els patògens bacterians amb una fase de dispersió ambiental han d'adaptar-se ràpidament i sobreviure en entorns diversos i canviants. El fitopatogen *R. solanacearum* té la capacitat de colonitzar diferents nínxols durant la seva vida parasitaria dins de les plantes hostes i com a bacteri lliure en el sòl i cursos d'aigua. Històricament, els estudis han centrat la seva atenció en el seu estil de vida parasitari, on múltiples anàlisis d'expressió gènica han identificat diversos determinants de virulència i la seva complexa regulació. No obstant això, les fases de vida lliure en l'ambient del patogen ha estat oblidat durant molt de temps. En aquest estudi, vam realitzar un anàlisi transcriptòmic de les bactèries recuperades de sòls i aigües, prèviament inoculats, per complementar els transcriptomes publicats anteriorment dins la planta. Els nostres resultats identifiquen l'ambient del sòl com la condició amb el perfil transcriptòmic més distintiu en tot el cicle de vida de *R. solanacearum*, descrivint més de 240 gens marcador d'aquesta condició. El metabolisme del nitrogen, les vies metabòliques del carboni alternatiu relacionades amb l'estrès i els gens de degradació de la lignina van ser trobats induïts juntament amb un assortiment de gens relacionats amb estrès. Aquests inclouen gens de manteniment de la homeòstasi del metall i gens relacionats amb l'estrès oxidatiu, que vam descriure com a essencials per a la supervivència bacteriana en el sòl. En contrast, l'expressió gènica en l'aigua va ser molt similar a la observada en el xilema durant la infecció amb una aturada metabòlica general i, sorprenentment, una alta inducció de la T3SS. Aquesta cascada de virulència va ser induïda independentment dels senyals de les plantes i depenia de la disponibilitat de nutrients i del pH. Curiosament, es va identificar un pH elevat com a possible senyal que governa l’expressió del T3SS en les etapes finals de la infecció. En aquest estudi, es proporciona el paisatge transcriptòmic complet del cicle de vida de *R. solanacearum* i s'identifiquen diversos factors que estableixen les bases per caracteritzar amb més detall les fases ambientals d'aquest important patogen.

4. CHAPTER 2

Gene expression in unexplored environmental niches reveals *Ralstonia solanacearum* genes essential to complete its life cycle

Roger de Pedro-Jové[1,2*], Jordi Corral[2*], Mercedes Rocafort[2], Marina Puigvert[1,2], Fatima Waqar[1,2], Cristina Vandecaveye[3], Alberto P. Macho[4], Núria S. Coll[2], Elena Orellano[3], Marc Valls[1,2]

[1] Department of Genetics, Microbiology and Statistics, University of Barcelona, Barcelona 08028, Catalonia, Spain.
[2] Centre for Research in Agricultural Genomics (CSIC-IRTA-UAB-UB), Bellaterra 08193, Catalonia, Spain.
[3] Área Biología Molecular, Facultad de Ciencias Bioquímicas y Farmacéuticas, Universidad Nacional de Rosario and Instituto de Biología Molecular y Celular de Rosario, Consejo Nacional de Investigaciones Científicas y Técnicas (CONICET), 2000 Rosario, Santa Fe, Argentina.
[4] Shanghai Centre for Plant Stress Biology, CAS Centre for Excellence in Molecular Plant Sciences, Chinese Academy of Sciences, Shanghai, 201602, China
* These authors contributed equally to this work

Correspondence to: marcvalls@ub.edu

Abstract

Bacterial pathogens with an environmental dispersal stage must rapidly adapt and survive in diverse and changing environments. The phytopathogen *R. solanacearum* has the ability to colonise different niches along its parasitic life inside the host plants and as free-living bacteria in the soil and waterways. Historically, reports have focused on its parasitic lifestyle where multiple gene expression analysis have identified many virulence determinants and its complex regulation. However, the environmental free-living stages of the bacteria have long been overlooked. In this study, we performed a transcriptomic analysis on bacteria recovered from inoculated soil and water to complement the previously published *in planta* transcriptomes. Our results identify the soil environment as the condition with the most distinct transcriptomic profile in all the life cycle of *R. solanacearum*, identifying over 240 marker genes of this condition. Nitrogen metabolism, alternative carbon metabolic pathways related to stress and lignin degradation genes were found upregulated together with an assortment of stress related genes. These include metal homeostasis maintenance and oxidative stress related genes, which we found to be essential for the bacterial survival in the soil. In contrast, gene expression in water was very similar to the one observed in the xylem during infection with a general metabolic shutdown and, surprisingly, a high induction of the T3SS. This virulence cascade was induced independently from the plant signals and was dependent on the nutrient availability and pH. Interestingly, high pH was identified as a potential signal governing the T3SS in late stages of infection. With this report provides the complete transcriptomic landscape of *R. solanacearum* life cycle and identifies multiple factors that set the basis to further characterise the environmental stages of this important pathogen.

Introduction

Whereas obligate pathogens rely on the stability of the host to thrive, environmental pathogens must adapt to maintain its capability to survive in a variety of environments, both inside and outside the host (Aussel, Beuzón and Cascales, 2016; Hassani, Durán and Hacquard, 2018). Bacterial survival to the surrounding environment demands a highly adaptive regulation to the everchanging conditions. Adaptation to temperature changes, nutrient availability, pH, and osmolarity are crucial to maintain the bacterial populations to infect new hosts (Leonard *et al.*, 2017; Wani *et al.*, 2022). Multiple bacterial plant and animal pathogens can survive outside the host. Animal pathogens such as *Listeria monocytogenes*, *Streptococcus pneumonia* or *Legionella pneumophila* have complex life cycles with an important environmental component crucial for its dispersion and infection (Li *et al.*, 2015; Vivant *et al.*, 2017; Aprianto *et al.*, 2018; Johansson and Freitag, 2019). All these pathogens are capable to finely tune their genetic programmes to endure extreme conditions in the air, soil, or waterways. Whereas this gene expression and regulation has been widely studied in animal pathogens, not much is known about it on plant pathogens.

Important plant pathogens are known to have environmental stages along their life cycle to which they must adapt. *Agrobacterium* spp. can remain in the soil as saprophyte like *Dickeya* spp., which can also survive associated to plant debris and insects (Perombelon and Kelman, 1980; Krimi *et al.*, 2002; Dessaux and Faure, 2018). Another example is *Pseudomonas syringae*, which colonises the aerial parts of the plant by living as epiphyte and disseminates through rainfall, insects or mechanical dispersion (Šantl-Temkiv *et al.*, 2015; Donati *et al.*, 2020). Only in *P. syringae* an extensive transcriptomic analysis has been conducted to compare the epiphytic and apoplastic life stages (Yu *et al.*, 2013). The transcriptomic profiling in the leave surface showed an upregulation of motility genes, chemosensing and production of surfactant compounds, among other genes to counter plant defences and prepare for plant infection (Yu *et al.*, 2013). *Ralstonia solanacearum* is one of the most interesting plant pathogens with a complex environmental lifestyle (Mansfield *et al.*, 2012). This bacterium can survive as a saprophyte in the soil, can remain for long periods of time in waterways and in association with reservoir hosts, a combination that can lead to important outbreaks in crop fields (Elphinstone, Stanford and Stead, 1998; Van Elsas *et al.*, 2000; Stevens *et al.*, 2018).

R. solanacearum is the causal agent of the bacterial wilt disease in over 200 plant species among them important commercial crops such as potato, tomato and ornamental roses (Osdaghi, 2020). This disease, in the past restricted to tropical and subtropical regions has nowadays caused important outbreaks in temperate regions due to the global rise in temperature (Cellier and Prior, 2010). *R. solanacearum* enters through the roots, moves through the apoplast until it reaches the xylem vessels where it proliferates clogging the water flow and eventually killing the plant (Yao and Allen, 2006; Digonnet *et al.*, 2012; Mori *et al.*, 2016; Tran *et al.*, 2016). This *in planta* stage of *R. solanacearum* has been widely studied and many of its virulence determinants and the regulation are well characterised (Genin and Denny, 2012; de Pedro-Jové *et al.*, 2021). However, many gaps remain on how *R. solanacearum* survives in the soil and waterways.

A remarkable persistence has been demonstrated for *R. solanacearum* in soil or irrigation waters (Van Elsas *et al.*, 2000; Van Overbeek *et al.*, 2004; Álvarez, López and Biosca, 2008). In fact, in a nutrient-limited environment such as water, bacterial cells were even able to proliferate keeping its ability to infect the plant intact. In line, bacterial cells can also survive in soil depleted of nutrients (Grey and Steck, 2001). Many environmental factors can impact the bacterial survival in the environment, however, *R. solanacearum* can trigger the viable but nonculturable (VBNC) as a survival mechanism in these stressful conditions. This mechanism present in many pathogenic and non-spore forming bacteria can be triggered by nutrient starvation, low temperature, heavy metals and oxidative stress (Um *et al.*, 2013). The resuscitation and return to culturability of bacterium in the VBNC stage has been demonstrated but the physiology and regulation of this state remains poorly characterised (Kong *et al.*, 2014; Kan *et al.*, 2019).

In this study, we have used the cold adapted *R. solanacearum* UY031 strain to analyse the transcriptomic changes that undergo *R. solanacearum* in the early stages of the life of the bacteria in soil and water to understand how the bacteria survives and adapt before becoming dormant. We have also included the previously published transcriptomic data to have an insight on the whole life cycle (de Pedro-Jové *et al.*, 2021). Our data shows that *R. solanacearum* deploys a very distinct genetic profile in the soil with important groups of upregulated genes related to adaptation and survival in this extreme environment. Moreover, bacteria living in the water environment shows a similar transcriptomic landscape of those bacteria living on the xylem of the dying plant with an unexpected induction of the type 3 secretion system.

Results

R. solanacearum displays a specific transcriptional reprogramming in soil and an expression profile in water similar to that found inside the xylem

To investigate the transcriptomic landscape of *Ralstonia solanacearum* outside the plant hosts we chose the environmental conditions where it is most commonly isolated: waterways and soil. Bacterial cells were resuspended in a commercial spring water, recovered at the most informative time on previous studies with other pathogens and total RNA extracted (Li *et al.*, 2015). For soil samples, *R. solanacearum* was inoculated a natural soil and total RNA directly isolated three days later, the time before plant infection occurs in our experimental conditions (de Pedro-Jové *et al.*, 2021) (Fig. S1A). To obtain a full gene expression landscape, RNA sequencing reads were analysed together with those previously obtained from *R. solanacearum* grown in rich medium or extracted from infected potato plants at three disease stages (de Pedro-Jové *et al.*, 2021) (Fig. S1A). Principal component analysis

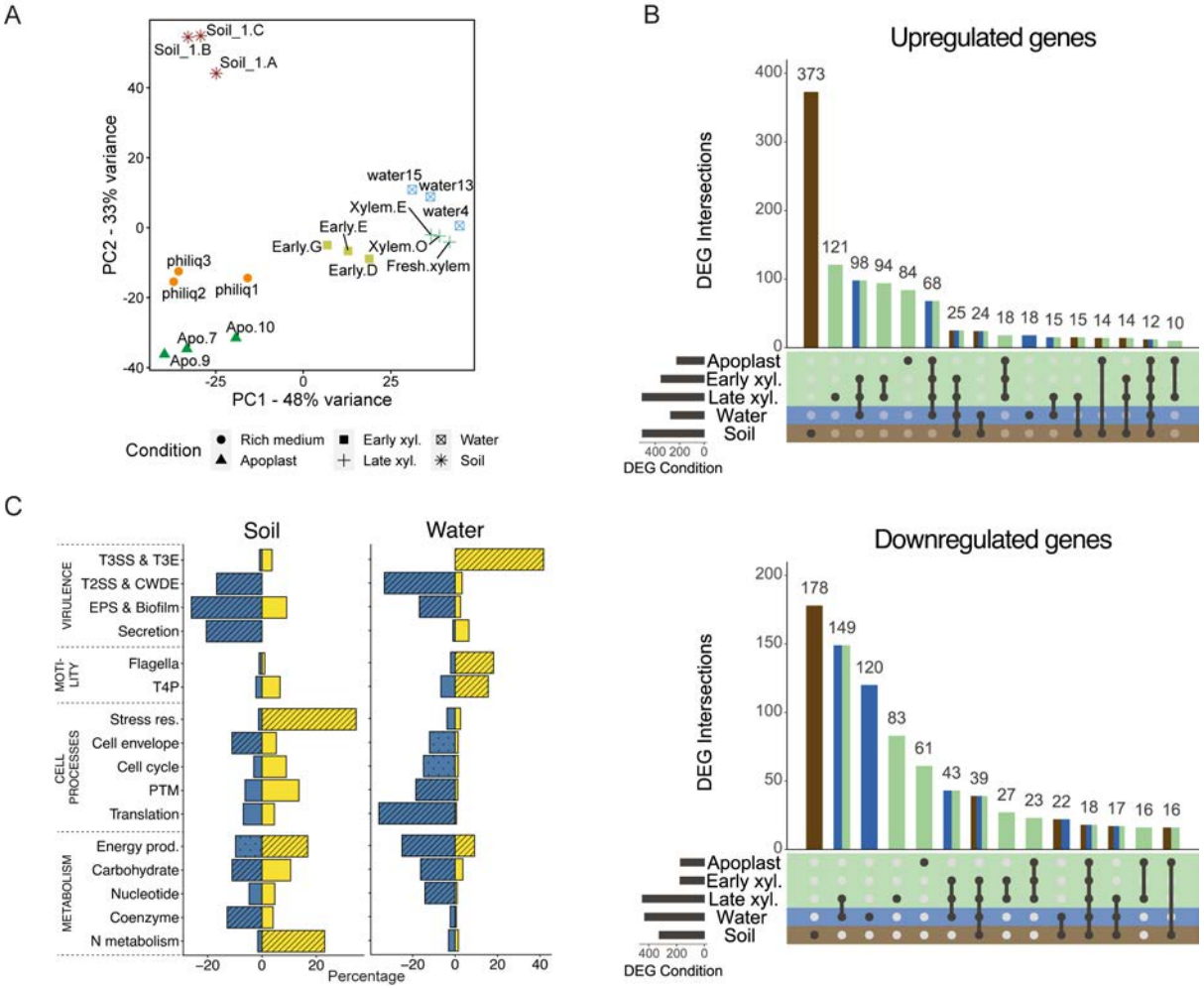

Figure 1. *R. solanacearum* transcriptomic profile in in vivo conditions. **A**) Two-dimensional Principal Component Analysis representation of expression data for all samples used in this study. Three biological replicates were analysed per condition. **B**) Shared and unique differentially expressed genes (DEG) across two environmental (soil - brown and water - blue) and three in planta conditions (Apoplast, Early and Late - green). Vertical bars represent DEG unique or shared between the indicated conditions (number above each bar). Only interactions with more than 10 genes are shown. Horizontal bars indicate total DEG per condition. DEGs were identified with DEseq2 (p-adj > 0.01, log2 FC ± 1.5) and plotted using UpsetR. **C**) Percentage of up- (yellow) and downregulated (blue) genes for each functional group in water and soil conditions. Categories were generated based on KEGG, COG and Uniprot information and grouped by functional similarity. Only significantly overrepresented categories (hypergeometric test p.value < 0.05 -line pattern- and < 0.01 -dotted pattern) in at least one of the conditions are shown. Short names for categories are as follows: Secretion (Intratrafficking and secretion), T4P (Type IV pili), PTM (Post-translational modification), Stress res. (Stress response), Translation (Translation and ribosome), Energy prod. (Energy production).

(PCA) already revealed good clustering of biological replicates, a clear differentiation of soil samples from the other conditions and similarity between water and xylem samples (Fig. 1A). 831 differentially expressed genes (DEGs, log_2 expression changes>1.5 vs rich medium, p.value<0.01) were identified in the soil, most of them (505) upregulated, while 701 DEGs were found in water samples, 2/3 of them downregulated (Fig. 1B, 1C and S1C). Comparison with *in planta* conditions (de Pedro-Jové *et al.*, 2021) confirmed that gene expression in soil was the most distinct with 373 and 178 unique genes up and downregulated only in this condition (Fig. 1B and 1C). On the contrary, most DEGs in water were shared with *in planta* conditions (98 up- and 149 downregulated also in late xylem and 68 also upregulated in all plant conditions), while only 18 genes were uniquely upregulated and 120 downregulated in water (Fig. 1B, 1C and Table S1).

To define robust marker genes for each step in the life cycle of *R. solanacearum*, we stringently selected genes with >2.5 log_2 expression changes in the condition of interest but not differentially expressed in any other condition (Table S2). In line with the previous results, 240 soil- specific and three water-specific marker genes were identified (Table 1 and S2). *Bona fide* markers specifically expressed inside the plant, were only found in the apoplast.

Table 1. Subset of representative marker genes from the soil condition classified according to their putative function. Locus names are presented without the preceding letters RSUY_.

Function		Locus_tag	FC	Name	Protein description
Stress response					
	Oxidative stress	*RS17495*	4.30	*ahpC*	alkyl hydroperoxide reductase subunit C
		RS17500	4.54	*ahpF*	alkyl hydroperoxide reductase subunit F
		RS04870	6.18	*katG*	catalase/peroxidase HPI
		RS14325	2.75	*gshB*	glutathione synthase
		RS14330	3.25	*gshA*	glutamate--cysteine ligase
	Metal homeostasis	*RS00665*	4.83	*copA*	heavy metal translocating P-type ATPase
		RS00670	4.58	*hmrR*	Cu(I)-responsive transcriptional regulator
		RS07025	4.04	*scU*	Fe-S cluster assembly scaffold
		RS07040	3.14	*hscB*	Fe-S protein assembly co-chaperone
		RS17525	2.89	*feoB*	ferrous iron transport protein B
		RS17530	3.89	*feoA*	ferrous iron transport protein A
		RS18860	3.39	*yusO*	MarR family transcriptional regulator
		RS18865	2.96	*corA*	magnesium and cobalt transport protein
		RS18870	2.64	*tag*	DNA-3-methyladenine glycosylase I
	Other/Putative	*RS00120*	3.73	*cstA*	carbon starvation protein A
		RS03790	3.30	*dps2*	DNA starvation/stationary phase protection protein
Soil metabolism					
	Degradation of aromatics	*RS00080*	3.34		dioxygenase
		RS02905	3.05	*paaI*	hydroxyphenylacetyl-CoA thioesterase
		RS02910	3.11	*paaG*	2-(1,2-epoxy-1,2-dihydrophenyl)acetyl-CoA isomerase
		RS18560	3.13	*paaB*	1,2-phenylacetyl-CoA epoxidase subunit B
		RS18565	2.70	*paaC*	phenylacetate-CoA oxygenase subunit
	Alternative TCA cycle	*RS08780*	3.04	*icl/aceA*	isocitrate lyase
		RS08800	2.80	*aceB*	malate synthase A
	Sugar metabolism	*RS17445*	2.86	*glgX*	glycogen debranching protein
		RS17460	2.81	*glgE*	DUF3416 domain-containing protein
		RS17465	3.86	*glgA*	glycogen synthase
		RS21000	3.20	*otsB*	trehalose-phosphatase
		RS21005	2.58	*otsA*	alpha,alpha-trehalose-phosphate synthase (UDP-forming)
	Other	*RS11540*	2.71		acyl-CoA dehydrogenase
Microbial competition					
		RS19530	2.75		type II toxin-antitoxin system RelE/ParE family toxin
		RS22595	2.67		type II toxin-antitoxin system Phd/YefM family antitoxin
Plant					
		RS01570	4.74	*sinR*	helix-turn-helix domain-containing protein
		RS14835	3.39	*puuR*	helix-turn-helix domain-containing protein

Stress response genes are strongly induced and support *R. solanacearum* survival in the soil

To characterise in an unbiased manner the transcriptional changes in soil, *R. solanacearum* genes were classified in functional groups based on COG categories and protein similarity, and the percentage of up- and down-regulated genes within each group and their enrichment were calculated (Fig. 1C and Table S3). The "Stress response" (35% of genes upregulated) and "Nitrogen metabolism" groups were clearly enriched in soil upregulated genes, while virulence and metabolism gene groups were all

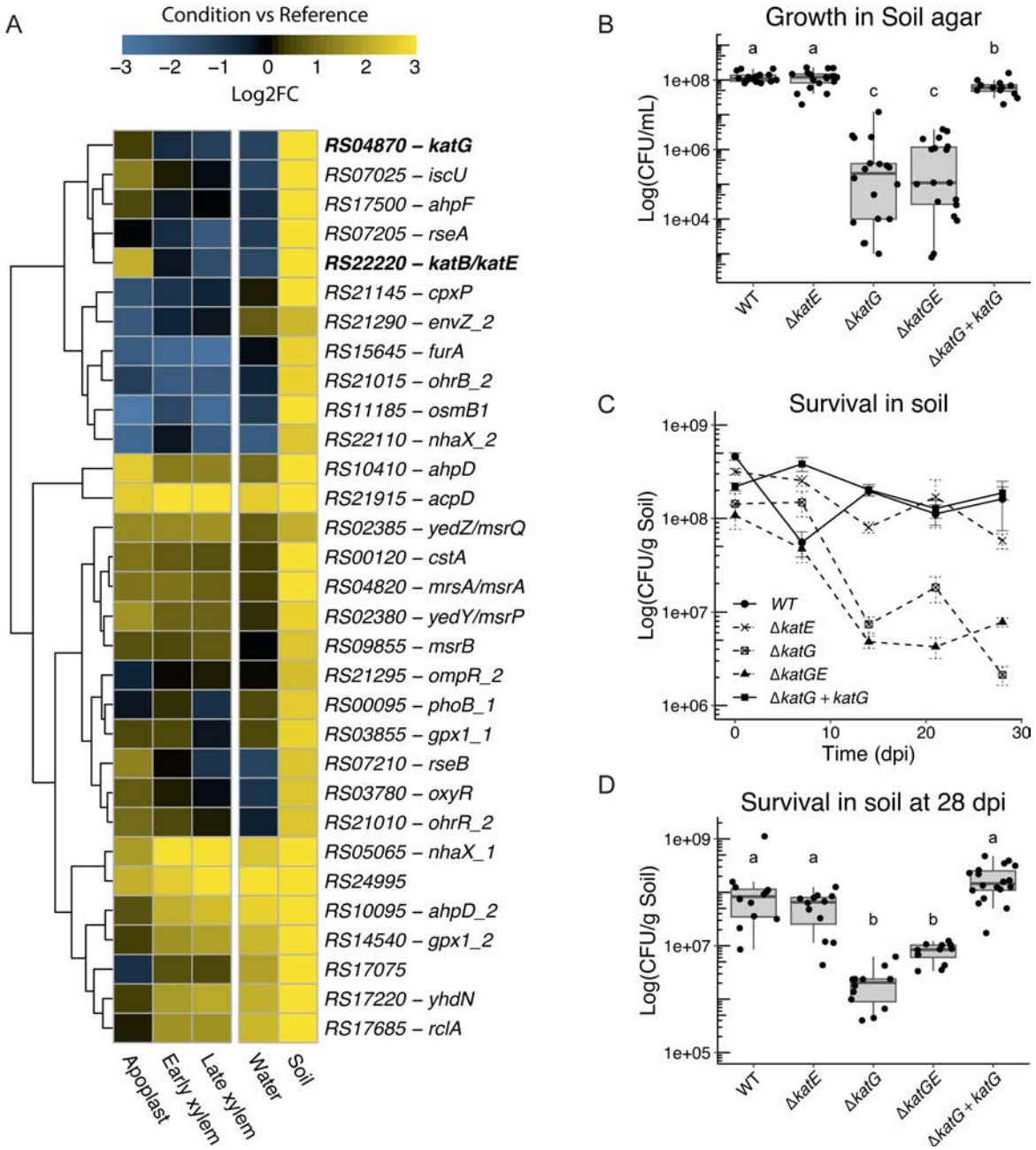

Figure 2. Stress response genes are important for *R. solanacearum* fitness in soil. A) Heatmap representation of gene $\log_2$ fold change with respect to the rich medium in the different conditions for stress response genes differentially upregulated in soil. The colour palette ranges from blue (downregulated) to yellow (upregulated genes), as indicated in the key. Locus names are presented without the preceding letters RSUY_. Genes selected for functional characterisation are shown in bold. **B**) Bacterial counts (Log CFU/mL) of wild type R. solanacearum (WT), single or mutiple catalase mutants (Δ*katE*, Δ*katG*, and Δ*katGE*), and the Δ*katG* complemented strain (Δ*katG-katG*) grown in soil agar. **C**) Bacterial survival (Log CFU/mL) in natural soil microcosms of the same strains used in B. **D**) Bacterial survival data (Log CFU/mL) in natural soil microcosms 28 days after inoculation. Different letters indicate significant differences according to one-way ANOVA (*p-value* < 0.1) followed by TukeyHSD statistical test.

enriched in downregulated genes (Fig. 1C and Table S3). GO term and KEGG pathways enrichment analyses yielded similar results, with “Metabolism in diverse environments”, “oxidative stress” and metal binding categories enriched in upregulated genes and terms related to secretion systems, ribosome and cell outer membrane enriched in downregulated genes (Fig. S2 and Table S4).

A closer scrutiny of the 240 soil marker genes (DEGs in soil not differentially expressed in water or *in planta*) reinforced the notion that *R. solanacearum* suffers a strong metabolic readjustment and induces stress-related genes in the soil (Table 1 and S2). Upregulated stress-related marker genes included most detoxifying ROS enzymes and stress genes related to inorganic ions, such as iron transporters and Fe-S related proteins (Table 1 and S2). Also upregulated were genes encoding iron sensors and regulators and other metal transporter and homeostasis genes (Table 1). Upregulated metabolism genes included: phenylacetate degradation genes; starvation and phosphate regulators or sensors; genes for glycogen, malate, and trehalose synthesis; two enzymes shortcutting the TCA cycle (isocitrate lyase and acyl-CoA dehydrogenase) and several metabolite transporters (Table 1). Other upregulated soil markers were involved in microbial competition (toxin/antitoxin and antibiotic protection/production genes). On the contrary, plant-related functions were specifically repressed in soil, since downregulated soil markers included genes encoding EPS formation, type IV pili, type I and II secretion system components as well as the two copies of the *egl* cell wall degrading enzymes. The biofilm and putrescine biosynthesis repressor genes *sinR* and *puuR* were upregulated markers, indicating that these plant-related activities are similarly downregulated in soil conditions (Table 1 and S2).

Heatmap representations also illustrated the specific expression of stress-response genes in soil, since most of them were upregulated in soil and downregulated in the other conditions (Fig. 2A) or downregulated in all *in vivo* conditions compared to *in vitro* growth in rich medium (Fig. S3A). To confirm the importance of stress response related genes for *R. solanacearum* fitness in the soil environment, we constructed deletion mutants for the genes encoding the ROS detoxifying enzymes in the genome: the catalase KatE and the catalase-peroxidase KatG. Growth of serial bacterial dilutions on soil-agar plates, which mimic this in soil conditions environment, showed that *R. solanacearum* strains with *ΔkatG* deletions grew significantly less than the wild type strain and growth was restored in a *katG* complemented strain (Fig. 2B). No differences were observed between the *ΔkatE* and the wild type and the *ΔkatE ΔkatE* grew comparably to the *ΔkatG* strain, suggesting no major role of KatE in soil. To investigate if bacterial survival in soil was affected, the mentioned bacterial strains were directly inoculated in natural soil microcosms at 10^8 colony forming units (CFUs) per g and viable cells were measured by plating soil-extracted bacteria throughout a 28-day period. In line with previous results, strains with *ΔkatG* deletions showed a significant decrease in viability, a phenotype clearly rescued by *katG* complementation, while no effect of the *katE* deletion was observed (Figs. 2C and 2D).

The Type 3 secretion system is strongly induced in water through a novel signalling pathway

Functional groups clearly enriched in water upregulated genes included “Type III Secretion system (T3SS) and type III effectors” (> 40% of the genes upregulated), “Flagella and Type IV pili” (~20% of genes upregulated) and “Energy Production” (Fig. 1C and Table S3). In contrast, the other gene groups involved in virulence were enriched in downregulated genes. These included “Type II secretion system” and “Cell wall degrading enzymes” (both with 30% of the genes downregulated) as well as “Exopolysaccharide and biofilm” (20% of genes downregulated). Most of the “Cell processes and metabolism” groups were also enriched in downregulated genes, especially “Translational and ribosome” (Fig. 1C and Table S3). Similarly, the GO/KEGG categories “flagellar”, “chemotaxis” and “protein secretion” were enriched amongst water upregulated genes (Fig. S2 and Table S4), while downregulated DEGs were enriched for metabolism, translation and “protein export” (Fig. S2).

T3SS genes are essential for *R. solanacearum* virulence and are strongly induced inside the plant (Boucher *et al.*, 1985; Monteiro, Genin, *et al.*, 2012; de Pedro-Jové *et al.*, 2021). It was thus surprising that *hrpG* and *hrpB,* the central activators of the T3SS regulatory cascade as well as most type III structural components (including the pilus subunit gene HrpY) (Fig. 3A) and most type III effector genes

appeared similarly upregulated in bacteria resuspended in water (Fig. 3B). To elucidate precisely how this induction signal was perceived, we measured expression of the downstream *hrpY* gene in strains

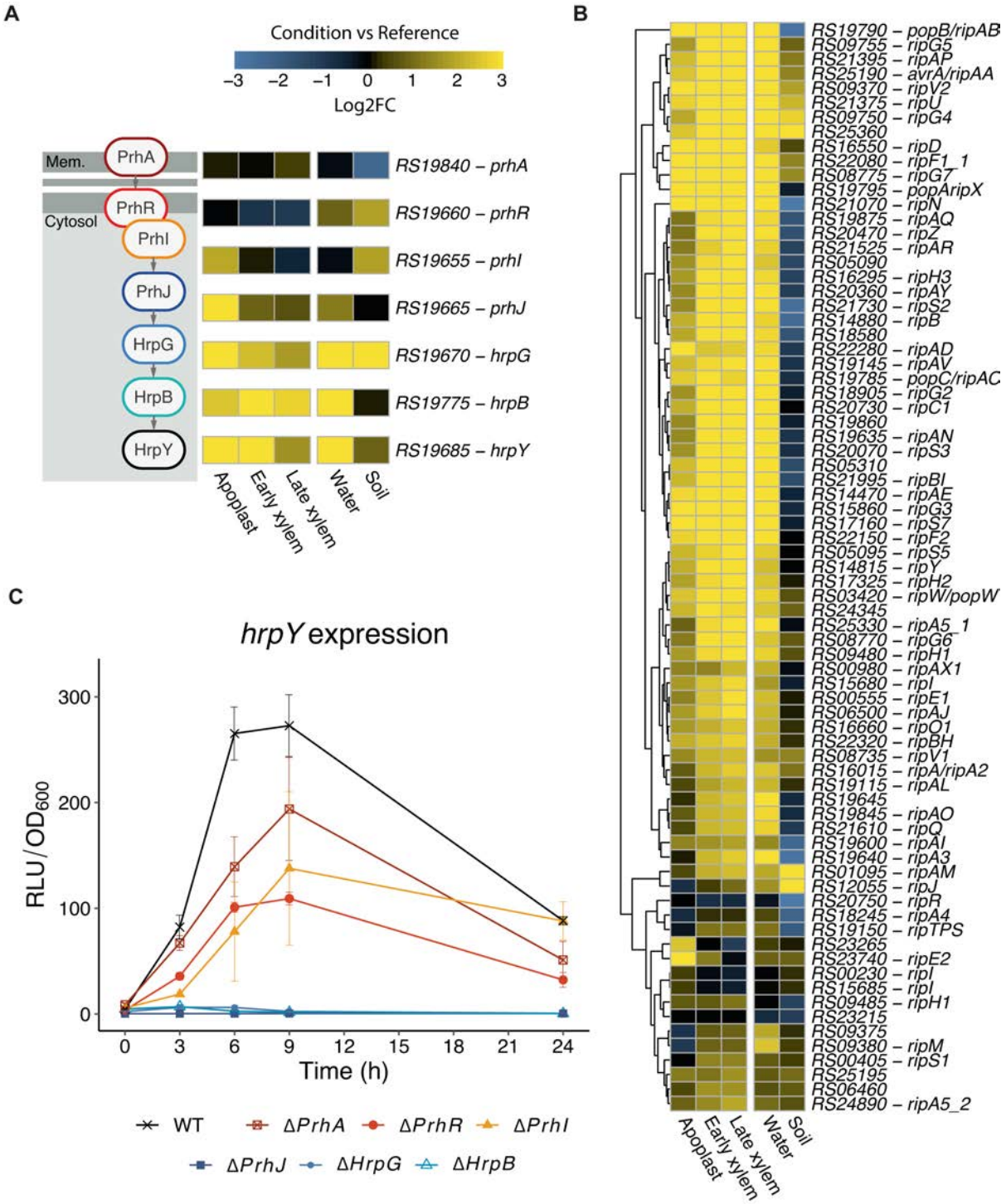

Figure 3. Induction of type III secretion system (T3SS) genes in water. A) Representation of the main components of the T3SS regulatory cascade and their expression in different conditions (log_2 fold change with respect to rich medium). **B**) Heatmap representation of the log2 fold change in expression with respect to growth in rich medium for type 3 effector genes in all conditions. The colour palette ranges from blue (downregulated) to yellow (upregulated genes) as indicated in the key. Locus names are presented without the preceding letters RSUY_. **C**) Time-course expression of the *PhrpY-Lux* reporter in strains disrupted for the different T3SS regulatory genes after resuspension in water. *R. solanacearum* cultures grown overnight in rich B medium were washed and diluted to OD_{600}=0.1 in water and luminescence and OD_{600} values were measured over a 24h period. Relative luminescence units (RLU) were normalised by bacterial concentration measured as OD_{600}. RLU values were divided by 1000 to facilitate visualisation.

disrupted for each of the known components and regulators of the T3SS regulatory cascade. Luminescence quantification of the *PhrpY-lux* promoter-reporter fusion showed that induction in water peaked after 6 to 9 hours and was abolished in the *ΔprhJ*, *ΔhrpG* or *ΔhrpB* deletion mutants with only a slight reduction compared to the wild type in the *ΔprhA, ΔprhR* and *ΔprhI* mutants (Fig. 3C). Thus, the newly discovered water induction signal is integrated in the T3SS regulatory cascade at the level of the PrhJ transcriptional regulator. The same result was obtained when *hrpB* induction was measured in different mutant backgrounds (Fig. S4).

Alkaline pH and starvation are the main T3SS inducers in water

Next, we decided to determine the precise environmental cues that induced the T3SS genes in water. Since water is almost depleted of nutrients and the mineral water used for transcriptomic experiments was slightly alkaline (pH ~8), we analysed whether these factors affected T3SS gene expression.

First, we measured expression of *hrpY* -encoding the main T3SS pilus component- and the upstream regulators involved in T3SS induction in water (*prhJ*, *hrpG* and *hrpB,* Fig. 3C) in the native mineral water or adjusted to neutral pH (Fig. 4A). To rule out changes due to bacterial growth, pH was measured for each culture (extreme values observed indicated in each case). This experiment showed that *hrpG, hrpB* and *hrpY*, but not *PrhJ* transcription was induced in water and that this induction was completely abolished at neutral pH (Fig. 4A). To prove that this was a general phenomenon, we repeated the experiment in waters from six different natural sources throughout the Iberian Peninsula, five of which were naturally alkaline (pH 8.1 to 8.8) and one neutral. Clear induction of *hrpG*, *hrpB* and *hrpY* was observed in all basic waters collected and neutralisation abolished these inductions (Fig. S4). On the contrary, while gene expression was almost undetectable in the naturally neutral water, its alkalinisation to pH=8 resulted in *hrpG*, *hrpB* and *hrpY* induction, demonstrating causality of basic pH in the induction of T3SS in water (Fig. 4B and S4).

Next, we investigated the importance of water nutrient scarcity in T3SS induction by measuring *hrpB* expression after addition of different volumes of rich medium into water (Fig. 4B). Progressive reduction of gene expression was observed with increasing concentrations of rich medium added, proving in a direct dose response that nutrient availability abolished T3SS induction in water (Fig. 4C).

Finally, the combined effect of the pH- and nutrient-dependent T3SS induction was tested on *hrpB* expression. This experiment revealed that basic pH and nutrient scarcity equally impacted T3SS induction and that the nutrient addition repression phenotype was epistatic to non-induction at neutral pH. (Fig. 4D).

The xylem sap becomes alkalinised during *R. solanacearum* infection

Low nutrients and high pH encountered in water may induce the T3SS because these conditions mimic those encountered by the bacterium *in planta*. It was known that the xylem sap contained limited nutrients (Zuluaga, Puigvert and Valls, 2013; Baroukh, Zemouri and Genin, 2022), but the pH found in the xylem during *R. solanacearum* infection is unknown. To investigate this, we grew a high number of tomato plants and inoculated them by drenching the soil with a suspension of *R. solanacearum* GMI1000. Non-inoculated plants grown in the same conditions were used as controls. Control or diseased plants were recovered, their disease symptoms recorded and xylem sap obtained from two stem sections of each plant: one from the hypocotyl just above the soil level and one from the top of the plant. pH and bacterial loads were measured for each of the xylem samples collected and the results were plotted representing xylem pH vs plant symptoms or xylem pH versus *R. solanacearum* concentrations in this compartment (Fig. 5). Non-inoculated plants showed slightly acidic xylem pHs and a higher pH was observed in almost all diseased plants, reaching pH=8 in heavily wilted or colonised plants. In addition, a positive correlation was clearly observed between xylem pH and both disease symptoms and bacterial loads (Fig. 5). In summary, *R. solanacearum* infection caused xylem alkalinisation, which was more apparent at the base of the stem than in apical parts, most likely because the bottom of the stem contains higher pathogen loads (Fig. 5) (Planas-Marquès *et al.*, 2020).

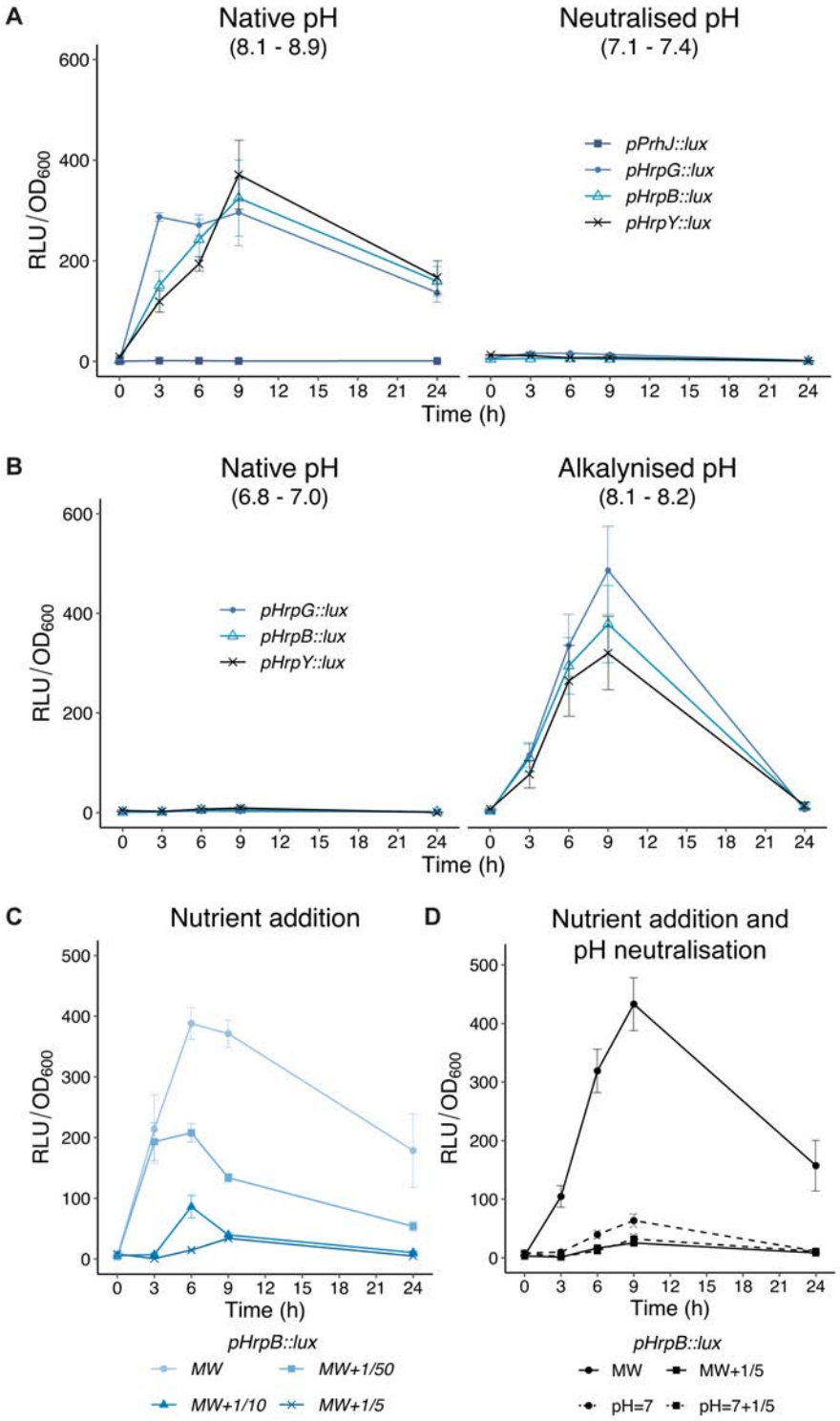

Figure 4. Alkaline pH and starvation induce the type 3 secretion system genes Time-course expression of *R. solanacearum* reporter strains in **A**) Native basic pH mineral water (water A) or the same water adjusted to neutral pH for *PprhJ-lux*, *PhrpG-lux*, *PhrpB-lux* and *PhrpY-lux* reporter strains or **B**) Native neutral water (water G) or the same water alkalinized to basic pH for *PhrpG-lux*, *PhrpB-lux* and *PhrpY-lux* reporter strains. For each time point, luminescence is indicated in relative units divided by 1000 (RLU) normalised by OD_{600}. **C**) Time-course expression of *hrpB* in water or the same water supplemented with increasing concentrations of rich B medium. Numbers indicate the fraction of rich medium vs the total volume. **D**) Time-course expression of *hrpB* in water, water neutralized to pH=7, water supplemented with 1/5 volume of rich B medium, or neutralized water supplemented with 1/5 volume of rich B medium. Water sources are indicated in the methods section.

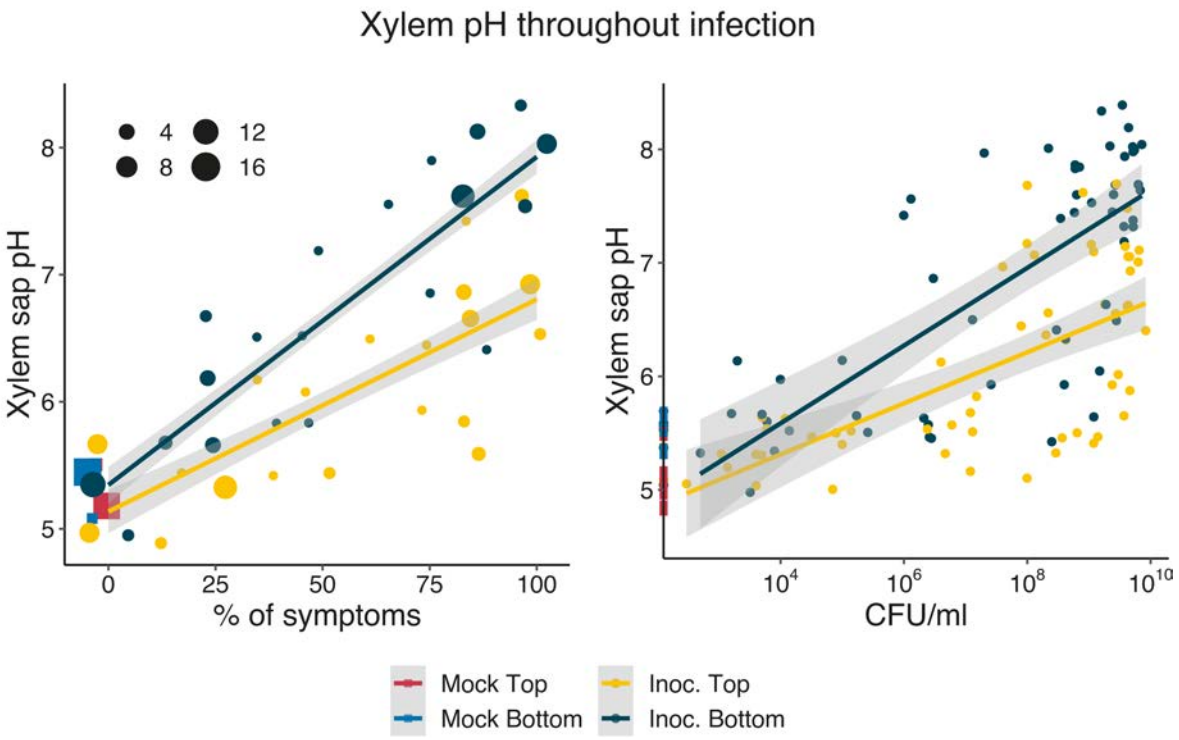

Figure 5. The pH of xylem sap is alkalinised during *R. solanacearum* infection. 3-week-old tomato plants were soil drench inoculated with *R. solanacearum* or mock treated with water and their symptoms recorded. Xylem samples from mock (square shapes) or inoculated tomato plants (Inoc., round shapes) were collected from the bottom or the top of the stem of plants at different disease stages and xylem pH and bacterial loads measured. Graphs represent xylem pH vs plant symptoms or xylem pH versus *R. solanacearum* content in the xylem. Shape sizes is proportional to the number of coincident points. Lines indicate correlation calculated with geom_smooth function from ggplot2 following a linear model ("lm").

Discussion

On our experimental design

Sampling time is key to capture the bacterial transcriptional adaptation to these new environmental conditions. In the case of water, samples were collected at 6 hours post inoculation (hpi), as transcriptional reprogramming in liquid medium occurs within the first hours. For example, in the human pathogen *Legionella pneumophila* it is at 6 hpi where they see the biggest amount of differentially expressed genes (Li *et al.*, 2015). Also, in our reporter gene expression analysis, it is around 6-9 hours when we see the most induction of the genes under study (Fig. 3B, Fig. 4). Once past that time and under stressful conditions, *R. solanacearum* and other bacterial species such as *Campylobacter jejuni* can enter the viable but non-culturable state in which bacteria is known to remain in a quiescent but active state (Bronowski *et al.*, 2017; Stevens *et al.*, 2018). For the soil samples, 3 days after inoculation were selected as it is the expected time when the bacterium enters the plant host (de Pedro-Jové *et al.*, 2021).

Soil shows the most distinct transcriptome whereas water samples are similar to the xylem condition

The PCA visualisation of the raw transcriptomic data (Fig. 1A) and the intersection graphs of the DEG under the different conditions (Fig. 1B) reveal two main observations regarding environmental conditions. First, soil transcriptomic changes are the most distinct, standing out with the highest number of up- and downregulated unique DEG. More than 350 genes are specifically deployed by *R. solanacearum* to adapt to the soil environment (Fig. 1B). Second, the transcriptomic program in water condition appears to share many characteristics with the gene expression of the xylem, as indicated by the PCA clustering and high number of co-expressed genes between the two conditions (Fig. 1A and 1B). Only among the downregulated DEG, the water condition shows 120 unique genes (Fig. 1B). All these differences correlated with the number of genes identified after a stringent filtering to look for marker genes of each condition (Table S2). Marker genes were almost exclusively identified in the *in planta* apoplast condition and, mostly, in the soil environment. The similarities between the water and xylem conditions hindered the identification of unique genes in these conditions (Table S2).

R. solanacearum employs different stress related genes to adapt and survive in the soil environment

In natural soils, bacterial cells must adapt to survive in a nutrient-limited environment and mitigate the multiple stresses they encounter. Bacteria must face many ROS-inducing agents, such as heavy metals, antimicrobial compounds, temperature and humidity fluctuations, which add to the internal oxidative stress induced by the growth of the bacterium in an environment with nutrient scarcity (McDougald *et al.*, 2002; Chattopadhyay *et al.*, 2011; Kim and Park, 2014; Abdul Rahman, Abdul Hamid and Nadarajah, 2021). The ability of soil-borne bacteria to respond to the various biotic and abiotic stresses that cause oxidative stress is of outmost importance for their survival.

In line with literature, stress response genes in *R. solanacearum* were enriched, with as much as 35% of the genes within the category being upregulated (Fig. 1C). Additionally, the GO/KEGG enrichment analysis on the upregulated DEG in soil yielded multiple gene functions related to oxidative stresses (Fig. S2). As expected, the genome of *R. solanacearum* encodes for a wealth of genes to cope with stressful conditions (Genin and Boucher, 2004; Flores-Cruz and Allen, 2009). Interestingly, almost all genes included in the stress response category were highly induced in soil (Fig. 2A and Fig. S3A). An important group of genes included in this category are the ROS detoxifying enzymes known to be important in the plant apoplast, where they play an essential role in detoxifying the plant defence oxidative burst (Bolwell, 2002). Furthemore, many of ROS detoxifying enzymes appeared among the marker genes of the soil, along with glutathione S-transferases (GST) proteins, all of which are crucial for redox homeostasis (Gallé *et al.*, 2021) (Table 1 and Table S2). One of most salient genes is the bifunctional catalase/peroxidase *katG* enzyme, which was identified as a marker in the soil with its expression increasing more than 6-fold compared to the reference medium (Table S2). Mutation of *katG*, but not the monofunctional catalase *katE*, resulted in a significant reduction of bacterial survival when challenged to grow in soil agar or in a soil microcosm. Additionally, there was no additive effect

when both genes were simultaneously deleted (Fig. 2B, 2C, 2D). The lack of phenotype observed in the *katE* mutant on the pathogen survival inside the plant apoplast had been previously described, despite its high expression levels and induction by the HrpG virulence regulator (Tondo *et al.*, 2020). Since the role of *katG* has not been tested inside the plant, it is still possible that it may be an important virulence factor. However, it is clear that KatG makes a significant contribution to the bacterial survival in the soil. In other soil-borne phytopathogens as *Erwinia amylovora*, both homologues played an important role in delaying the entrance of the bacterium in the VBNC state (Santander, Figàs-Segura and Biosca, 2018). It would be interesting to investigating whether the observed reduction in survival in the experiments, as determined by plating and counting the CFUs, was due to the early entrance of the bacteria into the VBNC state or because of their decline. Interestingly, a study on *R. solanacearum* demonstrated that catalase treatment could rescue the VBNC state in the microcosmos suggesting that lacking these enzymes could induce this state (Kong *et al.*, 2014). In any case, we have proven that oxidative stress is a major factor shaping the life of *R. solanacearum* in soil. In line, the pathogen has evolved a robust and redundant system to survive in these stressful conditions (Flores-Cruz and Allen, 2011).

Regarding the various stresses found in soil, several identified marker genes were related to metal homeostasis (Table 1 and Table S2). We identified genes associated to iron uptake and homeostasis, as well as genes involved in the biogenesis and protection of the Fe-S cluster proteins. These findings were further supported by the GO enrichment analysis, which also revealed enrichment of iron heme binding domains (Fig. S2). Domains that play an essential role in bacteria but are highly sensitive to oxidative stress (Nachin *et al.*, 2003). Also, copper transporters and its regulators were identified among the marker genes, a heavy metal to which *R. solanacearum* is known to tolerate (Ascarrunz *et al.*, 2011) (Table 1 and Table S2). A recent study in *R. solanacearum* showed that high iron levels in the medium can cause spontaneous mutants showing higher growth rates in stressful conditions and increased iron acquisition capacity but reduced virulence than wild type strains (Nakahara *et al.*, 2021). To sum up, excess of metals in the environment can generate an oxidative stress, which can only be countered by the deployment of the diverse metal homeostasis systems (Kim and Park, 2014). To finalise with the stress related genes, different genes involved in DNA repair were also identified among the marker genes (Table S2).

R. solanacearum reconfigures its metabolism to profit from soil nutrients

Two additional categories were enriched among the upregulated genes in the soil: the energy production and nitrogen metabolism (Fig. 1C). These findings were consistent with the GO/KEGG enriched terms related to metabolic adaptation, and nitrogen metabolism. The role of nitrogen metabolism, which includes nitrate respiration, assimilation and the detoxification of intermediate compounds, has been extensively studied in the xylem, where it is essential for the life and virulence of the bacterium (Dalsing and Allen, 2014; de Pedro-Jové *et al.*, 2021). Additionally, a research group investigated the impact of the high nitrogen concentrations resulting from the regular use of soil fertilisers in agriculture on the life of *R. solanacearum* in the soil (Giagnoni *et al.*, 2016). Remarkably, *R. solanacearum* can not only survive but also grow in the presence of abundant nitrogen (Wang, Liu and Ding, 2020), and it can also shape the bacterial composition of the soil (Wang *et al.*, 2018). Taking a closer look at the expression of nitrogen metabolism genes in soil, we observed higher expression values than in the xylem with the denitrification and detoxification pathways highly upregulated (Fig. S6 and Table S5).

The lack of accessible carbon sources in the soil (Soong *et al.*, 2020) promoted the induction of different regulatory proteins and metabolic pathways to obtain energy and adapt to this condition (Table S2). A DNA binding protein from starved cells (*dps*), described in *E. coli* and *A. tumefaciens*, proved to be crucial for protection under oxidative stress and challenging environmental conditions (Ceci *et al.*, 2003; Nair and Finkel, 2004). Interestingly, in *R. solanacearum*, *dps* was described to be induced in the rhizosphere upon plant exudate sensing and even higher under starvation conditions (Colburn-Clifford and Allen, 2010). Dps was necessary to tolerate oxidative stress and for full virulence *in planta* (Colburn-Clifford, Scherf and Allen, 2010). Curiously, the *dps* gene was among the soil marker genes showing a logFC > 3 (Table 1). The absence of plant exudates suggests that the expression of *dps* in soil might be triggered by starvation, indicating that soil is a challenging environment low in labile nutrients. Linked

with the lack of carbon sources, enrichment analysis identified among the downregulated genes, KEGG and GO terms related to the sugar metabolism (Fig. S2). Additionally, we also observed different GO terms related to translation and protein production, suggesting a general shutdown of bacterial metabolism in the soil (Fig. S2).

The glyoxylate cycle, an alternative to the tricarboxylic acid cycle (TCA), is a crucial metabolic strategy employed by several organisms that allows them to utilise alternative carbon sources in nutrient limited and stressful environments (Cronan, Jr. and Laporte, 2005; Ahn *et al.*, 2016). Two enzymes mediate the bypass of the TCA: the isocitrate lyase (*aceA*/*icl*) and the malate synthase A (*aceB*). Interestingly, both were identified as soil marker genes, and the associated KEGG pathway was found enriched (Table 1 and Fig. S2). The glyoxylate cycle utilises acetyl-CoAs as carbon source, and the enzyme acyl-CoA dehydrogenase, involved in the production of these molecules, was also identified as a marker of the soil condition (Table 1) (Fujita, Matsuoka and Hirooka, 2007). This alternative TCA pathway is activated to divert carbon away from energy production to gluconeogenesis (Maharjan *et al.*, 2005). In accordance, various enzymes involved in the glycogen biosynthesis were also upregulated together with trehalose biosynthetic genes (Table 1). Interestingly, both sugars were described to enhance cell viability under stressful conditions and growth restricting environments (Zevenhuizen, 1992; Wang and Wise, 2011; MacIntyre *et al.*, 2020). The glyoxylate cycle has been linked to virulence in other pathogens, but in the case of *R. solanacearum*, the pathway is not upregulated *in planta* (Table S2) where the pathogen has multiple sources of nutrition (Dunn, Ramírez-Trujillo and Hernández-Lucas, 2009; Lowe-Power, Khokhani and Allen, 2018).

A final pathway worth mentioning is the lignin degradation, which remains a poorly understood field in bacterial research. However, a study that surveyed the genomes of multiple gram-negative bacteria for lignin-degrading enzymes, discovered that *R. solanacearum* contained homologues of key enzymes of the pathway such the orthologue of pcaG (*RSUY_RS09205*), which was upregulated in soil (Table S5) (Bugg *et al.*, 2011). Consistent with this information, other enzymes such as a dioxygenase enzyme and multiple genes from the *paa* (phenylacetate catabolism) cluster that have been reported to break the aromatic ring of lignin compounds and facilitate their degradation, were identified among the marker genes (Table 1) (Grishin and Cygler, 2015; Sainsbury *et al.*, 2015; Rajkumari, Paikhomba Singha and Pandey, 2018; Xu *et al.*, 2022). The presence of all these enzymes suggest the capacity of *R. solanacearum* to degrade lignin, and their unique upregulation in the soil explains why no lignin degradation has been detected to date during infection (Lowe, Ailloud and Allen, 2015). Moreover, the breakdown of lignin results in the production of acetyl-CoA, the key molecules required for the glyoxylate cycle (Weng, Peng and Han, 2021), linking both metabolic pathways for efficient utilization of resources. Lignin degradation is also tightly linked to oxidative stress, as ROS induce the expression of *paa* genes. Additionally, several ROS detoxifying enzymes were reported to contribute to the lignin degradation (Sinsabaugh, 2010; Chen *et al.*, 2022). An alternative explanation to lignin degradation is the function reported for the *paa* gene cluster in degradation of antibiotics such as β-lactams, which could enhance bacterial survival in competition with other organisms (Crofts *et al.*, 2018). Related to this function, other genes related to microbial competition such as toxin/antitoxin, or antibiotic production and resistance genes, were identified as markers of the soil environment in line with previous publications (Hibbing *et al.*, 2010; Kobayashi, 2021) (Table 1 and Table S2).

Key genes for the virulence of *R. solanacearum in planta* are downregulated in the soil

In contrast to the challenging soil conditions where *R. solanacearum* seems to endure multiple biotic and abiotic stresses, and deploy various metabolic strategies for survival, the life of the bacteria *in planta* appears to be a buffet. Thus, most likely, the plant provides a relatively more favourable environment for *R. solanacearum* growth without major metabolic readjustments. Interestingly, related with the life *in planta*, we found a set of downregulated marker genes in soil involved in virulence. Among them we identified cell-wall degrading enzymes (*egl*), as well as genes related with biofilm formation such as the type IV pili, *nucA*, and the EPS operon (Table S2) (Mori *et al.*, 2016; Tran *et al.*, 2016). Related to the EPS operon, its putative repressor described in *Bacillus subtilis*, *sinR*, was an upregulated marker gene in soil (Colledge *et al.*, 2011). Similarly, the *purr* was also identified among the upregulated markers in soil (Table 1). This transcription factor was described in *E. coli* to inhibit putrescine production, a well-known metabolite that enhances plant colonisation in *R. solanacearum*

(Lowe-Power *et al.*, 2018). The identification of these downregulated genes, or upregulation of the repressors, links with the enrichment observed among the downregulated genes associated with T2SS & CWDE, EPS & Biofilm and Secretion (Fig. 1C). This stresses the tight control and compartmentalisation of the gene regulation in *R. solanacearum*.

R. solanacearum undergoes a general metabolic shutdown in the water environment

R. solanacearum has the ability to survive in waterways for extended periods, utilising them as a means of dispersion (Caruso *et al.*, 2005). Similar to what was described in the late xylem (de Pedro-Jové *et al.*, 2021), the bacterium inoculated in water experiences a general shutdown of its metabolism, translation and protein production as indicated by the enriched categories and GO/KEGG pathways among the downregulated genes (Fig. 1C and Fig. S2). Only a group of genes included in the KEGG pathway oxidative phosphorylation were enriched among the upregulated genes (Fig. S2). These genes coded for different cytochromes oxidases, which are also upregulated in almost all conditions (Fig. S2, Table S7 and Table S3). Cytochromes have been described in *R. solanacearum* as essential not only for the life of the bacterium inside the plant but also in the rhizosphere as these enzymes can function in microaerobic environments (Colburn-Clifford and Allen, 2010). This general shutdown could also be a preparation for the entering of the bacteria in the VBNC state.

Motility and the T3SS virulence cascade are highly induced in water

The motility category, T4P and the flagellar movement, and its corresponding terms in the GO/KEGG pathways were enriched among the upregulated genes in water (Fig. 1C, Fig. S2). This motility upregulation in liquid environments has also been reported in other pathogenic bacteria with a water dispersion strategy (Li *et al.*, 2015; Bronowski *et al.*, 2017; Vivant *et al.*, 2017). Similar to the soil environment, we observed a significant downregulation of the gene categories T2SS & CWDE and EPS & Biofilm. Unexpectedly, the category T3SS & T3E, a virulence hallmark of *R. solanacearum* and many pathogenic bacteria (Coburn, Sekirov and Finlay, 2007; Coll and Valls, 2013), appeared enriched among the upregulated genes (Fig. 1C). The canonical T3SS starts with the membrane receptor prhA, which is thought to sense an unknown plant signal and transduce it through the prhR, prhI and prhJ until it reaches the central regulator HrpG (Brito *et al.*, 2002). HrpG controls the downstream regulator HrpB, which triggers the transcriptional activation of the T3SS machinery, the *hrp* operon, and the T3E (Valls, Genin and Boucher, 2006) (Fig. 3A). In water, we detected a similar induction of the T3SS regulatory cascade as observed *in planta*, except that *prhJ* was not found upregulated (Fig. 3A). Furthermore, this induction is not limited to the regulatory genes but also to all the downstream T3E (Fig. 3B) and secretion machinery (Fig. S3B). To understand the reason this known virulence factor was triggered in water we decided to investigate the how and why of this induction. Interestingly, the induction of the T3SS cascade was abolished when *prhJ* and all the downstream regulators were knocked-out (Fig. 3C). As this gene did not show upregulation (Fig. 3A), it suggests that prhJ probably undergoes a post-translational modification, which will trigger the cascade and the downstream genes. Mutation of upstream genes from *prhJ* (*prhA*, *prhR* and *prhI*), showed a slight reduction in the activation of the T3SS (Fig. 3C), suggesting that there might be other cues modulating T3SS expression.

Interestingly, a similar activation bypassing the sensor protein PrhA was already described in *R. solanacearum* growing in minimal medium, in plant cell co-culture or in plant saps (Brito *et al.*, 1999; Zuluaga, Puigvert and Valls, 2013). In line with our results in water, around 6 hours, a rapid induction of HrpG was detected in xylem sap independently of plant cell contact. Also, this rapid response lacked the maintained induction led by the PrhA dependent activation as observed in our results (Fig. 3, 4, S4, and S5) (Zuluaga, Puigvert and Valls, 2013). In the same study, they discovered that none of the different sugars or amino acids present in plant saps were responsible of the induction (Zuluaga, Puigvert and Valls, 2013). Similarly, in the water environment, we observed an induction of the T3SS independent from plant signal or nutrients, as water is a nutrient-depleted medium with no plant cells. In our search for the environmental cue responsible of the activation of the T3SS the pH and nutrient scarcity were identified as potential signals (Fig. 4, Fig. S5). The various waters collected from different water sources showed a slightly alkalinised pH, which induced the T3SS and when pH was neutralised, the T3SS induction was abolished (Fig. 4A and Fig. S5). Interestingly, the only water with a natural neutral pH (Fig. 4B) behaved the other way around. In the native pH, no induction was observed and upon alkalinisation, the T3SS was induced. Regarding nutrient scarcity, the abolishment of the T3SS

induction was dose dependent (Fig. 4C). When pH and nutrient scarcity cues were combined, the additive effect was not clear as both signals greatly inhibit the T3SS separately (Fig. 4D). Interestingly, the T3SS induction was not durable in time but diminished after the peak at six to nine hours (Fig. 4D and Fig. S5). This pattern consistent with previously published data (Zuluaga, Puigvert and Valls, 2013), is reasonable as the T3SS machinery and effector production is an energetically expensive process for the bacterium (Sturm *et al.*, 2011). This could indicate that pH or nutritional crisis are important fast inducers of the T3SS to prepare the bacteria in case it encounters additional unknown cues or plant signals. If this is not the case, this induction would diminish until completely disappear.

Environmental cues triggering T3SS in water potentially modulate virulence *in planta*

As no plausible explanation was found to why the bacterium triggers T3SS in water, we tried to link the newly discovered environmental cues with the life of the bacterium *in planta*. Since nutrient composition inside the plant is difficult to modulate, we set out to investigate if a change in the pH is observed in plants infected with *R. solanacearum*. Surprisingly, as the infection progressed the pH of the xylem sap was alkalinised (Fig. 5). The pH increase correlated with both the visual criteria of measuring wilting symptoms, and with bacterial CFU quantification (Fig. 5). As observed, the basal pH of the xylem was around 5.5, and upon infection, it experienced a rapid alkalinisation reaching values of pH=8. Additionally, this alkalinisation was higher closer to the roots than in the upper parts of the plant, correlating with the usual bacterial distribution (Planas-Marquès *et al.*, 2020).

Interestingly, xylem sap alkalinisation has been previously reported when plants suffer from drought stress (Grunwald *et al.*, 2021). Tomato plants challenged with drought had an increase of the pH from 5 to 8, results almost identical to our observation (Wilkinson *et al.*, 1998; Verhage, 2021). As *R. solanacearum* disease symptoms are ultimately caused by clogging of the water flow and thus, drought, these similarities are somehow expected. We propose a hypothesis in which *R. solanacearum* would have evolved to sense basic pH as a cue to activate the T3SS in combination with other environmental and plant signals. In view of these results, we might have understood why in multiple transcriptomic studies the expression of the T3SS and T3E is detected at late stages of infection (de Pedro-Jové *et al.*, 2021; Du *et al.*, 2022; De Ryck, Van Damme and Goormachtig, 2023). Additionally, this would explain why the T3SS is not only induced at early time points when bacteria has not yet reached densities high enough to activate the HrpG repressor PhcA (Genin *et al.*, 2005).

Materials and Methods

Bacterial strains and plant growth conditions

A detailed list of all strains, plasmids and primers used in this work can be found in Table S6 The aggressive *Ralstonia solanacearum* strain UY031 (phylotype IIB, sequevar 1) isolated from potato tubers in Uruguay (Siri, Sanabria and Pianzzola, 2011) carrying the reporter Lux operon under control of the constitutive *psbA* promoter (*PpsbA-luxCDABE*) integrated in the genome (UY031 PpsbA-lux) was used in the transcriptomic analysis experiments (Monteiro, Genin, *et al.*, 2012). For the different reporter gene expression, soil growth and survival experiments, the *R. solanacearum* (or *R. pseudosolanacearum*) GMI1000 strain (phylotype I) was used. All the *R. solanacearum* strains were routinely grown at 28 °C in rich B medium (Monteiro, Genin, *et al.*, 2012) and *Escherichia coli* strains in Luria-Bertani (LB) medium at 37ºC. In all cases, the medium was supplemented with ampicillin (50 mg/L), kanamycin (50 mg/L), gentamicin (10 mg/L), or tetracycline (10 mg/L) when needed.

For *in planta* assays, tomato plants (*Solanum lycopersicum* cv. Marmande) were routinely grown in a 30:1:1 mix of Substrate 2 (Klasmann-Deilmann GmbH, Geeste, Germany), perlite and vermiculite for four weeks at 22 ºC and 60 % relative humidity (RH) under long-day photoperiod conditions (16 h light and 8 h darkness). Before bacterial inoculation, tomato plants were pre-acclimated for three days at 27 ºC under infection conditions (27 ºC, 12/12 h photoperiod and 60 %RH).

Bacterial sampling

For the reference rich B medium and the three *in planta* (Potato - *Solanum tuberosum* cv. Desirée) conditions (Apoplast, Early xylem and Late xylems) used for comparison, we recovered the previously published data in our group (Table S7 and S8). All information about the bacterial collection is described in detailed in the study (de Pedro-Jové *et al.*, 2021).

For the soil samples, the soil (soil:silica mixture) (Table S9) was autoclaved three times (approx. 3 h) to clean the substrate from living organism and to degrade as much as possible contaminant genomic material before the inoculation. Next, pots without plants containing approximately 200 g of soil were drenched with 40 ml of *R. solanacearum* UY031 PpsbA-lux at 10^8 colony forming units (CFU)/ml (OD_{600} = 0.1). Pots were incubated for three days at 27 ºC in 12/12 h photoperiod conditions at 60 %RH. A total of 5 g of soil was weighted and frozen in liquid nitrogen.

For the water samples, 100 µl of a 10^3 CFU/ml diluted overnight culture of *R. solanacearum* UY031 PpsbA-lux was plated on rich B medium supplemented with 0.5% glucose. After two days incubation at 28 ºC, the bacterial colonies were recovered by adding 1 ml followed by 500 µl of sterile mineral water (water A) (Table S9). The recovered bacteria washed twice and resuspended in 1 ml of mineral water. Then, the 1 ml of bacteria was inoculated to 49 ml of sterile mineral water in a 250 ml Erlenmeyer to a final concentration of $\sim 10^7$. The suspension was incubated at 28 ºC for 6 hours. After incubation, samples were centrifuged at 4 ºC, the supernatant discarded, and the pellet frozen in liquid nitrogen (Fig. S1A).

RNA extraction, sequencing, and library preparation

Total RNA from bacterial pellets of water samples was extracted using the SV Total RNA Isolation System kit (Promega) following manufacturer's instructions for gram-negative bacteria. For soil samples, the RNA PowerSoil® Total RNA Isolation Kit (MO BIO) was used supplemented with a Rigurous DNAse treatment using the TURBO DNA-free kit (Life Technologies, Ambion) following manufacturer's instructions. RNA concentration was measured with a ND-8000 Nanodrop, and RNA integrity was validated for all samples using the Agilent 2100 Bioanalyzer before sending for sequencing. Only high-quality RNA preparations, with RIN greater than 7.0, were used for paired end stranded RNA library construction. Three biological replicates per condition were subjected to bacterial rRNA depletion prior to sequencing on a HiSeq2000 Illumina System apparatus. Soil samples were sequenced by Macrogen Inc. and water samples by the Shangai PSC Genomics facility (Table S7).

The *novo* sequencing data will be available upon publication in the Sequence Read Archive under the Bio Project: (XXXX, accession codes XXXX).

Read alignment, mapping, and expression analysis

All the transcriptomic datasets used in this study (Table S8), were (re-)analysed following the same bioinformatic pipeline (Fig. S1B). First, raw RNA-seq data quality was evaluated with FastQC (v.0.11.5) (Andrews *et al.*, 2015) and later trimmed with trimGalore (v.0.6.1) (Moskvin *et al.*, 2011) with the paired (--paired) option to remove adaptors and low quality reads from the analysis. Since soil samples were sensible to contamination, potential rRNA contaminants were filtered out with the SortMeRNA software (v.4.2.0) (Kopylova, Noé and Touzet, 2012) with the default parameters and contaminant libraries. After removal, reads were mapped with Bowtie2 (v. 2.4.4) (Langmead and Salzberg, 2013) and the alignments quantified with the prokaryote counting software FADU (Feature Aggregate Depth Utility) (v. 1.8) (Fraser *et al.*, 2021) (Table S8 and Table S10). The NCBI's RefSeq version of the UY031 was used for the analysis (GCF_001299555.1_ASM129955v1).

Differential expression analyses was performed with Deseq2 (v. 1.34.0) (Love, Huber and Anders, 2014) package in R (v. 4.1.0) (R Core Team, 2021). Genes with |log2(fold-change)|>1.5 and adjusted *p-value* <0.01 were considered as differentially expressed (DEG) when compared to the rich B reference medium (Table S5). The UpsetR (Conway, Lex and Gehlenborg, 2017) R package (v. 1.4.0) was used to detect unique and intersections among the DEG in the different conditions. For condition comparison and clustering, Deseq2 transformed counts normalized for sample size were used to produce the Principal component analysis (Fig. 1A). To compare the DEG with previously published transcriptomic studies, we retrieved the data from Table S1 and S3 from (Vivant *et al.*, 2017), Table S1 to S3 from (Piveteau *et al.*, 2011) and Additional file 1 from (Li *et al.*, 2015). The protein .faa files of *Listeria monocytogenes* EGD-e (GCF_000196035.1_ASM19603v1_protein) and *Legionella pneumophila* JR32 (GCA_000008485.1_ASM848v1_protein) were downloaded from NCBI database and orthologs identified with OrthoFinder (v. 2.5.4) (Emms and Kelly, 2019).

Gene enrichment analysis and functional annotation

For the gene enrichment analysis, the UY031 genes were searched for associated Gene Ontology (GO) terms using the default annotation pipeline of the OmicsBox software (v. 2.2.4) (Götz *et al.*, 2008). For Kyoto Encyclopaedia of Genes and Genomes (KEGG) pathways, terms were downloaded from KEGG API (downloaded on December 12, 2022) (Table S4) (Kanehisa and Goto, 2000). For the enrichment analysis, the enricher function of the ClusterProfiler package (v. 4.2.2) (Yu *et al.*, 2012) was used in R.

To continue the functional characterisation, the UY031 genes were functionally categorised using the EggNOG-mapper (Cantalapiedra *et al.*, 2021) to retrieve the Cluster of Orthologous Groups (COG) categories. COG categorisation was curated with information from the KEGG and Uniprot databases (Kanehisa and Goto, 2000; Consortium *et al.*, 2023), together with previously published data (Table S5). The curated classification was used to conduct a hypergeometric test using the R stats package to detect enriched categories among the DEGs in the different categories (v. 4.1.0).

***R. solanacearum* mutant, complemented and reporter strain constructions**

Knockout deletion of the tandem genes coding for the *katGab* (*RSc0775*/*Rsc0776*) in *R. solanacearum* GMI1000 strain were obtained as previously described in (Tondo *et al.*, 2020). Briefly, the flanking regions were amplified (~1Kb) with compatible restriction sites and cloned into the pCM184 vector (Addgene) flanking the kanamycin resistance (Kan^R) cassette. The sequenced checked construct was linearised, naturally transformed into *R. solanacearum* and plated in rich B medium complemented with kanamycin for mutant selection (Bertolla *et al.*, 1997).

For the complementation constructs, the gateway pRCT destination vector, containing the tetracycline resistance cassette, was used (Monteiro, Solé, *et al.*, 2012). The complementation of the *KatGab* mutant was performed by amplifying the tandem *RSc0775/Rsc0776* genes with its promoter sequence.

The restriction sites for *Kpn*I and *Xba*I were introduced in the oligonucleotides for the later restriction cloning into the pRCT-GWY vector (Monteiro, Solé, *et al.*, 2012), creating the plasmid pRCT-PkatG-KatG. The final vector was linearized, naturally transformed into *R. solanacearum* knock-out mutants, and plated on Tetracycline rich B medium to select the transformed colonies (Bertolla *et al.*, 1997). All oligonucleotides used are listed in Table S6.

To obtain the reporter strains, the pRCG-PhrpY-lux (Puigvert *et al.*, 2019), pRCG-PhrpB-lux (Monteiro, Genin, *et al.*, 2012) and pRCG-PhrpG-lux (Zuluaga, Puigvert and Valls, 2013) vectors were *Sfi*I-digested, naturally transformed into the different *R. solanacearum* knockout mutants belonging to the T3SS regulatory pathway (Δ*prhA*, Δ*prhR*, Δ*prhI*, Δ*prhJ*, Δ*hrpG* and Δ*hrpB* (Table S6)), and selected in gentamicin-containing rich B medium. To construct the *prhJ* reporter strains, its promoter was PCR-amplified from the GMI1000 genome, by using oligonucleotides with the *Avr*II and *Kpn*I restriction sites flanking the sequence, and cloned into the pGEM-T-EASY vector (Life Technologies, Paisley, UK), obtaining the pG-PprhJ plasmid. The *prhJ* promoter was then excised from pG-PprhJ and cloned with the same restriction sites into the pRCG-GWY (Monteiro, Genin, *et al.*, 2012), creating the pRCG-PprhJ-GWY plasmid. Finally, to generate the pRCG-PprhJ-lux plasmid, a *Sfi*I-*Kpn*I fragment containing the entire *luxCDABE* operon, excised from the pRCGent-Pep-lux vector (Monteiro, Genin, *et al.*, 2012), was cloned into the same restriction sites of pRCG-PprhJ-lux. Finally, the plasmid was linearized, naturally transformed into the *R. solanacearum* GMI1000 WT and selected in gentamicin-containing rich B medium.

All PCRs were carried out by using the proofreading Q5® High-Fidelity DNA Polymerase (New Engand Biolabs). Validation of all knockouts, complemented and reporter strains was carried out by PCR amplification and sequencing with the appropriated oligonucleotides listed in Table S6.

Soil extract agar growth assay

Soil extract agar was prepared by mixing 400 g of soil in 1 liter of distilled water. The mix was autoclaved, kept at room temperature for 24 hours and centrifuged. The liquid phase was recovered free of soil particles, 15 g/L of agar added, and the pH adjusted to 6.8 - 7 before autoclaving (Leibniz Institute, 2023). Overnight cultures of *R. solanacearum* GMI1000 wild type (WT) and knock-out mutants grown in rich B medium were washed twice and resuspended in MQ water to a final concentration of 10^8 CFU/ml (OD_{600} = 0.1). Serial dilutions were plated on soil extract agar plates supplemented with appropriate antibiotics and incubated for 48 h at 28 °C. After, bacterial colonies were counted. Plating assays were performed in triplicate and at least three independent times.

Microcosm assay

For the microcosms assay, 15 g of soil was weight in separate 100-ml Enlermeyer and autoclaved. The *R. solanacearum* GMI1000 WT and knock-out mutants were grown overnight in rich B medium, washed twice and resuspended in MQ water. Then, 3.5 ml (corresponding to the field capacity of the soil) of the bacterial suspension was inoculated into the soil to reach a final concentration of ~3×10^8 CFU/g soil (Kong *et al.*, 2014). The flasks were incubated under regular infection conditions (27 °C, 12/12 h photoperiod and 60 %RH). At 0, 7, 14, 21 and 28 days post inoculation (dpi), bacterial survival was measured by collecting ~1 g of soil into Eppendorf tubes. The soil samples were weighted, homogenized in 1 ml of MQ water, and serial dilutions were carried out for plating onto modified antibiotic-containing SMSA medium (Elphinstone *et al.*, 1996). Colonies were counted after 48 h incubation at 28 ºC and normalised by the soil weight (CFU/g soil). Microcosms assays were performed in triplicate and at least three independent times.

Luminescence assay

Overnight cultures of the reporter strains in rich B medium supplemented with antibiotics were washed twice and resuspended in MQ water. Next, water (native pH or adjusted pH, neutralised with HCl and alkalinised with KOH) supplemented or not with rich B media (1/50, 1/10 or 1/5 final concentrations) were inoculated with the bacterial suspensions to a final concentration of 10^8 CFU/ml (OD_{600} = 0.1).

The bacterial suspensions in water were kept at 28°C with shaking at 180 rpm and aliquots were collected at 0, 3, 6, 9 and 24 hours post-inoculation (hpi) to measure luminescence and absorbance (Puigvert *et al.*, 2019). Luminescence results were expressed as relative light units (RLU) values divided by 1000 and normalized by the bacterial density (absorbance at OD_{600}). A FB-12 luminometer (Berthold Detection Systems, Pforzheim, Germany) and a V-1200 spectrophotometer (VWR, Radnor, PA) were used for the luminescence and absorbance measurements, respectively. Luminescence assays were performed in triplicate and at least three independent times.

Sap xylem pH assay

To measure the pH from the xylem sap, forty 4-week-old unwounded tomato plants were soil-soak inoculated with 40 ml bacterial suspension of *R. solanacearum* GMI1000 PpsbA-lux strain adjusted to a final concentration of 10^8 CFU/ml (OD_{600} = 0.1) (Morel *et al.*, 2018). Additionally, twenty plants were mock drenched with distilled water. Plants were kept under standard infection conditions (27 ºC, 12/12h photoperiod and 60 %RH) and wilting symptoms recorded on a disease index scale ranging from 0 % (no symptoms) to 100 % (wilted plant). Throughout the infection, two 3 cm-stem samples were collected per plant from the bottom (0.5 cm above the soil) and top (4^{th} internode). To extract the xylem sap, cut stems were centrifuged inside a tube. The pH was measured using pH-indicator strips pH 2.0 - 9.0 (Merck) and the sap was serial diluted and plated in rich B medium supplemented with appropriate antibiotics to count bacterial colonies.

Statistical analysis

All the statistical analysis were performed in R software. In each plot, the statistical test applied is detailed in the figure caption. A summary of all the statistical outputs is given in Table S11.

Supplementary Data

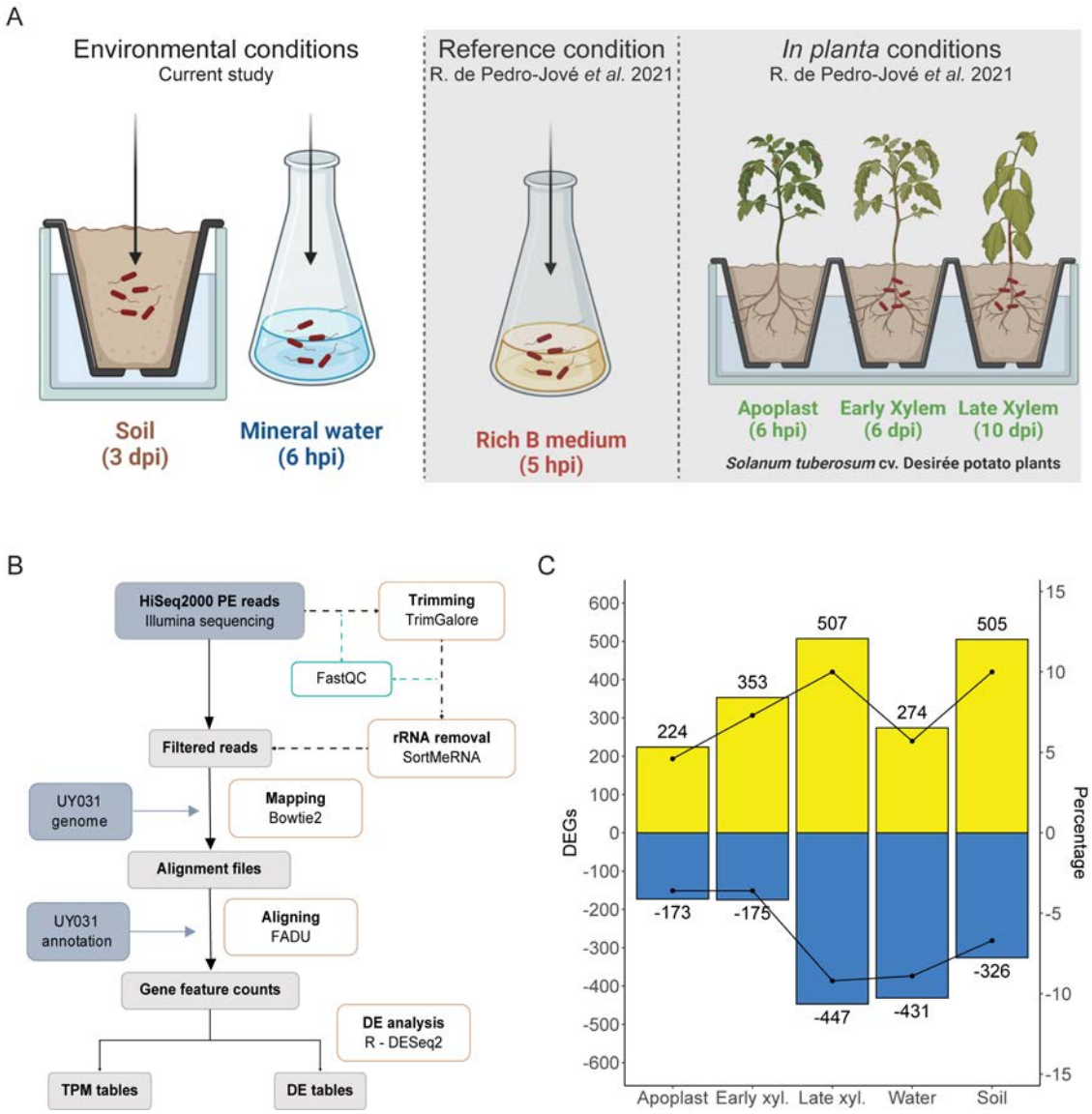

Supplementary Figure 1. Experimental set-up and DEGs. A) RNA sampling conditions from environmental samples (soil and mineral water), and those of previously obtained samples (the rich B medium reference condition and three in planta conditions; apoplast, early and late xylem). **B**) Transcriptomic analysis pipeline after sequencing. **C**) Deseq2 differentially expression analysis summary. The left Y axis of the bar plot indicates the amount of Up- (yellow) and Downregulated (blue) genes for each condition compared to the reference Rich B medium. The right Y axis, corresponding with the line plot, indicates the percentage of genes in the genome Up- or Downregulated in each condition tested.

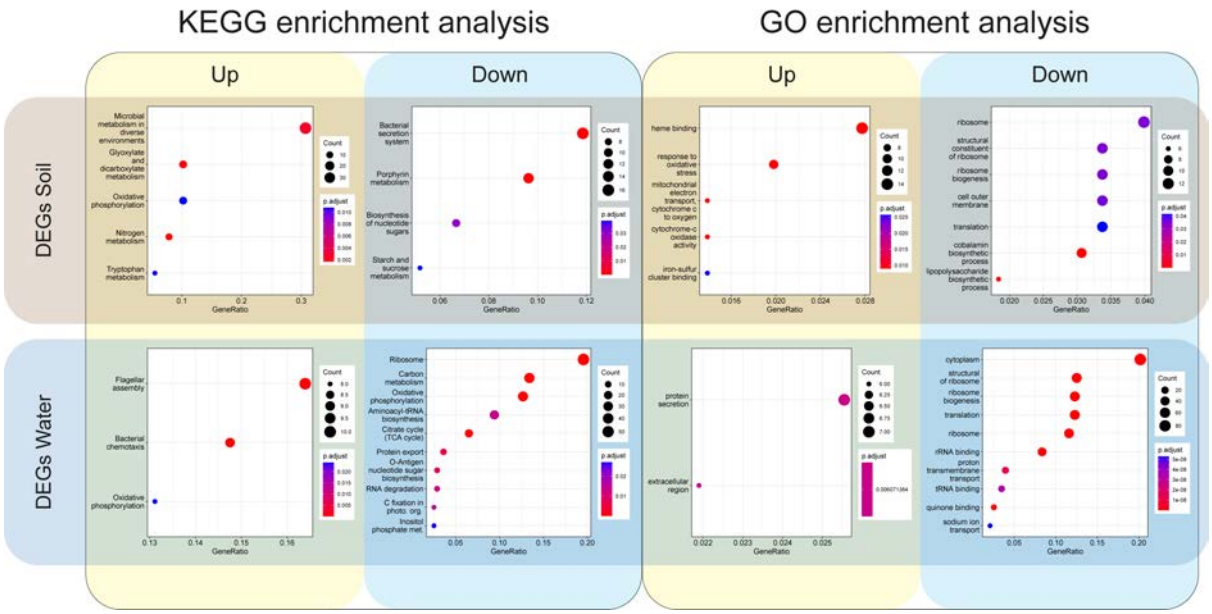

Supplementary Figure 2. GO and KEGG enrichment analyses of the environmental conditions. Dot plots of the KEGG (left) and GO (right) enrichment analyses of DEGs from soil (brown) and water (blue) conditions. Dot sizes represent the number of genes associated with each term and dot colour indicates the p. adjusted value. The gene ratio represented in the X axis is the proportion of associated genes to a term from the total gene set. The DEGs were extracted with DEseq2 using the thresholds: p-adj.value > 0.01 and log 2 FC ± 1.5 and ClusterProfiler was used to calculate the enrichment.

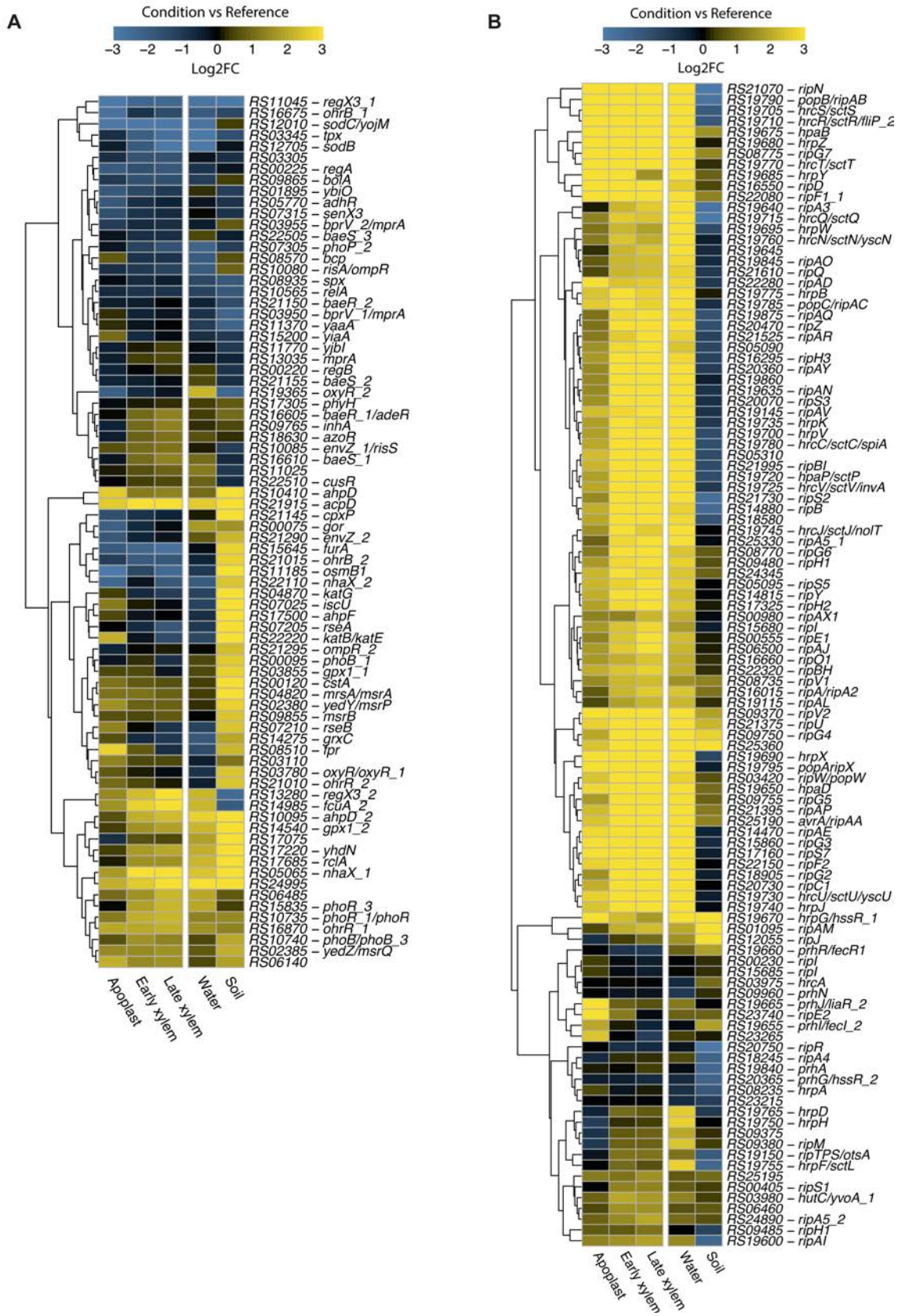

Supplementary Figure 3. Expression of all stress response and the type III secretion system (T3SS) and type III effector gene groups. Heatmap representation of gene $\log_2$ fold change with respect to the rich medium in the different conditions for **A**) All stress response genes and **B**) T3SS and T3E gene categories according to the curated classification (see Materials and Methods). The colour palette ranges from blue (downregulated) to yellow (upregulated genes) as indicated in the key. Locus names are presented without the preceding letters RSUY_.

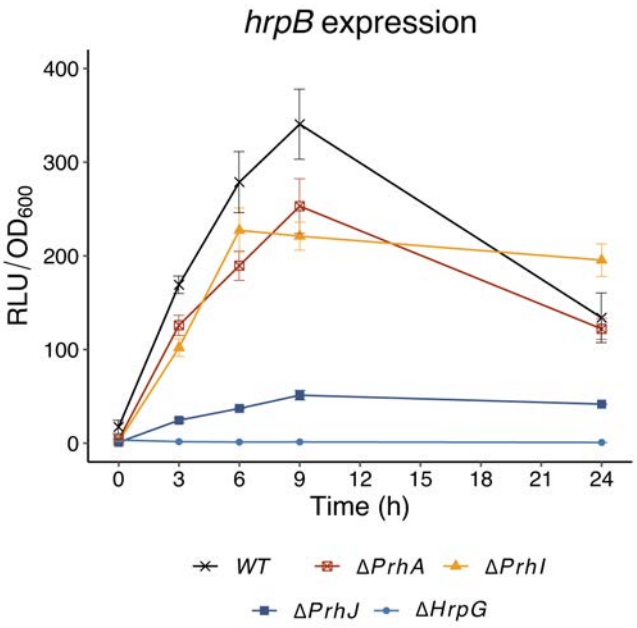

Supplementary Figure 4. Time-course expression of the *PhrpB-Lux* reporter in strains disrupted for the different T3SS regulatory genes after resuspension in water. *R. solanacearum* cultures grown overnight in rich B medium were washed and diluted to OD_{600}=0.1 in water and luminescence and OD_{600} values were measured over a 24h period. Relative luminescence units (RLU) were normalised by bacterial concentration measured as OD_{600}. RLU values were divided by 1000 to facilitate visualisation.

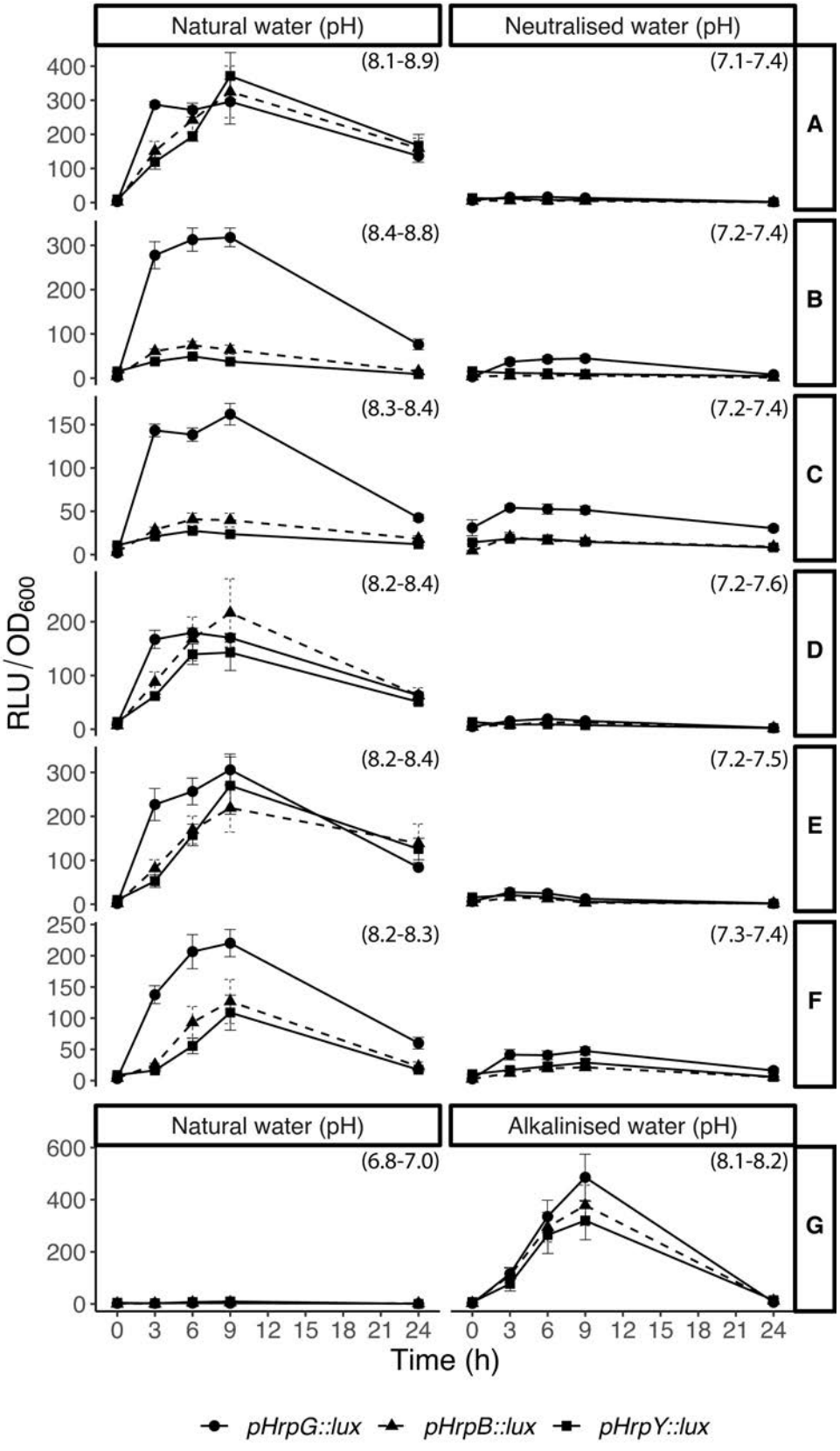

Supplementary Figure 5. Induction of the T3SS by basic pH in all natural water sources tested. Time-course expression of *prhG*, *hrpB* and *hrpY* reporter strains at native basic (A to F) or neutral pH (G) and after pH neutralisation with HCl or alkalinisation with KOH. For each time point, luminescence was measured (RLU) and normalised by OD_{600}. All values were divided by 1000 to facilitate visualisation. Water sources are indicated in the methods section.

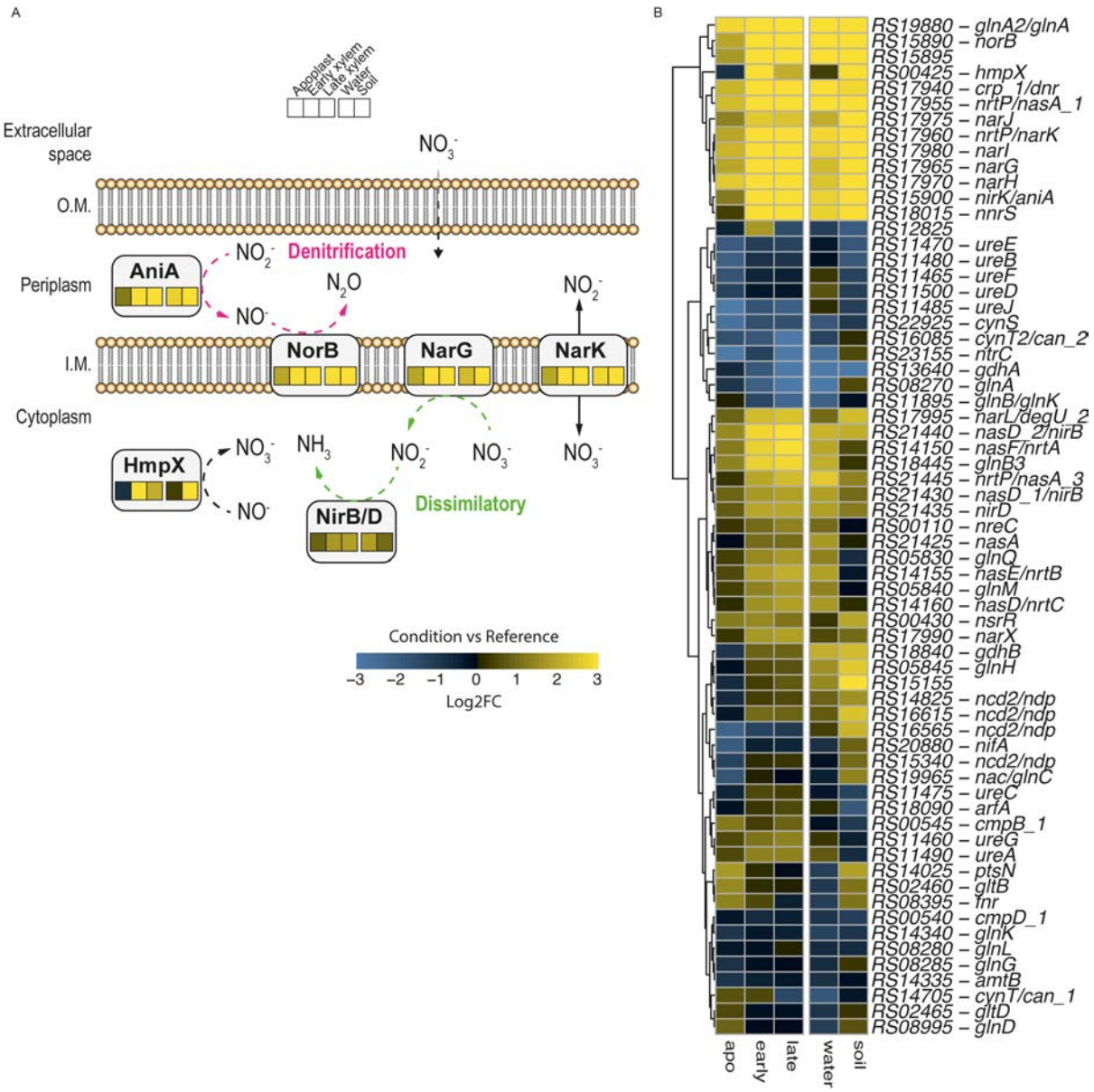

Supplementary Figure 6. Induction of nitrogen metabolism genes in soil. A) Representation of the main components of the nitrogen metabolism and their expression in different conditions (log_2 fold change with respect to rich medium, order as indicated above the illustration). Denitrification pathway is marked in pink, dissimilatory in green and detoxification by HmpX in black. O.M., Outer membrane and I.M., Inner membrane **B**) Heatmap representation of the log2 fold change in expression with respect to growth in rich medium for all the genes classified in the nitrogen metabolism group. The colour palette ranges from blue (downregulated) to yellow (upregulated genes) as indicated in the key. Locus names are presented without the preceding letters RSUY_.

Due to their length, the following Supplementary Tables may be found online in the following link: PhD_Roger.

Supplementary Table 1. List of genes corresponding to the intersections shown in the UpsetR plots (Fig. 1B).

Supplementary Table 4. Output tables of the KEGG and GO enrichment analysis conducted on general and exclusive up- and downregulated DEGs from water and soil conditions. The R package ClusterProfiler was used to conduct the analysis.

Supplementary Table 5. DEseq2 DEG analysis results from the the three in planta conditions (Apoplast, Early xyem and Late xylem) and the two environmental conditions (Soil and Water) using as reference the rich B medium. Only those genes with p-adj > 0.01, log2 FC ± 1.5 were considered differentially expressed. The curated classification of the UY031 genome is shown in the Supragroup and Group columns next to the Gene ID.

Supplementary Table 10. Reads output of the FADU aignment software for all the different conditions (some samples have technical replicates).

Supplementary Table 2. Marker genes filtering output of the different conditions. On top, the summary of the different steps of filtering and the remaining genes are detailed. The table on the bottom lists all the marker genes identified and, in more detail, the gene classification and operons (contiguous genes highlighted with the same colour) found in the soil marker genes. Only the summary is shown, the full table may be downloaded from PhD_Roger.

		|LFC|>1.5 p.adj<0.01	Not DEG in other conditions	|LFC|>1.5 only in the condifion	|LFC|>2.5
Apoplast	Upregulated	224	84	38	38
	Downregulated	173	61	15	11
Early	Upregulated	353	2	0	0
	Downregulated	175	1	0	0
Late	Upregulated	507	121	0	0
	Downregulated	447	83	5	5
Water	Upregulated	274	18	1	1
	Downregulated	431	120	16	2
Soil	Upregulated	505	373	198	161
	Downregulated	326	178	89	79

Supplementary Table 3. TAG enrichment analysis summary. Percentage of DEGs in each of the manually curated functional categories and the hypergeometric enrichment text are shown for the environmental soil and water conditions for the up- (_UP) and downregulated (_DOWN) genes. Hypergeometric statistical analysis was conducted in R package stats.

	Water		Soil	
	%	P.value	%	P.value
AminoAcid_DOWN	7.014028	0.954093	6.613226	0.575275
AminoAcid_UP	3.206413	0.997353	10.42084	0.529052
Carbohydrate_DOWN	16.26016	0.000101	10.97561	0.007353
Carbohydrate_UP	3.658537	0.945582	10.56911	0.504572
Cell cycle control_DOWN	14.92537	0.070761	2.985075	0.94657
Cell cycle control_UP	1.492537	0.980417	8.955224	0.714126
Cell envelope_DOWN	12.01923	0.072806	11.05769	0.011876
Cell envelope_UP	1.442308	0.999593	5.288462	0.997564
Coenzyme_DOWN	2.325581	0.999917	12.7907	0.002444
Coenzyme_UP	0.581395	0.999963	4.069767	0.999426
Defence mechanisms_DOWN	1.538462	0.999936	2.307692	0.994221
Defence mechanisms_UP	5.384615	0.610747	11.53846	0.380242
Energy_productionconversion_DOWN	25	6.82E-12	9.693878	0.067059
Energy_productionconversion_UP	9.183673	0.027617	16.83673	0.003394
EPS_Biofilm_DOWN	16.88312	0.017262	25.97403	8.92E-08
EPS_Biofilm_UP	2.597403	0.938242	9.090909	0.70656
Flagella_chemo_DOWN	2.12766	0.998523	1.06383	0.99867
Flagella_chemo_UP	18.08511	1.55E-05	1.06383	0.999972
Hormone biosynthesis_DOWN	0	1	20	0.142385
Hormone biosynthesis_UP	10	0.442033	0	1
Inorganic ion_DOWN	2.873563	0.999675	8.045977	0.282185
Inorganic ion_UP	3.448276	0.936166	11.49425	0.357213
Intratraficking, secretion_DOWN	1.075269	0.999844	20.43011	9.46E-06
Intratraficking, secretion_UP	6.451613	0.432286	0	1
Lipid_DOWN	8.87574	0.5466	7.100592	0.468906
Lipid_UP	3.550296	0.924471	5.325444	0.99432
Motility_DOWN	0	1	10	0.394281
Motility_UP	5	0.68906	0	1
Nitrogen metabolism_DOWN	3.076923	0.983394	1.538462	0.989588
Nitrogen metabolism_UP	1.538462	0.977959	23.07692	0.002278
Nucleotide_DOWN	14.15094	0.047182	4.716981	0.851703
Nucleotide_UP	0.943396	0.998067	4.716981	0.989576
Poorly_characterised_DOWN	3.38248	1	5.637467	0.963915
Poorly_characterised_UP	8.239376	1.99E-05	14.31049	1.12E-06
PTM_DOWN	18.51852	0.004598	6.17284	0.645672
PTM_UP	1.234568	0.991452	13.58025	0.220255
Replication, recombination and repair_DOWN	3.135889	0.999981	3.484321	0.995108
Replication, recombination and repair_UP	3.832753	0.941823	6.968641	0.985163
Secondary metabolism_DOWN	3.804348	0.998071	2.173913	0.998883
Secondary metabolism_UP	2.717391	0.981993	11.95652	0.279218
Signal transduction_DOWN	2.777778	0.99063	2.777778	0.960134
Signal transduction_UP	0	1	15.27778	0.125296
Stress response_DOWN	3.846154	0.975004	1.282051	0.995854
Stress response_UP	2.564103	0.941162	34.61538	6.58E-09
T2SS_CWDE_DOWN	33.33333	0.000166	16.66667	0.047675
T2SS_CWDE_UP	3.333333	0.826938	0	1
T3SS_DOWN	0	1	0.925926	0.99951
T3SS_UP	41.66667	5.52E-29	3.703704	0.997403
T4P_chemo_DOWN	6.666667	0.777967	2.222222	0.957295
T4P_chemo_UP	15.55556	0.01229	6.666667	0.863137
Transcription_DOWN	8.87574	0.5466	3.550296	0.975943
Transcription_UP	5.325444	0.625639	12.42604	0.22722
Translation and ribosome_DOWN	35.94771	6.33E-43	6.862745	0.498887
Translation and ribosome_UP	0.653595	1	4.575163	0.999957

Supplementary Table 6. Bacterial strains, plasmids, and oligos used in this work.

Strains		
Name	**Relevant characteristics***	**Source or reference**
R. solanacearum		
UY031 PpsbA-lux	Wild type strain (Phylotype IIB, sequevar 1) with *PpsbA-luxCDABE* from pRCG-PpsbA-lux, Gm^r	(Siri, Sanabria and Pianzzola, 2011)
GMI1000 WT	Wild type strain (Phylotype I, race 1 biovar 3)	(Boucher *et al.*, 1985)
Δ*katG*	GMI1000 strain with the *katGab* (*RSc0775*/*RSc0776*) genes substituted by a kanamicyn-resistance cassette, Km^r	This work
Δ*katG-katG*	Δ*katG* strain complemented with the *katGab* genes from pRCT-katGab, Km^r, Tc^r	This work
Δ*katE*	GMI1000 strain with the *katE* (*RSp1581*) gene substituted by a gentamicin-resistance cassette, Gm^r	(Tondo *et al.*, 2020)
Δ*katGE*	Δ*katE* strain with the *katG* (*RSc0775*/*RSc0776*) gene substituted by a kanamicyn-resistance cassette, Km^r, Gm^r	This work
GMI1000 PpsbA-lux	GMI1000 strain with *PpsbA-luxCDABE* from pRCG-PpsbA-lux, Gm^r	This work
GMI1000 PprhJ-lux	GMI1000 strain with *PprhJ-luxCDABE* from pRCG-PprhJ-lux, Gm^r	This work
GMI1000 PhrpG-lux	GMI1000 strain with *PhrpG-luxCDABE* from pRCG-PhrpG-lux, Gm^r	(Zuluaga, Puigvert and Valls, 2013)
GMI1000 PhrpB-lux	GMI1000 strain with *PhrpB-luxCDABE* from pRCG-PhrpB-lux, Gm^r	(Monteiro, Genin, *et al.*, 2012)
GMI1000 PhrpY-lux	GMI1000 strain with *PhrpY-luxCDABE* from pRCG-PhrpY-lux, Gm^r	(Puigvert *et al.*, 2019)
Δ*prhA*	*prhA* deletion mutant in the GMI1000 background, Sp^r, Sm^r	(Marenda *et al.*, 1998)
Δ*prhA* PhrpY-lux	*prhA* strain with *PhrpY-luxCDABE* from pRCG-PhrpY-lux, Sp^r, Sm^r, Gm^r	This work
Δ*prhA* PhrpB-lux	*prhA* strain with *PhrpB-luxCDABE* from pRCG-PhrpB-lux, Sp^r, Sm^r, Gm^r	This work
Δ*prhA* PhrpG-lux	*prhA* strain with *PhrpG-luxCDABE* from pRCG-PhrpG-lux, Sp^r, Sm^r, Gm^r	(Zuluaga, Puigvert and Valls, 2013)
Δ*prhR*	*prhR* deletion mutant in the GMI1000 background, Sp^r, Sm^r	(Arlat *et al.*, 1992)
Δ*prhR* PhrpY-lux	*prhA* strain with *PhrpY-luxCDABE* from pRCG-PhrpY-lux, Sp^r, Sm^r, Gm^r	This work
Δ*prhI*	*prhI* deletion mutant in the GMI1000 background, Sp^r, Sm^r	(Brito *et al.*, 2002)
Δ*prhI* PhrpY-lux	*prhI* strain with *PhrpY-luxCDABE* from pRCK-PhrpY-lux, Sp^r, Sm^r, Gm^r	This work
Δ*prhI* PhrpB-lux	*prhI* strain with *PhrpB-luxCDABE* from pRCG-PhrpB-lux, Sp^r, Sm^r, Gm^r	This work
Δ*prhI* PhrpG-lux	*prhI* strain with *PhrpG-luxCDABE* from pRCG-PhrpG-lux, Sp^r, Sm^r, Gm^r	(Zuluaga, Puigvert and Valls, 2013)
Δ*prhJ*	*prhJ* deletion mutant in the GMI1000 background, Sp^r, Sm^r	(Brito *et al.*, 1999)
Δ*prhJ* PhrpY-lux	*prhJ* strain with *PhrpY-luxCDABE* from pRCG-PhrpY-lux, Sp^r, Sm^r, Gm^r	This work
Δ*prhJ* PhrpB-lux	*prhJ* strain with *PhrpB-luxCDABE* from pRCG-PhrpB-lux, Sp^r, Sm^r, Gm^r	This work
Δ*prhJ* PhrpG-lux	*prhJ* strain with *PhrpG-luxCDABE* from pRCG-PhrpG-lux, Sp^r, Sm^r, Gm^r	(Zuluaga, Puigvert and Valls, 2013)
Δ*hrpG*	*hrpG* deletion mutant in the GMI1000 background	(Valls, Genin and Boucher, 2006)
Δ*hrpG* PhrpY-lux	*hrpG* strain with *PhrpY-luxCDABE* from pRCG-PhrpY-lux, Gm^r	This work
Δ*hrpG* PhrpB-lux	*hrpG* strain with *PhrpB-luxCDABE* from pRCG-PhrpB-lux, Gm^r	This work
Δ*hrpB*	*hrpB* deletion mutant in the GMI1000 background, Sp^r, Sm^r	(Genin *et al.*, 1992)
Δ*hrpB* PhrpY-lux	*hrpB* strain with *PhrpY-luxCDABE* from pRCG-PhrpY-lux, Sp^r, Sm^r, Gm^r	This work
Δ*hrpB* PhrpG-lux	*hrpB* strain with *PhrpG-luxCDABE* from pRCG-PhrpG-lux, Sp^r, Sm^r, Gm^r	This work

Plasmids		
Name	**Relevant characteristics**	**Source or reference**
pCM184-katGab::Km	Cloning pCM184 vector carrying kanamycin-resistance cassette flanked by upstream and downstream regions of *katGab* (*RSc0775*/*RSc0776*) genes from GMI1000, Km^r	This work
pRCT-GWY	Gateway pRCT destination vector carrying tetracycline-resistance cassette flanked by homologous regions to the GMI1000 genome, Ap^r, Tc^r	(Monteiro, Solé, *et al.*, 2012)
pRCT-katGab	Vector carrying the *katGab (RSc0775*/*RSc0776*) genes from GMI1000 cloned in *Kpn*I-*Xba*I in pRCT-GWY backbone, Tc^r	This work
pJET-oxyR::Km	Cloning vector carrying kanamycin-resistance cassette flanked by upstream and downstream regions of *oxyR* (*RSc2690)*gene from GMI1000, Km^r	(Valls, Genin and Boucher, 2006)
pRCT-PpsbA-GWY	Gateway pRCT destination vector carrying tetracycline-resistance cassette flanked by homologous regions to the GMI1000 genome, together with the *psbA* promoter from gene expression, Ap^r, Tc^r	(Valls, Genin and Boucher, 2006)
pRCT-PpsbA-oxyR	Vector carrying the *oxyR (RSc2690*) gene from GMI1000 cloned in pRCT-PpsbA-GWY backbone, Tc^r	This work
pRCG-PpsbA-lux	Vector carrying the *luxCDABE* operon flanked by homologous regions to the GMI1000 genome, together with the *psbA* promoter from gene expression, Ap^r, Tc^r	(Puigvert *et al.*, 2017)
pG-PphrJ	Cloning pGEM-T-EASY vector carrying the *prhJ* promoter from GMI1000, Ap^r	This work
pRCG-GWY	Gateway pRCG vector carrying gentamicin-resistance cassette flanked by homologous regions to the GMI1000 genome, Ap^r, Gm^r	(Monteiro, Solé, *et al.*, 2012)
pRCG-PprhJ-GWY	Vector carrying the *prhJ* promoter from GMI1000 cloned in *Avr*II-*Kpn*I in pRCG-GWY backbone, Gm^r	This work
pRCG-Pep-lux	Vector carrying the *luxCDABE* operon flanked by homologous regions to the GMI1000 genome, together with the *eps* promoter from gene expression, Ap^r, Tc^r	(Monteiro, Solé, *et al.*, 2012)
pRCG-PprhJ-lux	Vector carrying *luxCDABE* operon from pRCGent-Pep-lux cloned in *Kpn*I–*Not*I in pRCG-PprhJ backbone, Ap^r, Gm^r	This work
pRCG-PhrpY-lux	Vector carrying *the hrpY promoter* from GMI1000 cloned in *Avr*II–*Kpn*I in pRCG-PhrpB-lux backbone , Ap^r, Gm^r	(Puigvert *et al.*, 2017)

pRCG-PhrpB-lux	Vector carrying *luxCDABE* operon from pMU1* cloned in *Kpn*I–*Not*I in pRCG-PhrpB backbone, Ap^r, Gm^r	(Monteiro, Genin, *et al.*, 2012)
pRCG-PhrpG-lux	Vector carrying *luxCDABE* operon from pRCG-Pep-lux cloned in *Sfi*I–*Kpn*I in pRCG-PhrpG-GWY backbone, Ap^r, Gm^r	(Zuluaga, Puigvert and Valls, 2013)

Oligos

Name	**Sequence (5' to 3')****	**Application (Restriction site)**
KatG-EcoUpFw	tagaattcAGCGCTACGCAACGAAAC	KatGab KO - UP (*EcoR*I) and verification
KatG-KpnUpRv	taggtaccGGCATGCTTGAAAGGACACT	KatGab KO - UP (*Kpn*I)
KatG-HpaDwnFw	tagttaacCTGGGACAAGGTGATGAACC	KatGab KO - DOWN (*Hpa*I)
KatG-SacDwnRv	tagagctcGTGTCGCACGGCTGTATG	KatGab KO - DOWN (*Sac*I) and verification
KatGcomplFw	ggggtaccGTGATGGACCGGATGATGA	KatGab complementation (*Kpn*I)
KatGcomplRv	gctctagaGTGTGATGCCTGCTGTCG	KatGab complementation (*Xba*I)
PprhJFw	ccctaggTCACGGTGGTCCACAG	PrhJ promoter (*Avr*II)
PprhJRv	cggtaccACTTTCTCGTTGCAACTGG	PrhJ promoter (*Kpn*I)
glmS fwd (RscipUp2)	GGCGCGCTCAAGCTCAAGGA	Complemented and reporter strains verification
pRC rev (RscirUp1)	AGGAGCCTTTAATTGTATCGG	Complemented and reporter strains verification
pRC fwd (RscirDw1)	TGCTGCCACCGCTGAGCAAT	Complemented and reporter strains verification
Rsc0181 revII (RscipDw2)	CCTGGCTCGGCTGGACTTGC	Complemented and reporter strains verification

*****Km^r, Gm^r, Ap^r, Tc^r, Sp^r and Sm^r, stand for resistance to kanamycin, gentamicin, ampicillin, tetracycline, streptomycin and spectinomycin, respectively.

******Restriction endonuclease sites are indicated in lower and underlined case

Supplementary Table 7. Summarised information from the different transcriptomic datasets used in this study.

Sequencing	Condition	Bio Project	Ref.
Macrogen	Soil	XXXXX	This study
Shanghai PSC	Water	XXXXX	This study
Macrogen	Rich B medium liquid	PRJNA660623	(de Pedro-Jové *et al.*, 2021)
Shanghai PSC	Apoplast	PRJNA660623	
Shanghai PSC	Early xylem	PRJNA660623	
Shanghai PSC	Late xylem	PRJNA660623	

Supplementary Table 8. Summarised information of the final mapped reads per sample (one pair equal two reads).

Dataset	Condition	Sample	Raw reads	% removed	Clean reads	%sortRNA	Total recovered	% mapped	Map. reads	Coverage*
Macrogen	Rich B medium liquid	philiq1	57,246,756	1.7	56,298,486	0.4	56,053,008	98.1	54,976,790	1015.9
Macrogen	Rich B medium liquid	philiq2	65,092,176	0.6	64,722,746	0.7	64,268,276	97.0	62,340,228	1152.0
Macrogen	Rich B medium liquid	philiq3	61,483,242	0.5	61,190,784	1.3	60,425,028	96.6	58,382,662	1078.8
PSG	Apoplast	Apo-10	43,758,418	0.4	43,575,646	5.6	41,118,264	95.9	39,422,184	910.6
PSG	Apoplast	Apo-7	53,533,152	0.4	53,302,646	2.9	51,743,122	95.1	49,210,595	1136.7
PSG	Apoplast	Apo-9	49,890,054	0.4	49,685,954	5.6	46,919,384	94.0	44,082,641	1018.2
PSG	Early xylem	Early-D	47,108,788	0.5	46,865,410	6.9	43,610,148	95.0	41,449,626	957.4
PSG	Early xylem	Early-E	48,205,248	0.5	47,982,572	6.3	44,943,732	94.7	42,549,868	982.8
PSG	Early xylem	Early-G	50,315,990	0.5	50,077,572	11.0	44,578,220	88.4	39,418,704	910.5
PSG	Late xylem	Fresh-xylem	46,540,276	0.5	46,303,634	1.0	45,822,376	99.4	45,527,558	1051.6
PSG	Late xylem	Xylem-E	46,619,482	0.5	46,385,834	2.3	45,330,852	98.7	44,746,624	1033.6
PSG	Late xylem	Xylem-O	49,483,808	0.5	49,239,696	1.8	48,334,962	98.7	47,685,254	1101.4
PSG	Water	water13	33,359,014	0.4	33,215,970	9.8	29,975,128	98.4	29,489,531	681.2
PSG	Water	water15	43,586,412	0.3	43,451,338	21.9	33,933,240	97.7	33,152,775	765.8
PSG	Water	water4	47,910,516	0.6	47,645,840	0.2	47,528,556	98.9	47,005,742	1085.7
Macrogen	Soil	Soil_1-A	53,033,994	0.0	53,017,672	3.3	51,285,268	10.4	5,323,411	147.6
Macrogen	Soil	Soil_1-B	53,155,404	0.0	53,135,290	7.2	49,321,968	6.4	3,176,335	88.0
Macrogen	Soil	Soil_1-C	49,170,336	0.0	49,149,170	9.0	44,701,258	10.0	4,456,715	123.5

*An approximate coverage was calculated taking the whole genome (5.4 Mbp) as reference for the sake of comparing among samples.

Supplementary Table 9. List of waters and soil used in this work. Native pH and location (also illustrated in a map) is indicated for each water. Below, the chemical analysis of the soil and location is detailed (also illustrated in a map).

Mineral Water	Native pH	Location or reference
A	8.1-8.9	41.860429, 2.455151
B	8.4-8.8	42.561222, -6.583176
C	8.3-8.4	41.633048, 2.288612
D	8.2-8.4	41.729882, 1.848878
E	8.2-8.4	42.544268, -6.594719
F	8.2-8.3	41.392743, 1.935756
G	6.8-7.0	36.920797, -3.492753

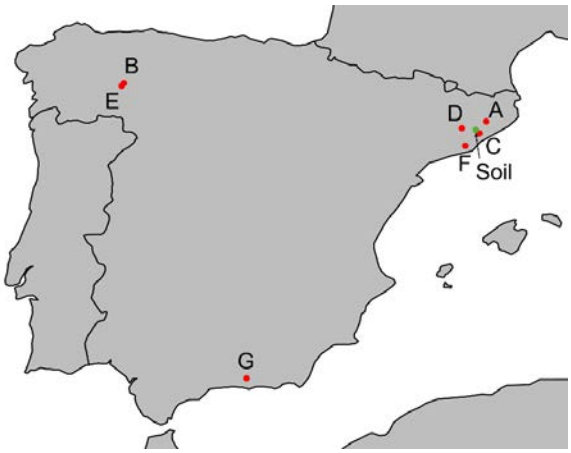

Soil chemical analysis
Location: 41.654514, 2.203791

Measured parameters	Result	Unit	Method	Evaluation
pH	7.1	pH	Potentiometry	Neutral
C.E.	0.352	dS/m	Electrometry	
Oxidable organic matter	4.67	%	Walkley.Black	Very high
Calcium carbonate equivalent	<5	% CaCO3 smn	Official Methods of Analysis M.A.P.A 1993	Inappreciable or non-calcareous
N-NO3	49.47	mg/Kg	Colorimetry	High
P Olsen	163	mg/Kg	Spectrophotometry UV-VIS	Very high
K (Ammonium acetate extraction)	576	mg/Kg	PNTS-009/ICP-MS	Very high
Mg (Ammonium acetate extraction)	300	mg/Kg	PNTS-009/ICP-MS	High
Ca (ExAmmonium acetate extraction)	1322	mg/Kg	PNTS-009/ICP-MS	Medium
Na (Ammonium acetate extraction)	40	mg/Kg	PNTS-009/ICP-MS	Not saline
S (Removable)	66	mg/Kg	ICP-MS	Medium
B (Removable)	1.06	mg/Kg	ICP-MS	High
Fe (Removable)	0.91	mg/Kg	ICP-MS	Low
Mn (Removable)	3.8	mg/Kg	ICP-MS	High
Zn (Removable)	2.17	mg/Kg	ICP-MS	High
Cu (Removable)	0.66	mg/Kg	ICP-MS	Medium
Mo (Removable)	0.02	mg/Kg	ICP-MS	Medium
Sand	61.2	%	USDA	
Slime	17.4	%	USDA	
Clay	21.4	%	USDA	

Supplementary Table 11. Statistical output files. Only significant results are shown

Figure 2B

One-way ANOVA

```
           Df    Sum Sq   Mean Sq F value Pr(>F)
Strain      4 2.623e+17 6.556e+16   47.76 <2e-16 ***
Residuals  79 1.085e+17 1.373e+15
---
Signif. codes:  0 ‘***’ 0.001 ‘**’ 0.01 ‘*’ 0.05 ‘.’ 0.1 ‘ ’ 1
```

TukeyHSD

```
  Tukey multiple comparisons of means
    95% family-wise confidence level

Fit: aov(formula = CFUSoil ~ Strain)

$Strain
                      diff        lwr       upr     p adj
KatE-WT          -3333333.3  -37813366  31146700 0.9988105
KatG-WT        -122164277.8 -156644311 -87684245 0.0000000
KatGE-WT       -122436900.0 -156916933 -87956867 0.0000000
KatG_Compl-WT   -57500000.0  -96049849 -18950151 0.0007374
KatG-KatE      -118830944.4 -153310977 -84350911 0.0000000
KatGE-KatE     -119103566.7 -153583600 -84623534 0.0000000
KatG_Compl-KatE  -54166666.7  -92716516 -15616818 0.0016968
KatGE-KatG        -272622.2  -34752655  34207411 0.9999999
KatG_Compl-KatG   64664277.8   26114429 103214127 0.0001109
KatG_Compl-KatGE  64936900.0   26387051 103486749 0.0001029
```

Figure 2D

One-way ANOVA

```
           Df    Sum Sq   Mean Sq F value  Pr(>F)
Strain      4 4.186e+17 1.046e+17    4.88 0.00176 **
Residuals  61 1.308e+18 2.144e+16
---
Signif. codes:  0 ‘***’ 0.001 ‘**’ 0.01 ‘*’ 0.05 ‘.’ 0.1 ‘ ’ 1
```

TukeyHSD

```
  Tukey multiple comparisons of means
    95% family-wise confidence level

Fit: aov(formula = CFU ~ Strain, data = micro28)

$Strain
                     diff        lwr       upr     p adj
KatE-WT        -103988942 -272040675  64062792 0.4180759
KatG-WT        -159474569 -327526302   8577164 0.0708356
KatGE-WT       -153770676 -321822409  14281057 0.0884236
KatG_Compl-WT    25955974 -127453568 179365516 0.9892877
KatG-KatE       -55485627 -223537360 112566106 0.8848955
KatGE-KatE      -49781735 -217833468 118269999 0.9194044
KatG_Compl-KatE  129944915  -23464626 283354457 0.1344559
KatGE-KatG        5703893 -162347840 173755626 0.9999807
KatG_Compl-KatG  185430543   32021001 338840085 0.0101863
KatG_Compl-KatGE 179726650   26317108 333136192 0.0137685
```

5. CHAPTER 3

PUBLICATION 2

KatE from the bacterial plant pathogen *Ralstonia solanacearum* is a monofunctional catalase controlled by HrpG that plays a major role in bacterial survival to hydrogen peroxide

Resum de la publicació 2 en català

“KatE from the bacterial plant pathogen *Ralstonia solanacearum* is a monofunctional catalase controlled by HrpG that plays a major role in bacterial survival to hydrogen peroxide”

“KatE és una catalasa monofuncional controlada per HrpG del patogen bacterià de plantes *Ralstonia solanacearum* que juga un paper essencial en la supervivència del bacteri contra peròxid d’hidrogen”

María Laura Tondo†, **Roger de Pedro-Jové**†, Agustina Vandecaveye, Laura Piskulic, Elena G. Orellano i Marc Valls

Referència: *Front. Plant Sci*. **11**:1156 (2020). https://doi.org/10.3389/fpls.2020.01156

Ralstonia solanacearum és l'agent causal de la malaltia del marciment bacterià en una àmplia gamma d'espècies vegetals. A més de les nombroses activitats bacterianes necessàries per a la invasió de l'hoste, les que estan involucrades en l'adaptació a l'ambient vegetal són clau per l’èxit de la infecció. L'habilitat de *R. solanacearum* per fer front a l'explosió oxidativa produïda per la planta és probablement una de les activitats requerides per créixer com a paràsit. Entre els múltiples enzims que neutralitzen l'estrès oxidatiu produït per les espècies reactives d'oxigen (ROS – *reactive oxygen species*) que codifica el genoma de *R. solanacearum* GMI1000, s'han identificat una sola catalasa monofuncional (KatE) i dues catalases bifuncionals KatG. En aquest treball, mostrem que aquestes activitats catalítiques estan actives en extractes proteics bacterians i que la funció de la catalasa monofuncional està associada a *katE*, com s'ha demostrat per la mutació del gen i la complementació del mutant. S'han utilitzat diferents estratègies per avaluar el paper de KatE en la fisiologia bacteriana i durant el procés d'infecció que causa el marciment bacterià. Mostrem que l'activitat de l'enzim és màxima durant el creixement exponencial *in vitro* i que aquesta regulació de la fase de creixement ocorre a nivell transcripcional. Els nostres estudis també demostren que l'expressió de *katE* és activada transcripcionalment per HrpG, un regulador central de *R. solanacearum* induït pel contacte amb cèl·lules vegetals. A més, revelem que, encara que les activitats catalítiques de KatE i KatG són induïdes pel tractament amb peròxid d'hidrogen, KatE té un major efecte sobre la supervivència bacteriana en condicions d’estrès oxidatiu i especialment en la resposta adaptativa de *R. solanacearum* a aquest estrès. El mutant del gen *katE* també va exhibir diferències en les característiques estructurals però no en la quantitat global de biofilm produït sobre superfícies abiòtiques, en comparació amb les cèl·lules salvatges. També s'ha estudiat el paper de la catalasa KatE durant la interacció amb la planta hoste, el tomàquet, revelant que la deleció d'aquest gen no té efecte sobre la virulència de *R. solanacearum* o sobre el creixement bacterià en teixits de fulla, el que suggereix el rol poc important d’aquesta catalasa en la capacitat de supervivència del bacteri dins la planta. El nostre treball proporciona la primera caracterització de les catalases de *R. solanacearum* i identifica KatE com una catalasa monofuncional genuïna amb un paper important en la protecció bacteriana contra l'estrès oxidatiu.

frontiers in Plant Science

ORIGINAL RESEARCH
published: 31 July 2020
doi: 10.3389/fpls.2020.01156

KatE From the Bacterial Plant Pathogen *Ralstonia solanacearum* Is a Monofunctional Catalase Controlled by HrpG That Plays a Major Role in Bacterial Survival to Hydrogen Peroxide

María Laura Tondo[1,2†], *Roger de Pedro-Jové*[3,4†], *Agustina Vandecaveye*[5], *Laura Piskulic*[6], *Elena G. Orellano*[1,5*] *and Marc Valls*[3,4*]

[1] Área Biología Molecular, Facultad de Ciencias Bioquímicas y Farmacéuticas, Universidad Nacional de Rosario, Rosario, Argentina, [2] Instituto de Ingeniería Ambiental, Química y Biotecnología Aplicada (INGEBIO), Facultad de Química e Ingeniería del Rosario, Pontificia Universidad Católica Argentina (UCA), Consejo Nacional de Investigaciones Científicas y Técnicas (CONICET), Rosario, Argentina, [3] Centre for Research in Agricultural Genomics (CSIC-IRTA-UAB-UB), Catalonia, Spain, [4] Department of Genetics, University of Barcelona, Barcelona, Spain, [5] Instituto de Biología Molecular y Celular de Rosario, Consejo Nacional de Investigaciones Científicas y Técnicas (CONICET), Rosario, Argentina, [6] Área Estadística y Procesamiento de Datos, Facultad de Ciencias Bioquímicas y Farmacéuticas, Universidad Nacional de Rosario, Rosario, Argentina

Ralstonia solanacearum is the causative agent of bacterial wilt disease on a wide range of plant species. Besides the numerous bacterial activities required for host invasion, those involved in the adaptation to the plant environment are key for the success of infection. *R. solanacearum* ability to cope with the oxidative burst produced by the plant is likely one of the activities required to grow parasitically. Among the multiple reactive oxygen species (ROS)-scavenging enzymes predicted in the *R. solanacearum* GMI1000 genome, a single monofunctional catalase (KatE) and two KatG bifunctional catalases were identified. In this work, we show that these catalase activities are active in bacterial protein extracts and demonstrate by gene disruption and mutant complementation that the monofunctional catalase activity is encoded by *katE.* Different strategies were used to evaluate the role of KatE in bacterial physiology and during the infection process that causes bacterial wilt. We show that the activity of the enzyme is maximal during exponential growth *in vitro* and this growth-phase regulation occurs at the transcriptional level. Our studies also demonstrate that *katE* expression is transcriptionally activated by HrpG, a central regulator of *R. solanacearum* induced upon contact with the plant cells. In addition, we reveal that even though both KatE and KatG catalase activities are induced upon hydrogen peroxide treatment, KatE has a major effect on bacterial survival under oxidative stress conditions and especially in the adaptive response of *R. solanacearum* to this oxidant. The *katE* mutant strain also exhibited differences in the structural characteristics of the biofilms developed on an abiotic surface in comparison to wild-type cells, but not in the overall amount of biofilm production. The role of catalase KatE during the interaction with its host

OPEN ACCESS

Edited by:
Benjamin Gourion, UMR2594 Laboratoire Interactions Plantes-Microorganismes (LIPM), France

Reviewed by:
Anna Katherine Block, Center for Medical, Agricultural and Veterinary Entomology, United States
Claudia S. L. Vicente, Instituto Nacional Investigaciao Agraria e Veterinaria (INIAV), Portugal

***Correspondence:**
Elena G. Orellano
orellano@ibr-conicet.gov.ar
Marc Valls
marcvalls@ub.edu

†*These authors have contributed equally to this work*

Specialty section:
This article was submitted to Plant Pathogen Interactions, a section of the journal Frontiers in Plant Science

Received: *21 May 2020*
Accepted: *16 July 2020*
Published: *31 July 2020*

Citation:
Tondo ML, de Pedro-Jové R, Vandecaveye A, Piskulic L, Orellano EG and Valls M (2020) KatE From the Bacterial Plant Pathogen Ralstonia solanacearum Is a Monofunctional Catalase Controlled by HrpG That Plays a Major Role in Bacterial Survival to Hydrogen Peroxide. Front. Plant Sci. 11:1156. doi: 10.3389/fpls.2020.01156

plant tomato is also studied, revealing that disruption of this gene has no effect on *R. solanacearum* virulence or bacterial growth in leave tissues, which suggests a minor role for this catalase in bacterial fitness *in planta*. Our work provides the first characterization of the *R. solanacearum* catalases and identifies KatE as a *bona fide* monofunctional catalase with an important role in bacterial protection against oxidative stress.

Keywords: *Ralstonia solanacearum*, bacterial wilt, oxidative burst, KatE catalase, host adaptation

INTRODUCTION

Ralstonia solanacearum is a gram-negative, soil-borne β-proteobacterium that causes the bacterial wilt disease in more than 200 plant species, including economically important food crops such as potato, tomato, peanut, and eggplant (Allen et al., 2004). In addition to its extremely wide host range, *R. solanacearum* exhibits an increasingly broad geographic distribution and is able to survive for long periods in waterways, soil and in symptomless or latently infected plants (Denny, 2006; Genin and Denny, 2012).

Upon interaction with a susceptible host, the pathogen initiates the infection by entering the roots. After colonisation of the intercellular spaces of the root cortex, the bacterium enters the xylem vessels, spreading rapidly, and systemically through the vascular system. Intensive bacterial multiplication and production of large amounts of exopolysaccharides (EPSs) blocks water traffic in vascular bundles, ultimately resulting in complete wilting, plant death, and the release of the pathogen back to the soil (Genin and Denny, 2012). *R. solanacearum* requires multiple virulence factors that act additively to facilitate infection of the host plant. Bacterial motility mediated by flagella and type IV pili, plant cell wall-degrading enzymes, and type II-secreted proteins enable bacterial penetration into root tissues. Secretion of type III effectors inside plant cells evades plant immune responses and allows disease development (Peeters et al., 2013). In the plant environment, *R. solanacearum* must overcome different types of metabolic stresses in order to survive and proliferate. One of these challenges is the exposure to plant-generated reactive oxygen species (ROS) that accumulate in the apoplast as part of the primary defence response to pathogen invasion (Lamb and Dixon, 1997).

ROS are unavoidable by-products of plant metabolic pathways generated as a result of successive one-electron reductions of molecular oxygen (O_2). Under physiological steady state conditions, ROS accumulation is prevented by the action of protective antioxidant systems often confined to specific compartments. However, adverse environmental factors including pathogen infection disturb this fine balance between production and scavenging of ROS leading to a rapid increase in intracellular ROS levels or "oxidative burst" (Apel and Hirt, 2004). In plants challenged with pathogenic microorganisms, including fungi, bacteria, and viruses, the oxidative burst proved to be one of the earliest events after elicitation (Wojtaszek, 1997). In the interaction of *R. solanacearum* with tomato plants, a single-phase ROS increase was detected at 24 h post-inoculation (hpi) of a susceptible cultivar, while a bi-phasic ROS generation with peak levels at 12 and 36 hpi was observed after infection of a resistant tomato variety (Mandal et al., 2011). The second phase of ROS accumulation, usually more prolonged and higher in magnitude, has been correlated with disease resistance *via* the hypersensitive response during incompatible and non-host interactions (Lamb and Dixon, 1997).

The oxidative burst fulfils multiple functions to plant cells undergoing pathogen attack. ROS promote the oxidative cross-linking of plant cell walls to slow pathogen entry and spread, and act as key signal molecules that mediate the activation of plant defence responses and systemic resistance (Lamb and Dixon, 1997). In addition, the high reactivity of ROS with cellular macromolecules, including DNA and proteins, make ROS effective antimicrobial agents capable of either killing the pathogen or slowing down its growth (Peng and Kuc, 1992). To counter-attack ROS, oxidative stress response genes were shown to be expressed in plant-associated bacteria during the interaction with their hosts (Smith et al., 1996; Santos et al., 2001; Okinaka et al., 2002; Saenkham et al., 2007; Tamir-Ariel et al., 2007). Particularly, an *in vivo* expression technology (IVET) screen performed in *R. solanacearum* during pathogenesis of tomato plants revealed that at least 15 out of 153 *in planta*-expressed genes encoded proteins involved in the oxidative stress response, further supporting the notion that an oxidative challenge is associated with plant infection (Brown and Allen, 2004; Flores-Cruz and Allen, 2009).

Hydrogen peroxide (H_2O_2), the major ROS of the oxidative burst, is an electrically neutral and relatively stable species that can penetrate through cell membranes and diffuse to reach distant cellular components (Wojtaszec, 1997). H_2O_2 concentrations must be kept at low levels inside bacterial cells due to its ability to oxidize ferrous ions to generate highly reactive hydroxyl radicals (·OH; Fenton reaction), and to react with iron-sulphur clusters of key metabolic enzymes (Mishra and Imlay, 2012). Among the bacterial enzymes evolved to remove ROS and avoid toxicity, catalases (E.C. 1.11.1.6; H_2O_2:H_2O_2 oxidoreductase) constitute the primary scavengers of H_2O_2 by catalyzing its dismutation to water and oxygen. Based on phylogenetic analyses, three distinct catalase families can be distinguished: typical (monofunctional) heme catalases (KatEs), bifunctional heme catalase-peroxidases (KatGs), and (non-heme) manganese catalases (MnCats) (Zámocky et al., 2012). Most sequenced bacterial genomes encode multiple catalase isozymes that operate in different physiological or environmental conditions (Mishra and Imlay, 2012). Induction of specific catalases has been observed when bacteria detect environmental ROS and

upon entry into the stationary phase (Loewen, 1997; Mishra and Imlay, 2012). In addition, recent reports have demonstrated the role of particular catalases during pathogenesis, enhancing the bacterial ability to overcome host-induced oxidative burst (Jittawuttipoka et al., 2009; Tondo et al., 2010; Mishra and Imlay, 2012). The available *R. solanacearum* GMI1000 genome encodes numerous predicted ROS-scavenging enzymes, including three putative catalases. The *RSc0775* (KatGb) and *RSc0776* (KatGa) open reading frames (ORFs) encode predicted bifunctional catalase-peroxidases in the bacterial chromosome; whereas *RSp1581* (KatE) codes for a predicted typical monofunctional catalase and is located in the megaplasmid, which harbors most *R. solanacearum* pathogenicity functions (Salanoubat et al., 2002; Genin and Denny, 2012).

Our previous transcriptomic studies in *R. solanacearum* extracted from roots of early infected potato plants indicated that the transcription of *katE* and, to a lesser extent, *katGb* is induced during plant colonisation compared to growth in rich medium (Puigvert et al., 2017). We also identified *katE* among the genes specifically induced by HrpG, a key *R. solanacearum* pathogenicity regulator that responds to direct bacterial contact with plant cells (Valls et al., 2006). In addition, *R. solanacearum* catalases are up-regulated by the transcriptional regulator OxyR, whose deletion impaired bacterial virulence (Flores-Cruz and Allen, 2011). These observations collectively suggest a role for catalases during the infection process, but the contribution of these enzymes to bacterial wilt disease has not been investigated.

Here we present a thorough study of the *R. solanacearum* KatE. We prove that this gene encodes a *bona fide* catalase enzyme responsible for one of the two catalase activities detected in this pathogen, describe its expression pattern and study its role during bacterial life *in planta*.

MATERIALS AND METHODS

Bacterial Strains, Plasmids, and Growth Conditions

Relevant characteristics of the plasmids and bacterial strains used in this work are described in **Table 1**. The wild-type strain GMI1000 of *R. solanacearum* and its *hrpG*-derivative have been previously described (Boucher et al., 1985; Valls et al., 2006). The complemented (*ΔhrpG* + *hrpG*) strain was obtained by electroporation of the *ΔhrpG* mutant with pLT-HrpG, a vector

TABLE 1 | Bacterial strains, plasmids, and primers used in this study.

Strain/plasmid	Relevant genotype and description	Source/reference
Ralstonia solanacearum		
GMI1000	Wild-type strain	Boucher et al., 1985
ΔkatE	*katE* deletion mutant in the GMI1000 background, Gm^r	This study
ΔkatE + *katE*	*ΔkatE* strain complemented with *katE* from pRCT-katE, Gm^r, Tc^r	This study
ΔhrpG	*hrpG* deletion mutant in the GMI1000 background	Valls et al., 2006
ΔhrpG + *hrpG*	*ΔhrpG* strain complemented with the overexpressing plasmid pLT-HrpG, Tc^r	This study
Escherichia coli		
JM109	*HsdR17 endA1 recal thi gyrA96 relA1 recA1 supE44* $\lambda^-\Delta$*(lac-proAB)*, [F', traD36, $proA^+B^+$, $lacI^qZ\Delta M15$]	Promega Corp.
Plasmids		
pGEM-T Easy	PCR cloning and sequencing vector, Ap^r	Promega Corp.
pGEM-UkatE	PCR-amplified (945-bp) *katE* upstream fragment, cloned in pGEM-T easy, Ap^r	This study
pGEM-DkatE	PCR-amplified (892-bp) *katE* downstream fragment, cloned in pGEM-T easy, Ap^r	This study
pCM351	Allelic exchange vector, Ap^r, Tc^r, Gm^r	Marx and Lidstrom, 2002
pCM-UDkatE	Upstream (945-bp) and downstream (892-bp) fragments of *katE* cloned into *Eco*RI/*Not*I and *Hpa*I/*Sac*I sites of pCM351, Ap^r, Tc^r, Gm^r	This study
pRCT	pRC containing tetracycline resistance and cloning sites, Ap^r, Cl^r, Tc^r	Monteiro et al., 2012b
pRCT-katE	PCR-amplified (1960-bp) fragment containing *katE* ORF and promoter sequence, cloned into *Hpa*I/*Bgl*II sites of pRCT, Ap^r, Cl^r, Tc^r	This study
pLT-HrpG	pLAFR3 derivative including the *HrpG* coding sequence under the control of the *Ptac* promoter	Valls et al., 2006
pJBA128	Vector containing *gfpmut3* under a constitutive *PlacUV5* promoter, Tc^r	Lee et al., 2005

Primer name	Sequence[a]	Amplified fragment
katEU-F	5' tagaattcGGATACTGACCGTTGCCATC 3' (*Eco*RI)	This study
katEU-R	5' tagcggccgcGAGTCTCCTGTGGGGATGAG 3' (*Not*I)	This study
katED-F	5' tagttaacGCTGCAGGACTGATGATGTG 3' (*Hpa*I)	This study
katED-R	5' tagagctcGGTCACGGATATCGAACCAC 3' (*Sac*I)	This study
UkatEU-F	5' GAATGCTTTCCGCCTTGATATC 3'	This study
Gent-R	5' CCTGCTGCGTAACATCGTTGC 3'	This study
ckatE-F	5' tagttaacTGTTTGAAGACGGTGACGTT 3' (*Hpa*I)	This study
ckatE-R	5' taagatctTCAGTCCTGCAGCTTCG 3' (*Bgl*II)	This study
katE_qPCR-F	5' TGAACAAGAACCCGGAGAAC 3'	This study
katE_qPCR-R	5' TGTCGGCATACGAGAAGATG 3'	This study

Ap^r, Gm^r, Tc^r: resistance to ampicillin (Ap), gentamicin (Gm) and tetracycline (Tc), respectively; PCR, polymerase chain reaction.
[a]Capital letters correspond to nucleotides of the R. solanacearum GMI1000 genome sequence and small letters to nucleotides added to facilitate cloning (restriction sites underlined).

that overexpress HrpG from the isopropyl-b-D-thiogalactopyranoside (IPTG)-inducible *Ptac* promoter. The plasmid and transformation procedures are described in (Valls et al., 2006). *R. solanacearum* strains were routinely grown at 28°C in tetrazolium chloride (TZC) agar plates (Kelman, 1954), complete BG medium (10 g/L bactopeptone, 1 g/L yeast extract, 1 g/L casamino acids, 0.5% glucose), or MP minimal medium supplemented with 20 mM L-glutamate as a carbon source (Plener et al., 2010). To induce HrpG expression in the complemented *ΔhrpG* + *hrpG* strain IPTG was added to the cultures at a final concentration of 100 mM. Gentamicin and tetracycline were used for selection of *R. solanacearum* strains (5 and 10 μg/mL in liquid and solid cultures, respectively). Bacterial growth was monitored by measuring optical density at 600 nm. *Escherichia coli* strains were grown at 37°C in Luria-Bertani (LB) broth supplemented with appropriate antibiotics (Sambrook and Russell, 2001).

Molecular Biology and Microbiological Techniques

Molecular cloning procedures, including DNA restriction and analysis, DNA ligation, preparation of competent cells, and transformation of *E. coli* by electroporation, were performed according to standard protocols (Ausubel et al., 1994; Sambrook and Russell, 2001). Plasmid DNA was isolated using Wizard Plus SV Minipreps DNA Purification System (Promega Corp., Madison, WI). Restriction enzymes, DNA ligase, and other DNA enzymes were used according to the manufacturers' recommendations. Total genomic DNA from *R. solanacearum* was isolated from fresh bacterial cultures as described by Chen and Kuo (Chen and Kuo, 1993). For RNA extraction and quantitative real-time PCR analysis, total RNA was extracted using the SV Total RNA Isolation Kit (Promega) following manufacturer's instructions for Gram-negative bacteria. cDNA was synthesized using the High Capacity cDNA reverse transcriptase kit (Applied Biosystems) following manufacturer's instructions. The Sybr Green Master Mix (Sigma Aldrich) was used for quantitative real-time PCR with the LightCycler 480 Instrument (Roche Life Science) using the katE_qPCR-F and katE_qPCR-R oligonucleotides as primers. Per each biological condition, duplicates were run and the phosphoserine aminotransferase gene (*serC*) was used as a reference gene for normalisation of expression as described in (Monteiro et al., 2012a).

Construction of the *R. solanacearum ΔkatE* Mutant and Complemented Strain

The *R. solanacearum ΔkatE* mutant strain was generated by inserting a gentamicin resistance cassette in substitution of the open reading frame *RSp1581* in the GMI1000 strain. Primers were designed in order to amplify 945-bp (primer pair katEU-F/katEU-R) and 892-pb (primer pair katED-F/katED-R) fragments located upstream and downstream of the gene *RSp1581*, respectively (**Table 1**). Specific restriction sites were incorporated to each primer to be used in subsequent cloning steps. PCR amplifications were performed with the proofreading Phusion DNA polymerase (New England Biolabs, Inc., Ipswich, MA, U.S.A.) following the manufacturer's conditions. The resulting fragments were cloned into pGEM-T easy (Promega Corp.) creating pGEM-UkatE and pGEM-DkatE for the upstream and downstream regions of the *katE* gene, respectively; and the identity of the inserts were confirmed by sequencing with vector primers SP6 and T7. Inserts were then excised by double digestion with *Eco*RI/*Not*I (upstream region) and *Hpa*I/*Sac*I (downstream region), and inserted into the multiple cloning sites of pCM351 (Marx and Lidstrom, 2002) on both sides of the gentamicin resistance cassette, creating pCM-UDkatE. This construction was then linearized by *Eco*RI and introduced into the wild type *R. solanacearum* GMI1000 by natural transformation following the protocol described by Boucher and associates (Boucher et al., 1985). Double recombination events were selected by gentamicin resistance on TZC agar plates and the correct insertion in the genome was confirmed by PCR using primers UkatEU-F and Gent-R, which hybridize upstream of the upper region used for the homologous recombination and in the gentamicin resistance cassette, respectively (**Table 1**). This mutant strain, denoted as *ΔkatE*, was used for phenotypic characterization.

For *ΔkatE* complementation, a 1960-bp DNA fragment containing the *katE* coding region and extending 430 pb upstream of the 5' end of the ORF was PCR amplified with primers ckatE-F and ckatE-R (**Table 1**). The amplified sequence included the putative promoter region of the *katE* gene as predicted with SoftBerry (www.softberry.com). This amplicon was double digested with *Hpa*I/*Bgl*II and cloned into the integration element of the suicide vector pRCT (Monteiro et al., 2012b) to generate recombinant plasmid pRCT-katE. This plasmid was then linearized by *Nco*I and introduced into the mutant strain *ΔkatE* by natural transformation as described above. Complemented strains were selected by tetracycline resistance on TZC agar plates. The complemented mutant strain selected for further studies was designated *ΔkatE* + *katE*.

Enzyme Activity Assay and Staining

R. solanacearum soluble cell extracts were prepared from 10 mL cultures harvested by centrifugation at 4,000 *g* for 10 min at 4°C. Bacteria were washed and resuspended in 500 μL of ice-cold 50 mM potassium phosphate buffer (pH 7.0) containing 1 mM PMSF, and then disrupted by intermittent sonication. Suspensions were clarified by centrifugation at 12,000 *g* for 20 min at 4°C. Protein concentrations in soluble cell extracts were determined by the Sedmak and Grossberg method (Sedmak and Grossberg, 1977) with bovine serum albumin as standard. Catalase activity in cell extracts was monitored through the decomposition of hydrogen peroxide by following the decrease in absorbance at 240 nm (Beers and Sizer, 1952). The assays were performed at 25°C in 50 mM potassium phosphate buffer (pH 7.0) containing 10 mM H_2O_2. To calculate the catalase specific activity an extinction coefficient of 43.6 M^{-1} cm^{-1} at 240 nm was used. One unit of catalase activity was defined as the amount of activity required to decompose 1 μmol of H_2O_2 per minute under the assay conditions.

For evaluation of catalase activity in gels, soluble protein extracts (15–25 μg) were separated by continuous electrophoresis in 8% (w/v) non-denaturing polyacrylamide gels in glycine buffer (pH 9.5). To eliminate the likelihood of multiple, potentially artifactual catalase bands, non-denaturing gels were electrophoresed

at a constant current of 10 mA. Staining for catalase activity was performed as previously described (Scandalios, 1968).

Peroxidase activity staining was performed according to Kang and associates (Kang et al., 1999) with some modifications. Briefly, aliquots of cell extracts containing 100 µg of soluble protein were electrophoresed on 8% (w/v) native polyacrylamide gels as previously described. Gels were then incubated in 0.1 M Tris-HCl (pH 7.5) containing 0.1 mg/mL 3,3'-diaminobenzidine, 9 mM H_2O_2, and 0.4 mg/mL $NiCl_2$ for approximately 30 min in the dark, until appearance of the bands.

Coomassie-stained gels were run in parallel to those used for catalase and peroxidase activity measurements to ascertain comparable protein loadings between samples.

Bacterial Survival in the Presence of Hydrogen Peroxide

To test bacterial resistance to hydrogen peroxide *R. solanacearum* overnight cultures were inoculated into fresh BG medium and grown to early exponential phase (6.5 h at 28°C and 200 rpm). Aliquots of the cultures were diluted and plated on BG-agar in order to quantify the bacterial population and then hydrogen peroxide was added to the cultures at final concentrations of 1 and 2.5 mM. After 15 min of exposure to the oxidant, samples were removed, washed once with fresh medium, serially diluted and plated on BG-agar plates.

For the induction experiments, *R. solanacearum* cultures were grown to early exponential phase (6.5 h) and incubated with sub-lethal concentrations of hydrogen peroxide (25, 50, and 100 µM) for an additional hour before being used in the killing experiments. After the induction treatment, aliquots of the cultures were washed, diluted and plated on BG-agar plates. Cultures were then treated with a lethal concentration of H_2O_2 (5 mM) for 15 min, after which samples were taken, washed once with fresh medium, serially diluted and plated on BG-agar plates.

In all cases, growth of liquid cultures was monitored spectrophotometrically by optical density at 600 nm (OD_{600}). Colonies were counted after 72 h incubation at 28°C. The percentage of survival was defined as the number of colony forming units (CFU) after treatment divided by the number of CFU prior to treatment ×100.

Biofilm Observation and Quantification

For analyses of biofilm formation *R. solanacearum* strains were modified to express the green fluorescent protein (GFP) by electroporation with plasmid pJBA128 (Lee et al., 2005). Saturated cultures of the GFP-labeled bacteria in BG medium were adjusted to an optical density at 600 nm of 0.1 and diluted 1:20 in fresh CPG medium (1 g/L casamino acids, 5 g/L glucose and 10 g/L bacteriological peptone). Then, 300 µL of the bacterial suspensions were placed onto chamber-covered glass slides (nu155411, Lab-Tek, NUNC, Naperville. IL, U.S.A.) that were statically incubated in a humidified PVC box at 28°C. All microscopic observations were performed on a Zeiss LSM880 confocal laser scanning microscope (Carl Zeiss, Jena, Germany) equipped with an argon laser and detector and filter sets for monitoring of GFP expression (excitation, 488 nm; emission, 517 nm). The images obtained were analyzed with ImageJ software (https://imagej.nih.gov).

Biofilm quantification analyses were carried out following crystal violet assay. In short, CPG overnight cultures were adjusted in CPG to an OD_{600} of 0.1. Next, 95 µL of fresh CPG and 5 µL of the adjusted culture to OD_{600} of 0.1 were added in each of the 96-well polystyrene microplates (Greiner, Kremsmünster, Austria) and incubated without shaking at 30°C during 24 h. After incubation, biomass growth was measured at OD_{600}. Next, 100 µL of 0.1% crystal violet stain was added to each well and incubated at room temperature for 30 min. Wells were washed three times with MQ-water and the stained biofilm was solubilised with 100 µL of 95% ethanol and measured at OD_{580}. Measurements were performed using SpectraMax multi-plate reader and the results normalised to biomass (OD_{580}/OD_{600}).

Pathogenicity and Bacterial Multiplication Assays in Tomato

The susceptible tomato (*Solanum lycopersicum*) cv. Marmande cultivar was grown under long-day light conditions at 25°C and 60% relative humidity. Prior to infection, three- to four-week-old plants were acclimated for 3 days at 27°C with constant light conditions (12 h light/12 h darkness). For the pathogenicity assays, plants not watered for two days were drench inoculated without root wounding with 40 mL of the bacterial suspension adjusted to 10^7 CFU/mL from an overnight culture. 20–25 plants were inoculated per strain and wilting symptoms were recorded per plant using an established semi-quantitative wilting scale ranging from 0 (no wilting) to 4 (death) (Monteiro et al., 2012b).

For bacterial growth assays *in planta*, tomato leaves were vacuum-infiltrated submerging the aerial plant into water or 10^5 CFU/mL bacterial suspensions for 20 s. In both cases, the adjuvant Silwet L-77 was added (80 µL/L suspension) to facilitate infiltration. At day 0 and 3 post infiltration, bacterial concentrations in the plant tissues were measured. To this end, three 5-mm diameter disks per biological replicate were taken from infiltrated leaves, homogenised and 10 µL of serial ten-fold dilutions were plated in selective plates. The plates were incubated at 28°C until colonies could be counted. Three biological replicas were used per bacterial strain.

Statistical Analyses

Quantitative analyses were performed with at least three independent biological samples. Data were subjected to a multifactorial mixed model ANOVA and Tukey's multiple comparison tests along with residual analysis and validation using Infostat software (Infostat 2006H, http://www.infostat.com.ar).

RESULTS

R. solanacearum RSp1581 Encodes an Active Monofunctional Catalase Induced During Exponential Growth

In order to investigate the role of *katE* in the *R. solanacearum* physiology and plant interaction, we generated a *katE* deletion mutant by genetic replacement of the *RSp1581* open reading

frame by a gentamicin resistance cassette in the GMI1000 strain background. The resulting mutant, named *ΔkatE*, exhibited typical colony morphology on tetrazolium chloride (TZC)-containing agar plates and similar growth curves to its wild-type parental strain, demonstrating that disruption of *katE* does not affect bacterial growth *in vitro* (**Supplementary Figure 1**).

To analyze the effect of *katE* deletion on *R. solanacearum* catalase activity, soluble protein extracts from cultures grown in BG medium to early exponential and stationary phase were separated on non-denaturing polyacrylamide gels and stained for catalase activity. As shown in **Figure 1A**, we detected two distinct catalase bands at both growth stages in the wild-type strain GMI1000. On the contrary, the upper, slow-migrating band was completely absent in the *ΔkatE* mutant, suggesting that this band corresponds to the KatE isozyme. As a final proof that the *RSp1581* open reading frame is functional and encodes this enzyme, complementation of *ΔkatE* with a single copy of the open reading frame under its own promoter restored the catalase activity pattern. Soluble protein extracts of the wild type, *ΔkatE* and complemented (*ΔkatE* + *katE*) strains were also run in parallel on a non-denaturing polyacrylamide gel stained for peroxidase activity (**Figure 1B**). This assay revealed that the fast-migrating catalase band detected in all three strains exhibits peroxidase activity as well, suggesting that it corresponds to one of the KatG isozymes identified in the *R. solanacearum* genome (Salanoubat et al., 2002). In adittion, the upper KatE band did not appear in the peroxidase assay further corroborating its monofunctional enzymatic nature.

The activity levels of KatE observed in native gels (**Figure 1A**) seemed to indicate that expression of this gene in *R. solanacearum* is regulated by growth phase, as previously reported for other bacterial species (Loewen, 1997; Vattanaviboon and Mongkolsuk, 2000; Tondo et al., 2010). To test this hypothesis, we measured the *katE* mRNA levels in early exponential and stationary phase cultures by quantitative real-time RT-PCR. As illustrated in **Figure 1C**, mRNA levels of *katE* significantly decreased in stationary wild type cells, being approximately 5-fold lower in the stationary phase with respect to early exponential growth phase. This expression pattern was similar in the complemented *ΔkatE* strain whereas expression was undetectable in the *katE* mutant.

KatE Expression Is Transcriptionally Activated by the HrpG Regulator

Using genome-wide expression analyses in *R. solanacearum*, we previously identified *katE* among a group of virulence and environmental adaptation genes specifically regulated by the HrpG transcriptional regulator (Valls et al., 2006). To better investigate the role of HrpG in the regulation of *katE*, we measured *katE* transcript levels in the wild-type GMI1000 strain, a *hrpG* deletion mutant (*ΔhrpG*) and the complemented mutant strain overexpressing this regulator (*ΔhrpG* + *hrpG*). *katE* mRNA levels were significantly lower in the *ΔhrpG* strain with respect to the wild-type or the complemented overexpressing strain (**Figure 2A**). This effect was more pronounced (significant differences in 95% Tukey HSD test) in minimal medium -known to specifically induce HrpG activity- than in cells grown in rich BG medium (**Figure 2A**). To evaluate the influence of this regulation at the protein level, we then measured the effect of *hrpG* on the catalase activity. Measurements of catalase activity in native polyacrylamide gels revealed the same expression pattern obtained for *katE* transcripts, with markedly lower levels in the *ΔhrpG* background that could be complemented by overexpression of this regulator (**Figure 2B**). These results show a clear correlation between *hrpG* and *katE* transcript levels and with the catalase activity as well.

R. solanacearum KatE Activity Is Enhanced Upon H_2O_2 Treatment and Protects Against Oxidative Stress

To assess the involvement of catalases in the *R. solanacearum* oxidative stress response, we exposed early exponential phase

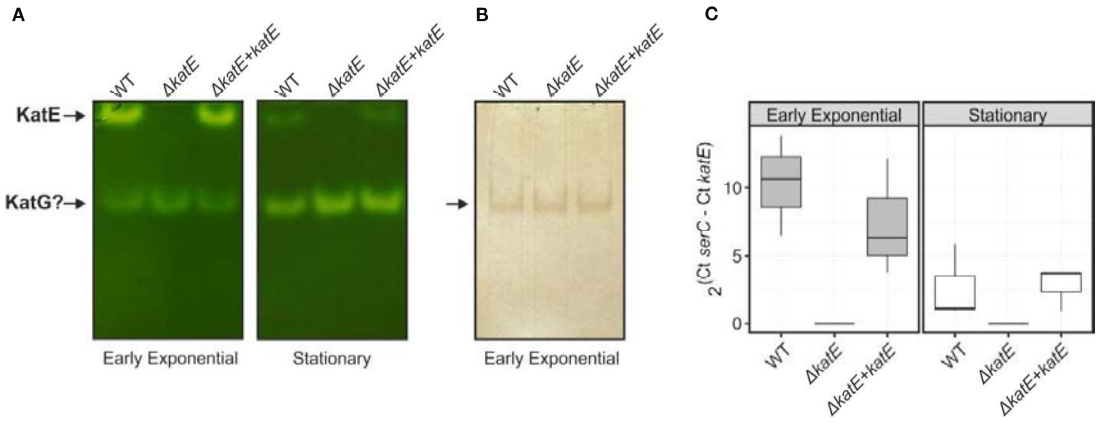

FIGURE 1 | Catalase/peroxidase activity patterns and *katE* expression in *R. solanacearum*. Equal amounts of total soluble protein extracts (25 μg) from wild-type GMI1000 strain (WT), the *katE* deletion mutant (*ΔkatE*), and the complemented (*ΔkatE* + *katE*) strain grown in BG medium to early exponential or stationary growth phases were separated on non-denaturing polyacrylamide gels stained for catalase **(A)** and peroxidase **(B)** activities. **(C)** *katE* mRNA levels measured by quantitative real-time PCR from cultures grown in the same conditions described in A. In the Y-axis is represented the $2^{\Delta Ct}$ normalised expression from three biological replicas with two technical replicas each. Experiments in A and B were repeated at least three times with similar results.

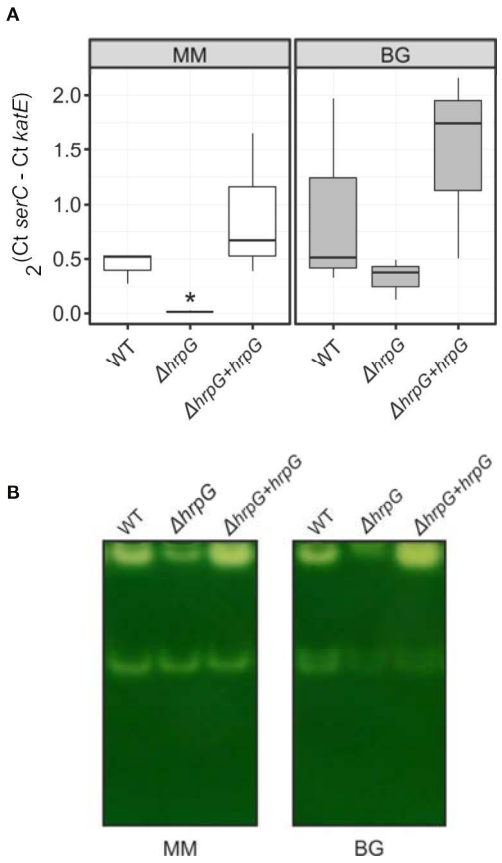

FIGURE 2 | Expression of *katE* in the wild-type (WT), *ΔhrpG* mutant, and complemented overexpressing (*ΔhrpG* + *hrpG*) strains. **(A)** mRNA levels of *katE* were measured by quantitative real-time PCR in RNAs extracted from *R. solanacearum* cells grown in rich BG or minimal medium supplemented with glutamate. In the Y-axis is represented the $2^{\Delta Ct}$ normalised expression from three biological replicas with two technical replicas each. The asterisk indicates the strain showing statistically significant differences to the other two strains tested in the same condition (95% Tukey HSD test). **(B)** Catalase activity patterns in native gels. Equal amounts of soluble proteins (25 μg) were separated by 8% non-denaturing PAGE and stained for catalase activity. A simultaneously run Coomassie-stained gel (not shown) indicated equal protein loadings between samples. This experiment was repeated three times with similar results.

cultures to a range of sub-lethal doses (25, 50, and 100 μM) of H_2O_2 for 1 h and the catalase activity patterns were compared to untreated control cultures on native polyacrylamide gels. As shown in **Figure 3A**, the activity of the two detected catalase bands increased upon H_2O_2 treatment, suggesting a clear induction of both isoforms under oxidative stress. To further evaluate the contribution of KatE to this response, we quantified the catalase activity levels in the wild type, the *ΔkatE* mutant and the complemented (*ΔkatE* + *katE*) strains grown in the conditions previously stated (**Figure 3B**). H_2O_2 treatment caused a ~5-fold increase of catalase activity in the wild-type strain, being this increment almost equivalent at all H_2O_2 concentrations tested. On the contrary, no catalase induction was observed in the *katE* mutant after peroxide exposure, suggesting an impaired ability to face the oxidative challenge.

Resistance of bacterial cells to lethal doses of H_2O_2 was then evaluated. As illustrated in **Figure 3C**, the *ΔkatE* mutant exhibited increased sensitivity to the oxidant compared to the parental wild-type strain, a phenotype that was more pronounced at higher H_2O_2 doses and maximal at the highest concentration tested (2.5 mM). Moreover, pre-adaptation of the cultures with a sub-lethal concentration of H_2O_2 (100 μM) led to a significant increase in the resistance of wild-type cells to an elevated dose (5 mM) of the agent (**Figure 3D**). This effect, commonly known as *adaptive response*, was not observed in the *ΔkatE* strain, which did not evidence higher tolerance to the oxidant after the adaptation treatment, reinforcing the notion that *katE* encodes the only catalase activity that contributes to bacterial adaptation to an oxidative environment.

Biofilm Formation Is Affected by the Deletion of *katE*

Bacterial antioxidant activities have been shown to influence biofilm formation (Kim et al., 2006; Simmons and Dybvig, 2015; Tondo et al., 2016). To analyze the structural characteristics of the *R. solanacearum* biofilm, we generated Green Fluorescent Protein (GFP)-labeled strain derivatives (**Table 1**) and observed their growth development on chambered cover glass slides by confocal laser scanning microscopy over a 5-day period. At two days post inoculation (dpi), formation of cell aggregates was apparent for the wild-type strain (**Figure 4A**), and a well-established biofilm with more complex structures was clearly observed at 5 dpi. In contrast, the *katE* mutant failed to form a structured biofilm after 5 days, exhibiting minor aggregation and reduced interstitial spaces. Besides observing the biofilm structure, we also quantified the amount of biofilm produced by measuring the intensity of crystal violet staining after growth on 96-well plates. As shown in **Figure 4B**, these experiments resulted in comparable quantities of biofilm in the wild type, the *katE* mutant and its genetically complemented derivative, demonstrating that KatE influences the development of biofilm structures but does not alter the overall amount of biofilm produced.

Pathogenicity Tests

As mentioned previously, *katE* transcription is activated by the master regulator of pathogenicity HrpG (**Figure 2**). In addition, our preliminary data show that *katE* from *R. solanacearum* strain UY031 is highly expressed when the bacterium grows in the plant apoplast and in the xylem (unpublished data). This information, together with our finding that catalase activity was key to survive oxidative stress led us to test whether it is required for *R. solanacearum* GMI1000 pathogenicity on tomato, its natural host. Plants of the susceptible tomato cultivar Marmande were inoculated with suspensions of the wild type, mutant, and complemented strains by soil drenching and symptom appearance was recorded over time (**Figure 5A**). No statistical differences in wilting symptoms in plants inoculated with the wild type, the *katE* disruption mutant or the complemented strain were observed in three biological replicas,

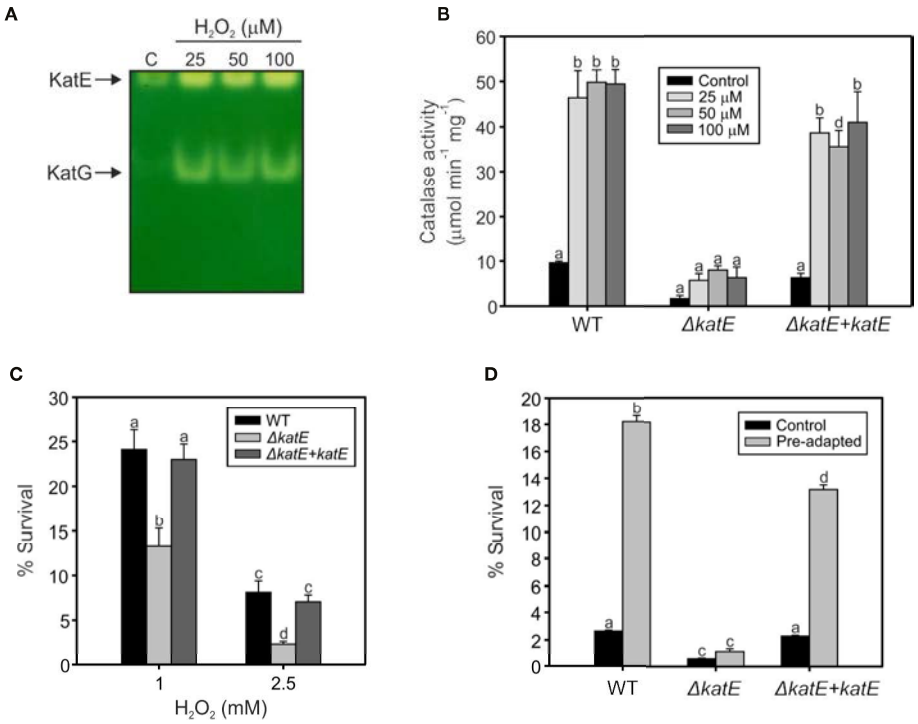

FIGURE 3 | Hydrogen peroxide response in wild type, the *ΔkatE* mutant, and its complemented counterpart. **(A)** Catalase activities detected after exposure to sub-lethal levels of hydrogen peroxide. Equal amounts (15 μg) of soluble protein extracts from early exponential phase cultures exposed to 25, 50, and 100 μM of H_2O_2 for 60 min, and from an untreated control (C), were separated on a native polyacrylamide gel stained for catalase activity. **(B)** Catalase activities quantified through H_2O_2 decomposition in soluble cell extracts obtained from cells treated as in A. **(C)** Sensitivity of *R. solanacearum* strains to 1 and 2.5 mM H_2O_2. Cells in early exponential phase of growth were exposed to the indicated concentrations of H_2O_2 for 15 min. The number of Colony Forming Units (CFU) was determined for each culture before and after the peroxide treatment by plating of appropriate dilutions. The percentage of survival is defined as the number of CFU after treatment divided by the number of CFU prior to H_2O_2 exposure ×100. **(D)** Sensitivity of pre-adapted cultures of WT, *ΔkatE*, and the complemented *ΔkatE* + *katE* strains to 5 mM H_2O_2. Exponential phase cultures were first adapted with 100 μM H_2O_2 for 60 min and then exposed to 5 mM H_2O_2 for 15 min. The number of CFU was determined for each culture before and after the 5 mM H_2O_2 treatment by plating of appropriate dilutions and percentage of survival calculated as the number of CFU after treatment divided by the number of CFU prior to treatment ×100. Data represent the mean and standard deviation of three independent experiments. Different letters indicate significant differences among strains and/or treatment according to the Tukey's multiple comparison test ($p<0.0001$).

suggesting no major role of the gene in the virulence of *R. solanacearum* GMI1000. The importance of apoplastic ROS led us to quantify whether bacterial fitness was affected during growth in this plant compartment. To this end, we infiltrated susceptible tomato leaves with solutions of the wild type, the *ΔkatE*, and the complemented strain and quantified bacterial concentrations in recovered leaf disk samples immediately after inoculation and at three days post inoculation (dpi). Results from a representative experiment are presented in **Figure 5B** and show that no differences in bacterial multiplication in the apoplast were observed for any of the three tested strains.

DISCUSSION

It has been shown that hydrogen peroxide is a central component of the oxidative burst during plant-pathogen interaction, as it accumulates in plants attacked by pathogenic microorganisms including fungi, bacteria and viruses (Baker and Orlandi, 1995; Wojtaszek, 1997). In this context, the antioxidant system adequacy by the invading microorganism must be fundamental to minimize the oxidative stress generated by the host plant, thus achieving the establishment of the infection. In this work, we demonstrated that monofunctional KatE and bifunctional KatG catalase activities can be detected in *R. solanacearum* soluble protein extracts using non-denaturing polyacrylamide gels (**Figure 1A**). Furthermore, a single mutant in the *katE* gene was generated and genetically complemented corroborating that the upper band revealed in the native gel corresponds to the KatE catalase.

We evaluated catalase activities during the different growth phases, detecting that the monofunctional catalase was induced during exponential growth (**Figures 1A, C**). These results collectively suggest that *katE* expression is growth phase regulated at the transcriptional level. Similar results were previously reported for other bacteria such as *E. coli, Xanthomonas campestris* pv. *campestris* and *Xanthomonas citri* subsp. *citri*, although the expression pattern of particular catalase isozymes may vary between species (Loewen, 1997; Vattanaviboon and Mongkolsuk,

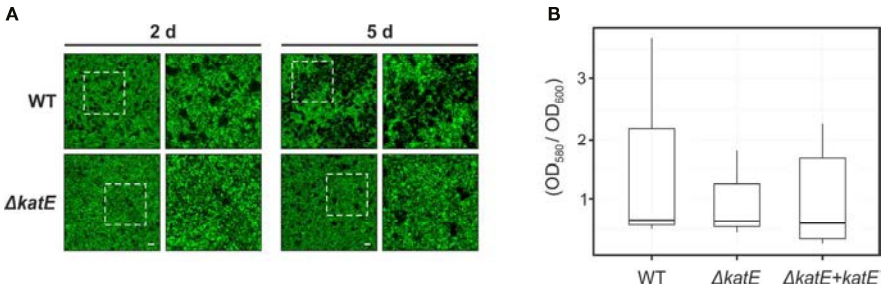

FIGURE 4 | Effect of *katE* disruption on *R. solanacearum* biofilm formation ability. **(A)** GFP-labeled wild-type and *ΔkatE* strains were grown on chambered cover slides and visualized under confocal laser scanning microscopy after 2 and 5 days of bacterial growth. Left panels show the biofilms developed at the bottom of the chambered cover slides with a magnification of 400X and right panels show a 2X zoom of the regions marked in the previous panels. Scale bars, 50 µm. **(B)** Biofilm quantification. Bacterial suspensions were grown for 24 h in 96 well plates at 30°C, stained with crystal violet and the biofilm was quantified as the OD_{580} normalized by the bacterial growth measured at OD_{600}. Boxplots of the values obtained per each tested strain from 5-6 biological replicas (N=5-6) are presented.

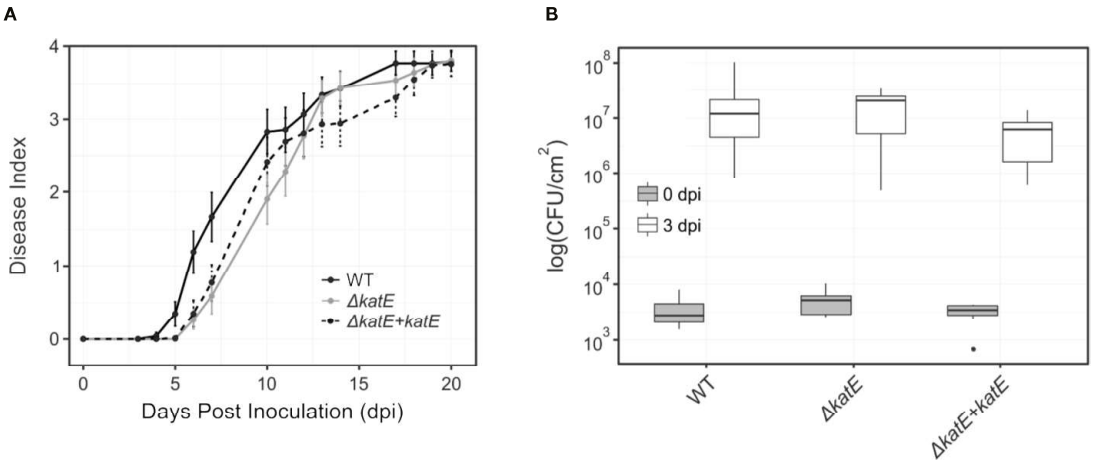

FIGURE 5 | Effect of *katE* in *R. solanacearum* virulence and fitness in the apoplast. **(A)** Bacterial pathogenicity assay on tomato. Wilting symptoms were recorded after soil-drench inoculation with the wild type *R. solanacearum* GMI1000 strain (black line), the *katE* disruption mutant derivative (grey line) and its complemented strain (dotted black line). Disease symptoms are plotted over time in a scale ranging from 0 (no symptoms) to 4 (wilted plant). Each data point represents the average of 20-25 plants and their standard errors. Three independent biological replicates were performed with similar results. **(B)** Bacterial growth in leave tissues. Tomato plants were vacuum infiltrated with 10^5 CFU/mL suspensions of GMI1000, the *katE* mutant, and the complemented strain. Leaf disks were sampled at day 0 and 3 post inoculation, and bacterial counts in the tissue were determined as CFU from plated dilutions normalized to the disk area sampled (N=3). All experiments were repeated three times with similar results.

2000; Tondo et al., 2010). In *X. citri* subsp. *citri*, *katE* gene was also regulated by growth phase but contrary to the pattern observed in *R. solanacearum*, it exhibited an strong induction in stationary phase cells (Tondo et al., 2010).

Our results show that *katE* is transcriptionally activated by HrpG but also responds to other inducing cues besides the growth phase, as shown by the higher transcriptional output observed upon growth in BG rich medium than in minimal medium, a condition known to induce HrpG activity (**Figure 2A**). This specific induction in rich medium independently of HrpG is corroborated by the high *katE* mRNA levels in the *ΔhrpG* mutant strain grown in this medium. Finally, *katE* expression seems to be controlled mostly at the transcriptional level, as the levels of the KatE enzyme mostly correlate with its mRNA abundance, although protein stability may be increased post-translationally in minimal medium, as indicated by the fact that it can be detected in the *ΔhrpG* mutant strain grown in this condition, where it shows minimal transcription levels (**Figures 2A, B**).

On the other hand, we studied the participation of the two *Ralstonia* catalases in the resistance against the oxidizing compound hydrogen peroxide. *R. solanacearum* exponential cultures were exposed to sub-lethal doses of peroxide, detecting

a clear induction of both catalase isoforms under oxidative stress (**Figure 3A**). These results are in agreement with those obtained by Florez-Cruz and Allen, who observed an OxyR-dependent induction of *katE* and *katG* mRNA levels after exposure to H_2O_2 (Flores-Cruz and Allen, 2009). Here, the contribution of KatE to this response was analyzed (**Figure 3B**). Quantification of *R. solanacearum* catalase activity in the *ΔkatE* mutant showed that it is almost residual and that its induction is undetectable (**Figure 3B**). The catalase activity was recovered in the complemented strain, where *katE* was reintroduced into the mutant background, and showing that KatE plays a significant role in the *R. solanacearum* protection to oxidative stress. To prove this, bacterial cultures were confronted to lethal doses of H_2O_2 detecting that the *ΔkatE* mutant was more susceptible to the oxidative compound than the wild type strain (**Figure 3C**). This is in agreement with the reported observations that disruption of the monofunctional catalase *katE* in *X. citri* subsp. *citri* and *katB* in *Pseudomonas syringae* pv. tomato DC3000 rendered these bacteria more susceptible to oxidative stress (Tondo et al., 2010; Guo et al., 2012). The other monofunctional catalase in *P. syringae* pv. tomato (KatE), which is clearly less induced by exposure to exogenous H_2O_2, also showed a minor role in resistance to the oxidative compound (Guo et al., 2012).

The adaptive response to oxidative agents has been previously proposed to play a fundamental role in plant-pathogen interactions, allowing bacteria to withstand increased oxidative stress conditions (Ausubel, 2005). Exposure to sub-lethal concentrations of oxidative stress agents usually have a priming effect on bacteria, which then tolerate higher doses of the same oxidant (adaptive response), and even others (cross-protection). These responses are due to the induction of numerous genes involved in oxidant removal and damage repair, including catalases (Demple, 1991; Tartaglia et al., 1991). Evaluation of this response in *R. solanacearum* showed that *katE* mutant does not significantly induce catalase activity upon treatment with low doses of H_2O_2 and its remained activity is not enough to protect bacteria against higher doses of the oxidant (**Figures 3B, D**). Consequently, even though KatG activity was found induced in peroxide-treated cultures according to in-gel catalase staining, our results suggest a minor role for the additional KatG catalases in the response to H_2O_2, being KatE the only catalase activity contributing to the bacterial adaptive response to an oxidative environment.

Our finding that KatE catalase activity was essential for survival in oxidative environments and the fact that ROS is a major player in plant defence responses (Wojtaszec, 1997; Flores-Cruz and Allen, 2009) led us to investigate its role in bacterial virulence. Surprisingly, we found no effect of the *katE* mutation on pathogenicity assays on tomato (**Figure 5A**). This could be due to the limited sensitivity of soil drench inoculation and disease scoring to detect minor differences in bacterial pathogenicity. An alternative explanation is that ROS accumulate mainly in the apoplast (Lamb and Dixon, 1997) and *R. solanacearum* grows mostly inside the xylem vessels of host plants. Thus, we measured the capacity of the bacterium to multiply in the tomato apoplast as a more quantitative measurement of its virulence and fitness. Again, disruption of *katE* did not cause any effect (**Figure 5B**). Although bacterial multiplication in the host is not always correlated with its aggressiveness (Angot et al., 2006), this result was somehow unexpected due to the important role played by the KatE catalase in *in vitro* protection to oxidative stress, a condition that is commonly encountered by bacteria inside the plant host (Lamb and Dixon, 1997).

In addition, the *katE* mutant strain did not show reduced ability to produce biofilms, another important trait for the wilting disease development (**Figure 4**). Biofilm-growing cells usually experience endogenous oxidative stress and many antioxidant systems were shown to be induced under this growth condition (Resch et al., 2005; Ram et al., 2005; Mikkelsen et al., 2007; Shanks et al., 2007; Chung et al., 2016). In fact, the role of catalase and superoxide dismutase in the development of mature biofilms was previously demonstrated in *X. citri* subsp. *citri* and *E. coli*, respectively (Kim et al., 2006; Tondo et al., 2016). According to our results, disruption of *katE* in *R. solanacearum* only alters the structure of the biofilm produced on an abiotic surface, but not the overall quantity of biofilm production. This is in agreement with previous reports indicating that perturbations of the physiological steady-state levels of ROS or the addition of catalase to the medium affects the quality and structural characteristics of the biofilms developed by *Azotobacter vinelandii* (Villa et al., 2012) and *Mycoplasma pneumoniae* (Simmons and Dybvig, 2015), with diverse effects on the amounts of biofilm produced.

However, the minor role that KatE seems to play *in planta* is in agreement with a previous screening for *R. solanacearum* genes essential for growth *in planta*, in which *katE* was not identified (Brown and Allen, 2004). The two possible explanations for the undetectable effect of *R. solanacearum katE* disruption on plant infection are, that ROS are not key players in the defence against this pathogen in tomato cv Marmande or that functional redundancy with other genes with catalase activity exists. The three catalases in *P. syringae* pv. tomato DC3000 are all plant induced and play non-redundant roles in virulence (Guo et al., 2012). Our results corroborate the hypothesis proposed by Guo *et al.* that catalases play different roles in each plant pathogen where they independently adapted to overcome the plant defensive production of H_2O_2. Our ongoing characterisation of the KatG catalases-peroxidases will be essential to shed light into this question.

DATA AVAILABILITY STATEMENT

All datasets presented in this study are included in the article/ **Supplementary Material**.

AUTHOR CONTRIBUTIONS

MLT, MV, and EO conceived and designed the work. MLT, RP-J, and AV performed the experiments. LP and RP-J contributed to

statistical analyses. EO and MV provided reagents and materials. All authors contributed to analysis and interpretation of results. MLT, RP-J, MV, and EO wrote the manuscript. All authors contributed to the article and approved the submitted version.

FUNDING

This work was supported by the Agencia Nacional de Promoción Científica y Tecnológica (ANPCyT PICT 2014-2487 to EO and PICT 2014-2485 to MLT) and the Spanish Ministry of Economy and Competitiveness (AGL2016-78002-R and PID2019-108595RB-I00 to MV). We also acknowledge financial support from the "Severo Ochoa Program for Centers of Excellence in R&D" (SEV/2015/0533), and the CERCA Program from the Catalan Government (Generalitat de Catalunya). The funders had no role in study design, data collection and analysis, decision to publish, or preparation of the manuscript. EO and MLT are staff members and AV is Fellow of the Consejo Nacional de Investigaciones Científicas y Técnicas (CONICET, Argentina).

ACKNOWLEDGMENTS

We are grateful to Núria S. Coll and the Bacterial Pathogens and Plant Cell Death Team (Center for Research in Agricultural Genomics, CRAG) for critical comments and Jordi Corral (Autonomous University of Barcelona) for useful suggestions. We also thank Rodrigo Vena (IBR-CONICET) for confocal microscopy analyses.

SUPPLEMENTARY MATERIAL

The Supplementary Material for this article can be found online at: https://www.frontiersin.org/articles/10.3389/fpls.2020.01156/full#supplementary-material

SUPPLEMENTARY FIGURE 1 | Growth curves of *R. solanacearum* GMI1000 wild-type (WT), *katE* mutant (*ΔkatE*) and complemented (*ΔkatE* + *katE*) strains in BG medium. *R. solanacearum* cultures were grown aerobically at 28°C with shaking at 200 rpm. Aliquots were taken at the indicated times and measured for colony-forming capacity by serial dilution and plating on BG-agar. Colonies were counted after 48 h incubation at 28°C.

REFERENCES

Allen, C., Prior, P., and Hayward, A. C. (2004). *Bacterial Wilt Disease and the Ralstonia solanacearum Species Complex* (St. Paul (Minnesota): American Phytopathological Society Press).

Angot, A., Peeters, N., Lechner, E., Vailleau, F., Baud, C., Gentzbittel, L., et al. (2006). *Ralstonia solanacearum* requires F-box-like domain-containing type III effectors to promote disease on several host plants. *Proc. Natl. Acad. Sci. U.S.A.* 103 (39), 14620–14625. doi: 10.1073/pnas.0509393103

Apel, K., and Hirt, H. (2004). Reactive oxygen species: metabolism, oxidative stress, and signal transduction. *Annu. Rev. Plant Biol.* 55, 373–399. doi: 10.1146/annurev.arplant.55.031903.141701

Ausubel, F. M., Brent, R., Kingston, R. E., Moore, D. D., Seidman, J. G., Smith, J. A., et al. (1994). *Current Protocols in Molecular Biology* (New York: John Wiley and Sons).

Ausubel, F. M. (2005). Are innate immune signaling pathways in plants and animals conserved? *Nat. Immunol.* 6, 973–979. doi: 10.1038/ni1253

Baker, C. J., and Orlandi, E. W. (1995). Active oxygen in plant pathogenesis. *Annu. Rev. Phytopathol.* 33, 299–321. doi: 10.1146/annurev.py.33.090195.001503

Beers, R. F. Jr, and Sizer, I. W. (1952). A spectrophotometric method for measuring the breakdown of hydrogen peroxide by catalase. *J. Biol. Chem.* 195, 133–140.

Boucher, C. A., Barberis, P. A., Trigalet, A. P., and Demery, D. A. (1985). Transposon mutagenesis of *Pseudomonas solanacearum*: Isolation of Tn5-induced avirulent mutants. *J. Gen. Microbiol.* 131, 2449–2457. doi: 10.1099/00221287-131-9-2449

Brown, D. G., and Allen, C. (2004). *Ralstonia solanacearum* genes induced during growth in tomato: an inside view of bacterial wilt. *Mol. Microbiol.* 53 (6), 1641–1660. doi: 10.1111/j.1365-2958.2004.04237.x

Chen, W. P., and Kuo, T. T. (1993). A simple and rapid method for the preparation of gram-negative genomic DNA. *Nucleic Acids Res.* 21, 2260. doi: 10.1093/nar/21.9.2260

Chung, C.-H., Fen, S., Yu, S.-C., and Wong, H. (2016). Influence of *oxyR* on growth, biofilm formation, and mobility of *Vibrio parahaemolyticus*. *Appl. Environ. Microbiol.* 82, 788–796. doi: 10.1128/AEM.02818-15

Demple, B. (1991). Regulation of bacterial oxidative stress genes. *Annu. Rev. Genet.* 25, 315–337. doi: 10.1146/annurev.ge.25.120191.001531

Denny, T. P. (2006). "Plant pathogenic Ralstonia species," in *Plant-Associated Bacteria*. Ed. S. S. Gnanamanickam (Dordrecht, The Netherlands: Springer), 573–644.

Flores-Cruz, Z., and Allen, C. (2009). *Ralstonia solanacearum* encounters an oxidative environment during tomato infection. *Mol. Plant-Microbe Interact.* 22, 773–782. doi: 10.1094/MPMI-22-7-0773

Flores-Cruz, Z., and Allen, C. (2011). Necessity of OxyR for the hydrogen peroxide stress response and full virulence in *Ralstonia solanacearum*. *Appl. Environ. Microbiol.* 77, 6426–6432. doi: 10.1128/AEM.05813-11

Genin, S., and Denny, T. P. (2012). Pathogenomics of the *Ralstonia solanacearum* species complex. *Annu. Rev. Phytopathol.* 50, 67–89. doi: 10.1146/annurev-phyto-081211-173000

Guo, M., Block, A., Bryan, C. D., Becker, D. F., and Alfano, J. R. (2012). *Pseudomonas syringae* catalases are collectively required for plant pathogenesis. *J. Bacteriol.* 194, 5054–5064. doi: 10.1128/JB.00999-12

Jittawuttipoka, T., Buranajitpakorn, S., Vattanaviboon, P., and Mongkolsuk, S. (2009). The catalase-peroxidase KatG is required for virulence of *Xanthomonas campestris* pv. campestris in a host plant by providing protection against low levels of H_2O_2. *J. Bacteriol.* 191, 7372–7377. doi: 10.1128/JB.00788-09

Kang, K.-S., Lim, C.-J., Han, T.-J., Kim, J.-C., and Jin, C.-D. (1999). Changes in the isozyme composition of antioxidant enzymes in response to aminotriazole in leaves of *Arabidopsis thaliana*. *J. Plant Biol.* 42, 187–193. doi: 10.1007/BF03030477

Kelman, A. (1954). The relationship of pathogenicity of *Pseudomonas solanacearum* to colony appearance in tetrazolium medium. *Phytopathology* 44, 693–695.

Kim, Y. H., Lee, Y., Kim, S., Yeom, J., Yeom, S., Seok, K. B., et al. (2006). The role of periplasmic antioxidant enzymes (superoxide dismutase and thiol peroxidase) of the Shiga toxin-producing *Escherichia coli* O157:H7 in the formation of biofilms. *Proteomics* 6, 6181–6193. doi: 10.1002/pmic.200600320

Lamb, C., and Dixon, R. A. (1997). The oxidative burst in plant disease resistance. *Annu. Rev. Plant Physiol. Plant Mol. Biol.* 48, 251–275. doi: 10.1146/annurev.arplant.48.1.251

Lee, B., Haagensen, J. A., Ciofu, O., Andersen, J. B., Hoiby, N., and Molin, S. (2005). Heterogeneity of biofilms formed by nonmucoid *Pseudomonas aeruginosa* isolates from patients with cystic fibrosis. *J. Clin. Microbiol.* 43, 5247–5255. doi: 10.1128/JCM.43.10.5247-5255.2005

Loewen, P. C. (1997). "Bacterial catalases," in *Oxidative Stress and the Molecular Biology of Antioxidant Defenses*. Ed. J. G. Scandalios (New York: Cold Spring Harbor Laboratory Press), 273–308.

Mandal, S., Das, R. K., and Mishra, S. (2011). Differential occurrence of oxidative burst and antioxidative mechanism in compatible and incompatible interactions of *Solanum lycopersicum* and *Ralstonia solanacearum*. *Plant Physiol. Biochem.* 49 (2), 117–123. doi: 10.1016/j.plaphy.2010.10.006

Marx, C. J., and Lidstrom, M. E. (2002). Broad-host-range *cre-lox* system for antibiotic marker recycling in Gram-negative bacteria. *Biotechniques* 33 (5), 1062–1067. doi: 10.2144/02335rr01

Mikkelsen, H., Duck, Z., Lilley, K. S., and Welch, M. (2007). Interrelationships between colonies, biofilms, and planktonic cells of *Pseudomonas aeruginosa*. *J. Bacteriol.* 189, 2411–2416. doi: 10.1128/JB.01687-06

Mishra, S., and Imlay, J. (2012). Why do bacteria use so many enzymes to scavenge hydrogen peroxide? *Arch. Biochem. Biophys.* 525 (2), 145–160. doi: 10.1016/j.abb.2012.04.014

Monteiro, F., Genin, S., van Dijk, I., and Valls, M. (2012a). A luminescent reporter evidences active expression of *Ralstonia solanacearum* type III secretion system genes throughout plant infection. *Microbiology* 158, 2107–2116. doi: 10.1099/mic.0.058610-0

Monteiro, F., Solé, M., van Dijk, I., and Valls, M. (2012b). A chromosomal insertion toolbox for promoter probing, mutant complementation, and pathogenicity studies in *Ralstonia solanacearum*. *Mol. Plant-Microbe Interact.* 25, 557–568. doi: 10.1094/MPMI-07-11-0201

Okinaka, Y., Yang, C.-H., Perna, N. T., and Keen, N. T. (2002). Microarray profiling of *Erwinia chrysanthemi* 3937 genes that are regulated during plant infection. *Mol. Plant-Microbe Interact.* 15, 619–629. doi: 10.1094/MPMI.2002.15.7.619

Peeters, N., Guidot, A., Vailleau, F., and Valls, M. (2013). *Ralstonia solanacearum*, a widespread bacterial plant pathogen in the post-genomic era. *Mol. Plant Pathol.* 14 (7), 651–662. doi: 10.1111/mpp.12038

Peng, M., and Kuc, J. (1992). Peroxidase-generated hydrogen peroxide as a source of antifungal activity *in vitro* and on tobacco leaf disks. *Phytopathology* 82, 696–699. doi: 10.1094/Phyto-82-696

Plener, L., Manfredi, P., Valls, M., and Genin, S. (2010). PrhG, a transcriptional regulator responding to growth conditions, is involved in the control of the type III secretion system regulon in *Ralstonia solanacearum*. *J. Bacteriol.* 192, 1011–1019. doi: 10.1128/JB.01189-09

Puigvert, M., Guarischi-Sousa, R., Zuluaga, P., Coll, N. S., Macho, A. P., Setubal, J. C., et al. (2017). Transcriptomes of *Ralstonia solanacearum* during root colonization of *Solanum commersonii*. *Front. Plant Sci.* 8, 370. doi: 10.3389/fpls.2017.00370

Ram, R. J., Verberkmoes, N. C., Thelen, M. P., Tyson, G. W., Baker, B. J., Blake, R. C., et al. (2005). Community proteomics of a natural microbial biofilm. *Science* 308, 1915–1920. doi: 10.1126/science.1109070

Resch, A., Rosenstein, R., Nerz, C., and Gotz, F. (2005). Differential gene expression profiling of *Staphylococcus aureus* cultivated under biofilm and planktonic conditions. *Appl. Environ. Microbiol.* 71, 2663–2676. doi: 10.1128/AEM.71.5.2663-2676.2005

Saenkham, P., Eiamphungporn, W., Farrand, S., Vattanaviboon, P., and Mongkolsuk, S. (2007). Multiple superoxide dismutases in *Agrobacterium tumefaciens*: functional analysis, gene regulation, and influence on tumorigenesis. *J. Bacteriol.* 189, 8807–8817. doi: 10.1128/JB.00960-07

Salanoubat, M., Genin, S., Artiguenave, F., Gouzy, J., Mangenot, S., Arlat, M., et al. (2002). Genome sequence of the plant pathogen *Ralstonia solanacearum*. *Nature* 415, 497–502. doi: 10.1038/415497a

Sambrook, J., and Russell, D. W. (2001). *Molecular Cloning: A Laboratory Manual* (New York: Cold Spring Harbor Laboratory Press).

Santos, R., Franza, T., Laporte, M. L., Sauvage, C., Touati, D., and Expert, D. (2001). Essential role of superoxide dismutase on the pathogenicity of *Erwinia chrysanthemi* strain 3937. *Mol. Plant-Microbe Interact.* 14, 758–767. doi: 10.1094/MPMI.2001.14.6.758

Scandalios, J. G. (1968). Genetic control of multiple molecular forms of catalase in maize. *Ann. N. Y. Acad. Sci.* 151, 274–293. doi: 10.1111/j.1749-6632.1968.tb11896.x

Sedmak, J. J., and Grossberg, S. E. (1977). A rapid, sensitive, and versatile assay for protein using Coomassie brilliant blue G250. *Anal. Biochem.* 79, 544–552. doi: 10.1016/0003-2697(77)90428-6

Shanks, R. M., Stella, N. A., Kalivoda, E. J., Doe, M. R., O'Dee, D. M., Lathrop, K. L., et al. (2007). A *Serratia marcescens* OxyR homolog mediates surface attachment and biofilm formation. *J. Bacteriol.* 189, 7262–7272. doi: 10.1128/JB.00859-07

Simmons, W. L., and Dybvig, K. (2015). Catalase enhances growth and biofilm production of *Mycoplasma pneumoniae*. *Curr. Microbiol.* 71 (2), 190–194. doi: 10.1007/s00284-015-0822-x

Smith, S. G., Wilson, T. J., Dow, J. M., and Daniels, M. J. (1996). A gene for superoxide dismutase from *Xanthomonas campestris* pv. campestris and its expression during bacterial-plant interactions. *Mol. Plant-Microbe Interact.* 9, 584–593. doi: 10.1094/mpmi-9-0584

Tamir-Ariel, D., Navon, N., and Burdman, S. (2007). Identification of genes in *Xanthomonas campestris* pv. vesicatoria induced during its interaction with tomato. *J. Bacteriol.* 189, 6359–6371. doi: 10.1128/JB.00320-07

Tartaglia, L. A., Storz, G., Farr, S. B., and Ames, B. N. (1991). "The bacterial adaptation to hydrogen peroxide stress," in *Oxidative stress, oxidants and antioxidant*. Ed. H. Sies (New York: Academic Press), 155–169.

Tondo, M. L., Petrocelli, S., Ottado, J., and Orellano, E. G. (2010). The monofunctional catalase KatE of *Xanthomonas axonopodis* pv. citri is required for full virulence in citrus plants. *PloS One* 5 (5), e10803. doi: 10.1371/journal.pone.0010803

Tondo, M. L., Delprato, M. L., Kraiselburd, I., Fernández Zenoff, M. V., Farías, M. E., and Orellano, E. G. (2016). KatG, the bifunctional catalase of *Xanthomonas citri* subsp. citri, responds to hydrogen peroxide and contributes to epiphytic survival on citrus leaves. *PloS One* 11 (3), e0151657. doi: 10.1371/journal.pone.0151657

Valls, M., Genin, S., and Boucher, C. (2006). Integrated regulation of the type III secretion system and other virulence determinants in *Ralstonia solanacearum*. *PloS Pathog.* 2 (8), e82. doi: 10.1371/journal.ppat.0020082

Vattanaviboon, P., and Mongkolsuk, S. (2000). Expression analysis and characterization of the mutant of a growth-phase- and starvation-regulated monofunctional catalase gene from *Xanthomonas campestris* pv. phaseoli. *Gene* 241, 259–265. doi: 10.1016/s0378-1119(99)00483-7

Villa, F., Remelli, W., Forlani, F., Gambino, M., Landini, P., and Cappitelli, F. (2012). Effects of chronic sub-lethal oxidative stress on biofilm formation by *Azotobacter vinelandii*. *Biofouling* 28 (8), 823–833. doi: 10.1080/08927014.2012.715285

Wojtaszek, P. (1997). Oxidative burst: an early plant response to pathogen infection. *Biochem. J.* 322 (3), 681–692. doi: 10.1042/bj3220681

Zámocky, M., Gasselhuber, B., Furtmüller, P. G., and Obinger, C. (2012). Molecular evolution of hydrogen peroxide degrading enzymes. *Arch. Biochem. Biophys.* 525 (2), 131–144. doi: 10.1016/j.abb.2012.01.017

Conflict of Interest: The authors declare that the research was conducted in the absence of any commercial or financial relationships that could be construed as a potential conflict of interest.

Supplementary Data

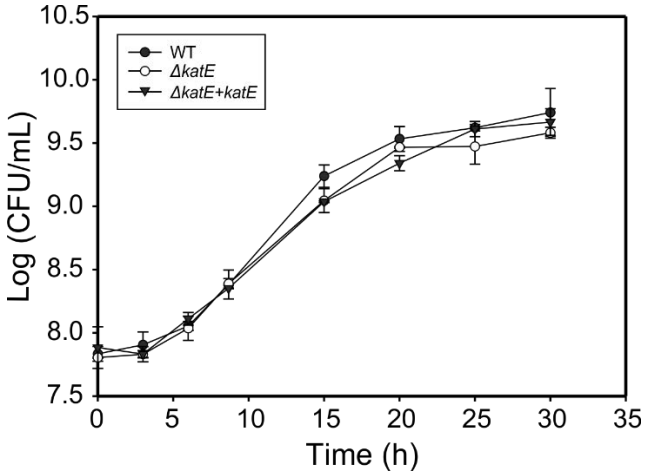

Supplementary Figure 1 | Growth curves of *R. solanacearum* GMI1000 wild-type (WT), *katE* mutant (Δ*katE*) and complemented (Δ*katE* + *katE*) strains in BG medium. *R. solanacearum* cultures were grown aerobically at 28 ºC with shaking at 200 rpm. Aliquots were taken at the indicated times and measured for colony-forming capacity by serial dilution and plating on BG-agar. Colonies were counted after 48 h incubation at 28 ºC

6. CHAPTER 4

DRAFT 2

The secretome of *Ralstonia solanacearum* within the host plant unravels a family of S8 serine proteases potentially involved in virulence

Resum de l'esborrany 2 en català

"The secretome of *Ralstonia solanacearum* within the host plant unravels a family of S8 serine proteases potentially involved in virulence"

"El secretoma de *Ralstonia solanacearum* dins la planta revela l'existència d'una família de proteases serines S8 potencialment involucrades en la virulència"

En aquest últim capítol, exposem els resultats preliminars de l'anàlisi proteòmic de les proteïnes secretades per *R. solanacearum* durant la infecció a l'interior del xilema i apoplast de la planta. Aquesta tècnica, utilitzada únicament *in vitro* en aquest patogen, ens permetrà tenir una visió més directa dels factors de virulència secretats pel patogen dins la planta. Després d'un filtratge estricte per eliminar aquelles proteïnes contaminants o producte de la lisis de la cèl·lula bacteriana, hem obtingut un conjunt de proteïnes potencialment secretades per *R. Solanacearum*. Entre aquestes, hi ha els esperats enzims de degradació de la paret cel·lular de planta, molt importants per virulència del patogen, i que ens demostren la robustesa del nostre anàlisis. Entre d'altres proteïnes molt interessants pel seu potencial en la virulència del bacteri, vam trobar diferents proteases serines S8. D'un total de quatre proteïnes S8 identificades al genoma, tres eren secretades. A més la seva activitat era enriquida tant en el xilema com en l'apoplast de la planta, suggerint la seva importància per la vida del bacteri dins la planta. Per descriure i caracteritzar aquesta família en detall, vam començar cercant la seva conservació i arquitectura proteica. Rsp0603 i Rsc3101 eren la parella més semblant constituïda de dominis serina no canònics, mentre que Rsc2653 i Rsc2654 contenien el domini serina amb la típica triada catalítica. A més totes quatre proteïnes es trobaven àmpliament conservades en els genomes de la majoria de soques de *R. Solanacearum*. A més a més Rsp0603 i Rsc3101 apareixien en múltiples estudis previs suggerint la seva importància, amb Rsp0603 regulada per el regulador de virulència HrpG. Per aquesta raó vam començar la caracterització per aquest últim parell de proteïnes. Els resultats preliminars dels experiments de virulència i d'eficàcia bioloògica del bacteri dins la planta, van demostrar que només quant tots dos gens eren eliminats alhora, hi havia diferencies respecte la soca salvatge. Aquests resultats eren un indici que aquestes proteïnes actuen de forma redundant o sinèrgica dins la planta per afavorir la infecció o el creixement del bacteri. Per últim, per acabar al caracterització de les proteases, vam decidir provar de posar a punt la purificació de Rsp0603. Tot i que les quantitats obtingudes no van ser en cap cas suficients per purificar, els estudis de producció ens van permetre arribar a la conclusió que té activitat proteasa ja que es va observar certa toxicitat i que Rsp0603 es processa igual que les proteïnes canòniques d'aquesta mateixa família d'altre organismes. Més experiments i optimització son necessaris per treure dades concloents, però els resultats recopilats fins al moment indiquen el potencial i importància de la família de les S8 proteases per *R. solanacearum*.

6. CHAPTER 4

The secretome of *Ralstonia solanacearum* within the host plant unravels a family of S8 serine proteases potentially involved in virulence

4.1 Results and discussion

4.1.1 Characterisation of the bacterial secretome in tomato during infection

Upon entering the host, *Ralstonia solanacearum* must navigate through the apoplast of epidermal and cortical root cells before reaching the xylem vessels, from where it will colonise the plant systemically. It is in these two compartments, the apoplast and the xylem, where the pathogen initiates different genetic programs to counter plant defence and achieve colonisation (Chapter 1) (Planas-Marquès *et al.*, 2020; de Pedro-Jové *et al.*, 2021). To continue the characterisation of the pathogen strategy to infect the plant, we decided to study its secretome inside the plant. This proteomic technique, primarily conducted *in vitro* (González *et al.*, 2007; Lonjon *et al.*, 2016), has rarely been applied to pathogenic organisms inside the plant (Kim *et al.*, 2013). In this study, we used previous xylem and apoplast proteomic data from *R. solanacearum* tomato infection in which both bacterial and plant proteins were identified through mass spectrometry analysis (Planas-Marquès *et al.*, 2018; Planas-Marquès, 2020). In those studies, the plant proteomic response to pathogen attack was analysed in depth, but bacterial proteins were overlooked as they were not the focus of study. Therefore, we recovered the datasets and reanalysed them to characterise the potential secretome of *R. solanacearum* inside the plant during infection. The xylem and apoplast sap samples were collected from mock- and *R. solanacearum* inoculated susceptible (*Solanum lycopersicum* cv. Marmande) and resistant (*Solanum lycopersicum* cv. Hawaii-7996) tomato varieties. While the bacterial loads in the apoplast sap did not differ between plant varieties, in the xylem, due to slower disease progression in resistant plants, the bacterial count at the sampling point was four logs bigger in susceptible varieties (Planas-Marquès *et al.*, 2018; Planas-Marquès, 2020).

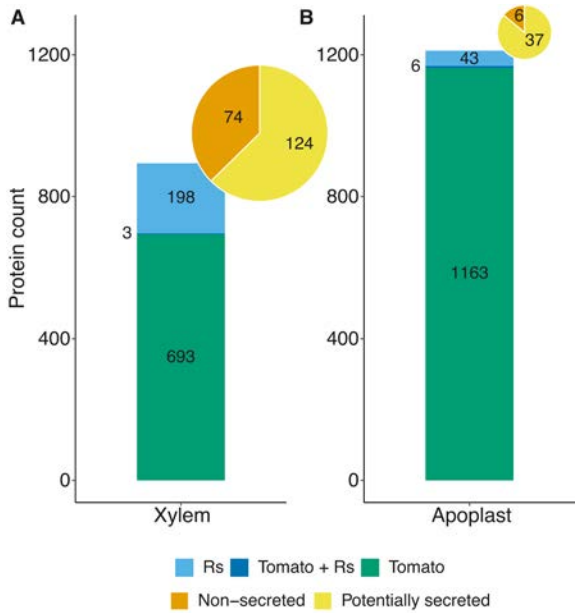

Figure 1. Summary of the proteomic filtering and classification of *R. solanacearum* identified proteins in the plant. The barplots indicate the protein groups belonging to either tomato, *R. solanacearum* (Rs) or shared between both organisms in the (**A**) xylem or (**B**) apoplast. The pie chart summarises the classification of *R. solanacearum* proteins in either non-secreted or potentially secreted.

The proteomic analysis identified, respectively, 198 and 43 *R. solanacearum* potentially secreted proteins in the xylem and apoplast after filtering out non-robust hits (Fig. 1) (detailed information in the Material and Methods). These numbers are related to the total amount of proteins detected, the more plant proteins identified, the lesser the chances for low abundance bacterial proteins to be detected (Fig. 1). At first glance, we noticed that plant variety barely affected protein composition in the apoplast, while 101 proteins (51% of the total) were exclusively found in the xylem of the susceptible variety (Fig. S1). Interestingly, these differences correlated with the higher bacterial loads in susceptible xylem sap at the sampling point (Planas-Marquès, 2020). To remove potential cytosolic contaminants resulting from bacterial death, we validated the secretory nature of the proteins through the cross of information with previous *in vitro* secretory studies and bioinformatic tools to predict

signal peptides (SP) and the final protein localisation (detailed information in the Material and Methods). This filtering was relaxed to keep most periplasmic proteins since the border between periplasm and extracellular space is sometimes unclear (Dalbey and Kuhn, 2012). Following this criterion, we filtered out 37% and 14% of the proteins in the xylem and apoplast respectively, keeping 124 proteins in the xylem and 37 proteins in the apoplast being potentially secreted (Fig. 1, Table S1, Table S2). The principal component analysis (PCA) plot of the normalised proteomic data both in the xylem and apoplast datasets still showed good clustering after the filtering (Fig. S2). The new filtered dataset got rid of the few unique proteins identified in the apoplast, becoming all apoplast proteins shared with the xylem secretome (Fig. 2A and Fig. S1A). Importantly, this curated list reduced the differences between the susceptible and resistant variety in the xylem by 20% and removed from the xylem's top enriched GO terms those unrelated with secreted proteins, such as translation and ribosome (Fig. 2A and Fig. S1B). In fact, both in the xylem and apoplast appeared similar enriched terms related to the presence of cell-wall degrading enzymes (CWDE), such as different hydrolase activities and carbohydrate metabolic process (Fig. 2B, Table S3). Unexpectedly, we also observed enrichment of the GO terms proteolysis and serine-type peptidase activity, which have not been linked to virulence in *R. solanacearum*. The over-representation analysis drawn in volcano plots showed that most proteins both in the apoplast and xylem were significantly more abundant in the susceptible variety. Moreover, this over-representation was not altered after the filtering of cytoplasmatic proteins, suggesting that these differences are an artifact derived from the different bacterial loads (Fig. S3).

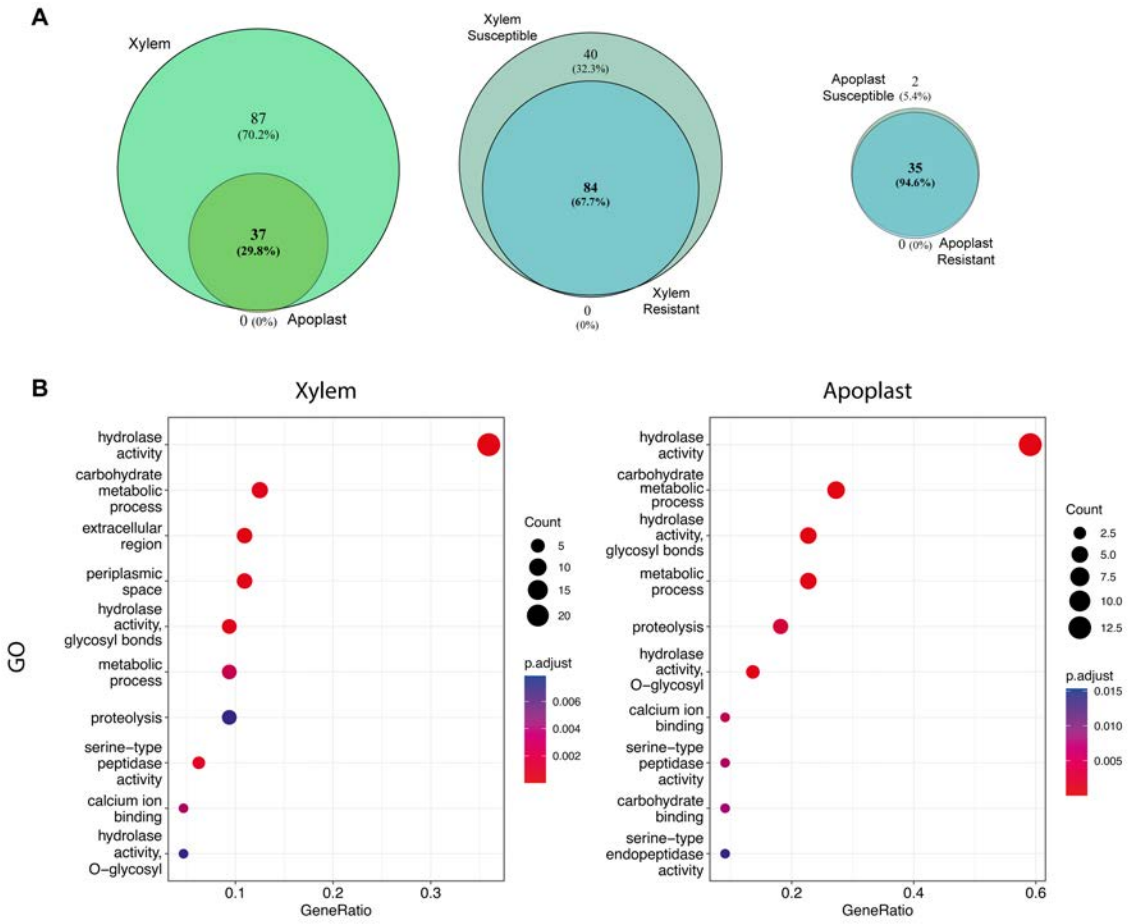

Figure 2. Identity and enrichment analysis of *R. solanacearum* secretome inside the plant. (**A**) Venn-diagrams representing the protein identity overlap between the whole xylem and apoplast secretome (left), and the differences between plant varieties (Susceptible vs. Resistant) within the xylem (centre) and apoplast (right) identified proteins. Non-imputed (non-normalised) proteomic data was considered to retrieve protein presence/absence between plant varieties. (**B**) GO terms enrichment analysis of the secreted proteins in the Xylem (left) and Apoplast (right) sap.

4.1.2 Description of the most abundant secreted proteins by *R. solancearum in planta*

As it is difficult to draw conclusions about abundances from the volcano plots results, we instead decided to retrieve the top 20 most abundant *R. solanacearum* proteins from each plant sap and variety. Overall, the most abundant proteins were almost the same among all the conditions, with a final list of 28 different proteins (Table 1). By far, the group of proteins more represented are CWDE, highlighting the importance of this group of enzymes for plant colonisation and infection. In fact, the two main cellulolytic (Cbha and Egl) and three pectolytic enzymes (Pme, PehB and PehC) can be found in the list together with other CWDE crucial for virulence (Liu *et al.*, 2005; Genin and Denny, 2012). Despite the ubiquity of CWDE, the Tek protein was the most abundant peptide identified *in planta*. This peptide, released from a precursor protein upon secretion, was previously identified as the most abundant secreted protein. However, Tek peptide has not been linked to virulence nor been associated with any known function (Denny *et al.*, 1996; Bocsanczy, Huguet-Tapia and Norman, 2017). An hemolysin-type protein stood out at the top 5, this protein shares homology with RTX-like toxin genes. This group of proteins, widespread among Gram-negative plant pathogens, have no established role but they are thought to be important for the bacterium ecological success (Van Sluys *et al.*, 2002; Genin and Boucher, 2004). Among other uncharacterised proteins, ABC transporters, signal peptide proteins and the described effector translocator RipF1 (or PopF1) (Meyer *et al.*, 2006; Peeters *et al.*, 2013), we identified several proteins with homology to interesting domain functions. Rsc2285 is a VirK protein, which is known to assist toxin secretion and is predicted to interact with multiple virulence proteins such as effectors. Altogether, its predicted role and wide preservation in plant pathogen lineages, hints towards the involvement of VirK in the modulation of plant immune response (Tapia-Pastrana *et al.*, 2012; Assis *et al.*, 2017). Rsp0745 is predicted to be a Hcp-like type VI secretion system machinery that might also act as type VI effector. In other pathogens, Hcp-like proteins have been linked to virulence and competition to other microorganisms (Haapalainen *et al.*, 2012). A function that could be important for *R. solanacearum* inside the plant to fully colonise the xylem niche and avoid microbial competition. Two more proteins that might be related to virulence were Rsc2353 and Rsp0161 that contain a PqaA-type and PepSY domain, respectively. The PqaA domains are alpha/beta hydrolases activated by a regulatory system known to regulate virulence genes. Also, this proteins have been described to confer resistance to antimicrobial compounds (Baker, Daniels and Morona, 1997). On the other hand, the PepSY domain, present in M4 peptidases has been linked to a potential protease inhibitory function (Yeats, Rawlings and Bateman, 2004). As plant proteases are crucial in defence response (Planas-Marquès *et al.*, 2018), it would be interesting to study whether they can be inhibited by PepSY proteins. Finally, among multiple other proteases such as an S10 probable carboxypeptidase protein, we found on the top 10 two putative S8 serine peptidases, Rsc3101 and Rsp0603, also called subtilisin-like enzymes or subtilases, belonging to the serine-peptidase GO term that appeared previously enriched both in the xylem and apoplast (Fig. 2B). The S8 family includes mostly secreted enzymes from eukaryotes, archaea and bacteria with diverse substrates and biological activities. Many contribute to nonselective protein catabolic processes, whereas others catalyse highly specific protein cleavages (Shinde and Thomas, 2011). While serine proteases have been widely characterised in pathogenic fungi (Li *et al.*, 2017), only few bacterial subtilases have been linked to virulence to date. For example, *Vibrio cholerae* IvaP alters host proteins in the gut (Howell *et al.*, 2019) and B Streptococcal C5a Peptidase helps on host invasion (Cheng *et al.*, 2002). In bacterial phytopathogens, the involvement of proteases in virulence is less understood, and whereas some other protease families have been linked with virulence (Figaj *et al.*, 2019; Verma and Teper, 2022), no virulence-related subtilases have been characterised to date.

Table 1. *R. solanacearum* most abundant secreted proteins. The top-20 most abundant proteins from each plant background and plant sap were retrieved ending up with a list of 28 most abundant secreted proteins. The protein abundance in each conditions is represented as the average of the log_2 transformed LFQ. CWDE are highlighted in grey and proteases in blue. Nd values indicate non-detected proteins.

		XYLEM		APOPLAST		
UniprotKB ID	*Gene ID*	**Susceptible**	**Resistant**	**Susceptible**	**Resistant**	*Annotation*
Q8XR59	RSp1002	30.1	28.1	26.1	26.5	Tek signal peptide protein (tek)
Q8XS97	RSp0583	29.1	25.8	22.6	23.1	Glucanase (cbhA) (GH6)
Q8XS78	RSp0603	28.6	25.7	24.0	23.8	Probable serine protease protein (S8)
Q8XT20	RSp0295	28.6	26.1	23.9	23.9	Putative hemolysin-type protein
P58601	RSp0138	27.6	25.0	23.4	23.2	Pectinesterase (pme) (GH28)
Q8XRJ8	RSp0833	27.2	23.6	22.7	22.5	Polygalacturonase (pehC) (GH28)
Q8XUT4	RSc3101	27.2	24.4	22.4	22.3	Putative serine protease protein (S8)
Q8XYK2	RSc1756	27.2	23.8	24.3	23.9	Exo-poly-galacturonosidase (pehB) (GH28)
Q8XT54	RSp0261	27.1	23.5	*nd*	*nd*	Putative transmembrane protein
P58599	RSp0162	27.1	23.5	22.9	22.6	Endoglucanase (egl) (GH5)
Q8XPM8	RSp1610	27.0	23.6	20.8	19.4	Uncharacterized protein
Q8XX75	RSc2241	26.9	24.4	21.1	20.6	Polygalactosaminidase or related (GH114)
Q8XQI5	RSp1240	26.8	23.3	23.6	23.4	Murein transglycosylase (GH103)
Q8XS79	RSp0602	26.8	23.0	22.7	22.6	Probable signal peptide protein
Q8XSE4	RSp0532	26.5	23.9	22.1	22.2	Putative aminopeptidase protein (M1)
Q8XX33	RSc2285	26.2	22.5	23.4	23.1	Putative signal peptide protein (VirK)
Q8XRT6	RSp0745	26.2	23.4	21.5	21.1	Uncharacterized protein (T6SSE Hcp)
Q8Y0P0	RSc1003	26.1	23.4	20.0	19.9	Probable carboxypeptidase protein (S10)
Q8XPT2	RSp1555	26.0	23.7	*nd*	*nd*	Secreted protein popf1 (T3E PopF1)
Q8Y255	RSc0481	25.4	23.3	23.6	22.0	Amino-acid-binding (Pbp) abc transporter
Q8XTE4	RSp0169	24.7	23.4	21.8	19.9	Putative transmembrane protein
Q8XWW7	RSc2353	24.9	23.3	22.3	20.2	Probable signal peptide protein (PepSY)
Q8XVW0	RSc2717	23.4	21.6	23.8	22.7	Probable signal peptide protein (YceI-like)
Q8XU93	RSc3300	24.1	22.0	23.3	21.9	Putative amino-acid transport protein
Q8XTF1	RSp0161	22.1	18.4	22.8	22.0	Putative transmembrane protein (PqaA-type)
Q8XVV9	RSc2718	21.1	19.9	22.5	21.2	Probable signal peptide protein (YceI-like)
Q8XV73	RSc2958	24.2	21.6	21.9	20.3	Probable signal peptide protein (MlaC -like)
Q8XT40	RSp0275	21.8	19.6	21.5	21.4	Putative glycosyl hydrolase family (GH18)

4.1.3 Comparison of the secretome of *R. solanacearum* with previous omics studies

To determine whether the abundance of the secreted proteins of *R. solanacearum* identified *in planta* correlated with previous omics data, we compared the *in planta* secretome with proteomic studies conducted *in vitro* (Zuleta, 2001; González *et al.*, 2007; Lonjon *et al.*, 2016, 2020) and *in planta* gene expression data (C1) (de Pedro-Jové *et al.*, 2021). Overall, in the apoplast, all proteins identified *in planta* were also identified in the *in vitro* proteomic studies. However, 25% of the proteins identified in the xylem were not detected *in vitro*, which does not necessarily mean that the protein is not present in that condition (Nesvizhskii and Aebersold, 2005). Next, we investigated the correlation between abundances in plant saps and *in vitro*. We used the Lonjon *et al.* (2016) dataset, as it was the most complete, and plotted their normalised abundances with both the susceptible and resistant plant varieties datasets (Fig. S4). In all cases there was a conserved trend, in which abundance did not seem to differ importantly between *in planta* and *in vitro*. Interestingly, there were some proteins, both in susceptible and resistant saps, that stood out as being more abundant *in planta* (proteins above the trend line, Fig. S4). Among them the top 20 proteins described before: the CWDEs, the hemolysin-like protein, and the serine proteases. Rsp0603 serin protease was one of the proteins with the most different abundance being on the top *in planta* but very low *in vitro*.

To compare with the previous expression data, we crossed the protein abundance with the transcriptomic data from the early xylem or apoplast, the conditions most relatable (Fig. S5). A high dispersion was observed indicating a big difference between the gene expression and the final amount of secreted proteins. An expected result taking into account the multiple processes

that modulate transcription and translation together with the different post-translational modifications that can affect the protein stability and secretion (de Sousa Abreu *et al.*, 2009). Regardless of the differences, a similar pattern was observed to that of the proteomic comparison, with the most abundant proteins *in planta* being more represented than expected by the gene expression data (proteins above the trend line, Fig. S5). Again, one of the outstanding proteins was Rsp0603, which suggests its important role for the life of the bacterium in plants. These differences observed between proteomic and transcriptomic data also emphasizes the importance of the combination of different omics tools to have the complete picture on the multiple layers governing gene expression and protein production.

4.1.4 Conservation and description of the subtilases family in *R. solanacearum*

The secreted serine proteases caught our attention for being not only detected, but among the most abundant proteins in the xylem and apoplast fluids (Table 1, Table S1 and Table S2). Also, the enrichment of the GO term “serine-type peptidase activity” in both plant compartments (Fig 2, Table S3) suggested a potential role of this group of proteases for the life of the bacteria inside the plant. Another S8 protease, Rsc2654, was identified as secreted in the xylem as it was also part of the enriched serine-type protease GO term (Table S1, Table S3). To understand the extent and importance of this protein family in the genome of *R. solanacearum*, the entire genome was searched for S8 serine proteases to ensure that none had been lost due to misannotation. Surprisingly, only four subtilases were identified in the whole *R. solanacearum* proteome, with Rsc2653, neighbouring Rsc2654, being the only one not detected in our secretome, but identified in previous evolutionary and proteomic studies (Zuleta, 2001; Siezen, Renckens and Boekhorst, 2007). Once identified, we retrieved the amino acid sequences of the four proteases and aligned them. From the alignment, we built the sequence identity matrix and constructed a maximum-likelihood phylogenetic tree adding as outgroup the S10 protease detected in the secretome (Rsc1003) (Fig. 3A). The four proteins grouped in two clear clades, which related with the percentage of identity among the proteases. Rsp0603 and Rsc3101 showed a high identity of 78%, even rising to 86% if we measured similarity. This high percentage of identity suggested that these genes are paralogues, one located in the main chromosome (Rsc3101) and the other in the megaplasmid (Rsp0603). The remaining two proteases, Rsc2654 and Rsc2653, showed a sequence identity of 32% and a similarity of 44% (Fig. 3A). Despite this similarity, the fact that they cluster together in the chromosome suggested that these genes were originated from a tandem duplication event, a common feature of subtilisin-like proteins in other organisms (Li *et al.*, 2017; Schaller *et al.*, 2018). Next, we decided to investigate the conservation of the four subtilases in the different strains of *R. solanacearum*. We used the amino acid sequences to run a BLASTp search against the protein files of the different strains. S8 proteases seemed to be well conserved among the different *R. solanacearum* strains with all the proteins sharing from 85% to 100% identity (Fig. S6, Table S4). Overall, possibly due to misannotation, few proteins were missing in just a handful of strains, being Rsp0603 the top missing protein in 10 different strains (Fig. S6). The potential duplication events occurred in the S8 proteases family and its conservation in different strains hinted towards the importance of this family in *R. solanacearum*.

We then set to analyse the protein architecture of the different S8 proteases and conducted an in-depth search in the literature to understand the potential role of the family (Fig. 3B and Table 2). Correlating with identity and phylogeny results, we found that Rsc2654 and 2653 on one side, and Rsp0603 and Rsc3101 on the other had clear different domain architectures. On one hand, Rsc2653 and Rsc2654 both showed a canonical subtilase domain with the typical catalytic triad (D, H and S), an N-termini signal peptide, and a MprA C-termini protease domain. This plasma membrane GlyGly-CTERM anchoring domain is the recognition sequence for protein sorting and cleavage by rhombosortases, a protease found in tandem (Rsc2655) with their targets in *R. solanacearum*. It is hypothesised that anchorage to the plasma membrane is another layer of control, since only when the rhombosortase is active, the protein will be released into the

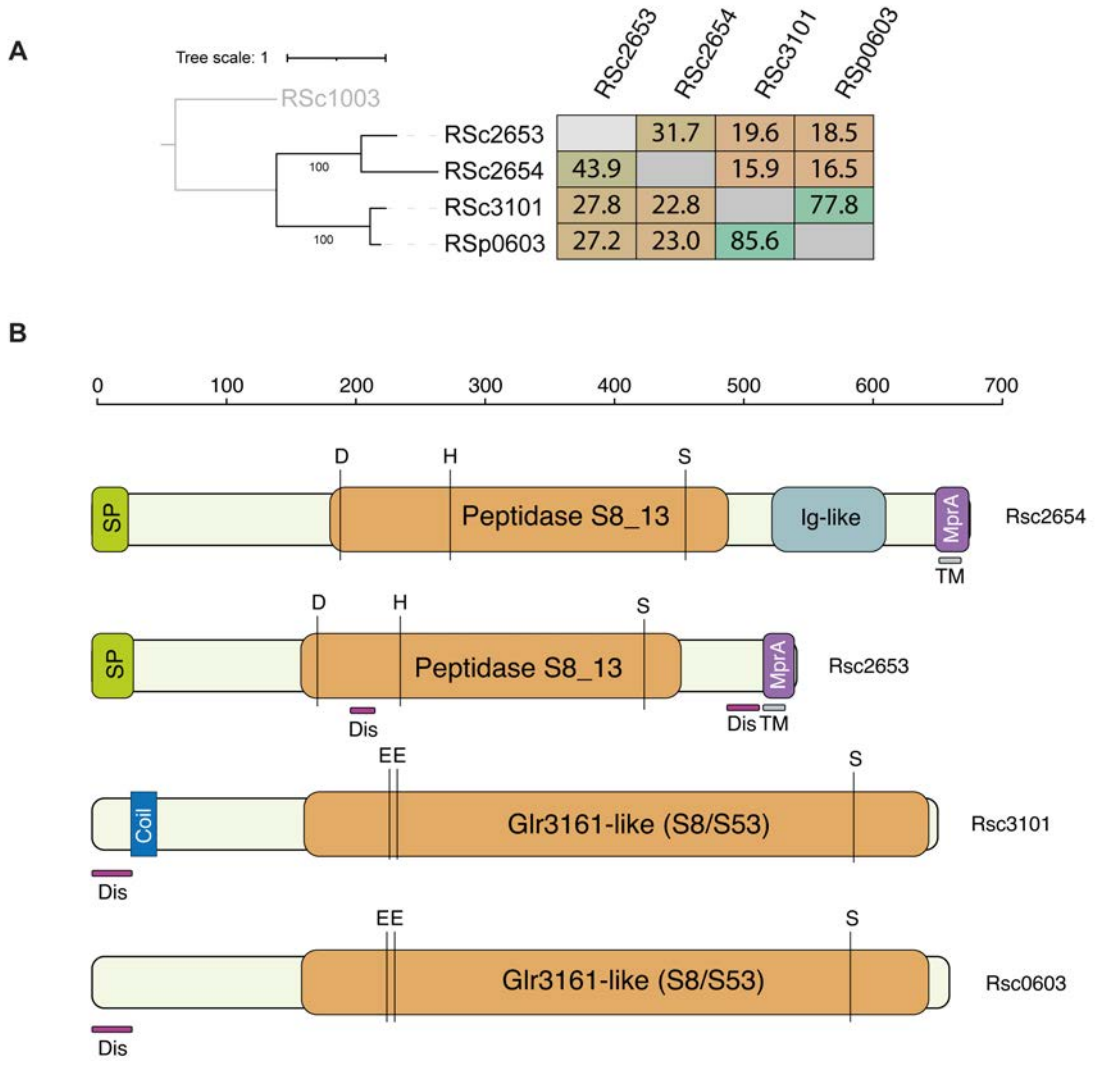

Figure 3. S8 serine proteases family evolution, conservation and domain architecture in *R. solanacearum*. (**A**) The aminoacidic sequences of the S8 serine proteases and, as outgroup the Rsc1003 carboxypeptidase, were retrieved for alignment and construction of a maximum-likelihood tree. Bootstrap values are displayed below each branch. On the right side of the phylogenetic tree, the similarity (bottom-left) and identity (top right) matrices derived from the alignment are displayed. Numbers are coloured from orange to green scale to indicate lower to higher % of similarity or identity. (**B**) Schematic domain organisation of the S8 serine proteases family. The scale on the top indicates the aminoacidic length. The different letters, (D-H-S, or E-E-S) are the predicted catalytic sites. SP, Signal Peptide; Dis, Disordered region; TM, Transmembrane domain; Ig-like, Immunoglobulin-like.

surrounding medium (Haft and Varghese, 2011). Moreover, Rsc2654 has an additional Ig-like domain, involved in protein-protein interactions (Potapov *et al.*, 2004). Regarding the literature search, no previous information was found for Rsc2653 suggesting its minor role in the life of the bacterium inside the plan. In contrast, Rsc2654 was identified in an *in vivo* expression technology (IVET) assay. In short, this technology uses the host as a selective environment to screen for *in planta* expressed genes (Table 2)(Brown and Allen, 2004). On the other hand, the second pair of proteins Rsp0603 and Rsc3101, have a non-canonical Glr3161-like domain. This domain is found in uncharacterised and, possibly, non-peptidase proteins of the S8 family that do not conserve the active sites residues. In this case only the serine is conserved. These proteins don't have a predicted signal peptide, but they contain a predicted disordered region in the N-termini of the sequence (Fig. 3B). This pair of proteins, together with Rsc2654, were also identified in the IVET assay, proving the robustness of the proteomic data. More related with the putative role as virulence factors, Rsp0603 and Rsc3101 were identified as positively regulated by the core

virulence HrpG transcription factor (Valls, Genin and Boucher, 2006). Both genes were also identified to be repressed by PhcA, another important virulence regulator that responds to cell density via quorum sensing (Table 2)(Khokhani *et al.*, 2017). Rsp0603 was by far the most interesting protease being identified as positively regulated by efpR, another regulator of virulence determinants (Capela *et al.*, 2017), upregulated in potato roots upon infection (Puigvert *et al.*, 2017) and of being a target for glycosylation (Table 2). Interestingly, protein glycosylation was also found to be crucial for *R. solanacearum* pathogenesis (Elhenawy *et al.*, 2015). To deepen into the characterisation and function of this family, we decided to start the characterisation with Rsp0603 and Rsc3101, the clade with the most percentage of identity (Fig. 3A) and with the most hints suggesting a potential role in the fitness and/or virulence of the bacteria in planta.

Table 2. Summary of the literature search and characteristics of the S8 serine proteases family.

		Non-canonical		Canonical		
		RSp0603	RSc3101	RSc2654	RSc2653	Ref.
Secretome	Xylem					
	Apoplast					
Regulation	hrpG					(Valls, Genin and Boucher, 2006)
	PhcA					(Khokhani et al., 2017)
	EfpR					(Capela et al., 2017)
Other	IVET					(Brown and Allen, 2004)
	Glycosilation					(Elhenawy et al., 2015)
	Root transcriptome					(Puigvert et al., 2017)
	AA length	663	664	679	543	
	Signal peptide	No	No	Yes	Yes	

4.1.4 Role of S8 serine proteases in the fitness and virulence of the bacteria *in planta*

The information found about Rsp0603 and Rsc3101 pointed towards their importance for the life of the bacteria inside the host plant. To test if their role was linked to virulence, we performed a pathogenicity test in which plants were drenched inoculated with the wild type, the single Δ*Rsp0603* and Δ*Rsc3101*, or the double mutant, and the wilting symptoms scored through time (Fig. 4A). Despite the slight increase at early time points of Δ*Rsp0603* and the delayed wilting symptoms observed in the double mutant, variability among different experiments (data not shown) was too high to draw any clear conclusions. More experiments are needed to see if the trend observed in the double mutant is consistent. In case the delayed wilting symptoms are maintained, this would indicate that both proteases act synergically to cause virulence inside the plant.

Despite a gene deletion mutant might show no evident effect on the virulence of the pathogen, its function might still be important for the fitness of the bacteria inside the plant apoplast, as previously reported for the DNA translocator protein *recA* (Mercier *et al.*, 2009). To test if this was the case of our pair of serine proteases, tomato leaves were infiltrated with the wild type and mutant strains, and samples recovered at day 0 and 3 post infiltration to measure bacterial growth. Interestingly, a slight significant reduction was observed for the bacterial multiplication of the double mutant compared to the wild type (Fig. 4B). This indicates that whereas they might not have a huge effect on virulence, these proteases are important for the survival of the bacterial cells inside the plant apoplast. Also, the protease pair seems to act synergically or have redundant functions as the protease single mutants did not show any growth defect. To confirm these preliminary differences, a complementation of the double mutant strain must be conducted to check if the phenotype is recovered. Overall, the weak phenotype observed in virulence combined

with the growth defect in the double mutant hints towards the role of these pair of proteases during the host infection of *R. solanacearaum*. Besides confirming the results, the addition of the other known S8 proteases in the study would be useful to check if the whole family has a similar function

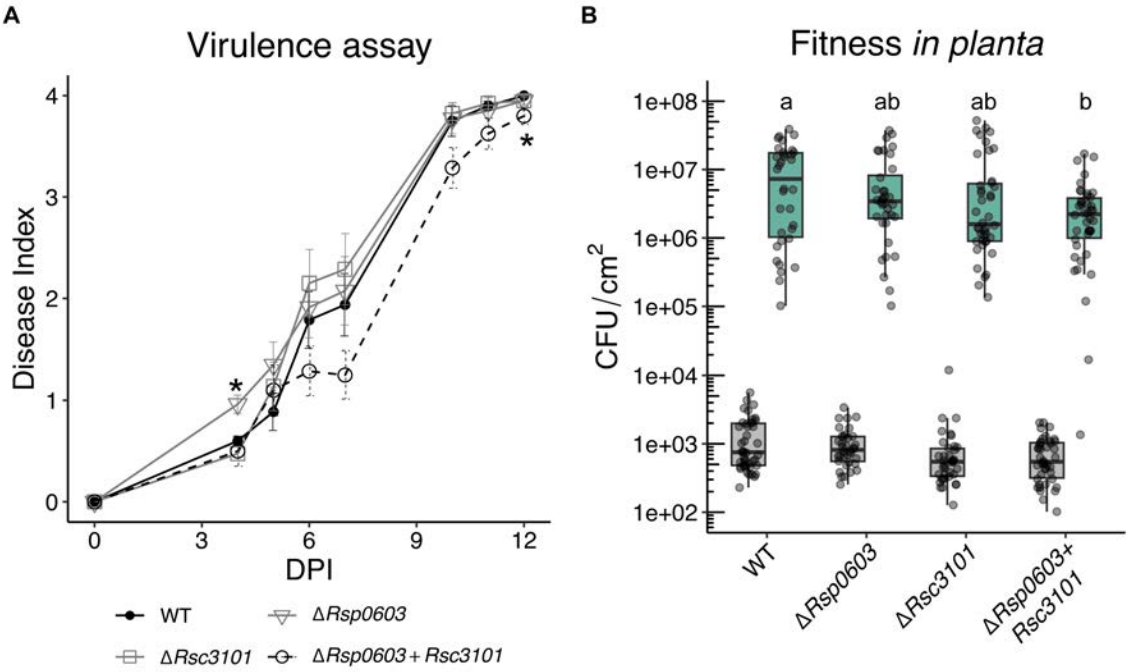

Figure 4. Effect of *Rsp0603* and *Rsc3101* in *R. solanacearum* virulence and fitness in the apoplast. (**A**) Bacterial virulence assay on tomato. The wilting symptoms of the wild type (WT), single Δ*Rsp0603* and Δ*Rsc3101*, and double mutant strains were recorded over time and plotted in a scale ranging from 0 (no symptoms) to 4 (wilted plant). Each data point represents the average of 20 plants and the standard errors. With asterisks are marked the significantly different points determined by one-way ANOVA (*p.value* < 0.05). (**B**) Bacterial growth in the tomato leaves apoplast. Tomato plants were vacuum infiltrated with the bacterial suspensions of the different wilt type, single and double mutants. Leaf disks were recovered at day 0 and 3 and the bacterial growth quantified by plating. The bacterial loads were normalised to the disk area sampled (N=3) and a total of four plants were used in each experiment. At least three biological replicates of the experiment were conducted. DPI; Days post inoculation. The different letters indicate significant differences according to the one-way ANOVA (*p.value* < 0.05) followed by TukeyHSD test. The detailed output of the statistical analysis is detailed in Table S6.

and act redundantly inside the plant.

4.1.3 Production and test expression of S8 serine proteases

To continue with the protein function characterisation and to try to elucidate its activity, we decided to express the proteins as a first step to purify them. By purifying the protein, we could investigate whether they have peptidase activity, as both have a non-canonical serine domain, their putative interactors, or targets inside the plant. We selected the widely used heterologous system of *E. coli* for the first trial expression. We decided to start with Rsp0603 to first optimise the system.

For the heterologous expression of our proteins in *E. coli* two different vectors were used, the pOPIN GoldenGate modular assembly system (Bentham *et al.*, 2021) and the commercial pCold vector (Takara). For the modular system, the gene of interest, *Rsp0603*, was combined with the Protein G B1 domain (GB1) (Song *et al.*, 2022) and Maltose binding protein (MBP) (Pryor and Leiting, 1997) solubility tags fused to 6xHis, and inserted into the backbone vectors under the control of the inducible T7 promoter. *E. coli* BL21 and Shuffle strains were transformed, and samples collected at 0, 2, 3, 4, 5 hours, and overnight after IPTG induction. We checked Rsp0603 protein production in the soluble and insoluble fractions of the cell lysates.

With the GB1 tag, in all the different constructs and strains, the highest expression was at the time point 0h before induction or at 2 hours after induction (Fig. 5A). This means that the system was very leaky and that upon induction the protein production did not increase but diminished, and/or the protein was degraded over time. Moreover, the protein was mostly found in the insoluble fraction. Also, whereas the BL21 strain lysates showed a protein size around the expected one, the protein seemed to be degraded in the Shuffle strain (Fig. S7A). With the MBP tag, the results were quite similar. This time the protein was also produced before induction, but it was accumulated over time only in the insoluble fraction. Some bands could be found in the soluble fraction on the overnight lysates that most likely correspond to subproducts of the protein degradation (Fig. 5B). Again, the protein was degraded in the Shuffle strain and most of the bands visualised in the western blot were most likely degradation products (Fig. S7B). Overall, neither the GB1 nor the MBP solubility tags seemed to help to solubilise our protein or avoid its precipitation into inclusion bodies and in case some was detected, it was not visible in the Coomassie (Fig. 5, Fig. S7). The mutation of the conserved serine of the catalytic site to an alanine (S589A) caused the stabilisation of the protein and the increase of the protein found in the insoluble fractions (Fig. S7C). However, only with the MBP tag, we could see some degradation pattern in the soluble fraction that was anyway not visible in the Coomassie (Fig. S7D). It is worth mentioning that in all cases the detected band was slightly higher than expected, a difference that can be due to the predicted glycosylation of the protein (Elhenawy *et al.*, 2015).

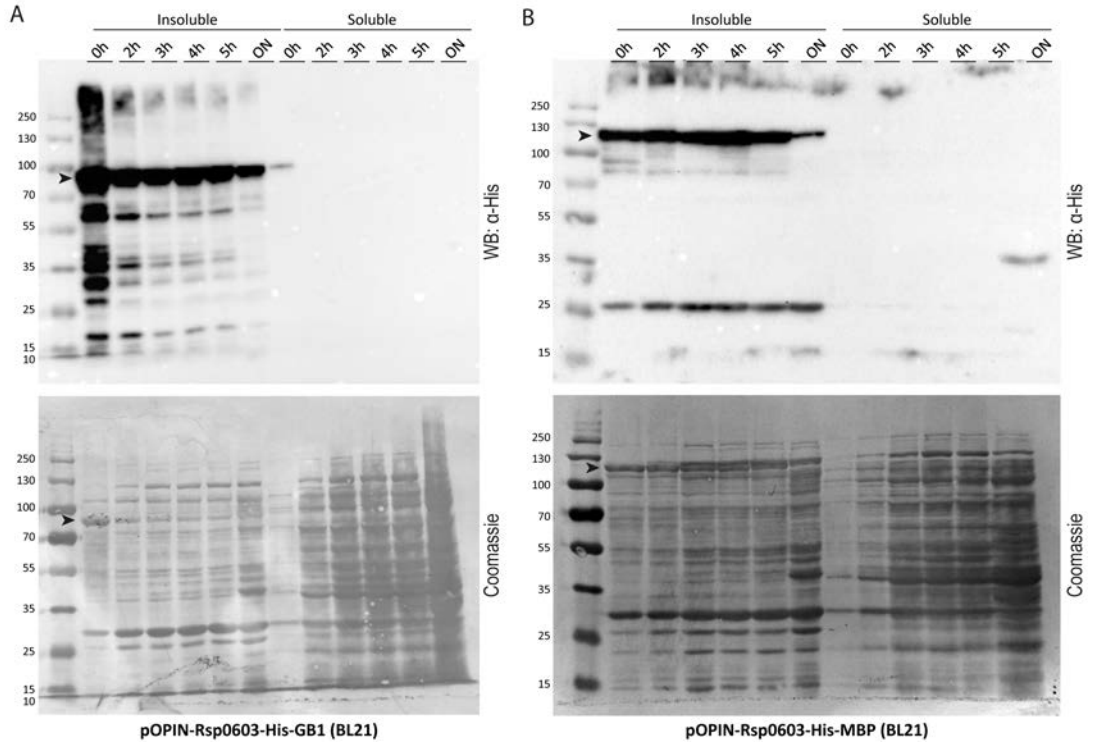

Figure 5. Protein test expression in *E. coli*. Protein test expression of Rsp0603 fused to (**A**) His-GB1 or (**B**) His-MBP in E. coli BL21 strain using the pOPIN system. Protein samples were collected at 0, 2, 3, 4, 5 hours and overnight (ON) and insoluble/soluble fraction visualised via western blotting using α-His-HRP antibody. Below the western blot images, membranes stained with Coomassie to visualise the proteins are shown. Approximate expected size indicated by an arrow: Rsp0603-His-GB1 (80 KDa) and Rsp0603-His-MBP (113 KDa).

Before moving to another system we tried the pCold vector, which is optimised for production of proteins at low temperatures and carries a glutathione S-transferase (GST) tag that helps to solubilise the protein (Harper and Speicher, 2011). BL21 strain was transformed, and samples collected before and after 24h of induction. As observed before, the induction reduced the total

amount of proteins compared to the non-induced cell lysate. Again, the mutant version of the protein showed an increased stability, being present in the western blots after induction with IPTG (Fig. S8A, S8B). In all cases proteins detected in the soluble fractions were barely visible in the Coomassie. The degradation of the wild type versions of the protein or its presence in inclusion bodies upon IPTG induction and the higher stability of the mutant versions led us to believe that Rsp0603 might be toxic for the bacteria due to its unknown catalytic function. Also, we concluded that *E. coli* might not be the most suitable system to produce these proteins.

On view of the insolubility of the Rsp0603 in *E. coli*, we decided to explore two alternative systems: (1) *N. benthamiana* transient expression, which can yield big amounts of proteins and allow us to visualise if our proteins have a phenotype *in planta* and (2) the overexpression of the protein in the native system *R. solanacearum*.

To express the Rsp0603 in *N. benthamiana*, the Greengate modular system (Lampropoulos *et al.*, 2013) was used to construct a vector carrying *Rsp0603* with an mCherry-HA tag and a Signal Peptide (SP) for secretion to the apoplast (α-amylase and Chintinase IV). Since these proteins are predicted to be secreted to the apoplast, we decided to include the SP to ensure that they were properly directed to their natural expected destination. We included a non-SP construct as a control for phenotype observation and, also, for protein production intracellularly in case it happened to be more efficiently produced inside the cells. These constructs were transformed in

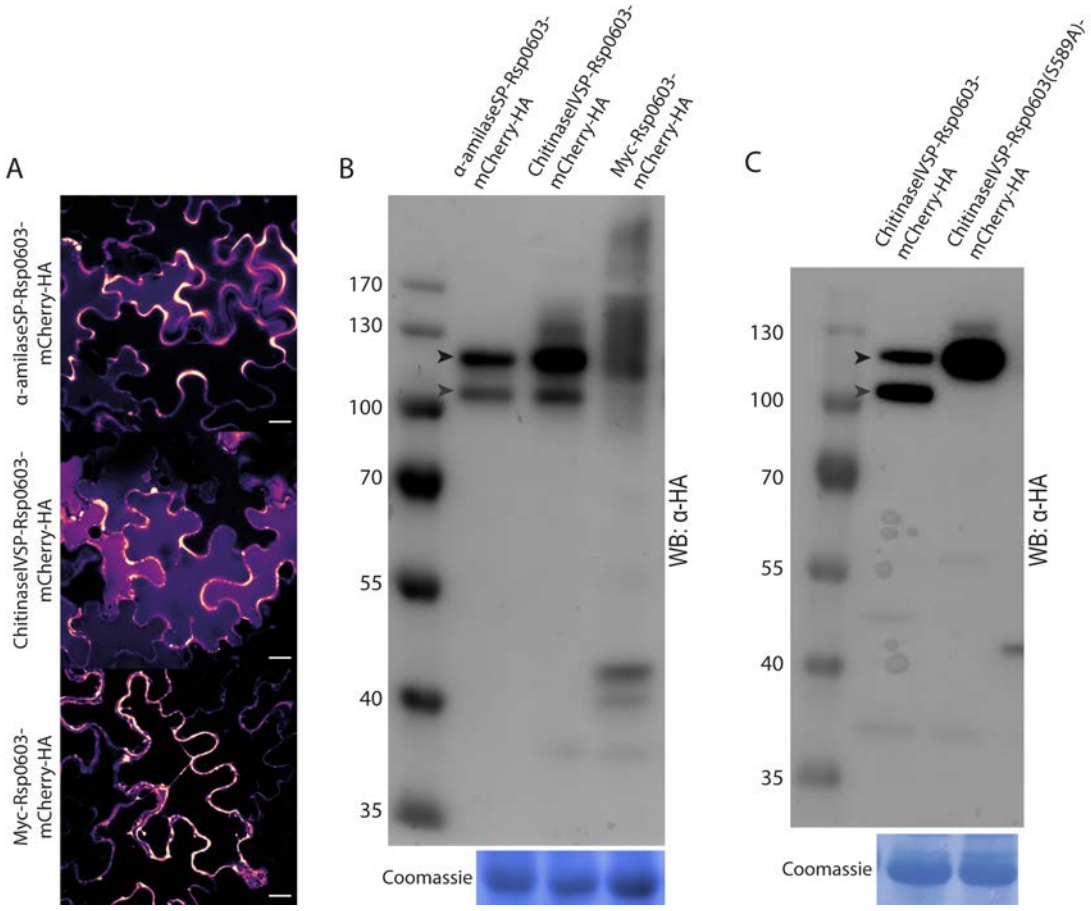

Figure 6. **Test expression of Rsp0603 in *Nicotiana benthamiana*.** Transient protein expression in N. bentamiana RDR6i plants agroinfiltrated with Rsp0603-HA-mCherry with the signal peptides α-amilase, Chitinase IV or no signal peptide (myc) were visualised (**A**) via confocal microscopy images (Scale bars represent 20 μm) or (**B**) western blotting using α-HA-HRP antibody after protein extraction. Approximate expected size of 105 KDa. (**C**) Western blot visualisation of the protein extraction of *N. benthamiana* plants agroinfiltrated with the wild type and the mutant (S258A) version of Rsp0603 with the ChitinaseIV SP. The α-HA-HRP antibody was used for visualisation. The arrows indicate the putative full-length (expected size of 105 KDa) and the processed version (expected size of 90 KDa).

Agrobacterium tumefaciens and transiently expressed in *N. benthamiana*. Before protein extraction, we visualised the constructs under the confocal microscope. Since we were expressing a bacterial protein inside the plant, in all cases the expression was quite low and very patchy. The constructs with SP showed a quite distinctive distribution within the cytosol (visualised as cytosolic strands), and possibly plasma membrane localisation and/or apoplastic. Also, we observed a ubiquitous signal inside the cell, which could be the protein being internalised and degraded into the vacuole (Cheng *et al.*, 2002) (Fig. 6). In contrast, the control construct without SP showed a clear cytosolic distribution. We then extracted the proteins and visualised them by western blot (Fig. 6). In the SP constructs, we consistently found two bands which could indicate a processing of the protein, whereas in the one without SP a smear was observed which could indicate the post-translational modification of this protein, possibly for degradation (Myeku and Figueiredo-Pereira, 2011). Since we were interested in the putative processing of the protein, we repeated the transient expression with the α-amylase SP construct carrying the wild type or mutant version of *Rsp0603*. Interestingly, the processing was no longer observed in the mutant version, which indicated that the mutated Serine residue is important for the protein processing in the plant (Fig. 6).

A feature shared between bacterial and plant subtilases, related to their processing, is their synthesis as prepropeptides. This protein family is synthesised carrying a SP and a self-cleaved prodomain that aids in the folding and serves as an autoinhibitory domain (Bryan, 2002; Schaller, Stintzi and Graff, 2012; Howell *et al.*, 2019). Although Rsp0603 or Rsc3101 lack a predicted prodomain and have a non-canonical S8 domain, we investigated whether the identified peptides in the plant could provide evidence of the processing of these proteins. To this end, we mapped the identified peptides in the xylem to the protein aminoacidic sequence using the webtool Peptigram (Manguy *et al.*, 2017). Interestingly, no peptides mapped to the region between the N termini and the amino acid in the position ~150, together with a gap inside the protein (Fig. 7, Fig. S9). The gap inside the protein could be linked to the trypsin bias, since the cutting sites were not very abundant and too large or small peptides can be lost (data not shown) (Tran *et al.*, 2011). However, this was not the case of the N termini of the protein (data not shown), suggesting that these proteases are likely processed. Also, the difference in size between the full length and the protein lacking the first 150 amino acids is about 15 KDa, which coincides with the band size difference observed in the western blot (Fig. 6). In *E. coli*, there might be some processing, but the low expression, degradation and the unspecific bands in the soluble fraction might mask this processing.

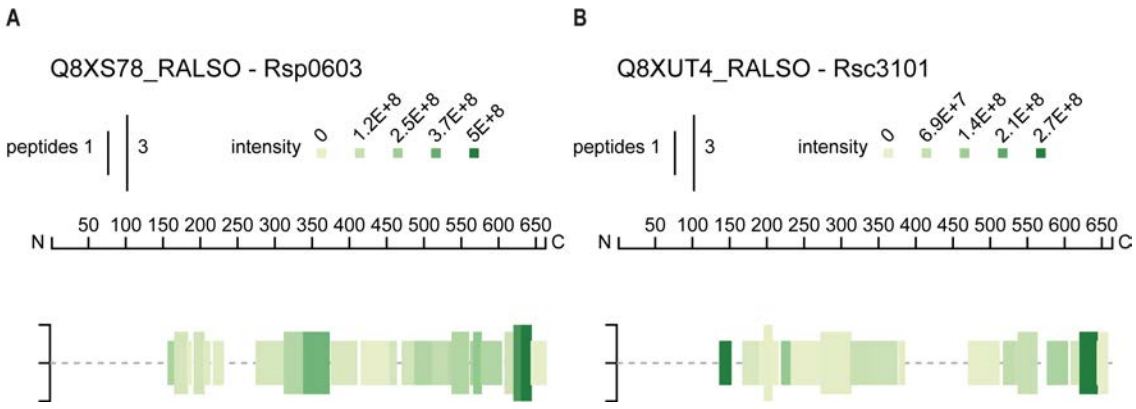

Figure 7. **Peptigram profile of Rsp0603 and Rsc3101.** Mapping of the identified peptides in the proteomics data of (A) Rsp0603 and (B) Rsc3101, adding the different samples intensities from the analysis. A green bar is drawn for each protein residue covered by at least an identified peptide. The height of the bar is proportional to the amount of peptides that cover the specified position and the colour intensity is proportional to the summed ion intensities of the identified peptides in that position. The webtool Peptigram (v.1.0.1) was used to create the plots. The mapping per samples can be found in Fig. S9.

Despite the observation of protein processing in *N. benthamiana*, the proteins could not be detected after Coomassie staining (Fig. S8C), which made us discard this technique for protein production. The other strategy on the table was the protein overexpression in *R. solanacearum*. The plasmids used derived from the chromosomal insertion pRCT vector from (Monteiro, Solé, *et al.*, 2012). The vector carrying the constitutive promoter (*Ppsba*) and *Rsp0603* was transformed in the Δ*Rsp0603* mutant background. Unfortunately, the protein extraction and concentration from the supernatant was not optimised and we only managed to obtain very faint bands, possibly due to the protein degradation along the precipitation process (Fig. S8D).

To sum up, it would be interesting to continue investigating the protein processing seen *in planta* and to optimise the production to purify the protein by optimising codon usage. By doing so, we could investigate in more detail its processing and possibly unravel its function inside the plant. Also, another heterologous system worth considering is *Bacillus subtilis*, known to secrete and produce high amounts of proteins with different levels of toxicity, among them subtilases (Degering *et al.*, 2010; Ursino *et al.*, 2020). However, in the best-case scenario, we would like to optimise and purify the protein from *R. solanacearum* itself to have the protein with all the different post-translation modifications that it might have in the native system.

4.2 Materials and Methods

4.2.1 Data collection and proteomic analysis

The proteomic data used in this work was obtained and partially analysed in the lab (Planas-Marquès *et al.*, 2018; Planas-Marquès, 2020). The data was originated from a proteomic study to unravel plant proteases involved in the defence against the phytopathogen *Ralstonia solanacearum* GMI1000 strain. Briefly, proteins were extracted from the xylem and apoplast of susceptible (var. Marmande) and resistant (var. Hawaii 7996) tomato (*Solanum lycopersicum*) plants of mock and *R. solanacearum* inoculated plants. After extraction, the plant sap was filtered through a 0.22 µm filter to remove any plant debris and bacterial cells. All samples were processed by in-solution trypsin digestion and analysed by LC-MS/MS.

After peptide identification, protein abundance was quantified by label-free quantification (LFQ), and samples were quality checked with RawMeat and the raw files searched with Andromeda against the UniProt Reference Proteomes of *Solanum lycopersicum* (UP000004994_4081.fasta, 33952 entries, download 31/5/2017) and *Ralstonia solanacearum* GMI1000 (UP000001436_267608.fasta, 5001 entries, downloaded 31/5/2017). Raw data was further analysed in Perseus (v.1.6.12.0) software from MaxQuant (Tyanova *et al.*, 2016). Potential contaminants were filtered out and stringent parameters were applied to remove non-robust detections. First, only protein groups with at least two unique peptides were kept for analysis. Second, only protein groups detected in all three biological apoplast replicates or four (out of five) xylem biological replicates in at least one condition (variety x treatment) were kept. All protein groups that did not fulfil both requirements were filtered out. *R. solanacearum* proteins were subset after annotating the proteins using the default annotation file for *R. solanacearum* and *S. lycopersicum* downloaded from Perseus webpage. Missing values were imputed from a normal distribution using default parameters and differentially accumulated proteins detected by false discovery rate corrected (FDR<0.05) t-test. The output imputed and non-imputed table were exported from Perseus for further analysis (Table S1, Table S2).

To remove the contaminants resulting from bacterial lysis (e.g. ribosomal proteins) we validated the secretory nature of our list of protein. Analysis were carried with SignalP 5.0 (Almagro Armenteros *et al.*, 2019) to detect canonical signal peptides, and the SecretomeP 2.0 server (Bendtsen *et al.*, 2005), for non-classical secreted proteins (Table S1, Table S2). Additionally, we used the protein localisation prediction tools BUSCA (Savojardo *et al.*, 2018), PSORTb 3.0.2 (Yu *et al.*, 2010), and LocTree3 (Goldberg *et al.*, 2014) to determine the putative localisation of our proteins of interest. This information was combined with the extensive secretory analysis performed by (Zuleta, 2001). Finally, proteins were classified as potentially secreted or contaminants. In general lines, if secreted in Zuleta (2001), proteins were only removed if they did not have a predicted signal peptide and were predicted to be in the cytoplasm. If they were not identified in Zuleta (2001), proteins were kept unless they had no signal peptide and predicted to be in the cytoplasm or unknown by two out of three predictors, unless predicted to be secreted by any of the software. This flexible criterion was even manually curated to keep or remove proteins that we were considered badly annotated (Table S1, Table S2).

4.2.2 Enrichment analysis

GO terms associated to *R. solanacearum* GMI1000 strain were downloaded from QuikGO (Binns *et al.*, 2009) (24298 entries, downloaded 16/10/2020) whereas KEGG pathways were recovered through the KEGG API (Kanehisa and Goto, 2000) (4383 entries, downloaded 16/10/2020). For the enrichment analysis, we used the enricher function of the ClusterProfiler (v3.18.0) package (Yu *et al.*, 2012) in R (v4.0.3 (R Core Team, 2021)) and the dotplot function included in the same package to represent the enrichment results.

4.2.3 Hidden Markov Model (HMM) search and protein domain architecture prediction

HMM models to search for subtilases was downloaded (Peptidase_S8.hmm, ver. 23, downloaded 13/11/2020) from Pfam (Mistry *et al.*, 2021). Using the HMMER software (v. 3.3.2) (Eddy, 2011), we used the default command to search against the secreted list of proteins and the whole proteome of *R. solanacearum*. To determine the protein domains of our proteins of interest the online tools InterPro (Blum *et al.*, 2021) and Conserved Domain Database (Marchler-Bauer and Bryant, 2004) were used.

4.2.4 Phylogenetic and conservation analysis

Amino acid sequences of interest were retrieved, and aligned using MAFFT (v. 7.453) (Katoh and Standley, 2013) with G-INS-I strategy (--globalpair and --maxiterate 1000). Aligned sequences were inputted to RaxML (v. 8.2.12) (Stamatakis, 2014) to find the best Maximum-likelihood phylogenetic tree (-f a). The automated protein model selection (-m PROTGAMMAAUTO) and rapid bootstrapping parameters (-# 100) were used. The output tree was uploaded to iTol webtool (v. 6.6) (Letunic and Bork, 2021) for visualisation and modification. To construct protein similarity and identity matrices, protein amino acid sequences were aligned by pairs in the global alignment online tool Needle (EMBOSS) (Madeira *et al.*, 2022).

4.2.5 Bacterial growth and construction of *R. solanacearum* gene knock-out and complemented strains

R. solanacearum GMI1000 wild-type or mutant strains were regularly grown at 30 ºC in rich B medium with 0.5% glucose (Monteiro, Genin, *et al.*, 2012) and supplemented with the appropriate antibiotics. *Escherichia coli* and *Agrobacterium tumefaciens* were grown at 37ºC in Luria-Bertani broth (Bertani, 1951) or 28 ºC in Yeast Extract Broth medium, respectively, supplemented with the appropriate antibiotics. All strains used are listed in Table S5.

Generation of mutant strains was done by inserting a resistance cassette in substitution of the open reading frames of the genes of interest as described in (Yu *et al.*, 2004). Briefly, in a first round of PCRs, approximately one kilobase fragment upstream and downstream of the gene of interest were amplified in parallel to the resistance cassette, adding compatible overhangs to the primers. The second round PCR consisted of an overlap PCR to combine the resistance cassette with the genomic fragments flanking the gene of interest. In the third round, the whole overlap product was amplified to obtain enough DNA. The resulting fragment was inserted in a pJET1.2 (CloneJET PCR cloning kit, ThermoFisher Scientific) and checked by sequencing. The resulting plasmid was linearised and introduced into *R. solanacearum* wild-type by natural transformation (Boucher *et al.*, 1985). Recombination events were selected by growing the transformed bacteria into selective media and checked by PCR.

For complementation, the coding sequences of the gene of interest was amplified with *attB* overhangs, the amplicon was transformed into pDonor-207 with the BP Clonase (ThermoFischer Scientific) and checked by sequencing. The gene of interest was finally transferred to the destination suicide vector pRCT (Monteiro, Solé, *et al.*, 2012) by an LR reaction (ThermoFischer Scientific) under the control of the constitutive promoter p*Psba* (Table S5), and finally transformed into the strain of interest of *R. solanaecarum*.

4.2.6 Plant material and bacterial assays

The susceptible tomato (*S. lycopersicum* var. Marmande) was grown on soil (Substrate 2, Klasmann-Deilmann GmbH) mixed with perlite and vermiculite (30:1:1). Plants were grown under long-day conditions (16 h light / 8 h darkness) at 22 ºC and 60% relative humidity. Two days prior to infection, plants were transferred to acclimate to chambers at 27 ºC under 12h/12h light/night photoperiod and 60% relative humidity.

For pathogenicity assays, plants were drenched inoculated with 40 ml of the bacterial suspension adjusted at 10^8 colony forming units (CFU)/ml from an overnight culture. Wilting symptoms were recorded with a semi-quantitative wilting scale ranging from 0 (no symptoms) to 4 (completely wilted plant). For bacterial growth assays *in planta*, tomato leaves were vacuum infiltrated with water or a bacterial suspension at 10^5 CFU/ml. 80 µl/l of Silwett-77 adjuvant was added to facilitate infiltration. A total of three 5-mm diameter disks were collected, homogenised in water, and 10 µl of serial ten-fold dilutions plated in selective plates. The plates were incubated at 28 ºC and colonies counted and normalised by the leaf disk area.

4.2.7 *E. coli* test expression analysis

For the pOPIN expression system (Bentham *et al.*, 2021), the gene of interest was amplified with compatible overhangs containing BsaI sites. The gene was combined and ligated with the backbones and the tag of interest. The resulting vectors (Table S5) were transformed to *E. coli* BL21 and Shuffle strains and cells grown at 37ºC and 30ºC respectively. The overnight cultures were adjusted to OD_{600}=0.1 and induced with Isopropyl β-D-1-thiogalactopyranoside (IPTG) at 1 mM when OD_{600}=0.6 was reached. An aliquot was collected at 0, 2, 3, 4, 5 hours and overnight, aliquots were centrifuged, and the bacterial pellet stored for processing.

For the pCold system, the genes of interest were amplified with compatible restriction enzymes overhangs and cloned into the commercial pCold vector (Takara Bio Inc). This vector was later transformed into the *E. coli* chemically competent BL21 expression strain (Table S5). An overnight culture was diluted to OD_{600}=0.1 with fresh medium and grown at 37ºC with shaking until OD_{600} reached 0.6. Then, the protein production was induced by adding 1 mM IPTG and transferred to 15 ºC for overnight growth. After 16 hours, aliquots were collected, centrifuged and bacterial pellets stored.

The collected pellets were resuspended in PBS and sonicated on ice. The lysates were centrifuged at 25,000 xg for 20 min to separate soluble and insoluble fractions. These fractions were mixed with protein loading dye, boiled, and loaded into an SDS-PAGE to check via western blot the expression of the protein of interest.

4.2.8 Transient expression in *Nicotiana benthamiana*, microscopy visualisation and protein extraction

Plant expression vectors were assembled through GreenGate cloning strategy (Lampropoulos *et al.*, 2013). To this end, the coding sequence of the genes of interest was amplified with the correct overhangs and combined with the modules to construct the different expression plasmids detailed in Table S5. The expression vectors were transformed on the electrocompetent *Agrobacterium tumefacients* ASE strain containing the pSOUP binary vector. For the transient expression in *N. benthamiana*, bacteria were collected from YEB plates and resuspended in water. After two washes, cells were resuspended in induction buffer (10 mM $MgCl_2$, 10 mM MES, and 150 µM acetosyringone), adjusted to an OD_{600} of 0.5 and incubated at 28 ºC for few hours. *Agrobacterium* strains were hand inoculated with a blunt-end syringe into the leaves of three- to four-week-old *N. benthamiana* plants. Three days post inoculation protein expression in infiltrated leaves was checked with an Olympus FV1000 inverted confocal microscope with a x63/water objective using the 543 nm laser to excite and visualise the mCherry fluorophore. Afterwards, plant tissue was frozen in liquid N_2 for processing.

Frozen material was ground with mortar and pestle for protein extraction. For every 500 mg of tissue, 2 ml of extraction buffer (50 Mm HEPES pH 7.3, 150 mM NaCl, 0.5% Nonidet P-40, 10% glycerol, 1 mM EDTA pH 8, 5 mM DTT, 1% PVPP and 1× Protease inhibitor cocktail (Sigma, P599)) was added, mix thoroughly, and centrifuged for 10 min at 14,000 xg at 4 ºC. The supernatant was transfer to a new tube and mixed with protein loading dye, boiled, and loaded on an SDS-PAGE gel. The protein was visualized via western blot analysis.

4.2.9 *R. solanacearum* test secretion

For secretion studies, bacterial cultures of the complementation/overexpression strains were grown overnight at 28ºC. Bacteria was then centrifuged at 5000 xg for 10 minutes at 4ºC and the medium fraction (supernatant) was separated from the pellet. Culture supernatants were filtered through a 0.22 µm-pore membrane to eliminate residual cell contamination before protein precipitation. To precipitate the proteins, trichloroacetic acid was added to a final concentration of 25% and the solution incubated overnight at 4 ºC. The next day, the tubes were centrifuged at 6000 xg for 30 min. at 4ºC and the supernatant discarded. The protein pellet was washed twice with 90% acetone, dried, resuspended with PBS and mixed with protein loading dye. Samples were boiled and loaded on an SDS-PAGE gel. The protein was visualised via western blot.

4.2.10 Statistical analysis

All the statistical analysis were performed in R software. In each plot, the statistical test applied is detailed in the figure caption. The compilation of all statistical analysis outputs are shown in Table S6.

4.3 Supplementary Data

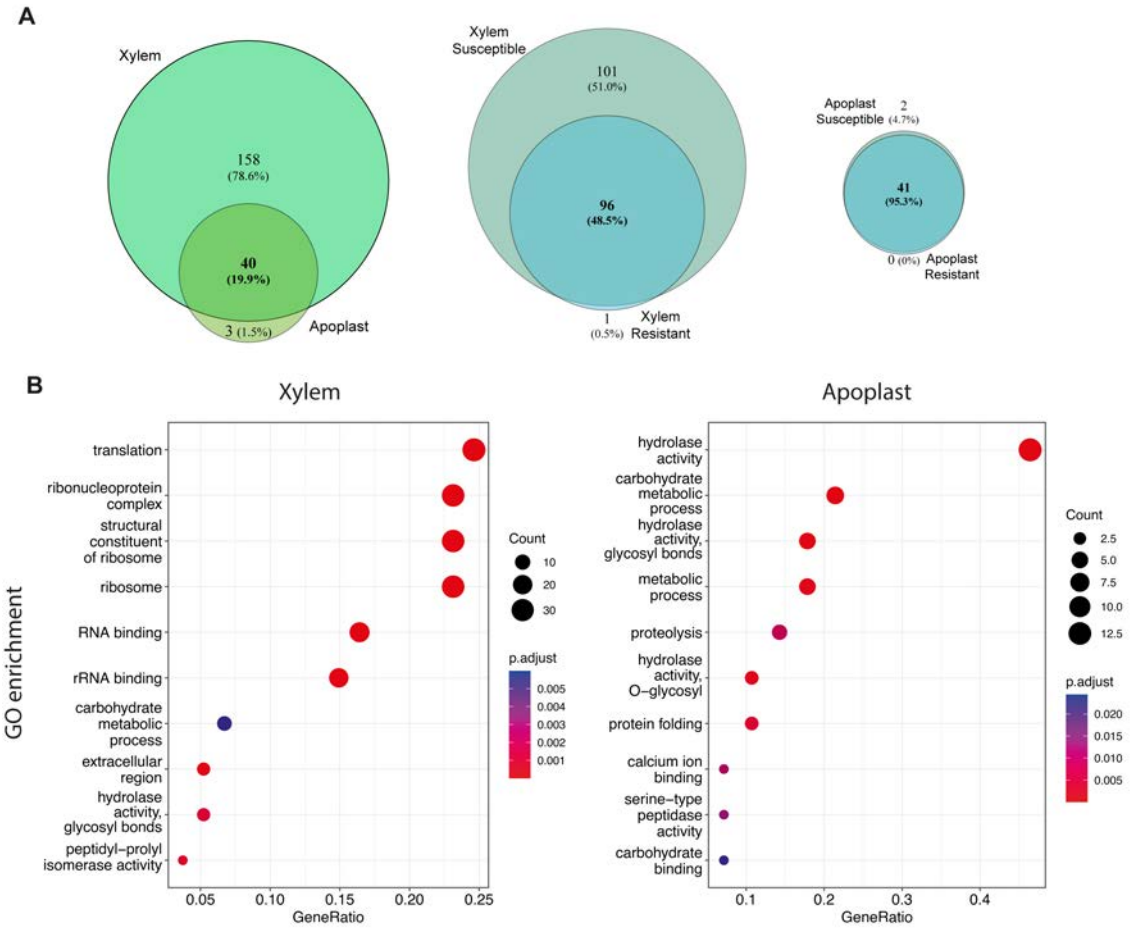

Supplementary Figure 1. Identity and enrichment analysis of *R. solanacearum* pre-filtered proteome inside the plant. (**A**) Venn-diagrams representing the protein identity overlap between all bacterial proteins identified in the xylem and apoplast (left), and the differences between plant varieties (Susceptible vs. Resistant) within the xylem (centre) and apoplast (right) proteins. Non-imputed (non-normalised) proteomic data was considered to retrieve protein presence/absence between plant varieties. (**B**) GO terms enrichment analysis of the secreted proteins in the Xylem (left) and Apoplast (right) sap.

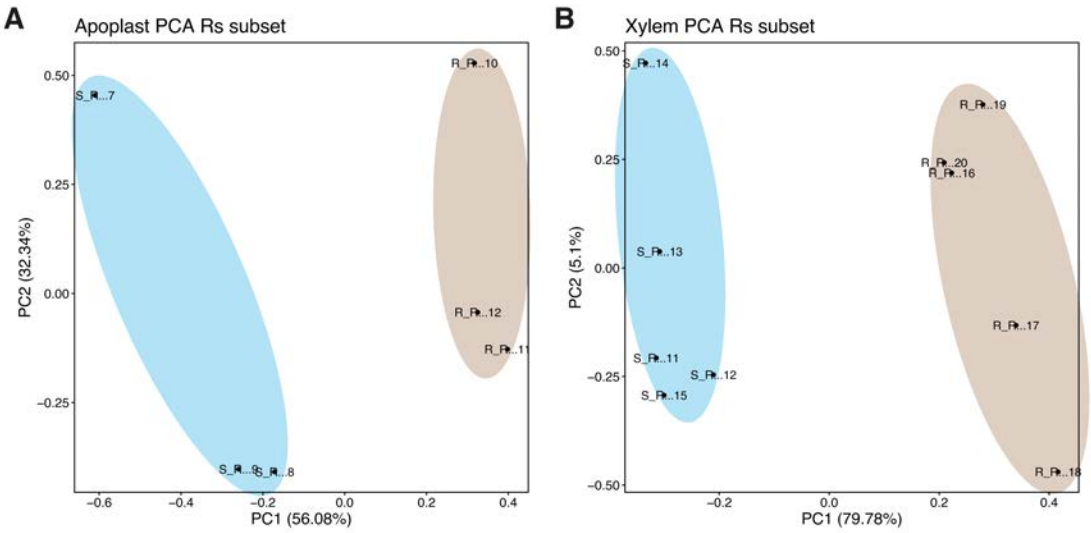

Supplementary Figure 2. Two-dimensional Principal Component Analysis (PCA) of the xylem and apoplast filtered proteome. PCA plots of the (**A**) apoplast and (**B**) xylem of the normalised protein abundance of the final filtered datasets.

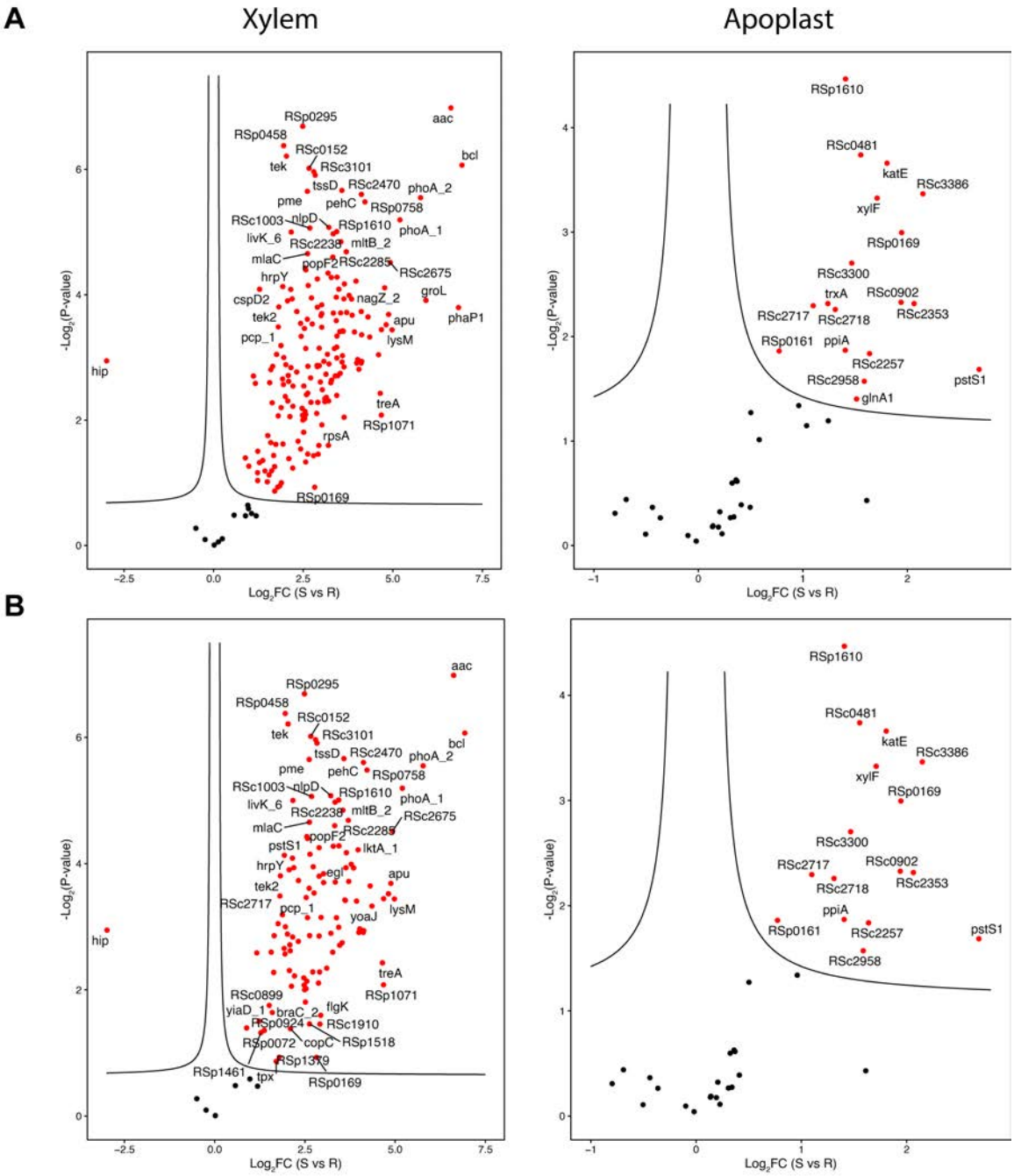

Supplementary Figure 3. Identification of the differentially abundant proteins by plant variety. Volcano plots from before (**A**) and after (**B**) filtering out the cytoplasmatic proteins. The volcano plots show the relation between the p-value (y-axis) and fold change (FC) (x-axis) of susceptible vs. resistant plant varieties of the xylem (left) or apoplast (right) proteins. The red dots indicate the differentially accumulated proteins determined by T-test (FDR q-value < 0.05) using the Persus software.

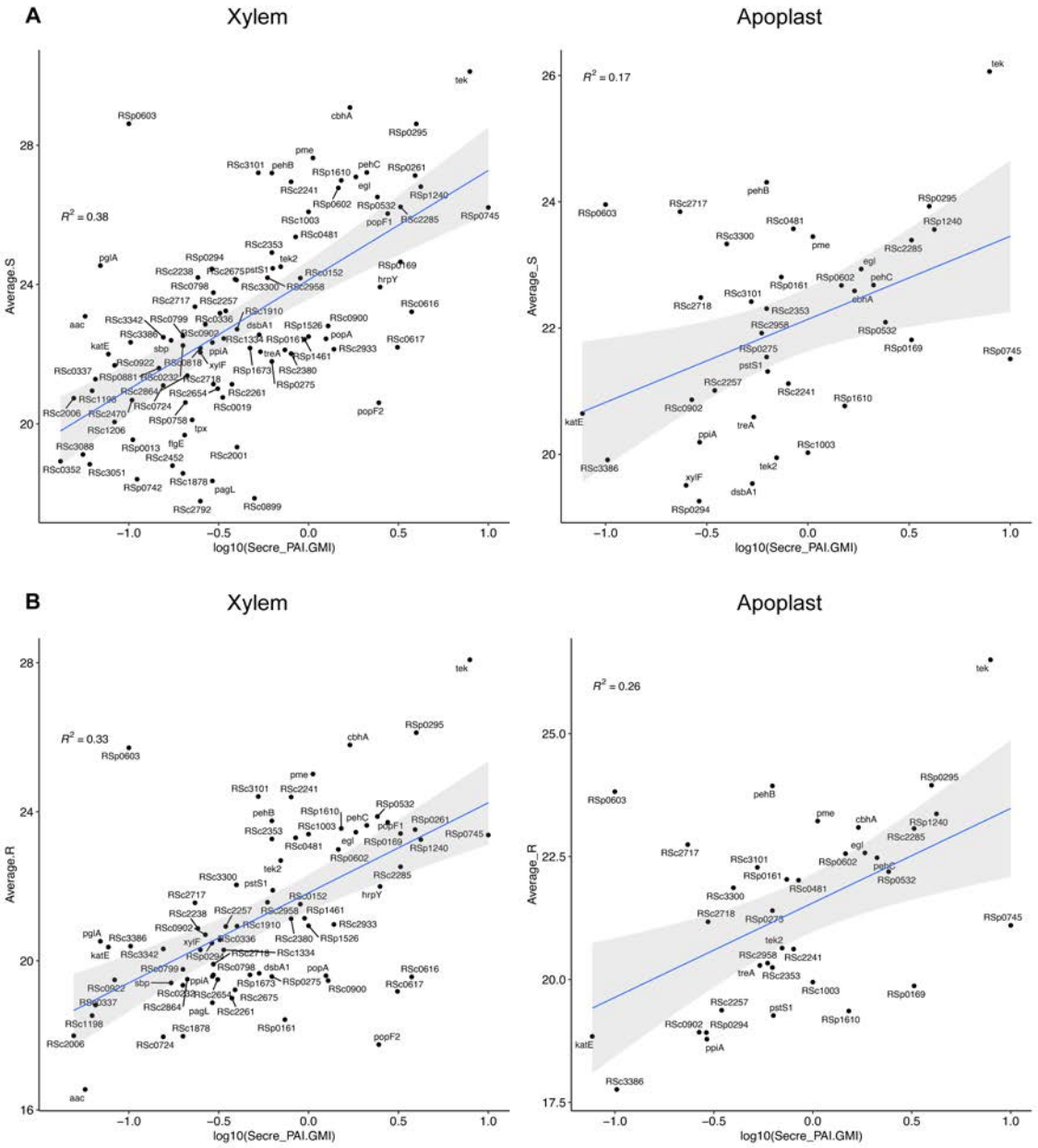

Supplementary Figure 4. Comparison of protein abundances between the in planta and in vitro proteomic datasets. The averaged log2 transformed LFQ protein abundance (y-axis) in the (**A**) susceptible and (**B**) resistant plant variety from the xylem (left) and the apoplast (right) were plotted against the $\log_{10}$ of the protein abundance index (PAI) from Lonjon et al. (2016) (x-axis). Regression line determined in R is shown (R^2 = determination coefficient) in each plot.

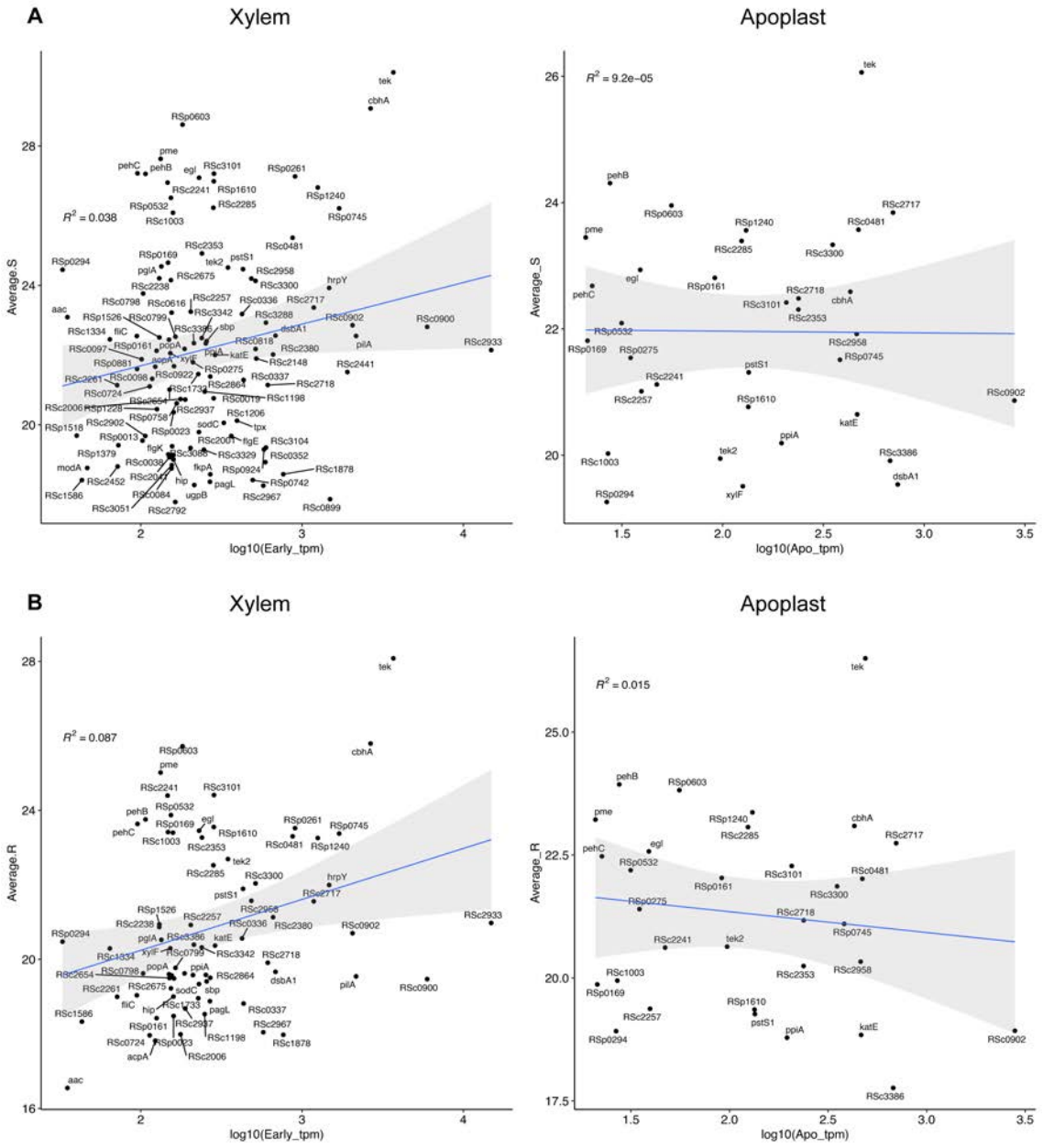

Supplementary Figure 5. Comparison between protein abundance and gene expression. The averaged log2 transformed LFQ protein abundance (y-axis) in the (**A**) susceptible and (**B**) resistant plant varieties from the xylem (left) and the apoplast (right) were plotted against the $\log_{10}$ TPM (Transcripts per kilobase million) gene expression data from the early xylem (left) and the apoplast (right), respectively, from de Pedro-Jové et al., (2021). Regression line determined in R is shown (R^2 = determination coefficient) in each plot.

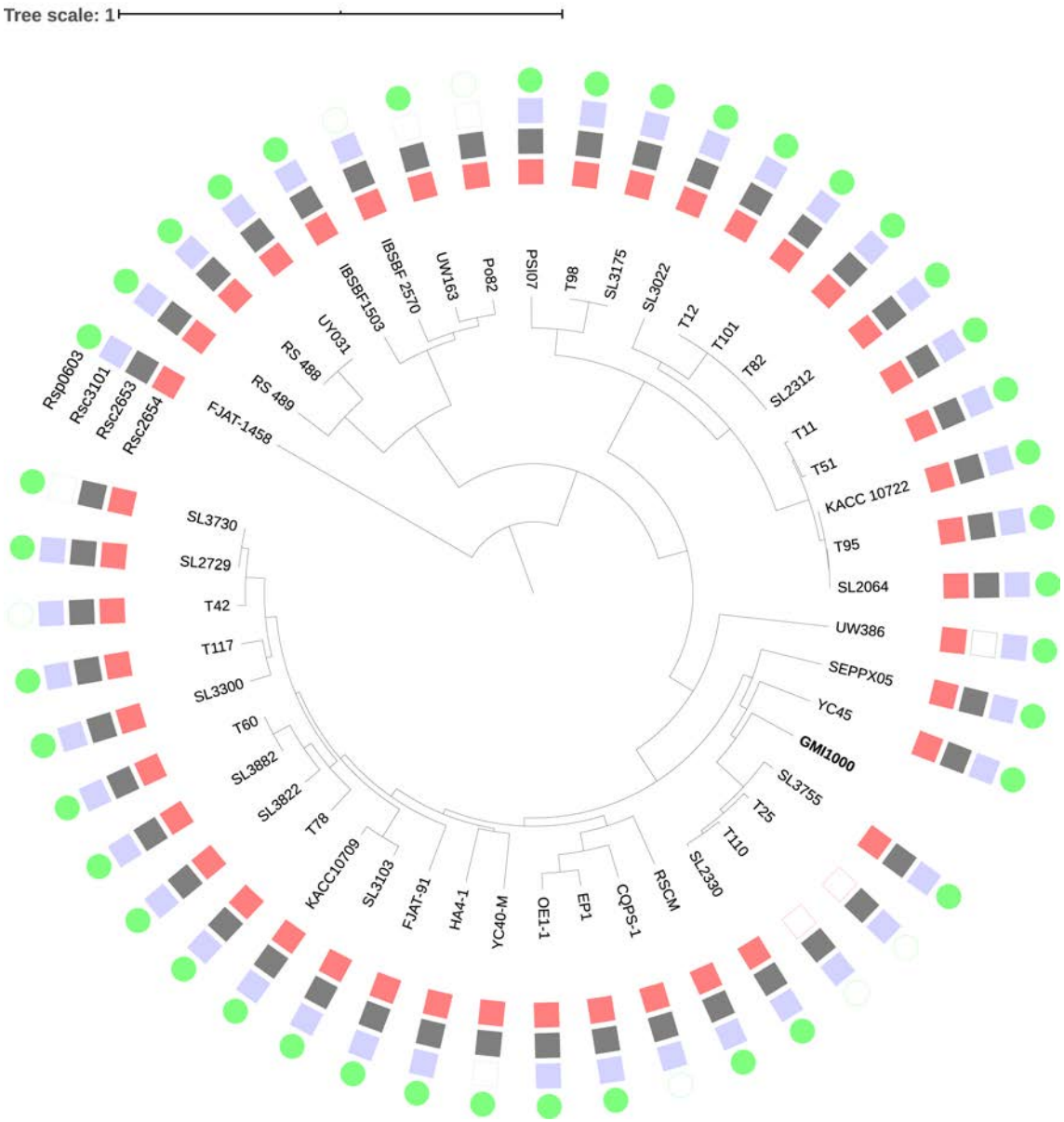

Supplementary Figure 6. S8 serine proteases family conservation along the *R. solanacearum* species complex. The aminoacidic sequences of S8 serine proteases family from the GMI1000 strain were retrieved and BlastP conducted against the different available *R. solanacearum* predicted protein files. The proteases located in the chromosome (Rsc3101, Rsc2653 and Rsc2654) and megaplasmid (Rsp0603) of GMI1000 (in bold) are indicated as a square or circle, respectively. The positive blast searches are indicated as filled squares or circles. The R. solanacearum strains phylogenetic tree was downloaded from the NCBI. The blast output data of the best hits in each strain is detailed in Table S4.

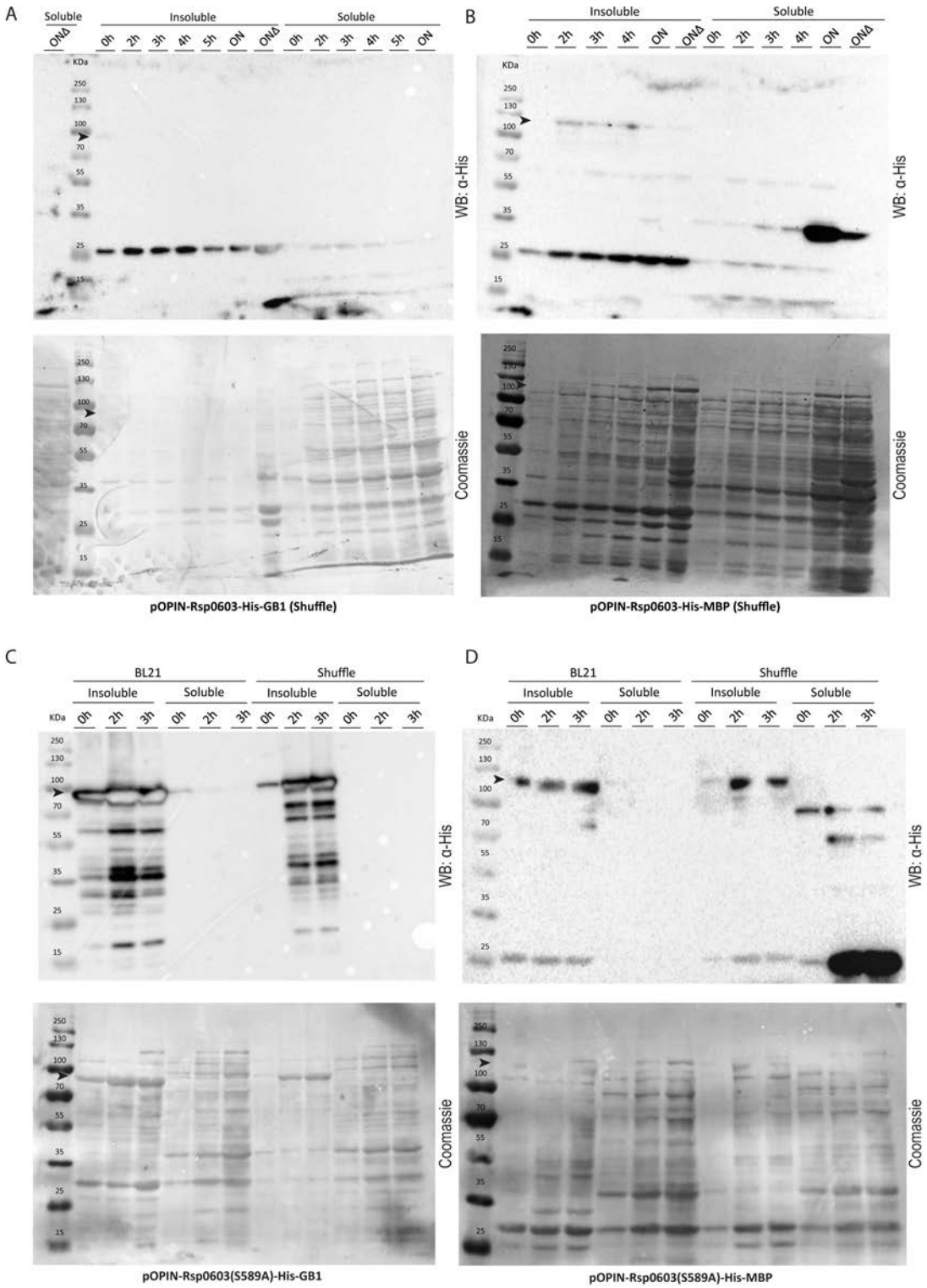

Supplementary Figure 7. Protein test expression of the wild-type or mutant (S258A) version of Rsp0603 in *E. coli*. (**A, B**) Protein expression of wild-type Rsp0603 fused to (**A**) His-GB1 or (**B**) His-MBP in E. coli Shuffle strain using the pOPIN system. Soluble and insoluble fractions of protein samples were collected at 0, 2, 3, 4, 5 hours and overnight (ON, ONΔ) and visualised via western blotting using α-His-HRP antibody. (**C, D**) Protein expression of the mutant (S258A) version of Rsp0603 fused to (**C**) His-GB1 or (**D**) His-MBP in E. coli BL21 (left) or Shuffle (right) strain using the pOPIN system. Below the western blot images, membranes stained with Coomassie to visualise the proteins are shown. Approximate expected size indicated by an arrow: Rsp0603-His-GB1 (80 KDa) and Rsp0603-His-MBP (113 KDa).

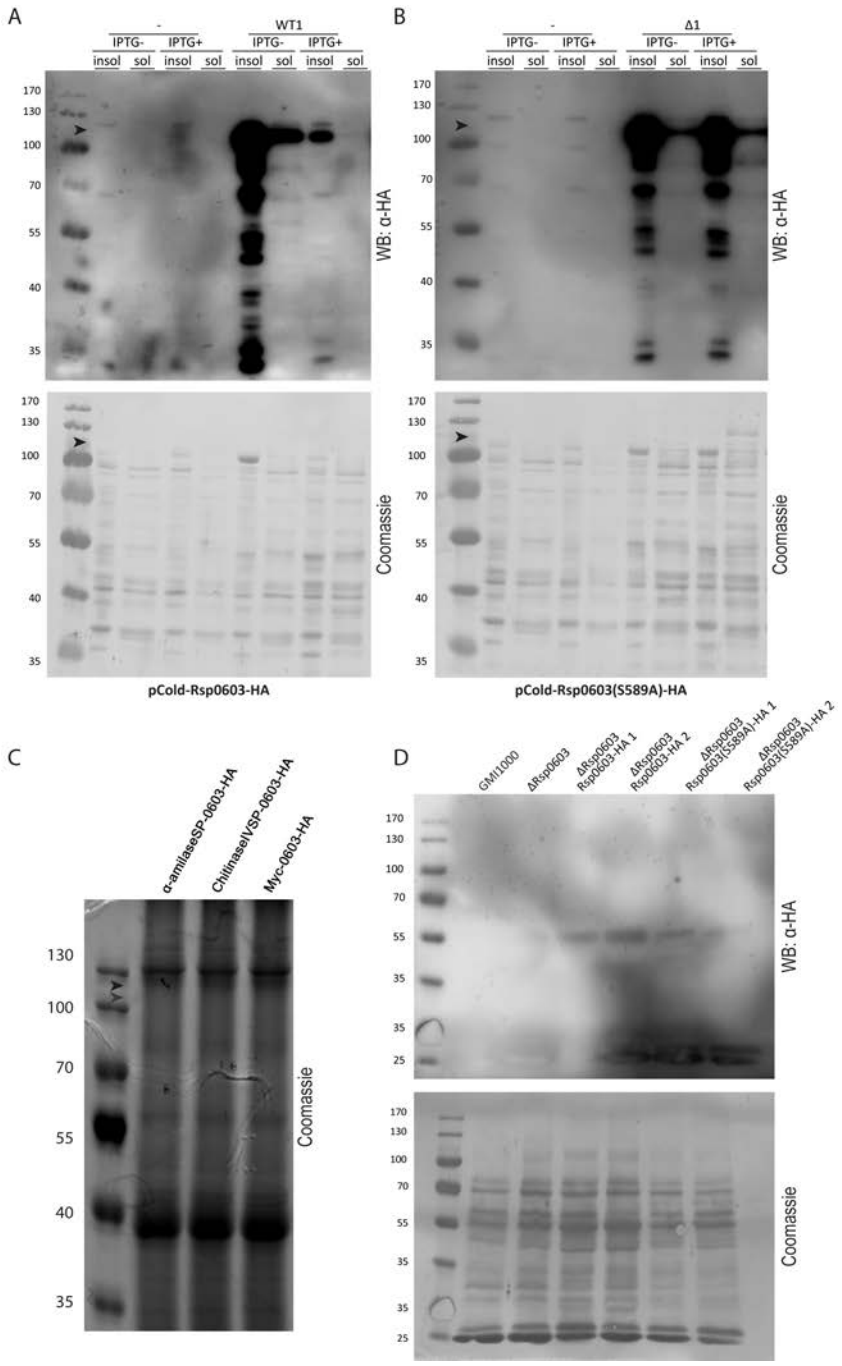

Supplementary Figure 8. Test expression of Rsp0603 using different expression systems. (**A, B**) Protein expression of (**A**) wild-type or (**B**) mutant (S258A) version of Rsp0603 in *E. coli* BL21 strain using the pCold system. Soluble and insoluble fractions of protein samples collected 24 hours with and without induction (IPTG-/+) and visualised via western blotting using α-HA-HRP antibody. Below the western blot images, membranes stained with Coomassie to visualise the proteins are shown. Approximate expected size: Rsp0603-GST-HA (95 KDa) (**C**) Coomassie staining of the Western Blot membranes shown in Fig. 6B. Approximate expected size of 105 KDa. (**D**) Rsp0603 expression in R. solanacearum. The wild type GMI1000, and the mutant background Δ*Rsp0603* were used as control. The mutant background was complemented with the wild type (Rsp0603-HA, two clones) and the mutant (S258A) version of Rsp0603 (Rsp0603(S258A)-HA, two clones) to detect the protein. The supernatant of bacteria grown for 24h was precipitated and visualised using the α-HA-HRP antibody. Below the western blot images, membranes stained with Coomassie to visualise the proteins are shown. Approximate expected size indicated by an arrow: Rsp0603-HA (80 KDa)

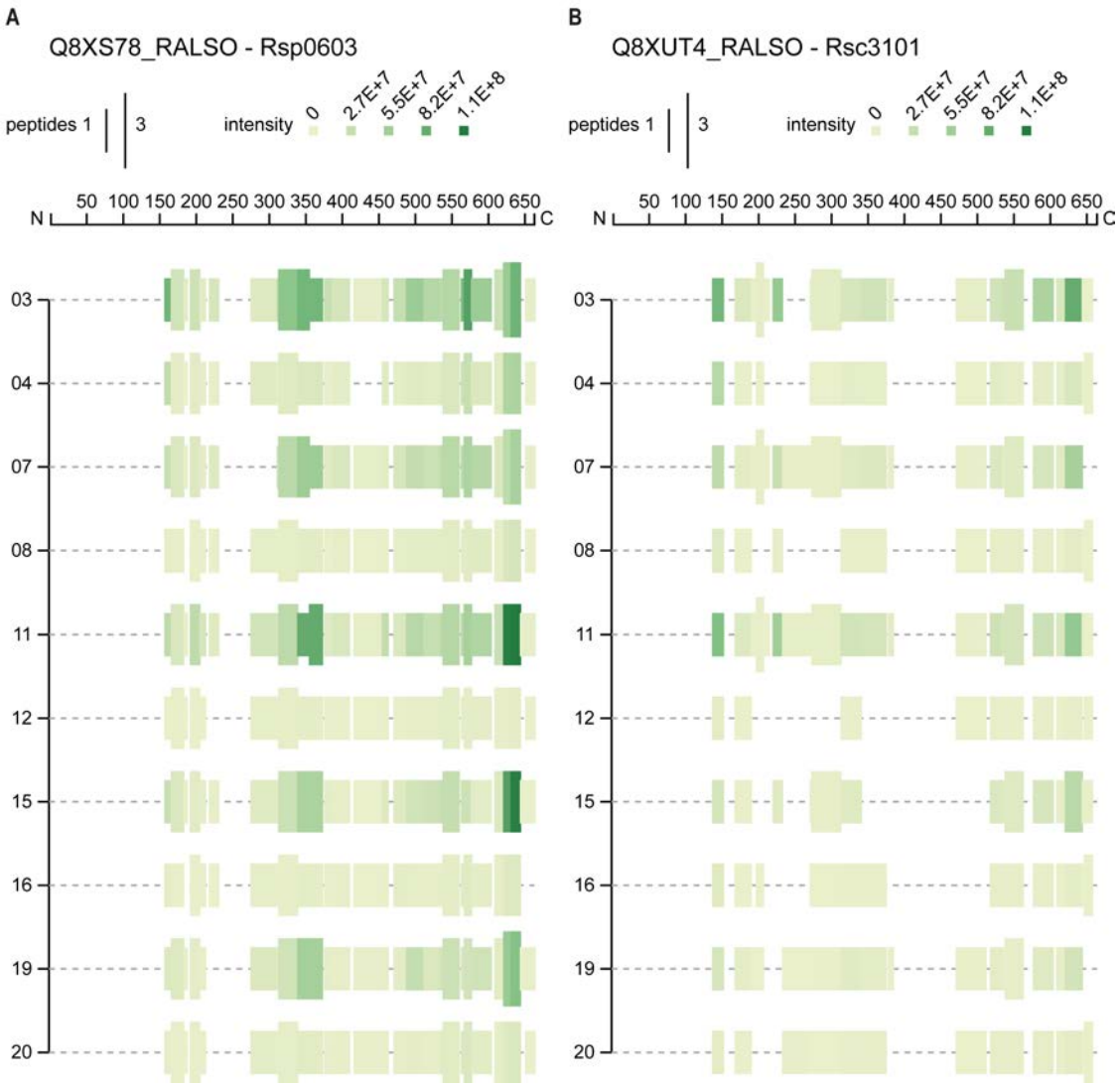

Supplementary Figure 9. Peptigram profile of Rsp0603 and Rsc3101. Mapping of the identified peptides in the proteomics data of (A) Rsp0603 and (B) Rsc3101. For each protein residue covered by an identified peptide, a green bar is drawn. The height of the bar is proportional to the amount of peptides that cover the specified position and the colour intensity is proportional to the summed ion intensities of the identified peptides in that position. Each sample is represented on a separate line (xylem samples have been selected for the visualisation). The webtool Peptigram (v.1.0.1) was used to create the plots.

Due to their length, the following Supplementary Tables may be found online in the following link: PhD_Roger.

Supplementary Table 1: List of filtered putative secreted proteins in the Xylem sap.

Supplementary Table 2: List of filtered putative secreted proteins in the Apoplast sap.

Supplementary Table 3. Output tables of the GO enrichment analysis conducted on the filtered protein datasets of the Xylem and Apoplast saps. The R package ClusterProfiler was used to conduct the analysis. Only the summary is shown, the full table may be sent upon request.

	GO ID	Description	GenRat.	BgRatio	pvalue	p.adjust	qvalue	Count
Xylem	0005576	extracellular region	7/64	19/3671	1.50E-08	8.39E-07	5.52E-07	7
	0016787	hydrolase activity	23/64	396/3671	6.80E-08	1.90E-06	1.25E-06	23
	0042597	periplasmic space	7/64	45/3671	9.45E-06	0.000158	0.000104	7
	0016798	hydrolase activity, acting on glycosyl bonds	6/64	31/3671	1.16E-05	0.000158	0.000104	6
	0005975	carbohydrate metabolic process	8/64	66/3671	1.41E-05	0.000158	0.000104	8
	0008236	serine-type peptidase activity	4/64	13/3671	5.34E-05	0.000499	0.000328	4
	0008152	metabolic process	6/64	58/3671	0.000441	0.003529	0.002322	6
	0005509	calcium ion binding	3/64	11/3671	0.000755	0.005284	0.003476	3
	0004553	hydrolase activity, hydrolyzing O-glycosyl compounds	3/64	13/3671	0.001276	0.007884	0.005187	3
	0006508	proteolysis	6/64	72/3671	0.001408	0.007884	0.005187	6
	0030246	carbohydrate binding	3/64	15/3671	0.00198	0.010082	0.006633	3
	0004252	serine-type endopeptidase activity	3/64	18/3671	0.003421	0.015967	0.010504	3
	0008233	peptidase activity	5/64	65/3671	0.005078	0.021876	0.014392	5
	0110165	cellular anatomical entity	3/64	25/3671	0.008842	0.035367	0.023268	3
	0009288	bacterial-type flagellum	3/64	26/3671	0.009872	0.036856	0.024248	3
	0009279	cell outer membrane	4/64	51/3671	0.011373	0.039805	0.026187	4
	0019867	outer membrane	3/64	28/3671	0.012135	0.039975	0.0263	3
Apoplast	0016787	hydrolase activity	13/22	396/3671	4.45E-08	1.38E-06	8.43E-07	13
	0016798	hydrolase activity, acting on glycosyl bonds	5/22	31/3671	7.30E-07	1.13E-05	6.92E-06	5
	0005975	carbohydrate metabolic process	6/22	66/3671	1.60E-06	1.65E-05	1.01E-05	6
	0008152	metabolic process	5/22	58/3671	1.77E-05	0.000137	8.40E-05	5
	0004553	hydrolase activity, hydrolyzing O-glycosyl compounds	3/22	13/3671	5.14E-05	0.000319	0.000195	3
	0006508	proteolysis	4/22	72/3671	0.000762	0.003937	0.002406	4
	0005509	calcium ion binding	2/22	11/3671	0.001825	0.008084	0.004941	2
	0008236	serine-type peptidase activity	2/22	13/3671	0.00257	0.009958	0.006087	2
	0030246	carbohydrate binding	2/22	15/3671	0.003434	0.01183	0.00723	2
	0004252	serine-type endopeptidase activity	2/22	18/3671	0.00495	0.015346	0.00938	2
	0005576	extracellular region	2/22	19/3671	0.005513	0.015536	0.009496	2
	0008233	peptidase activity	3/22	65/3671	0.006417	0.016576	0.010132	3

Supplementary Table 4. Summary of the BlastP searches of the S8 serien proteases of *R. solanacearum* GMI1000 strain in other strains of the RSSC. The NCBI protein ID, the percentage of identity (%id) and the percentatge of coverage (%co) is indicated for each protein and strain. Only the summary is shown, the full table may be sent upon request.

	Rsc2654			Rsc2653			Rsc3101			Rsp0603		
	Protein	%id	%co	Protein	%id	%co	Protein	%id	%co	Protein	%id	%co
CQPS-1	WP_058907898.1	98.235	100	WP_058907899.1	99.816	100	WP_071623917.1	98.795	100			
EP1	WP_020832604.1	97.804	100	WP_043897787.1	99.632	100	WP_071507738.1	98.946	100	WP_071507938.1	99.246	100
FJAT-1458	WP_020832604.1	97.804	100	WP_071895428.1	99.079	100	WP_071623917.1	98.795	100	WP_071508290.1	99.397	100
FJAT-91	WP_069079115.1	98.382	100	WP_019718304.1	99.632	100	WP_071508400.1	99.096	100	WP_016727722.1	99.548	100
GMI1000												
HA4-1	WP_111374732.1	99.412	100	WP_111374733.1	99.079	100	WP_071012351.1	98.946	100	WP_111374789.1	99.397	100
IBSBF_2570	WP_150396433.1	85.609	100	WP_150396434.1	93.394	99	WP_150396336.1	89.039	100			
IBSBF1503	WP_014616211.1	85.316	100	WP_042548972.1	93.53	99	WP_042548943.1	89.608	100	WP_039552775.1	90.09	100
KACC_10722	WP_075463488.1	86.784	100	WP_075463489.1	94.475	100	WP_075463175.1	88.705	100	WP_075466391.1	86.015	100
KACC10709	WP_069079115.1	98.382	100	WP_069079114.1	99.079	100	WP_069079179.1	98.946	100	WP_069079556.1	99.237	99
OE1-1	WP_020832604.1	97.804	100	WP_043897787.1	99.632	100	WP_071507738.1	98.946	100	WP_071507938.1	99.246	100
Po82	WP_014616211.1	85.316	100	WP_042567429.1	93.9	99						
PSI07	WP_013211572.1	86.404	100	WP_013211573.1	94.659	100	WP_013211140.1	86.898	100	WP_048816975.1	86.466	100
RS_488	WP_003263080.1	86.784	100	WP_003263079.1	92.791	99	WP_003262077.1	89.458	100	WP_039557708.1	88.138	100
RS_489	WP_013205222.1	86.068	95	WP_097908848.1	92.279	99	WP_013204879.1	89.307	100	WP_097909451.1	87.952	100
RSCM	WP_058907898.1	98.235	100	WP_058907899.1	99.816	100	WP_058908059.1	99.247	100	WP_058908819.1	99.246	100
SEPPX05	WP_087451100.1	98.529	100	WP_028860938.1	99.632	100	WP_058908059.1	99.247	100	WP_087452563.1	98.793	100
SL2064	WP_075463488.1	86.784	100	WP_075463489.1	94.475	100	WP_075463175.1	88.705	100	WP_075466391.1	86.015	100
SL2312	WP_118882662.1	86.131	100	WP_118882663.1	94.843	100	WP_118882495.1	88.855	100	WP_118884388.1	86.165	100
SL2330	WP_118872031.1	98.529	100	WP_118872032.1	99.448	100	WP_118871970.1	99.247	100	WP_087452563.1	98.793	100
SL2729	WP_118909152.1	98.235	100	WP_019718304.1	99.632	100	WP_071508400.1	99.096	100	WP_071508290.1	99.397	100
SL3022	WP_134927036.1	87.092	99	WP_134927037.1	94.659	100	WP_134926815.1	88.554	100	WP_134928043.1	86.165	100
SL3103	WP_118941035.1	98.454	95	WP_019718304.1	99.632	100	WP_069079179.1	98.946	100	WP_069079556.1	99.237	99
SL3175	WP_118869217.1	86.257	100	WP_078222007.1	95.028	100	WP_013211140.1	86.898	100	WP_048816975.1	86.466	100
SL3300	WP_069079115.1	98.382	100	WP_019718304.1	99.632	100	WP_071508400.1	99.096	100	WP_071508290.1	99.397	100
SL3730	WP_118909152.1	98.235	100	WP_019718304.1	99.632	100				WP_071508290.1	99.397	100
SL3755	WP_118872031.1	98.529	100	WP_118872032.1	99.448	100	WP_118871970.1	99.247	100	WP_058908819.1	99.246	100
SL3822	WP_069079115.1	98.382	100	WP_019718304.1	99.632	100	WP_071508400.1	99.096	100	WP_071508290.1	99.397	100
SL3882	WP_069079115.1	98.382	100	WP_019718304.1	99.632	100	WP_071508400.1	99.096	100	WP_071508290.1	99.397	100
T101	WP_118882662.1	86.131	100	WP_118882663.1	94.843	100	WP_118882495.1	88.855	100	WP_118884388.1	86.165	100
T11	WP_075463488.1	86.784	100	WP_075463489.1	94.475	100	WP_075463175.1	88.705	100	WP_075466391.1	86.015	100
T110				WP_151347316.1	99.263	100	WP_118871970.1	99.247	100			
T117	WP_069079115.1	98.382	100	WP_019718304.1	99.632	100	WP_071508400.1	99.096	100	WP_071508290.1	99.397	100
T12	WP_118882662.1	86.131	100	WP_118882663.1	94.843	100	WP_118882495.1	88.855	100			
T25				WP_118872032.1	99.448	100	WP_118871970.1	99.247	100	WP_058908819.1	99.246	100
T42	WP_118909152.1	98.235	100	WP_019718304.1	99.632	100	WP_071508400.1	99.096	100			
T51	WP_075463488.1	86.784	100	WP_075463489.1	94.475	100	WP_075463175.1	88.705	100	WP_075466391.1	86.015	100
T60	WP_069079115.1	98.382	100	WP_019718304.1	99.632	100	WP_071508400.1	99.096	100	WP_071508290.1	99.397	100
T78	WP_069079115.1	98.382	100	WP_019718304.1	99.632	100	WP_071508400.1	99.096	100	WP_071508290.1	99.397	100
T82	WP_118882662.1	86.131	100	WP_118882663.1	94.843	100	WP_118882495.1	88.855	100	WP_118884388.1	86.165	100
T95	WP_075463488.1	86.784	100	WP_075463489.1	94.475	100	WP_075463175.1	88.705	100	WP_075466391.1	86.015	100
T98	WP_118869217.1	86.257	100	WP_078222007.1	95.028	100	WP_013211140.1	86.898	100	WP_048816975.1	86.466	100
UW163	WP_014616211.1	85.316	100	WP_042567429.1	93.9	99						
UW386	WP_138928705.1	94.698	100				WP_064048284.1	96.687	100	WP_138929890.1	94.729	100
UY031	WP_003263080.1	86.784	100	WP_003263079.1	92.791	99	WP_003262077.1	89.458	100	WP_039557708.1	88.138	100
YC40-M	WP_064820688.1	96.434	94	WP_043897787.1	99.632	100						
YC45	AKZ25739.1	99.411	100	AKZ25738.1	99.816	100	AKZ25317.1	99.096	100			

Supplementary Table 5. Bacterial strains, plasmids, and oligos used in this work.

Strains		
Name	**Relevant characteristics**	**Source or reference**
E. coli		
TOP10	Chemically Competent Cell used for cloning	
BL21	Chemically Competent Cell ideal for heterologous expression systems based on the T7 promoter	
Shuffle	Chemically Competent Cell ideal for heterologous expression optimised for correct folding of active proteins with disulfide bonds	
A. tumefaciens		
ASE pSoup	Electrocompetent *A. tumefaciens* containing the pSoup to enable binary plasmid replication	
R. solanacearum		
GMI1000	Wild type strain (Phylotype I) (0^R)	
GMI1000 *ΔRsp0603*	Wild type GMI1000 strain with the *Rsp0603* cds replaced by GenR cassete (G^R)	This work
GMI1000 *ΔRsc3101*	Wild type GMI1000 strain with the *Rsp3101* cds replaced by KanR cassete (K^R)	This work
GMI1000 *ΔRsp0603ΔRsc3101*	Wild type GMI1000 strain with the *Rsp0603* and *Rsc3101* cds replaced by GenR and KanR cassete, respectively (G^R, K^R)	This work
GMI1000 *ΔRsp0603-Rsp0603-HA*	Wild type GMI1000 strain with the *Rsp0603* cds replaced by GenR cassete, complemented with the native version of the *Rsp0603 cds* (G^R, T^R)	This work
GMI1000 *ΔRsp0603-Rsp0603(S589A)-HA*	Wild type GMI1000 strain with the Rsp0603 cds replaced by GenR cassete, complemented with the *Rsp0603* Serine 589 residue mutated to Alanine (G^R, T^R)	This work
Plasmids		
Name	**Relevant characteristics**	**Source or reference**
pDONOR207	Gateway donor vector (G^R)	Invitrogen
pJET1.2/blunt	CloneJET Cloning vector (Ap^R)	Thermo Scientific™
pCold	pCold DNA cold-shock expression system (Ap^R)	Takara
pRCT-PpsbA-GWY	Gateway vector carrying tetracycline cassette flanked by homologous regions to the GMI1000 genome of a permissive site for complementation (Ap^r, Tc^r)	This work
pOPIN-Rsp0603-His-GB1	pOPIN backbone carrying *Rsp0603* cds fused to His-GB1 (Ap^R)	This work
pOPIN-Rsp0603-His-MBP	pOPIN backbone carrying *Rsp0603* cds fused to His-MBP (Ap^R)	This work
pOPIN-Rsp0603(S589A)-His-GB1	pOPIN backbone carrying *Rsp0603(S589A)* cds fused to His-GB1 (Ap^R)	This work
pOPIN-Rsp0603(S589A)-His-MBP	pOPIN backbone carrying *Rsp0603(S589A)* cds fused to His-MBP (Ap^R)	This work
pCold-Rsp0603-HA	pCold backbone carrying *Rsp0603-HA* (Ap^R)	This work
pCold-Rsp0603(S589A)-HA	pCold backbone carrying *Rsp0603(S589A)-HA* (Ap^R)	This work
Pro35S::myc-Rsp0603-mCherry-HA	Greengate modular system carrying c-Myc tag, fused to *Rsp0603-mCherry-HA* (Sm^R)	This work
Pro35S::aAmilaseSP-Rsp0603-mCherry-HA	Greengate modular system carrying a-AmilaseSP, fused to *Rsp0603-mCherry-HA* (Sm^R)	This work
Pro35S::ChitinaseIVSP-Rsp0603-mCherry-HA	Greengate modular system carrying ChitinaseIVSP, fused to *Rsp0603-mCherry-HA* (Sm^R)	This work
Pro35S::ChitinaseIVSP-Rsp0603(S589A)-mCherry-HA	Greengate modular system carrying ChitinaseIVSP, fused to *Rsp0603(S589A)-mCherry-HA* (Sm^R)	This work

Supplementary Table 6. Statistical output files. Only significant results are shown.

Figure 4A

TP4

ANOVA

```
            Df Sum Sq Mean Sq F value  Pr(>F)
Strain       3  3.046  1.0154   5.484 0.00183 **
Residuals   76 14.072  0.1852
---
Signif. codes:
0 ‘***’ 0.001 ‘**’ 0.01 ‘*’ 0.05 ‘.’ 0.1 ‘ ’ 1
  Tukey multiple comparisons of means
    95% family-wise confidence level
Fit: aov(formula = DI ~ Strain, data = ano)
$Strain
             diff         lwr        upr     p adj
0603-WT    0.3625  0.005066172  0.7199338 0.0455710
3101-WT   -0.1250 -0.482433828  0.2324338 0.7949786
2d-WT     -0.1000 -0.457433828  0.2574338 0.8827382
3101-0603 -0.4875 -0.844933828 -0.1300662 0.0032847
2d-0603   -0.4625 -0.819933828 -0.1050662 0.0058331
2d-3101    0.0250 -0.332433828  0.3824338 0.9977800
```

TP10

ANOVA

```
            Df Sum Sq Mean Sq F value Pr(>F)
Strain       3   3.75   1.249    2.58 0.0597 .
Residuals   76  36.78   0.484
---
Signif. codes:
0 ‘***’ 0.001 ‘**’ 0.01 ‘*’ 0.05 ‘.’ 0.1 ‘ ’ 1
  Tukey multiple comparisons of means
    95% family-wise confidence level
Fit: aov(formula = DI ~ Strain, data = ano)
$Strain
             diff        lwr        upr     p adj
0603-WT    0.0250 -0.5528982 0.60289822 0.9994704
3101-WT    0.0750 -0.5028982 0.65289822 0.9862628
2d-WT     -0.4625 -1.0403982 0.11539822 0.1616813
3101-0603  0.0500 -0.5278982 0.62789822 0.9958268
2d-0603   -0.4875 -1.0653982 0.09039822 0.1281740
2d-3101   -0.5375 -1.1153982 0.04039822 0.0776152
```

TP12

ANOVA

```
            Df Sum Sq Mean Sq F value Pr(>F)
Strain       3   0.45 0.15000    2.78 0.0467 *
Residuals   76   4.10 0.05395
---
Signif. codes:
0 ‘***’ 0.001 ‘**’ 0.01 ‘*’ 0.05 ‘.’ 0.1 ‘ ’ 1
  Tukey multiple comparisons of means
    95% family-wise confidence level
Fit: aov(formula = DI ~ Strain, data = ano)
$Strain
             diff        lwr          upr     p adj
0603-WT    -0.05 -0.2429353  0.142935257 0.9041078
3101-WT    -0.05 -0.2429353  0.142935257 0.9041078
2d-WT      -0.20 -0.3929353 -0.007064743 0.0392516
3101-0603   0.00 -0.1929353  0.192935257 1.0000000
2d-0603    -0.15 -0.3429353  0.042935257 0.1818388
2d-3101    -0.15 -0.3429353  0.042935257 0.1818388
```

Figure 4B

TP3

ANOVA

```
              Df   Sum Sq   Mean Sq F value Pr(>F)
Strain         3 1.09e+15 3.635e+14   3.565 0.0157 *
Residuals    152 1.55e+16 1.020e+14
---
Signif. codes:
0 ‘***’ 0.001 ‘**’ 0.01 ‘*’ 0.05 ‘.’ 0.1 ‘ ’ 1
  Tukey multiple comparisons of means
    95% family-wise confidence level
Fit: aov(formula = CFU ~ Strain, data = fit_3)
$Strain
               diff       lwr        upr     p adj
0603-WT   -2694545.8  -8877114  3488022.2 0.6702771
3101-WT   -2040311.1  -7997983  3917360.5 0.8102556
2d-WT     -7157174.0 -13114846 -1199502.4 0.0114828
3101-0603   654234.8  -5303437  6611906.4 0.9918773
2d-0603   -4462628.1 -10420300  1495043.5 0.2134948
2d-3101   -5116862.9 -10840809   607082.8 0.0975115
```

7. GENERAL DISCUSSION

7. GENERAL DISCUSSION

Ralstonia solanacearum is one of the most devastating plant pathogens worldwide, infecting over 200 plant species and causing severe economic losses in agricultural production (Hayward, 1991; Mansfield *et al.*, 2012). In this work we set to characterise the transcriptomic landscape of the phylotype IIB-1 UY031 strain, described as highly aggressive on potato (Siri, Sanabria and Pianzzola, 2011). First, by unravelling the gene expression landscape throughout plant infection (Chapter 1 or C1). Second, by filling the knowledge gaps of its life cycle by studying the transcriptional adaptation of *R. solanacearum* in the overlooked soil and water environmental stages (Chapter 2 or C2). The second part of the thesis delves on the characterisation of specific genes potentially involved in virulence and/or fitness of *R. solanacearum*. We studied the role of the catalase KatE in detail (Chapter 3 or C3) and started the description and characterisation of the subtilisin-like protein family of *R. solanacearum*, highly accumulated inside the plant during infection (Chapter 4 or C4).

7.1 Transcriptomic studies as a tool to understand gene expression dynamics

As introduced, many different virulence factors have been identified in *R. solanacearum* and the regulation networks governing their expression studied in detail (Schell, 2000; Genin and Denny, 2012). However, preliminary gene expression studies were mostly conducted *in vitro,* and the resulting observations were not fitting with the real gene expression observed during infection (Jacobs *et al.*, 2012; Monteiro *et al.*, 2012). For example, *hrp* expression *in planta* was observed at late stages of infection, contradicting the early assumption that this system was only expressed in low bacterial densities during early infection (Genin *et al.*, 2005). The advancement and easy access to high throughput transcriptomic technologies has provided a useful platform to study *R. solanacearum* gene expression and regulation networks *in planta*. However, transcriptomic studies conducted before this work only captured the gene expression in specific *in planta* conditions such as root apoplast (Puigvert *et al.*, 2017) or bacteria living in the xylem at the onset of infection (Jacobs *et al.*, 2012; Dalsing *et al.*, 2015; Meng *et al.*, 2015; Ailloud *et al.*, 2016; Khokhani *et al.*, 2017). The knowledge gathered on the complex gene expression regulation networks, suggests an everchanging transcriptional landscape reliant on cell density, plant molecules, metabolic cues and environmental signals that cannot be captured in a single sampling point (Álvarez, Biosca and López, 2010). To overcome the constraint of previous transcriptomic studies, we designed an experimental setup to provide a detailed expression dynamics of the whole *R. solanacearum* life cycle (C1 and C2).

To study the transcriptomic landscape of *R. solanacearum* inside the plant, bacteria were sampled in a time course manner from the apoplast and the xylem in the early and late stages of infection. The major problem of the root apoplast bacterial transcriptome was the low yield of bacterial RNA and the difficulty to not contaminate samples with bacteria from other tissues. To overcome this problem, we used the leaf apoplast as a paradigm of the root apoplast, where bacteria is described to behave similarly and deploy similar strategies (Hikichi, 2016). Also, our sampling points were optimised to obtain similar bacterial loads in the apoplast and the xylem vessels to understand the niche adaptation without the added variable of bacterial densities. Despite these limitations, leaf apoplast samples were the most comparable to the previously published root apoplast. Moreover, different virulence genes such as motility were found induced in this condition as previously reported (Kang *et al.*, 2002; Corral *et al.*, 2020; de Pedro-Jové *et al.*, 2021) (C1). Briefly, based on the differential expression analysis, we could identify four different genetic programmes deployed by the pathogen inside the plant: (1) genes expressed throughout the plant infection, (2) genes specifically induced in the apoplast, (3) genes induced during the growth of the bacteria in the xylem, and (4) genes unique of the late xylem condition (de Pedro-Jové *et al.*, 2021) (C1). Of interest is this late xylem condition, in which *R. solanacearum* was recently described to escape the xylem pits and invade the surrounding parenchyma cells (Planas-Marquès *et al.*, 2020).

As an environmental pathogen, *R. solanacearum* can spend most of its life outside the plant in the soil or moving through the waterways. These are crucial stages of its life cycle that have only been superficially studied to quantify its persistence and survival along time (Van Elsas *et al.*, 2000, 2001). However, there is no knowledge about the transcriptional changes that facilitate adaptation and survival in these conditions. To complete the whole transcriptional landscape throughout the life cycle of *R. solanacearum*, we sampled bacteria inoculated in the soil and water (C2). As we wanted to capture the early adaptation to these environmental conditions before bacterial cells entered the VBNC state (Van Overbeek *et al.*, 2004), we recovered soil samples after three days, when plant infection is supposed to occur (de Pedro-Jové *et al.*, 2021) (C1), and water samples after six hours. In the case of water, the sampling point was selected based on the time point with most transcriptional changes in a previous transcriptomic study in the pathogen *Legionella pneumophila* growing in water (Li *et al.*, 2015). Remarkably, as observed in *L. pneumophila*, the peak of gene expression changes in *R. solanacearum* was also observed around six to nine hours (C2, Fig. 3, 4, S4 and S5). In the study of the environmental conditions, we identified the soil as the most distinct condition, and observed a high similarity of the water condition to the late xylem (or out of the xylem) condition (C2, Fig. 1).

The use of GO terms or KEGG pathways enrichment analysis are a valuable strategy to unbiasedly search for overrepresented gene functions among the different condition. However, this enrichment relies on limited well-known pathways in the KEGG or to GO terms based on homology to model organisms that usually fail to be associated to genes with a similar function due to the high diversity of bacterial genomes (Torto-Alalibo, Collmer and Gwinn-Giglio, 2009; Law, Kale and Murali, 2021). Among the orphan genes not considered in this enrichment analysis we find crucial virulence or fitness genes of *R. solanacearum*. Therefore, in both transcriptomic studies (C1 and C2) manually curated categories were constructed to define a set of genes known to be involved in virulence (C1) or to fully classify the genes of *R. solanacearum* into the different categories including the different virulence and fitness determinants (C2).

7.2 Decoding the genetic reprogramming of virulence and fitness determinants during the life cycle of *R. solanacearum*

Studying the complete life cycle rather than isolated niches strengthens the biological relevance of the observations and highlights the importance and dynamism of the different virulence and fitness factors. Moreover, for the first time, the addition of the environmental transcriptomic data has allowed to ascribe a broader role to genes previously only linked to virulence and life *in planta* of *R. solanacearum*.

7.2.1 Regulation of the T3SS and related T3E

One of our main observations was the induction of the T3SS regulators and downstream triggered genes like the T3E (Coll and Valls, 2013). Interestingly, in C1 we found out that the T3SS cascade has a sequential activation *in planta* with *hrpG* induction by the *prhI and prhJ* peaking in the apoplast, and the downstream regulator *hrpB* induced in the xylem together with the *hrp* operon and most of the T3E (Figure 1). In the apoplast, the expression of the regulatory *prh* and *hrpG* genes was most llikely triggered by the canonical plant cell contact cascade starting at PrhA (Marenda *et al.*, 1998; Brito *et al.*, 2002). Interestingly, the high induction of the downstream *hrpB* regulator in the xylem is also triggered independently from the PrhA through unknown signals present in the minimal medium or in plant sap (Figure 1). This also reinforces

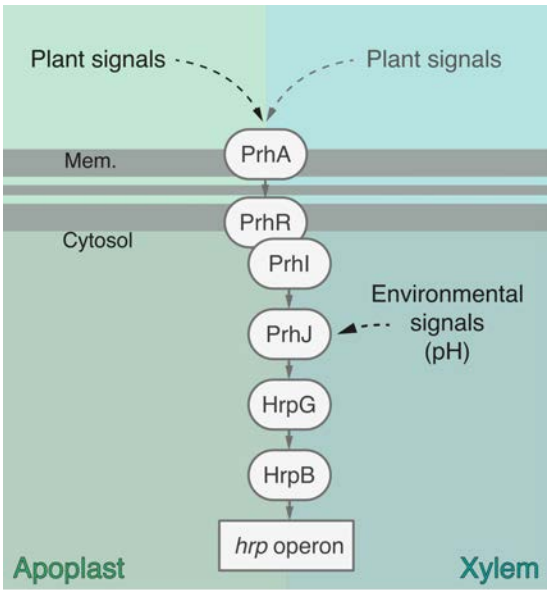

Figure 1. Main inputs modulating T3SS cascade in *R. solanacearum* during host infection in the Apoplast and Xylem.

the idea that the HrpG and HrpB regulators might play different roles in different compartments during infection (Vasse *et al.*, 2000; Valls, Genin and Boucher, 2006) and further disagrees with the initial hypothesis that T3SS and downstream genes were solely required for the initial stages of infection due to its repression under high bacterial densities (Yoshimochi *et al.*, 2009; Monteiro *et al.*, 2012). Regarding the T3SS regulation in the environment (C2, Fig. 3), we stumbled upon an unexpected activation of this virulence system. In soil, only *hrpG* amongst the whole cascade or downstream genes was highly induced, reinforcing the idea of a network of regulators rather than a cascade, and the functional differentiation of the different T3SS core regulators (Valls, Genin and Boucher, 2006).

Strikingly, we observed an induction in water of the T3SS cascade at the *hrpG* level, and of all downstream regulatory proteins, triggering the *hrp* operon and T3E expression (C2, Fig. 3 and S3). A closer look at the different components of the T3SS regulatory cascade made us hypothesise that the water cues were sensed though the *prhJ*, which in its turn triggered all the downstream cascade (C2, Fig. 3). Interestingly, alternative induction pathways independent of plant cell contact, have been observed for a long time but, at the time, these signals could not be identified (Brito *et al.*, 1999; Zuluaga, Puigvert and Valls, 2013). In our study we identified two environmental cues modulating the T3SS in water: first, the pH and second, starvation. The nutrient supply or the neutralisation of alkali pH abolished the T3SS induction observed in the water. Although this environmental induction was not prolonged (C2, Fig. 3, 4, S4 and S5) possibly due to the costly production of all the downstream machinery and effectors (Sturm *et al.*, 2011), we could not find a reasonable answer to why the bacterium could need this virulence system in water. One of our hypotheses was that these same newly discovered environmental cues were also important for the virulence *in planta*. Interestingly, a gradual alkalinisation of pH was observed along infection going from pH 5.5 on healthy plant to pH values around 8 when plants were completely wilted (C2, Fig. 5). This alkalinisation was also observed during drought stress, a stress also induced by the bacterial wilt disease (Wilkinson *et al.*, 1998; Grunwald *et al.*, 2021). Our hypothesis is that, besides the early plant triggered activation of the T3SS, which leads to high expression of the HrpG regulator, later signals such as pH could synergically help to induce *hrpB* and the T3SS machinery and effectors (Figure 1). On the other hand, the higher *hrpG* induction seen in the apoplast and in soil cold be linked with the proteins described to be part of its regulon (Valls, Genin and Boucher, 2006). For example, different CWDE, attachment related proteins, phytohormone production and different protection enzymes like ROS detoxifying enzymes could be of paramount importance for the early colonisers of the plant. This correlates with the observation that *hrpG* mutants despite being highly infective were unable to transit through the root endodermis, reinforcing the hypothesis of the role of this regulator for early vascular invasion (Vasse *et al.*, 2000). In soil, different genes induced by the HrpG regulon were found highly upregulated such as exopolysaccharide synthesis repressor (*epsR*) or different detoxifying enzymes whereas others, such as the CWDE *egl*, were clearly downregulated (C2). This implies an unknown regulatory complex which could further tune the HrpG regulon described *in vitro* or *in planta*.

Linking the expression pattern of T3E and their role *in planta* can be sometimes tricky due to their simultaneous activation during infection and their functional redundancy (Lei *et al.*, 2020; De Ryck, Van Damme and Goormachtig, 2023). Some effectors have a differentiated expression pattern such as the poorly characterised *ripE2*, that seems apoplast specific, but most effectors showed high expression throughout the plant infection with most of them highly induced in the xylem (C1, Fig. 3 and C2, Fig. 3). Some of these effectors are the *ripAB* (*popB*) and *ripAC* (*popC*) that have been described to modulate plant defence by interfering, respectively, with the gene targets of C^{2+} and salicylic acid signalling pathways (Zheng *et al.*, 2019; Qi *et al.*, 2022), or by suppressing ETI and ubiquitination (Figure 2) (Yu *et al.*, 2020, 2022). Also, the induced AWR (RipA) or GALA (RipG) families are required for full virulence, with RipA5 (AWR5) effector targeting the conserved target of rapamycin (TOR) pathway, a switch regulator between growth and stress response (Solé *et al.*, 2012; Popa *et al.*, 2016), and different RipG effectors predicted to interfere with proteasome degradation (Figure 2) (Remigi *et al.*, 2011). The effector genes *ripE1*, *ripB* and *ripAY* were also expressed throughout the infection and even higher in the xylem sap. The three of them have been functionally characterised to interfere, in this order, with

jasmonate signalling (Sang *et al.*, 2020), ROS production and cytokinin pathways (Cao *et al.*, 2022), and to supress ETI immune responses (Figure 2) (Sang *et al.*, 2020). Finally, the highly induced in all *in planta* conditions *ripN*, *ripD* and *ripAD* effector genes, are known to suppress or interfere with PTI (Figure 2) (Sun *et al.*, 2019; Jeon *et al.*, 2020). In contrast, *ripI* and *ripTPS,* which induce the plant biosynthesis of the bacterial nutrient sources GABA and trehalose, respectively (Figure 2), showed low expression throughout infection (C1, Fig. 3) (Poueymiro *et al.*, 2014; Xian *et al.*, 2020). The observed low expression could be a sign of their tight regulation since overproduction of these metabolites has been linked to defence response and cell death (Wang *et al.*, 2019; Laili *et al.*, 2021).

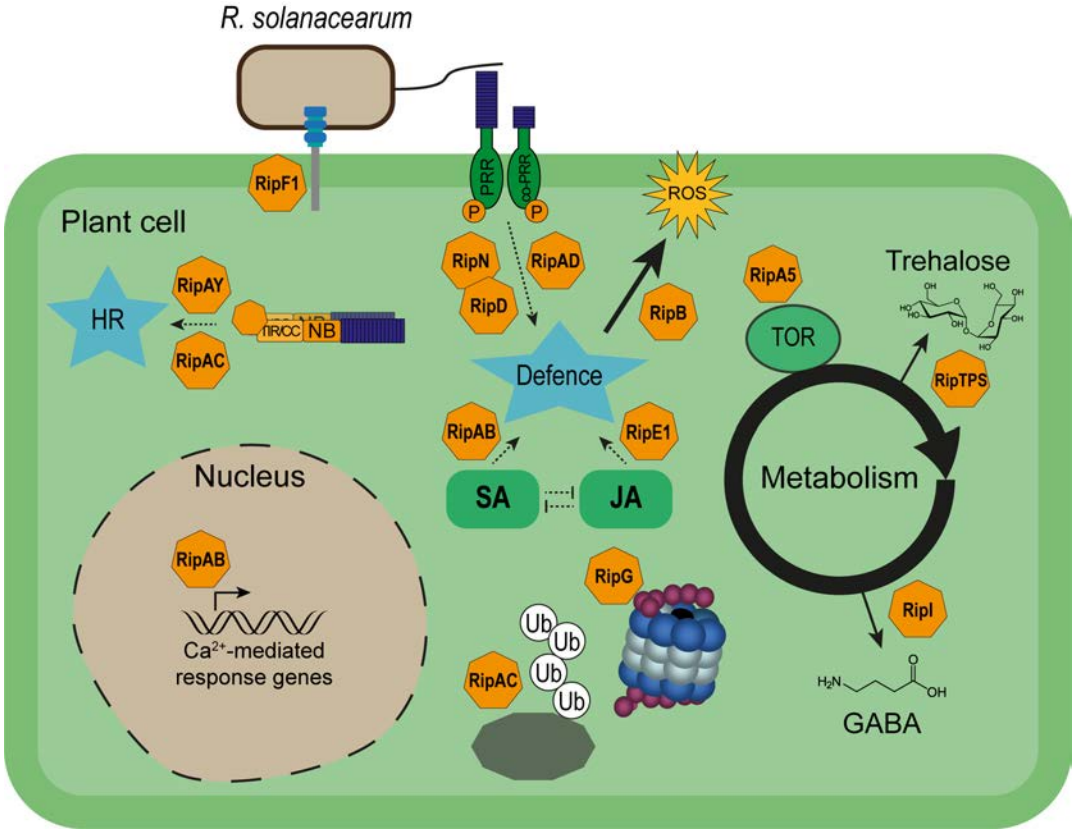

Figure 2. Schematic representation of the known functions of T3E from *R. solanacearum* inside the plant cell during infection. Abbreviations can be found in the text except for HR, Hypersensitive response; SA, Salicylic acid; JA, Jasmonic acid; Ub, Ubiquitin; GABA, gamma-aminobutyric acid and ROS, Reactive oxygen species.

In the water condition, there was a general induction of T3E similar to the expression observed *in planta*, which contrasted with the T3E repression in soil (C2, Fig. 3). Surprisingly, a high expression of *ripAM* and *ripJ* was specifically observed in the soil environment. Only *ripAM* has been linked to virulence in potato (Zheng *et al.*, 2019) and to be secreted independently from the helper *hrp* associated (*hpa*) proteins (Lonjon *et al.*, 2016). An important feature that could facilitate its secretion in a context where the T3SS is not fully active. However, the putative function of these effectors in soil is a mystery. Overall, characterisation of *R. solanacearum* effectors is still a complex research field hindered by the multiple hosts and pathogen diversity (Landry *et al.*, 2020; De Ryck, Van Damme and Goormachtig, 2023). A deeper characterisation of the disease progression combined with information on the T3E expression and secretion will be key to comprehend their multiple roles during the life cycle of *R. solanacearum*.

7.2.2 ROS detoxification throughout *R. solanacearum* life cycle

Upon pathogen recognition, plants rapidly respond with an apoplastic ROS burst used as defence signalling and to challenge pathogen survival (Saijo, Loo and Yasuda, 2018). The ROS molecules, which include superoxide, hydroxyl radicals and hydrogen peroxide, can cause severe damage to the cells leading to DNA mutation and eventually cell death (Imlay, 2008). As expected, *R. solanacearum*

contains several detoxifying enzymes, or ROS scavenging genes, to cope with this oxidative burst. Many genes were found to be highly expressed in the plant environment such as the alkyl hydroperoxide reductases *ahp* (Flores-Cruz and Allen, 2011). Also, the differential expression analysis identified few genes that were specifically expressed in the apoplast, such as the catalases (*katE* and *katG*), the peroxidase *bcp* or the known oxidative stress response regulator *oxyR* (C2, Fig. 2) (Flores-Cruz and Allen, 2009, 2011). The induction of stress-related genes in water followed the same pattern as in the xylem condition, thus reinforcing the idea of the similarity between these two conditions. In soil, many more stress-related genes were found induced and to even higher fold changes (C2, Fig. 2 and S3). Moreover, other genes related to protection in harsh environments such as Fe-S clusters, used as an oxidizing source, or heavy metal homeostasis proteins were recurrently found in the soil (Imlay, 2008) (C2, Table 1). All these results suggest that, in addition to playing a crucial role for the growth of *R. solanacearum* inside the plant (Colburn-Clifford, Scherf and Allen, 2010; Flores-Cruz and Allen, 2011), ROS scavenging enzymes are also required for the survival of the pathogen in the soil environment.

Due to the importance of ROS scavenging enzymes in the life cycle of *R. solanacearum*, we conducted a detailed characterisation of the catalase family. This involved an in-depth study of the role of the monofunctional catalase *katE* (C3), as well as preliminary analysis on the bifunctional catalase-peroxidase *katG* (C2), which provided a comprehensive overview of the role of these enzymes in the life cycle of *R. solanacearum*. In C3, we detected the catalase activity of both KatG and KatE enzymes in polyacrylamide gels of the protein extracts, and we demonstrated the importance of katE in detoxifying high concentrations of H_2O_2 *in vitro* (C3, Fig. 3). However, deletion mutants of *katE* did not exhibit any impact on virulence or fitness of the bacterium *in planta* (C3, Fig. 5), or in their survival in the soil (C2, Fig. 2). On the contrary deletion of the bifunctional catalase-peroxidase *katG* reduced the ability of the bacterium to survive in the soil environment (C2, Fig, 2). Moreover, unpublished data showed that KatG also contributes to the detoxification of H_2O_2 *in vitro*, acting in a redundant manner with katE at low H_2O_2 concentrations (Invernón Garrido, 2023). Additionally, KatG was also important for the fitness of the bacteria inside the plant independently of KatE catalase activity (Invernón Garrido, 2023). This surprised us as it is *katE*, and not *katG*, the enzyme positively regulated by the regulator HrpG and the one that showed higher expression *in planta* (Valls, Genin and Boucher, 2006; de Pedro-Jové *et al.*, 2021). However, monofunctional catalase mutants usually behave as the wild types, as the peroxidase activity is preferentially used at low H_2O_2 concentrations. Only when peroxidases are saturated, or no donors are available, the function of catalases can be visualised (Mishra and Imlay, 2012). This suggests that H_2O_2 inside the plant, or in the soil environment, might not reach concentrations high enough for KatE to be required as there are multiple other detoxifying enzymes, such as KatG, that act primarily for its detoxification. Although KatE might have minor roles such as biofilm formation (C3, Fig. 4), it would be interesting to uncover the other roles of KatE in the life cycle of *R. solanacearum*.

7.2.3 Metabolic adaptation to the changing environments of *R. solanacearum*

Despite the upregulation of many virulence factors during the late stages of infection, we observed a general metabolic shutdown accompanied by downregulation of transcription and translation which was consistently seen in the water environment and to a lesser extent in soil (C1, Fig. 1 and 2, and C2, Fig. 1 and S2). Despite this general downregulation, nitrogen metabolism was found to be important for the xylem and the soil environment. The combination of the rapid oxygen consumption and the encounter of low oxygen environments force *R. solanacearum* to use other molecules such as nitrate for respiration (Dalsing *et al.*, 2015). Additionally, *R. solanacearum* also has the machinery to assimilate and detoxify the intermediate nitrogen reactive species (Dalsing and Allen, 2014; Truchon *et al.*, 2023). Detoxification of nitrogen reactive species could also be crucial to counter plant defence responses (Mur *et al.*, 2017) or to survive and thrive in agricultural soils containing high nitrogen (Wang, Liu and Ding, 2020).

In addition to the necessity of nitrogen metabolism in the soil environment, *R. solanacearum* must also deal with a general scarcity of nutrients including carbon sources such as sugars. To overcome this

challenge, the pathogen induces metabolic pathways to utilise alternative carbon substrates. Plant debris mainly constituted of lignin is a highly stable compound that can be degraded by multiple soil microorganisms, among them *R. solanacearum*, which was predicted to possess the enzymes for its utilisation (Bugg *et al.*, 2011). In the soil condition, dioxygenases, and multiple genes from the phenylacetate pathway (*paa*), involved in the cleavage of the lignin aromatic ring (Teufel *et al.*, 2010; Bugg *et al.*, 2011), were identified as marker upregulated genes (C2, Table 1). Interestingly, the end product of the lignin polymer degradation acetyl-CoA is the main input of the glyoxylate cycle (Maharjan *et al.*, 2005; Weng, Peng and Han, 2021). This variation of the tricarboxylic acid cycle (TCA) was also highly induced in the soil with its two main enzymes, isocitrate lyase and malate synthase, found among the marker soil genes. This alternative cycle can bypass the TCA to redirect the use of carbon for energy production to the gluconeogenesis (Dunn, Ramírez-Trujillo and Hernández-Lucas, 2009). Interestingly, biosynthetic genes of the glycogen pathway and of the derived sugar trehalose were upregulated in the soil (C2, Table 1). Both compounds have been described to enhance bacterial survival in challenging environments under osmotic and oxidative stresses like the ones encountered in the soil environment (Wang and Wise, 2011; Ahn *et al.*, 2016; MacIntyre *et al.*, 2020).

Figure 3. Graphical representation of the gene groups expression (Glyoxylate cycle, T3SS, Nitrogen metabolism, Stress response genes Type IV pili and Flagella) along the life cycle of *R. solanacearum*. The colours range from dark purple (high expression) to light purple (low expression).

7.2.4 Role of motility and attachment in the life cycle of *R. solanacearum*

R. solanacearum displays swimming and twitching motility, which involved the use of flagellum or T4P, respectively. Both of them were required for full virulence during soil soaked inoculation, but whereas twitching *pilA* mutants (deficient in the T4P) were impaired throughout all the infection process, flagellar mutants only showed an effect during initial root colonisation (Tans-Kersten, Huang and Allen, 2001; Kang *et al.*, 2002; Corral *et al.*, 2020). Consistent with this information, flagellar and twitching genes were highly induced in the apoplast with twitching induction maintained throughout infection (C1, Fig. 4). In the water environment, we also observed enrichment of swimming and twitching motility, an upregulation observed in other bacterial pathogens that move through water (C2, Fig. S2) (Li *et al.*, 2015; Bronowski *et al.*, 2017; Vivant *et al.*, 2017). In the soil, only few genes related to motility were upregulated, with the exception of the highly upregulated T4P, required for the pathogen to adhere to different surfaces (C2, Table S5) (Kang *et al.*, 2002).

Our results have shed light on the complex gene expression dynamics in the pathogen, which allows its adaptation to the various ecological niches it encounters throughout its life cycle in both the plant and the environment. We have described *R. solanacearum* metabolic preferences, as well as the importance of different virulence and fitness factors not only during the infective stage, but also under previously unknown environmental conditions.

7.3 Secretome analysis as an approach to discover novel virulence factors in *R. solanacearum*

In C4, we focused our attention on proteomics/secretomics analysis as a novel and different approach to study *R. solanacearum* virulence and/or fitness factors *in planta*. When analysing transcriptomic data, useful information is gathered on the expression of key genes and its regulation in different conditions. However, a portion of the information is missed due to the many steps in between a gene is transcribed and the protein is produced. Although translation in bacteria is not as complex as in eukaryotic organisms, proteins that are synthesised can also be post-translationally modified or degraded, and only a subset of them will eventually be secreted (de Sousa Abreu *et al.*, 2009; Vogel and Marcotte, 2012). Consonant with this information, the comparison of the gene expression data and the protein abundance of the secreted proteins showed very low correlation (C4, Fig. S5). Thus, having information on the proteomic level, and even better at the subset of proteins secreted by *R. solanacearum* during infection, might provide a more direct representation of the gene functions deployed by the bacterium to infect the plant.

7.3.1 Characterisation of the *R. solanacearum* secretome during plant infection

The proteomic data from leaf apoplast and xylem sap obtained from mock and *R. solanacearum* inoculated plants were previously analysed to elucidate plant defence response to pathogen infection (Planas-Marquès *et al.*, 2018; Planas-Marquès, 2020). In C4 of this thesis we reanalysed the data to change the focus to the bacterial proteins potentially secreted in the apoplast and xylem, the two main plant-pathogen battlegrounds in the plant (Planas-Marquès *et al.*, 2020). It is interesting to note that despite the differences in the total amount of proteins, all apoplastic proteins were also detected in the xylem, and the enrichment analysis of both proteins sets yielded very similar results. These similarities suggest a comparable behaviour of the bacterium in terms of secreted proteins in the plant environments at the early stages of infection. As expected, GO terms related to hydrolases were the most abundant ones (C4, Fig. 2). These activities correspond to the CWDE, also referred to glycoside hydrolases, known to degrade (or hydrolyse) glycosidic bonds from the plant cell wall (Drula *et al.*, 2022). This enrichment correlated with the proteins retrieved by looking at the 20 most abundant proteins from each plant sap and variety. In this list, the CWDE were the most represented group of proteins secreted by *R. solanacearum*. Among them, we found different cell wall remodelling enzymes such as glucanases, pectinesterases and polygalacturonases (C4, Table 1). Interestingly, the combined action of these enzymes allow the degradation of the big diversity of polysaccharides present in plant cell walls such as cellulose, hemicellulose and pectin (Vorwerk, Somerville and Somerville, 2004). The collective function of these enzymes is needed for plant colonisation and for full virulence as shown by

deletion mutants of multiple CWDE in *R. solanacearum* (Liu *et al.*, 2005). However, these enzymes can also release cell derived compounds sense as elicitors (or DAMP) that trigger plant defence responses (Nakaho and Allen, 2009). This observation emphasise the importance of the cell wall as an critical physical barrier for plant-pathogen interactions (Vorwerk, Somerville and Somerville, 2004; Planas-Marquès *et al.*, 2020).

Besides the known CWDE, an interesting protein identified among the most abundant ones only in the xylem was RipF1 (or PopF1). This effector was described to act as a translocator, possibly creating the pore in the host membrane, and to help in the secretion of T3E such as RipAA (or AvrA). Interestingly, the mutant strain lacking RipF1 was not virulent *in planta* suggesting that it might also promote the secretion of other effectors (Figure 2) (Meyer *et al.*, 2006). Among the most abundant, we also identified different proteins containing domains that could be interesting to study for their potential link to virulence. A hemolysin toxin, VirK protein, a T6SS effector, or PqaA-type protein have not been fully characterised in *R. solanacearum* but all were found in other organisms to modulate plant defence, effector protein secretion, and ecological success upon competition with other microorganisms (Baker, Daniels and Morona, 1997; Genin and Boucher, 2002; Van Sluys *et al.*, 2002; Haapalainen *et al.*, 2012; Assis *et al.*, 2017). One protein that caught our interest was the PepSY peptidase, a domain that has been linked to protease inhibition in other organisms (Yeats, Rawlings and Bateman, 2004). In plant defence, plant proteases play a crucial role by perceiving and attacking the invading pathogen or by being part of the signalling cascade (van der Hoorn and Jones, 2004). Interestingly, plant pathogens such as *Phytophtora* spp. can counter the action of these proteases by secreting protease inhibitors such as EPI1 or EPI10 (Tian, Benedetti and Kamoun, 2005; Jashni *et al.*, 2015; Ekchaweng *et al.*, 2017). Hence, it would be interesting to investigate whether this PepSY peptidase can inhibit plant proteases and thus protect bacteria and enhance plat colonisation.

Finally, Rsp0603 and Rsc3101 showed up in the most abundant protein list, both predicted to be S8 serine proteases. Interestingly, their activity was also enriched together with the hydrolases in the GO terms enrichment analysis (C4, Fig. 2), suggesting their importance for the life of the bacterium inside the plant. For this reason, we decided to study this protein family in more detail.

7.3.2 Conservation and function of the S8 serine proteases in *R. solanacearum*

A total of four S8 serine proteases or subtilases were identified in the genome of *R. solanacearum*, with three of them found secreted inside the plant (Rsp0603, Rsc3101 and Rsc2654) , and the forth being potentially secreted (Rsc2653) (Zuleta, 2001). The proteins clearly grouped in two clades based on sequence similarity (C4, Fig. 3). On one side, Rsp0603 and Rsc3101 clade showed over 85% similarity and, on the other, the proteins in tandem Rsc2653 and Rsc2654, more than 40% similarity. Interestingly, these two paralogue pairs were widely conserved among the complete sequenced genomes of different *R. solanacearum* strains, hinting towards the importance of this protein family. Their protein architecture was again conserved between the protein pairs. On one hand Rsc2653 and Rsc2654 contained the canonical subtilase domain with the typical catalytic triad (D, H and S), and a C termini domain that is recognised and processed by another putative protease located in tandem (Rsc2655), thought to be a post-translational modulation of the protein activity (Haft and Varghese, 2011). On the other hand, Rsp0603 and Rsc3101 showed a non-canonical domain with only the S residue of the triad conserved. An in-depth search of information on these proteins allowed us to find interesting information, which again pointed towards the importance of this family (C4, Table 2). In short, the three proteases found in our study to be secreted were also identified in an *in vivo* experiment to search for expressed genes *in planta*. Moreover, the most interesting pair were the noncanonical proteases with Rsp0603 being the one found to be regulated by the HrpG, PhcA and EfpR virulence regulators, to be found overexpressed in the roots upon infection and glycosylated.

According with the various clues pointing towards their importance in the life of the bacteria inside the plant, differences were observed when both genes of the noncanonical subtilases (Rsp0603 and Rsc3101) were mutated (C4, Fig. 4). The double mutant exhibited delayed symptoms that, although the

considerable variability among replicates, suggest a possible defect in virulence. Additionally, the growth of this mutant within the leaf apoplast was lower when compared to the wild type or single mutant strains, indicating its reduced fitness. The fact that phenotypes are only visible when both genes are simultaneously mutated indicated that either they have redundant functions or that they act synergically. Despite these preliminary results, more replicates are needed and, ideally, the triple or quadruple mutant needed to further characterise and rule out functional redundancy among the constituents of the subtilases family.

To functionally characterise the secreted *R. solanacearum* subtilases, we decided to purify the proteins, we selected promising Rsp0603 to set up the purification system (C4, Fig. 5, 6, S7 and S8). Unfortunately, the trials to purify Rsp0603 were not successful, and the protein was mostly found insoluble and in very small amounts or degraded in the heterologous production systems of *E. coli* and *N. benthamiana*, or in the native system, *R. solanacearum*. The fact that the “catalytic” dead version of the protein, in which the conserved serine was exchanged by an alanine, showed a slight increase in the stability and solubility, suggest the potential toxicity and protease activity of Rsp0603. Moreover, expression analysis in *N. benthamiana* of the native and catalytic mutant version of Rsp0603 allowed us to discover that the serine residue is necessary for the protein processing, validating the protease activity hypothesis (C4, Fig. 6). The observation of two bands indicated that even though Rsp0603 don’t have a predicted prodomain, this protein seems to be processed the same way as described for the different constituents of the subtilases family (C4, Fig. 7) (Howell *et al.*, 2019). Despite the impossibility to obtain the purified version of the protein, we gathered sufficient evidences that supports the importance of these proteins for the infection process of *R. solanacearum*. The efficient expression of this protein will be key to elucidate its putative interactors and its function inside the plant.

In this final chapter, we have taken the first steps towards the use of *in planta* secretomic data to discover new virulence factors in *R. solanacearum*. Despite the suboptimal experimental set up of the proteomic analysis due to the varying bacterial loads, we were able to consistently identify several bacterial proteins, including various CWDE, and multiple proteins with potential roles in virulence. These findings demonstrate the robustness of our secretomic data and the usefulness of these kind of analysis to further explore the proteins secreted by the bacteria inside the plant.

8. CONCLUSIONS

8. CONCLUSIONS

I. To determine *R. solanacearum* transcriptomic landscape during infection

1. Dynamic transcriptional changes during *R. solanacearum* host infection can be condensed in four specific genetic programmes: genes expressed in all *in planta* conditions, in the apoplast, in the xylem or only at late stages in the xylem.
2. Induction of the Type III Secretion System (T3SS) cascade follows a sequential activation with the highest expression of the core hrpB and most of the T3E taking place in the xylem.
3. *R. solanacearum* induces motility genes throughout infection with flagellar-associated genes being more expressed in the apoplast.
4. Nitrogen respiration, denitrification and detoxification are highly induced in the plant xylem.
5. Several ROS scavenging enzymes are induced throughout infection.

II. To determine *R. solanacearum* transcriptomic landscape in the environment

6. *R. solanacearum* deploys the most distinct transcriptome profile during soil adaptation, whereas gene expression in the environmental water condition is very similar to the *in planta* xylem condition.
7. Stress-related genes such as metal homeostasis and oxidative stress response genes are highly induced in the soil environment.
8. Absence of the catalase-peroxidase *katG* results in impaired growth of *R. solanacearum* in soil.
9. Nitrogen respiration, denitrification and detoxification pathway shows a higher induction than in the xylem condition.
10. The glyoxylate pathway genes (alternative to the TCA) are highly induced in the soil, together with the putative genes responsible of degrading aromatic compounds of lignin.
11. *R. solanacearum* suffers a general metabolism shutdown in the water environment.
12. The T3SS cascade and all downstream T3E are highly induced in water through an alternative activation via *prhJ*.
13. The T3SS induction is not prolonged and is dependent on basic pH and starvation. This induction can be abolished by nutrient availability and pH neutralisation.
14. Plants infected by *R. solanacearum* suffer an alkalinisation of the pH to levels similar to those in which T3SS is induced in water.

III. To functionally characterise candidate *R. solanacearum* virulence and/or fitness genes

IIIa. To functionally characterise the catalase KatE

15. The catalase KatE show catalase activity *in vitro* and protects *R. solanacearum* against oxidative stress.
16. KatG disruption affects biofilm formation but shows no difference in virulence or growth in planta with the wild type strain.

IIIb. To decipher the function of the serine proteases during infection

17. Secretome analysis proves to be a useful approach to identify proteins potentially involved in the virulence of *R. solanacearum*.
18. The most abundant *R. solanacearum* secreted proteins during infection include multiple proteins such as CWDE and two S8 serine proteases.
19. The S8 serine protease family is widely conserved in the different *R. solanacearum* strains with the two paralogues pairs, Rsp0603/Rsc3101 and Rsc2653/Rsc2654 showing a noncanonical and canonical subtilisin protease domain, respectively. Rsc2653 is the only protein of the family not detected in the secretomic analysis.
20. Absence of both Rsp0603 and Rsc3101 proteases results in reduced virulence and growth *in planta*.
21. The predicted catalytic serine-589 of Rsp0603 is necessary for the processing of the protein in *N. benthamiana*.

RESUM EN CATALÀ

RESUM EN CATALÀ

Les pèrdues causades per patògens de plantes són una gran amenaça per a l'agricultura i la seguretat alimentària en tot el món. En el context de la globalització i el canvi climàtic, l'aparició i la dispersió de patògens resistents a les estratègies de control convencionals provoquen brots destructius. Un dels fitopatògens bacterians més importants és *R. solanacearum*, l'agent causal de la malaltia del marciment bacterià, que afecta a més de 200 espècies de plantes. *R. solanacearum* colonitza el sistema vascular de les plantes i bloqueja el flux d'aigua secretant exopolisacàrids, el que provoca el marciment. A més, pot persistir i dispersar-se fàcilment a través del sòl i les vies d'aigua contaminades. S'han estudiat molts factors de virulència diferents, però manca una comprensió exhaustiva de la regulació transcripcional durant el cicle de vida d'aquest patogen. La gran variabilitat genètica i fenotípica d'aquest patogen tradicionalment tropical ha portat a la seva propagació i establiment en regions temperades. Per prevenir la seva dispersió i dissenyar estratègies de gestió eficients, inexistents fins ara, és de vital importància comprendre a fons el procés d'infecció i dispersió del patogen.

En aquesta tesi ens vam proposar caracteritzar el paisatge transcriptòmic de *R. solanacearum* per desxifrar nous determinants de virulència i d'eficàcia biològica desplegats pel patogen durant tot el seu cicle de vida. En els dos primers capítols, vam estudiar el perfil d'expressió gènica del bacteri durant diferents etapes d'infecció de les plantes (Capítol 1 o C1) i de les etapes ambientals del sòl i l'aigua (Capítol 2 o C2). En general, hem identificat un perfil d'expressió dinàmic de diferents gens de metabolisme i virulència al llarg del cicle de vida del patogen. Consistent amb anàlisis anteriors, vam identificar que el sistema de secreció de tipus III (T3SS) també està transcripcionalment actiu en les etapes tardanes de la infecció i, inesperadament, també a l'aigua. Curiosament, vam identificar el pH alcalí com un senyal que activa l'expressió del T3SS a l'aigua, que pot estar relacionada amb l'alcalinització del pH durant la infecció dins de la planta. A més, vam validar l'expressió de diferents factors de virulència en planta, com la motilitat flagel·lar o T4P durant la infecció. Al sòl, vam identificar l'expressió de múltiples vies metabòliques i gens relacionats amb l'estrès que són necessaris per a la vida de la bacteri al sòl. Entre ells, vam descriure la inducció de gens relacionats amb la degradació de la lignina i vies metabòliques alternatives per sintetitzar molècules de carboni relacionades amb la tolerància a l'estrès.

Els dos últims capítols tenen com a objectiu caracteritzar i descriure gens específics potencialment implicats en la virulència i/o la supervivència de *R. solanacearum*. Al Capítol 3 (C3), vam estudiar detalladament el paper de la catalasa KatE. Vam demostrar la seva importància per a la detoxificació del peròxid d'hidrogen, però vam descobrir que, possiblement degut a la redundància, la seva mutació no té cap efecte biològic en la virulència o en la vida de la bacteri a l'interior de la planta. Finalment, al Capítol 4 (C4), vam adoptar una aproximació diferent estudiant el secretoma de *R. solanacearum* dins l'apoplast i el xilema de la planta. Es van identificar moltes proteïnes potencials relacionades amb la virulència, però ens vam centrar en la descripció de la família de proteïnes de proteases serina S8. Els resultats preliminars suggereixen que les proteases S8, altament acumulades durant la infecció, podrien estar involucrades en la vida de la bacteri dins de la planta.

En resum, aquesta tesi proporciona un fonament sòlid per estudiar i caracteritzar factors de virulència i supervivència importants per al cicle de vida del bacteri. A més, hem iniciat la descripció i caracterització de diferents factors de virulència potencials importants per a la bacteri. Tota aquesta informació podria ser útil en el futur per tenir un coneixement exhaustiu del patogen i dissenyar noves estratègies eficients de gestió i control de la malaltia.

REFERENCES

Abdul Rahman, N. S. N., Abdul Hamid, N. W. and Nadarajah, K. (2021) ‘Effects of Abiotic Stress on Soil Microbiome’, *International Journal of Molecular Sciences*, 22(16), p. 9036. doi: 10.3390/ijms22169036.

Aguilar-Marcelino, L. *et al.* (2020) ‘Using molecular techniques applied to beneficial microorganisms as biotechnological tools for controlling agricultural plant pathogens and pest’, in *Molecular Aspects of Plant Beneficial Microbes in Agriculture*. Elsevier, pp. 333–349. doi: 10.1016/B978-0-12-818469-1.00027-4.

Ahmed, W. *et al.* (2022) ‘Ralstonia solanacearum, a deadly pathogen: Revisiting the bacterial wilt biocontrol practices in tobacco and other Solanaceae’, *Rhizosphere*, 21, p. 100479. doi: 10.1016/j.rhisph.2022.100479.

Ahn, S. *et al.* (2016) ‘Role of glyoxylate shunt in oxidative stress response’, *Journal of Biological Chemistry*, 291(22), pp. 11928–11938. doi: 10.1074/jbc.M115.708149.

Ailloud, F. *et al.* (2015) ‘Comparative genomic analysis of Ralstonia solanacearum reveals candidate genes for host specificity’, *BMC Genomics*, 16(1), pp. 1–11. doi: 10.1186/s12864-015-1474-8.

Ailloud, F. *et al.* (2016) ‘In planta comparative transcriptomics of host-adapted strains of Ralstonia solanacearum’, *PeerJ*, 2016(1). doi: 10.7717/peerj.1549.

Ajwa, H. *et al.* (2010) ‘Properties of Soil Fumigants and Their Fate in the Environment’, in *Hayes’ Handbook of Pesticide Toxicology*. Academic Press, pp. 315–330. doi: 10.1016/B978-0-12-374367-1.00009-4.

Aldon, D. *et al.* (2000) ‘A bacterial sensor of plant cell contact controls the transcriptional induction of Ralstonia solanacearum pathogenicity genes’, *The EMBO Journal*, 19(10), pp. 2304–2314. doi: 10.1093/EMBOJ/19.10.2304.

Almagro Armenteros, J. J. *et al.* (2019) ‘SignalP 5.0 improves signal peptide predictions using deep neural networks’, *Nature Biotechnology*, 37(4), pp. 420–423. doi: 10.1038/s41587-019-0036-z.

Álvarez, B., Biosca, E. G. and López, M. M. (2010) ‘On the life of Ralstonia solanacearum, a destructive bacterial plant pathogen’, *Technology and education topics in applied microbiology and microbial biotechnology*, pp. 267–279. Available at: https://pdfs.semanticscholar.org/aa85/77e213e2977a0e4eb739795e3fea51187181.pdf?_ga=2.156465595.1055873898.1504096691-1311319012.1504096691.

Álvarez, B., López, M. M. and Biosca, E. G. (2007) ‘Influence of native microbiota on survival of Ralstonia solanacearum phylotype II in river water microcosms’, *Applied and Environmental Microbiology*, 73(22), pp. 7210–7217. doi: 10.1128/AEM.00960-07.

Álvarez, B., López, M. M. and Biosca, E. G. (2008) ‘Survival strategies and pathogenicity of Ralstonia solanacearum phylotype II subjected to prolonged starvation in environmental water microcosms’, *Microbiology*, 154(11), pp. 3590–3598. doi: 10.1099/mic.0.2008/019448-0.

Álvarez, B., López, M. M. and Biosca, E. G. (2019) ‘Biocontrol of the Major Plant Pathogen Ralstonia solanacearum in Irrigation Water and Host Plants by Novel Waterborne Lytic Bacteriophages’, *Frontiers in Microbiology*, 10, p. 2813. doi: 10.3389/fmicb.2019.02813.

Álvarez, E. *et al.* (2015) *Production of Clean Planting Material for Managing Platain Diseases*. Available at: https://www.researchgate.net/publication/279180567_Production_of_Clean_Planting_Material_for_Managing_Plantain_Diseases#fullTextFileContent (Accessed: 14 February 2023).

An, S. Q. *et al.* (2019) ‘Mechanistic insights into host adaptation, virulence and epidemiology of the phytopathogen Xanthomonas’, *FEMS Microbiology Reviews*. Oxford University Press, pp. 1–32. doi: 10.1093/femsre/fuz024.

Andrews, S. *et al.* (2015) *FastQC. A quality control tool for high throughput sequence data. Babraham Bioinformatics*, *Babraham Institute*. Available at: https://www.bioinformatics.babraham.ac.uk/projects/fastqc/%0Ahttp://www.bioinformatics.bbsrc.ac.uk/projects/fastqc/.

Aprianto, R. *et al.* (2018) ‘High-resolution analysis of the pneumococcal transcriptome under a wide range of infection-relevant conditions’, *Nucleic Acids Research*, 46(19), pp. 9990–10006. doi: 10.1093/nar/gky750.

Araud-Razou, I. *et al.* (1998) ‘Detection and visualization of the major acidic exopolysaccharide of Ralstonia solanacearum and its role in tomato root infection and vascular colonization’, *European Journal of Plant Pathology*, 104(8), pp. 795–809. doi: 10.1023/A:1008690712318.

Arlat, M. *et al.* (1992) ‘Transcriptional organization and expression of the large hrp gene cluster of Pseudomonas solanacearum.’, *Molecular plant-microbe interactions : MPMI*, pp. 187–193. doi: 10.1094/MPMI-5-187.

Ascarrunz, S. D. M. *et al.* (2011) ‘Quick adaptation of Ralstonia Solanacearum to copper stress to recover culturability and growth in water and soil’, *Brazilian Journal of Microbiology*, 42(2), p. 576. doi: 10.1590/S1517-838220110002000023.

Assis, R. D. A. B. *et al.* (2017) ‘Identification and analysis of seven effector protein families with different adaptive and evolutionary histories in plant-associated members of the Xanthomonadaceae’, *Scientific Reports*, 7(1), pp. 1–17. doi: 10.1038/s41598-017-16325-1.

Aussel, L., Beuzón, C. R. and Cascales, E. (2016) ‘Meeting report: Adaptation and communication of bacterial pathogens’, *Virulence*, 7(4), pp. 481–490. doi: 10.1080/21505594.2016.1152441.

Bacete, L. *et al.* (2018) ‘Plant cell wall-mediated immunity: cell wall changes trigger disease resistance responses’, *Plant Journal*, 93(4), pp. 614–636. doi: 10.1111/tpj.13807.

Baker, S. J., Daniels, C. and Morona, R. (1997) ‘PhoP/Q regulated genes in Salmonella typhi: Identification of melittin sensitive mutants’, *Microbial Pathogenesis*, 22(3), pp. 165–179. doi: 10.1006/mpat.1996.0099.

Baroukh, C., Zemouri, M. and Genin, S. (2022) ‘Trophic preferences of the pathogen Ralstonia solanacearum and consequences on its growth in xylem sap’, *MicrobiologyOpen*, 11(1). doi: 10.1002/mbo3.1240.

Bendtsen, J. D. *et al.* (2005) ‘Non-classical protein secretion in bacteria’, *BMC Microbiology*, 5(1), p. 58. doi: 10.1186/1471-2180-5-58.

Bentham, A. R. *et al.* (2021) ‘pOPIN-GG: A resource for modular assembly in protein expression vectors’, *bioRxiv*, p. 2021.08.10.455798. doi: 10.1101/2021.08.10.455798.

Berendsen, R. L., Pieterse, C. M. J. and Bakker, P. A. H. M. (2012) ‘The rhizosphere microbiome and plant health’, *Trends in Plant Science*. Elsevier Current Trends, pp. 478–486. doi: 10.1016/j.tplants.2012.04.001.

Bertani, G. (1951) ‘Studies on Lysogenesis I’, *Journal of Bacteriology*, 62(3), pp. 293–300. doi: 10.1128/jb.62.3.293-300.1951.

Bertolla, F. *et al.* (1997) ‘Conditions for natural transformation of Ralstonia solanacearum’, *Applied and Environmental Microbiology*, 63(12), pp. 4965–4968. doi: 10.1128/aem.63.12.4965-4968.1997.

Bhatt, G. and Denny, T. P. (2004) ‘Ralstonia solanacearum iron scavenging by the siderophore staphyloferrin B is controlled by PhcA, the global virulence regulator’, *Journal of Bacteriology*, 186(23), pp. 7896–7904. doi: 10.1128/JB.186.23.7896-7904.2004.

Binns, D. *et al.* (2009) ‘QuickGO: A web-based tool for Gene Ontology searching’, *Bioinformatics*, 25(22), pp. 3045–3046. doi: 10.1093/bioinformatics/btp536.

Blum, M. *et al.* (2021) ‘The InterPro protein families and domains database: 20 years on’, *Nucleic Acids Research*, 49(D1), pp. D344–D354. doi: 10.1093/nar/gkaa977.

Bocsanczy, A. M. *et al.* (2022) ‘Identification of candidate type 3 effectors that determine host specificity associated with emerging Ralstonia pseudosolanacearum strains’, *European Journal of Plant Pathology*, 163(1), pp. 35–50. doi: 10.1007/s10658-021-02455-w.

Bocsanczy, A. M., Huguet-Tapia, J. C. and Norman, D. J. (2017) ‘Comparative genomics of ralstonia solanacearum identifies candidate genes associated with cool virulence’, *Frontiers in Plant Science*,

8. doi: 10.3389/fpls.2017.01565.

Bolwell, G. P. (2002) ‘The apoplastic oxidative burst in response to biotic stress in plants: a three-component system’, *Journal of Experimental Botany*, 53(372), pp. 1367–1376. doi: 10.1093/jexbot/53.372.1367.

Boucher, C. A. *et al.* (1985) ‘Transposon mutagenesis of Pseudomonas solanacearum: Isolation of Tn5-induced avirulent mutants’, *Journal of General Microbiology*, 131(9), pp. 2449–2457. doi: 10.1099/00221287-131-9-2449.

Brito, B. *et al.* (1999) ‘prhJ and hrpG, two new components of the plant signal-dependent regulatory cascade controlled by PrhA in Ralstonia solanacearum.’, *Molecular microbiology*, 31(1), pp. 237–51. doi: 10.1046/j.1365-2958.1999.01165.x.

Brito, B. *et al.* (2002) ‘A signal transfer system through three compartments transduces the plant cell contact-dependent signal controlling Ralstonia solanacearum hrp genes’, *Molecular Plant-Microbe Interactions*, 15(2), pp. 109–119. doi: 10.1094/MPMI.2002.15.2.109.

Bronowski, C. *et al.* (2017) ‘Campylobacter jejuni transcriptome changes during loss of culturability in water’, *PLOS ONE*. Edited by Y.-F. Chang, 12(11), p. e0188936. doi: 10.1371/journal.pone.0188936.

Brown, D. G. and Allen, C. (2004) ‘Ralstonia solanacearum genes induced during growth in tomato: An inside view of bacterial wilt’, *Molecular Microbiology*, 53(6), pp. 1641–1660. doi: 10.1111/j.1365-2958.2004.04237.x.

Brown, D. G., Swanson, J. K. and Allen, C. (2007) ‘Two Host-Induced Ralstonia solanacearum Genes, acrA and dinF , Encode Multidrug Efflux Pumps and Contribute to Bacterial Wilt Virulence’, *Applied and Environmental Microbiology*, 73(9), pp. 2777–2786. doi: 10.1128/AEM.00984-06.

Brumbley, S. M., Carney, B. F. and Denny, T. P. (1993) ‘Phenotype conversion in Pseudomonas solanacearum due to spontaneous inactivation of PhcA, a putative LysR transcriptional regulator’, *Journal of Bacteriology*, 175(17), pp. 5477–5487. doi: 10.1128/jb.175.17.5477-5487.1993.

Brumbley, S. M. and Denny, T. P. (1990) ‘Cloning of wild-type Pseudomonas solanacearum phcA, a gene that when mutated alters expression of multiple traits that contribute to virulence’, *Journal of Bacteriology*, 172(10), pp. 5677–5685. doi: 10.1128/jb.172.10.5677-5685.1990.

Brutus, A. *et al.* (2010) ‘A domain swap approach reveals a role of the plant wall-associated kinase 1 (WAK1) as a receptor of oligogalacturonides’, *Proceedings of the National Academy of Sciences of the United States of America*, 107(20), pp. 9452–9457. doi: 10.1073/pnas.1000675107.

Bryan, P. N. (2002) ‘Prodomains and protein folding catalysis’, *Chemical Reviews*, 102(12), pp. 4805–4815. doi: 10.1021/CR010190B/ASSET/IMAGES/MEDIUM/CR010190BE00009.GIF.

Buddenhagen, I., Sequeira, L. and Kelman, A. (1962) ‘Designation of races in Pseudomonas solanacearum’, *Phytopathology*, 52, p. 726. Available at: https://cir.nii.ac.jp/crid/1570009750240715392 (Accessed: 5 February 2023).

Bugg, T. D. H. *et al.* (2011) ‘Pathways for degradation of lignin in bacteria and fungi’, *Natural Product Reports*, 28(12), p. 1883. doi: 10.1039/c1np00042j.

Cantalapiedra, C. P. *et al.* (2021) ‘eggNOG-mapper v2: Functional Annotation, Orthology Assignments, and Domain Prediction at the Metagenomic Scale’, *Molecular Biology and Evolution*, 38(12), pp. 5825–5829. doi: 10.1093/molbev/msab293.

Cao, P. *et al.* (2022) ‘A conserved type III effector RipB is recognized in tobacco and contributes to Ralstonia solanacearum virulence in susceptible host plants’, *Biochemical and Biophysical Research Communications*, 631, pp. 18–24. doi: 10.1016/j.bbrc.2022.09.062.

Cao, Y. *et al.* (2018) ‘Antagonism of Two Plant-Growth Promoting Bacillus velezensis Isolates Against Ralstonia solanacearum and Fusarium oxysporum’, *Scientific Reports*, 8(1), pp. 1–14. doi: 10.1038/s41598-018-22782-z.

Capela, D. *et al.* (2017) ‘Recruitment of a Lineage-Specific Virulence Regulatory Pathway Promotes Intracellular Infection by a Plant Pathogen Experimentally Evolved into a Legume Symbiont’,

Molecular Biology and Evolution, 34(10), pp. 2503–2521. doi: 10.1093/molbev/msx165.

Carmeille, A. *et al.* (2006) 'Identification of QTLs for Ralstonia solanacearum race 3-phylotype II resistance in tomato', *Theoretical and Applied Genetics*, 113(1), pp. 110–121. doi: 10.1007/s00122-006-0277-3.

Caruso, P. *et al.* (2005) 'Seasonal variation of Ralstonia solanacearum biovar 2 populations in a Spanish river: Recovery of stressed cells at low temperatures', *Applied and Environmental Microbiology*, 71(1), pp. 140–148. doi: 10.1128/AEM.71.1.140-148.2005.

Castillo, J. A. and Greenberg, J. T. (2007) 'Evolutionary dynamics of Ralstonia solanacearum', *Applied and Environmental Microbiology*, 73(4), pp. 1225–1238. doi: 10.1128/AEM.01253-06.

Ceci, P. *et al.* (2003) 'The Dps Protein of Agrobacterium tumefaciens Does Not Bind to DNA but Protects It toward Oxidative Cleavage', *Journal of Biological Chemistry*, 278(22), pp. 20319–20326. doi: 10.1074/jbc.M302114200.

Cellier, G. *et al.* (2012) 'Phylogeny and population structure of brown rot- and Moko disease-causing strains of Ralstonia solanacearum phylotype II', *Applied and Environmental Microbiology*, 78(7), pp. 2367–2375. doi: 10.1128/AEM.06123-11.

Cellier, G. and Prior, P. (2010) 'Deciphering phenotypic diversity of Ralstonia solanacearum strains pathogenic to potato', *Phytopathology*, 100(11), pp. 1250–1261. doi: 10.1094/PHYTO-02-10-0059.

Chapman, M. R. and Kao, C. C. (1998) 'Epsr modulates production of extracellular polysaccharides in the bacterial wilt pathogen Ralstonia (Pseudomonas) solanacearum', *Journal of Bacteriology*, 180(1), pp. 27–34. doi: 10.1128/jb.180.1.27-34.1998.

Chattopadhyay, M. K. *et al.* (2011) 'Increase in oxidative stress at low temperature in an antarctic Bacterium', *Current Microbiology*, 62(2), pp. 544–546. doi: 10.1007/s00284-010-9742-y.

Chen, D. *et al.* (2017) 'Complete Genome Sequence of Ralstonia solanacearum FJAT-91, a High-Virulence Pathogen of Tomato Wilt', *Genome Announcements*, 5(37). doi: 10.1128/GENOMEA.00900-17.

Chen, S. *et al.* (2022) 'A soil-borne Mn(II)-oxidizing bacterium of Providencia sp. exploits a strategy of superoxide production coupled to hydrogen peroxide consumption to generate Mn oxides', *Archives of Microbiology*, 204(3), pp. 1–14. doi: 10.1007/s00203-022-02771-7.

Cheng, C. *et al.* (2013) 'Plant immune response to pathogens differs with changing temperatures', *Nature Communications*, 4(1), pp. 1–9. doi: 10.1038/ncomms3530.

Cheng, Q. *et al.* (2002) 'The group B streptococcal C5a peptidase is both a specific protease and an invasin', *Infection and Immunity*, 70(5), pp. 2408–2413. doi: 10.1128/IAI.70.5.2408-2413.2002.

Cheng, Y. T., Zhang, L. and He, S. Y. (2019) 'Plant-Microbe Interactions Facing Environmental Challenge', *Cell Host & Microbe*, 26(2), pp. 183–192. doi: 10.1016/J.CHOM.2019.07.009.

Chilton, M. D. *et al.* (1977) 'Stable incorporation of plasmid DNA into higher plant cells: the molecular basis of crown gall tumorigenesis', *Cell*, 11(2), pp. 263–271. doi: 10.1016/0092-8674(77)90043-5.

Chinchilla, D. *et al.* (2006) 'The Arabidopsis receptor kinase FLS2 binds flg22 and determines the specificity of flagellin perception', *Plant Cell*, 18(2), pp. 465–476. doi: 10.1105/tpc.105.036574.

Cho, H. *et al.* (2019) 'Prediction of host-specific genes by pan-genome analyses of the Korean Ralstonia solanacearum species complex', *Frontiers in Microbiology*, 10(MAR), p. 506. doi: 10.3389/fmicb.2019.00506.

Choi, J. *et al.* (2014) 'Identification of a plant receptor for extracellular ATP', *Science*, 343(6168), pp. 290–294. doi: 10.1126/science.343.6168.290.

Clough, S. J., Lee, K. E., *et al.* (1997) 'A two-component system in Ralstonia (Pseudomonas) solanacearum modulates production of PhcA-regulated virulence factors in response to 3-hydroxypalmitic acid methyl ester', *Journal of Bacteriology*, 179(11), pp. 3639–3648. doi: 10.1128/jb.179.11.3639-3648.1997.

Clough, S. J., Flavier, A. B., *et al.* (1997) 'Differential expression of virulence genes and motility in Ralstonia (Pseudomonas) solanacearum during exponential growth', *Applied and Environmental Microbiology*, 63(3), pp. 844–850. doi: 10.1128/aem.63.3.844-850.1997.

Coburn, B., Sekirov, I. and Finlay, B. B. (2007) 'Type III secretion systems and disease', *Clinical Microbiology Reviews*, 20(4), pp. 535–549. doi: 10.1128/CMR.00013-07.

Colburn-Clifford, J. and Allen, C. (2010) 'A cbb3-Type Cytochrome C Oxidase Contributes to Ralstonia solanacearum R3bv2 Growth in Microaerobic Environments and to Bacterial Wilt Disease Development in Tomato', *Molecular Plant-Microbe Interactions*, 23(8), pp. 1042–1052. doi: 10.1094/MPMI-23-8-1042.

Colburn-Clifford, J. M., Scherf, J. M. and Allen, C. (2010) 'Ralstonia solanacearum Dps contributes to oxidative stress tolerance and to colonization of and virulence on tomato plants', *Applied and Environmental Microbiology*, 76(22), pp. 7392–7399. doi: 10.1128/AEM.01742-10.

Coll, N. S. and Valls, M. (2013) 'Current knowledge on the Ralstonia solanacearum type III secretion system', *Microbial Biotechnology*, 6(6), pp. 614–620. doi: 10.1111/1751-7915.12056.

Colledge, V. L. *et al.* (2011) 'Structure and organisation of SinR, the master regulator of biofilm formation in Bacillus subtilis', *Journal of Molecular Biology*, 411(3), pp. 597–613. doi: 10.1016/j.jmb.2011.06.004.

Consortium, T. U. *et al.* (2023) 'UniProt: the Universal Protein Knowledgebase in 2023', *Nucleic acids research*, 51(D1), pp. D523–D531. doi: 10.1093/nar/gkac1052.

Conway, J. R., Lex, A. and Gehlenborg, N. (2017) 'UpSetR: An R package for the visualization of intersecting sets and their properties', *Bioinformatics*, 33(18), pp. 2938–2940. doi: 10.1093/bioinformatics/btx364.

Corral, J. *et al.* (2020) 'Twitching and Swimming Motility Play a Role in Ralstonia solanacearum Pathogenicity', *mSphere*, 5(2), pp. 1–16. doi: 10.1128/msphere.00740-19.

Coupat-Goutaland, B. *et al.* (2011) 'Ralstonia solanacearum virulence increased following large interstrain gene transfers by natural transformation', *Molecular Plant-Microbe Interactions*, 24(4), pp. 497–505. doi: 10.1094/MPMI-09-10-0197.

Crofts, T. S. *et al.* (2018) 'Shared strategies for β-lactam catabolism in the soil microbiome', *Nature Chemical Biology*, 14(6), pp. 556–564. doi: 10.1038/s41589-018-0052-1.

Cronan, Jr., J. E. and Laporte, D. (2005) 'Tricarboxylic Acid Cycle and Glyoxylate Bypass', *EcoSal Plus*, 1(2). doi: 10.1128/ecosalplus.3.5.2.

Cunnac, S., Boucher, C. and Genin, S. (2004) 'Characterization of the cis-Acting Regulatory Element Controlling HrpB-Mediated Activation of the Type III Secretion System and Effector Genes in Ralstonia solanacearum', *Journal of Bacteriology*, 186(8), pp. 2309–2318. doi: 10.1128/JB.186.8.2309-2318.2004.

Dalbey, R. E. and Kuhn, A. (2012) 'Protein Traffic in Gram-negative bacteria - how exported and secreted proteins find their way', *FEMS Microbiology Reviews*, 36(6), pp. 1023–1045. doi: 10.1111/j.1574-6976.2012.00327.x.

Dalsing, B. L. *et al.* (2015) 'Ralstonia solanacearum uses inorganic nitrogen metabolism for virulence, ATP production, and detoxification in the oxygen-limited host xylem environment', *mBio*, 6(2), pp. 1–13. doi: 10.1128/mBio.02471-14.

Dalsing, B. L. and Allen, C. (2014) 'Nitrate Assimilation Contributes to Ralstonia solanacearum Root Attachment, Stem Colonization, and Virulence', *Journal of Bacteriology*, 196(5), pp. 949–960. doi: 10.1128/JB.01378-13.

Degering, C. *et al.* (2010) 'Optimization of Protease Secretion in Bacillus subtilis and Bacillus licheniformis by Screening of Homologous and Heterologous Signal Peptides', *Applied and Environmental Microbiology*, 76(19), p. 6370. doi: 10.1128/AEM.01146-10.

Delaspre, F. *et al.* (2007) 'The Ralstonia solanacearum pathogenicity regulator HrpB induces 3-

hydroxy-oxindole synthesis', *Proceedings of the National Academy of Sciences of the United States of America*, 104(40), pp. 15870–15875. doi: 10.1073/pnas.0700782104.

Denne, N. L. *et al.* (2021) 'Ralstonia solanacearum Effectors Localize to Diverse Organelles in Solanum Hosts', *Phytopathology*, 111(12), pp. 2213–2226. doi: 10.1094/PHYTO-10-20-0483-R.

Denny, T. (2006) 'Plant pathogenic Ralstonia species', in *Plant-Associated Bacteria*. Dordrecht: Springer Netherlands, pp. 573–644. doi: 10.1007/978-1-4020-4538-7_16.

Denny, T. . *et al.* (1994) 'Phenotype conversion of Pseudomonas solanacearum: its molecular basis and potential function', in Allsopp, D., Colwell, R. R., and Hawksworth, D. L. (eds) *Bacterial wilt: the disease and its causative agent, Pseudomonas solanacearum*. CAB INTERNATIONAL, pp. 137–143.

Denny, T. P. (1995) 'Involvement of bacterial polysaccharides in plant pathogenesis', *Annual Review of Phytopathology*. Annual Reviews 4139 El Camino Way, P.O. Box 10139, Palo Alto, CA 94303-0139, USA, pp. 173–197. doi: 10.1146/annurev.py.33.090195.001133.

Denny, T. P. *et al.* (1996) 'Cloning and characterization of tek, the gene encoding the major extracellular protein of Pseudomonas solanacearum', *Molecular Plant-Microbe Interactions*, 9(4), pp. 272–281. doi: 10.1094/MPMI-9-0272.

Denny, T. P. and Baek, S.-R. (1991) 'Genetic Evidence that Extracellular Polysaccharide Is a Virulence Factor of Pseudomonas solanacearum', *Molecular Plant-Microbe Interactions*, 4(2), p. 198. doi: 10.1094/mpmi-4-198.

Desaint, H. *et al.* (2021) 'Fight hard or die trying: when plants face pathogens under heat stress', *New Phytologist*, 229(2), pp. 712–734. doi: 10.1111/NPH.16965.

Dessaux, Y. and Faure, D. (2018) 'Niche construction and exploitation by Agrobacterium: How to survive and face competition in soil and plant habitats', *Current Topics in Microbiology and Immunology*, 418, pp. 55–86. doi: 10.1007/82_2018_83.

Digonnet, C. *et al.* (2012) 'Deciphering the route of Ralstonia solanacearum colonization in Arabidopsis thaliana roots during a compatible interaction: Focus at the plant cell wall', *Planta*, 236(5), pp. 1419–1431. doi: 10.1007/s00425-012-1694-y.

Dillon, M. M. *et al.* (2019) 'Molecular evolution of Pseudomonas syringae type iii secreted effector proteins', *Frontiers in Plant Science*, 10. doi: 10.3389/fpls.2019.00418.

Donati, I. *et al.* (2020) 'Pseudomonas syringae pv. actinidiae: Ecology, Infection Dynamics and Disease Epidemiology', *Microbial Ecology*, 80(1), pp. 81–102. doi: 10.1007/s00248-019-01459-8.

Drula, E. *et al.* (2022) 'The carbohydrate-active enzyme database: Functions and literature', *Nucleic Acids Research*, 50(D1), pp. D571–D577. doi: 10.1093/nar/gkab1045.

Du, H. *et al.* (2022) 'Dual RNA-seq Reveals the Global Transcriptome Dynamics of Ralstonia solanacearum and Pepper (Capsicum annuum) Hypocotyls During Bacterial Wilt Pathogenesis', *Phytopathology*, 112(3), pp. 630–642. doi: 10.1094/PHYTO-01-21-0032-R.

Dunn, M. F., Ramírez-Trujillo, J. A. and Hernández-Lucas, I. (2009) 'Major roles of isocitrate lyase and malate synthase in bacterial and fungal pathogenesis', *Microbiology*, 155(10), pp. 3166–3175. doi: 10.1099/mic.0.030858-0.

Eddy, S. R. (2011) 'Accelerated profile HMM searches', *PLoS Computational Biology*, 7(10). doi: 10.1371/journal.pcbi.1002195.

Eisfeld, C. *et al.* (2022) 'Removal of bacterial plant pathogens in columns filled with quartz and natural sediments under anoxic and oxygenated conditions', *Water Research*, 220, p. 118724. doi: 10.1016/j.watres.2022.118724.

Ekchaweng, K. *et al.* (2017) 'The plant defense and pathogen counterdefense mediated by Hevea brasiliensis serine protease HbSPA and Phytophthorapalmivora extracellular protease inhibitor PpEPI10', *PLoS ONE*, 12(5), p. e0175795. doi: 10.1371/journal.pone.0175795.

Elhenawy, W. *et al.* (2015) 'Protein O-linked glycosylation in the plant pathogen Ralstonia solanacearum', *Glycobiology*, 26(3), pp. 301–311. doi: 10.1093/glycob/cwv098.

Elphinstone, J. G. *et al.* (1996) ‘Sensitivity of different methods for the detection of Ralstonia solanacearum in potato tuber extracts’, *EPPO Bulletin*, 26(3–4), pp. 663–678. doi: 10.1111/j.1365-2338.1996.tb01511.x.

Elphinstone, J. G. (2005) ‘The current bacterial wilt situation: A global overview’, in *Bacterial wilt disease and the Ralstonia solanacearum species complex*. American Phytopathological Society (APS Press), pp. 9–28.

Elphinstone, J. G., Stanford, H. and Stead, D. E. (1998) ‘Survival and transmission of Ralstonia solanacearum in aquatic plants of Solatium dulcamara and associated surface water in England1’, *EPPO Bulletin*, 28(1–2), pp. 93–94. doi: 10.1111/j.1365-2338.1998.tb00709.x.

Van Elsas, J. D. *et al.* (2000) ‘Survival of Ralstonia solanacearum biovar 2, the causative agent of potato brown rot, in field and microcosm soils in temperate climates’, *Phytopathology*, 90(12), pp. 1358–1366. doi: 10.1094/PHYTO.2000.90.12.1358.

Van Elsas, J. D. *et al.* (2001) ‘Effects of ecological factors on the survival and physiology of Ralstonia solanacearum bv. 2 in irrigation water’, *Canadian Journal of Microbiology*, 47(9), pp. 842–854. doi: 10.1139/cjm-47-9-842.

Elsayed, T. R. *et al.* (2020) ‘Biocontrol of Bacterial Wilt Disease Through Complex Interaction Between Tomato Plant, Antagonists, the Indigenous Rhizosphere Microbiota, and Ralstonia solanacearum’, *Frontiers in Microbiology*, 10, p. 2835. doi: 10.3389/fmicb.2019.02835.

Emms, D. M. and Kelly, S. (2019) ‘OrthoFinder: Phylogenetic orthology inference for comparative genomics’, *Genome Biology*, 20(1). doi: 10.1186/s13059-019-1832-y.

EPPO (2018) ‘PM 7/21 (2) Ralstonia solanacearum , R. pseudosolanacearum and R. syzygii (Ralstonia solanacearum species complex)’, *EPPO Bulletin*, 48(1), pp. 32–63. doi: 10.1111/epp.12454.

EPPO (2023) *EPPO Global Database*. Available at: https://gd.eppo.int/ (Accessed: 28 February 2023).

Fasnacht, M. and Polacek, N. (2021) ‘Oxidative Stress in Bacteria and the Central Dogma of Molecular Biology’, *Frontiers in Molecular Biosciences*, 8, p. 392. doi: 10.3389/fmolb.2021.671037.

Ferreira, V. *et al.* (2017) ‘Interspecific potato breeding lines display differential colonization patterns and induced defense responses after Ralstonia solanacearum infection’, *Frontiers in Plant Science*, 8, p. 1424. doi: 10.3389/fpls.2017.01424.

Figaj, D. *et al.* (2019) ‘The role of proteases in the virulence of plant pathogenic bacteria’, *International Journal of Molecular Sciences*, 20(3). doi: 10.3390/ijms20030672.

Flavier, A. B., Ganova-Raeva, L. M., *et al.* (1997) ‘Hierarchical autoinduction in Ralstonia solanacearum: Control of acyl- homoserine lactone production by a novel autoregulatory system responsive to 3-hydroxypalmitic acid methyl ester’, *Journal of Bacteriology*, 179(22), pp. 7089–7097. doi: 10.1128/jb.179.22.7089-7097.1997.

Flavier, A. B., Clough, S. J., *et al.* (1997) ‘Identification of 3-hydroxypalmitic acid methyl ester as a novel autoregulator controlling virulence in Ralstonia solanacearum’, *Molecular Microbiology*, 26(2), pp. 251–259. doi: 10.1046/j.1365-2958.1997.5661945.x.

Flavier, A. B., Schell, M. A. and Denny, T. P. (1998) ‘An RpoS (σ(s)) homologue regulates acylhomoserine lactone-dependent autoinduction in Ralstonia solanacearum’, *Molecular Microbiology*, 28(3), pp. 475–486. doi: 10.1046/j.1365-2958.1998.00804.x.

Flemming, H.-C. and Wingender, J. (2010) ‘The biofilm matrix’, *Nature Reviews Microbiology*, 8(9), pp. 623–633. doi: 10.1038/nrmicro2415.

Flores-Cruz, Z. and Allen, C. (2009) ‘Ralstonia solanacearum Encounters an Oxidative Environment During Tomato Infection’, *Molecular Plant-Microbe Interactions®*, 22(7), pp. 773–782. doi: 10.1094/MPMI-22-7-0773.

Flores-Cruz, Z. and Allen, C. (2011) ‘Necessity of OxyR for the hydrogen peroxide stress response and full virulence in Ralstonia solanacearum’, *Applied and Environmental Microbiology*, 77(18), pp.

6426–6432. doi: 10.1128/AEM.05813-11.

Fortnum, B. A. and Martin, S. B. (1998) ‘Disease Management Strategies for Control of Bacterial Wilt of Tobacco in the Southeastern USA’, in *Bacterial Wilt Disease*. Springer, Berlin, Heidelberg, pp. 394–402. doi: 10.1007/978-3-662-03592-4_60.

Francl, L. J. (2001) ‘The Disease Triangle: A Plant Pathological Paradigm Revisited.’, *The Plant Health Instructor*. doi: 10.1094/phi-t-2001-0517-01.

Fraser, C. M. *et al.* (2021) ‘Host-Microbe Biology FADU : a Quanti fi cation Tool for Prokaryotic Transcriptomic Analyses’, (September 2020), pp. 1–16.

Fujita, Y., Matsuoka, H. and Hirooka, K. (2007) ‘Regulation of fatty acid metabolism in bacteria’, *Molecular Microbiology*, 66(4), pp. 829–839. doi: 10.1111/j.1365-2958.2007.05947.x.

Furusawa, A. *et al.* (2019) ‘Ralstonia solanacearum colonization of tomato roots infected by Meloidogyne incognita’, *Journal of Phytopathology*, 167(6), pp. 338–343. doi: 10.1111/jph.12804.

Gabius, H. (2002) ‘The sugar code: functional lectinomics’, *Biochimica et Biophysica Acta (BBA) - General Subjects*, 1572(2–3), pp. 165–177. doi: 10.1016/S0304-4165(02)00306-9.

Gallé, Á. *et al.* (2021) ‘Crosstalk between the redox signalling and the detoxification: GSTs under redox control?’, *Plant Physiology and Biochemistry*, 169, pp. 149–159. doi: 10.1016/j.plaphy.2021.11.009.

García, R. O., Kerns, J. P. and Thiessen, L. (2019) ‘Ralstonia solanacearum Species Complex: A Quick Diagnostic Guide’, *Plant Health Progress*, 20(1), pp. 7–13. doi: 10.1094/PHP-04-18-0015-DG.

Garg, R. P. *et al.* (2000) ‘Multicomponent transcriptional regulation at the complex promoter of the exopolysaccharide I biosynthetic operon of Ralstonia solanacearum’, *Journal of Bacteriology*, 182(23), pp. 6659–6666. doi: 10.1128/JB.182.23.6659-6666.2000.

Geng, R. *et al.* (2022) ‘Comprehensive Analysis Reveals the Genetic and Pathogenic Diversity of Ralstonia solanacearum Species Complex and Benefits Its Taxonomic Classification’, *Frontiers in Microbiology*, 13, p. 1708. doi: 10.3389/fmicb.2022.854792.

Genin, S. *et al.* (1992) ‘Evidence that the hrpB gene encodes a positive regulator of pathogenicity genes from Pseudomonas solanacearum’, *Molecular Microbiology*, 6(20), pp. 3065–3076. doi: 10.1111/j.1365-2958.1992.tb01764.x.

Genin, S. *et al.* (2005) ‘Control of the Ralstonia solanacearum Type III secretion system (Hrp) genes by the global virulence regulator PhcA’, *FEBS Letters*, 579(10), pp. 2077–2081. doi: 10.1016/j.febslet.2005.02.058.

Genin, S. (2010) ‘Molecular traits controlling host range and adaptation to plants in Ralstonia solanacearum’, *New Phytologist*, 187(4), pp. 920–928. doi: 10.1111/j.1469-8137.2010.03397.x.

Genin, S. and Boucher, C. (2002) ‘Ralstonia solanacearum: Secrets of a major pathogen unveiled by analysis of its genome’, *Molecular Plant Pathology*, 3(3), pp. 111–118. doi: 10.1046/j.1364-3703.2002.00102.x.

Genin, S. and Boucher, C. (2004) ‘Lessons learned from the genome analysis of Ralstonia solanacearum’, *Annual Review of Phytopathology*, 42, pp. 107–134. doi: 10.1146/annurev.phyto.42.011204.104301.

Genin, S. and Denny, T. P. (2012) ‘Pathogenomics of the ralstonia solanacearum species complex’, *Annual Review of Phytopathology*, 50, pp. 67–89. doi: 10.1146/annurev-phyto-081211-173000.

Ghosh, S. and O’Connor, T. J. (2017) ‘Beyond paralogs: The multiple layers of redundancy in bacterial pathogenesis’, *Frontiers in Cellular and Infection Microbiology*, 7(NOV), p. 467. doi: 10.3389/fcimb.2017.00467.

Giagnoni, L. *et al.* (2016) ‘Availability of different nitrogen forms changes the microbial communities and enzyme activities in the rhizosphere of maize lines with different nitrogen use efficiency’, *Applied Soil Ecology*, 98, pp. 30–38. doi: 10.1016/j.apsoil.2015.09.004.

van Gijsegem, F. *et al.* (1995) 'The hrp gene locus of Pseudomonas solanacearum, which controls the production of a type III secretion system, encodes eight proteins related to components of the bacterial flagellar biogenesis complex', *Molecular Microbiology*, 15(6), pp. 1095–1114. doi: 10.1111/J.1365-2958.1995.TB02284.X.

Van Gijsegem, F. *et al.* (2002) 'Genetic dissection of the Ralstonia solanacearum hrp gene cluster reveals that the HrpV and HrpX proteins are required for Hrp pilus assembly', *Molecular Microbiology*, 44(4), pp. 935–946. doi: 10.1046/j.1365-2958.2002.02936.x.

Goldberg, T. *et al.* (2014) 'LocTree3 prediction of localization', *Nucleic Acids Research*, 42(W1). doi: 10.1093/nar/gku396.

González, A. *et al.* (2011) 'Detection and functional characterization of a large genomic deletion resulting in decreased pathogenicity in Ralstonia solanacearum race 3 biovar 2 strains', *Environmental Microbiology*, 13(12), pp. 3172–3185. doi: 10.1111/j.1462-2920.2011.02636.x.

González, E. T. *et al.* (2007) 'Using the Ralstonia solanacearum tat secretome to identify bacterial wilt virulence factors', *Applied and Environmental Microbiology*, 73(12), pp. 3779–3786. doi: 10.1128/AEM.02999-06.

González, E. T. and Allen, C. (2003) 'Characterization of a Ralstonia solanacearum operon required for polygalacturonate degradation and uptake of galacturonic acid', *Molecular Plant-Microbe Interactions*, 16(6), pp. 536–544. doi: 10.1094/MPMI.2003.16.6.536.

Götz, S. *et al.* (2008) 'High-throughput functional annotation and data mining with the Blast2GO suite', *Nucleic Acids Research*, 36(10), pp. 3420–3435. doi: 10.1093/nar/gkn176.

Graham, J. and Lloyd, A. B. (1979) 'Survival of potato strain (race 3) of Pseudomonas solanacearum in the deeper soil layers', *Australian Journal of Agricultural Research*, 30(3), pp. 489–496. doi: 10.1071/AR9790489.

Graham, J., Lloyd, A. B. and Jones, D. A. (1979) 'Survival of Pseudomonas solanacearum Race 3 in Plant Debris and in Latently Infected Potato Tubers', *Phytopathology*, 69(10), p. 1100. doi: 10.1094/phyto-69-1100.

Graham, T. L., Sequeira, L. and Huang, T. S. R. (1977) 'Bacterial lipopolysaccharides as inducers of disease resistance in tobacco', *Applied and Environmental Microbiology*, 34(4), pp. 424–432. doi: 10.1128/aem.34.4.424-432.1977.

Grey, B. E. and Steck, T. R. (2001) 'The Viable but Nonculturable State of Ralstonia solanacearum May Be Involved in Long-Term Survival and Plant Infection', *Applied and Environmental Microbiology*, 67(9), pp. 3866–3872. doi: 10.1128/AEM.67.9.3866-3872.2001/ASSET/7E623F7C-7054-4E3B-B053-D9B0ED58A74F/ASSETS/GRAPHIC/AM0910117004.JPEG.

Grishin, A. M. and Cygler, M. (2015) 'Structural organization of enzymes of the phenylacetate catabolic hybrid pathway', *Biology*. Multidisciplinary Digital Publishing Institute, pp. 424–442. doi: 10.3390/biology4020424.

Grunwald, Y. *et al.* (2021) 'Arabidopsis leaf hydraulic conductance is regulated by xylem sap pH, controlled, in turn, by a P-type H+-ATPase of vascular bundle sheath cells', *Plant Journal*, 106(2), pp. 301–313. doi: 10.1111/tpj.15235.

Guarischi-Sousa, R. *et al.* (2016) 'Complete genome sequence of the potato pathogen Ralstonia solanacearum UY031', *Standards in Genomic Sciences*, 11(1), pp. 1–8. doi: 10.1186/s40793-016-0131-4.

Guidot, A. *et al.* (2009) 'Horizontal gene transfer between ralstonia solanacearum strains detected by comparative genomic hybridization on microarrays', *ISME Journal*, 3(5), pp. 549–562. doi: 10.1038/ismej.2009.14.

Haapalainen, M. *et al.* (2012) 'Hcp2, a secreted protein of the phytopathogen Pseudomonas syringae pv. tomato DC3000, is required for fitness for competition against bacteria and yeasts', *Journal of Bacteriology*, 194(18), pp. 4810–4822. doi: 10.1128/JB.00611-12.

Habe, I. *et al.* (2019) 'QTL analysis of resistance to bacterial wilt caused by *Ralstonia solanacearum*

in potato', *Breeding Science*, 69(4), pp. 592–600. doi: 10.1270/jsbbs.19059.

Hacquard, S. *et al.* (2016) 'Survival trade-offs in plant roots during colonization by closely related beneficial and pathogenic fungi', *Nature Communications*, 7(1), pp. 1–13. doi: 10.1038/ncomms11362.

Haft, D. H. and Varghese, N. (2011) 'GlyGly-CTERM and rhombosortase: A C-terminal protein processing signal in a many-to-one pairing with a rhomboid family intramembrane serine protease', *PLoS ONE*, 6(12). doi: 10.1371/journal.pone.0028886.

Harper, S. and Speicher, D. W. (2011) 'Purification of proteins fused to glutathione S-transferase.', *Methods in molecular biology (Clifton, N.J.)*, 681, pp. 259–280. doi: 10.1007/978-1-60761-913-0_14.

Hassani, M. A., Durán, P. and Hacquard, S. (2018) 'Microbial interactions within the plant holobiont', *Microbiome*. BioMed Central, p. 58. doi: 10.1186/s40168-018-0445-0.

Hayes, M. M., MacIntyre, A. M. and Allen, C. (2017) 'Complete genome sequences of the plant pathogens Ralstonia solanacearum type strain K60 and R. solanacearum race 3 biovar 2 strain UW551', *Genome Announcements*, 5(40). doi: 10.1128/genomeA.01088-17.

Hayward, A. C. (1964) 'Characteristics of Pseudomonas solanacearum', *Journal of Applied Bacteriology*, 27(2), pp. 265–277. doi: 10.1111/J.1365-2672.1964.TB04912.X.

Hayward, A. C. (1991) 'Biology and epidemiology of bacterial wilt caused by Pseudomonas solanacearum', *Annual review of phytopathology. Vol. 29*, 29, pp. 65–87. doi: 10.1146/annurev.py.29.090191.000433.

Hernández-Romero, D., Solano, F. and Sanchez-Amat, A. (2005) 'Polyphenol oxidase activity expression in Ralstonia solanacearum', *Applied and Environmental Microbiology*, 71(11), pp. 6808–6815. doi: 10.1128/AEM.71.11.6808-6815.2005.

Hibbing, M. E. *et al.* (2010) 'Bacterial competition: surviving and thriving in the microbial jungle', *Nature Reviews Microbiology*, 8(1), pp. 15–25. doi: 10.1038/nrmicro2259.

Hikichi, Y. (2016) 'Interactions between plant pathogenic bacteria and host plants during the establishment of susceptibility', *Journal of General Plant Pathology*. Springer Tokyo, pp. 326–331. doi: 10.1007/s10327-016-0680-9.

Hirsch, J. *et al.* (2002) 'Delayed symptom development in ein2-1, an Arabidopsis ethylene-insensitive mutant, in response to bacterial wilt caused by Ralstonia solanacearum', *Phytopathology*, 92(10), pp. 1142–1148. doi: 10.1094/PHYTO.2002.92.10.1142.

van der Hoorn, R. AL and Jones, J. D. G. (2004) 'The plant proteolytic machinery and its role in defence', *Current Opinion in Plant Biology*, 7(4), pp. 400–407. doi: 10.1016/j.pbi.2004.04.003.

Howell, M. *et al.* (2019) 'Functional characterization of a subtilisin-like serine protease from Vibrio cholerae', *Journal of Biological Chemistry*, 294(25), pp. 9888–9900. doi: 10.1074/jbc.RA119.007745.

Huang, J. *et al.* (1995) 'A complex network regulates expression of eps and other virulence genes of Pseudomonas solanacearum', *Journal of Bacteriology*, 177(5), pp. 1259–1267. doi: 10.1128/jb.177.5.1259-1267.1995.

Huang, J. *et al.* (1998) 'Joint transcriptional control of xpsR, the unusual signal integrator of the Ralstonia solanacearum virulence gene regulatory network, by a response regulator and a LysR-type transcriptional activator', *Journal of Bacteriology*, 180(10), pp. 2736–2743. doi: 10.1128/jb.180.10.2736-2743.1998.

Huang, J., Denny, T. P. and Schell, M. A. (1993) 'vsrB, a regulator of virulence genes of Pseudomonas solanacearum, is homologous to sensors of the two-component regulator family', *Journal of Bacteriology*, 175(19), pp. 6169–6178. doi: 10.1128/jb.175.19.6169-6178.1993.

Huang, J. and Schell, M. (1995) 'Molecular characterization of the eps gene cluster of Pseudomonas solanacearum and its transcriptional regulation at a single promoter', *Molecular Microbiology*, 16(5), pp. 977–989. doi: 10.1111/j.1365-2958.1995.tb02323.x.

Huang, Q. and Allen, C. (1997) 'An exo-poly-α-D-galacturonosidase, PehB, is required for wild-type

virulence of Ralstonia solanacearum', *Journal of Bacteriology*, 179(23), pp. 7369–7378. doi: 10.1128/jb.179.23.7369-7378.1997.

Imlay, J. A. (2008) 'Cellular Defenses against Superoxide and Hydrogen Peroxide', *Annual Review of Biochemistry*, 77(1), pp. 755–776. doi: 10.1146/annurev.biochem.77.061606.161055.

Invernón Garrido, A. (2023) *The catalase/peroxidase KatG is important for the survival of Ralstonia solanacearum in soil and in planta*. Universitat de Barcelona.

Ishikawa, Y. *et al.* (2019) 'Activation of Ralfuranone/Ralstonin Production by Plant Sugars Functions in the Virulence of Ralstonia solanacearum', *ACS Chemical Biology*, 14(7), pp. 1546–1555. Available at: https://pubs.acs.org/sharingguidelines (Accessed: 12 February 2023).

Jacobs, J. M. *et al.* (2012) 'The in planta transcriptome of Ralstonia solanacearum: Conserved physiological and virulence strategies during bacterial wilt of tomato', *mBio*, 3(4), pp. 1–11. doi: 10.1128/mBio.00114-12.

Janse, J. D. (2012) 'Review on brown rot (Ralstonia solanacearum race 3, biovar 2, phylotype IIB) epidemiology and control in the Netherlands since 1995: A success story of integrated pest management', *Journal of Plant Pathology*, 94(2), pp. 257–272. Available at: https://www.jstor.org/stable/45156035#metadata_info_tab_contents (Accessed: 5 February 2023).

Jashni, M. K. *et al.* (2015) 'The battle in the apoplast: Further insights into the roles of proteases and their inhibitors in plant–pathogen interactions', *Frontiers in Plant Science*, 6(AUG), p. 584. doi: 10.3389/fpls.2015.00584.

Jeon, H. *et al.* (2020) 'Ralstonia solanacearum Type III Effectors with Predicted Nuclear Localization Signal Localize to Various Cell Compartments and Modulate Immune Responses in Nicotiana spp.', *The Plant Pathology Journal*, 36(1), pp. 43–53. doi: 10.5423/PPJ.OA.08.2019.0227.

Johansson, J. and Freitag, N. E. (2019) ' Regulation of Listeria monocytogenes Virulence ', *Microbiology Spectrum*, 7(4). doi: 10.1128/microbiolspec.gpp3-0064-2019.

Jones, J. D. G. and Dangl, J. L. (2006) 'The plant immune system', *Nature*, 444(7117), pp. 323–329. doi: 10.1038/nature05286.

Kai, K. *et al.* (2015) 'Methyl 3-Hydroxymyristate, a Diffusible Signal Mediating phc Quorum Sensing in Ralstonia solanacearum', *ChemBioChem*, 16(16), pp. 2309–2318. doi: 10.1002/cbic.201500456.

Kan, Y. *et al.* (2019) 'Induction and Resuscitation of the Viable but Non-culturable (VBNC) State in Acidovorax citrulli, the Causal Agent of Bacterial Fruit Blotch of Cucurbitaceous Crops', *Frontiers in Microbiology*, 10(MAY), p. 1081. doi: 10.3389/FMICB.2019.01081/BIBTEX.

Kanehisa, M. and Goto, S. (2000) *KEGG: Kyoto Encyclopedia of Genes and Genomes*, *Nucleic Acids Research*. Nucleic Acids Res. doi: 10.1093/nar/28.1.27.

Kang, Y. *et al.* (2002) 'Ralstonia solanacearum requires type 4 pili to adhere to multiple surfaces and for natural transformation and virulence', *Molecular Microbiology*, 46(2), pp. 427–437. doi: 10.1046/j.1365-2958.2002.03187.x.

Kang Yaowei *et al.* (1994) 'Dramatically reduced virulence of mutants of Pseudomonas solanacearum defective in export of extracellular proteins across the outer membrane', *Molecular Plant-Microbe Interactions*, 7(3), pp. 370–377. doi: 10.1094/mpmi-7-0370.

Kao, C. C., Barlow, E. and Sequeira, L. (1992) 'Extracellular polysaccharide is required for wild-type virulence of Pseudomonas solanacearum', *Journal of Bacteriology*, 174(3), pp. 1068–1071. doi: 10.1128/jb.174.3.1068-1071.1992.

Kashyap, A. *et al.* (2021) 'Blocking intruders: inducible physico-chemical barriers against plant vascular wilt pathogens', *Journal of Experimental Botany*. Edited by D. Ort, 72(2), pp. 184–198. doi: 10.1093/jxb/eraa444.

Kashyap, A. *et al.* (2022) 'Induced ligno-suberin vascular coating and tyramine-derived hydroxycinnamic acid amides restrict Ralstonia solanacearum colonization in resistant tomato', *New Phytologist*, 234(4), pp. 1411–1429. doi: 10.1111/nph.17982.

Katoh, K. and Standley, D. M. (2013) ‘MAFFT multiple sequence alignment software version 7: Improvements in performance and usability’, *Molecular Biology and Evolution*, 30(4), pp. 772–780. doi: 10.1093/molbev/mst010.

Kaur, S. *et al.* (2022) ‘How do plants defend themselves against pathogens-Biochemical mechanisms and genetic interventions’, *Physiology and Molecular Biology of Plants*. Springer, pp. 485–504. doi: 10.1007/s12298-022-01146-y.

Kelman, A. (1954) ‘The relationship or pathogenicity in Pseudomonas solanacearum to colony appearance on a tetrazolium medium’, *Phytopathology*, 44(19), p. 693.

Khokhani, D. *et al.* (2017) ‘A Single Regulator Mediates Strategic Switching between Attachment/Spread and Growth/Virulence in the Plant Pathogen Ralstonia solanacearum’, *mBio*. Edited by A. K. Vidaver, 8(5). doi: 10.1128/mBio.00895-17.

Kim, J. and Park, W. (2014) ‘Oxidative stress response in Pseudomonas putida’, *Applied Microbiology and Biotechnology*, 98(16), pp. 6933–6946. doi: 10.1007/s00253-014-5883-4.

Kim, S. G. *et al.* (2013) ‘In-depth insight into in vivo apoplastic secretome of rice-Magnaporthe oryzae interaction’, *Journal of Proteomics*, 78, pp. 58–71. doi: 10.1016/j.jprot.2012.10.029.

Kobayashi, K. (2021) ‘Diverse LXG toxin and antitoxin systems specifically mediate intraspecies competition in Bacillus subtilis biofilms’, *PLoS Genetics*, 17(7), p. e1009682. doi: 10.1371/journal.pgen.1009682.

Kocharova, N. A. *et al.* (1993) ‘Sudies of O-specific polysaccharide chains of Pseudomonas solanacearum lipopolysaccharides consisting of structually different repeating units.’, *Carbohydrate Research*, 250(2), pp. 275–287. doi: 10.1016/0008-6215(93)84006-R.

Kong, H. G. *et al.* (2014) ‘Induction of the Viable but Nonculturable State of Ralstonia solanacearum by Low Temperature in the Soil Microcosm and Its Resuscitation by Catalase’, *PLOS ONE*, 9(10), p. e109792. doi: 10.1371/JOURNAL.PONE.0109792.

Kopylova, E., Noé, L. and Touzet, H. (2012) ‘SortMeRNA: Fast and accurate filtering of ribosomal RNAs in metatranscriptomic data’, *Bioinformatics*, 28(24), pp. 3211–3217. doi: 10.1093/bioinformatics/bts611.

Krimi, Z. *et al.* (2002) ‘Seasonal fluctuations and long-term persistence of pathogenic populations of Agrobacterium spp. in soils’, *Applied and Environmental Microbiology*, 68(7), pp. 3358–3365. doi: 10.1128/AEM.68.7.3358-3365.2002.

Kubicek, C. P., Starr, T. L. and Glass, N. L. (2014) ‘Plant cell wall-degrading enzymes and their secretion in plant-pathogenic fungi’, *Annual Review of Phytopathology*, 52(1), pp. 427–451. doi: 10.1146/annurev-phyto-102313-045831.

Laili, N. *et al.* (2021) ‘Role of trehalose synthesis in ralstonia syzygii subsp. Indonesiensis PW1001 in inducing hypersensitive response on eggplant (solanum melongena cv. senryo-nigou)’, *Plant Pathology Journal*, 37(6), pp. 566–579. doi: 10.5423/PPJ.OA.06.2021.0087.

Lampropoulos, A. *et al.* (2013) ‘GreenGate - A novel, versatile, and efficient cloning system for plant transgenesis’, *PLoS ONE*, 8(12), p. 83043. doi: 10.1371/journal.pone.0083043.

Landry, D. *et al.* (2020) ‘The large, diverse, and robust arsenal of Ralstonia solanacearum type III effectors and their in planta functions’, *Molecular Plant Pathology*, 21(10), pp. 1377–1388. doi: 10.1111/mpp.12977.

Langmead, B. and Salzberg, S. (2013) ‘Bowtie2’, *Nature methods*, 9(4), pp. 357–359. doi: 10.1038/nmeth.1923.Fast.

Lavale, S. A. *et al.* (2022) ‘Two decades of omics in bacterial wilt resistance in Solanaceae, what we learned?’, *Plant Stress*, 5, p. 100099. doi: 10.1016/j.stress.2022.100099.

Law, J. N., Kale, S. D. and Murali, T. M. (2021) ‘Accurate and efficient gene function prediction using a multi-bacterial network’, *Bioinformatics*, 37(6), pp. 800–806. doi: 10.1093/bioinformatics/btaa885.

Lebeau, A. *et al.* (2011) ‘Bacterial wilt resistance in tomato, pepper, and eggplant: Genetic resources

respond to diverse strains in the Ralstonia solanacearum species complex', *Phytopathology*, 101(1), pp. 154–165. doi: 10.1094/PHYTO-02-10-0048.

Lei, N. *et al.* (2020) 'Super-Multiple Deletion Analysis of Type III Effectors in Ralstonia solanacearum OE1-1 for Full Virulence Toward Host Plants', *Frontiers in Microbiology*, 11(July), pp. 1–10. doi: 10.3389/fmicb.2020.01683.

Leibniz Institute (2023) *German Collection of Microorganisms and Cell Cultures GmbH: List of Media for Microorganisms*. Available at: https://www.dsmz.de/collection/catalogue/microorganisms/culture-technology/list-of-media-for-microorganisms (Accessed: 27 February 2023).

Lemaga, B. *et al.* (2005) 'Integrated control of potato bacterial wilt in Eastern Africa: the experience of African highlands initiative', in *Bacterial wilt disease and the Ralstonia solanacearum species complex*. American Phytopathological Society (APS Press), pp. 145–157.

Leonard, S. *et al.* (2017) 'Plant–phytopathogen interactions: bacterial responses to environmental and plant stimuli', *Environmental Microbiology*, 19(5), pp. 1689–1716. doi: 10.1111/1462-2920.13611.

Letunic, I. and Bork, P. (2021) 'Interactive tree of life (iTOL) v5: An online tool for phylogenetic tree display and annotation', *Nucleic Acids Research*, 49(W1), pp. W293–W296. doi: 10.1093/nar/gkab301.

Li, C. H. *et al.* (2014) 'Roles of different forms of lipopolysaccharides in ralstonia solanacearum pathogenesis', *Molecular Plant-Microbe Interactions*, 27(5), pp. 471–478. doi: 10.1094/MPMI-08-13-0248-R.

Li, J. *et al.* (2017) 'Phylogenomic evolutionary surveys of subtilase superfamily genes in fungi', *Scientific Reports*, 7(1), pp. 1–15. doi: 10.1038/srep45456.

Li, L. *et al.* (2015) 'Transcriptomic changes of Legionella pneumophila in water', *BMC Genomics*, 16(1), pp. 1–21. doi: 10.1186/s12864-015-1869-6.

Liu, H. *et al.* (2001) 'Twitching motility of Ralstonia solanacearum requires a type IV pilus system', *Microbiology*, 147(12), pp. 3215–3229. doi: 10.1099/00221287-147-12-3215.

Liu, H. *et al.* (2005) 'Pyramiding unmarked deletions in Ralstonia solanacearum shows that secreted proteins in addition to plant cell-wall-degrading enzymes contribute to virulence', *Molecular Plant-Microbe Interactions*, 18(12), pp. 1296–1305. doi: 10.1094/MPMI-18-1296.

Liu, Y. *et al.* (2022) 'Mutation in phcA Enhanced the Adaptation of Ralstonia solanacearum to Long-Term Acid Stress', *Frontiers in Microbiology*, 13. doi: 10.3389/fmicb.2022.829719.

Lonjon, F. *et al.* (2016) 'Comparative secretome analysis of ralstonia solanacearum type 3 secretion-Associated mutants reveals a fine control of effector delivery, essential for bacterial pathogenicity', *Molecular and Cellular Proteomics*, 15(2), pp. 598–613. doi: 10.1074/mcp.M115.051078.

Lonjon, F. *et al.* (2020) 'HpaP Sequesters HrpJ, an Essential Component of Ralstonia solanacearum Virulence That Triggers Necrosis in Arabidopsis', *Molecular Plant-Microbe Interactions*, 33(2), pp. 200–211. doi: 10.1094/MPMI-05-19-0139-R.

Love, M. I., Huber, W. and Anders, S. (2014) 'Moderated estimation of fold change and dispersion for RNA-seq data with DESeq2', *Genome Biology*, 15(12), pp. 1–21. doi: 10.1186/s13059-014-0550-8.

Lowe-Power, T. M. *et al.* (2016) 'Degradation of the plant defense signal salicylic acid protects Ralstonia solanacearum from toxicity and enhances virulence on tobacco', *mBio*, 7(3). doi: 10.1128/mBio.00656-16.

Lowe-Power, T. M. *et al.* (2018) 'Metabolomics of tomato xylem sap during bacterial wilt reveals Ralstonia solanacearum produces abundant putrescine, a metabolite that accelerates wilt disease', *Environmental Microbiology*, 20(4), pp. 1330–1349. doi: 10.1111/1462-2920.14020.

Lowe-Power, T. M., Khokhani, D. and Allen, C. (2018) 'How Ralstonia solanacearum Exploits and Thrives in the Flowing Plant Xylem Environment', *Trends in Microbiology*, 26(11), pp. 929–942. doi: 10.1016/j.tim.2018.06.002.

Lowe, T. M., Ailloud, F. and Allen, C. (2015) 'Hydroxycinnamic acid degradation, a broadly conserved

trait, protects Ralstonia solanacearum from chemical plant defenses and contributes to root colonization and virulence', *Molecular Plant-Microbe Interactions*, 28(3), pp. 286–297. doi: 10.1094/MPMI-09-14-0292-FI.

Ma, L. *et al.* (2018) 'Biological control tobacco bacterial wilt and black shank and root colonization by bio-organic fertilizer containing bacterium Pseudomonas aeruginosa NXHG29', *Applied Soil Ecology*, 129, pp. 136–144. doi: 10.1016/j.apsoil.2018.05.011.

Macho, A. P. *et al.* (2010) 'A competitive index assay identifies several Ralstonia solanacearum type III effector mutant strains with reduced fitness in host plants', *Molecular Plant-Microbe Interactions*, 23(9), pp. 1197–1205. doi: 10.1094/MPMI-23-9-1197.

Macho, A. P. (2016) 'Subversion of plant cellular functions by bacterial type-III effectors: Beyond suppression of immunity', *New Phytologist*, 210(1), pp. 51–57. doi: 10.1111/nph.13605.

MacIntyre, A. M. *et al.* (2020) 'Trehalose Synthesis Contributes to Osmotic Stress Tolerance and Virulence of the Bacterial Wilt Pathogen Ralstonia solanacearum', *Molecular Plant-Microbe Interactions*, 33(3), pp. 462–473. doi: 10.1094/MPMI-08-19-0218-R.

Madeira, F. *et al.* (2022) 'Search and sequence analysis tools services from EMBL-EBI in 2022', *Nucleic Acids Research*, 50(W1), pp. W276–W279. doi: 10.1093/nar/gkac240.

Maharjan, R. P. *et al.* (2005) 'The role of isocitrate lyase and the glyoxylate cycle in Escherichia coli growing under glucose limitation', *Research in Microbiology*, 156(2), pp. 178–183. doi: 10.1016/j.resmic.2004.09.004.

Manguy, J. *et al.* (2017) 'Peptigram: A Web-Based Application for Peptidomics Data Visualization', *Journal of Proteome Research*, 16(2), pp. 712–719. doi: 10.1021/acs.jproteome.6b00751.

Mansfield, J. *et al.* (2012) 'Top 10 plant pathogenic bacteria in molecular plant pathology', *Molecular Plant Pathology*. John Wiley & Sons, Ltd, pp. 614–629. doi: 10.1111/j.1364-3703.2012.00804.x.

Marchler-Bauer, A. and Bryant, S. H. (2004) 'CD-Search: Protein domain annotations on the fly', *Nucleic Acids Research*, 32(WEB SERVER ISS.). doi: 10.1093/nar/gkh454.

Marenda, M. *et al.* (1998) 'PrhA controls a novel regulatory pathway required for the specific induction of Ralstonia solanacearum hrp genes in the presence of plant cells', *Molecular Microbiology*, 27(2), pp. 437–453. doi: 10.1046/j.1365-2958.1998.00692.x.

Mattick, J. S. (2002) 'Type IV Pili and Twitching Motility', *Annual Review of Microbiology*, 56(1), pp. 289–314. doi: 10.1146/annurev.micro.56.012302.160938.

McDougald, D. *et al.* (2002) 'Defences against oxidative stress during starvation in bacteria', *Antonie van Leeuwenhoek, International Journal of General and Molecular Microbiology*, 81(1–4), pp. 3–13. doi: 10.1023/A:1020540503200.

McGarvey, J. A. *et al.* (1998) 'Analysis of Extracellular Polysaccharide I In Culture and In Planta Using Immunological Methods: New Insights and Implications', in *Bacterial Wilt Disease*. Springer, Berlin, Heidelberg, pp. 157–163. doi: 10.1007/978-3-662-03592-4_23.

McGarvey, J. A., Denny, T. P. and Schell, M. A. (2007) 'Spatial-Temporal and Quantitative Analysis of Growth and EPS I Production by Ralstonia solanacearum in Resistant and Susceptible Tomato Cultivars', *https://doi.org/10.1094/PHYTO.1999.89.12.1233*, 89(12), pp. 1233–1239. doi: 10.1094/PHYTO.1999.89.12.1233.

Meng, F. (2013) 'Ralstonia Solanacearum Species Complex and Bacterial Wilt Disease', *Journal of Bacteriology & Parasitology*, p. 510. doi: 10.4172/2155-9597.1000e119.

Meng, F. *et al.* (2015) 'Comparative transcriptome analysis reveals cool virulence factors of Ralstonia solanacearum race 3 biovar 2', *PLoS ONE*, 10(10). doi: 10.1371/journal.pone.0139090.

Meng, F., Yao, J. and Allen, C. (2011) 'A MotN mutant of Ralstonia solanacearum is hypermotile and has reduced virulence', *Journal of Bacteriology*, 193(10), pp. 2477–2486. doi: 10.1128/JB.01360-10.

Mercier, A. *et al.* (2009) 'Influence of DNA conformation and role of comA and recA on natural transformation in Ralstonia solanacearum', *Canadian Journal of Microbiology*, 55(6), pp. 762–770.

doi: 10.1139/W09-025.

Meyer, D. *et al.* (2006) ‘PopF1 and PopF2, two proteins secreted by the Type III protein secretion system of Ralstonia solanacearum, are translocators belonging to the HrpF/NopX family’, *Journal of Bacteriology*, 188(13), pp. 4903–4917. doi: 10.1128/JB.00180-06.

Milling, A., Babujee, L. and Allen, C. (2011) ‘Ralstonia solanacearum extracellular polysaccharide is a specific elicitor of defense responses in wilt-resistant tomato plants’, *PLoS ONE*, 6(1), p. e15853. doi: 10.1371/journal.pone.0015853.

Mishra, S. and Imlay, J. (2012) ‘Why do bacteria use so many enzymes to scavenge hydrogen peroxide?’, *Archives of Biochemistry and Biophysics*, 525(2), pp. 145–160. doi: 10.1016/j.abb.2012.04.014.

Mistry, J. *et al.* (2021) ‘Pfam: The protein families database in 2021’, *Nucleic Acids Research*, 49(D1), pp. D412–D419. doi: 10.1093/nar/gkaa913.

Miya, A. *et al.* (2007) ‘CERK1, a LysM receptor kinase, is essential for chitin elicitor signaling in Arabidopsis’, *Proceedings of the National Academy of Sciences of the United States of America*, 104(49), pp. 19613–19618. doi: 10.1073/PNAS.0705147104/SUPPL_FILE/05147FIG5.PDF.

Montanaro, L. *et al.* (2011) ‘Extracellular DNA in biofilms’, *International Journal of Artificial Organs*. SAGE PublicationsSage UK: London, England, pp. 824–831. doi: 10.5301/ijao.5000051.

Monteiro, F., Solé, M., *et al.* (2012) ‘A chromosomal insertion toolbox for promoter probing, mutant complementation, and pathogenicity studies in Ralstonia solanacearum’, *Molecular Plant-Microbe Interactions*, 25(4), pp. 557–568. doi: 10.1094/MPMI-07-11-0201.

Monteiro, F., Genin, S., *et al.* (2012) ‘A luminescent reporter evidences active expression of Ralstonia solanacearum type III secretion system genes throughout plant infection’, *Microbiology (United Kingdom)*, 158(8), pp. 2107–2116. doi: 10.1099/mic.0.058610-0.

Morel, A. *et al.* (2018) ‘Plant pathogenicity phenotyping of Ralstonia solanacearum strains’, in *Methods in Molecular Biology*. Methods Mol Biol, pp. 223–239. doi: 10.1007/978-1-4939-7604-1_18.

Mori, Y. *et al.* (2016) ‘The vascular plant-pathogenic bacterium R alstonia solanacearum produces biofilms required for its virulence on the surfaces of tomato cells adjacent to intercellular spaces’, *Molecular Plant Pathology*, 17(6), pp. 890–902. doi: 10.1111/mpp.12335.

Mori, Y. *et al.* (2018) ‘Involvement of ralfuranones in the quorum sensing signalling pathway and virulence of Ralstonia solanacearum strain OE1-1’, *Molecular Plant Pathology*, 19(2), pp. 454–463. Available at: https://onlinelibrary.wiley.com/doi/full/10.1111/mpp.12537 (Accessed: 11 February 2023).

Moskvin, O. V. *et al.* (2011) *Rhodobase, a meta-analytical tool for reconstructing gene regulatory networks in a model photosynthetic bacterium*, *BioSystems*. doi: 10.1016/j.biosystems.2010.10.017.

Mukaihara, T., Tamura, N. and Iwabuchi, M. (2010) ‘Genome-wide identification of a large repertoire of Ralstonia solanacearumType III effector proteins by a new functional screen’, *Molecular Plant-Microbe Interactions*, 23(3), pp. 251–262. doi: 10.1094/MPMI-23-3-0251.

Mur, L. A. J. *et al.* (2017) ‘Moving nitrogen to the centre of plant defence against pathogens.’, *Annals of botany*, 119(5), pp. 703–709. doi: 10.1093/aob/mcw179.

Myeku, N. and Figueiredo-Pereira, M. E. (2011) ‘Dynamics of the Degradation of Ubiquitinated Proteins by Proteasomes and Autophagy’, *Journal of Biological Chemistry*, 286(25), pp. 22426–22440. doi: 10.1074/jbc.M110.149252.

Nachin, L. *et al.* (2003) ‘SufC: An unorthodox cytoplasmic ABC/ATPase required for [Fe-S] biogenesis under oxidative stress’, *EMBO Journal*, 22(3), pp. 427–437. doi: 10.1093/emboj/cdg061.

Nair, S. and Finkel, S. E. (2004) ‘Dps protects cells against multiple stresses during stationary phase’, *Journal of Bacteriology*, 186(13), pp. 4192–4198. doi: 10.1128/JB.186.13.4192-4198.2004.

Nakahara, H. *et al.* (2021) ‘Induction of spontaneous phenotype conversion in Ralstonia solanacearum by addition of iron compounds in liquid medium’, *Journal of Microbiological Methods*,

186, p. 106233. doi: 10.1016/j.mimet.2021.106233.

Nakaho, K. and Allen, C. (2009) ‘A pectinase-deficient ralstonia solanacearum strain induces reduced and delayed structural defences in tomato xylem’, *Journal of Phytopathology*, 157(4), pp. 228–234. doi: 10.1111/j.1439-0434.2008.01467.x.

Nakano, M. and Mukaihara, T. (2018) ‘Ralstonia solanacearum type iii effector ripal targets chloroplasts and induces jasmonic acid production to suppress salicylic acid-mediated defense responses in plants’, *Plant and Cell Physiology*, 59(12), pp. 2576–2589. doi: 10.1093/pcp/pcy177.

Nesvizhskii, A. I. and Aebersold, R. (2005) ‘Interpretation of shotgun proteomic data: The protein inference problem’, *Molecular and Cellular Proteomics*, 4(10), pp. 1419–1440. doi: 10.1074/mcp.R500012-MCP200.

Newman, M.-A. *et al.* (2007) ‘Priming, induction and modulation of plant defence responses by bacterial’, *Journal of endotoxin research*, 13(2), pp. 69–84.

Ngou, B. P. M. *et al.* (2021) ‘Mutual potentiation of plant immunity by cell-surface and intracellular receptors’, *Nature*, 592(7852), pp. 110–115. doi: 10.1038/s41586-021-03315-7.

Notti, R. Q. *et al.* (2015) ‘A common assembly module in injectisome and flagellar type III secretion sorting platforms’, *Nature Communications*, 6(1), pp. 1–11. doi: 10.1038/ncomms8125.

Occhialini, A. *et al.* (2005) ‘Genome-Wide Analysis of Gene Expression in Ralstonia solanacearum Reveals That the hrpB Gene Acts as a Regulatory Switch Controlling Multiple Virulence Pathways’, *Molecular Plant-Microbe Interactions*®, 18(9), pp. 938–949. doi: 10.1094/MPMI-18-0938.

Oerke, E. C. and Dehne, H. W. (2004) ‘Safeguarding production - Losses in major crops and the role of crop protection’, *Crop Protection*, 23(4), pp. 275–285. doi: 10.1016/j.cropro.2003.10.001.

Olsson, K. (1976) ‘Experience of Brown Rot Caused by Pseudomonas solanacearum (Smith) Smith in Sweden’, *EPPO Bulletin*, 6(4), pp. 199–207. doi: 10.1111/j.1365-2338.1976.tb01546.x.

Omae, N. and Tsuda, K. (2022) ‘Plant-Microbiota Interactions in Abiotic Stress Environments’, *Molecular Plant-Microbe Interactions*. American Phytopathological Society, pp. 511–526. doi: 10.1094/MPMI-11-21-0281-FI.

Orgambide, G. *et al.* (1991) ‘High heterogeneity of the exopolysaccharides of Pseudomonas solanacearum strain GMI 1000 and the complete structure of the major polysaccharide’, *Journal of Biological Chemistry*, 266(13), pp. 8312–8321. doi: 10.1016/s0021-9258(18)92977-7.

Osdaghi, E. (2020) *Ralstonia solanacearum (bacterial wilt of potato). Invasive Species Compendium*, *Cabi*. doi: 10.1079/CABICOMPENDIUM.45009.

Van Overbeek, L. S. *et al.* (2004) ‘The low-temperature-induced viable-but-nonculturable state affects the virulence of Ralstonia solanacearum Biovar 2’, *Phytopathology*, 94(5), pp. 463–469. doi: 10.1094/PHYTO.2004.94.5.463.

Parks, D. H. *et al.* (2018) ‘A standardized bacterial taxonomy based on genome phylogeny substantially revises the tree of life’, *Nature Biotechnology*, 36(10), p. 996. doi: 10.1038/nbt.4229.

de Pedro-Jové, R. *et al.* (2021) ‘Dynamic expression of Ralstonia solanacearum virulence factors and metabolism-controlling genes during plant infection’, *BMC Genomics*, 22(1). doi: 10.1186/s12864-021-07457-w.

Peeters, N. *et al.* (2013) ‘Repertoire, unified nomenclature and evolution of the Type III effector gene set in the Ralstonia solanacearum species complex’, *BMC Genomics*, 14(1). doi: 10.1186/1471-2164-14-859.

Perombelon, M. C. M. and Kelman, A. (1980) ‘Ecology of the Soft Rot Erwinias’, *Annual Review of Phytopathology*, 18(1), pp. 361–387. doi: 10.1146/annurev.py.18.090180.002045.

Peyraud, R. *et al.* (2016) ‘A Resource Allocation Trade-Off between Virulence and Proliferation Drives Metabolic Versatility in the Plant Pathogen Ralstonia solanacearum’, *PLoS Pathogens*, 12(10), p. e1005939. doi: 10.1371/journal.ppat.1005939.

Piveteau, P. *et al.* (2011) ‘Changes in gene expression during adaptation of Listeria monocytogenes to the soil environment’, *PLoS ONE*, 6(9). doi: 10.1371/journal.pone.0024881.

Planas-Marquès, M. *et al.* (2018) ‘Protease Activities Triggered by Ralstonia solanacearum Infection in Susceptible and Tolerant Tomato Lines’, *Molecular and Cellular Proteomics*, 17(6), pp. 1112–1125. doi: 10.1074/mcp.RA117.000052.

Planas-Marquès, M. *et al.* (2020) ‘Four bottlenecks restrict colonization and invasion by the pathogen Ralstonia solanacearum in resistant tomato’, *Journal of Experimental Botany*, 71(6), pp. 2157–2171. doi: 10.1093/jxb/erz562.

Planas-Marquès, M. (2020) *Quantitative proteomic approaches for the characterization of bacterial wilt resistance mechanisms in tomato*. Universitat de Barcelona.

Plener, L. *et al.* (2010) ‘PrhG, a transcriptional regulator responding to growth conditions, is involved in the control of the type III secretion system regulon in Ralstonia solanacearum’, *Journal of Bacteriology*, 192(4), pp. 1011–1019. doi: 10.1128/JB.01189-09.

Plener, L. *et al.* (2012) ‘Metabolic adaptation of Ralstonia solanacearum during plant infection: A methionine biosynthesis case study’, *PLoS ONE*, 7(5). doi: 10.1371/journal.pone.0036877.

Popa, C. *et al.* (2016) ‘The effector AWR5 from the plant pathogen Ralstonia solanacearum is an inhibitor of the TOR signalling pathway’, *Scientific Reports*, 6. doi: 10.1038/srep27058.

Potapov, V. *et al.* (2004) ‘Protein-protein recognition: Juxtaposition of domain and interface cores in immunoglobulins and other sandwich-like proteins’, *Journal of Molecular Biology*, 342(2), pp. 665–679. doi: 10.1016/j.jmb.2004.06.072.

Poueymiro, M. *et al.* (2014) ‘A Ralstonia solanacearum type III effector directs the production of the plant signal metabolite trehalose-6-phosphate’, *mBio*, 5(6). doi: 10.1128/mBio.02065-14.

Prior, P. *et al.* (2016) ‘Genomic and proteomic evidence supporting the division of the plant pathogen Ralstonia solanacearum into three species’, *BMC Genomics*, 17(1), pp. 1–11. doi: 10.1186/s12864-016-2413-z.

Prior, P. and Fegan, M. (2005) ‘Recent developments in the phylogeny and classification of ralstonia solanacearum’, *Acta Horticulturae*, 695(695), pp. 127–136. doi: 10.17660/ActaHortic.2005.695.14.

Prokchorchik, M. *et al.* (2020) ‘Host adaptation and microbial competition drive Ralstonia solanacearum phylotype I evolution in the Republic of Korea’, *Microbial Genomics*, 6(11), pp. 1–12. doi: 10.1099/mgen.0.000461.

Pryor, K. D. and Leiting, B. (1997) ‘High-level expression of soluble protein in Escherichia coli using a His6-tag and maltose-binding-protein double-affinity fusion system’, *Protein expression and purification*, 10(3), pp. 309–319. doi: 10.1006/PREP.1997.0759.

Puigvert, M. *et al.* (2017) ‘Transcriptomes of ralstonia solanacearum during root colonization of solanum commersonii’, *Frontiers in Plant Science*, 8. doi: 10.3389/fpls.2017.00370.

Puigvert, M. *et al.* (2019) ‘Type III secretion inhibitors for the management of bacterial plant diseases’, *Molecular Plant Pathology*, 20(1), pp. 20–32. doi: 10.1111/mpp.12736.

Qi, P. *et al.* (2022) ‘A Ralstonia solanacearum effector targets TGA transcription factors to subvert salicylic acid signaling’, *Plant Cell*, 34(5), pp. 1666–1683. doi: 10.1093/plcell/koac015.

R Core Team (2021) ‘R: A Language and Environment for Statistical Computing’. Vienna, Austria: R Foundation for Statistical Computing. Available at: https://www.r-project.org/.

Raetz, C. R. H. and Whitfield, C. (2002) ‘Lipopolysaccharide Endotoxins’, *Annual Review of Biochemistry*, 71(1), pp. 635–700. doi: 10.1146/annurev.biochem.71.110601.135414.

Rajkumari, J., Paikhomba Singha, L. and Pandey, P. (2018) ‘Genomic insights of aromatic hydrocarbon degrading Klebsiella pneumoniae AWD5 with plant growth promoting attributes: a paradigm of soil isolate with elements of biodegradation’, *3 Biotech*, 8(2), p. 118. doi: 10.1007/s13205-018-1134-1.

Rakha, M. *et al.* (2020) ‘Development of interspecific hybrids between a cultivated eggplant resistant to bacterial wilt (Ralstonia solanacearum) and eggplant wild relatives for the development of rootstocks’, *Plants*, 9(10), pp. 1–13. doi: 10.3390/plants9101405.

Ratnayake, A. S. (2002) *Screening for physiological characteristics that contribute to the virulence of Ralstonia solanacearum GMI1000*. University of Georgia. Available at: https://esploro.libs.uga.edu/esploro/outputs/graduate/Screening-for-physiological-characteristics-that-contribute-to-the-virulence-of-Ralstonia-solanacearum-GMI1000/9949334156302959.

Remenant, B. *et al.* (2011) ‘Ralstonia syzygii, the blood disease bacterium and some asian R. solanacearum strains form a single genomic species despite divergent lifestyles’, *PLoS ONE*, 6(9). doi: 10.1371/journal.pone.0024356.

Remigi, P. *et al.* (2011) ‘Functional diversification of the GALA type III effector family contributes to Ralstonia solanacearum adaptation on different plant hosts’, *New Phytologist*, 192(4), pp. 976–987. doi: 10.1111/j.1469-8137.2011.03854.x.

Rivard, C. L. and Louws, F. J. (2008) ‘Grafting to manage soilborne diseases in heirloom tomato production’, *HortScience*, 43(7), pp. 2104–2111. doi: 10.21273/hortsci.43.7.2104.

Roberts, D. P., Denny, T. P. and Schell, M. A. (1988) ‘Cloning of the egl gene of Pseudomonas solanacearum and analysis of its role in phytopathogenicity.’, *Journal of bacteriology*, 170(4), pp. 1445–1451. doi: 10.1128/jb.170.4.1445-1451.1988.

Roux, B. *et al.* (2015) ‘Genomics and transcriptomics of Xanthomonas campestris species challenge the concept of core type III effectome’, *BMC Genomics*, 16(1). doi: 10.1186/s12864-015-2190-0.

Le Roux, C. *et al.* (2015) ‘A receptor pair with an integrated decoy converts pathogen disabling of transcription factors to immunity’, *Cell*, 161(5), pp. 1074–1088. doi: 10.1016/j.cell.2015.04.025.

Rubenstein Sabbagh, C. R. *et al.* (2019) ‘Pangenomic type III effector database of the plant pathogenic Ralstonia spp.’, *PeerJ*, 7(8), p. e7346. doi: 10.7287/peerj.preprints.27726.

De Ryck, J., Van Damme, P. and Goormachtig, S. (2023) ‘From prediction to function: Current practices and challenges towards the functional characterization of type III effectors’, *Frontiers in Microbiology*, 14, p. 238. doi: 10.3389/fmicb.2023.1113442.

Safni, I. *et al.* (2014) ‘Polyphasic taxonomic revision of the Ralstonia solanacearum species complex: Proposal to emend the descriptions of Ralstonia solanacearum and Ralstonia syzygii and reclassify current R. syzygii strains as Ralstonia syzygii subsp. syzygii subsp. nov., R. s’, *International Journal of Systematic and Evolutionary Microbiology*, 64(Pt_9), pp. 3087–3103. doi: 10.1099/ijs.0.066712-0.

Saijo, Y., Loo, E. P. iian and Yasuda, S. (2018) ‘Pattern recognition receptors and signaling in plant–microbe interactions’, *The Plant Journal*, 93(4), pp. 592–613. doi: 10.1111/TPJ.13808.

Saile, E. *et al.* (1997) ‘Role of extracellular polysaccharide and endoglucanase in root invasion and colonization of tomato plants by Ralstonia solanacearum’, *Phytopathology*, 87(12), pp. 1264–1271. doi: 10.1094/PHYTO.1997.87.12.1264.

Sainsbury, P. D. *et al.* (2015) ‘Chemical intervention in bacterial lignin degradation pathways: Development of selective inhibitors for intradiol and extradiol catechol dioxygenases’, *Bioorganic Chemistry*, 60, pp. 102–109. doi: 10.1016/j.bioorg.2015.05.002.

Salanoubat, M. *et al.* (2002) ‘Genome sequence of the plant pathogen Ralstonia solanacearum’, *Nature*, 415(6871), pp. 497–502. doi: 10.1038/415497A.

Salgon, S. *et al.* (2017) ‘Eggplant resistance to the Ralstonia solanacearum species complex involves both broad-spectrum and strain-specific quantitative trait loci’, *Frontiers in Plant Science*, 8, p. 828. doi: 10.3389/fpls.2017.00828.

Salguero-Linares, J. and Coll, N. S. (2019) ‘Plant proteases in the control of the hypersensitive response’, *Journal of Experimental Botany*, 70(7), pp. 2087–2095. doi: 10.1093/jxb/erz030.

Sang, Y. *et al.* (2020) ‘Intra-strain Elicitation and Suppression of Plant Immunity by Ralstonia solanacearum Type-III Effectors in Nicotiana benthamiana’, *Plant Communications*, 1(4), p. 100025.

doi: 10.1016/j.xplc.2020.100025.

Santander, R. D., Figàs-Segura, À. and Biosca, E. G. (2018) ‘Erwinia amylovora catalases KatA and KatG are virulence factors and delay the starvation-induced viable but non-culturable (VBNC) response’, *Molecular Plant Pathology*, 19(4), pp. 922–934. doi: 10.1111/mpp.12577.

Šantl-Temkiv, T. *et al.* (2015) ‘Characterization of airborne ice-nucleation-active bacteria and bacterial fragments’, *Atmospheric Environment*, 109, pp. 105–117. doi: 10.1016/j.atmosenv.2015.02.060.

Savary, S. *et al.* (2019) ‘The global burden of pathogens and pests on major food crops’, *Nature Ecology and Evolution*, 3(3), pp. 430–439. doi: 10.1038/s41559-018-0793-y.

Savojardo, C. *et al.* (2018) ‘BUSCA: An integrative web server to predict subcellular localization of proteins’, *Nucleic Acids Research*, 46(W1), pp. W459–W466. doi: 10.1093/nar/gky320.

Schaller, A. *et al.* (2018) ‘From structure to function – a family portrait of plant subtilases’, *New Phytologist*, 218(3), pp. 901–915. doi: 10.1111/nph.14582.

Schaller, A., Stintzi, A. and Graff, L. (2012) ‘Subtilases – versatile tools for protein turnover, plant development, and interactions with the environment’, *Physiologia Plantarum*, 145(1), pp. 52–66. doi: 10.1111/J.1399-3054.2011.01529.X.

Schell, M. A. (2000) ‘Control of virulence and pathogenicity genes of Ralstonia solanacearum by an elaborate sensory network’, *Annual Review of Phytopathology*, 38, pp. 263–292. doi: 10.1146/annurev.phyto.38.1.263.

Schell, M. A., Roberts, D. P. and Denny, T. P. (1988) ‘Analysis of the Pseudomonas solanacearum polygalacturonase encoded by pglA and its involvement in phytopathogenicity.’, *Journal of bacteriology*, 170(10), pp. 4501–4508. doi: 10.1128/jb.170.10.4501-4508.1988.

Scholthof, K. B. G. (2007) ‘The disease triangle: Pathogens, the environment and society’, *Nature Reviews Microbiology*, 5(2), pp. 152–156. doi: 10.1038/nrmicro1596.

Sebastià, P. *et al.* (2021) ‘The Bacterial Wilt Reservoir Host Solanum dulcamara Shows Resistance to Ralstonia solanacearum Infection’, *Frontiers in Plant Science*, 12, p. 2408. doi: 10.3389/fpls.2021.755708.

Shinde, U. and Thomas, G. (2011) ‘Insights from Bacterial Subtilases into the Mechanisms of Intramolecular Chaperone-Mediated Activation of Furin’, in *Methods in Molecular Biology*. Humana Press Inc., pp. 59–106. doi: 10.1007/978-1-61779-204-5_4.

Shrivastava, S. and Mande, S. S. (2008) ‘Identification and functional characterization of gene components of type VI secretion system in bacterial genomes’, *PLoS ONE*, 3(8), p. e2955. doi: 10.1371/journal.pone.0002955.

Siezen, R. J., Renckens, B. and Boekhorst, J. (2007) ‘Evolution of prokaryotic subtilases: Genome-wide analysis reveals novel subfamilies with different catalytic residues’, *Proteins: Structure, Function and Genetics*, 67(3), pp. 681–694. doi: 10.1002/prot.21290.

Singh, S. K. *et al.* (2022) ‘Microbial enhancement of plant nutrient acquisition’, *Stress Biology*, 2(1), pp. 1–14. doi: 10.1007/s44154-021-00027-w.

Sinsabaugh, R. L. (2010) ‘Phenol oxidase, peroxidase and organic matter dynamics of soil’, *Soil Biology and Biochemistry*, 42(3), pp. 391–404. doi: 10.1016/J.SOILBIO.2009.10.014.

Siri, M. I., Sanabria, A. and Pianzzola, M. J. (2011) ‘Genetic diversity and aggressiveness of Ralstonia solanacearum strains causing bacterial wilt of potato in Uruguay’, *Plant Disease*, 95(10), pp. 1292–1301. doi: 10.1094/PDIS-09-10-0626.

Van Sluys, M. A. *et al.* (2002) ‘Comparative genomic analysis of plant-associated bacteria’, *Annual Review of Phytopathology*, 40, pp. 169–189. doi: 10.1146/annurev.phyto.40.030402.090559.

Smith, E. F. (1896) ‘A Bacterial Disease of the Tomato, Eggplant, and Irish Potato (Bacillus solanacearum n. sp.)’, *U. S Departement of Agriculture*, 12(December), pp. 5–28.

Solé, M. *et al.* (2012) ‘The awr gene family encodes a novel class of Ralstonia solanacearum type III

effectors displaying virulence and avirulence activities', *Molecular Plant-Microbe Interactions*, 25(7), pp. 941–953. doi: 10.1094/MPMI-12-11-0321.

Song, S. J. *et al.* (2022) 'The B1 Domain of Streptococcal Protein G Serves as a Multi-Functional Tag for Recombinant Protein Production in Plants', *Frontiers in Plant Science*, 13, p. 1023. doi: 10.3389/FPLS.2022.878677/BIBTEX.

Soong, J. L. *et al.* (2020) 'Microbial carbon limitation: The need for integrating microorganisms into our understanding of ecosystem carbon cycling', *Global Change Biology*, 26(4), pp. 1953–1961. doi: 10.1111/gcb.14962.

de Sousa Abreu, R. *et al.* (2009) 'Global signatures of protein and mRNA expression levels', *Molecular BioSystems*, 5(12), pp. 1512–1526. doi: 10.1039/b908315d.

Stamatakis, A. (2014) 'RAxML version 8: A tool for phylogenetic analysis and post-analysis of large phylogenies', *Bioinformatics*, 30(9), pp. 1312–1313. doi: 10.1093/bioinformatics/btu033.

Stevens, L. H. *et al.* (2018) 'Survival of Ralstonia solanacearum and Ralstonia pseudosolanacearum in drain water', *EPPO Bulletin*, 48(1), pp. 97–104. doi: 10.1111/epp.12450.

Sturm, A. *et al.* (2011) 'The cost of virulence: Retarded growth of salmonella typhimurium cells expressing type iii secretion system 1', *PLoS Pathogens*, 7(7), p. e1002143. doi: 10.1371/journal.ppat.1002143.

Sudakevitz, D. *et al.* (2004) 'A new Ralstonia solanacearum high-affinity mannose-binding lectin RS-IIL structurally resembling the Pseudomonas aeruginosa fucose-specific lectin PA-IIL', *Molecular Microbiology*, 52(3), pp. 691–700. doi: 10.1111/j.1365-2958.2004.04020.x.

Sudakevitz, D., Imberty, A. and Gilboa-Garber, N. (2002) 'Production, properties and specificity of a new bacterial L-fucose- and D-arabinose-binding lectin of the plant aggressive pathogen Ralstonia solanacearum, and its comparison to related plant and microbial lectins', *Journal of Biochemistry*, 132(2), pp. 353–358. doi: 10.1093/oxfordjournals.jbchem.a003230.

Sun, Y. *et al.* (2019) 'The Ralstonia solanacearum effector RipN suppresses plant PAMP-triggered immunity, localizes to the endoplasmic reticulum and nucleus, and alters the NADH/NAD + ratio in Arabidopsis', *Molecular Plant Pathology*, 20(4), pp. 533–546. doi: 10.1111/mpp.12773.

Tan, X. *et al.* (2019) 'Complete genome sequence of sequevar 14m ralstonia solanacearum strain ha4-1 reveals novel type iii effectors acquired through horizontal gene transfer', *Frontiers in Microbiology*, 10(AUG), p. 1893. doi: 10.3389/FMICB.2019.01893/BIBTEX.

Tans-Kersten, J., Guan, Y. and Allen, C. (1998) 'Ralstonia solanacearum pectin methylesterase is required for growth on methylated pectin but not for bacterial wilt virulence', *Applied and Environmental Microbiology*, 64(12), pp. 4918–4923. doi: 10.1128/aem.64.12.4918-4923.1998.

Tans-Kersten, J., Huang, H. and Allen, C. (2001) 'Ralstonia solanacearum needs motility for invasive virulence on tomato', *Journal of Bacteriology*, 183(12), pp. 3597–3605. doi: 10.1128/JB.183.12.3597-3605.2001.

Tapia-Pastrana, G. *et al.* (2012) 'VirK is a periplasmic protein required for efficient secretion of plasmid-encoded toxin from enteroaggregative Escherichia coli', *Infection and Immunity*, 80(7), pp. 2276–2285. doi: 10.1128/IAI.00167-12.

Teufel, R. *et al.* (2010) 'Bacterial phenylalanine and phenylacetate catabolic pathway revealed', *Proceedings of the National Academy of Sciences of the United States of America*, 107(32), pp. 14390–14395. doi: 10.1073/pnas.1005399107.

Thompson, M. G. *et al.* (2020) 'Agrobacterium tumefaciens: A Bacterium Primed for Synthetic Biology', *BioDesign Research*. AAAS. doi: 10.34133/2020/8189219.

Thoms, D., Liang, Y. and Haney, C. H. (2021) 'Maintaining symbiotic homeostasis: How do plants engage with beneficial microorganisms while at the same time restricting pathogens?', *Molecular Plant-Microbe Interactions*. American Phytopathological Society, pp. 462–469. doi: 10.1094/MPMI-11-20-0318-FI.

Tian, M., Benedetti, B. and Kamoun, S. (2005) 'A second Kazal-like protease inhibitor from Phytophthora infestans inhibits and interacts with the apoplastic pathogenesis-related protease P69B of tomato', *Plant Physiology*, 138(3), pp. 1785–1793. doi: 10.1104/pp.105.061226.

Tondo, M. L. *et al.* (2020) 'KatE From the Bacterial Plant Pathogen Ralstonia solanacearum Is a Monofunctional Catalase Controlled by HrpG That Plays a Major Role in Bacterial Survival to Hydrogen Peroxide', *Frontiers in Plant Science*, 11. doi: 10.3389/fpls.2020.01156.

Torto-Alalibo, T., Collmer, C. W. and Gwinn-Giglio, M. (2009) 'The Plant-Associated Microbe Gene Ontology (PAMGO) Consortium: community development of new Gene Ontology terms describing biological processes involved in microbe-host interactions', *BMC Microbiology*, 9(Suppl 1), p. S1. doi: 10.1186/1471-2180-9-S1-S1.

Toruño, T. Y., Stergiopoulos, I. and Coaker, G. (2016) 'Plant-Pathogen Effectors: Cellular Probes Interfering with Plant Defenses in Spatial and Temporal Manners', *Annual review of phytopathology*, 54, p. 419. doi: 10.1146/ANNUREV-PHYTO-080615-100204.

Tran, B. Q. *et al.* (2011) 'Addressing trypsin bias in large scale (Phospho)proteome analysis by size exclusion chromatography and secondary digestion of large post-trypsin peptides', *Journal of Proteome Research*, 10(2), pp. 800–811. doi: 10.1021/pr100951t.

Tran, T. M. *et al.* (2016) 'Extracellular DNases of Ralstonia solanacearum modulate biofilms and facilitate bacterial wilt virulence', *Environmental Microbiology*, 18(11), pp. 4103–4117. doi: 10.1111/1462-2920.13446.

Truchon, A. N. *et al.* (2023) 'Plant-Pathogenic Ralstonia Phylotypes Evolved Divergent Respiratory Strategies and Behaviors To Thrive in Xylem', *mBio*. Edited by M. Whiteley. doi: 10.1128/mbio.03188-22.

Tyanova, S. *et al.* (2016) 'The Perseus computational platform for comprehensive analysis of (prote)omics data', *Nature Methods*. Nature Publishing Group, pp. 731–740. doi: 10.1038/nmeth.3901.

Ujita, Y. *et al.* (2019) 'Signal Production and Response Specificity in the phc Quorum Sensing Systems of Ralstonia solanacearum Species Complex', *ACS Chemical Biology*, 14(10), pp. 2243–2251. doi: 10.1021/acschembio.9b00553.

van Ulsen, P. *et al.* (2014) 'Type V secretion: From biogenesis to biotechnology', *Biochimica et Biophysica Acta (BBA) - Molecular Cell Research*, 1843(8), pp. 1592–1611. doi: 10.1016/j.bbamcr.2013.11.006.

Um, H. Y. *et al.* (2013) 'Altered Gene Expression and Intracellular Changes of the Viable But Nonculturable State in Ralstonia solanacearum by Copper Treatment', *The plant pathology journal*, 29(4), pp. 374–385. doi: 10.5423/PPJ.OA.07.2013.0067.

Ursino, E. *et al.* (2020) 'Bacillus subtilis as a host for mosquitocidal toxins production', *Microbial Biotechnology*, 13(6), p. 1972. doi: 10.1111/1751-7915.13648.

Valls, M., Genin, S. and Boucher, C. (2006) 'Integrated Regulation of the Type III Secretion System and Other Virulence Determinants in Ralstonia solanacearum', *PLoS Pathogens*. Edited by J. Dangl, 2(8), p. e82. doi: 10.1371/journal.ppat.0020082.

Vasse, J. *et al.* (2000) 'The hrpB and hrpG Regulatory Genes of Ralstonia solanacearum Are Required for Different Stages of the Tomato Root Infection Process', *Molecular Plant-Microbe Interactions®*, 13(3), pp. 259–267. doi: 10.1094/MPMI.2000.13.3.259.

Vasse, J., Frey, P. and Trigalet, A. (1995) 'Microscopic studies of intercellular infection and protoxylem invasion of tomato roots by Pseudomonas solanacearum', *Molecular Plant-Microbe Interactions*, 8(2), pp. 241–251. doi: 10.1094/MPMI-8-0241.

Verhage, L. (2021) 'Pump it up! How xylem sap pH controls water transport in leaves', *The Plant Journal*, 106(2), pp. 299–300. doi: 10.1111/tpj.15265.

Verma, R. K. and Teper, D. (2022) 'Immune recognition of the secreted serine protease ChpG restricts the host range of Clavibacter michiganensis from eggplant varieties', *Molecular Plant*

Pathology, 23(7), pp. 933–946. doi: 10.1111/mpp.13215.

Villa, J. E. *et al.* (2005) 'Phylogenetic relationships of Ralstonia solanacearum species complex strains from Asia and other continents based on 16S rDNA, endoglucanase, and hrpB gene sequences', *Journal of General Plant Pathology*, 71(1), pp. 39–46. doi: 10.1007/s10327-004-0156-1.

Vivant, A. L. *et al.* (2017) 'Transcriptomic analysis of the adaptation of Listeria monocytogenes to lagoon and soil matrices associated with a piggery environment: Comparison of expression profiles', *Frontiers in Microbiology*, 8(SEP), pp. 1–16. doi: 10.3389/fmicb.2017.01811.

Vogel, C. and Marcotte, E. M. (2012) 'Insights into the regulation of protein abundance from proteomic and transcriptomic analyses', *Nature Reviews Genetics*, 13(4), pp. 227–232. doi: 10.1038/nrg3185.

Vorholt, J. A. (2012) 'Microbial life in the phyllosphere', *Nature Reviews Microbiology*. Nature Publishing Group, pp. 828–840. doi: 10.1038/nrmicro2910.

Vorwerk, S., Somerville, S. and Somerville, C. (2004) 'The role of plant cell wall polysaccharide composition in disease resistance', *Trends in Plant Science*, 9(4), pp. 203–209. doi: 10.1016/j.tplants.2004.02.005.

Wairuri, C. K. *et al.* (2012) 'Ralstonia solanacearum needs Flp pili for virulence on potato', *Molecular Plant-Microbe Interactions*, 25(4), pp. 546–556. doi: 10.1094/MPMI-06-11-0166.

Wang, G. *et al.* (2019) 'Resistance against Ralstonia solanacearum in tomato depends on the methionine cycle and the γ-aminobutyric acid metabolic pathway', *Plant Journal*, 97(6), pp. 1032–1047. doi: 10.1111/tpj.14175.

Wang, J. F. *et al.* (2000) 'Resistance of tomato line Hawaii7996 to Ralstonia solanacearum Pss4 in Taiwan is controlled mainly by a major strain-specific locus', *Molecular Plant-Microbe Interactions*, 13(1), pp. 6–13. doi: 10.1094/MPMI.2000.13.1.6.

Wang, L. and Wise, M. J. (2011) 'Glycogen with short average chain length enhances bacterial durability', *Naturwissenschaften*. Springer, pp. 719–729. doi: 10.1007/s00114-011-0832-x.

Wang, N. *et al.* (2019) 'Plant root exudates are involved in Bacillus cereusAR156 mediated biocontrol against Ralstonia solanacearum', *Frontiers in Microbiology*, 10(JAN), p. 98. doi: 10.3389/fmicb.2019.00098.

Wang, R. *et al.* (2018) 'Bacterial community structure and functional potential of rhizosphere soils as influenced by nitrogen addition and bacterial wilt disease under continuous sesame cropping', *Applied Soil Ecology*, 125, pp. 117–127. doi: 10.1016/j.apsoil.2017.12.014.

Wang, Y. *et al.* (2021) 'A bacterial effector protein uncovers a plant metabolic pathway involved in tolerance to bacterial wilt disease', *Molecular Plant*, 14(8), pp. 1281–1296. doi: 10.1016/j.molp.2021.04.014.

Wang, Y., Liu, Y. and Ding, W. (2020) 'The phenotype and pathogenicity of Ralstonia solanacearum transformed under prolonged stress of excessive exogenous nitrogen', *Journal of Phytopathology*, 168(3), pp. 175–183. doi: 10.1111/jph.12879.

Wani, A. K. *et al.* (2022) 'Microbial adaptation to different environmental conditions: molecular perspective of evolved genetic and cellular systems', *Archives of Microbiology*, 204(2), p. 144. doi: 10.1007/s00203-022-02757-5.

Weng, C., Peng, X. and Han, Y. (2021) 'Depolymerization and conversion of lignin to value-added bioproducts by microbial and enzymatic catalysis', *Biotechnology for Biofuels*, 14(1), p. 84. doi: 10.1186/s13068-021-01934-w.

Wenneker, M. *et al.* (1999) 'Ralstonia (Pseudomonas) solanacearum race 3 (biovar 2) in surface water and natural weed hosts: First report on stinging nettle (Urtica dioica)', *European Journal of Plant Pathology*, 105(3), pp. 307–315. doi: 10.1023/A:1008795417575.

Westman, S. M. *et al.* (2019) 'Defence priming in Arabidopsis – a Meta-Analysis', *Scientific Reports*, 9(1), pp. 1–13. doi: 10.1038/s41598-019-49811-9.

Wicker, E. *et al.* (2009) 'Epidemiological evidence for the emergence of a new pathogenic variant of

ralstonia solanacearum in martinique (French West Indies)', *Plant Pathology*, 58(5), pp. 853–861. doi: 10.1111/j.1365-3059.2009.02098.x.

Wicker, E. *et al.* (2012) 'Contrasting recombination patterns and demographic histories of the plant pathogen Ralstonia solanacearum inferred from MLSA', *ISME Journal*, 6(5), pp. 961–974. doi: 10.1038/ismej.2011.160.

Wilkinson, S. *et al.* (1998) 'Effects of xylem pH on transpiration from wild-type and flacca tomato leaves: A vital role for abscisic acid in preventing excessive water loss even from well-watered plants', *Plant Physiology*, 117(2), pp. 703–709. doi: 10.1104/pp.117.2.703.

Wright, C. A. and Beattie, G. A. (2004) 'Pseudomonas syringae pv. tomato cells encounter inhibitory levels of water stress during the hypersensitive response of Arabidopsis thalian', *Proceedings of the National Academy of Sciences of the United States of America*, 101(9), pp. 3269–3274. doi: 10.1073/pnas.0400461101.

Wu, D. *et al.* (2019) 'A Plant Pathogen Type III Effector Protein Subverts Translational Regulation to Boost Host Polyamine Levels', *Cell Host and Microbe*, 26(5), pp. 638-649.e5. doi: 10.1016/j.chom.2019.09.014.

Xian, L. *et al.* (2020) 'A Bacterial Effector Protein Hijacks Plant Metabolism to Support Pathogen Nutrition', *Cell Host and Microbe*, 28(4), pp. 548-557.e7. doi: 10.1016/j.chom.2020.07.003.

Xin, X. F. *et al.* (2016) 'Bacteria establish an aqueous living space in plants crucial for virulence', *Nature*, 539(7630), pp. 524–529. doi: 10.1038/nature20166.

Xin, X. F., Kvitko, B. and He, S. Y. (2018) 'Pseudomonas syringae: What it takes to be a pathogen', *Nature Reviews Microbiology*. Nature Publishing Group, pp. 316–328. doi: 10.1038/nrmicro.2018.17.

Xu, J. *et al.* (2011) 'Complete Genome Sequence of the Plant Pathogen Ralstonia solanacearum Strain Po82', *Journal of Bacteriology*, 193(16), pp. 4261–4262. doi: 10.1128/JB.05384-11.

Xu, Z. *et al.* (2022) 'Understanding of bacterial lignin extracellular degradation mechanisms by Pseudomonas putida KT2440 via secretomic analysis', *Biotechnology for Biofuels and Bioproducts*, 15(1), pp. 1–16. doi: 10.1186/s13068-022-02214-x.

Yabuuchi, E. *et al.* (1995) 'Transfer of Two Burkholderia and an Alcaligenes Species to Ralstonia Gen. Nov.: Proposal of Ralstonia pickettii (Ralston, Palleroni and Doudoroff 1973) Comb. Nov., Ralstonia solanacearum (Smith 1896) Comb. Nov. and Ralstonia eutropha (Davis 1969) Comb. No', *MICROBIOLOGY and IMMUNOLOGY*, 39(11), pp. 897–904. doi: 10.1111/j.1348-0421.1995.tb03275.x.

Yadeta, K. A. and Thomma, B. P. H. J. (2013) 'The xylem as battleground for plant hosts and vascular wilt pathogens', *Frontiers in Plant Science*, 4(APR), p. 97. doi: 10.3389/FPLS.2013.00097/BIBTEX.

Yamada, K. *et al.* (2016) 'Regulation of sugar transporter activity for antibacterial defense in Arabidopsis', *Science*, 354(6318), pp. 1427–1430. doi: 10.1126/science.aah5692.

Yan, J. *et al.* (2022) 'RasI/R Quorum Sensing System Controls the Virulence of Ralstonia solanacearum Strain EP1', *Applied and Environmental Microbiology*. Edited by H. Nojiri, 88(15). doi: 10.1128/aem.00325-22.

Yao, J. and Allen, C. (2006) 'Chemotaxis is required for virulence and competitive fitness of the bacterial wilt pathogen Ralstonia solanacearum', *Journal of Bacteriology*, 188(10), pp. 3697–3708. doi: 10.1128/JB.188.10.3697-3708.2006.

Yeats, C., Rawlings, N. D. and Bateman, A. (2004) 'The PepSY domain: A regulator of peptidase activity in the microbial environment?', *Trends in Biochemical Sciences*, 29(4), pp. 169–172. doi: 10.1016/j.tibs.2004.02.004.

Yoshimochi, T. *et al.* (2009) 'The global virulence regulator PhcA negatively controls the Ralstonia solanacearum hrp regulatory cascade by repressing expression of the PrhIR signaling proteins', *Journal of Bacteriology*, 191(10), pp. 3424–3428. doi: 10.1128/JB.01113-08.

Yu, G. *et al.* (2012) 'ClusterProfiler: An R package for comparing biological themes among gene

clusters', *OMICS A Journal of Integrative Biology*, 16(5), pp. 284–287. doi: 10.1089/omi.2011.0118.

Yu, G. *et al.* (2020) 'A bacterial effector protein prevents mapk-mediated phosphorylation of sgt1 to suppress plant immunity', *PLoS Pathogens*. Edited by Yuanchao Wang, 16(9), p. e1008933. doi: 10.1371/journal.ppat.1008933.

Yu, G. *et al.* (2022) 'The Arabidopsis E3 ubiquitin ligase PUB4 regulates BIK1 and is targeted by a bacterial type-III effector', *The EMBO Journal*, 41(23), p. e107257. doi: 10.15252/embj.2020107257.

Yu, J. H. *et al.* (2004) 'Double-joint PCR: A PCR-based molecular tool for gene manipulations in filamentous fungi', *Fungal Genetics and Biology*, 41(11), pp. 973–981. doi: 10.1016/j.fgb.2004.08.001.

Yu, N. Y. *et al.* (2010) 'PSORTb 3.0: Improved protein subcellular localization prediction with refined localization subcategories and predictive capabilities for all prokaryotes', *Bioinformatics*, 26(13), pp. 1608–1615. doi: 10.1093/bioinformatics/btq249.

Yu, X. *et al.* (2013) 'Transcriptional responses of Pseudomonas syringae to growth in epiphytic versus apoplastic leaf sites', *Proceedings of the National Academy of Sciences of the United States of America*, 110(5). doi: 10.1073/pnas.1221892110.

Yu, X. *et al.* (2017) 'From Chaos to Harmony: Responses and Signaling upon Microbial Pattern Recognition', *Annual Review of Phytopathology*. Annual Reviews, pp. 109–137. doi: 10.1146/annurev-phyto-080516-035649.

Yuliar, Nion, Y. A. and Toyota, K. (2015) 'Recent Trends in Control Methods for Bacterial Wilt Diseases Caused by Ralstonia solanacearum', *Microbes and environments*, 30(1), pp. 1–11. doi: 10.1264/jsme2.ME14144.

Zevenhuizen, L. P. T. M. (1992) 'Levels of trehalose and glycogen in Arthrobacter globiformis under conditions of nutrient starvation and osmotic stress', *Antonie van Leeuwenhoek*, 61(1), pp. 61–68. doi: 10.1007/BF00572124.

Zhang, L. *et al.* (2012) 'TssM is essential for virulence and required for type VI secretion in Ralstonia solanacearum', *Journal of Plant Diseases and Protection*, 119(4), pp. 125–134. doi: 10.1007/BF03356431/METRICS.

Zhang, L. *et al.* (2014) 'TssB is essential for virulence and required for Type VI secretion system in Ralstonia solanacearum', *Microbial Pathogenesis*, 74(1), pp. 1–7. doi: 10.1016/j.micpath.2014.06.006.

Zhang, Y. *et al.* (2013) 'Functional analysis of Ralstonia solanacearum PrhG regulating the hrp regulon in host plants', *Microbiology (United Kingdom)*, 159(8), pp. 1695–1704. doi: 10.1099/MIC.0.067819-0/CITE/REFWORKS.

Zhang, Y. *et al.* (2019) 'Involvement of a PadR regulator PrhP on virulence of Ralstonia solanacearum by controlling detoxification of phenolic acids and type III secretion system', *Molecular Plant Pathology*, 20(11), pp. 1477–1490. doi: 10.1111/mpp.12854.

Zheng, X. *et al.* (2019) 'A systematic screen of conserved Ralstonia solanacearum effectors reveals the role of RipAB, a nuclear-localized effector that suppresses immune responses in potato', *Molecular Plant Pathology*, 20(4), pp. 547–561. doi: 10.1111/mpp.12774.

Zhou, X. *et al.* (2022) 'Cross-kingdom synthetic microbiota supports tomato suppression of Fusarium wilt disease', *Nature communications*, 13(1), p. 7890. doi: 10.1038/s41467-022-35452-6.

Zuleta, M. C. (2001) *Identification of Ralstonia solanacearum exoproteins secreted by the type two secretion system using proteomic techniques*, *Phd Thesis*. University of Georgia.

Zuluaga, A. P., Puigvert, M. and Valls, M. (2013) 'Novel plant inputs influencing Ralstonia solanacearum during infection', *Frontiers in Microbiology*, 4(NOV), p. 349. doi: 10.3389/fmicb.2013.00349.

ANNEX

Chapter 4

Identification of Type III Secretion Inhibitors for Plant Disease Management

Roger de Pedro Jové, Pau Sebastià, and Marc Valls

Abstract

Bacterial plant pathogens are among the most devastating threats to agriculture. To date, there are no effective means to control bacterial plant diseases due to the restrictions in the use of antibiotics in agriculture. A novel strategy under study is the use of chemical compounds that inhibit the expression of key bacterial virulence determinants. The type III secretion system is essential for virulence of many Gram-negative bacteria because it injects into the plant host cells bacterial proteins that interfere with their immune system. Here, we describe the methodology to identify bacterial type III secretion inhibitors, including a series of protocols that combine *in planta* and in vitro experiments. We use *Ralstonia solanacearum* as a model because of the number of genetic tools available in this organism and because it causes bacterial wilt, one of the most threatening plant diseases worldwide. The procedures presented can be used to evaluate the effect of different chemical compounds on bacterial growth and virulence.

Key words Bacterial plant pathogens, Type III secretion system, *Ralstonia solanacearum*, Chemical inhibitors, Plants, Protocols, Immunodetection, In vitro inhibitory test

1 Introduction

Bacteria can cause a range of diseases in economically important crops, leading to important losses. *Ralstonia solanacearum*, the causal agent of bacterial wilt, is one of the most devastating plant pathogens worldwide. The lack of effective means to control bacterial diseases and block the spread of these pathogens urge for new control strategies. The use of antibiotics and copper-based compounds is nowadays banned or tightly regulated in many countries [1, 2]. Using compounds that inhibit specific bacterial virulence factors is a promising and sustainable strategy.

The type III secretion system (T3SS) is one of the most distinctive hallmarks of Gram-negative bacterial pathogens. These pathogens use the T3SS to inject small molecules called effectors

Roger de Pedro Jové and Pau Sebastià contributed equally to this work.

Glenn R. Hicks and Chunhua Zhang (eds.), *Plant Chemical Genomics: Methods and Protocols*, Methods in Molecular Biology, vol. 2213, https://doi.org/10.1007/978-1-0716-0954-5_4,

inside the plant cell. Bacterial type III effectors (T3Es) hijack plant defense mechanisms and manipulate different metabolic pathways to successfully colonize the host [3]. Mutant bacteria devoid of the T3SS are totally nonpathogenic so that a possible strategy to inhibit bacterial virulence is to use chemical compounds that block the expression of this secretion system and impede bacterial colonization throughout the plant [4–6].

In this protocol, we present a stepwise guide to assess the ability of different chemical compounds to transcriptionally downregulate the expression of key T3SS genes and to test if they could be used as a means to decrease the virulence of the tested pathogens *in planta*.

2 Materials

2.1 Plant Growth

1. *Nicotiana benthamiana*; *Nicotiana tabacum*; and *Solanum lycopersicum* cv. Marmande.
2. Soil mix: Peat soil substrate n°2 + vermiculite + perlite (*see* **Note 1**).
3. Plant growth chambers with temperature, humidity, and photoperiod control.

2.2 Bacterial Strains and Growth

1. *Ralstonia solanacearum* GMI1000 reporter strains for transcription of *hrpB* (*PhrpB*::*luxCDABE*), *psbA* (*PpsbA*::*luxCDABE*), and *hrpY* (*PhrpY*::*luxCDABE*). *R. solanacearum* GMI1000 *PpsbA*::*avrA*-HA.
2. B medium: 10 g/L bacteriological peptone, 1 g/L yeast extract, and 1 g/L casamino acids. Add 1.5% agar for solid media before autoclaving. Before plating, add 0.5% glucose and 0.005% triphenyltetrazolium chloride (TTC). Supplement with the appropriate antibiotics (*see* **Notes 2** and **3**).
3. Boucher's minimal medium [7]: To prepare 1 L of 2× Boucher's medium, mix 100 mL of 5× M63 medium (10 g/L $(NH_4)_2SO_4$, 68 g/L KH_2PO_4, and 2.5 mg/L $FeSO_4{\cdot}7H_2O$, pH 7 with KOH) with 405 µL of 1 M $MgSO_4{\cdot}7H_2O$ and adjust to 1 L with sterile distilled water. Before use, dilute to 1× with sterile distilled water (or 2× agar on water for plates). Supplement with 20 mM glutamate and appropriate antibiotics.

2.3 T3SS Inhibition Test In Vitro

1. Potential type III secretion inhibitory compound to test.
2. DMSO.
3. Incubator at 28 °C with rotor.
4. Luminometer.
5. Spectrophotometer.

2.4 Effect of the Tested Compound on Bacterial T3E Secretion

1. Sucrose.
2. Congo red.
3. 0.22-μM filter.
4. 10-mL syringe.
5. 25% trichloroacetic acid.
6. 90% acetone.
7. Phosphate-buffered saline (PBS) 1×: 8 g/L NaCl, 0.201 g/L KCl, 1.42 g/L Na_2HPO_4, 0.272 g/L KH_2PO_4.
8. 4× Laemmli buffer.
9. Digital sonifier.
10. Primary anti-HA rat monoclonal antibody conjugated to horseradish peroxidase (HRP) in Tris-buffered saline (TBS) with 0.1% Tween-20 and 1% skimmed milk (*see* **Note 4**).
11. Coomassie blue.
12. LAS-4000 mini system.

2.5 In Planta Experiments

1. Blunt-end syringe.
2. 100% ethanol.
3. Leaf disk puncher.
4. Potter S homogenizer.

3 Methods

3.1 Plant and Bacterial Growth

3.1.1 N. benthamiana/ N. tabacum

1. Sow *N. benthamiana* or *N. tabacum* seeds in a pot at 26 °C and 14 h light/10 h darkness.
2. After 10 days, transfer each seedling to individual pots.
3. After 10 days, transfer each individual plant to single big pots. These plants will be ready for assays after 3 weeks (*see* **Notes 5** and **6**).

3.1.2 Solanum lycopersicum *cv. Marmande*

1. Sterilize Marmande tomato seeds with a sterile solution containing 1:3.33 of commercial bleach (4.7% concentrated) and 0.05% triton. Keep the seeds in the solution for 10 min. Wash with sterile distilled water at least five times.
2. Sow the sterilized seeds and cover with plastic film.
3. Keep the plants in the growth chamber at 22 °C, 16 h light and 8 h darkness for 1 week, until tomato seedlings emerge and touch the plastic film on top.
4. Transfer each tomato seedling to individual soil pots with the soil mix and let them grow for 3 weeks in a chamber at 22 °C and 16 h light and 8 h darkness (*see* **Note 5**).

3.1.3 *Ralstonia solanacearum*

1. Streak the bacterial strain from a glycerol stock at −80 °C on B medium supplemented with antibiotics for 2 days at 28 °C.
2. Pick a single colony and incubate in liquid B or minimal media.

3.2 In Vitro T3SS Inhibitor Screening in Ralstonia solanacearum

1. Grow an overnight pre-culture in liquid B media supplemented with antibiotics (*see* **Notes 7** and **8**).
2. Centrifuge the overnight pre-culture in 2-mL Eppendorf tubes at RT for 1 min at maximum speed, discard the supernatant, and resuspend the bacterial pellet in 1 mL of sterile distilled H_2O.
3. Measure the OD_{600} with a spectrophotometer (*see* **Note 9**).
4. Adjust to a final OD_{600} of 0.3 adding the right pre-culture volume to a culture tube containing 1.5 mL of fresh Boucher's minimal medium supplemented with 20 mM glutamate, antibiotic, and 100 mM inhibitory test compound/DMSO (*see* **Note 10**).
5. Mix by vortexing for a few seconds and incubate in a shaker.
6. Measure luminescence at times 0, 4, 6, 8 and 24 h transferring 200 μL from each tube into a 1.5-mL Eppendorf tube and quantifying light emission from the reporter in the luminometer. For each time point, measure as well OD_{600} in a spectrophotometer by transferring the 200 μL into a cuvette containing 800 μL of distilled water (*see* **Notes 11–13**).

3.3 Effect of the Tested Compound on Bacterial T3E Secretion

1. From an overnight culture of liquid B medium supplemented with antibiotics, adjust to a final OD_{600} of 0.2 (2×10^8 CFUs/mL) in a final volume of 10 mL of minimal medium supplemented with antibiotics, 10 mM glutamate, 10 mM sucrose, 100 μg/mL congo red (*see* **Note 14**), and 100 μg/mL of the test inhibitor compound (or 10 μL of DMSO as a control).
2. Incubate at room temperature for 12–14 h (or until OD_{600} reaches 1).
3. Transfer the culture to a 50-mL falcon tube and centrifuge at 4000 × *g* for 10 min.
4. Filter the supernatant through a 0.22-μM filter with a syringe in order to remove any bacteria. The bacterial pellet is also kept at −20 °C for further analysis.
5. Add 10 mL of cold 25% TCA to the filtered supernatant and let it precipitate all night long at 4 °C.
6. Centrifuge at 6000 × *g* for 30 min at 4 °C and discard the supernatant.
7. Wash the protein pellet (it will contain all secreted proteins in the medium) twice with cold 90% acetone and let it dry at RT.

8. Resuspend the protein pellet in 100 µL of PBS 1×. Mix 15 µL of this solution with 15 µL of Laemmli buffer.
9. Recover the frozen bacterial pellet, freeze–thaw 3–4 times (−80 °C—RT cycles), resuspend in 1 mL of 1× PBS, and sonicate the cells using a sonifier (*see* **Note 15**). Mix 15 µL of the mixture with 15 µL of Laemmli buffer.
10. Boil the samples for 5 min and load it on SDS-PAGE (it will be a 100× concentration from initial culture).
11. The presence of particular proteins in the extracts can be analyzed by immunoblot using an antibody against the protein of interest. Coomassie-stained sodium dedecylsulfate-polyacrylamide gel electrophoresis (SDS-PAGE) membranes can be visualized using a LAS-4000 mini system (*see* Fig. 1).

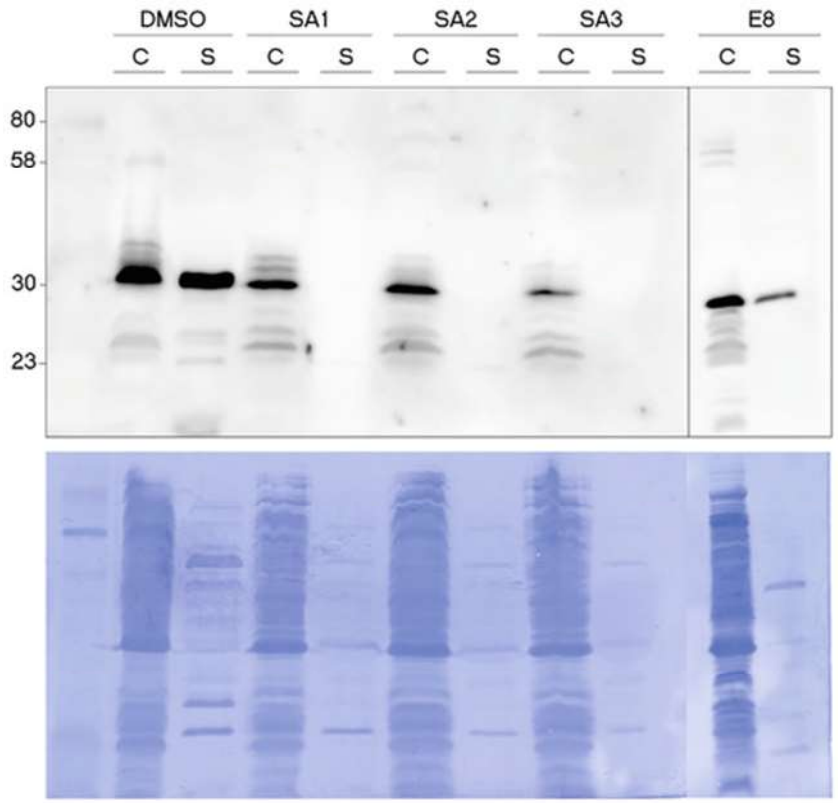

Fig. 1 Immunoblot of the secreted T3 effector (in this case, AvrA-HA) after treatment with four different inhibitory compounds (SA1-3 and E8) or the control (DMSO). The cytosolic (C) and secreted (S) fractions were separated by centrifugation. The protein of interest was detected with anti-HA antibody. Coomassie blue-stained membranes (below) used in the western blotting are also shown. (Reproduced from [9] with permission of John Wiley and Sons)

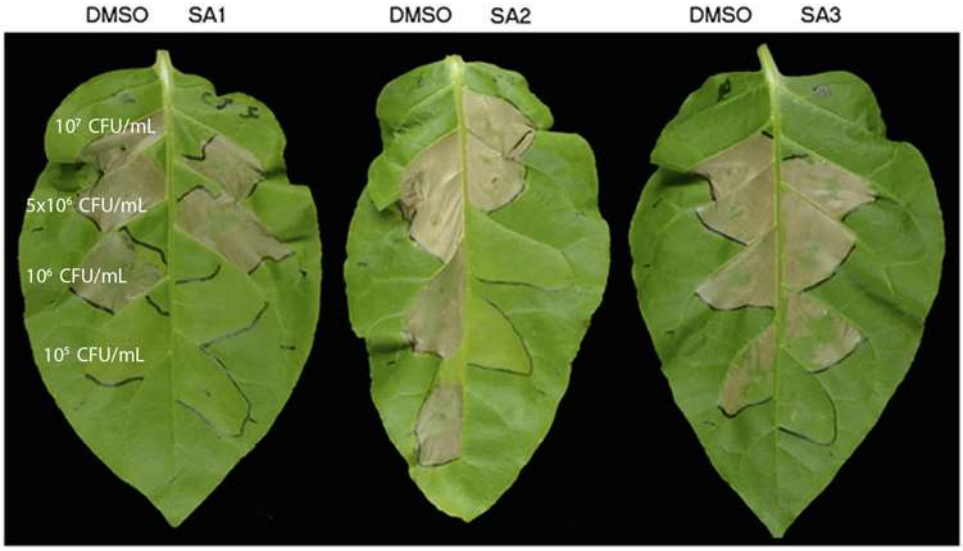

Fig. 2 *N. benthamiana* leaves infiltrated with serial dilutions of *R. solanacearum* preincubated with inhibitory compounds (in this case, SA1, SA2, SA3) or with a control solution (DMSO). Leaves were photographed 2 days post-infiltration. (Reproduced from [9] with permission of John Wiley and Sons)

3.4 In Vivo T3E Translocation Test Using Hypersensitive Response Assays

1. To the overnight culture of the desired bacterial strain (e.g., *R. solanacearum* GMI1000) in Boucher's minimal medium supplemented with 20 mM glutamate and antibiotic, add the tested inhibitory compound at 100 μM (or with DMSO for the nontreated condition) and incubate for 8 h.
2. Centrifuge at maximum speed for 8 min and discard the supernatant.
3. Resuspend bacterial pellet with sterile distilled water and measure the OD_{600}. Make serial dilutions ranging from 10^7 to 10^5 CFUs/mL (*see* **Note 16**).
4. Leaf-infiltrate *N. benthamiana* and *N. tabacum* plants with a blunt-end syringe following a predesigned scheme (*see* **Note 17** and Fig. 2).
5. The first signs of hypersensitive responses are visible 12 h post-infiltration, but they can be better appreciated when the dead tissue is totally dry, so the pictures are taken 2 days post-infiltration in *N. tabacum*, and 5 days post-infiltration in *N. benthamiana* (*see* **Note 18**).

3.5 Compound Effect on Bacterial Fitness In Planta

1. Grow an overnight pre-culture in liquid B medium supplemented with antibiotics.
2. Measure the OD_{600} of the pre-culture and adjust a bacterial suspension to 10^5 CFU/mL ($OD_{600} = 0.0001$) with autoclaved tap water supplemented with each test compound at 100 μM (or DMSO alone for control condition).

3. Hand-infiltrate 4 tomato leaves per tested compound with a blunt-end syringe (*see* **Note 19**).
4. Place the infiltrated plants in the growth chamber for 1 h at 27 °C and 60% relative humidity.
5. At time 0 (just after infiltration) and at 4 days post-infiltration (d.p.i.), collect 2 leaf discs (5 mm diameter) from the infiltrated area of six independent leaves. Combine in a 1.5-mL Eppendorf tube the disks from 2 leaves (4 disks total) to generate three biological replicates.
6. Homogenize the plant material with a Potter S homogenizer in 200 µL of sterile distilled water (*see* **Note 20**).
7. Add 800 µL of sterile distilled water to each Eppendorf tube.
8. Place the plants back in the growth chamber.
9. Prepare tenfold dilutions from the leaf homogenates (*see* **Note 21**).
10. Plate 10 µL drops of the 4 dilutions on plates of B medium (containing TTC and glucose) supplemented with antibiotics and incubate at 28 °C for 1–2 days to count colonies (*see* **Note 22**).

3.6 Effect of the T3 Secretion Inhibitor on Bacterial Virulence to Plants

1. Grow an overnight pre-culture in liquid B medium supplemented with antibiotics.
2. For each treatment, wound the roots of 12 plants grown in independent pots with a 1-mL pipette tip by making 4 holes in the soil around the stem. Water each plant with 40 mL of a bacterial suspension containing 10^8 CFUs/mL supplemented with 100 µM of the compound to test or DMSO (*see* **Note 23**).
3. Record wilting symptoms during 9 days after infection for each plant using a semiquantitative scale ranging from 0 (no wilting) to 4 (death) (*see* **Note 24**).

4 Notes

1. For 24 individual square pots mix: 7 L of peat soil, 0.2 L of vermiculite, and 0.2 L of perlite.
2. For gentamicin and tetracycline, use half of the recommended concentration in liquid media (e.g., 10 µg/mL gentamicin in solid medium and 5 µg/mL in liquid medium).
3. Keep the TTC solution and tetracycline away from direct light contact. Glucose strongly enhances exopolysaccharide production and TTC turns red through bacterial metabolism, so wild-type *R. solanacearum* colonies appear red with a thick mucus halo in this medium. Spontaneous nonmucous mutants (usually rare) are nonpathogenic and can be discarded.

4. The anti-HA antibody (clone 3F10) from Roche, Switzerland, works well for us at 1:4000 dilution. Anti-HA antibodies from our resources might work as well, and we recommend testing for ideal dilutions before use.
5. To acclimate the plants, 2 days prior to bacterial inoculation, transfer them to the infection growth chamber (27 °C and 60% humidity).
6. For HR assays, plants should not be stressed. Clear signs of stress are chlorotic leaves and flowering. To avoid this, do not water in excess, and always use high-intensity light. Plants can be grown at 24–26 °C without any difference.
7. Minimal medium is appropriate when type III secretion gene expression has to be induced (e.g., *PhrpY::lux*). B medium is appropriate when high growth is desired, or expression of the type III secretion genes has to be repressed.
8. Normally, 10 mL of overnight culture should be enough to prepare 20 tubes for the inhibition test.
9. We recommend measuring OD_{600} from 1/10 dilutions of overnight cultures to avoid saturation, as spectrophotometers usually measure linearly between 0.01 and 2.
10. To ease the experiment, prepare these minimal media culture tubes the day before and store at 4 °C. Pre-warm the media before use.
11. Use a cuvette with the same growth medium as blank to calibrate the spectrophotometer.
12. This protocol can be scaled up to 96-well plates in case a larger set of inhibitors has to be tested. For growth measurements, a transparent bottom plate must be used. For luminescence measurements, use white opaque plates, which help reflecting luminescence and amplify the signal. The 96-well plates can be measured using a Spectramax M3 from Molecular Devices.
13. Luminescence measurements allow quantification of the transcriptional output at different time points, and OD_{600} measurements quantify bacterial growth to normalize luminescence per cell and rule out eventual inhibitory or bacteriostatic effects of the tested compounds.
14. Congo red enhances bacterial protein secretion through the type III secretion system [8].
15. We normally sonicate for 90s at 30% amplification and 10s ON/OFF intervals using a digital sonifier, Model 250/450 (BRANSON, USA). The required sonication time and intervals can vary for different sonifiers.
16. In *R. solanacearum*, an $OD_{600} = 1$ usually corresponds to 10^9 CFUs/mL.

17. It is recommended to randomize the infiltration of the bacterial dilutions in different leaves in order to get rid of eventual position effects. Infiltrate in the inter-vein areas to avoid a mixture of treatments.
18. For a better HR cell death visualization, the treated leaves can be bleached using 100% ethanol in a water bath at 60 °C for 20 min.
19. Tomato plants can be vacuum-infiltrated instead using Silwett as an adjuvant to facilitate infiltration (80 μL/L). Usually, 20–30 s of vacuum infiltration is enough per tomato plant, but timings might change in other plant species depending on the hardness of their leaves. A change in the leaf color to dark green indicates proper vacuum infiltration.
20. We use the mechanic drill with a plastic pestle, but a tissue lyser with beads or a classical mortar can also be used.
21. To ease manipulation, it is advisable to perform dilutions in 96-well plates using a multichannel pipette by transferring 10 μL into 90 μL of sterile distilled H_2O consecutively. Make sure to mix well each dilution.
22. For colony count, make sure that colonies are well separated. Bacterial growth is calculated as recovered CFU/cm^2 (area depends on the size of the leaf disk puncher).
23. In order to facilitate plant infection, it is better to stop watering them 2 days prior to inoculation.
24. Wilting symptoms are recorded based on a scale from 0 to 4: 0 = no wilting, 1 = 25% of the leaves wilted, 2 = 50% of the leaves wilted, 3 = 75% of the leaves wilted, and 4 = 100% of the leaves wilted. It is recommended that the same person carries out the whole symptom recording to avoid biases.

References

1. Duffy B, Schärer HJ, Bünter M et al (2005) Regulatory measures against Erwinia amylovora in Switzerland. EPPO Bull 35:239–244. https://doi.org/10.1111/j.1365-2338.2005.00820.x
2. MacKie KA, Müller T, Kandeler E (2012) Remediation of copper in vineyards—a mini review. Environ Pollut 167:16–26. https://doi.org/10.1016/j.envpol.2012.03.023
3. Büttner D (2016) Behind the lines-actions of bacterial type III effector proteins in plant cells. FEMS Microbiol Rev 40:894–937. https://doi.org/10.1093/femsre/fuw026
4. Hudson DL, Layton AN, Field TR et al (2007) Inhibition of type III secretion in *Salmonella enterica* serovar typhimurium by small-molecule inhibitors. Antimicrob Agents Chemother 51:2631–2635. https://doi.org/10.1128/AAC.01492-06
5. Kauppi AM, Nordfelth R, Uvell H et al (2003) Targeting bacterial virulence: inhibitors of type III secretion in Yersinia. Chem Biol 10:241–249. https://doi.org/10.1016/s1074-5521(03)00046-2
6. Muschiol S, Bailey L, Gylfe A et al (2006) A small-molecule inhibitor of type III secretion inhibits different stages of the infectious cycle of chlamydia trachomatis. Proc Natl Acad Sci U S A 103:14566–14571. https://doi.org/10.1073/pnas.0606412103
7. Boucher CA, Barberis PA, Demery DA (1985) Transposon mutagenesis of pseudomonas

solanacearum: isolation of Tn5-induced Avirulent mutants. Microbiology 131:2449–2457. https://doi.org/10.1099/00221287-131-9-2449

8. Bahrani FK, Sansonetti PJ, Parsot C (1997) Secretion of Ipa proteins by Shigella flexneri: inducer molecules and kinetics of activation. Infect Immun 65:4005–4010
9. Solé M, Puigvert M, Davis RA et al (2018) Type III secretion inhibitors for the management of bacterial plant diseases. Mol Plant Pathol 20:20–32. https://doi.org/10.1111/mpp.12736

Journal of Experimental Botany
doi:10.1093/jxb/eraa610 Advance Access Publication 21 January, 2021

RESEARCH PAPER

A genome-wide association study reveals cytokinin as a major component in the root defense responses against *Ralstonia solanacearum*

Alejandro Alonso-Díaz[1], Santosh B. Satbhai[2,3,*], Roger de Pedro-Jové[1], Hannah M. Berry[4,5] Christian Göschl[2], Cristiana T. Argueso[4], Ondrej Novak[6], Wolfgang Busch[2,3], Marc Valls[1,7] and Núria S. Coll[1,†]

[1] Centre for Research in Agricultural Genomics (CSIC-IRTA-UAB-UB), Bellaterra, Barcelona, Spain
[2] Gregor Mendel Institute (GMI), Austrian Academy of Sciences, Vienna Biocenter (VBC), Dr Bohr-Gasse 3, Vienna 1030, Austria
[3] Salk Institute For Biological Studies, Plant Molecular and Cellular Biology Laboratory, 10010 N Torrey Pines Rd, La Jolla, CA 92037, USA
[4] Department of Bioagricultural Sciences and Pest Management, Colorado State University, Fort Collins, CO 80523, USA
[5] Cell and Molecular Biology, Colorado State University, Fort Collins, CO 80523, USA
[6] Laboratory of Growth Regulators, Olomouc, The Czech Republic
[7] Genetics Department, University of Barcelona, Barcelona, Spain

*Present address: Department of Biological Sciences, Indian Institute of Science Education and Research (IISER) Mohali, Punjab, India.
† Correspondence: nuria.sanchez-coll@cragenomica.es

Received 9 October 2020; Editorial decision 21 December 2020; Accepted 19 January 2021

Editor: Steven Spoel, University of Edinburgh, UK

Abstract

Bacterial wilt caused by the soil-borne pathogen *Ralstonia solancearum* is economically devastating, with no effective methods to fight the disease. This pathogen invades plants through their roots and colonizes their xylem, clogging the vasculature and causing rapid wilting. Key to preventing colonization are the early defense responses triggered in the host's root upon infection, which remain mostly unknown. Here, we have taken advantage of a high-throughput *in vitro* infection system to screen natural variability associated with the root growth inhibition phenotype caused by *R. solanacearum* in Arabidopsis during the first hours of infection. To analyze the genetic determinants of this trait, we have performed a genome-wide association study, identifying allelic variation at several loci related to cytokinin metabolism, including genes responsible for biosynthesis and degradation of cytokinin. Further, our data clearly demonstrate that cytokinin signaling is induced early during the infection process and cytokinin contributes to immunity against *R. solanacearum*. This study highlights a new role for cytokinin in root immunity, paving the way for future research that will help in understanding the mechanisms underpinning root defenses.

Keywords: Bacterial wilt, cytokinin, defense, GWAS, hormones, immune system, *Ralstonia solanacearum*, root, salicylic acid.

Introduction

Plant hormones are extremely important for the regulation of the plant defense against pathogens (Pieterse *et al.*, 2012). Several studies have shown that the accumulation of salicylic acid (SA) induces plant defense against biotrophic pathogens (Shigenaga and Argueso, 2016), whereas jasmonic acid (JA) and ethylene are essential against necrotrophs. The crosstalk between JA and abscisic acid (ABA) induces plant defense against herbivores and insects (Pieterse *et al.*, 2012). The synergistic or antagonistic interaction between the different hormone signaling pathways enables the plant to fine-tune defense responses to the pathogen that are effective while minimizing damage or yield penalties (Pieterse *et al.*, 2009).

Cytokinin is a plant hormone traditionally associated with plant growth and development (Mok, 1994; Sa *et al.*, 2001; Wybouw and De Rybel, 2019) with an emerging role in plant immunity. Cytokinin has been shown to participate in defense against various plant pathogens, including fungi (Argueso *et al.*, 2012; Gupta *et al.*, 2020), bacteria (Choi *et al.*, 2010; Naseem *et al.*, 2012; Pieterse *et al.*, 2012). and viruses (Clarke *et al.*, 1998a; Pogány *et al.*, 2004). Furthermore, application of exogenous cytokinin results in an increase of callose production in *Arabidopsis thaliana* (henceforth, Arabidopsis) infected with *Pseudomonas syringae* or treated with the flagellin-derived defense elicitor flg22 (Choi *et al.*, 2010). Tight regulation of cytokinin levels is essential to determine the precise signaling outcome. Treatments with low concentrations of exogenous cytokinin result in greater susceptibility to infection with the oomycete *Hyaloperonospora arabidopsidis* in Arabidopsis, and also to infection with *Blumeria graminis* in wheat. In contrast, treatments with higher levels of cytokinin increase resistance of plants to these and other pathogens (Argueso *et al.*, 2012; Babosha, 2009; Gupta *et al.*, 2020).

Importantly, cytokinin signaling in immunity is greatly intertwined with SA signaling. It has been observed that increased resistance to *H. arabidopsidis* induced by cytokinin treatment is mediated by SA accumulation and the activation of SA-dependent defense genes (Choi *et al.*, 2010; Argueso *et al.*, 2012). Mechanistically, it has been shown that the ARR2 (ARABIDOPSIS RESPONSE REGULATOR 2), a major transcription factor of the cytokinin signal transduction pathway, physically interacts with TGA3, a transcription factor from the SA signaling pathway (Choi *et al.*, 2010). The interaction of these two transcription factors is regulated by NPR1 (NON-EXPRESSOR OF PATHOGENESIS-RELATED PROTEINS 1), leading to changes in *PR1* expression and plant immune status (Choi *et al.*, 2010). More recently, it has been shown that cytokinin treatment of tomato leaves induces resistance against fungi in an SA-dependent manner (Gupta *et al.*, 2020). Although sparse, current evidence indicates that the crosstalk between cytokinin and SA signaling pathways is very important for plant immune responses (Choi *et al.*, 2010; Argueso *et al.*, 2012).

The majority of studies analyzing the role of cytokinin in plant defense have been performed using foliar pathogens (Clarke *et al.*, 1998a; Pogány *et al.*, 2004; Choi *et al.*, 2010; Argueso *et al.*, 2012; Naseem *et al.*, 2012; Pieterse *et al.*, 2012; Gupta *et al.*, 2020). In contrast, the role of cytokinin in root defenses remains mostly unexplored.

Ralstonia solanacearum is a natural soil-borne bacterial vascular pathogen that infects many plant species, including Arabidopsis, and it is the causative agent of bacterial wilt, a disease of devastating economic impact worldwide. *Ralstonia solanacearum* invades plants through the roots, moving centripetally until it reaches the xylem. Xylem colonization allows movement of the bacteria up into the stem, causing a rapid and permanent obstruction of the vasculature (Hayward, 1991; Planas-Marquès *et al.*, 2020). Many genetic tools are available to study this pathogen, since it has been widely used as a model species for plant–pathogen interactions in the last decades (Mansfield *et al.*, 2012; Coll and Valls, 2013).

Transcriptomic analyses of Arabidopsis roots infected with the bacterial pathogen *R. solanacearum* show expression of cytokinin biosynthetic genes at early time points [6 hours post-infection (hpi)] (Zhao *et al.*, 2019), while cytokinin-degrading genes are expressed at later stages of infection (after 72 h) in *Medigaco truncatula* roots infected with *R. solanacearum* (Moreau *et al.*, 2014). Interestingly, Arabidopsis plants lacking the redundant negative regulator of cytokinin signaling ARR6 showed increased resistance to the fungal pathogen *Plectosphaerella cucumerina* but increased susceptibility to *R. solanacearum* (Bacete *et al.*, 2020). However, these phenotypes did not occur as a direct result of the interactions between cytokinin signaling and classical hormone-based defense pathways.

In previous work, we set up an *in vitro* system to study Arabidopsis early root phenotypes caused by *R. solanacearum* infection: root growth inhibition, root hair formation, and root tip cell death (Lu *et al.*, 2018). This robust method revealed genetic determinants of the interaction both from the bacterial virulence and plant defense sides at very early stages of infection, which were masked in classic pathogenicity assays. Here, we have taken advantage of the high-throughput potential of this *in vitro* system to screen the natural variation of the root growth inhibition phenotype across 430 Arabidopsis accessions representative of the worldwide genetic variation of this species and determine the gene(s) responsible for this trait using genome-wide association (GWA) mapping.

Thanks to the large number of Arabidopsis accessions that have been sequenced and genotyped, this model plant has great potential for genome-wide association study (GWAS) analyses (Atwell *et al.*, 2010). Previous studies using GWAS and natural genetic variation have detected genetic variants associated with resistance to abiotic stress (Bac-Molenaar *et al.*, 2015; Kalladan *et al.*, 2017; Satbhai *et al.*, 2017; Li *et al.*, 2019), root development (Meijón *et al.*, 2014), or flowering time (Aranzana *et al.*, 2005). GWAS has also been shown to be a very powerful tool to unravel genomic regions associated with the natural

variation of disease resistance of various plants against different pathogens, for example Arabidopsis against *Pseudomonas syringae* (Aranzana *et al.*, 2005; Atwell *et al.*, 2010; Iakovidis *et al.*, 2016), and *Xanthomonas campestris* (Huard-Chauveau *et al.*, 2013) and *Botrytis cinerea* (Corwin *et al.*, 2016; Thoen *et al.*, 2017), or *Glycine max* against *Fusarium virguliforme* (Wen *et al.*, 2014), among others. Importantly, a GWAS has been recently used to study the temperature-dependent genetic variation that underscores resistance of Arabidopsis against *R. solanacearum* (Aoun *et al.*, 2017). Finally, GWAS has also highlighted the importance of hormonal crosstalk between SA and ABA in the JA pathway involved in defense in Arabidopsis (Proietti *et al.*, 2018). Taking advantage of GWAS, we have identified cytokinin signaling as an important component in the root growth inhibition phenotype caused by *R. solanacearum* in Arabidopsis, contributing to root defenses against the pathogen.

Materials and methods

Plant material

A collection of 430 *A. thaliana* ecotypes (Supplementary Table S1) provided by the Molecular Plant Biology Stock from the Gregor Mendel Institute (Vienna, Austria) was used for GWAS. The Arabidopsis mutant lines used in this study have been previously described in Kiba *et al.* (2013) (*cyp735a1* and *cyp735a2*) and Caesar *et al.* (2011) (*ahk2*, *ahk3*, and *ahk4/cre1*). Transgenic line *TCSn::GFP* has been described in Zürcher *et al.* (2013). The *eds16 TCSn::GFP* line was obtained by crossing the *eds16* mutant (Dewdney *et al.*, 2000) to the TCSn::GFP transgenic line and screening F_2 plants for the presence of *TCSn::GFP* by selection on Murashige and Skoog (MS) plates supplemented with BASTA and for *eds16* using PCR primers that can detect the *eds16* mutation (*eds16 Fwd*, CCTGAGAGACTATTCCAAAGGAC; *eds16 Rev*, ACTCTGAAGATGGGTCACTTCC). Homozygous seeds were used in all the assays.

Plant and bacterial growth conditions for GWAS

Seeds were surface sterilized for 2 h in open 1.5 ml Eppendorf tubes in a sealed box containing chlorine gas generated from 125 ml of 10% w/v sodium hypochlorite and 3.5 ml of 37% hydrochloric acid. For stratification, sterile seeds were kept at 4 °C for 72 h in the dark. After that, seeds were put on agar plates containing MS (Duchefa Biochemie B.V., Haarlem, The Netherlands) and 0.8% agar (Becton, Dickinson and Co., Franklin Lakes, NJ, USA). The placement of the seeds was guided by a printout of a seed-planting grid schematic (Supplementary Fig. S1) placed below the plate. Each plate contained two accessions with six seeds per accession. To account for positional effects within and between the Petri dishes, we plated 12 seeds for each accession over two plates in a permutated block design. Plates were positioned in racks that oriented the plates in a vertical position to a growth chamber constantly kept at 21 °C and a 16 h light/8 h dark cycle, with a light intensity of 120 µmol m^{-2} s^{-1} during the light period. Plants were inoculated as described in the section below '*In vitro* inoculation assays'.

Image acquisition

Root images were obtained using CCD flatbed scanners (EPSON Perfection V600 Photo, Seiko Epson Co., Nagano, Japan). The BRAT (Busch-lab Root Analysis Toolchain) image acquisition tool on a standard desktop computer running Ubuntu Linux allowed the simultaneous control of the scanners (Slovak *et al.*, 2014). Scans were performed with a resolution of 1200×1200 dpi, resulting in an image size of 6000×6000 pixels (36 MP) for each of our 12×12 cm agar plates. To enhance image quality, scanning was performed in a dark room and with the scanner lid open.

Genome-wide association mapping

We measured median and mean total root length values of 430 Arabidopsis accessions after *R. solanacearum* infection using BRAT (n=2) to conduct GWA using an accelerated mixed model (EMMAX) (Kang *et al.*, 2010) followed by EMMA (Kang *et al.*, 2008) for the most significant associations among all accessions studied The GWA was performed on a cluster, with algorithms identical to those used in the GWAPP Web interface (Seren *et al.*, 2012). Single nucleotide polymorphisms (SNPs) with minor allele counts ≥10 were considered. The significance of SNP associations was determined at a 5% false discovery rate (FDR) threshold computed by the Benjamini–Hochberg–Yekutieli method (Benjamini and Hochberg, 1995).

Broad-sense heritability calculation

All individuals that were measured were used to calculate the broad-sense heritability (H^2=VG/VP), which is defined as the proportion of phenotypic variation (VP) due to genetic variation (VG) (estimated from the between-line phenotypic variance).

Gene Ontology analysis

The GO-finder website (https://go.princeton.edu/) was used for Gene Ontology (GO) analysis. Genes solely 'inferred from electronic annotation associations' were excluded from the analysis.

In vitro inoculation assays

Seeds were surface sterilized with a solution containing 30% bleach and 0.02% Triton X-100 for 10 min, washed five times with Milli-Q water, and sown (20 seeds per plate) on agar plates containing MS (Duchefa Biochemie B.V.) and 0.8% agar (Becton, Dickinson and Co.). Sown plates were stratified at 4 °C in the dark for 2 days. Plates were then transferred to chambers and grown vertically for 7 d under constant conditions of 21–22 °C, 60% humidity, and a 16 h light/8 h dark photoperiod with a light intensity of 120 µmol m^{-2} s^{-1} during the light period.

Ralstonia solanacearum GMI1000 was grown at 28 °C in solid or liquid rich B medium (0.1% yeast extract, 1% bacto pectone, and 0.1% casamino acids) (Becton, Dickinson and Company). For inoculation, *R. solanacearum* GMI1000 was collected by centrifugation (1500 rcf, 5 min) from overnight liquid cultures at 28 °C, resuspended with water, and adjusted to a final OD_{600} of 0.001 corresponding to 10^6 colony-forming units (CFU) ml^{-1}. Arabidopsis seedlings grown on plates as detailed above were inoculated with 5 µl of the bacterial solution, which was applied 1 cm above the root tip, as described previously (Digonnet *et al.*, 2012). Plates were then sealed with micropore tape (3M Deutschland GmbH, Neuss, Germany) and transferred to a controlled growth chamber at 25 °C, 60% humidity, and a 12 h light/12 h dark photoperiod with a light intensity of 120 µmol m^{-2} s^{-1} during the light period.

For the analysis of root growth inhibition and root hair formation, pictures were taken 48–72 hpi with an Olympus DP71 stereomicroscope (Olympus, Center Valley, PA, USA) at ×11.5. To analyze green fluorescent protein (GFP) root expression, roots from seedlings grown on plates were collected 48 hpi and photographed with a Leica DM6 epifluorescence microscope (Leica, Wetzlar, Germany). In order to quantify GFP fluorescence, the Leica Application Suite X (LAS X) software was used.

A 0.1 cm section of the maturation zone was selected and GFP intensity was quantified as relative units and presented as the average of all roots measured. Three independent biological replicates were performed and, for each replica, 24 (Fig. 2) or 10 (Fig. 5) roots per condition were used.

Exogenous cytokinin and salicylic acid application

For *R. solanacearum in vitro* root inoculation assays that included exogenous application of hormones, 7-day-old seedlings were transferred from MS agar plates to fresh MS agar plates supplemented with different hormone concentrations (25 nM and 50 nM kinetin; 1.5 µM and 7.5 µM SA) from Duchefa Biochemie. Roots were inoculated 24 h later as described above.

Pathogenicity assays

Ralstonia solanacearum pathogenicity tests were carried out using the soil-drench method (Monteiro *et al.*, 2012). Briefly, Arabidopsis was grown for 4 weeks in Jiffy pots (Jiffy Group, Lorain, OH, USA) in a controlled chamber at 22 °C, 60% humidity, and an 8 h light/16 h dark photoperiod. Jiffys were drilled three times with a wooden stick and immediately submerged for 30 min into a solution of overnight-grown *R. solanacearum* adjusted to OD_{600}=0.1 corresponding to 10^8 CFU ml^{-1} with distilled water (35 ml of bacterial solution per plant). Inoculated plants were transferred to trays containing a thin layer of soil drenched with the same *R. solanacearum* solution and kept in a chamber at 27 °C, 60% humidity, and 12 h light/12 h dark. Plant wilting symptoms were recorded every day and expressed according to a disease index scale (0, no wilting; 1, 25% wilted leaves; 2, 50%; 3, 75%; and 4, death) (Supplementary Fig. S5). At least 30 plants per condition were used in each assay, and at least three replicates were performed for every experiment.

Quantitative reverse transcription–PCR (RT–qPCR)

Roots were collected from *R. solanacearum*-infected or water-treated Arabidopsis plants at 0, 24, and 48 hpi. Briefly, roots from ~40 seedlings were cut and pooled. Roots were rapidly washed in water and dried before freezing in liquid nitrogen. Samples were stored at –80 °C. RNA was extracted using the Maxwell 16 LEV Plant RNA Kit (Promega, Australia) according to the manufacturer´s recommendations. RNAs were treated with DNase-free RNase (Promega, Australia) and the concentration measured with an ND-8000 Nanodrop. cDNA was synthesized from 2 µg of RNA using the High Capacity cDNA Reverse Transcription Kit (Applied Biosystems, USA) according to the manufacturer's instructions. According to the SYBR Green PCR mix instructions (Roche, Switzerland), 2.5 µl of cDNA were used in a final reaction volume of 10 µl in the LightCycler 480 System (Roche, Switzerland). Melting curves and relative quantification of target genes were determined using the software LightCycler V1.5 (Roche, Switzerland). The amplification program was set to an initial step of 10 min at 95 °C followed by 45 cycles using 95 °C for 10 s, 60 °C for 30 s, and 72 °C for 30 s. All samples were run in triplicate for each biological replicate, and the target gene was normalized to the endogenous control gene Arabidopsis tubulin β-1 chain (*At1g75780*). To visualize the data, we calculated the fold change of each biological replicate in 24 h and 48 h samples by normalizing to the ΔCt of time point 0 hpi of the mock and infected samples separately. The statistical analysis of the normalized data was performed using the 'rstatix' R package (ver. 0.6.0). To test for differences in gene expression between mock and infected samples, the normalized data were tested for normality and homogeneity of variances. If these two requirements were fulfilled, the parametric *t*-test was performed for each time point to compare between mock and infected samples. All primer sequences used were obtained from previous publications and are listed in Supplementary Table S6. qPCR analysis conforms to the Minimum Information for Publication of Quantitative Real-Time PCR Experiments (MIQE) guidelines (Bustin *et al.*, 2009).

Cytokinin analysis (LC-MS/MS)

Arabidopsis plants were grown in pots with sand for 5 weeks in a controlled chamber at 22 °C, 60% humidity, and an 8 h light/16 h dark photoperiod, with a light intensity of 120 µmol m^{-2} s^{-1} during the light period. The sand in the pots was drilled three times with a wooden stick and immediately irrigated with bacterial solution of overnight-grown *R. solanacearum* adjusted to OD_{600}=0.1 with distilled water (50 ml of bacterial solution per plant). Trays with plant pots infected were transferred to a chamber at 27 °C, 60% humidity, and 12 h light/1 2h dark. Then, at 4–7 days post-inoculation (dpi), inoculated roots were washed with distilled water and dried with filter paper. After that, the root samples were weighed and stored at –80 °C. Four biological replicates with 20 mg each were used each time (0, 4, and 7 dpi). Cytokinin levels were measured as described previously (Poitout *et al.*, 2018).

Results

Genome-wide association mapping reveals several loci associated with cytokinin metabolism in Arabidopsis roots infected with R. solanacearum

Infection of Arabidopsis roots with *R. solanacearum* GMI1000 *in vitro* results in root growth inhibition. We previously observed natural variation of this phenotype across a small population of Arabidopsis accessions (Lu *et al.*, 2018). To identify loci responsible for this natural variation, we performed a GWAS using a collection of 430 Arabidopsis accessions representative of the worldwide genetic variation of this species (Supplementary Fig. S1; Supplementary Table S1). Arabidopsis seeds were sown on agar plates following the scheme presented in Supplementary Fig. S1 to ensure randomization. After 7 d, seedlings were inoculated 1 cm over the root tip with a 5 µl droplet of a 10^6 CFU ml^{-1} suspension of *R. solanacearum* GMI1000. Images of seedlings were then acquired using scanners every day for 5 d to measure root length and to monitor the impact on root growth caused by *R. solanacearum* infection *in vitro*. Differences in root length between accessions were monitored after infection and subsequently analyzed.

To identify sequence variation in genomic regions associated with the variation of the root growth inhibition phenotype caused by the *R. solanacearum* root infection, we conducted GWA mapping using the Arabidopsis 250K SNP chip data (Horton *et al.*, 2012) with a mixed model correcting for population structure (Seren *et al.*, 2012) and the root growth data described in Supplementary Table S2. Because we were interested in the root growth responses upon *R. solanacearum* root infection, we focused our analysis on root growth rates. The broad-sense heritability (H^2) of these traits ranged from 10% to 55% with an average of 36% (Supplementary Table S3). We observed 20 unique SNPs significantly associated with the root growth responses to *R. solanacearum* infection using a 5% Benjamini–Hochberg threshold (Supplementary Table

S4). The most significant of these associations (SNP 15401974, chromosome 5; *P*-value 1.64×10^{-9}; FDR 5.6×10^{-5}) was found for two root growth rate measurements: the mean of the relative root growth rate between day 2 and day 3 (Fig. 1A); and the median of the relative root growth rate between day 4 and day 5 (Fig. 1B). Because this SNP displayed the most significant *P*-value and was found in traits relating to two different days of the time course, we concluded that it might be important in explaining the root growth phenotypic variation between accessions. While this SNP is located within the 5 kb upstream region of multiple genes (*At5g38450* and *At5g38460*) (Supplementary Fig. S2), the highest level of

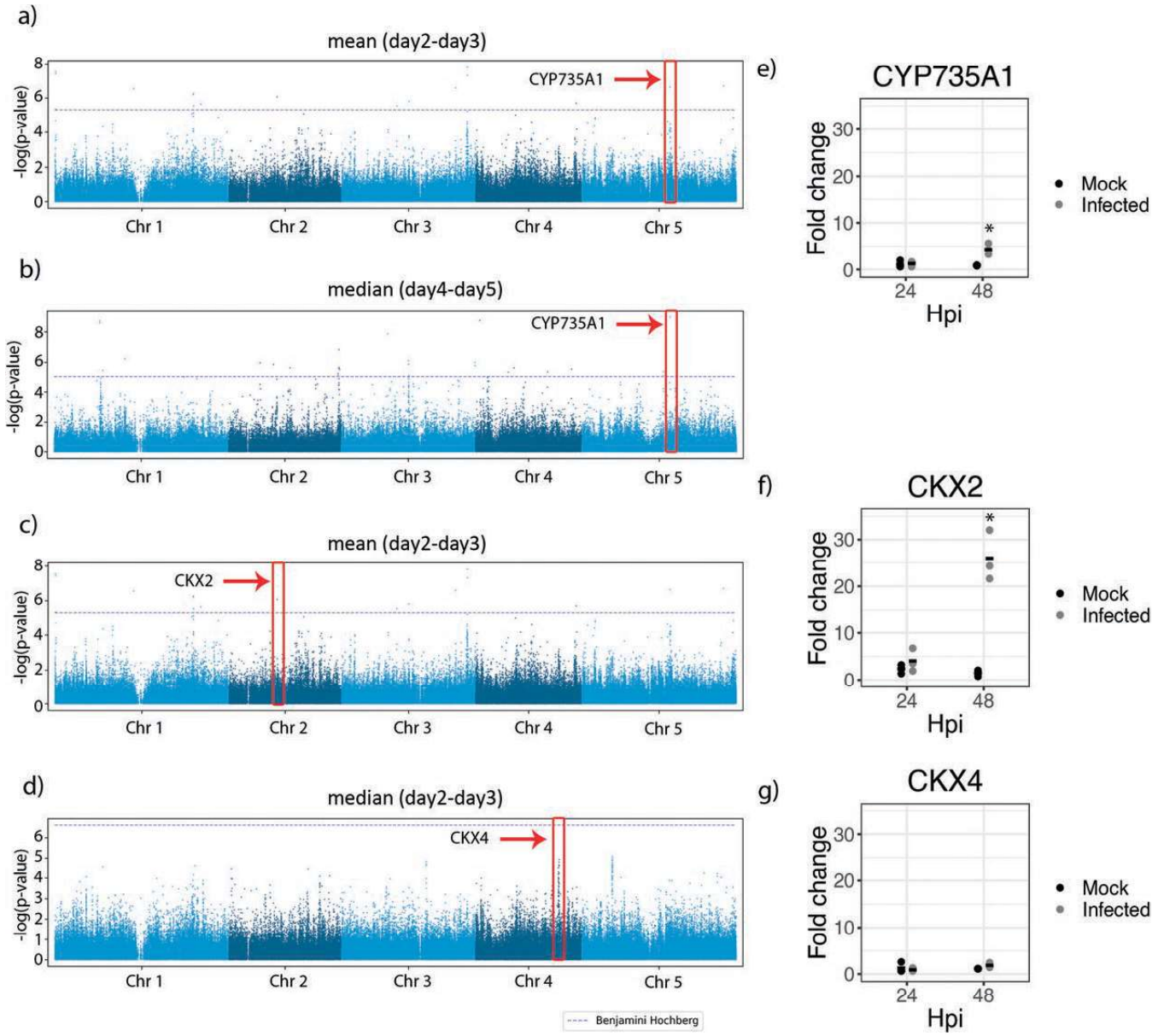

Fig. 1. GWA analysis reveals association of cytokinin metabolism genes with root growth inhibition caused by *R. solanacearum* infection of Arabidopsis roots. (A–D) Manhattan plots of GWA results for root growth traits. Different colors represent different chromosomes. The horizontal dashed lines correspond to a nominal *P*<0.05 significance threshold after Benjamini–Hochberg correction. Solid red boxes highlight the SNPs with the highest *P*-values in: (A) mean relative root growth rate between day 2 and day 3 (*P*-value 2.42E-07); (B) median root growth rate between day 4 and day 5 (*P*-value 1.64E-09); (C) mean relative root growth rate between day 2 and day 3 (*P*-value 8.89E-07); and (C) median root growth rate between day 2 and day 3 (*P*-value 6.55E-07). Fold change values of the quantitative PCR analysis of (E) *CYP735A1*, (F) *CKX2*, and (G) *CKX4* using *TUBULIN* as control. Asterisks indicate statistically significant differences in a paired Student's *t*-test (*P<0.05) between 48 hpi and normalizing by the values of the time point control (0 h hpi).

linkage disequilibrium in any gene of this region with the top SNP can be observed for an SNP in the *At5g38450* gene (Pearson coefficient of correlation r=0.39). This gene encodes a cytokinin hydroxylase (*CYP735A1*) that catalyzes the biosynthesis of the cytokinin *trans*-zeatin (Takei *et al.*, 2004). Another analysis guided our focus towards the cytokinin pathway: when conducting a GO enrichment analysis of genes in 10 kb proximity to SNPs associated with root growth rate upon infection (EMMAX P-value $<10^{-6}$) (Supplementary Table S4), we found the process cytokinin catabolism to be significantly enriched (P-value 0.00025; FDR 4.86%; Supplementary Table S5). These included two additional genes associated with cytokinin metabolism, the cytokinin oxidases *At2g19500* (*CKX2*) and *AT4G29740* (*CKX4*). *CKX2* is upstream of an SNP significantly associated with mean relative root growth rate between day 2 and day 3 (SNP 8436350; chromosome 2; P-value 8.89×10^{-7}; FDR 0.015) (Fig. 1C) and *CKX4* is upstream of an SNP marginally associated with median root growth rate between day 2 and day 3 (SNP 14577216; chromosome 4; P-value 6.55×10^{-7}; FDR 0.101) (Fig. 1D). Both genes code for proteins that catalyze the degradation of cytokinins (Mok and Mok, 2001).

Next, we analyzed the level of expression of *CYP735A1*, *CKX2*, and *CKX4* in Arabidopsis Col-0 roots. This ecotype was selected for further analysis because it has been widely used for pathogenicity assays using *R. solanacearum*, many genetic resources are available, and it is susceptible to the widely available GMI1000 strain, with a clearly observable root inhibition phenotype that appears at early stages of infection (Lu *et al.*, 2018; Supplementary Fig. S3). Quantitative PCR was used to compare plants infected with *R. solanacearum* and mock-treated plants at 0, 24, and 48 h post-treatment. *Ralstonia solanacearum* infection consistently induced expression of two of these three genes (*CYP735A1* and *CKX2*) at 48 hpi (Fig. 1E–G), indicating a potential involvement of cytokinin signaling in plant root defenses against this bacterial pathogen.

Early R. solanacearum *infection induces cytokinin signaling in Arabidopsis roots.*

Next, we analyzed whether *R. solanacearum* infection resulted in an increase of cytokinin content in Arabidopsis Col-0 roots. For this, we measured the levels the cytokinins *trans*-zeatin, *cis*-zeatin, and isopentenyladenine, as well as total cytokinins using LC-MS/MS. We could observe a significant increase in *trans*- and *cis*-zeatin, as well as total cytokinins after infection (Fig. 2A–D). We could only detect significant increases at later stages of infection (4 and 7 dpi), probably due to the sensitivity constraints of the measurement method.

In order to more specifically investigate the early effects of *R. solanacearum* infection on root cytokinin signaling, we took advantage of a more sensitive approach by analyzing expression of the synthetic Arabidopsis cytokinin reporter *TWO COMPONENT SIGNALING SENSOR* new (*TCSn*) fused to GFP (*TCSn::GFP*) (Zürcher *et al.*, 2013). Arabidopsis seedlings stably expressing *TCSn::GFP* were grown vertically on MS medium during 7 d and then roots were inoculated with *R. solanacearum* (see the Materials and methods). Infection resulted in a strong induction of *GFP* expression driven by the cytokinin signaling reporter *TCSn* in the vasculature of the root maturation zone (Fig. 2B, C). The intensity of the *GFP* induction caused by *R. solanacearum* infection at 48 hpi was four times higher than in the water control, which clearly indicated that cytokinin signaling is engaged in root responses to *R. solanacearum* invasion (Fig. 2D).

Plants affected in cytokinin biosynthesis and perception display enhanced susceptibility towards R. solanacearum

If cytokinin levels and cytokinin signaling are important for root defense responses against *R. solanacearum*, it would be expected that impairment of cytokinin biosynthesis results in enhanced susceptibility to the pathogen. To address this question, we performed pathogenicity assays on knockout mutants of the cytokinin biosynthetic enzymes CYP735A1 and CYP735A2, which do not display any apparent phenotype (Kiba *et al.*, 2013). For this, 4-week-old Arabidopsis plants were inoculated with *R. solanacearum* GMI1000 by soil drenching, and symptoms were evaluated over time following a disease index scale (Lu *et al.*, 2018). Both *cyp735a1* and *cyp735a2* showed earlier wilting disease symptoms and were dramatically more susceptible to *R. solanacearum* than wild-type plants (Fig. 3A). This clearly indicates that cytokinin biosynthesis is involved in defense responses against *R. solanacearum*.

Based on this, we hypothesized that cytokinin perception would be equally important for immune responses against *R. solanacearum*. To test this idea, we performed pathogenicity assays on knockout mutants of the sensor histidine kinases AHK2, AHK3, and CRE1/AHK4, which act as cytokinin receptors (Ueguchi *et al.*, 2001; Higuchi *et al.*, 2004). All three cytokinin receptor mutants *ahk2*, *ahk3*, and *cre1/ahk4*, which grow normally on soil (Ueguchi *et al.*, 2001; Higuchi *et al.*, 2004), displayed enhanced susceptibility to *R. solanacearum* infection (Fig. 3B), indicating that perception of cytokinin is an important component of defense responses during *R solanacearum* infection.

Exogenous cytokinin application partially reverts R. solanacearum*-induced early root phenotypes*

Our next goal was to determine whether exogenous cytokinin application could counteract the effects caused by *R. solanacearum* infection using the *in vitro* early root phenotypes as a measurable output (root growth inhibition and root hair production) (Lu *et al.*, 2018). For this, 7-day-old seedlings grown *in vitro* were transferred to fresh MS medium supplemented with different concentrations of the natural

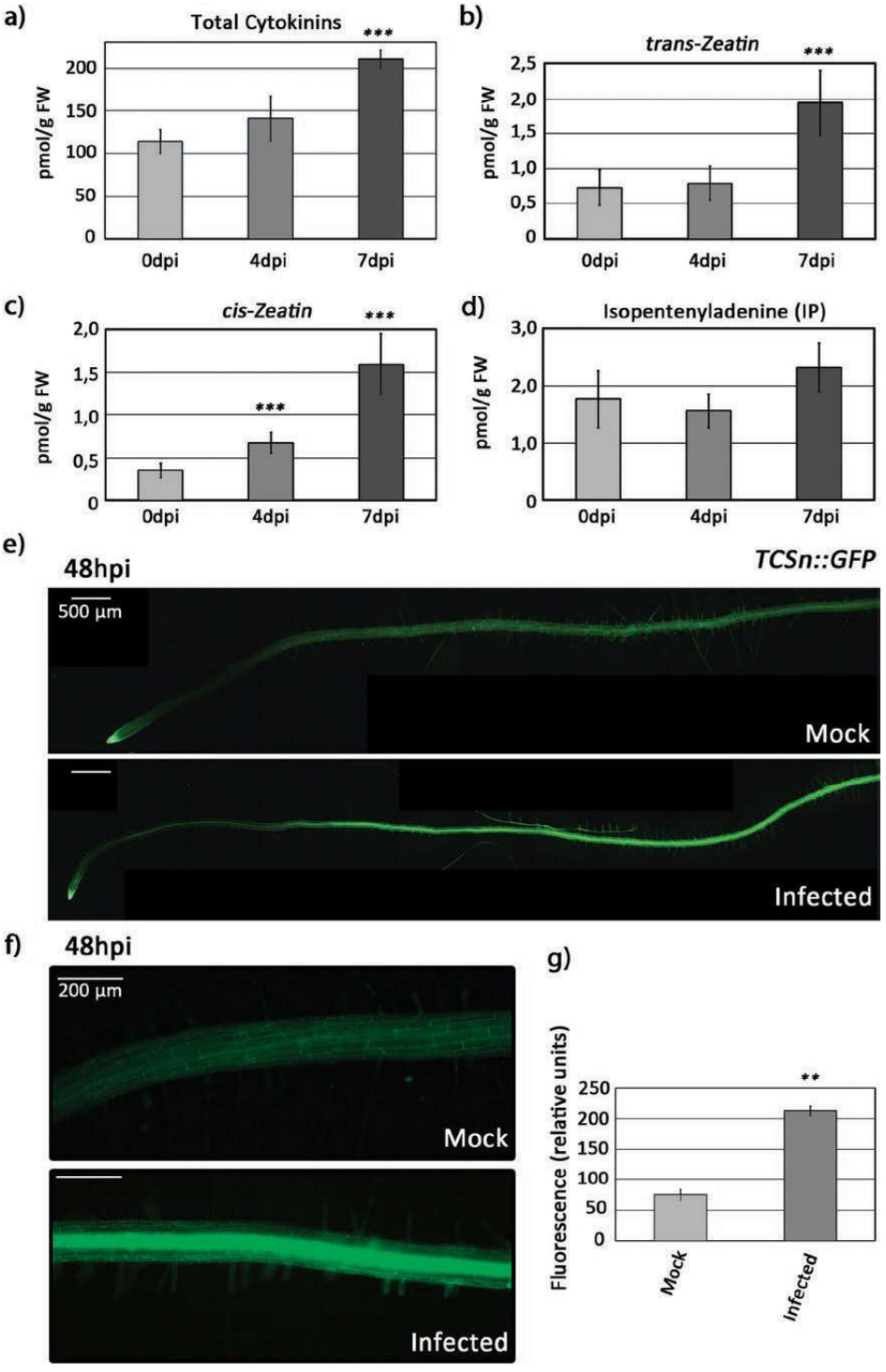

Fig. 2. Early *R. solanacearum* infection induces cytokinin signaling in Arabidopsis Col-0 roots. Four-week-old Col-0 plants were inoculated with *R. solanacearum*, and (A) total cytokinin, (B) *trans*-zeatin, (C) *cis*-zeatin, and (D) isopentenyladenine concentrations were analyzed in inoculated root tissues at the indicated times (0, 4, and 7 dpi) by LC-MS/MS using four biological replicates. Error bars correspond to SEs. Asterisks indicate statistically significant differences between 4 and 7 dpi and the control (0 dpi) in a paired Student's *t*-test (***P <0.001). (E–G) Six-day-old seedlings stably expressing the cytokinin signaling marker *TCSn::GFP* were inoculated with *R. solanacearum* or water, and roots at 48 hpi were observed under an epifluorescence microscope. *TCSn::GFP* signal in (E) whole roots and (F) the root maturation zone. (G) Quantification of the fluorescence intensity on the maturation zone (F) corresponds to the average GFP intensity from 24 individual roots per condition, calculated using the LAS X software. The experiment was repeated three times with similar results. Error bars correspond to SEs. Asterisks indicate statistically significant differences between 48 hpi and the control (0 hpi) in a paired Student's *t*-test (**P<0.01).

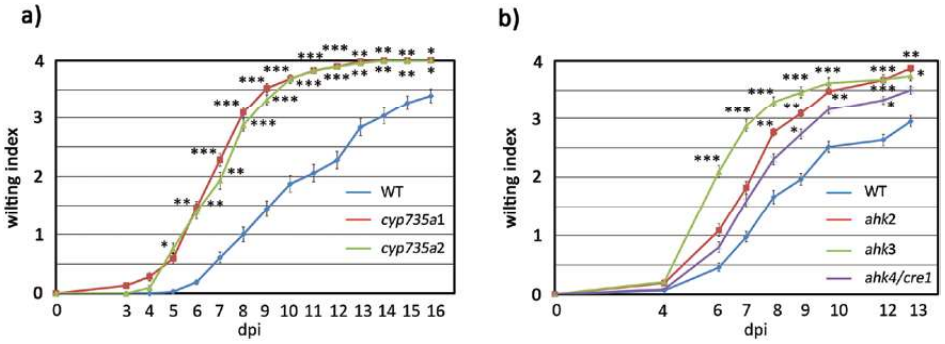

Fig. 3. Cytokinin biosynthesis and perception are important for the plant response against *R. solanacearum* root infection. Four-week-old plants were soil-drench inoculated with *R. solanacearum* and symptoms were measured over time using a disease index on a scale of 1 to 4 (0=no wilting, 1=25% wilted leaves, 2=50%, 3=75%, and 4=death). (A) Wild-type Col-0 and *trans*-zeatin biosynthesis mutants *cyp735a1* and *cyp735a2*. (B) Wild-type Col-0 and cytokinin sensor histidine kinase mutant genes (*ahk2*, *ahk3*, and *ahk4/cre1*). Each experiment was repeated at least three times obtaining similar results, using 24 plants per experiment. Error bars correspond to SEs. Asterisks indicate statistically significant differences between the wild type and different mutant lines in a paired Student's *t*-test (**P*<0.05, ***P*<0.01, ****P*<0.001).

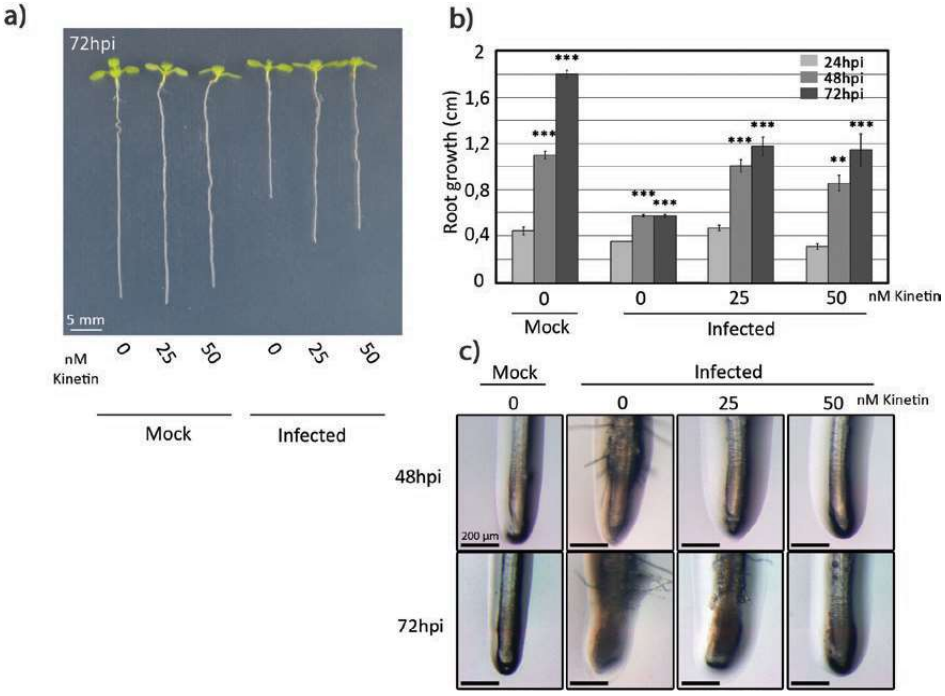

Fig. 4. Exogenous cytokinin application partially reverts *R. solanacearum*-induced early root phenotypes. Seven-day-old Col-0 seedlings were grown for 24 h in MS medium supplemented with kinetin (0, 25, and 50 nM) and were inoculated with *R. solanacearum* or water. (A) An image of representative plants was obtained using a stereoscope 72 h after infection or mock treatment. (B) Root growth was measured at the indicated time points. (C) Images of representative roots were obtained using a stereoscope at the indicated time points after infection. Error bars correspond to SEs. Asterisks indicate statistically significant differences between 24, 48, and 72 hpi in a paired Student's *t*-test (***P*<0.01, ****P*<0.001).

cytokinin kinetin (0, 25, and 50 nM). After 24 h, roots were pin-inoculated with *R. solanacearum* 1 cm above the root tip, and root growth inhibition and root hair production were monitored over time. Interestingly, kinetin supplementation (both 25 nM and 50 nM concentrations) resulted in partial reversion of the root growth inhibition phenotype caused by *R. solanacearum in vitro* (Fig. 4A, B). Whereas untreated inoculated seedlings stopped growing at 24 hpi, kinetin-treated inoculated seedlings kept growing, although to a lesser extent than non-infected roots. In addition, root hair production resulting from *R. solanacearum* infection was also inhibited by the kinetin pre-treatment (Fig. 4C). This effect was more pronounced when using a higher kinetin dose (50 mM), where no root hairs were observed. In contrast, the lower dose resulted in delayed but visible root hair production. We can thus conclude that kinetin pre-treatment at concentrations between 25 nM

and 50 nM can alleviate the early root *in vitro* phenotypes caused by *R. solanacearum* infection, without causing toxicity to the plants. This indicates that cytokinin contributes to the onset of early responses that take place upon *R. solanacearum* infection in the root.

Salicylic acid contributes to cytokinin signaling in Arabidopsis roots in response to R. solanacearum *infection*

A crosstalk between cytokinins and SA has been previously shown to regulate plant defenses against pathogens infecting leaves, such as *Pseudomonas syringae* (Choi *et al.*, 2010), *Hyalopenospora arabidopsidis* (Argueso *et al.*, 2012), *Botrytis cinerea*, and *Oidium neolycopersici* (Gupta *et al.*, 2020). However, whether a crosstalk between these hormones in root defenses takes place has not been determined. Previous *R. solanacearum* pathogenicity tests have not detected differences in susceptibility between wild-type and SA-deficient plants (*sid2* mutant or *NahG* transgenic lines, carrying an SA-degrading enzyme) (Hirsch *et al.*, 2002; Hernández-Blanco *et al.*, 2007; Hanemian *et al.*, 2016). However, exogenously applied SA had a clear effect on the root phenotypes induced by *R. solanacearum* infection *in vitro*. Seven-day-old seedlings were transferred for 24 h to MS medium supplemented with different SA concentrations (0, 1, 5, and 7.5 μM). We observed that SA concentrations >1 μM (5 μM and 7.5 μM) caused root growth inhibition of up to 50% of untreated seedlings (Supplementary Fig. S4A), as reported in previous studies (Pasternak *et al.*, 2019). Therefore, we performed *R. solanacearum in vitro* inoculation assays only on seedlings pre-treated with 1 μM SA, which did not cause any obvious effect on root growth before inoculation. Seven-day-old seedlings were transferred to MS medium supplemented with 1 μM SA and, 24 h later, roots were inoculated with *R. solanacearum* and monitored over time for root growth inhibition and root hair production. Exogenous application of 1 μM SA partially reverted the root inhibitory phenotype caused by *R. solanacerum* infection (Fig. 5A). On the other hand, 1 μM SA did not have any significant effect on root hair production (Supplementary Fig. S4b). Root hair production was partly inhibited only when higher SA concentrations (5, 7.5, and 1 μM) were exogenously supplied prior to *R. solanacearum* infection (Supplementary Fig. S2b). Considering that these concentrations affect root growth under normal conditions (Supplementary Fig. S2A), root hair inhibition may be a pleiotropic growth/development phenotype derived from SA toxicity rather than the result of SA modulation of defense responses to *R. solanacearum*.

To ascertain whether SA contributes to the cytokinin signaling involved in the response of Arabidopsis Col-0 roots to *R. solanacearum* root infection, we tested if impairing SA signaling would result in a decrease of cyokinin signaling outputs. For this, we quantified expression of *TCSn::GFP* in transgenic lines in a wild-type or an *eds16* mutant background, which is impaired in SA biosynthesis upon pathogen challenge (Dewdney *et al.*, 2000). *TCSn::GFP* expression after infection is reduced when SA signaling is suppressed, compared with the wild type. This can be observed at the whole-root level (Fig. 5B) and in a magnified area of the root maturation zone (Fig. 5C). Fluorescence quantification shows that in *eds16* mutant plants, *TCSn::GFP* expression is 25% lower than in a *TCSn::GFP* wild-type background (Fig. 5D). This indicates that SA signaling affects cytokinin signaling in response to *R. solanacearum* infection, pointing towards a potential cytokinin–SA crosstalk occurring in roots in response to infection with soil-borne pathogens. Further research in this area will clarify the possibility of a cytokinin–SA crosstalk during responses to pathogens in roots.

Discussion

Role of cytokinin in the interaction between R. solanacearum *and Arabidopsis*

In this study, we have taken advantage of GWAS to understand the genetic nature of the root phenotypic changes induced by *R. solanacearum* on Arabidopsis roots during early stages of infection. GWAS has been previously used to understand the basis of resistance against *R. solanacearum* in Arabidopsis under different temperatures and inoculation conditions (Aoun *et al.*, 2017). The study by Aoun and colleagues used wilt disease index rates over time as a trait to underscore temperature-dependent genetic diversity. At lower temperatures (27 °C) the main resistance quantitative trait locus (QTL) identified was RPS4/RRS1-R, a plant immune receptor pair with a very well-known role in resistance of Arabidopsis to *R. solanacearum* (Deslandes *et al.*, 2002; Le Roux *et al.*, 2015; Sarris *et al.*, 2015). In addition to that, this study revealed a new potential susceptibility gene at higher temperatures (30 °C), strictosidine synthase-like 4 (SSL4), which encodes a protein with structural similarities to animal proteins involved in immunity (Aoun *et al.*, 2017). This study highlights the power of GWAS in revealing new potential sources of resistance to be engineered into crops.

Our study focuses on the same Arabidopsis–*R. solanacearum* pathosystem but from a different angle. At the very early stages of infection (2–3 dpi), *R. solanacearum* infection results in quick root growth inhibition, root hair formation, and root meristem cell death, which can be easily observed and screened in *in vitro* inoculation assays. We detected natural variation associated with these phenotypes among a small subset of accessions representative of Arabidopsis diversity (Lu *et al.*, 2018). Based on that observation and on the fact that the initial stages of plant colonization by *R. solanacearum* are poorly understood, despite being important for establishment of the bacteria inside the plant, we took advantage of GWAS to analyze the genetic diversity associated with one of these

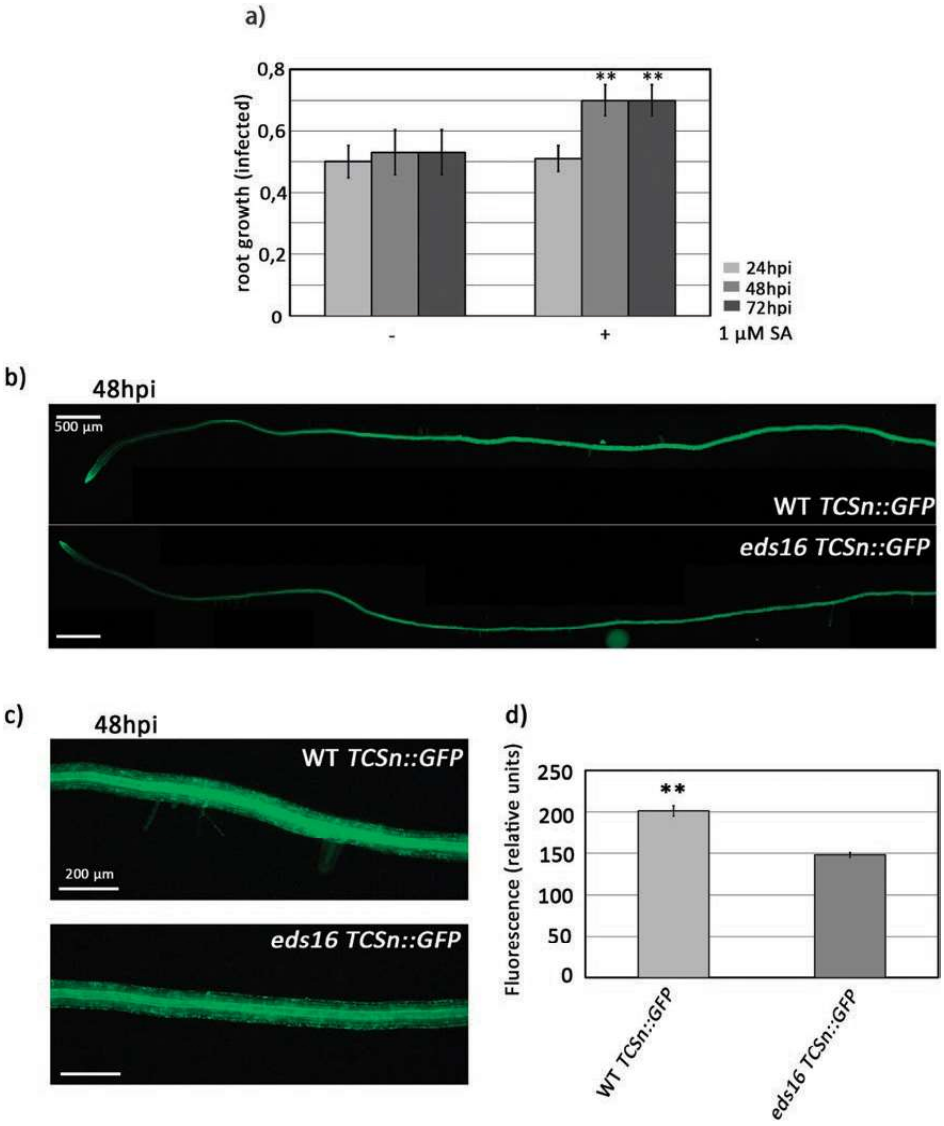

Fig. 5. SA contributes to cytokinin signaling in roots in response to *R. solanacearum* infection. (A) Seven-day-old Col-0 wild-type seedlings were grown for 24 h in MS medium supplemented with SA (0 µM and 1 µM) and were then inoculated with *R. solanacearum*. Root growth was measured. Error bars correspond to SEs. Asterisks indicate statistically significant differences between 24, 48, and 72 hpi in a paired Student's *t*-test (**P<0.01). (B–D) Six-day-old seedlings stably expressing the cytokinin signaling marker *TCSn::GFP* in the Col-0 and *eds16* background were inoculated with *R. solanacearum*, and at 48 hpi roots were observed under an epifluorescence microscope. *TCSn::GFP* signal in (B) whole roots and (C) the root maturation zone. This experiment was performed twice using 10 plants per genotype in each experiment. (D) Quantification of the fluorescence intensity on the maturation zone (C) corresponds to the average GFP intensity from 10 individual roots per condition calculated using the LAS X software. The experiment was repeated three times with similar results. Error bars correspond to the SE. Asterisks indicate statistically significant differences between 48 hpi and the control (0 hpi) in a paired Student's *t*-test (**P<0.01).

traits: root growth inhibition. Root hair formation and root meristem cell death were not included in GWAS because the technology at hand did not allow precise measurement of these traits.

Using GWAS, we screened root growth inhibition at different time points after infection on a large number of Arabidopsis accessions and focused on three candidate loci in the close proximity of SNPs that are significantly associated with this phenotype (Fig. 1A–C). These three genes are involved in the metabolism of cytokinin: *CYP735A1* in biosynthesis (Takei *et al.*, 2004), and *CKX2* and *CKX4* in cytokinin degradation (Mok and Mok, 2001). Gene expression analysis by qPCR showed that the expression of these genes in Col-0 roots was consistently induced by *R. solanacearum* at 48 hpi (Fig. 1E, F). Although the genes involved in cytokinin degradation, *CKX2* and *CKX4*, have not been investigated further in this work, they might participate in modulating the increased cytokinin levels in response to *R. solanacearum* infection.

Our data are in line with previous data underscoring a potential role for cytokinins in plant defense against *R. solanacearum*. RNA sequencing results show induction of genes involved in cytokinin synthesis (*CYP735A2*, *LOG2*, and *LOG6*), degradation (*CKX2*, *CKX3*, and *CKX5*), and response regulation (*ARR3*, *ARR4*, *ARR5*, *ARR7*, and *ARR16*) in Arabidopsis Col-0 roots at early time points after *R. solanacearum* infection (Zhao *et al.*, 2019). Moreover, genes controlling cytokinin metabolism (*LOG* and *CKX*), signaling (*ARR* genes). and perception (*CRE1*) have been shown to be differentially expressed in roots of the susceptible A17 *Medicago truncatula* genotype after infection with *R. solanacearum* (Moreau *et al.*, 2014). Importantly, Arabidopsis plants deficient in ARR6 show altered cell wall composition and are more susceptible to infection with *R. solanacearum* (Bacete *et al.*, 2020). Interestingly, Aoun *et al.* (2017) found two cytokinin-related genes among their top SNPs obtained upon infection with *R. solanacearum* at high temperatures (30 °C): the signal receptor AHK3 and the cytokinin response factor CRF2. In agreement with this, we have found that *ahk3* knockout mutants are more susceptible to *R. solanacearum* than the wild-type control (Fig. 3B).

Coupled to these increases in cytokinin-regulated gene expression, we observed an activation of cytokinin signaling in the root 48 hpi with *R. solanacearum*, as evidenced by expression of the reporter *TCSn::GFP* (Fig. 2E–G). Together, these data indicate that *R. solanacearum* triggers cytokinin production in the root by means of induction of gene expression of cytokinin biosynthetic genes, which is accompanied by activation of cytokinin signaling; in parallel, cytokinin degradation genes are up-regulated, to ensure a timely response and a tight regulation of cytokinin levels in the plant as has been described in the literature (Rashotte *et al.*, 2003; Brenner *et al.*, 2012).

Furthermore, we could observe an increase of cytokinin levels in the root after infection (Fig. 2A–D), albeit at later stages of infection, since at early stages reliable detection was challenging. When assessing which cytokinin forms were most abundant, we could detect that *R. solanacearum* resulted in an increase in both *trans*- and *cis*-zeatin levels, whereas the levels of isopentenyladenine did not show significant changes. The fact that *trans*-zeatin was among the most abundant forms was not surprising, since it is one of the most active forms of cytokinin in plants (Sakakibara, 2006). In contrast, *cis*-zeatin has always been regarded as an isomer with lower activity in plants. In fact, the study of *cis*-zeatin in the context of plant–pathogen interactions has only been addressed in the *Nicotiana tabacum*–*Pseudomonas syringae* pathosystem, where the exogenous addition of this isomer promotes the resistance of the plant against the pathogen (Groβkinsky *et al.*, 2011). Our data indicate that cytokinin may play a role in root defense against *R. solanacearum*, with *cis*- and *trans*-zeatin as two potentially important cytokinin forms for this defense function.

Taking advantage of the genetic resources available for Arabidopsis, we tested whether cytokinin synthesis and/or perception participated in defense against *R. solanacearum*. For this, we carried out pathogenicity tests, comparing a variety of mutants with defects in cytokinin perception (*ahk2*, *ahk3*, and *ahk4/cre1*) and biosynthesis (*cyp735a1* and *cyp735a2*). Our data clearly showed that both cytokinin synthesis and perception participate in defense against *R. solanacearum*, as defects in either pathway result in enhanced susceptibility towards the pathogen (Fig. 3).

Furthermore, application of low concentrations of the cytokinin kinetin partially reversed the phenotypes caused by *R. solanacearum* infection in Arabidopsis roots (Fig. 4). A plausible explanation could be that exogenous cytokinin application induces the expression of defense-related genes in the root, as we have shown here (Fig. 1F, G) similar to what has been previously reported for leaves (Rashotte *et al.*, 2003; Choi *et al.*, 2010; Argueso *et al.*, 2012). In fact, high doses of cytokinin were shown to induce resistance in Arabidopsis against the oomycete *H. arabidopsidis* (Argueso *et al.*, 2012), against *P. syringae* in Arabidopsis (Choi *et al.*, 2010), or even against virus replication in *Phaseolus vulgaris* (Clarke *et al.*, 1998b). In our root system, low doses of cytokinin were sufficient to partially prevent the root phenotypes caused by *R. solanacearum*. We did not use high doses of cytokinin because they have been shown to inhibit primary root (To *et al.*, 2004; Argyros *et al.*, 2008) growth.

The impact of SA on the cytokinin signaling involved in the response of Arabidopsis roots to R. solanacearum *infection*

Previous research, performed mostly in shoot tissue, showed that the role of cytokinins in plant immunity is deeply related to SA signaling, with a clear crosstalk between the two signaling pathways taking place (Choi *et al.*, 2010; Argueso *et al.*, 2012; Gupta *et al.*, 2020). Choi *et al.* demonstrated that the SA-dependent TGA3 transcription factor binds to the response regulator ARR2, which is modulated by cytokinin signaling, to generate a complex that binds to the PR1 promoter and promotes defense against *P. syringae* (Choi *et al.*, 2010). Also, it has been shown that cytokinin regulates plant immunity against the oomycete *H. arabidopsidis* through the elevation of defense responses that are dependent on SA (Argueso *et al.*, 2012).

Here, we addressed whether SA had any impact on cytokinin signaling induced as part of the defense responses against root-invading pathogens and root immunity. Although the SA-deficient plants show the same level of susceptibility to *R. solanacearum* as the wild type (Hirsch *et al.*, 2002; Hernández-Blanco *et al.*, 2007; Hanemian *et al.*, 2016), previous reports indicate that SA may participate in defense against this pathogen. For instance, RRS1-R-mediated defense in Arabidopsis ecotype Niederzenz-1 is orchestrated by SA (Deslandes *et al.*, 2002). Additionally, SA partly contributes to the enhanced tolerance to *R. solanacearum* observed in the Arabidopsis mutant *wat1* (*Walls are Thin1*) (Denancé *et al.*, 2013). Further, SA

participates in defense of other plant species to *R. solanacearum*, such as in tomato-resistant varieties Hawaii 7996 and CRA 66 (Baichoo and Jaufeerally-Fakim, 2016), and in tobacco (Lowe-Power *et al.*, 2016; Liu *et al.*, 2017).

It has been previously reported that treatments with SA or its analog BTH [benzo(1,2,3)thiadiazole-7-carbothioic acid *S*-methyl ester] are potent activators of plant defenses against various pathogens both in leaves (Achuo *et al.*, 2002; Herman *et al.*, 2008; War *et al.*, 2011; Azami-Sardooei *et al.*, 2013; Bektas and Eulgem, 2015; Kouzai *et al.*, 2018) and in roots (Attard *et al.*, 2010; Chuberre *et al.*, 2018). We found that exogenous SA application results in a partial reversion of the *in vitro* root phenotypes caused by *R. solanacearum* infection (Fig. 5A), similar to that we observed after cytokinin treatment (Fig. 4A, B). Our results indicate that SA might also contribute to root defenses against *R. solanacearum* at early stages of infection.

Although evidence is still limited, our results point towards the existence of an SA–cytokinins crosstalk in Arabidopsis roots after infection, since *R. solanacearum*-triggered expression of the cytokinin marker *TCSn::GFP* is significantly reduced by SA depletion in the *eds16* mutant when compared with wild-type plants (Fig. 5B–D). These data demonstrate that in the context of root infection, SA levels affect cytokinin signaling and, in turn, cytokinin signaling could modulate SA levels, although evidence proving the effects of cytokinin on SA signaling is still limited in this system. This indicates that cross-talk between the cytokinin and SA pathways in response to pathogens could also take place in response to *R. solanacearum* in roots and might affect defense response outcomes. Whether cytokinins, SA, and their crosstalk have a more general role in immunity against root-invading pathogens will be interesting to explore in the future.

Together, our data demonstrate that cytokinins participate in defense against *R. solanacearum* and are involved in the early root phenotypes caused by the pathogen at early stages of infection. While it is known that cytokinin plays a very important role in defense against bacteria, fungi, or viruses (Clarke *et al.*, 1998a; Pogány *et al.*, 2004; Choi *et al.*, 2010; Großkinsky *et al.*, 2011; Argueso *et al.*, 2012), our findings highlight a novel role for cytokinin in root immunity. Defenses in the root remain vastly unexplored and our study adds evidence indicating that pathogen perception in the root activates cytokinin metabolism and signaling, which modulates plant immunity contributing to plant defense.

Supplementary data

The following supplementary data are available at *JXB* online.

Fig. S1. Genome-wide association study experimental scheme.

Fig. S2. Zoom-in of SNP positions.

Fig. S3. Ecotype distribution based on root growth data after infection with *R. solanacearum*.

Fig. S4. Role of SA in *R. solanacearum* infection.

Fig. S5. Disease index scale of Arabidopsis plants after *R. solanacearum* infection.

Table S1. Ecotypes used in this study.

Table S2. Root growth data.

Table S3. Heritability rates.

Table S.4 Top SNPs.

Table S5. Gene Ontology (GO) analysis.

Table S6. Primers used for quantitative PCR.

Acknowledgements

We are grateful to Hitoshi Sakakibara (RIKEN Center, Yokohama, Japan) for *cyp735a1* and *cyp735a2*, and to Klaus Harter (Center for Plant Molecular Biology, Tübingen, Germany) for *ahk2*, *ahk3*, and *ahk4/cre1*. We thank Saul Lema and Marc Planas-Marquès for inspiring discussions on the topic. We thank Ling Zhang (Salk Institute) for the calculation of broad-sense heritability estimate, and Martí Bernardo (CRAG) for his help with data visualization and statistics. This work was supported by the Spanish Ministry of Economy and Competitiveness grant nos RyC 2014-16158, AGL2016-78002-R, and PID2019-108595RB-I00/AEI/10.13039/501100011033 to NSC, and through the 'Severo Ochoa Programme for Centres of Excellence in R&D' (SEV-2015-0533). We also acknowledge financial support from the CERCA Programme/Generalitat de Catalunya, from the Austrian Academy of Sciences through the Gregor Mendel Institute (WB and SBS) and from funding for CTA and HMB by the United States Department of Agriculture (USDA) grant no. COL00781. We acknowledge support of the publication fee by the CSIC Open Access Publication Support Initiative through its Unit of Information Resources for Research (URICI).

Author contributions

AA-D designed the research, performed the research, analyzed and interpreted data, and wrote the manuscript. SBS performed the research, analyzed data, and edited the manuscript. RdP-J performed the research and analyzed data. HMB performed the research, analyzed data, and edited the manuscript. CG performed the research and analyzed data. CTA designed the research, interpreted data, and edited the manuscript. ON performed the research and analyzed data. WB designed the research, interpreted data, and edited the manuscript. MV designed the research, analyzed and interpreted data, and edited the manuscript. NSC designed the research, analyzed and interpreted data, and wrote the manuscript.

Data availability

The data that support the findings of this study are available from the corresponding author, NSC, upon reasonable request.

References

Achuo AE, Audenaert K, Meziane H, Höfte M. 2002. The SA-dependent defense pathway is active against different pathogens in tomato and tobacco. Mededelingen (Rijksuniversiteit te Gent. Fakulteit van de Landbouwkundige en Toegepaste Biologische Wetenschappen) **67**, 149–157.

Aoun N, Tauleigne L, Lonjon F, Deslandes L, Vailleau F, Roux F, Berthomé R. 2017. Quantitative disease resistance under elevated

temperature: genetic basis of new resistance mechanisms to *Ralstonia solanacearum*. Frontiers in Plant Science **8**, 1387.

Aranzana MJ, Kim S, Zhao K, *et al.* 2005. Genome-wide association mapping in Arabidopsis identifies previously known flowering time and pathogen resistance genes. PLoS Genetics **1**, e60.

Argueso CT, Ferreira FJ, Epple P, To JP, Hutchison CE, Schaller GE, Dangl JL, Kieber JJ. 2012. Two-component elements mediate interactions between cytokinin and salicylic acid in plant immunity. PLoS Genetics **8**, e1002448.

Argyros RD, Mathews DE, Chiang YH, Palmer CM, Thibault DM, Etheridge N, Argyros DA, Mason MG, Kieber JJ, Schaller GE. 2008. Type B response regulators of Arabidopsis play key roles in cytokinin signaling and plant development. The Plant Cell **20**, 2102–2116.

Attard A, Gourgues M, Callemeyn-Torre N, Keller H. 2010. The immediate activation of defense responses in Arabidopsis roots is not sufficient to prevent *Phytophthora parasitica* infection. New Phytologist **187**, 449–460.

Atwell S, Huang YS, Vilhjálmsson BJ, *et al.* 2010. Genome-wide association study of 107 phenotypes in *Arabidopsis thaliana* inbred lines. Nature **465**, 627–631.

Azami-Sardooei Z, Seifi HS, De Vleesschauwer D, Höfte M. 2013. Benzothiadiazole (BTH)-induced resistance against *Botrytis cinerea* is inversely correlated with vegetative and generative growth in bean and cucumber, but not in tomato. Australasian Plant Pathology **42**, 485–490.

Babosha AV. 2009. Regulation of resistance and susceptibility in wheat–powdery mildew pathosystem with exogenous cytokinins. Journal of Plant Physiology **166**, 1892–1903.

Bacete L, Mélida H, López G, Dabos P, Tremousaygue D, Denancé N, Miedes E, Bulone V, Goffner D, Molina A. 2020. Arabidopsis response regulator 6 (ARR6) modulates plant cell-wall composition and disease resistance. Molecular Plant-Microbe Interactions **33**, 767–780.

Bac-Molenaar JA, Fradin EF, Becker FF, Rienstra JA, van der Schoot J, Vreugdenhil D, Keurentjes JJ. 2015. Genome-wide association mapping of fertility reduction upon heat stress reveals developmental stage-specific QTLs in *Arabidopsis thaliana*. The Plant Cell **27**, 1857–1874.

Baichoo Z, Jaufeerally-Fakim Y. 2016. *Ralstonia solanacearum* upregulates marker genes of the salicylic acid and ethylene signaling pathways but not those of the jasmonic acid pathway in leaflets of Solanum lines during early stage of infection. European Journal of Plant Pathology **147**, 615–625.

Bektas Y, Eulgem T. 2015. Synthetic plant defense elicitors. Frontiers in Plant Science **5**, 804.

Benjamini Y, Hochberg Y. 1995. Controlling the false discovery rate: a practical and powerful approach to multiple testing. Journal of the Royal Statistical Society: Series B (Methodological) **57**, 289–300.

Brenner WG, Ramireddy E, Heyl A, Schmülling T. 2012. Gene regulation by cytokinin in Arabidopsis. Frontiers in Plant Science **3**, 8.

Bustin SA, Benes V, Garson JA, *et al.* 2009. The MIQE guidelines: minimum information for publication of quantitative real-time PCR experiments. Clinical Chemistry **55**, 611–622.

Caesar K, Thamm AM, Witthöft J, Elgass K, Huppenberger P, Grefen C, Horak J, Harter K. 2011. Evidence for the localization of the Arabidopsis cytokinin receptors AHK3 and AHK4 in the endoplasmic reticulum. Journal of Experimental Botany **62**, 5571–5580.

Choi J, Huh SU, Kojima M, Sakakibara H, Paek KH, Hwang I. 2010. The cytokinin-activated transcription factor ARR2 promotes plant immunity via TGA3/NPR1-dependent salicylic acid signaling in Arabidopsis. Developmental Cell **19**, 284–295.

Chuberre C, Plancot B, Driouich A, Moore JP, Bardor M, Gügi B, Vicré M. 2018. Plant immunity is compartmentalized and specialized in roots. Frontiers in Plant Science **9**, 1692.

Clarke SF, Burritt DJ, Jameson PE, Guy PL. 1998*a*. Influence of plant hormones on virus replication and pathogenesis-related proteins in *Phaseolus vulgaris* L. infected with white clover mosaic potexvirus. Physiological and Molecular Plant Pathology **53**, 195–207.

Clarke SF, Burritt, DJ, McKenzie MJ, Jameson PE, Guy PL. 1998*b*. Influence of white clover mosaic potexvirus infection on the endogenous cytokinin content of bean. Plant Physiology **120**, 547–552.

Coll NS, Valls M. 2013. Current knowledge on the *Ralstonia solanacearum* type III secretion system. Microbial Biotechnology **6**, 614–620.

Corwin JA, Copeland D, Feusier J, Subedy A, Eshbaugh R, Palmer C, Maloof J, Kliebenstein DJ. 2016. The quantitative basis of the Arabidopsis innate immune system to endemic pathogens depends on pathogen genetics. PLoS Genetics **12**, e1005789.

Denancé N, Ranocha P, Oria N, *et al.* 2013. Arabidopsis *wat1* (*walls are thin1*)-mediated resistance to the bacterial vascular pathogen, *Ralstonia solanacearum*, is accompanied by cross-regulation of salicylic acid and tryptophan metabolism. The Plant Journal **73**, 225–239.

Deslandes L, Olivier J, Theulieres F, Hirsch J, Feng DX, Bittner-Eddy P, Beynon J, Marco Y. 2002. Resistance to *Ralstonia solanacearum* in *Arabidopsis thaliana* is conferred by the recessive RRS1-R gene, a member of a novel family of resistance genes. Proceedings of the National Academy of Sciences, USA **99**, 2404–2409.

Dewdney J, Reuber TL, Wildermuth MC, Devoto A, Cui J, Stutius LM, Drummond EP, Ausubel FM. 2000. Three unique mutants of Arabidopsis identify *eds* loci required for limiting growth of a biotrophic fungal pathogen. The Plant Journal **24**, 205–218.

Digonnet C, Martinez Y, Denance N, Chasseray M, Dabos P, Ranocha P, Marco Y, Jauneau A, Goffner D. 2012. Deciphering the route of *Ralstonia solanacearum* colonization in *Arabidopsis thaliana* roots during a compatible interaction: focus at the plant cell wall. Planta **236**, 1419–1431.

Großkinsky DK, Novak O, Roitsch T, *et al.* 2011. Cytokinins mediate resistance against *Pseudomonas syringae* in tobacco through increased antimicrobial phytoalexin synthesis independent of salicylic acid signaling. Plant Physiology **157**, 815–830.

Gupta R, Pizarro L, Leibman-Markus M, Marash I, Bar M. 2020. Cytokinin response induces immunity and fungal pathogen resistance, and modulates trafficking of the PRR LeEIX2 in tomato. Molecular Plant Pathology **21**, 1287–1306.

Hanemian M, Barlet X, Sorin C, *et al*. 2016. Arabidopsis CLAVATA1 and CLAVATA2 receptors contribute to *Ralstonia solanacearum* pathogenicity through a miR169-dependent pathway. New Phytologist **211**, 502–515.

Hayward AC. 1991. Biology and epidemiology of bacterial wilt caused by *Pseudomonas solanacearum*. Annual Review of Phytopathology **29**, 65–87.

Herman MA, Davidson JK, Smart CD. 2008. Induction of plant defense gene expression by plant activators and *Pseudomonas syringae* pv. tomato in greenhouse-grown tomatoes. Phytopathology **98**, 1226–1232.

Hernández-Blanco C, Feng DX, Hu J, *et al*. 2007. Impairment of cellulose synthases required for Arabidopsis secondary cell wall formation enhances disease resistance. The Plant Cell **19**, 890–903.

Higuchi M, Pischke MS, Mähönen AP, *et al.* 2004. In planta functions of the Arabidopsis cytokinin receptor family. Proceedings of the National Academy of Sciences, USA **101**, 8821–8826.

Hirsch J, Deslandes L, Feng DX, Balagué C, Marco Y. 2002. Delayed symptom development in *ein2-1*, an arabidopsis ethylene-insensitive mutant, in response to bacterial wilt caused by *Ralstonia solanacearum*. Phytopathology **92**, 1142–1148.

Horton MW, Hancock AM, Huang YS, *et al.* 2012. Genome-wide patterns of genetic variation in worldwide *Arabidopsis thaliana* accessions from the RegMap panel. Nature Genetics **44**, 212–216.

Huard-Chauveau C, Perchepied L, Debieu M, Rivas S, Kroj T, Kars I, Bergelson J, Roux F, Roby D. 2013. An atypical kinase under balancing selection confers broad-spectrum disease resistance in Arabidopsis. PLoS Genetics **9**, e1003766.

Iakovidis M, Teixeira PJ, Exposito-Alonso M, *et al.* 2016. Effector-triggered immune response in *Arabidopsis thaliana* is a quantitative trait. Genetics **204**, 337–353.

Kalladan R, Lasky JR, Chang TZ, Sharma S, Juenger TE, Verslues PE. 2017. Natural variation identifies genes affecting drought-induced abscisic acid accumulation in *Arabidopsis thaliana*. Proceedings of the National Academy of Sciences, USA **114**, 11536–11541.

Kang HM, Sul JH, Service SK, Zaitlen NA, Kong SY, Freimer NB, Sabatti C, Eskin E. 2010. Variance component model to account for

sample structure in genome-wide association studies. Nature Genetics **42**, 348–354.

Kang HM, Zaitlen NA, Wade CM, Kirby A, Heckerman D, Daly MJ, Eskin E. 2008. Efficient control of population structure in model organism association mapping. Genetics **178**, 1709–1723.

Kiba T, Takei K, Kojima M, Sakakibara H. 2013. Side-chain modification of cytokinins controls shoot growth in Arabidopsis. Developmental Cell **27**, 452–461.

Kouzai Y, Noutoshi Y, Inoue K, Shimizu M, Onda Y, Mochida K. 2018. Benzothiadiazole, a plant defense inducer, negatively regulates sheath blight resistance in *Brachypodium distachyon*. Scientific Reports **8**, 17358.

Le Roux C, Huet G, Jauneau A, *et al.* 2015. A receptor pair with an integrated decoy converts pathogen disabling of transcription factors to immunity. Cell **161**, 1074–1088.

Li B, Sun L, Huang J, Göschl C, Shi W, Chory J, Busch W. 2019. GSNOR provides plant tolerance to iron toxicity via preventing iron-dependent nitrosative and oxidative cytotoxicity. Nature Communications **10**, 3896.

Liu Q, Liu Y, Tang Y, Chen J, Ding W. 2017. Overexpression of *NtWRKY50* increases resistance to *Ralstonia solanacearum* and alters salicylic acid and jasmonic acid production in tobacco. Frontiers in Plant Science **8**, 1–12.

Lowe-Power TM, Jacobs JM, Ailloud F, Fochs B, Prior P, Allen C. 2016. Degradation of the plant defense signal salicylic acid protects *Ralstonia solanacearum* from toxicity and enhances virulence on tobacco. MBio **7**, 1–12.

Lu H, Lema A S, Planas-Marquès M, Alonso-Díaz A, Valls M, Coll NS. 2018. Type III secretion-dependent and -independent phenotypes caused by *Ralstonia solanacearum* in *Arabidopsis* roots. Molecular Plant-Microbe Interactions **31**, 175–184.

Mansfield J, Genin S, Magori S, *et al.* 2012. Top 10 plant pathogenic bacteria in molecular plant pathology. Molecular Plant Pathology **13**, 614–629.

Meijón M, Satbhai SB, Tsuchimatsu T, Busch W. 2014. Genome-wide association study using cellular traits identifies a new regulator of root development in Arabidopsis. Nature Genetics **46**, 77–81.

Mok DW, Mok MC. 2001. Cytokinin metabolism and action. Annual Review of Plant Physiology and Plant Molecular Biology **52**, 89–118.

Mok MC. 1994. Cytokinins and plant development—an overview. In: Mok DWS, Mok M, eds. Cytokinins—chemistry, activity, and function. Boca Raton, FL: CRC Press, 155–166.

Monteiro F, Genin S, van Dijk I, Valls M. 2012. A luminescent reporter evidences active expression of *Ralstonia solanacearum* type III secretion system genes throughout plant infection. Microbiology (Reading) **158**, 2107–2116.

Moreau S, Fromentin J, Vailleau F, Vernié T, Huguet S, Balzergue S, Frugier F, Gamas P, Jardinaud MF. 2014. The symbiotic transcription factor MtEFD and cytokinins are positively acting in the *Medicago truncatula* and *Ralstonia solanacearum* pathogenic interaction. New Phytologist **201**, 1343–1357.

Naseem M, Philippi N, Hussain A, Wangorsch G, Ahmed N, Dandekar T. 2012. Integrated systems view on networking by hormones in Arabidopsis immunity reveals multiple crosstalk for cytokinin. The Plant Cell **24**, 1793–1814.

Pasternak T, Groot EP, Kazantsev FV, Teale W, Omelyanchuk N, Kovrizhnykh V, Palme K, Mironova VV. 2019. Salicylic acid affects root meristem patterning via auxin distribution in a concentration-dependent manner. Plant Physiology **180**, 1725–1739.

Pieterse CM, Leon-Reyes A, Van der Ent S, Van Wees SC. 2009. Networking by small-molecule hormones in plant immunity. Nature Chemical Biology **5**, 308–316.

Pieterse CMJ, Leon-Reyes A, Zamioudis C, Van Wees SCM, Van der Does D. 2012. Hormonal modulation of plant immunity. Annual Review of Cell and Developmental Biology **28**, 489–521.

Planas-Marquès M, Kressin JP, Kashyap A, Panthee DR, Louws FJ, Coll NS, Valls M. 2020. Four bottlenecks restrict colonization and invasion by the pathogen *Ralstonia solanacearum* in resistant tomato. Journal of Experimental Botany **71**, 2157–2171.

Pogány M, Koehl J, Heiser I, Elstner EF, Barna B. 2004. Juvenility of tobacco induced by cytokinin gene introduction decreases susceptibility to *Tobacco necrosis virus* and confers tolerance to oxidative stress. Physiological and Molecular Plant Pathology **65**, 39–47.

Poitout A, Crabos A, Petřík I, Novák O, Krouk G, Lacombe B, Ruffel S. 2018. Responses to systemic nitrogen signaling in Arabidopsis roots involve trans-zeatin in shoots. The Plant Cell **30**, 1243–1257.

Proietti S, Caarls L, Coolen S, Van Pelt JA, Van Wees SCM, Pieterse CMJ. 2018. Genome-wide association study reveals novel players in defense hormone crosstalk in Arabidopsis. Plant, Cell & Environment **41**, 2342–2356.

Rashotte AM, Carson SDB, To JPC, Kieber JJ. 2003. Expression profiling of cytokinin action in Arabidopsis. Plant Physiology **132**, 1998–2011. the author

Sa G, Mi M, He-chun Y, Ben-ye L, Guo-feng L, Kang C. 2001. Effects of *ipt* gene expression on the physiological and chemical characteristics of *Artemisia annua* L. Plant Science **160**, 691–698.

Sakakibara H. 2006. Cytokinins: activity, biosynthesis, and translocation. Annual Review of Plant Biology **57**, 431–449.

Sarris PF, Duxbury Z, Huh SU, *et al.* 2015. A plant immune receptor detects pathogen effectors that target WRKY transcription factors. Cell **161**, 1089–1100.

Satbhai SB, Setzer C, Freynschlag F, Slovak R, Kerdaffrec E, Busch W. 2017. Natural allelic variation of FRO2 modulates Arabidopsis root growth under iron deficiency. Nature Communications **8**, 15603.

Seren, Ü., Vilhjálmsson, B. J., Horton, M. W., Meng, D., Forai, P., Huang, Y. S., Nordborg, M. 2012. GWAPP: a web application for genome-wide association mapping in Arabidopsis. The Plant Cell **24**, 4793–4805.

Shigenaga AM, Argueso CT. 2016. No hormone to rule them all: interactions of plant hormones during the responses of plants to pathogens. Seminars in Cell & Developmental Biology **56**, 174–189.

Slovak R, Göschl C, Su X, Shimotani K, Shiina T, Busch W. 2014. A scalable open-source pipeline for large-scale root phenotyping of Arabidopsis. The Plant Cell **26**, 2390–2403.

Takei K, Yamaya T, Sakakibara H. 2004. Arabidopsis *CYP735A1* and *CYP735A2* encode cytokinin hydroxylases that catalyse the biosynthesis of *trans*-zeatin. Journal of Biological Chemistry **279**, 41866–41872.

Thoen MP, Davila Olivas NH, Kloth KJ, *et al.* 2017. Genetic architecture of plant stress resistance: multi-trait genome-wide association mapping. New Phytologist **213**, 1346–1362.

To JP, Haberer G, Ferreira FJ, Deruère J, Mason MG, Schaller GE, Alonso JM, Ecker JR, Kieber JJ. 2004. Type-A Arabidopsis response regulators are partially redundant negative regulators of cytokinin signaling. The Plant Cell **16**, 658–671.

Ueguchi C, Koizumi H, Suzuki T, Mizuno T. 2001. Novel family of sensor histidine kinase genes in *Arabidopsis thaliana.* Plant & Cell Physiology **42**, 231–235.

War, A. R., Paulraj, M. G., War, M. Y., & Ignacimuthu, S. 2011. Role of salicylic acid in induction of plant defense system in chickpea (*Cicer arietinum*). Plant Signaling and Behavior **6**, 1787–1792.

Wen Z, Tan R, Yuan J, *et al.* 2014. Genome-wide association mapping of quantitative resistance to sudden death syndrome in soybean. BMC Genomics **91**, 574–581.

Wybouw B, De Rybel B. 2019. Cytokinin—a developing story. Trends in Plant Science **24**, 177–185.

Zhao C, Wang H, Lu Y, *et al.* 2019. Deep sequencing reveals early reprogramming of arabidopsis root transcriptomes upon *Ralstonia solanacearum* infection. Molecular Plant-Microbe Interactions **32**, 813–827.

Zürcher E, Tavor-Deslex D, Lituiev D, Enkerli K, Tarr PT, Müller B. 2013. A robust and sensitive synthetic sensor to monitor the transcriptional output of the cytokinin signaling network *in planta*. Plant Physiology **161**, 1066–1075.

frontiers in Plant Science

ORIGINAL RESEARCH
published: 10 November 2021
doi: 10.3389/fpls.2021.755708

The Bacterial Wilt Reservoir Host *Solanum dulcamara* Shows Resistance to *Ralstonia solanacearum* Infection

Pau Sebastià[1†], Roger de Pedro-Jové[1,2†], Benoit Daubech[1], Anurag Kashyap[1], Núria S. Coll[1] and Marc Valls[1,2]*

[1] Centre for Research in Agricultural Genomics (CSIC-IRTA-UAB-UB), Bellaterra, Spain, [2] Department of Genetics, University of Barcelona, Barcelona, Spain

Ralstonia solanacearum causes bacterial wilt, a devastating plant disease, responsible for serious losses on many crop plants. *R. solanacearum* phylotype II-B1 strains have caused important outbreaks in temperate regions, where the pathogen has been identified inside asymptomatic bittersweet (*Solanum dulcamara*) plants near rivers and in potato fields. *S. dulcamara* is a perennial species described as a reservoir host where *R. solanacearum* can overwinter, but their interaction remains uncharacterised. In this study, we have systematically analysed *R. solanacearum* infection in *S. dulcamara*, dissecting the behaviour of this plant compared with susceptible hosts such as tomato cv. Marmande, for which the interaction is well described. Compared with susceptible tomatoes, *S. dulcamara* plants (i) show delayed symptomatology and bacterial progression, (ii) restrict bacterial movement inside and between xylem vessels, (iii) limit bacterial root colonisation, and (iv) show constitutively higher lignification in the stem. Taken together, these results demonstrate that *S. dulcamara* behaves as partially resistant to bacterial wilt, a property that is enhanced at lower temperatures. This study proves that tolerance (i.e., the capacity to reduce the negative effects of infection) is not required for a wild plant to act as a reservoir host. We propose that inherent resistance (impediment to colonisation) and a perennial habit enable bittersweet plants to behave as reservoirs for *R. solanacearum*.

Keywords: bacterial wilt, *Ralstonia solanacearum*, disease resistance, reservoir host plants, vascular reinforcements, overwintering

OPEN ACCESS

Edited by:
Adi Avni,
Tel Aviv University, Israel

Reviewed by:
Guido Sessa,
Tel Aviv University, Israel
Antonio Cellini,
University of Bologna, Italy

***Correspondence:**
Marc Valls
marcvalls@ub.edu

† These authors have contributed equally to this work

Specialty section:
This article was submitted to Plant Pathogen Interactions, a section of the journal Frontiers in Plant Science

Received: *09 August 2021*
Accepted: *04 October 2021*
Published: *10 November 2021*

Citation:
Sebastià P, de Pedro-Jové R, Daubech B, Kashyap A, Coll NS and Valls M (2021) The Bacterial Wilt Reservoir Host Solanum dulcamara Shows Resistance to Ralstonia solanacearum Infection. Front. Plant Sci. 12:755708. doi: 10.3389/fpls.2021.755708

INTRODUCTION

Alternate or reservoir hosts are non-target organisms that can harbour high amounts of pathogens for long periods of time and serve as an inoculum source for further infections on the primary host (Haydon et al., 2002; Morris et al., 2009). However, the term "reservoir host" has been also applied to natural or economically unimportant hosts or to hosts where infections are always non-pathogenic (Haydon et al., 2002). In many important crop diseases, non-agricultural reservoirs have also been proposed to enhance the adaptive potential of pathogens and influence disease epidemiology (Mueller et al., 2012; Monteil et al., 2013; Thinakaran et al., 2015; McCann, 2020).

For instance, *Pseudomonas syringae* isolated from wild species was shown to potentially develop into novel crop pathovars in a few evolutionary steps (Monteil et al., 2013; Bartoli et al., 2015), and experimental evolution experiments with *Ralstonia solanacearum* demonstrated high fitness gains when this pathogen was inoculated on distant hosts (Guidot et al., 2014).

Ralstonia solanacearum is the agent causing the devastating bacterial wilt disease in over 200 plant species, including economically important crops such as potato, tomato, peanut, eggplant, and banana (Hayward, 1994; Mansfield et al., 2012; Coll and Valls, 2013). *R. solanacearum* can survive in the soil and waterways (Van Elsas et al., 2000; Álvarez et al., 2008a), from where it infects plants through the roots and colonises the xylem tissue, blocking water flow and causing plant wilting (Hayward, 1991; Schell, 2000). The disease is endemic in tropical and subtropical areas, but *R. solanacearum* phylotype II-B1 (formerly race 3 biovar 2) strains are adapted to cooler temperatures and have caused important outbreaks in temperate regions (Elphinstone, 1996; Janse et al., 2004; Champoiseau et al., 2009).

Survival and overwintering of *R. solanacearum* in temperate regions appears to rely on infection of perennial reservoir host plants because its persistence in the soil is limited (Olsson, 1976; Shamsuddin et al., 1978; Elphinstone, 1996). Bittersweet (*Solanum dulcamara*) is a common holarctic perennial weed that has been proposed to play a reservoir role in the persistence and spread of *R. solanacearum* based on several observations. Firstly, common incidences of *R. solanacearum* in *S. dulcamara* have been described along waterways (Kempenaar et al., 1998), and most disease outbreaks were related to watercourses in which infected *S. dulcamara* plants were present (Olsson, 1976; Elphinstone, 1996; Janse et al., 1998). Secondly, winter persistence of *R. solanacearum* in waterways correlated with the presence of the pathogen in *S. dulcamara* plants growing near them (Olsson, 1976; Elphinstone et al., 1998; Caruso et al., 2005). Thirdly, *R. solanacearum* was shown to colonise asymptomatically the roots and vascular tissue of *S. dulcamara* plants in the wild, and infected plants were shown to release the bacterium onto surface water *via* aquatic roots (Olsson, 1976; Elphinstone, 1996; Janse, 1996). Besides *S. dulcamara, R. solanacearum* phylotype IIB sequevar 1 strain have been found growing asymptomatically in the wild with other weeds that act as sources of inoculum to infect potato fields. These include *Solanum nigrum* (Olsson, 1976), *Solanum cinereum* (Graham and Lloyd, 1978), *Urtica dioica* in Europe (Wenneker et al., 1999), and a number of wild species from the Ugandan highlands (Tusiime et al., 1997). In China, tropical *R. solanacearum* strains were also identified in the weed *Ageratum conyzoides* L., often showing wilting symptoms (She et al., 2013).

The interactions between *R. solanacearum* and its cultivated hosts have been well-characterised, but little is known about the behaviour of this pathogen inside wild hosts. *R. solanacearum* inoculation on *S. dulcamara* in laboratory conditions has been previously reported (Wenneker et al., 1999; Álvarez et al., 2008b; Jacobs et al., 2013). A first assay screening a large number of plant species found that 66% of *S. dulcamara* plants inoculated through soil drenching became infected (Álvarez et al., 2008b). However, the authors classified this plant as tolerant to bacterial wilt because colonisation was only apparent in 25% of the plants, in which the bacterium occupied a few xylem vessels or occasionally all xylem bundles (Álvarez et al., 2008b). In another report, wilting was more apparent after soil drench inoculations, and *S. dulcamara* plants showed intermediate symptomatology compared with susceptible (Bonny Best) and resistant (Hawaii 7996) tomato plants (Jacobs et al., 2013). In a third study, all plants became infected and 97% showed symptoms when the bacterium was directly inoculated in the stem. However, symptomatology and pathogen presence was restricted to inoculated shoots, indicating slow or no spreading of the bacterium throughout the plant (Wenneker et al., 1999). In this same study, only 13–19% of the plants were infected and 9% showed symptoms when plants were soil-drench inoculated (Wenneker et al., 1999). In summary, *S. dulcamara* presents highly variable symptomatology in response to *R. solanacearum* depending on the inoculation method, although it usually shows an intermediate behaviour between a susceptible and a resistant host. The mechanisms responsible for this partial restriction of colonisation by *R. solanacearum* have not yet been described.

In this study, we have undertaken a thorough characterisation of the interaction between *R. solanacearum* and its wild host *S. dulcamara*. We describe the localisation of the pathogen during the infection process and the symptomatology on the plant at different temperatures and compare this interaction with that established on susceptible tomato (cv. Marmande) and potato (cv. Desirée) plants.

MATERIALS AND METHODS

Plant and Bacterial Materials and Growth Conditions

Bittersweet (*S. dulcamara*) plants were grown from seeds harvested from wild specimens in Vidrà (NE Catalonia, Spain). The susceptible tomato (*Solanum lycopersicum* cv. Marmande) and susceptible potato (*Solanum tuberosum* cv. Desirée) plants used in this study are commercially available.

For pot experiments, *S. dulcamara* and *S. lycopersicum* cv. Marmande seeds were surface-sterilised in 35% bleach and 0.02% Triton-X 100 for 10 min and then rinsed with sterile distilled water five times before sowing them in soil (Substrate 2, Klasmann-Deilmann GmbH) mixed with perlite and vermiculite (30:1:1) and grown under controlled conditions for 3 weeks under a long-day photoperiod (16 h light/8 h dark) and under a light intensity of 120–150 $\mu mol \cdot m^{-2} \cdot s^{-1}$ at 22°C and 60% humidity. For optimal germination, *S. dulcamara* seeds were stratified at 4°C for 2 weeks before transferring them to 22°C. *S. tuberosum* cv. Desirée potato plants were propagated *in vitro* (Puigvert et al., 2017) and 2-week old apex was sown in the same soil mixture described above and grown in the same conditions.

All infection assays were performed using the *R. solanacearum* strain UY031 (phylotype IIB, sequevar 1) isolated from potato tubers in Uruguay (Siri et al., 2011), carrying either the synthetic *luxCDABE* operon or the GFPuv gene, both under the control of the constitutive *psbA* promoter (Monteiro et al., 2012). Bacteria were routinely grown at 28–30°C in rich B medium in liquid

cultures supplemented with gentamicin (10 μg/ml) and the same medium, supplemented with 0.5% glucose and 50 mg/l of triphenyl tetrazolium chloride for growth on semi-solid agar plates (Monteiro et al., 2012).

Plant Inoculation and Pathogenicity Assays

For soil-soaking and stem inoculation assays, plants were grown for 3–4 weeks. Soil-soaking root inoculations were performed by pouring 40 ml of 10^8 colony-forming units (CFU)·ml^{-1} (OD_{600} = 0.1) of bacterial suspension on every plant pot without disturbing the roots. Infected plants were kept in a growth chamber set at 27°C (exceptionally 20°C when indicated) and scored for wilting symptoms using a scale from 0 to 4, 0 = healthy plant with no wilt, 1 = 25%, 2 = 50%, 3 = 75% of the leaves wilted, and 4 = total wilting. Disease indexes were calculated by averaging the disease score of each plant of the experiment ($n > 15$) as indicated in previous publications with *S. dulcamara*, tomato, and potato (Álvarez et al., 2008b; Siri et al., 2011; Planas-Marquès et al., 2020). Stem-inoculation assays were performed by applying a 5 μl droplet of a 10^6 CFU·ml^{-1} (OD_{600} = 0.001) bacterial solution twice with a sterile 0.3 × 13 mm needle (30GX 1/2″, BD Microlance, Becton Dickinson) to the wounds caused at the base of the petiole after removal of the first true leaf. After inoculation, plants were kept in a growth chamber set at 27°C unless otherwise specified and scored for wilting symptoms as described before (Monteiro et al., 2012).

To quantify the bacterial content inside the shoots, 2 cm sections were excised from above the taproot (soil-soaked plants) or above the inoculation point (stem-inoculated plants), weighed, and incubated for at least 30 min in a sterile 2-ml Eppendorf tube with 300 μl of sterile distilled water to let the bacterium ooze from the tissue. Luminescence was measured from the tubes containing excised tissue with a luminometer (FB 12, Berthold Detection Systems) to determine the bacterial concentrations since luminescence was proven to strongly correlate with bacterial density (Planas-Marquès et al., 2020). To measure bacterial counts in the root, plants inoculated as described were uprooted from day 1 to day 4 post-inoculation, and the roots were rinsed with distilled water. Approximately 1–2 cm of root below the tap root were cut and ground. Tissue was weighed and CFUs were counted as described above. Dilution plating of samples on rich B medium and CFU counting 24 h later was performed in some cases to verify luminescence results.

Assessment of Bacterial Colonisation

Plant colonisation by *R. solanacearum* was assessed using the luminescent and fluorescent strains described above. Plant stems inoculated with the luminescent strain were sliced using a sterile razor blade obtaining internode sections just below and above the petiole where inoculation had been carried out. One millimetre thick transversal cuts and 1 cm long longitudinal cuts were placed flat on a square plate and visualised using a live imaging system (ChemiDoc Touch Imaging System, Bio-Rad) using a 5-min exposure time with 3 × 3 sensitivity. Images were processed using Image Lab software (Bio-Rad). Soil-soak inoculated plants with the luminescent strain were photographed by placing the whole plant in a Fuji Film LAS4000 light imager system with a 15-min exposure time.

Stem-inoculated plants with the fluorescent strain were dissected as described before and photographed using binocular microscopy equipped with a UV fluorescent lamp (BP330-385 BA420 filter) and an SZX16 stereomicroscope equipped with a DP71 camera system (Olympus) using the following settings: GFP filter, 10 s exposure time, ISO 1/800. Soil-soaked plants with the fluorescent strain were photographed with a Leica DM6 microscope. Bright field or fluorescence images merging the UV channel for plant structures (blue) and the GFP channel for bacteria (green) were automatically assembled by the microscope software to obtain single images including the whole root section.

Quantification of the black signal (luminescence) or the green channel (fluorescence) in the pictures was quantified using the Fiji software (United States National Institutes of Health).

Tissue Stainings

After producing root wounds with a 1 ml pipette tip, the plants were soil-soaked with a bacterial solution of 10^7 CFU·g^{-1} (OD_{600} = 0.01). The day the plants showed an adequate disease index, the taproots were transversally sliced. Then four to five slices per plant were placed in a 1.5-ml tube with 70% ethanol for at least 7 days to remove the chlorophyll. For lignin staining, individual taproot slices were placed on a microscope slide and incubated with two drops of phloroglucinol HCl for about 1 min, then rinsed with 70% ethanol, and a cover slide was placed on top for visualisation in the upright microscope (Leica DM6) bright-field (Pomar et al., 2004). Mock-infected plants were inoculated with water. Lignin quantification was performed by selecting the vascular area in tomato and potato plants and comparing it with the same area in *S. dulcamara* plants using ImageJ software. Images were converted to a greyscale (eight-bit image) and the mean grey value was calculated.

For suberin staining, individual *S. dulcamara,* tomato cv. Marmande and potato cv. Desirée taproot slices were placed in a well containing a Sudan IV solution for 5 min and then rinsed in another well with 70% ethanol as described (Kashyap et al., 2021). Clean slices were placed on a slide and visualised with the UV filter on a Leica DM6 microscope.

Statistical Analyses

Statistical analyses were performed using Statgraphics software. All statistical tests are indicated in the respective figure legends.

RESULTS

Solanum dulcamara Shows an Enhanced Capacity to Withstand *R. solanacearum* Infection in Comparison With Tomato cv. Marmande

To analyse the symptomatology caused by *R. solanacearum* in *S. dulcamara* and compare its behaviour with that of tomato, we inoculated plants in controlled conditions using two different

methods. First, we used a more naturalistic root inoculation method by soaking the soil with a bacterial solution without causing any wounding to plants, after which the plants were kept at 27°C, and then the wilting symptoms were recorded over time. All susceptible tomato Marmande plants were completely wilted 14 days post-inoculation (dpi), while the symptoms just started to appear in *S. dulcamara* (**Figure 1A**). By 28 dpi, less than half of the *S. dulcamara* plants had completely wilted, showing a clear delay in the development of the disease with respect to tomato plants (*p-value* < 0.0001; **Figure 1A**).

The second method used was direct bacterial inoculation inside the plant stem vasculature, a more aggressive procedure that skips the first infection steps (root entry and vascular colonisation). As expected, disease progression was faster after stem inoculation and all the tomato plants were completely wilted at 8 dpi. *S. dulcamara* plants still showed a clear delay in disease progression after stem inoculation (*p-value* < 0.0001): first symptoms were apparent only by day 8, although most plants were completely wilted by 14 dpi (**Figure 1B**). Interestingly, an important proportion of *S. dulcamara* plants remained asymptomatic at the end of our experiments, especially when soil inoculation was performed. Quantification of bacterial loads in the stem over time showed an overall correlation with disease symptoms (**Figures 1C,D**). In soil-drench

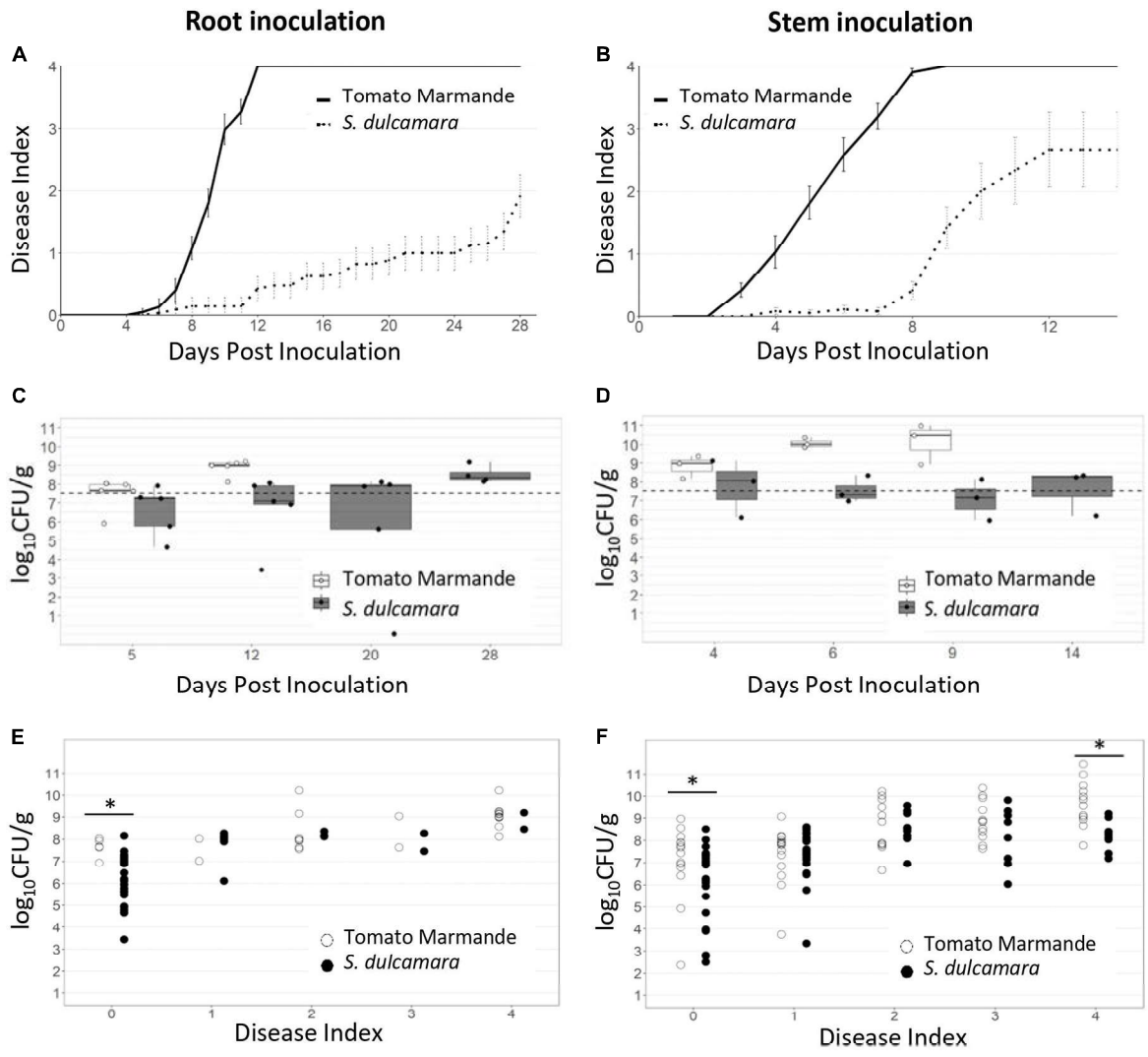

FIGURE 1 | Bacterial wilt evaluation in *S. dulcamara* and tomato cv. Marmande plants. Plants of the wild reservoir host *S. dulcamara* and tomato susceptible to bacterial wilt were root inoculated by soil soaking **(A,C,E)** or stem inoculated **(B,D,F)** with *R. solanacearum* UY031 carrying a luminescent reporter. **(A,B)** Wilting symptoms were recorded over time using a scale from 0 (no wilting) to 4 (completely wilted). *n* = 30–35 plants per plant species. **(C,D)** Bacterial concentrations in the stem at different time points from plants in panels **(A,B)**, respectively. *n* = 4–8 plants per sampling day. **(E,F)** Bacterial content in relation to wilting symptoms for each plant individual analysed of the two species. *n* = 30 plant samples analysed for each species. Bacterial counts are expressed as log CFUs·g^{-1} tissue. *indicates statistical differences (*p value* < 0.05, *T*-student significant test). The experiments in panels **(A,C)** were repeated three times with similar results. The experiment in panels **(B,D)** was repeated twice with similar results.

inoculations, when tomato plants were almost completely wilted (12 dpi), the bacterial concentrations in their stems were $\sim 10^9$ CFU·g^{-1}, significantly higher than the $\sim 10^7$ CFU·g^{-1} found in *S. dulcamara*, which only showed minor symptoms at this time point (**Figure 1C**). Similar results with bacterial concentrations were obtained in stem inoculation experiments although these plants displayed higher bacterial contents, especially at late disease stages, since structural barriers present in roots are circumvented in this inoculation method (**Figure 1D**).

To precisely determine the bacterial concentrations that the two plant species could withstand inside their tissues, we took the data from all biological replicas and plotted bacterial content in relation to wilting symptoms for each plant analysed. This representation clearly showed that, irrespective of the inoculation method, *S. dulcamara* and susceptible tomato bore similar bacterial concentrations at intermediate wilting stages (**Figures 1E,F**). However, two clear differences were observed: (i) as hinted before, at early disease stages (disease index = 1) *S. dulcamara* plants showed lower bacterial colonisation, and (ii) bacterial loads rarely exceeded 10^9 CFU·g^{-1} in *S. dulcamara*, whereas they often overcame these levels in tomato plants, leading to statistical differences when plants were completely wilted. The differences in the late disease stages were more apparent in stem inoculation experiments because this more aggressive inoculation method resulted in a higher proportion of plants showing symptoms and becoming totally wilted (disease index 4) compared with natural root inoculations by soil drenching (**Figures 1E,F**). In summary, *S. dulcamara* plants displayed delayed bacterial wilt symptom development compared with susceptible tomato plants, with most of the individuals surviving infection in the timeframe of our experiments. In addition, lower *R. solanacearum* concentrations were observed in the stems of *S. dulcamara* at early and late disease stages, suggesting delayed colonisation and restriction to bacterial growth.

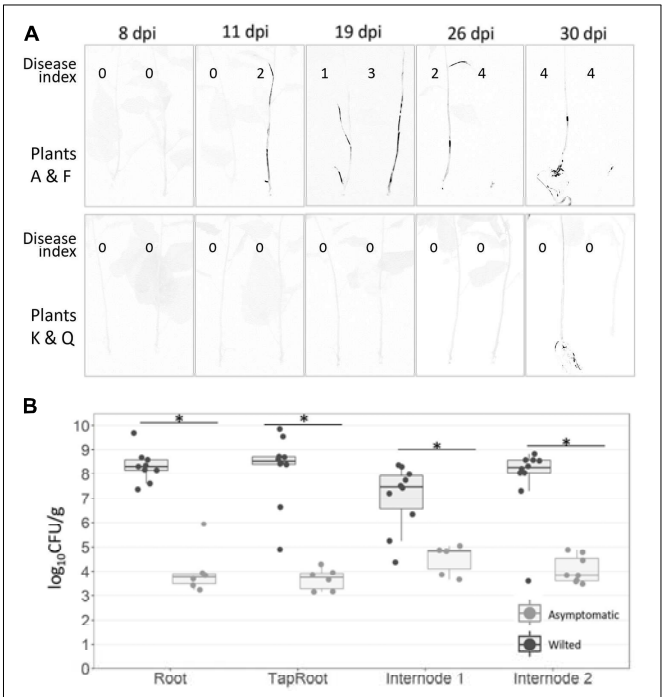

FIGURE 2 | Bacterial colonisation and multiplication in stem-inoculated *S. dulcamara* and tomato cv. Marmande plants. **(A)** Non-destructive live luminescence imaging of four representatives *S. dulcamara* plants throughout a 30-day period after root inoculation with a luminescent *R. solanacearum* strain. Two symptomatic (A & F) and two asymptomatic (K & Q) plants are shown. Luminescent bacteria are detected in darker areas. Wilting symptoms (Disease index = 0–4) are indicated next to each plant inside the images. **(B)** *R. solanacearum* concentrations measured at the root, taproot, internode 1 (2–3 cm above the inoculation point) and 2 (6–9 cm above the inoculation point) in *S. dulcamara* plants uprooted 30 days post-inoculation (dpi) with the luminescent reporter strain. The results from asymptomatic (disease index 0) and symptomatic (disease index 1–4) plants are shown separately. Bacterial counts were calculated from tissue luminescence and are expressed as log CFUs·g^{-1} tissue. *indicates statistical differences (p-value < 0.05, T-student significant test).

A High Proportion of *S. dulcamara* Plants Show Long-Lasting Latent Infections

Ralstonia solanacearum infection heterogeneity amongst different plant individuals is common. To analyse the progression of bacterial colonisation and disease symptoms in single plants over time, we took advantage of the luminescent *R. solanacearum* strain used in this work, which could be visualised non-destructively inside plant tissues (Cruz et al., 2014). Stem inoculations were used in these experiments to reduce the high stochasticity of root inoculations and to facilitate infection so that a significant proportion of plants become completely wilted. Live imaging and symptom recording of whole plants were carried out along a 30-day period, after which the plants were uprooted to visualise bacterial content in the roots. As observed before, in this experiment, half of the *S. dulcamara* plants showed symptoms, and half of them remained asymptomatic at the end of the assay (**Figure 2A** and **Supplementary Figure 1**). Bacterial colonisation paralleled the onset of disease symptoms in wilting plants (**Figure 2A** top panel) and was always undetectable in the aerial tissues of asymptomatic plants (**Figure 2A** bottom panel). Interestingly, *R. solanacearum* latent infections were detected in the most asymptomatic plants (four out of six plants **Supplementary Figure 1**), which displayed detectable luminescence in the root at 30 dpi (**Figure 2A** bottom panel and **Supplementary Figure 1**). Quantification of the black signal from the pictures in S1 showed that the area colonised by bacteria positively correlates with the disease symptoms, except in totally wilted plants where tissue collapse and drying causes bacterial death (**Supplementary Figure 2**). For a more sensitive and quantitative analysis, the bacterial contents of root and stem sections of plants uprooted at 30 dpi were calculated. The results proved that *R. solanacearum* was present in all tissues analysed from asymptomatic *S. dulcamara* plants, although bacterial concentrations were in almost all cases four orders of magnitude lower than that in symptomatic plants (**Figure 2B**).

In summary, long-term challenging of *S. dulcamara* with *R. solanacearum* always resulted in two distinct behaviours: plants with apparent bacterial colonisation and disease symptoms

and plants that remained symptomless even after direct stem inoculation, but which always carried latent bacterial infections.

Ralstonia solanacearum Movement Is Restricted in *S. dulcamara* Tissues Compared With Susceptible Tomato cv. Marmande

We have previously demonstrated that resistant tomato varieties can restrict *R. solanacearum* root colonisation and hamper bacterial vertical and horizontal movements in the stem (Planas-Marquès et al., 2020). Thus, we hypothesised that this mechanism could be also active in *S. dulcamara* and cause the observed delay in symptom appearance and infection latency. Next, we evaluated if *S. dulcamara* plants restricted bacterial movement in the stems compared with susceptible tomatoes. To better compare bacterial behaviour in the two hosts, we stem-inoculated a large number of plants with the luminescent reporter strain and observed bacterial distribution in their stems by grouping the plants according to disease stage. The whole 4-to-5-week-old plants could not be imaged because of size limitations and reduced sensitivity due to stem thickness. Thus, we obtained stem sections of internodes one to four from plants and imaged the top and bottom slices of each section and the remaining stem longitudinally divided in two. Representative pictures presented in **Figure 3A** show that luminescence matched the location of xylem bundles and was less intense in *S. dulcamara* plants compared with tomatoes at early disease stages. Quantification of the luminescence signal (**Supplementary Figure 3A**) corroborated this result, supporting the lower bacterial loads previously observed in asymptomatic *S. dulcamara* (**Figures 1E,F**). In addition, the luminescence of xylem bundles tended to decrease with height in *S. dulcamara*, while it remained constant in the susceptible tomato plants (**Figure 3A**), suggesting stronger restriction to vertical bacterial movement along the vessels in *S. dulcamara*.

To further analyse if *S. dulcamara* restricts the horizontal spread of *R. solanacearum* to neighbouring xylem and parenchyma tissues, we observed shoot sections of plants stem-inoculated with a GFP-tagged strain (Cruz et al., 2014) using fluorescence microscopy. Representative images of internode cuts above the inoculation point showed that the bacterium was slightly more confined to the vasculature in *S. dulcamara,* and that a lower number of xylem vessels appeared fluorescent in this species with respect to tomato plants at comparable disease stages (**Figure 3B**). Despite the differences observed in asymptomatic plants, quantification of the fluorescence intensity in diseased plants (**Supplementary Figure 3B**) showed that colonisation was comparable in tomato and *S. dulacamara* plants displaying similar symptomatology.

Since stem inoculation skips the initial stages of infection, and to determine whether *R. solanacearum* root entry and colonisation were also restricted in *S. dulcamara* plants, we carried out a root inoculation experiment. Briefly, plants were inoculated with the luminescent reporter strain by soil drenching and the bacterial counts were measured at short times after inoculation (1–4 dpi). As can be observed in **Supplementary Figure 4**, bacterial concentrations were comparable at early time points, demonstrating no difference in root entry. However, statistically lower bacterial loads were observed in *S. dulcamara* roots at 4 dpi, proving that the root tissues of *S. dulcamara* also limit *R. solanacearum* colonisation.

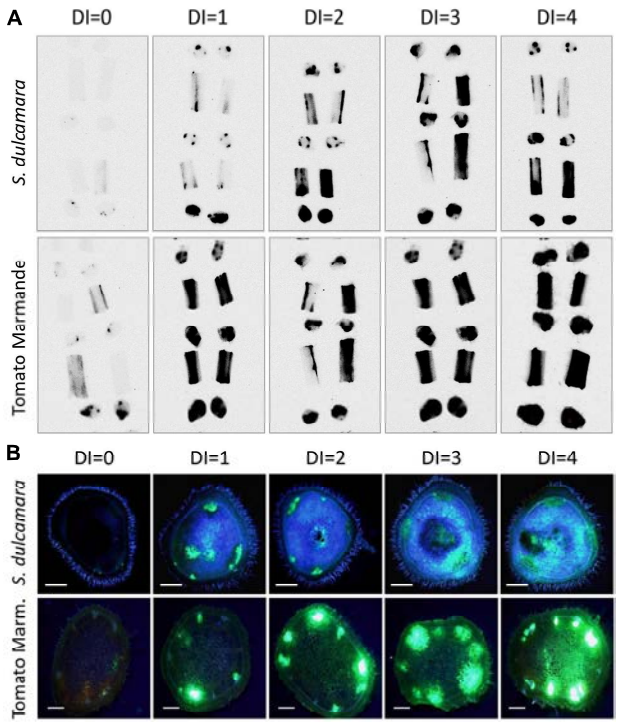

FIGURE 3 | *R. solanacearum* distribution in stems of inoculated *S. dulcamara* and tomato cv. Marmande plants. **(A)** Representative luminescence imaging photographs at different wilting stages (Disease index 0–4) of stem sections from *S. dulcamara* (top panel) and tomato (bottom panel) plants stem-inoculated with luminescent *R. solanacearum*. Luminescent bacteria are detected as dark areas in transversal and longitudinal sections of plant internodes 1–4 organised bottom to top. Inoculation points are indicated by an arrow. **(B)** Representative fluorescence microscopy images of stem sections from *S. dulcamara* (top panel) and tomato (bottom panel) plants stem-inoculated with an *R. solanacearum* strain constitutively expressing GFP. Inoculations were performed at the base of the first true leaf and transversal sections obtained in the first internode, 2 cm above the inoculation point. Scale bars indicate 0.5 mm.

Taken together, the assessment of bacterial colonisation in shoots and roots of both hosts suggests that *S. dulcamara* plants cope better with bacterial wilt because they have the ability to effectively restrict pathogen movement and colonisation inside their tissues.

Solanum dulcamara Displays Dramatically Reduced Bacterial Wilt Symptoms and Bacterial Colonisation at 20°C

Solanum dulcamara has been demonstrated to be a reservoir plant host in which *R. solanacearum* can overwinter (Olsson, 1976; Elphinstone et al., 1998; Janse et al., 1998; Wenneker et al., 1999; Caruso et al., 2005). To test the plant behaviour at

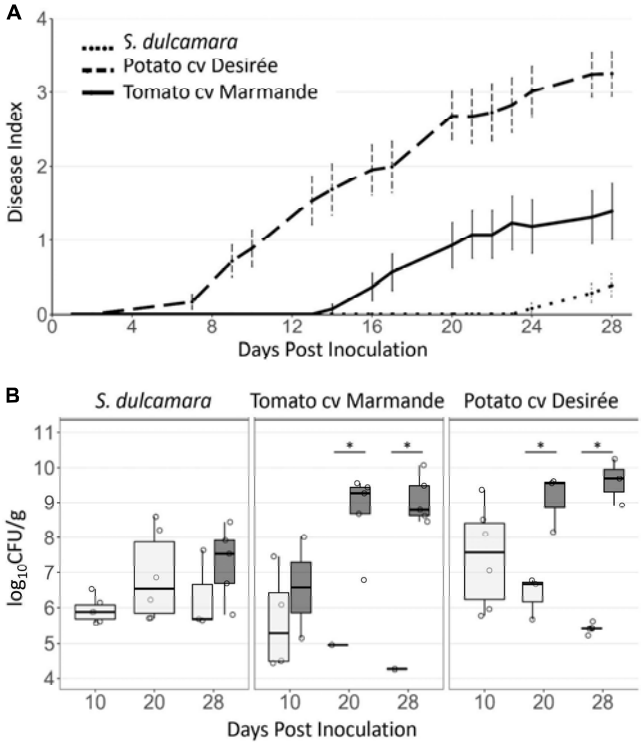

FIGURE 4 | Influence of temperature on bacterial wilt symptomatology in *S. dulcamara* and susceptible tomato and potato varieties. **(A)** Bacterial wilt symptom development (0 = asymptomatic to 4 = completely wilted) after soil-drench inoculation in *S. dulcamara,* tomato cv. Marmande and potato cv. Desirée plants inoculated with the *R. solanacearum* luminescent reporter and kept at 20°C. *n* = 30–35 plants per species. **(B)** Bacterial concentrations at the taproot level quantified by measuring the luminescence at 10, 20 and 28 dpi from *S. dulcamara*, susceptible tomato cv. Marmande, and susceptible potato cv. Desirée inoculated as in panel **(A)**. Results are grouped according to disease symptoms: asymptomatic (grey, disease index 0) and symptomatic (white, disease indices 1–4). *n* = 4–8 plants per sampling day and condition. *indicates statistical differences (*p* value < 0.05, *T*-student significant test).

lower temperatures that mimic those encountered in temperate environments, *S. dulcamara* and tomato plants kept at 20°C were soil-soak inoculated with luminescent *R. solanacearum,* and the symptoms and bacterial loads in the stems were evaluated over time. A temperature of 20°C was chosen as the lower temperature, compared with 27°C to avoid strong effects on plant or pathogen growth. To rule out specific effects of lower temperatures on the tomato-control plants, susceptible potato plants (cv. Desirée), which are adapted to cooler conditions than tomatoes (Ingram and McCloud, 1984), were also included in this experiment. Few days after inoculation, the first tomato plants started to wilt, followed by the first potato plants 2 weeks after inoculation. By 30 dpi, around 50% of the potatoes and over 25% of the tomatoes were completely wilted (**Figure 4A**), in accordance with previous results in tomatoes inoculated at these temperatures with a closely related II-B1 strain (Milling et al., 2009). On the contrary, all *S. dulcamara* plants survived the infection at 30 dpi with only a few of them (six out of 25) showing mild wilting symptoms in individual leaves (disease index <0.5, **Figure 4A**). Quantification of bacterial levels in the stem over time correlated with wilting, showing overall lower bacterial titres in *S. dulcamara* than in susceptible tomato or potato plants (**Figure 4B**). Since most plants remained asymptomatic throughout the experimental period, bacterial concentrations were calculated separately for asymptomatic and symptomatic plants. Symptomatic plants carried bacterial counts above 10^7 CFUs·g^{-1} in all species, concentrations being the lowest in *S. dulcamara* because disease symptoms were less developed in this species compared with the two susceptible crops. For instance, 30 days after inoculation *R. solanacearum* counts reached a maximum of 5×10^8 CFUs·g^{-1} in *S. dulcamara*, whereas wilted potato and tomato plants harboured up to 10^{10} CFUs·g^{-1} (**Figure 4B**).

In conclusion, cooler temperatures slowed down disease development in all species, but this effect was more pronounced in *S. dulcamara*, which always survived the disease in the tested period while holding mostly asymptomatic (latent) bacterial infections.

Solanum dulcamara Contains a Constitutively and Highly Lignified Xylem

The colonisation pattern of *R. solanacearum* in *S. dulcamara* compared with tomato cv. Marmande suggested that the former may contain vascular structures or components that make bacterial movement difficult. Lignin is one of the main components of the secondary plant cell wall, and it has been

described to play an important role as a structural defence mechanism in resistant tomato varieties against *R. solanacearum* (Nakaho et al., 2000; Ishihara et al., 2012; Kashyap et al., 2021). Therefore, we tested whether *S. dulcamara* xylem vessels presented differential lignin accumulation in their cell walls compared with susceptible tomato and potato plants. Taproot sections obtained 9 days after mock or soil inoculation with the *R. solanacearum* GFP reporter strain were stained with phloroglucinol HCl to identify lignified structures. This revealed constitutive and conspicuous lignification of the *S. dulcamara* vasculature, whereas, in susceptible tomato and potato plants, the parenchyma cells surrounding the vascular cylinder did not appear lignified (**Figure 5A**). In addition, while lignification remained stable in *S. dulcamara* after *R. solanacearum* infection, both tomato and Desirée plants showed a significant decrease in lignin accumulation upon *R. solanacearum* infection (**Figure 5A**), as previously described (Kashyap et al., 2021). To avoid the effect of lower bacterial concentrations usually found in *S. dulcamara* tissues, plants that contained comparable bacterial colonisation, as assessed by bacterial GFP fluorescence, were used for staining (**Figure 5A** lower panel). Quantification of the lignin stain intensity in mock and infected plants clearly confirmed a decrease in inoculated tomato and potato that was not observed in *S. dulcamara* plants (**Figure 5B**). The same results were observed after lignin staining from samples obtained at 6 dpi (**Supplementary Figure 3**), when bacterial colonisation was still low (**Supplementary Figure 3A** lower panel).

We have recently described (Kashyap et al., 2021) that suberin plays an important role in tomato resistance to bacterial wilt. To evaluate if this compound had an effect on the *S. dulcamara* restriction to *R. solanacearum* colonisation, we also stained inoculated or mock-treated stem sections with Sudan IV, which binds to the aliphatic domain of suberin to produce a reddish-brown colouration. No detectable increase in the accumulation of suberin was observed in *S. dulcamara* or in the susceptible plants after infection or mock treatment, as shown in **Supplementary Figure 6**.

In sum, *S. dulcamara* presented a constitutive accumulation of lignin in the xylem vessels and surrounding parenchyma that was not reduced upon pathogen infection as observed in susceptible tomato and potato, which may explain a higher restriction of bacterial colonisation in this species.

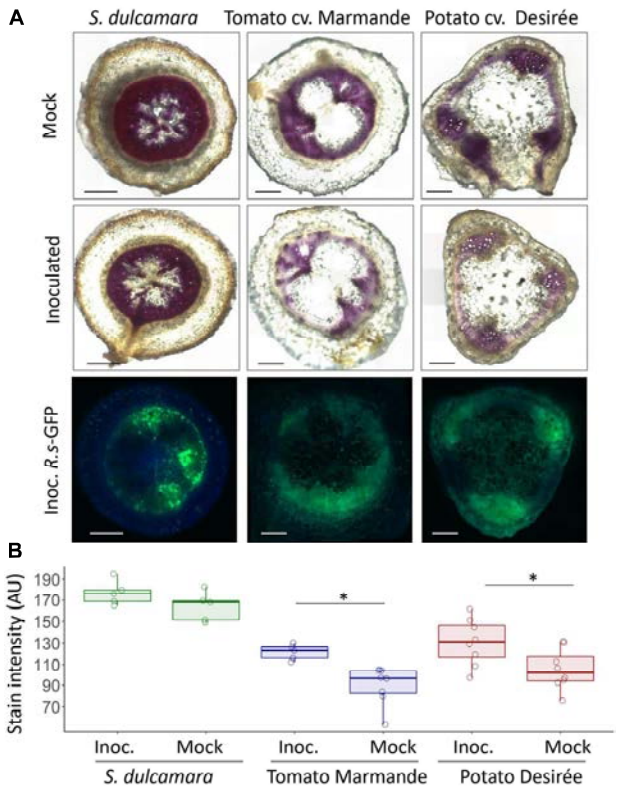

FIGURE 5 | Lignification of *S. dulcamara*, Tomato cv. Marmande and *S. tuberosum* cv. Desirée tissues upon *R. solanacearum* infection. **(A)** Representative composed images of *S. dulcamara*, tomato, and potato taproot transversal sections obtained 9 days after inoculation with *R. solanacearum*-GFP or mock treatment. First and second row: microscope bright-field images after lignin staining with phloroglucinol HCl (magenta colouration). Third row: fluorescence microscopy images after inoculation to assess the extent of bacterial colonisation. Images were obtained using a Leica DM6 microscope. Scale bars indicate 0.5 mm. **(B)** Quantification of the phloroglucinol HCL stain -indicative of lignin content- in the vascular area from the images shown in A performed with the ImageJ software. *indicates statistical differences (p-value < 0.05; T-student significant test $\alpha = 0.05$).

DISCUSSION

Solanum dulcamara Shows Partial Resistance to Bacterial Wilt

It has been established that plants display two main types of defence against pathogens: resistance, which is the ability of the host to limit pathogen multiplication; and tolerance, defined as the ability of the host to reduce the negative effects of infection (Clarke, 1986; Pagán and García-Arenal, 2020). However, the term tolerance has often been used incorrectly to describe partial levels of plant resistance. To differentiate bona fide tolerance from partial resistance a key aspect is that tolerance implies that the plant shows less symptoms or yield effects at equivalent levels of pathogen loads (Pagán and García-Arenal, 2020). According to these definitions, *S. dulcamara* shows some degree of resistance to bacterial wilt and no tolerance to the pathogen. A clear proof that tolerance does not play a role in the response of *S. dulcamara* to *R. solanacearum* is that all direct and indirect quantifications *R. solanacearum* inside *S. dulacamara* plants are comparable with those observed in tomato plants showing similar symptoms (**Figures 1E,F**, **2** and **Supplementary Figures 2**, **3**, **6**). The only exception to this is totally wilted plants, where bacterial populations declined, likely due to the lack of humidity in dry dead tissues (e.g., plant F, **Figure 2A**).

Several observations support that *S. dulcamara* plants display partial resistance to bacterial wilt (**Table 1**). First, irrespective of the inoculation method used, *S. dulcamara* showed delayed symptomatology (**Figures 1A,B**), delayed stem colonisation (**Figures 1C,D**), and slightly delayed root

TABLE 1 | Schematic comparison of the interaction at different levels between *R. solanacearum* and a susceptible tomato, *S. dulcamara*, and a resistant tomato.

	Susceptible tomato	*S. dulcamara*	Resistant tomato
Disease symptoms	+++	++	±
Bacterial levels in roots	+++	++	+
Bacterial levels in stems	+++	++	+
Bacterial vertical spread	+++	++	+
Bacterial horizontal spread	+++	++	+
Symptoms at lower temp.	++	±	NT
Structural reinforcements	±	++	+++

±: few or inexistent; +: low levels; ++: intermediate levels; +++: high levels; NT: not tested.

colonisation (**Supplementary Figure 4**). These phenotypes are similar but less pronounced than those observed in resistant tomato cv. Hawaii 7996 (**Table 1** and Planas-Marquès et al., 2020). Further proofs of this are that an important proportion of *S. dulcamara* plants remained asymptomatic when tomatoes were completely wilted and that stem inoculation and large numbers had to be used to obtain enough plants at advanced disease stages to compare with susceptible tomatoes.

Second, *S. dulcamara* restricted *R. solanacearum* vertical movement in the stem. A luminescent *R. solanacearum* reporter strain was able to entirely colonise susceptible tomato, while in *S. dulcamara* plants the upper stem displayed less pathogen colonisation (**Figures 2**, **3A**). In accordance with this, it has been described in *S. dulcamara* that symptomatology and pathogen presence was restricted only to shoots directly inoculated, indicating slow or no spreading of the bacterium throughout the plant (Wenneker et al., 1999). We previously reported similar behaviour, although clearly more apparent (**Table 1**) in resistant tomatoes (Planas-Marquès et al., 2020).

Third, bacterial movement between xylem vessels was also limited in *S. dulcamara* compared with susceptible tomatoes (**Figure 3B**). This could explain the stem colonisation delay observed, as *S. dulcamara* restricts *R. solanacearum* to specific xylem vessels, while others remain pathogen-free, a behaviour also reported for the resistant tomato (Planas-Marquès et al., 2020).

Taken together, our results confirm previous studies that reported *S. dulcamara* as partially resistant to bacterial wilt, although it was misleadingly described as tolerance. Discrepancies amongst previous reports where infection rates varied from 100 to 66% and 13 to 19% (Wenneker et al., 1999; Álvarez et al., 2008b; Jacobs et al., 2013) can be explained by the different inoculation methods used, by different assay conditions (e.g., temperature and inoculum), and/or by genetic differences amongst the plant accessions used.

Solanum dulcamara Carries Latent *R. solanacearum* Infections at 20°C

Three conditions are required for the establishment and development of plant diseases: a virulent pathogen, a susceptible host, and permissive environmental conditions (McNew, 1960). We thus explored the behaviour of *S. dulcamara* resistance to bacterial wilt when plants are grown and inoculated at lower temperatures. A decrease in temperature resulted in delayed symptom appearance and bacterial colonisation in both the susceptible hosts and in *S. dulcamara* (**Figure 4**) and the difference in resistance between them was maintained. This indicates that the ability of a pathogen to cause disease is compromised at a lower temperature, as has been described for many pathosystems. Thus, in these conditions, *S. dulcamara* plants displayed a stronger resistance to the disease, as all plants survived a month after inoculation and only very few of them showed minor wilting symptoms (**Figure 4A** and **Table 1**), but they all carried asymptomatic (latent) infections (**Figure 4B**).

Tolerance to disease, i.e., the ability to keep high bacterial levels without showing symptoms, has been proposed as a key trait for plants to act as reservoir hosts, providing a source of pathogen inoculum that spreads when environmental conditions become appropriate (Roberts and Heesterbeek, 2020). Based on our findings with *S. dulcamara* (**Table 1**), we propose that resistance, i.e., limiting pathogen colonisation, could also enable plants to act as reservoirs. Intermediate resistance would be required in this case for two reasons: first, it would allow a limited amount of pathogen to colonise and survive under unfavourable environmental conditions, such as winter temperatures, as latent infections inside the plant, and second, when environmental conditions favour disease (high temperature in our case), the pathogen could overcome resistance in some plants, multiplying to high numbers and spreading to other hosts. These two conditions could not take place if plants were either fully resistant or tolerant. This theory is supported by the original description of *S. dulcamara* as a symptomless *R. solanacearum* carrier in the wild (Olsson, 1976; Hayward, 1991), and studies show that environmental conditions can break resistance to the disease. For instance, in eucalypt, *R. solanacearum* usually behaves as a latent colonist, and only in the presence of other stressing factors the pathogen is able to proliferate and cause disease (Coutinho and Wingfield, 2017).

Constitutive Xylem Lignification in an *S. dulcamara* Is Likely Responsible for Its Resistance to *R. solanacearum*

Observation of *S. dulcamara* stem transversal sections indicated a highly lignified xylem compared with susceptible tomato and potato varieties (**Figure 5** and **Supplementary Figure 5**). This is in accordance with previous reports that lignin biosynthesis genes were upregulated in the bacterial wilt resistant tomato variety LS-89 upon *R. solanacearum* infection (Ishihara et al., 2012). Furthermore, we have recently shown striking differences in lignin composition between susceptible (Marmande) and resistant (Hawaii 7996) tomatoes, which indicate that the properties of paravascular lignin may be key for resistance to bacterial wilt (Kashyap et al., 2021).

Interestingly, *S. dulcamara* lignification was already high in mock-treated plants and was not affected by infection (**Figure 5** and **Supplementary Figure 5**), whereas susceptible tomato and

potato plants reduced their lignin content significantly both at 6 and 9 dpi upon *R. solanacearum* inoculation. This constitutive lignification and the irrelevance of suberin components, whose levels are comparable with susceptible plants (**Supplementary Figure 6**), are key differences in the factors controlling *S. dulcamara* resistance compared with tomato H7996, where suberin components play a major role (Kashyap et al., 2021). The fact that *S. dulcamara* is a perennial, with the ensuing secondary growth present in these plants (Caldwell, 2016), may explain the high lignification of its tissues, which must be even more pronounced in wild plants- and that this phenomenon is not inducible like in the annual tomato plants.

The correlation observed between resistance to infection and the presence of cell wall reinforcements both in resistant tomato and in the wild *S. dulcamara* plants indicates that lignification hinders *R. solanacearum* movement throughout the plant tissues and entry in the xylem vessels. This would explain the delay in symptom appearance compared with susceptible tomatoes (**Figures 1A,B**) and also account for the low bacterial content in inoculated plants that remained healthy (**Figures 1C–F**). Microscopically, cell wall reinforcements could have a major contribution to the stronger bacterial restriction in specific xylem vessels and decreased spread to neighbouring parenchyma cells, as observed in *S. dulcamara* compared with tomato cv. Marmande (**Figure 3**). Restriction of *R. solanacearum* infection to primary xylem vessels while secondary xylem vessels remain functional (Esau, 1977) could explain why *S. dulcamara* better survives the infection. Restricting pathogen movement is an important mechanism for resistance against *R. solanacearum* in tomato (Caldwell et al., 2017; Planas-Marquès et al., 2020) and potato (Cruz et al., 2014) that is also conserved in grapevine against *Xylella fastidiosa* (Chatterjee et al., 2008).

In summary, strong preexisting lignified xylem vessels present in *S. dulcamara* are likely the factor that supports its resistance to *R. solanacearum* and allows it to behave like a reservoir host. The generation of *S. dulcamara* mutants in lignin biosynthesis genes would be extremely useful to confirm this hypothesis.

DATA AVAILABILITY STATEMENT

The original contributions presented in the study are included in the article/**Supplementary Material**, further inquiries can be directed to the corresponding author.

AUTHOR CONTRIBUTIONS

MV, PS, NC, and AK conceived and designed the work. PS, AK, RP-J, and BD performed the experiments and statistical analyses. MV and NC provided reagents and materials. PS, RP-J, and MV analysed the results and edited the figures. MV, PS, and NC wrote the manuscript. All authors have made a substantial, direct and intellectual contribution to the work, and approved it for publication.

FUNDING

This work was supported by the Spanish Ministry of Economy and Competitiveness (AGL2016-78002-R) and the Ministry of Science and Innovation PID2019-108595RB-I00/AEI/10.13039/501100011033. We also acknowledge financial support from the "Severo Ochoa Program for Centers of Excellence in R&D" (SEV-2015-0533 and CEX2019-000902-S), and the CERCA Program from the Catalan Government (Generalitat de Catalunya). The funders had no role in study design, data collection and analysis, decision to publish, or preparation of the manuscript. PS held an INPHINIT Programme fellowship from Fundació "La Caixa" and AK was a recipient of a Netaji Subhas - Indian Council of Agricultural Research (ICAR) International Fellowship. RP-J received FI and FPU fellowships from Generalitat de Catalunya and the Ministry of Education and Professional Formation, respectively. BD have received funding from the European Union's Horizon 2020 Research and Innovation Programme under the Marie Skłodowska-Curie Grant Agreement No. 945043.

ACKNOWLEDGMENTS

The authors are grateful to all the members of the Bacterial Pathogens and Plant Cell Death Team (Center for Research in Agricultural Genomics, CRAG), especially to Marc Planas for their technical assistance and critical comments.

SUPPLEMENTARY MATERIAL

The Supplementary Material for this article can be found online at: https://www.frontiersin.org/articles/10.3389/fpls.2021.755708/full#supplementary-material

REFERENCES

Álvarez, B., López, M. M., and Biosca, E. G. (2008a). Survival strategies and pathogenicity of *Ralstonia solanacearum* phylotype II subjected to prolonged starvation in environmental water microcosms. *Microbiology* 154, 3590–3598. doi: 10.1099/mic.0.2008/019448-0

Álvarez, B., Vasse, J., Le-Courtois, V., Trigalet-Démery, D., López, M. M., and Trigalet, A. (2008b). Comparative behavior of *Ralstonia solanacearum* biovar 2 in diverse plant species. *Phytopathology* 98, 59–68. doi: 10.1094/PHYTO-98-1-0059

Bartoli, C., Lamichhane, J. R., Berge, O., Guilbaud, C., Varvaro, L., Balestra, G. M., et al. (2015). A framework to gauge the epidemic potential of plant pathogens in environmental reservoirs: the example of kiwifruit canker. *Mol. Plant Pathol.* 16, 137–149. doi: 10.1111/mpp.12167

Caldwell, D. (2016). *The Role of Root Anatomy and Root Architecture in Resistance to Ralstonia solanacearum*. Ph. D. thesis. West Lafayette: Purdue University.

Caldwell, D., Kim, B. S., and Iyer-Pascuzzi, A. S. (2017). *Ralstonia solanacearum* differentially colonizes roots of resistant and susceptible tomato plants. *Phytopathology* 107, 528–536. doi: 10.1094/PHYTO-09-16-0353-R

Caruso, P., Palomo, J. L., Bertolini, E., Álvarez, B., López, M. M., and Biosca, E. G. (2005). Seasonal variation of *Ralstonia solanacearum* biovar 2 populations in a Spanish river: recovery of stressed cells at low temperatures. *Appl. Environ. Microbiol.* 71, 140–148. doi: 10.1128/AEM.71.1.140-148.2005

Champoiseau, P. G., Jones, J. B., and Allen, C. (2009). *Ralstonia solanacearum* Race 3 biovar 2 causes tropical losses and temperate anxieties. *Plant Health Progr.* 10:35. doi: 10.1094/PHP-2009-0313-01-RV

Chatterjee, S., Newman, K. L., and Lindow, S. E. (2008). Cell-to-cell signaling in Xylella fastidiosa suppresses movement and xylem vessel colonization in grape. *Mol. Plant-Microbe Interact.* 21, 1309–1315. doi: 10.1094/MPMI-21-10-1309

Clarke, D. D. (1986). Tolerance of parasites and disease in plants and its significance in host-parasite interactions. *Adv. Plant Pathol.* 5, 161–198.

Coll, N. S., and Valls, M. (2013). Current knowledge on the *Ralstonia solanacearum* type III secretion system. *Microb. Biotechnol.* 6, 614–620. doi: 10.1111/1751-7915.12056

Coutinho, T. A., and Wingfield, M. J. (2017). *Ralstonia solanacearum* and r. Pseudosolanacearum on eucalyptus: opportunists or primary pathogens? *Front. Plant Sci.* 8:761. doi: 10.3389/fpls.2017.00761

Cruz, A. P. Z., Ferreira, V., Pianzzola, M. J., Siri, M. I., Coll, N. S., and Valls, M. (2014). A novel, sensitive method to evaluate potato germplasm for bacterial wilt resistance using a luminescent *Ralstonia solanacearum* reporter strain. *Mol. Plant Microbe Interact.* 27, 277–285. doi: 10.1094/MPMI-10-13-0303-FI

Elphinstone, J. G. (1996). Survival and possibilities for extinction of *Pseudomonas solanacearum* (Smith) Smith in cool climates. *Potato Res.* 39, 403–410. doi: 10.1007/BF02357946

Elphinstone, J. G., Stanford, H., Stead, D. E., and Hutton, S. (1998). Survival and transmission of *Ralstonia solanacearum* in aquatic plants of Solanum dulcamara and associated surface water in England. *EPPO Bull.* 94, 93–94. doi: 10.1111/j.1365-2338.1998.tb00709.x

Esau, K. (1977). *Anatomy of Seed Plants*, 2nd Edn. New York: John Wiley & Sons Ltd. doi: 10.2307/2418500

Graham, J., and Lloyd, A. B. (1978). Solanum cinereum R. Br., a wild host of *Pseudomonas solanacearum* biotype II. *J. Aust. Inst. Agric. Sci.* 44, 124–126.

Guidot, A., Jiang, W., Ferdy, J. B., Thébaud, C., Barberis, P., Gouzy, J., et al. (2014). Multihost experimental evolution of the pathogen *ralstonia solanacearum* unveils genes involved in adaptation to plants. *Mol. Biol. Evol.* 31, 2913–2928. doi: 10.1093/molbev/msu229

Haydon, D. T., Cleaveland, S., Taylor, L. H., and Laurenson, M. K. (2002). Identifying reservoirs of infection: a conceptual and practical challenge. *Emerg. Infect. Dis.* 8, 1468–1473. doi: 10.3201/eid0812.010317

Hayward, A. C. (1991). Biology and Epidemiology of Bacterial Wilt caused by *Pseudomonas solanacearum*. *Ann. Rev. Phytopathol.* 29, 65–87. doi: 10.1146/annurev.py.29.090191.000433

Hayward, A. C. (1994). "The hosts of *Pseudomonas solanacearum*," in *Bacterial Wilt: the Disease and Its Causative Agent, Pseudomonas solanacearum*, eds A. Hayward and G. Hartman (Wallingford: CAB International), 9–24.

Ingram, K. T., and McCloud, D. E. (1984). Simulation of Potato Crop Growth and Development 1. *Crop Sci.* 24, 21–27. doi: 10.2135/cropsci1984.0011183X002400010006x

Ishihara, T., Mitsuhara, I., Takahashi, H., and Nakaho, K. (2012). Transcriptome analysis of quantitative resistance-specific response upon *Ralstonia solanacearum* infection in Tomato. *PLoS One* 7:e46763. doi: 10.1371/journal.pone.0046763

Jacobs, J. M., Milling, A., Mitra, R. M., Hogan, C. S., Ailloud, F., Prior, P., et al. (2013). *Ralstonia solanacearum* requires pops, an ancient avre-family effector, for virulence and to overcome salicylic acid-mediated defenses during tomato pathogenesis. *mBio* 4, e00875–13. doi: 10.1128/mBio.00875-13

Janse, J. D. (1996). Potato brown rot in western Europe – history, present occurrence and some remarks on possible origin, epidemiology and control strategies. *EPPO Bull.* 26, 679–695. doi: 10.1111/j.1365-2338.1996.tb01512.x

Janse, J. D., Araluppan, F. A. X., Schans, J., Wenneker, M., and Westerhuis, W. (1998). "Experiences with bacterial brown rot *Ralstonia solanacearum* biovar 2, race 3 in the Netherlands," in *Bacterial Wilt Disease*, eds P. Prior, C. Allen, and J. Elphinstone (Berlin: Springer), 146–152. doi: 10.1007/978-3-662-03592-4_21

Janse, J. D., Van Den Beld, H. E., Elphinstone, J., Simpkins, S., Tjou-Tam-Sin, N. N. A., and Van Vaerenbergh, J. (2004). Introduction to Europe of *Ralstonia solanacearum* biovar 2, race 3 in Pelargonium zonale cuttings. *J. Plant Pathol.* 86, 147–155.

Kashyap, A., Capellades, M., Zhang, W., Srinivasan, S., Laromaine, A., Serra, O., et al. (2021). Induced ligno-suberin vascular coating and tyramine-derived hydroxycinnamic acid amides restrict *Ralstonia solanacearum* colonization in resistant tomato roots. *bioRxiv* [Preprint]. doi: 10.1101/2021.06.15.448549

Kempenaar, C., Groeneveld, R. M. W., Lotz, L. A. P., Wenneker, M., and Janse, J. D. (1998). Ecology and control of bittersweet in relation to brown rot. *Gewasbescherming* 29, 119–123.

Mansfield, J., Genin, S., Magori, S., Citovsky, V., Sriariyanum, M., Ronald, P., et al. (2012). Top 10 plant pathogenic bacteria in molecular plant pathology. *Mol. Plant Pathol.* 13, 614–629. doi: 10.1111/j.1364-3703.2012.00804.x

McCann, H. C. (2020). Skirmish or war: the emergence of agricultural plant pathogens. *Curr. Opin. Plant Biol.* 50, 147–152. doi: 10.1016/j.pbi.2020.06.003

McNew, G. L. (1960). "The nature, origin, and evolution of parasitism," in *Plant Pathology: An Advanced Treatise*, eds J. G. Horsfall and A. E. Dimond (New York: Academic Press), 19–69.

Milling, A., Meng, F., Denny, T. P., and Allen, C. (2009). Interactions with hosts at cool temperatures, not cold tolerance, explain the unique epidemiology of *Ralstonia solanacearum* race 3 biovar 2. *Phytopathology* 99, 1127–1134. doi: 10.1094/PHYTO-99-10-1127

Monteil, C. L., Cai, R., Liu, H., Mechan Llontop, M. E., Leman, S., Studholme, D. J., et al. (2013). Nonagricultural reservoirs contribute to emergence and evolution of *Pseudomonas* syringae crop pathogens. *New Phytol.* 199, 800–811. doi: 10.1111/nph.12316

Monteiro, F., Solé, M., Van Dijk, I., and Valls, M. (2012). A chromosomal insertion toolbox for promoter probing, mutant complementation, and pathogenicity studies in *Ralstonia solanacearum*. *Mol. Plant Microbe Interact.* 25, 557–568. doi: 10.1094/MPMI-07-11-0201

Morris, C. E., Bardin, M., Kinkel, L. L., Moury, B., Nicot, P. C., and Sands, D. C. (2009). Expanding the paradigms of plant pathogen life history and evolution of parasitic fitness beyond agricultural boundaries. *PLoS Pathog.* 5:e1000693. doi: 10.1371/journal.ppat.1000693

Mueller, E. E., Groves, R. L., and Gratton, C. (2012). Crop and non-crop plants as potential reservoir hosts of Alfalfa mosaic virus and cucumber mosaic virus for spread to commercial snap bean. *Plant Dis.* 96, 506–514. doi: 10.1094/PDIS-02-11-0089

Nakaho, K., Hibino, H., and Miyagawa, H. (2000). Possible mechanisms limiting movement of *Ralstonia solanacearum* in resistant tomato tissues. *J. Phytopathol.* 148, 181–190. doi: 10.1046/j.1439-0434.2000.00476.x

Olsson, K. (1976). Experience of Brown Rot Caused by *Pseudomonas solanacearum* (Smith) Smith in Sweden. *EPPO Bull.* 6, 199–207. doi: 10.1111/j.1365-2338.1976.tb01546.x

Pagán, I., and García-Arenal, F. (2020). Tolerance of plants to Pathogens: a unifying view. *Ann. Rev. Phytopathol.* 58, 1–20. doi: 10.1146/annurev-phyto-010820-012749

Planas-Marquès, M., Kressin, J. P., Kashyap, A., Panthee, D. R., Louws, F. J., Coll, N. S., et al. (2020). Four bottlenecks restrict colonization and invasion by the pathogen *Ralstonia solanacearum* in resistant tomato. *J. Exp. Bot.* 71, 2157–2171. doi: 10.1093/jxb/erz562

Pomar, F., Novo, M., Bernal, M. A., Merino, F., and Barceló, A. R. (2004). Changes in stem lignins (monomer composition and crosslinking) and peroxidase are related with the maintenance of leaf photosynthetic integrity during Verticillium wilt in Capsicum annuum. *New Phytol.* 163, 111–123. doi: 10.1111/j.1469-8137.2004.01092.x

Puigvert, M., Guarischi-Sousa, R., Zuluaga, P., Coll, N. S., Macho, A. P., Setubal, J. C., et al. (2017). Transcriptomes of *Ralstonia solanacearum* during root colonization of solanum commersonii. *Front. Plant Sci.* 8:370. doi: 10.3389/fpls.2017.00370

Roberts, M. G., and Heesterbeek, J. A. P. (2020). Characterizing reservoirs of infection and the maintenance of pathogens in ecosystems. *J. R. Soc. Interface* 17:20190540. doi: 10.1098/rsif.2019.0540

Schell, M. A. (2000). Control of virulence and pathogenicity genes of *Ralstonia solanacearum* by an elaborate sensory network. *Ann. Rev. Phytopathol.* 38, 263–292. doi: 10.1146/annurev.phyto.38.1.263

Shamsuddin, N., Lloyd, A. B., and Graham, J. (1978). Survival of the potato strain of *Pseudomonas solanacearum* in soil. *J. Aust. Inst. Agric. Sci.* 44, 212–215.

She, X. M., He, Z. F., Luo, F. F., and Li, H. P. (2013). First report of bacterial wilt caused by *Ralstonia solanacearum* on Ageratum conyzoides in China. *Plant Dis.* 97, 418–418. doi: 10.1094/PDIS-08-12-0780-PDN

Siri, M. I., Sanabria, A., and Pianzzola, M. J. (2011). Genetic diversity and aggressiveness of *Ralstonia solanacearum* strains causing bacterial wilt of potato in Uruguay. *Plant Dis.* 95, 1292–1301. doi: 10.1094/PDIS-09-10-0626

Thinakaran, J., Pierson, E., Kunta, M., Munyaneza, J. E., Rush, C. M., and Henne, D. C. (2015). Silverleaf nightshade (*Solanum elaeagnifolium*), a reservoir host for 'Candidatus Liberibacter *solanacearum*', the putative causal agent of zebra chip disease of potato. *Plant Dis.* 99, 910–915. doi: 10.1094/PDIS-12-14-1254-RE

Tusiime, G., Adipala, E., Opio, F., and Bhagsari, A. S. (1997). "Weeds as latent hosts of *Ralstonia solanacearum* in highland Uganda: implications to development of an integrated control package for bacterial wilt," in *Bacterial Wilt Disease: Molecular and Ecological Aspects*, eds P. Prior, C. Allen, and J. Elphinstone (Berlin: Springer-Verlag), 413–419. doi: 10.1007/978-3-662-03592-4_63

Van Elsas, J. D., Kastelein, P., Van Bekkum, P., Van der Wolf, J. M., De Vries, P. M., and Van Overbeek, L. S. (2000). Survival of *Ralstonia solanacearum* biovar 2, the causative agent of potato brown rot, in field and microcosm soils in temperate climates. *Phytopathology* 90, 1358–1366. doi: 10.1094/PHYTO.2000.90.12.1358

Wenneker, M., Verdel, M. S. W., Groeneveld, R. M. W., Kempenaar, C., Van Beuningen, A. R., and Janse, J. D. (1999). Ralstonia (*Pseudomonas*) *solanacearum* race 3 (biovar 2) in surface water and natural weed hosts: first report on stinging nettle (Urtica dioica). *Eur. J. Plant Pathol.* 105, 307–315. doi: 10.1023/A:1008795417575

Conflict of Interest: The authors declare that the research was conducted in the absence of any commercial or financial relationships that could be construed as a potential conflict of interest.

Publisher's Note: All claims expressed in this article are solely those of the authors and do not necessarily represent those of their affiliated organizations, or those of the publisher, the editors and the reviewers. Any product that may be evaluated in this article, or claim that may be made by its manufacturer, is not guaranteed or endorsed by the publisher.